

April 2022

Proposition 1 Delta Stewardship Council Contract Award 18203



# Synthesis of Juvenile Steelhead Responses to Hydrodynamic Conditions in the Sacramento-San Joaquin Delta

Prepared for Delta Stewardship Council and State Water Contractors



April 2022

Proposition 1 Delta Stewardship Council Contract Award 18203

# Synthesis of Juvenile Steelhead Responses to Hydrodynamic Conditions in the Sacramento-San Joaquin Delta

**Prepared for**

State Water Contractors  
1121 L Street, Suite 1050  
Sacramento, California 95814

Delta Stewardship Council  
Delta Science Program  
715 P Street, 15 - 300  
Sacramento, California 95814

**Prepared by**

Anchor QEA, LLC  
33 New Montgomery Street, Suite 1210  
San Francisco, California 94105



# TABLE OF CONTENTS

<b>Executive Summary.....</b>	<b>1</b>
Summary of Key Results.....	2
SST Metrics.....	3
Management Implications.....	4
Recommendations for Future Studies:.....	5
<b>1   Introduction .....</b>	<b>1</b>
1.1   Acknowledgements.....	4
<b>2   Methods .....</b>	<b>6</b>
2.1   Project Process .....	6
2.2   Study Area.....	7
2.3   Hydrodynamic Modeling Overview .....	9
2.3.1   UnTRIM Bay-Delta Model .....	9
2.3.2   Hydrodynamic Model Simulation Periods.....	14
2.3.3   Hydrodynamic Variables.....	15
2.3.4   Evaluation of Turner Cut Net Flow.....	22
2.4   Steelhead Data Analysis.....	23
2.4.1   Tagging and Telemetry Data .....	23
2.4.2   Fish Transition Modeling .....	25
2.4.3   Covariates.....	27
<b>3   Results.....</b>	<b>32</b>
3.1   UnTRIM.....	32
3.1.1   Correlation Analysis.....	32
3.1.2   Exports and Net Water Flow Through Turner Cut.....	34
3.2   Head of Old River.....	40
3.2.1   Model Selection .....	41
3.2.2   Fifteen-Minute Transitions.....	46
3.2.3   Example Period Transition Probabilities .....	49
3.3   Turner Cut .....	53
3.3.1   Model Selection .....	53
3.3.2   Fifteen-Minute Transitions.....	56
3.3.3   Example Period Transition Probabilities .....	59
3.4   Water Project Area.....	60

3.4.1	Model Selection .....	61
3.4.2	Fifteen-Minute Transitions.....	68
3.4.3	Example Period Transition Probabilities .....	72
<b>4</b>	<b>Discussion .....</b>	<b>79</b>
4.1	Steelhead Behavioral Responses.....	79
4.1.1	Head of Old River.....	80
4.1.2	Turner Cut.....	82
4.1.3	Water Project Area.....	84
4.2	Approach.....	86
4.2.1	Data Limitations.....	87
4.2.2	SST Metrics.....	88
4.2.3	Similar Analyses .....	89
<b>5</b>	<b>Conclusions .....</b>	<b>91</b>
5.1	Management Implications.....	94
5.2	Recommendations.....	96
<b>6</b>	<b>References .....</b>	<b>100</b>

## TABLES

Table 2-1	Date Ranges of Fish Detections and Periods During Which Hydrodynamic Variables Were Extracted from the Hydrodynamic Model Predictions .....	14
Table 2-2	Hydrodynamic Variables Generated from the Hydrodynamic Model Predictions ....	16
Table 2-3	Date Ranges When HOR Barrier Was Installed Each Year .....	29
Table 3-1	Head of Old River Junction Model Selection Results.....	42
Table 3-2	Best Fit Head of Old River Model Parameter Estimates.....	45
Table 3-3	Turner Cut Junction Model Selection Results.....	54
Table 3-4	Best Fit Turner Cut Model Parameter Estimates.....	55
Table 3-5	Water Project Area Model Selection Results .....	62
Table 3-6	Best Fit Water Project Area Model Parameter Estimates.....	63

## FIGURES

Figure 2-1	Study Area .....	7
Figure 2-2	High-Resolution UnTRIM San Francisco Bay-Delta Model Domain, Bathymetry, and Locations of Model Boundary Conditions .....	10
Figure 2-3	Locations of Stations Used for Meteorological Boundary Conditions .....	13
Figure 2-4	Time Series of Delta Outflow and X2 for Water Years Encompassing Each Simulation Year .....	15
Figure 2-5	Direction of Positive Cross-Sectional Water Flow Around Head of Old River .....	17
Figure 2-6	Direction of Positive Cross-Sectional Water Flow Around Turner Cut .....	18
Figure 2-7	Direction of Positive Cross-Sectional Water Flow Around Water Project Area .....	19
Figure 2-8	Location of Cross Section in Turner Cut and Individual Hydrophones from 2016.....	21
Figure 2-9	Locations of Cross-Section Centers in the Vicinity of Each Hydrophone Array .....	22
Figure 2-10	Daily Presence of Juvenile Steelhead in Study Areas .....	25
Figure 2-11	Schematic of Multistate Models and State Transition Matrices .....	27
Figure 3-1	Predicted Net Flow During 2016 .....	35
Figure 3-2	Predicted Net Flow During 2013 .....	36
Figure 3-3	Relationship Between Predicted Net Flow Through Turner Cut and Toward the Export Facilities .....	37
Figure 3-4	Data-Based Net Flow During 2016 .....	38
Figure 3-5	Data-Based Net Flow During 2013 .....	39
Figure 3-6	Relationship Between Data-Based Flow Through Turner Cut and Water Exports .....	40
Figure 3-7	Distribution of HOR Junction Observed State-to-State Transitions with and Without the Barrier Installed .....	41
Figure 3-8	Head of Old River Junction Best Fit Model Covariate Slope Coefficient Estimates....	43
Figure 3-9	Net Flow Effect on the 15-Minute Transition Probability of Actively Migrating Smolts from HOR (State U) .....	46
Figure 3-10	Net Flow and Barrier Effect on 15-Minute Transition Probabilities for Active Migrators and Non-Migrators .....	47
Figure 3-11	Tide Flow Effect on the 15-Minute Transition Probability of Actively Migrating Smolts .....	48
Figure 3-12	Tide Flow and Barrier Effect on 15-Minute Transition Probabilities for Active Migrators and Non-Migrators .....	48
Figure 3-13	Distributary Tide Flow Effect on the 15-Minute Transition Probability of Actively Migrating Smolts with No Barrier .....	49
Figure 3-14	Example Transition Probabilities over a 3-Day Period: May 22 to May 24, 2012.....	50
Figure 3-15	Flow Conditions at HOR over a 3-Day Period: May 22 to May 24, 2012 .....	51
Figure 3-16	Example Transition Probabilities over a 3-Day Period: March 17 to March 19, 2016.....	52

Figure 3-17	Flow Conditions over a 3-Day Period: March 17 to March 19, 2016 .....	52
Figure 3-18	Distribution of Turner Cut Junction Observed State-to-State Transitions .....	53
Figure 3-19	Turner Cut Junction Best Fit Model Covariate Slope Coefficient Estimates.....	56
Figure 3-20	Net Flow Effect on 15-Minute Transition Probabilities .....	57
Figure 3-21	Tide Flow Effect on 15-Minute Transition Probabilities .....	58
Figure 3-22	Distributary Tide Flow Effect on 15-Minute Transition Probabilities.....	58
Figure 3-23	Example Period Transition Probabilities over a 3-Day Period: May 2 to May 4, 2016 .....	59
Figure 3-24	Flow Conditions over a 3-Day Period: May 2 to May 4, 2016 .....	60
Figure 3-25	Distribution of Water Project Area Observed State-to-State Transitions .....	61
Figure 3-26	Water Project Area Best Fit Model Covariate Slope Coefficient Estimates.....	64
Figure 3-27	Predicted Depth-Averaged Water Temperature in the Water Project Area: March 21, 2016 .....	66
Figure 3-28	Net Flow in West Canal and Corresponding Clifton Court Forebay Radial Gate Operation in March 2014.....	67
Figure 3-29	Tide Flow Effect on 15-Minute Transition Probabilities from CVP (State C).....	68
Figure 3-30	Net Flow Effect on 15-Minute Transition Probabilities from CCF Radial Gates (State R).....	69
Figure 3-31	Tide Flow Effect on 15-Minute Transition Probabilities from CCF Radial Gate (State R).....	69
Figure 3-32	Net Flow Effect on 15-Minute Transition Probabilities from West Canal (State W)...	70
Figure 3-33	Tide Flow Effect on 15-Minute Transition Probabilities from West Canal (State W) .	71
Figure 3-34	Release Day Effect on 15-Minute Transition Probabilities in the WPA .....	72
Figure 3-35	Example Transition Probabilities from CVP (State C): April 17 to April 23, 2015.....	73
Figure 3-36	Example Transition Probabilities from CCF Radial Gates (State R): April 17 to April 23, 2015 .....	74
Figure 3-37	Example Transition Probabilities from Downstream in West Canal (State D): April 17 to April 23, 2015 .....	74
Figure 3-38	Flow and Temperature Conditions: April 17 to April 23, 2015.....	75
Figure 3-39	Example Period Transition Probabilities from Upstream at CVP (State C): March 20 to March 26, 2016.....	76
Figure 3-40	Example Period Transition Probabilities from CCF Radial Gate (State R): March 20 to March 26, 2016 .....	76
Figure 3-41	Example Period Transition Probabilities from Downstream in West Canal (State W): March 20 to March 26, 2016.....	77
Figure 3-42	Flow and Temperature Conditions: March 20 to March 26, 2016.....	78

## **APPENDICES**

- Appendix A Stakeholder Workshop
- Appendix B Hydrodynamic Model Output Memorandum
- Appendix C Hydrodynamic Model Validation
- Appendix D Supplemental Fish Data and Model Outputs

## ABBREVIATIONS

AIC	Akaike's information criterion
BAAQMD	Bay Area Air Quality Management District
Bay-Delta	San Francisco Bay and Sacramento-San Joaquin Delta
CCF	Clifton Court Forebay
CCWD	Contra Costa Water District
CDEC	California Data Exchange Center
cfs	cubic feet per second
CIMIS	California Irrigation Management Information System
CVP	Central Valley Project
Delta	Sacramento-San Joaquin Delta
DICU	Delta Island Consumptive Use
DSM2	Delta Simulation Model 2
DWR	California Department of Water Resources
HOR	Head of Old River
I:E	inflow to export ratio
km	kilometer
m	meter
m/s	meters per second
m <sup>3</sup> /s	cubic meters per second
mainstem	SJR mainstem
mm	millimeter
NARR	North American Regional Reanalysis
NAVD88	North American Vertical Datum of 1988
NOAA	National Oceanic and Atmospheric Administration
NOAA NARR	NOAA North American Regional Reanalysis
OR	Old River
PSU	practical salinity unit
RMSD <sub>n</sub>	normalized root-mean-square difference
SJR	San Joaquin River
SMSCG	Suisun Marsh Salinity Control Gates
steelhead	California Central Valley steelhead
SWP	State Water Project
TC	Turner Cut
ubRMSD	unbiased root-mean-square difference
UnTRIM Bay-Delta model	Unstructured Nonlinear Tidal Residual Intertidal Mudflat Bay-Delta hydrodynamic model

USGS	U.S. Geological Survey
VIF	variance inflation factor
WCL	West Canal
WPA	water project export facilities area



## Executive Summary

This study combined detailed 3D hydrodynamic model predictions with juvenile steelhead (*Oncorhynchus mykiss*) telemetry data to investigate how hydrodynamic conditions affect steelhead movement through the Sacramento-San Joaquin Delta (Delta). The study was designed to evaluate what can be learned about steelhead behavior based on hydrodynamic conditions at small scales important to fish at key routing junctions and sites using acoustic telemetry data collected in the San Joaquin River (SJR) and South Delta from 2011 through 2016.

A majority (38 of 43) of studies conducted in the Delta between 2006 and 2016 evaluated Chinook salmon (*O. tshawytscha*), but only 5 evaluated steelhead (Perry et al. 2016). Buchanan et al. (2021) reported on results of survival analysis of all 6 years of the juvenile steelhead telemetry dataset used in our analysis. Given the Endangered Species Act status of steelhead and limited information on steelhead behavior within the Delta, additional analysis of steelhead was needed to inform water management discussions and support Collaborative Science and Adaptive Management Program (CSAMP) objectives. Our study evaluated steelhead movement using all 6 years of telemetry data that included different water years and water project operations.

A high-resolution 3D hydrodynamic model (UnTRIM) was used to predict hydrodynamic conditions throughout the Delta during the 6 years when telemetry data on juvenile steelhead were collected by the U.S. Bureau of Reclamation. The telemetry data were analyzed to understand where hydrophone locations and detection records were robust enough to support analyses of fish movement. Based on this review and discussions with CSAMP scientists, three areas of interest were evaluated: (1) the distributary mainstem junction at Head of Old River (HOR); (2) the distributary mainstem junction at Turner Cut (TC); and (3) the Inner Delta Water Project Area (WPA).

For an area to be evaluated, the same or similarly located acoustic receivers must have been deployed in multiple years. At HOR, acoustic receivers were deployed upstream and downstream of the junction on the mainstem, and downstream of the junction on Old River, in roughly the same location from 2011 to 2016. At TC junction, receivers were deployed upstream and downstream in the mainstem and in TC in 2013, 2015, and 2016. In the WPA, receivers were deployed at the inlet to the Central Valley Project (CVP) facilities, at the radial gate inlet to Clifton Court Forebay (CCF) at the State Water Project, and in West Canal in 2014, 2015, and 2016. At each location, state transition probabilities during short (15 minutes) and long example periods (3 or 5 days) were evaluated.

This analysis used a multistate Markov model that estimated fish movements, also referred to as transitions, from one state to another (e.g., from upstream to downstream in the main channel, or into a distributary channel). Using this multistate model together with variables from a well-calibrated 3D hydrodynamic model, as well as fish-specific and other environmental variables (e.g., time of day, rock barrier presence), provided insight into the different hydrodynamic variables that

are most predictive of juvenile steelhead transitions at the locations evaluated. Where feasible based on the available data, we also evaluated five metrics identified by the Salmon Scoping Team (SST) to potentially help refine water project operations to improve juvenile salmonid survival through the Delta.

Overall, the pairing of a detailed hydrodynamic simulation model with acoustic telemetry data was successful. It was used to evaluate steelhead transitions in a multistate modeling framework where fish transitions among states were evaluated at two distributary junctions from the mainstem SJR to the inner and South Delta, and at the WPA. The outcome of the analyses was an increased understanding of how juvenile steelhead movement at the three locations studied relates to specific hydrodynamic conditions and management actions.

## Summary of Key Results

Key findings from the analyses conducted at each location are as follows.

### Head of Old River

- Fish generally stayed in the SJR when the barrier was installed and moved into Old River when the barrier was not installed.
- When the barrier was installed:
  - There was more variability in the percentage of fish classified as active migrants (range from 24% to 97%), compared to when it was not installed (range from 73% to 91%).
  - During one period in May 2012, active migrants had an 80% chance of moving downstream after 3 hours, while non-migrants did not reach an 80% chance of transitioning downstream until 1.7 days.
- Over short time periods, fish were more likely to move downstream on the SJR rather than into Old River when net flows were high (generally during high water years) on the SJR, even when the barrier was not installed.
- During low flow years, tidal flow had more influence on the probability of transitioning at the 15-minute timescale, with fish generally moving downstream with the ebb tide and “backtracking” on the flood tide. The Old River tidal flow was only a factor when the barrier was not installed.
- The interactive effect between barrier and time of day could indicate altered behavioral patterns because of the barrier, such as foraging or predator avoidance.

### Turner Cut

- Few fish entered TC, but those that did were more likely to enter during flood tide flow into TC. The tidal component of flow had the strongest influence on fish transitions in the TC junction among the three areas evaluated.

- Over three-quarters of fish that had previously been designated as actively migrating at HOR continued to move through the TC junction at approximately the same rate as was observed at HOR.
- Juvenile steelhead were generally more likely to move during the day.
- Although the range of mainstem net flow was limited (-55 to 72 cubic meters per second) during the 3 years of telemetry data available at this location, net flow was the strongest predictor of upstream-to-downstream movement.
- The analyses evaluated total flow, net flow, and tidal flow at each location (where total = net + tidal). Water project exports influenced net flow through TC. This finding is in contrast with earlier findings by the SST and published results by other researchers that found little influence of water project operations on flow in TC. The magnitude of net flow in TC influenced how “reversed” the total flow became during flood tides, which in turn increased the chance of fish entering TC.

### **Water Project Area**

- Fish in this area displayed longer residence time and a lack of directional movement, unlike the other two areas where one transition direction had a much higher rate. Additionally, fish had higher probabilities of transitioning in the direction of tidal flows.
- Of the total number of fish detected in the WPA, 30.7% ended up in the CVP salvage tank. The probability of this happening over time increased with high reverse net flow. Since net flow was reversed for the entire study period evaluated at this location (2014 to 2016), all fish experienced some level of reverse net flow.
- Fish were more likely to move away (either direction) from the entrance to CCF (i.e., the radial gates) when net flow in West Canal was low, probably because the radial gates are generally closed when net flow is low.
- Temperature, source water, and tidal flows are highly dynamic in this area. Temperature fluctuations related to source water and tidal flow were influential in the model, but we were not able to isolate the effects on fish movement. Data were only available in critical or below normal water years (Table 2-1). The influence of these interacting variables requires further investigation.
- Fish released into the SJR after the HOR barrier was installed (i.e., later release day) were more likely to transition toward CVP in the WPA, potentially a result of taking a longer route down the SJR and generally moving in a southward direction through the Inner Delta.

### **SST Metrics**

Several metrics identified by the SST were removed from consideration during initial data exploration due to high correlation with other covariates that were modeled, or due to the metrics not aligning with the fine scale needed for analyses of movement and behavior. However, Qwest was shown to

have a high correlation with local flow conditions that were incorporated into the model in some areas (e.g.,  $R > 0.9$  for Qwest and mainstem flow at TC). Also, total export flows were highly correlated with net flow in West Canal ( $R > -0.95$ ). Depth-averaged percent Sacramento River water, percent SJR water, and percent Mokelumne River water were evaluated in the hydrodynamic and state transition models but were not included in the best fit models of fish transitions for the three areas evaluated.

## Management Implications

Management implications from the analyses conducted at each location are as follows.

### Head of Old River

The strategy of installing the barrier to prevent fish from taking the Old River migration route through the Delta is successful.

- **Basis:** Our analysis shows that the barrier being installed creates a high chance that actively migrating fish will not enter Old River, but also increases the chance that fish will backtrack from downstream to upstream on the mainstem SJR at the HOR junction. The observed proportion of transitions from upstream of the HOR junction into Old River increased from 3% when the barrier was installed to 54% when the barrier was not installed. There was more variability in the percentage of fish classified as active migrators (range from 24% to 97%) when the barrier was installed compared to when it was not installed (range from 73% to 91%), potentially indicating that the barrier is affecting fish behavior. The presence of the barrier has been shown to be a primary factor that increases survival on the SJR route because of the way it diverts both fish and flow into the mainstem SJR (Buchanan et al. 2021). However, the barrier could potentially lower survival if it delays fish migration. Additionally, the barrier appeared to alter diel movement patterns, with fish being less likely to make downstream transitions during the day when the barrier was installed.

### Turner Cut

Adjust the timing of water project operations during daytime such that net flow during ebb tides is enhanced and exports do not coincide with flood tide flows at TC. This would increase the proportion of fish staying on the mainstem SJR and not entering TC. This may also allow fish to move through the area more quickly (i.e., increase the probability of upstream fish transitioning downstream). These changes would result in higher survival (Buchanan et al. 2021).

Alter the physical conditions at TC such that steelhead are less likely to enter TC on a flood tide. This could include altering the physical structure of the entrance to TC or installing some type of non-physical barrier that alters the behavior of juvenile steelhead and reduces the proportion of fish

entering TC. If successful, these physical or non-physical changes would result in higher survival (Buchanan et al. 2021).

- **Basis:** UnTRIM modeling showed the net flow in TC and total tidally averaged export flow are highly correlated ( $R \sim 0.9$ ) for 2013, 2015, and 2016 (dry, critical, and below normal water years, respectively; Table 2-1). Fish modeling results show that flood tide flows increase the chance of fish entering TC, but when net flow is lower, flood tides are more likely to be reversed. We also observed a relationship between an increase in predicted flow toward the export facilities and an increase in net flow down TC when all 6 years of the study are considered together.

## Water Project Area

No direct management implications were identified for the WPA, but information potentially of management interest includes the following:

- Fish have a longer residence time in this area than HOR or TC, and 31% of the fish detected here ended up in the CVP salvage tank. The State Water Project salvage tank was not outfitted with a hydrophone and the number of tagged fish ending up at this location is unknown. High reverse net flow increased the probability of transitioning from CVP to the CVP salvage tank to more than 80% after approximately 2.5 days. Long residence times in the area likely increase exposure to predation, but also the potential for being collected at salvage facilities.
- Fish were more likely to move away (either direction) from the entrance to CCF (i.e., radial gates) when net flow in West Canal was low.
- Fish generally displayed a lack of directional movement, but transitions appeared to be in the direction of tidal flows (ebb and flood).
- One notable observation that may warrant further investigation is that fish released after the HOR barrier was installed (i.e., later release day) were more likely to move toward the CVP. Buchanan et al. (2021) conducted a preliminary analysis showing that the salvage subroutine may increase survival because it shortens route length. If trucking of salvaged fish has a higher route survival than other longer routes through the Inner Delta, this might be a positive factor.

## Recommendations for Future Studies:

The following recommended studies were identified:

1. Conduct additional fine-scale, juvenile steelhead acoustic telemetry studies at HOR, TC, and WPA.
2. Conduct additional fine-scale, juvenile salmonid acoustic telemetry studies at additional important locations in the Delta.

3. Integrate the multistate model results from this study with routing and final fate analysis conducted by others and water management strategies.
4. Incorporate results from the predictive multistate model, routing, and final fate analysis into life cycle models to assess population-level effects.
5. Conduct additional flow-based analyses at TC.
6. Conduct acoustic telemetry studies on wild juvenile steelhead of different age classes.

Additional telemetry information should be collected to evaluate key hypotheses on juvenile steelhead behavior at locations of interest in the Delta. This should be done under various inflow levels and export operations. Information should be analyzed by using the multistate modeling approach (Recommendations 1, 2, and 5); related to available information on routing and survival (Recommendation 3); and extended to population-level effects if possible (Recommendation 4). The analyses conducted were based on large, hatchery-origin steelhead. Similar information on natural-origin steelhead should also be collected based on steelhead smolts captured and tagged at existing traps (Recommendation 6). Additional telemetry information on Chinook salmon could be collected at the same time using the same hydrophone locations to develop additional information on fine scale movements and behavior of salmon.

Completing this significant analytical step for steelhead provides the linkage between acoustic data and life cycle modeling needed to integrate observed fish behavior and water project alternatives in a quantitative framework to assess effects on fish at the population level. The additional studies we recommend would allow for further exploration of the effects of exports and alternative water management strategies on salmonids. Given that the spatial domain of the UnTRIM hydrodynamic model covers the entire Delta, behavioral responses of fish can be evaluated using our approach for any location in the Delta that is deemed important for water management and fish routing and survival objectives if telemetry data are available to support the analysis.

## 1 Introduction

The Collaborative Science and Adaptive Management Program (CSAMP) was formed in 2013 to focus on science and adaptive management issues related to current and future operations of the State Water Project (SWP) and Central Valley Project (CVP). This includes addressing emerging science and information needs regarding water management and species of concern in the Sacramento–San Joaquin Delta (Delta) and upriver, including actions to improve the resiliency of delta smelt and salmonids.

The Collaborative Adaptive Management Team (CAMP) was formed to support CSAMP and is composed of managers and senior-level scientists. To assist CAMP and address CSAMP goals, the Salmon Scoping Team (SST) was formed and staffed by state and federal resource agencies, environmental interests, and public water agencies. SST was tasked by CAMP with reviewing and synthesizing the available scientific information on salmon and steelhead routing and survival through the Delta and addressing a set of specific management questions. SST produced a two-volume report in early 2017 summarizing the review. SST concluded that through-Delta survival has been consistently low for San Joaquin River (SJR) Chinook salmon (*Oncorhynchus tshawytscha*) and more variable for Sacramento River Chinook salmon, and that survival data are limited for steelhead (*Oncorhynchus mykiss*; SST 2017a).

Starting in 2011, a 6-year study of steelhead routing and survival from the SJR through the Delta was funded by the U.S. Bureau of Reclamation (Reclamation) and implemented. The study was required as part of the National Oceanic and Atmospheric Administration (NOAA) National Marine Fisheries Service's (NMFS's) Biological Opinion (BO) on Long-Term Coordinated Operation of the CVP and SWP. Reasonable and Prudent Alternative (RPA) Action IV.2.2 in the BO specified that Reclamation undertake experiments utilizing acoustic-tagged salmonids to identify proportional causes of mortality due to flows, exports, and other project and non-project adverse effects on steelhead smolts out-migrating from the San Joaquin Basin and through the southern Delta (NOAA 2009).

As the steelhead telemetry data became available each year, the data were processed and analyzed, and annual reports were produced (e.g., USBR 2018b, which covered study year 2012). The annual reports focused on survival, routing, and travel time through the system from the point of release at Durham Ferry, California, to Chipps Island, California. SST's review included results from the first 2 years of study. Based on data from 2011 and 2012, survival of acoustic-tagged juvenile steelhead migrating from the SJR was 0.54 and 0.32, respectively, which was greater than that of fall-run Chinook salmon during those years (0.02 and 0.03, respectively; SST 2017a).

Since the SST report was completed, Buchanan et al. (2021) reported on results of analysis of all 6 years of study. Point estimates of through-Delta survival from Mossdale Bridge to Chipps Island ranged from 0.06 for the May 2014 release to 0.69 for the March 2011 release; annual estimates were lowest in 2013 (0.14) and highest in 2011 (0.54).

Perry et al. (2016) reviewed anadromous salmonid literature pertaining to the Delta that included 43 studies published between 2006 and 2016. The studies evaluated predation, feeding success, growth rates, life history, and survival. Of these studies, 38 evaluated Chinook salmon but only 5 evaluated steelhead.

Recent work to understand salmonid behaviors when migrating through the Delta has used individual-based particle tracking models (e.g., the enhanced particle tracking model [ePTM]) that rely on numerical algorithms to describe fish behavior. However, agent-based particle tracking models are intended to capture system-scale migration dynamics (Sridharan et al. 2018). Salmonids respond to environmental conditions using their sensory systems; therefore, the scale of these systems (i.e., fish body length) is much finer than can be provided by 1D hydrodynamic models of the Delta used in particle tracking models.

One recommendation by SST was that assessing salmonid behavior at specific times and locations may require the application of more refined and sophisticated 2D or 3D hydrodynamic simulation models (SST 2017a). MacWilliams et al. (2015) describe the Unstructured Nonlinear Tidal Residual Intertidal Mudflat Bay-Delta hydrodynamic model (UnTRIM Bay-Delta model), a high-resolution 3D model developed for the San Francisco Bay and Sacramento-San Joaquin Delta (Bay-Delta) system. Bever and MacWilliams (2016) demonstrated that combining detailed hydrodynamic modeling using UnTRIM with long-term fisheries data provided new and significant insights into hydrodynamic conditions most likely to affect delta smelt catch. There are several advantages of using simulated data, compared to observed data from gage and monitoring stations, in this type of analysis. These include no missing periods of data, high data quality, extensive spatial coverage that can address specific focal areas being analyzed, and a wide array of variables in this type of model that can be used in fisheries analysis.

Historically, California Central Valley steelhead (steelhead) were found from the upper Sacramento River south to Kings River and, possibly, the Kern River system (Yoshiyama et al. 1996). Lindley et al. (2006) estimated that at least 81 steelhead populations were distributed throughout the tributaries of the Sacramento and San Joaquin rivers. Presently, dams block access to 80% of historically available habitat and to all historical spawning habitat for approximately 38% of the historical populations of steelhead (Lindley et al. 2006). On January 5, 2006, the distinct population segment (DPS) of steelhead was listed as threatened under the Endangered Species Act (ESA; Federal Register 2006). The listing status was not changed in the most recent 5-year status review conducted by NMFS in 2016 (Federal Register 2016). The SJR and Delta hydrologic unit are designated as critical habitat for steelhead (NOAA 2005).

Given the ESA status of steelhead and limited information on steelhead behavior and survival within and through the Delta, additional analysis of steelhead was needed to inform water management discussions and support CSAMP objectives. In 2019, the study team proposed a study under Delta Science Proposal Solicitation for Proposition 1 Watershed and Delta Ecosystem Restoration Grant Programs, titled "Evaluating Juvenile Salmonid Behavioral Responses to Hydrodynamic Conditions in the Sacramento-San

Joaquin Delta," which focused exclusively on juvenile steelhead responses to hydrodynamic conditions. The study team is composed of the State Water Contractors, Anchor QEA, and the U.S. Geological Survey (USGS). The timing of the proposal reflected the availability of a complete set of tag files from the 6-year telemetry study and the existing and well-calibrated UnTRIM (MacWilliams et al. 2015), which has been applied successfully in the Delta for evaluating fish management questions.

The study takes a different approach to understanding salmonid migration behavior than ePTM and has different goals and spatial scales. The study is not focused on system-scale migration dynamics. It was designed to inform what can be learned about steelhead behavior relative to hydrodynamic conditions at small scales important to fish at key routing junctions and sites within the Delta based on acoustic telemetry data collected from 2011 through 2016. An improved understanding of what is influencing steelhead behavior at junctions and, thus, route selection through the Delta, is needed to help CSAMP and CAMT interpret how water management and barrier operations in the Delta affect local hydrodynamic conditions in steelhead migration pathways.

The study was also developed to inform whether acoustic data collected from a hydrophone deployment designed to measure routing and survival through the entire Delta could identify local behavioral patterns at key locations important to water project management, or whether additional, fine-scale studies and hydrophone deployments similar to that implemented by Holleman et al. (2022) are needed. Another primary objective of the study was to evaluate whether existing data from studies of routing and survival through the entire Delta could be used to understand steelhead behavior at specific locations within the Delta.

In addition to RPA Action IV.2.2, RPA Action IV.2.1 identified targeted levels of export volume dependent on SJR flow at Vernalis (i.e., inflow to export ratio [I:E]). RPA IV.2.3 identified target discharge levels through the Old and Middle River (OMR) corridor during winter and spring (i.e., OMR flow management; NOAA 2009).

CAMT tasked SST with assessing a total of 13 specific management questions, of which 8 could be addressed with the available information. These included the annual January 1 onset of OMR reverse-flow management and alternative flow metrics. SST identified the following five metrics that could be developed and tested to potentially help refine water project operations to improve juvenile salmonid survival through the Delta (SST 2017b):

- Qwest
- Hydraulic residence times
- Percentage time flow that is positive (i.e., in a downstream direction) in Old River, Middle River, and other South Delta locations
- Proportion of CVP exports relative to total export level

- Proportion of Sacramento River water arriving at the export facilities relative to the total volume of Sacramento River flow entering the Delta

The study team proposed to assess these metrics as part of the analysis, where possible.

The process used when implementing the project is described in Section 2.1. As an overview, the complete set of acoustic telemetry data from the 6-year study was obtained and reviewed to assess detection histories, sample sizes, and differences among study years. Key hypotheses and focal areas of interest were assembled and discussed with CAMT's newly formed Salmon Subcommittee (SSC). The study team then selected key UnTRIM variables and the analytical approach that would be used, a multistate model that tracks fish transitions from one state to another (e.g., from upstream to downstream in a channel). Preliminary results were then presented to interested parties in a 2-day workshop in November 2021. Based on feedback received during the workshop, additional analyses were conducted. The methods, results, and recommendations from the study are described in the following sections.

## 1.1 Acknowledgements

This project was funded by the Delta Science Program via funding provided by the California Department of Fish and Wildlife through the Delta Science Proposal Solicitation (Proposition 1–2019/20) for Watershed and Delta Ecosystem Restoration Grant Programs under Contract Award 18203. The contributing authors include Sydney Gonsalves (Anchor QEA), Aaron Bever (Anchor QEA), Michelle Havey (Anchor QEA), Michael MacWilliams (Anchor QEA), and John Ferguson (Anchor QEA). The study team includes Russell Perry (USGS), John Plumb (USGS), Mike Dodrill (USGS), and Adam Pope (USGS).

The study team acknowledges the significant contribution throughout the implementation of the study from both team members and external supporters and collaborators. These included Ben Geske (Delta Stewardship Council), Linda Standlee (State Water Contractors), Darcy Austin (State Water Contractors), Alison Collins (Metropolitan Water District), Rebecca Buchanan (University of Washington), Josh Israel (Reclamation), and multiple members of the SSC from various agencies and entities. In addition, through Alison Collins' support and leadership, the Metropolitan Water District provided funding that enabled the study team to present and discuss preliminary findings in a workshop setting to interested parties and scientists. A list of workshop participants is provided in Appendix A.

Telemetry data used in this evaluation were provided by Reclamation and processed with an additional predator filter implemented by Rebecca Buchanan. The processed telemetry data used in this evaluation were provided to Delta Stewardship Council and State Water Contractors at the completion of this study and can be made available upon request. The full telemetry dataset will be

posted to the Environmental Research Divisions Data Access Program (ERDDAP) in 2022. Hydrodynamic variables were extracted from the hydrodynamic model for time periods that overlapped with the telemetry data during each year simulated. These data have been posted to the Environmental Data Initiative as described in Appendix B.

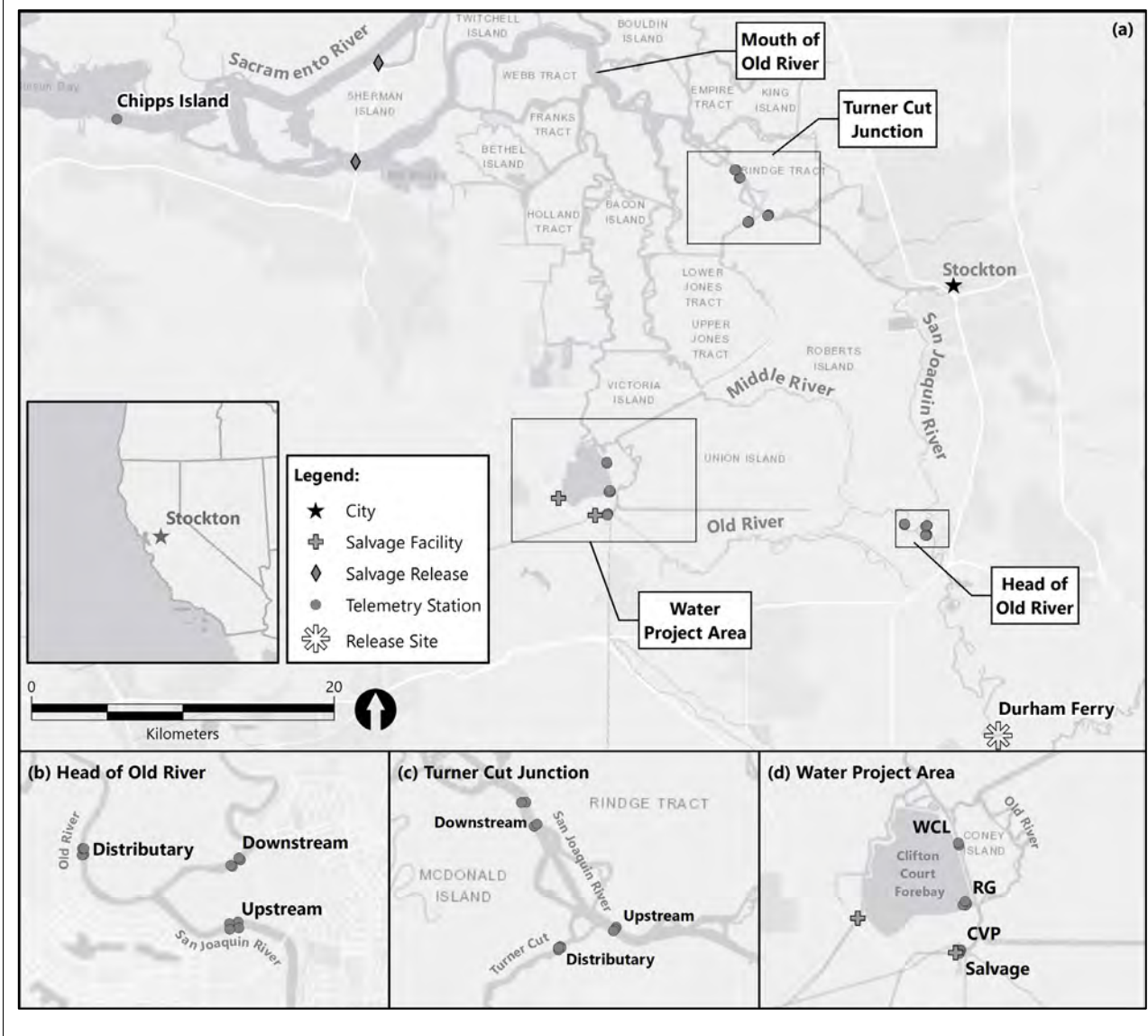
## 2 Methods

### 2.1 Project Process

Implementation of the study began with obtaining data files for all 6 years of acoustic telemetry studies from Reclamation and conducting initial tag data exploration to understand years and locations that could be assessed using the detection data and hydrophone array locations. A predator filter, previously designed to distinguish juvenile steelhead smolts and behavior, was received from Rebecca Buchanan. This was followed with an identification of key hypotheses from previous reports, including SST (2017a), to guide the approach, and coordination with stakeholders through two meetings with CAMT's newly formed SSC to discuss the hypotheses and identify focal study locations (Figure 2-1). The SSC stakeholders suggested areas of interest for analysis that were then checked against telemetry data coverage.

A review of the literature and discussions with partners at USGS resulted in a decision to model fish transitions using a continuous-time multistate Markov model (Jackson 2011). This was done by integrating UnTRIM run outputs with the telemetry and tagging data to assess behavioral responses of steelhead in identified study areas to key hydrodynamic variables. Data for times and locations from UnTRIM runs were selected based on the available acoustic telemetry data, sites, and conditions shown in previous acoustic studies to influence behavior and route selection, and discussions with SSC. Preliminary modeling results were presented to interested parties in a 2-day workshop in November 2021 (Appendix A). Based on feedback received during the workshop, additional analyses were conducted, results were finalized, and recommendations were developed based on the final set of results.

**Figure 2-1**  
**Study Area**



## 2.2 Study Area

The Delta is formed at the confluence of the south-flowing Sacramento River, the north-flowing SJR, and several other tributaries, including the Mokelume and Cosumne rivers. Approximately 50% of the total surface runoff in California flows to the Delta (Lund et al. 2007). Historically, the Delta consisted of approximately 3,000 square kilometers of tule marsh and low-lying forested island that connected meandering channels from California's Central Valley to the Suisun, San Pablo, and San Francisco bays, which connect to the Pacific Ocean (Luoma et al. 2015).

Habitat in the Delta is now highly modified, with levees allowing drained lands in the Delta to be used primarily for agriculture, with areas of rural to urban development (Luoma et al. 2015). The complex water infrastructure in the Delta supplies drinking water to approximately two-thirds of California residents (DWR 2022) and supports a nearly \$50 billion-per-year agricultural economy (CDFA 2020). Physical changes, altered flows, water removal, nutrient and contaminant inputs, warming climate, and non-native plants and fish species have been the primary causes of increasingly challenging conditions for salmonids in the SJR and Delta since the late 1800s (Nichols et al. 1986; Luoma et al. 2015).

Out-migrating juvenile steelhead enter the South Delta at Mossdale Bridge near Lathrop, California, and must travel approximately 88 kilometers (km) on the SJR mainstem (mainstem) or through the Inner Delta to Chipps Island at the entry to Suisun Bay. During this journey, juvenile steelhead encounter a number of riverine distributary junctions, as well as human-made canals, sloughs, and side channels (Figure 2-1). Behavior and conditions at these junctions determine routing through the Delta and overall survival (Perry et al. 2010, 2013; Buchanan et al. 2021).

The Head of Old River (HOR) and Turner Cut (TC) are two Delta junctions evaluated in this analysis. The confluence of the SJR and Old River is approximately 4.6 km downstream (north) of Mossdale Bridge and is the first junction encountered by juvenile steelhead after entering the Delta. Routing choice at this junction is important because it determines whether fish will take one of two main migration routes: continuing north on the mainstem or turning westward into the Inner Delta and toward the state and federal water project export facilities area (WPA). TC joins the mainstem along the Stockton Deepwater Shipping Channel, approximately 12 km downstream of downtown Stockton, California. TC represents another opportunity for juvenile steelhead to enter the Inner Delta, where there is a high risk of predation (Nobriga and Freyer 2007, Michel et al. 2020) or make their way through a series of waterways, either to the WPA or back to the mainstem (Buchanan et al. 2021).

The WPA is not a typical junction like HOR and TC, but is, instead, a convergence of multiple waterways in the southwestern Delta including Old River, Grant Line Canal, West Canal, and Victoria Canal, with inlets to federal water export facilities (CVP) and, through Clifton Court Forebay (CCF) radial gates, to state water export facilities (SWP). Routing in this area is thought to be strongly driven by both export pumping and tidal influences (SST 2017a). Fish that travel northward on West Canal and continue north along Old River can leave the Inner Delta by reentering the northern downstream end of the SJR and completing their migration toward Chipps Island. However, fish may be entrained at the state or federal water project facilities. Some entrained fish are collected and salvaged at the federal Tracy Fish Collection Facility or the state Skinner Fish Facility. Salvaged fish are trucked to a release point approximately 20 km upstream of Chipps Island, a route that may increase survival (Buchanan et al. 2021).

## 2.3 Hydrodynamic Modeling Overview

This section documents the hydrodynamic model used to predict environmental conditions throughout the Bay-Delta and, specifically, the environmental conditions collocated with the telemetry data (described in Section 3.1.1). An overview of the UnTRIM Bay-Delta hydrodynamic model is presented first, followed by a description of the periods simulated using the hydrodynamic model, then a description of the hydrodynamic variables extracted from the hydrodynamic model predictions for use in evaluating the effects of hydrodynamics on the behavior of acoustically tagged juvenile steelhead in the Delta. These hydrodynamic variables are predictions of different environmental conditions, such as water flow, salinity, and water temperature, that occurred at the same time as the telemetry data were collected. As such, these represent predictions of the physical conditions a fish would have experienced at any given time and place.

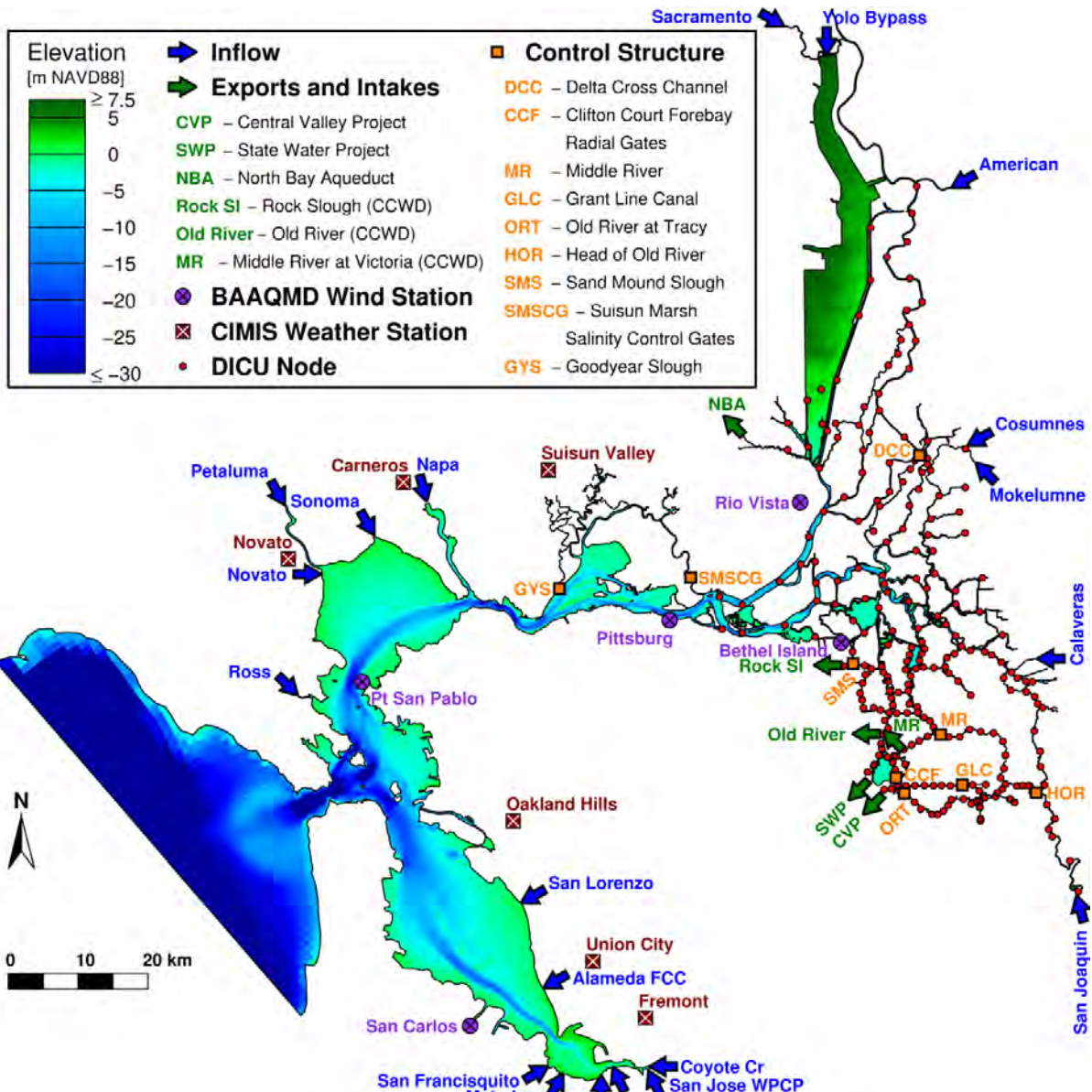
### 2.3.1 *UnTRIM Bay-Delta Model*

The high-resolution UnTRIM Bay-Delta model is a 3D hydrodynamic model of the Bay-Delta, which has been developed using the UnTRIM hydrodynamic model (MacWilliams et al. 2007, 2008, 2009, 2015). The UnTRIM Bay-Delta model extends from the Pacific Ocean through the entire Delta. The model takes advantage of the grid flexibility allowed in an unstructured mesh by gradually varying grid cell sizes, beginning with large grid cells in the Pacific Ocean and gradually transitioning to finer grid resolution in the smaller channels of the Delta. This approach offers significant advantages in terms of numerical efficiency and accuracy. It allows for local grid refinement for detailed analysis of local hydrodynamics, while still incorporating the overall hydrodynamics of the larger estuary in a single model.

The model is highly spatially resolved in the Delta and resolves the operational components of the radial gates leading into CCF (MacWilliams and Gross 2013) and gates and temporary barriers in the Delta. The resulting model has more than 130,000 horizontal grid cells and more than 1 million 3D grid cells (Figure 2-2).

**Figure 2-2**

**High-Resolution UnTRIM San Francisco Bay-Delta Model Domain, Bathymetry, and Locations of Model Boundary Conditions**



Note:

Evaporation and precipitation data are from California Irrigation Management Information System weather stations.

The UnTRIM Bay-Delta model has previously been applied to evaluate possible delta smelt swimming behaviors (Gross et al. 2021) and evaluate water flow through junctions in the tidal portion of the Sacramento River (Bever and MacWilliams 2016). The UnTRIM Bay-Delta model has also

previously been applied to evaluate potential effects of summer reoperation of the Suisun Marsh Salinity Control Gates (SMSCG) to better understand how summer SMSCG operation would affect salinity in Suisun Marsh and Suisun Bay during both above- and below-normal water years (Anchor QEA 2018a) and to evaluate the effects of the 2018 SMSCG Action (Anchor QEA 2019a).

The UnTRIM Bay-Delta model has also been applied to the Bay-Delta as part of the Delta Risk Management Strategy (MacWilliams and Gross 2007), several studies to evaluate the mechanisms behind the Pelagic Organism Decline (e.g., MacWilliams et al. 2008), the Bay-Delta Conservation Plan (MacWilliams and Gross 2010), and an examination of X2 and the Low Salinity Zone (MacWilliams et al. 2015). The UnTRIM Bay-Delta model was also applied in the U.S. Fish and Wildlife Service's evaluation of how changing the position of X2 impacts the water temperature in the Low Salinity Zone (Anchor QEA 2019b).

The UnTRIM Bay-Delta model has also been applied for a range of studies by the U.S. Army Corps of Engineers, including the Hamilton Wetlands Restoration Project (MacWilliams and Cheng 2007), the *Sacramento River Deep Water Ship Channel Deepening Study* (MacWilliams et al. 2009), the *San Francisco Bay to Stockton Navigation Project Deepening Study* (MacWilliams et al. 2014), and the *South San Francisco Bay Shoreline Study* (MacWilliams et al. 2012).

The UnTRIM Bay-Delta model has been calibrated using water level, flow, salinity, and water temperature data collected in the Bay-Delta in numerous previous studies (e.g., MacWilliams et al. 2008, 2009; MacWilliams and Gross 2010; MacWilliams et al. 2015; MacWilliams et al. 2016; Anchor QEA 2018b, 2019). The model has been shown to accurately predict salinity, water temperature, tidal flows, and water levels throughout the Bay-Delta under a wide range of conditions. This report documents the model validation for water flow, salinity, and water temperature for a subset of the available locations from Suisun Bay through the Delta (Appendix C).

### **2.3.1.1 River Inflow Source Tracking**

The UnTRIM Bay-Delta model allows for the addition of a conservative tracer to the inflows of the hydrodynamic model. For this study, freshwater inflows to the Delta were tagged with different tracers to allow tracking of the movement of the different source waters throughout the Bay-Delta. These tracers were used to evaluate the time-varying percent of Sacramento River water, SJR water, and Mokelumne River water at the hydrophone locations. These rivers were selected for evaluation and possible inclusion in the fish transition models because the Sacramento River is the largest source of freshwater to the Bay-Delta, the tagged fish were generally released in the SJR, and the fish were reared in the Mokelumne River.

### **2.3.1.2 Temperature Modeling Background**

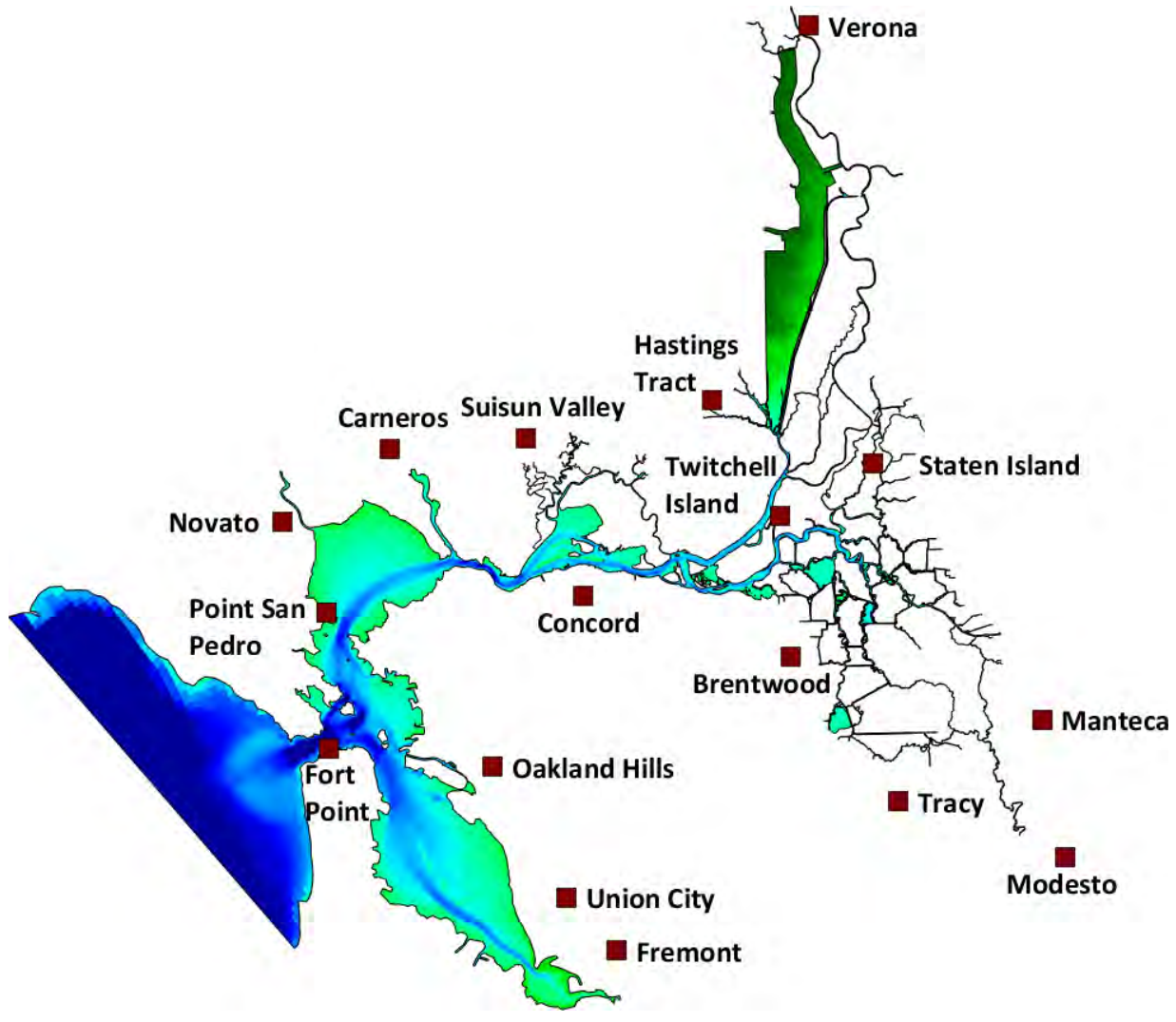
The UnTRIM Bay-Delta model predicts water temperature throughout the Bay-Delta. Input parameters for the temperature model include both observed meteorological variables and the

observed temperature of water inflows to the Bay-Delta from tributaries. This section details temperature modeling of the Bay-Delta using the UnTRIM Bay-Delta model.

Water temperature was modeled using surface heat fluxes, temperature inflows from tributaries and water treatment plants, and water temperature at the Pacific Ocean open boundary. The surface heat flux represents the net heating or cooling of the water based on meteorological conditions and surface water temperature. The surface heat flux is calculated at each time step and model grid cell following Octavio et al. (1977) and as described in Deltares (2014). In the heat flux formulation, the air temperature, incoming short-wave radiation, relative humidity, and cloud cover are specified based on observed data. The heat losses from the water due to evaporation, back radiation, and convection were computed by the model. The heat flux prescribed at the water surface is the net of the calculated incoming and outgoing heat fluxes and acts to warm or cool the water.

The meteorological boundary conditions for temperature modeling used a combination of California Irrigation Management Information System (CIMIS; DWR 2018) and NOAA North American Regional Reanalysis (NARR; NOAA NARR 2018) data. Hourly air temperature, incoming short-wave radiation, and relative humidity were obtained from 16 CIMIS stations around the Bay-Delta (Figure 2-3). Data from nearby CIMIS stations were used when data at individual stations were not available. The hourly air temperature was also obtained from the NOAA San Francisco Fort Point location (9414290), with the other meteorological variables for this location obtained from nearby CIMIS stations. The percent cloud cover was specified using NOAA NARR gridded data (an approximately 32-km grid) because cloud cover was not available from CIMIS. The 3-hourly NARR cloud cover from the closest gridded data point to each CIMIS station was interpolated to hourly data and combined with the CIMIS data for model boundary conditions.

**Figure 2-3**  
**Locations of Stations Used for Meteorological Boundary Conditions**



Daily averaged temperatures for each inflow were based on USGS (2020) and California Department of Water Resources (DWR) California Data Exchange Center (CDEC) data (2020), when available. The average water temperature for each of the 12 months of a year was calculated from time series of available data and used for the inflow temperature when observed data were not available. The monthly averaged temperature from nearby inflows was applied for inflows and water treatment plants when no temperature data were available. The open boundary water temperature was specified using daily temperature observations from the Farallon Islands (SCCOOS 2020), approximately 20 km west of the tidal ocean boundary.

### *2.3.2 Hydrodynamic Model Simulation Periods*

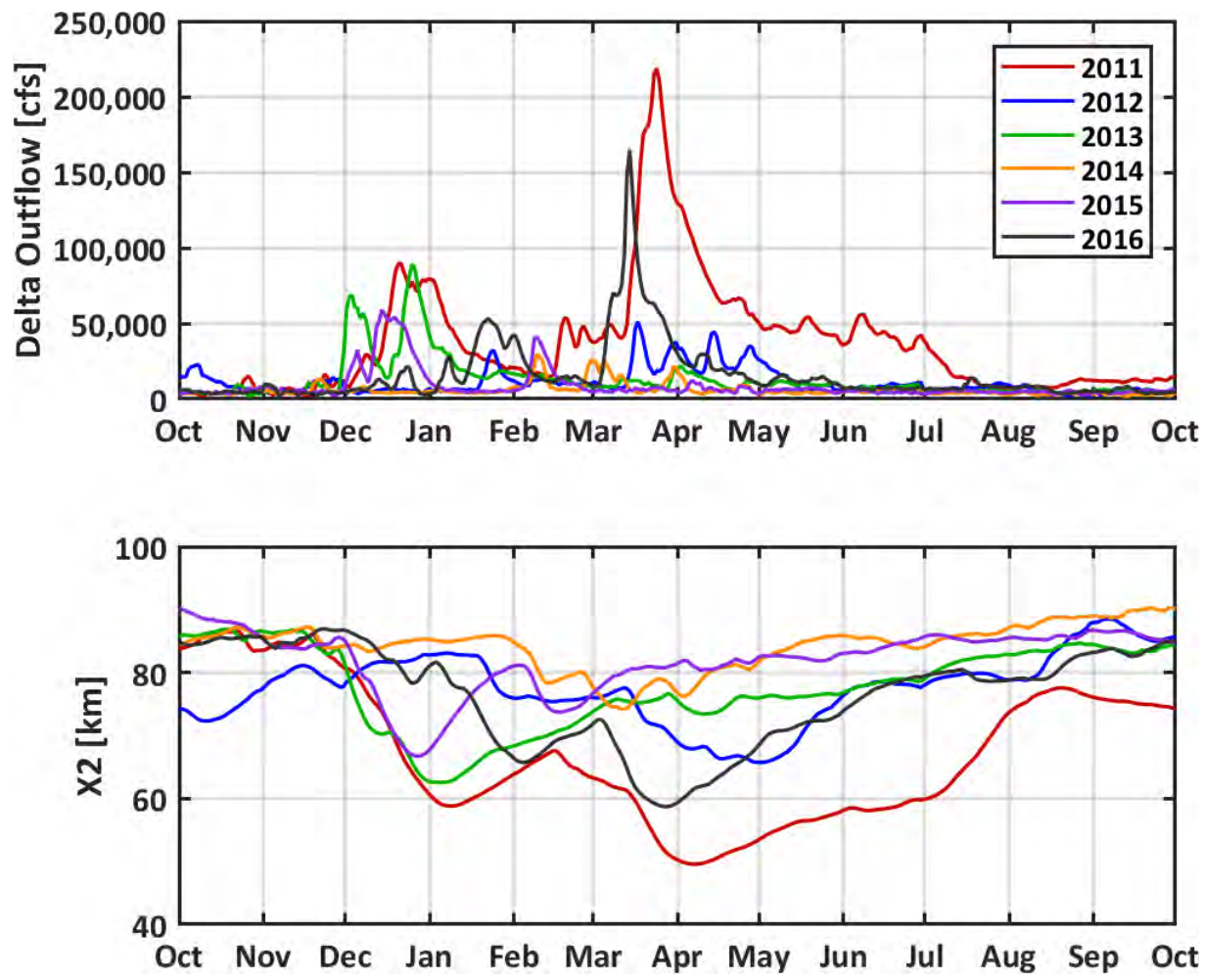
The hydrodynamic model was used to simulate periods during each of the 6 years when the telemetry data were available for predicting environmental conditions at the hydrophone locations. The simulation years were 2011, 2012, 2013, 2014, 2015, and 2016 (Table 2-1). These years spanned a large range in Delta outflow and X2 (Figure 2-4) and ranged from critical to wet water years. The hydrodynamic model simulations spanned the complete date range of the available hydrophone data in each year and started at least 2.25 months before the first fish detection in each year. The simulation of at least 2.25 months before the start of the telemetry data allowed the model to spin up prior to the start of the telemetry data.

**Table 2-1**  
**Date Ranges of Fish Detections and Periods During Which Hydrodynamic Variables Were Extracted from the Hydrodynamic Model Predictions**

<b>Year</b>	<b>Water Year Type</b>	<b>Date Range of Fish Detections at Hydrophones</b>	<b>Date Range of Extracted Hydrodynamic Model Output</b>
2011	Wet	March 22 to July 27, 2011	March 1 to August 1, 2011
2012	Below normal	March 27 to August 3, 2012	March 1 to August 6, 2012
2013	Dry	March 6 to July 26, 2013	March 1 to August 1, 2013
2014	Critical	March 26 to August 8, 2014	March 1 to August 10, 2014
2015	Critical	March 4 to July 1, 2015	March 1 to July 4, 2015
2016	Below normal	February 24 to June 29, 2016	February 1 to July 1, 2016

**Figure 2-4**

**Time Series of Delta Outflow and X2 for Water Years Encompassing Each Simulation Year**



Notes:

Complete water years are shown for reference.  
Delta outflow and X2 are from Dayflow (DWR 2022).

### 2.3.3 Hydrodynamic Variables

Hydrodynamic variables were extracted from the hydrodynamic model for time periods that overlapped with the telemetry data during each year simulated. These hydrodynamic variables represent predictions of the physical conditions a fish would have experienced at any given time. Using the hydrodynamic model to predict the environmental conditions a fish would have experienced has the benefit of providing the environmental conditions at the locations of the telemetry data on the short timescales of the telemetry data. Using the hydrodynamic model predictions also allows for the incorporation of a wider range of environmental conditions than would be available had only observational data been considered. For example, using hydrodynamic

model predictions allows for the use of instantaneous and time-varying water flow through all the channels of a junction. It supports an examination of how changes in water flow on tidal timescales may affect fish routing through an individual junction.

A range of variables representative of the conditions at each of the hydrophone arrays was extracted from the hydrodynamic model predictions for use with the fish telemetry data. Some of the hydrodynamic variables were extracted directly from the hydrodynamic model predictions, and some were calculated from other hydrodynamic model variables. Eight output variables were extracted directly from the hydrodynamic model predictions, and four variables were calculated from other variables in the model (Table 2-2). The hydrodynamic model output is available on the Environmental Data Initiative data portal (EDI 2022). While each of these hydrodynamic variables was considered for possible use in the fish transition models, each fish transition model ultimately used the hydrodynamic variables that best predicted the fish transitions at the considered junctions. As a result, not all the hydrodynamic variables were used in the final fish transition models.

**Table 2-2**  
**Hydrodynamic Variables Generated from the Hydrodynamic Model Predictions**

Type	Variable (Unit)	Frequency
Directly extracted from model cross sections	Cross-sectional water flow ( $\text{m}^3/\text{s}$ )	90 seconds and tidally averaged
Directly extracted from model at discrete locations	Depth-averaged salinity (PSU)	3 minutes and tidally averaged
	Depth-averaged water temperature ( $^{\circ}\text{C}$ )	
	Water depth (m)	
	Depth-averaged current speed (m/s)	
	Depth-averaged percent Sacramento River water (%)	
	Depth-averaged percent SJR water (%)	
	Depth-averaged percent Mokelumne River water (%)	
Calculated	OMR flow ( $\text{m}^3/\text{s}$ )	90 seconds and tidally averaged
	Qwest ( $\text{m}^3/\text{s}$ )	
	Flow toward SWP and CVP exports ( $\text{m}^3/\text{s}$ )	
	I:E ratio (unitless)	Daily

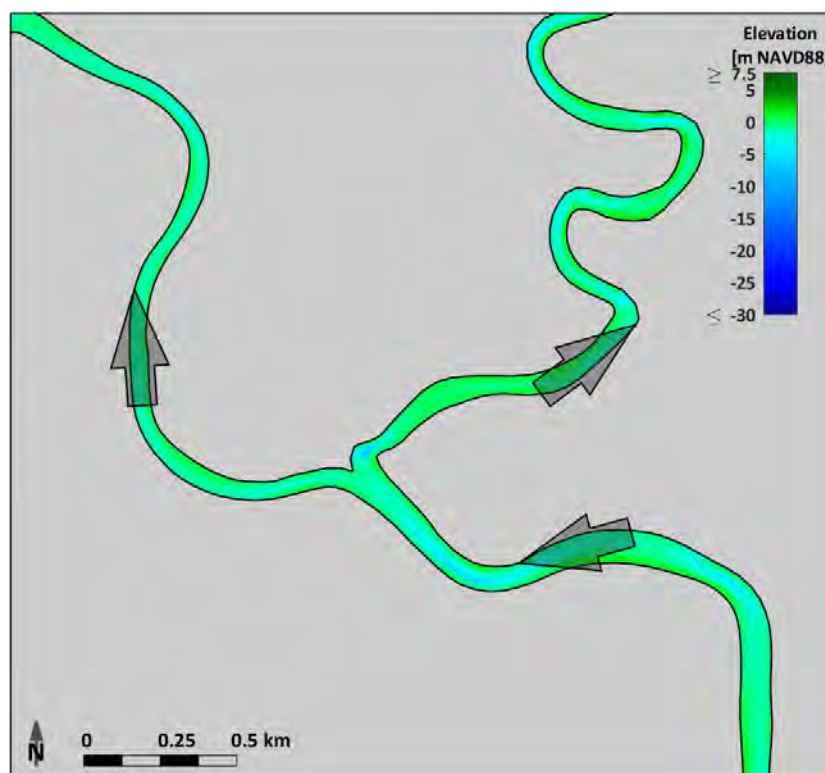
### 2.3.3.1 Output Variables Extracted Directly from Hydrodynamic Model

Water flow in the study area was extracted from the hydrodynamic model as the total cross-sectional water flow. Cross-sectional water flow is the predicted rate of water flow through a cross section across a channel. The predicted cross-sectional flows correspond to the flows past sets of hydrophones (hydrophone arrays). The direction of water flow was indicated by the sign of the flow to preserve information on how water flowed through junctions and channels

(Figures 2-5, 2-6, and 2-7). Water flow was extracted from the hydrodynamic model every 90 seconds. Both the 90-second instantaneous values and the tidally averaged (24.8-hour average) values were considered in the fish transition models. The tidally averaged water flow is representative of the net flow over a tidal period. Tidal average values were calculated by performing a 24.8-hour running average twice.

Depth-averaged salinity, depth-averaged water temperature, water depth, and depth-averaged current speed were extracted from the model predictions at discrete locations in the vicinity of each hydrophone array. Depth-averaged percent Sacramento River water, depth-averaged percent SJR water, and depth-averaged percent Mokelumne River water were also extracted from the model predictions at discrete locations in the vicinity of each hydrophone array. These hydrodynamic variables are time series of modeled environmental conditions at individual locations. Variables based on discrete locations were extracted from the hydrodynamic model every 3 minutes, and the tidally averaged values were also considered in the fish transition models. The tidally averaged values are representative of the average over a tidal period.

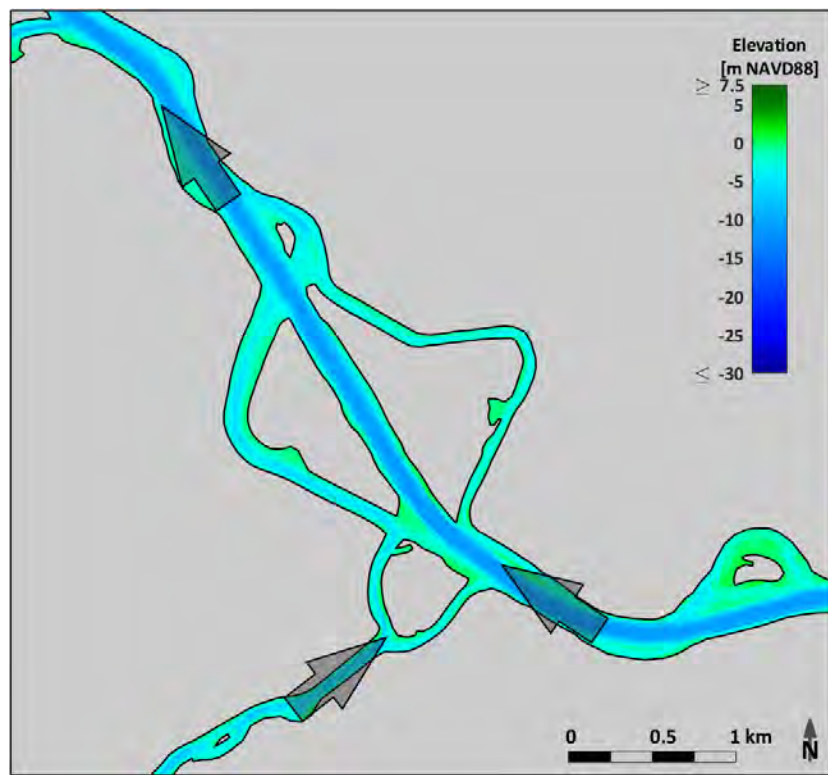
**Figure 2-5**  
**Direction of Positive Cross-Sectional Water Flow Around Head of Old River**



Note:  
The hydrodynamic model grid is shown as the background.

**Figure 2-6**

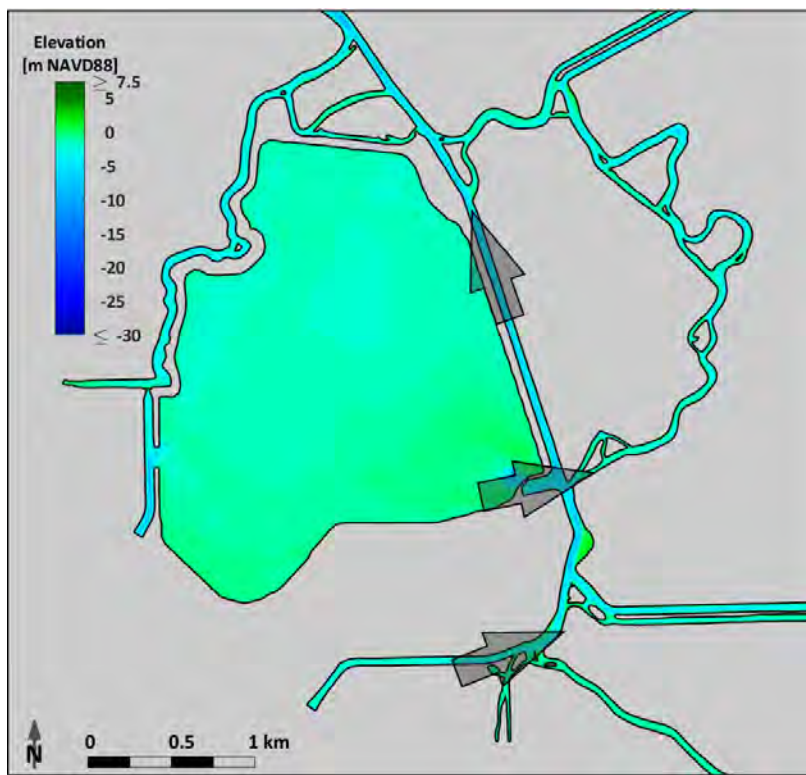
**Direction of Positive Cross-Sectional Water Flow Around Turner Cut**



Note:

The hydrodynamic model grid is shown as the background.

**Figure 2-7**  
**Direction of Positive Cross-Sectional Water Flow Around Water Project Area**



Note:  
The hydrodynamic model grid is shown as the background.

### 2.3.3.2 Output Variables Calculated from Multiple Hydrodynamic Model Variables

Four variables were calculated from the hydrodynamic model predictions for evaluation in the fish transition models (Table 2-2). This section summarizes how those variables were calculated.

The OMR flow is the combined cross-sectional water flow through Old River and Middle River. The calculated OMR flow retains the direction of flow, toward the San Francisco Bay (north) or toward the SWP and CVP export facilities (south), to provide additional information past simply the magnitude of the water flow. OMR flow was calculated by adding the 90-second hydrodynamic model predictions of the flow through the Old River at Bacon Island and Middle River at Middle River locations. These locations are nearest to the "OLD" and "MRE" hydrophone arrays. Both the 90-second instantaneous values and tidally averaged values were calculated for possible use in the fish transition models.

Qwest is the cross-sectional flow past Jersey Point in the SJR. The Qwest considered in this study was calculated from the instantaneous hydrodynamic model output as the predicted flow past Jersey

Point, not using the daily water balance method used by DWR. Qwest was calculated from the hydrodynamic model predictions every 90 seconds, and both the 90-second instantaneous values and tidally averaged values were calculated for possible use in the fish transition models.

Flow toward SWP and CVP export facilities is the water flow toward these major export facilities. This flow was calculated as the water flow at model cross sections near the entrance to CCF (SWP) and in the channel leading to the CVP Bill Jones Pumping Plant. The flow toward the exports retains the direction of flow to provide additional information past simply the magnitude of the water flow. Flow toward the exports was calculated from the hydrodynamic model every 90 seconds, and both the instantaneous values and tidally averaged values were extracted every 90 seconds.

The I:E is the ratio of SJR inflow (I) to combined exports from the CVP and SWP (E). The I:E is calculated as I divided by E. The inflow is daily inflow from the SJR, and the flow exported from the SWP and CVP is the daily flow toward the export facilities. As such, I:E was calculated as a daily value. The I:E becomes infinite and then undefined if the flow toward the exports ever approaches zero or equals zero, respectively, limiting the usefulness of I:E on short timescales.

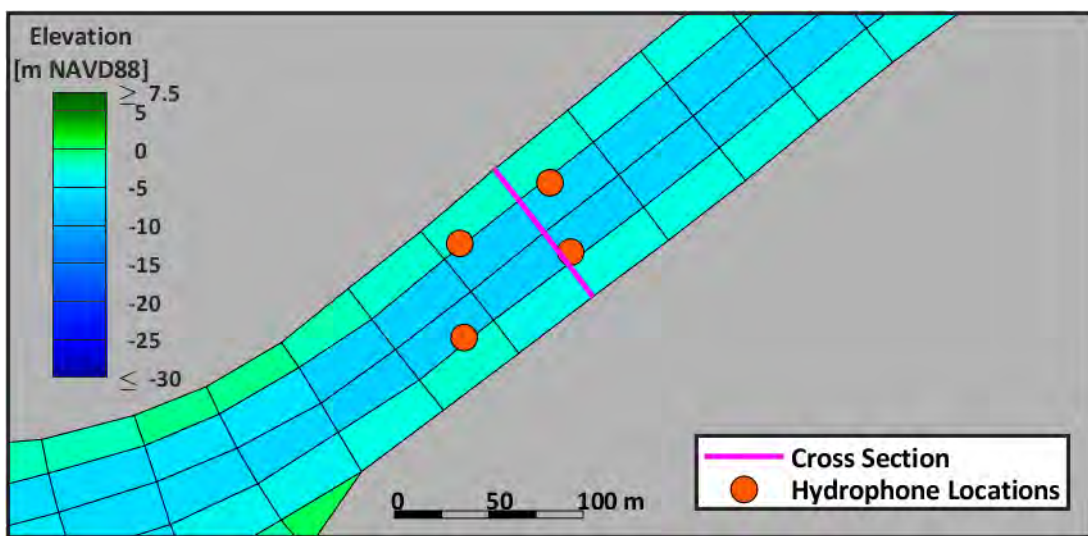
### **2.3.3.3 Locations of Hydrodynamic Variables**

Cross-sectional water flow and the hydrodynamic variables at discrete locations were extracted from the hydrodynamic model in the vicinity of each hydrophone array. Cross sections for water flow were specified to run approximately through the center of the hydrophone arrays (Figures 2-8 and 2-9). The variables extracted at discrete locations (except for current speed) were extracted at the center of the cross sections (Figure 2-9). The correlation of the values extracted at each of the individual hydrophone locations to those extracted at the center of the cross sections was evaluated (Section 4.1).

The values at the individual hydrophone locations were highly correlated to the values at the center of the cross sections for salinity, water temperature, percent source water, and water depth. Because the depth-averaged current speed at each hydrophone location was slightly less correlated to the cross-section centers, the depth-averaged current velocity was extracted at two locations for each set of hydrophones. The depth-averaged current speed was extracted both at the center of the water flow cross sections for consistency with the other hydrodynamic variables, and at a location near the deepest model grid cell at the center of the channel to provide additional information for the fish transition models. Current speed varies laterally across the channel, so these predicted current speeds should not be interpreted to represent the spatially varying current speed across the entire channel or through a junction.

**Figure 2-8**

**Location of Cross Section in Turner Cut and Individual Hydrophones from 2016**

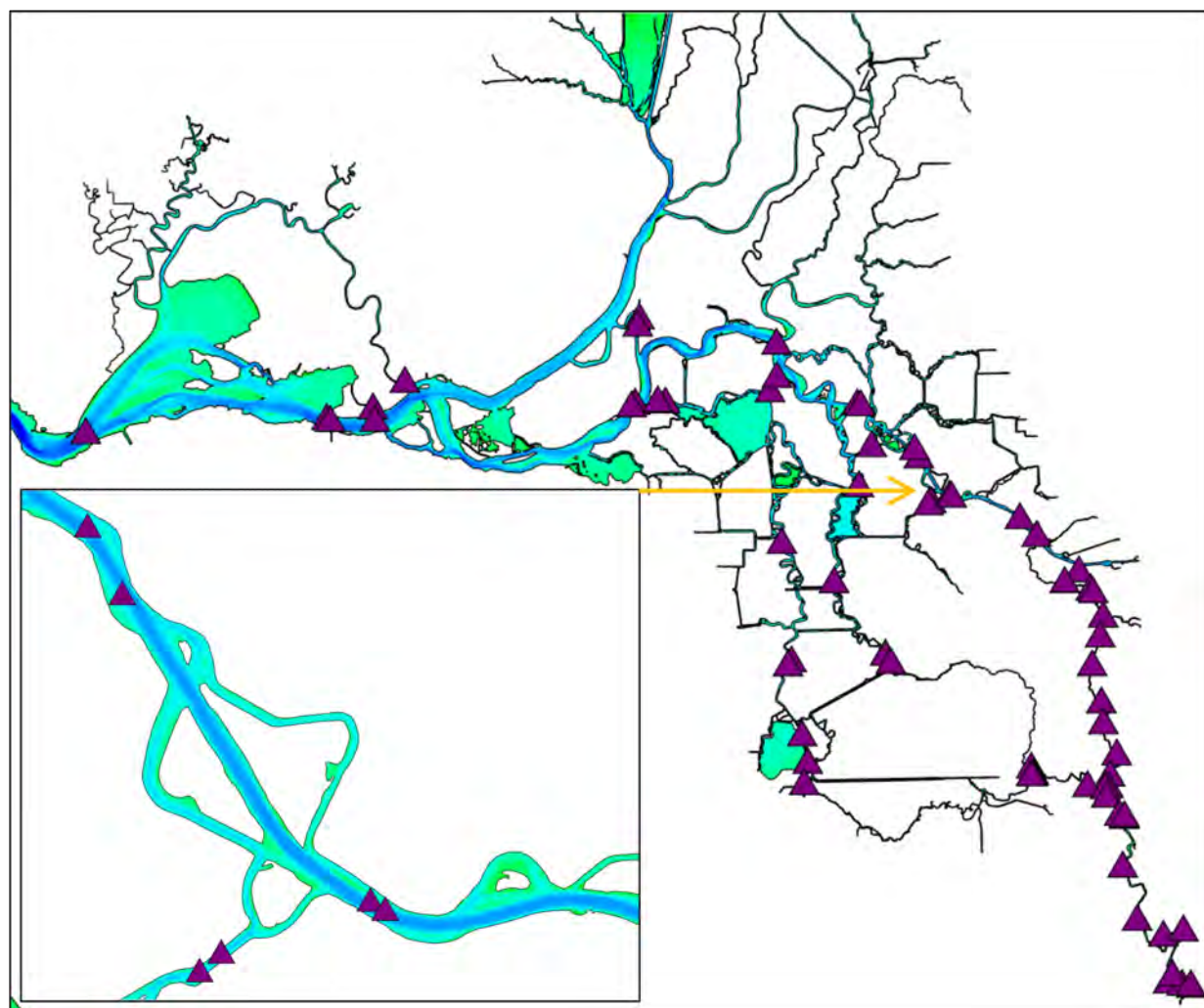


Note:

The hydrodynamic model grid is shown as the background.

**Figure 2-9**

**Locations of Cross-Section Centers in the Vicinity of Each Hydrophone Array**



Note:

Figure shows the complete set of cross sections for all years. Individual cross sections may not be applicable to all considered years because some hydrophone array locations varied between years.

#### 2.3.4 Evaluation of Turner Cut Net Flow

Net (tidally averaged) water flow in TC is hypothesized to be influential for fish entering TC (Section 3.3). Although TC is located relatively distant from the CVP and SWP export facilities compared to the HOR junction and the WPA, net flow through TC was evaluated to determine whether there is an influence of water exports from the CVP and SWP on net flow through TC.

In this analysis, the predicted net flow through TC was compared to the predicted net flow toward the export facilities, to determine whether there was a relationship between changes in exports and

changes in predicted net flow through TC. The predicted net flow toward the SWP and CVP export facilities was calculated as described in Section 2.3.3.2. This analysis evaluated the net flows in TC and the net flow toward the exports over the date range when fish were detected at the hydrophones from each of the 6 years (Table 2-1). Data-based water flow through TC was then used to confirm any relationships determined from the predicted flows.

The USGS data-based flow through TC (USGS Station 11311300, CDEC Station TRN) was daily-averaged and compared to the daily exports from the SWP and CVP, to determine whether a relationship between exports and net flows in Tuner Cut was present in the observational data. The data-based analysis was conducted over the same date ranges in each of the 6 years used in the analysis of the predicted net flows.

The predicted net flow through the SJR upstream and downstream of TC was plotted with the SJR inflow at Vernalis to put the net flows in TC and the exports in perspective with the SJR inflow. The large variations in flow magnitude make it difficult to directly compare the time series flows visually. As a result, the flows were also normalized so they all range between -1 and 1 over the date range plotted.

Non-normalized net flow through TC was also compared to net flow toward the SWP and CVP export facilities using basic statistics to determine if there was a significant relationship between exports and net flow through TC. A significant relationship was classified as having a Spearman rank correlation (Yue et al. 2002)  $p$  of less than 0.05. A non-parametric rank correlation was used to test for significance to exclude assumptions about data distribution inherent in a parametric test. Correlation was evaluated using Spearman's  $\rho$  ( $R_s$ ). The slope of any relationship between TC net flow and exports was calculated using the Theil-Sen non-parametric method (Theil 1950; Sen 1968; Gocic and Trajkovic 2013), commonly referred to as the Sen's slope. The Sen's slope was used on plots to visualize any trend in TC net flow versus exports and is not meant as a predictive method for estimating TC net flow from exports.

## 2.4 Steelhead Data Analysis

### 2.4.1 Tagging and Telemetry Data

An existing juvenile steelhead acoustic telemetry dataset was used for this study (Buchanan 2018a, 2018b, 2018c; USBR 2018a, 2018b, 2018c). The full telemetry dataset will be posted to the Environmental Research Divisions Data Access Program (ERDDAP) in 2022. Fish were obtained from the Mokelumne River Hatchery, which is one of three artificial propagation programs for steelhead. From 2011 to 2016, 958 to 2,196 fish per year were surgically implanted with acoustic transmitters and released in the SJR at Durham Ferry. In 2011, fish were implanted with Hydroacoustic Technology, Inc., acoustic tags, while in 2012 through 2016, VEMCO acoustic tags were used.

Juvenile steelhead fork lengths ranged from 97 to 396 millimeters (mm), with annual averages ranging between 212 and 277 mm (Buchanan et al. 2021). Tagging was performed by DWR at the Skinner Fish Protection Facility in 2011 and at the Mokelumne River Hatchery from 2012 to 2016. Acoustic data were collected by stationary hydrophone and receiver arrays deployed throughout the Delta. The number of individual receivers deployed ranged from 68 in 2011 to 177 in 2016.

Acoustic tags generally have high detection probability. Detection probabilities were generally >90%, though in some years, individual arrays had probabilities as low as 30% (Buchanan 2018a, 2018b, 2018c; USBR 2018a, 2018b, 2018c). Detection probabilities <100% can result from debris or structures that block line of sight, tag failure, receiver malfunction, noise sources, or shallow water or hard surfaces that cause errors from reflected acoustic signals. In most cases, multiple hydrophones were deployed in a line or array to improve coverage of the stream channel and increase detection probability. However, in 2011, only single hydrophones were deployed at some locations.

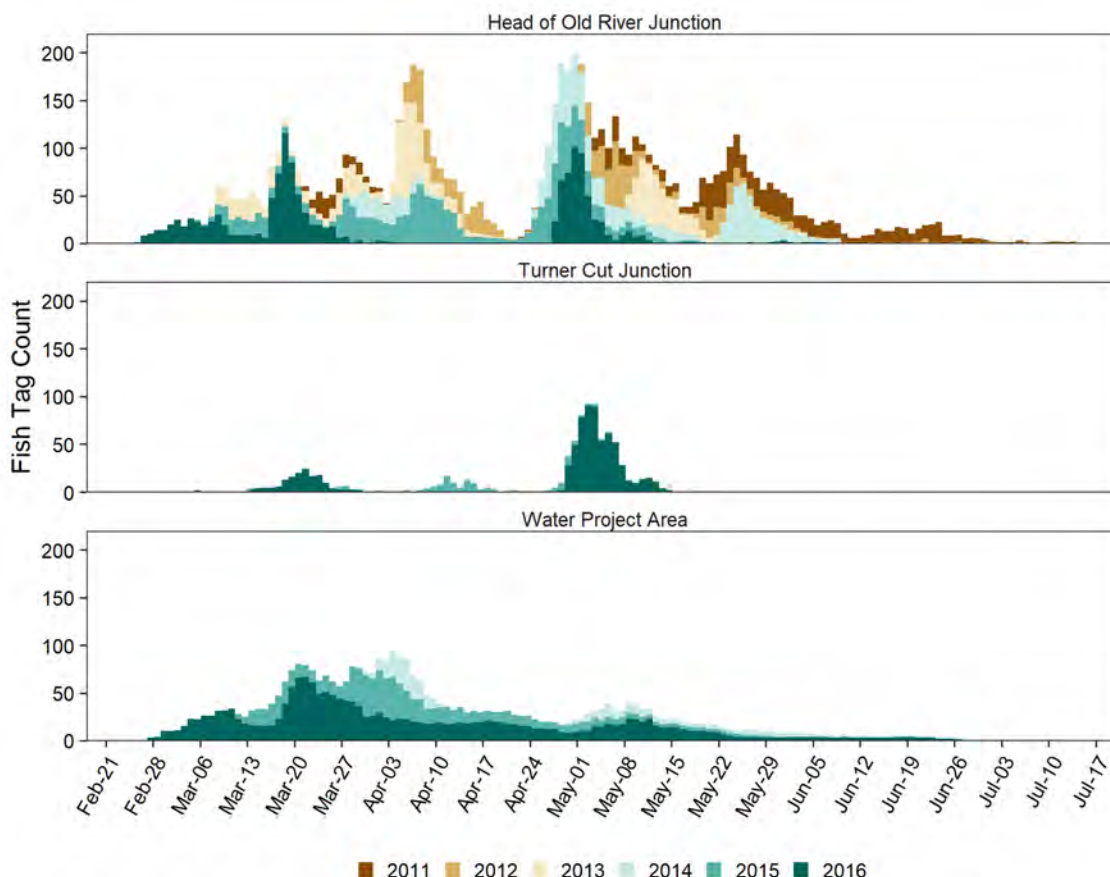
Raw acoustic receiver detection data were processed into detection events for each tag by the USGS laboratory in Cook, Washington (2011), or Sacramento, California (2012 to 2016). A detection event was defined as a series of detections by one or more acoustic receivers at a single location with 15 minutes or less between detections. A fish was considered to be continuously present at a location during a detection event.

A predator filter based on assumed behavioral differences between juvenile steelhead and resident predatory fish such as juvenile and subadult bass was applied by Rebecca Buchanan (University of Washington). Criteria for the predator filter were spatially explicit and included fish speed, residence time, number of upstream transitions, total travel time, and movement against flow. Further descriptions of field and data processing methods, including tagging, tag surgeon effects on fish survival, tag-life analysis, and predator filter development, are described by Buchanan et al. (2021), Buchanan (2018a, 2018b, 2018c) and Reclamation (USBR 2018a, 2018b, 2018c).

For this study, a subset of steelhead telemetry data was selected in the three areas of interest: the distributary mainstem junctions at HOR and TC, and the Inner Delta WPA. In some cases, extended smolt detection histories were still present in the data before the individual fish was classified as a predator upon its next upstream or transition. These likely represent predator detections that did not yet trigger the predator filter. Steelhead smolts are strong swimmers and are more difficult to distinguish from predators than other juvenile salmonids, such as Chinook salmon (Appendix A; ESA and AECOM 2018). Therefore, extended detection histories were censored at 10 days for mainstem junctions (HOR and TC) and at 20 days in the WPA. Fish presence in each area is shown in Figure 2-10, and summary tables are provided in Appendix D. For the HOR junction, further detail on when the barrier was installed is shown in Appendix D, Figure D.1-1a. The HOR barrier had a major influence on which route fish took through the South Delta and, therefore, where fish detections occurred in both the TC junction and WPA, but it was not installed during all 6 years.

For an area to be evaluated, the same or similarly located acoustic receivers must have been deployed in multiple years. At HOR, receivers were deployed upstream and downstream of the junction on the mainstem and downstream of the junction on Old River in roughly the same location from 2012 to 2016. In 2011, a single receiver was deployed approximately 2.2 km farther upstream of the junction on the mainstem. This difference in location was accounted for during modeling (Section 3.2). Acoustic receivers at TC junction were deployed upstream and downstream in the mainstem and in TC in 2013, 2015, and 2016. In the WPA, receivers were deployed at the inlet to the CVP facilities, at the radial gate inlet to CCF at the SWP, and in West Canal in 2014, 2015, and 2016.

**Figure 2-10**  
**Daily Presence of Juvenile Steelhead in Study Areas**



## 2.4.2 Fish Transition Modeling

Fish transitions were modeled using a continuous-time multistate Markov model (Jackson 2011) in which individuals move from state  $r(t)$  at time  $t$  to state  $s(t + dt)$  at time  $t + dt$ . Upon entering a river junction (HOR and TC), each tagged fish was assigned to one of three transient states that represent

upstream (U) or downstream (D) locations on the mainstem or the distributary channel (T; Figure 2-11A). For analysis of WPA, states were designated as upstream Old River at CVP export (C), radial gate entry to CCF (R), and downstream in West Canal (W). For WPA, a fourth absorbing state was added to represent fish detected in the CVP salvage tank (V; Figure 2-11B).

Transitions between states are described by a transition rate matrix  $Q(t)$  with elements  $q_{rs}(t)$  that represent the instantaneous risk of transitioning from state  $r$  to state  $s$  (Figure 2-11). In Markov models,  $q_{rs}(t)$  is assumed to be independent of the observed history of the process up to the time just before  $t$  (i.e.,  $t-1$ ; Jackson 2011). Times between state transitions are assumed to be exponentially distributed random variables with rate  $\lambda = q_{rs}$  and with a mean time to transition of  $1/\lambda = 1/q_{rs}$ . Data for the analysis represented a time series of occupied states for each fish,  $S(t=0)$ ,  $S(t=1)$ , ...,  $S(t=n)$  for  $t = 0, 1, \dots, n$  timesteps after first entering an area.

The model included panel-type observations for all timesteps of no detection, as well as detections following a gap of >15 minutes, since the time of fish arrival to a location is arbitrary. A second observation type, indicating a known transition time, was used for detections on consecutive timesteps at the same state (i.e., during a single detection event) since the fish was assumed to be continuously present. Additionally, state  $s(t)$  was allowed to remain unknown or censored if there was no detection of a fish at timestep  $t$  (Kock et al. 2018). In this case, the true state could have been any of the transient states in the model. This allows time-varying covariates to change on timesteps for which the fish state is unknown. Therefore, the set of possible states in the model was  $S \in (U, D, T)$  for HOR and TC and  $S \in (U, R, D, V)$  at WPA.

The structure of the model allows transition rates to be expressed as a function of time-varying covariates. To add covariates, the elements of  $Q$  can be replaced with new elements that are a function of the time-changing covariates. The elements of the transition rate matrix can then be described in the form of a proportional hazard model (Equation 1).

### **Equation 1**

$$q_{rs}(z_i(t)) = q_{rs}^0 \exp(\beta_{rs}^T z_i(t))$$

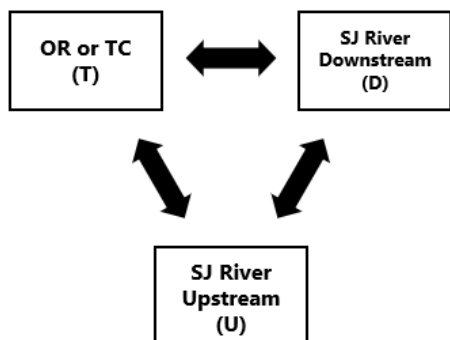
where:

- $z_i(t)$  = a vector of covariates for individual  $i$  at time  $t$
- $q_{rs}^0$  = baseline hazard rate
- $\beta_{rs}$  = a vector of slope coefficients for  $k$  covariates
- $\exp(\beta_{rs,k})$  = hazard ratio for the  $k$ th covariate

The multistate models were fit using the “msm Package” version 1.6.8 (Jackson 2011, 2019) in R version 4.1.2 (R Core Team 2021), which uses the maximum likelihood estimation method to estimate model parameters and standard errors.

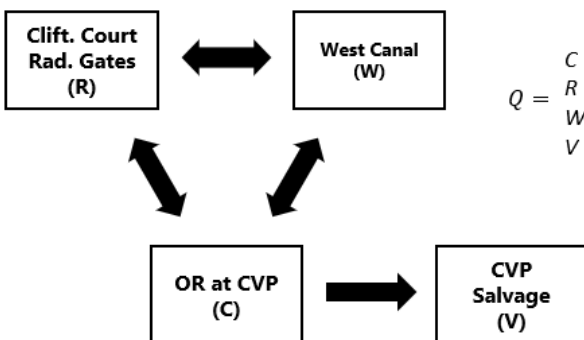
**Figure 2-11**  
**Schematic of Multistate Models and State Transition Matrices**

A



$$Q = \begin{matrix} & U & D & T \\ U & -(q_{UD} + q_{UT}) & q_{UD} & q_{UT} \\ D & q_{DU} & -(q_{DU} + q_{DT}) & q_{DT} \\ T & q_{TU} & q_{TD} & -(q_{TU} + q_{TD}) \end{matrix}$$

B



$$Q = \begin{matrix} & C & R & W & V \\ C & -(q_{CR} + q_{CW} + q_{CV}) & q_{CR} & q_{CW} & q_{CV} \\ R & q_{RC} & -(q_{RC} + q_{RW}) & q_{RW} & 0 \\ W & q_{WC} & q_{WR} & 0 & 0 \\ V & 0 & 0 & 0 & 0 \end{matrix}$$

Notes:

Panel A is the schematic of the multistate model and state transition matrix used to estimate transition rates ( $q_{rs}$ ) of steelhead smolts at HOR and TC. States are defined as San Joaquin (SJ) River upstream (U), SJ River downstream (D), and the Old River or TC distributary (T).

Panel B is the schematic of the multistate model and state transition matrix used to estimate transition rates of steelhead smolts in the Inner Delta WPA. States are defined as Old River at CVP (C), radial gates at Clifton (Clift.) Court Forebay (R), West Canal (W), and CVP Salvage Tank (V).

### 2.4.3 Covariates

We hypothesized that environmental, operational, and fish-specific factors could affect transition rates and included these covariates in varying combinations in the models. Simulated environmental

and operational data from the UnTRIM Bay-Delta model were used as covariates and were generated as described in Section 2.3. Environmental conditions were described by river flow (discharge), water temperature, and percent source river water (e.g., SJR). To disentangle the influence of riverine flow from tidal flow, the tidally averaged flow was calculated as described in Section 2.3.3.1 to be representative of riverine “net flow” (Net). Deviations from net flow (total flow minus net flow) represent the tidal component of flow (Tide). Water temperature and percent source river water were decomposed in a similar manner to distinguish between fish responses to daily and seasonal trends.

Larger scale operation metrics such as OMR flow, Qwest, total flow toward exports, and I:E ratio were removed from consideration. This occurred during data exploration and was due to several factors. Some metrics were found to be highly correlated with local flow conditions (e.g.,  $R > 0.9$  for Qwest and mainstem flow at TC); were calculated at a location far removed from the location of our analyses and, therefore, were less relevant to the local spatial scale of the analysis (e.g., total export flow calculated 30 km from HOR); or did not contain the temporal resolution needed for the fine-scale analysis being conducted (I:E, calculated daily). Depth-averaged current speed was removed from consideration because it is highly correlated with flow and may make model interpretation more difficult for management applications because these applications are based on flow (not current speed). Other local environmental variables generated by UnTRIM were also removed from consideration, either for being highly correlated with flow (e.g.,  $R > 0.7$  for water depth and flow) or for being low and nearly constant in the areas evaluated (e.g., salinity).

The fish-specific variables fork length, release day, and migrator status were also considered. Migrator status was considered at the most upstream junction, HOR, to distinguish between actively migrating juvenile steelhead and those that showed signs of extended rearing before eventual outmigration or possible residualization. Active migrants were those fish that moved through the junction quickly enough to be consistent with the 1.4- to 34.9-day range of travel time from HOR to Chipps Island documented by Buchanan et al. (2021). The possibility of either life history was not excluded by the predator filter (USBR 2018a).

Prior studies of migrating smolts have identified nocturnal migration behavior (Chapman et al. 2013), yet others have found increases in activity during the day (Smith et al. 2020). We considered diel migration patterns in smolt behavior by including a binary variable (Day) representing day or night. Day and night were based on the daily sunrise and sunset times for central Delta latitude and longitude coordinates, using R package’s “suncalc” (Thieurmel and Elmarhraoui 2019).

Two additional covariates were considered at HOR. Migrating juvenile salmonids are thought to have lower survival on the Inner Delta “Old River Route” because of exposure to the water project facilities, though recent studies have found this may not be the case for steelhead (Buchanan et al. 2021). To prevent juvenile salmonids from taking this route, in most years, management agencies have installed a rock barrier across the entrance to the Old River distributary. During the telemetry data

collection period, the barrier was in place from early April to early June in 2012, 2014, 2015, and 2016. Exact dates for barrier installation and removal for each year relative to fish presence are provided in Table 2-3.

The presence or absence of the rock barrier was indicated with a binary variable (Barrier). As described in Section 2.4.1, telemetry stations were generally deployed in similar locations each year, with the exception of the upstream station at HOR in 2011, when it was located farther upstream. To account for this difference, an indicator variable for 2011 was included. For the WPA, Barrier was also considered because it determined the routing and timing for smolts to reach this area. A variable indicating whether the CCF radial gates were open or closed was also included.

**Table 2-3**  
**Date Ranges When HOR Barrier Was Installed Each Year**

Year	Date Range of Fish Detections at Hydrophones
2011	Not installed
2012	April 1 to June 4, 2012
2013	Not installed
2014	April 8 to June 9, 2014
2015	April 3 to June 1, 2015
2016	April 1 to June 1, 2016

Due to the limited sample size for some state transitions, covariate effects were only included for transitions well represented in the data for each area being evaluated (Figure 2-10). At HOR, covariate effects were modeled for  $q_{UD}$ ,  $q_{UT}$ ,  $q_{DU}$ , and  $q_{DT}$ . At TC, covariate effects were modeled for  $q_{UD}$ ,  $q_{UT}$ , and  $q_{DU}$ . For WPA, covariate effects were modeled for all allowed transitions. The same covariate structure was assumed for all state transitions when fitting each model. Between 10 and 15 alternative models were fit for each area, and the simplest model assumed that all transition rates were constant.

At HOR, the covariate model first included the barrier and 2011 effects (both singularly and together) and compared these models with a no-covariate model. The most highly supported model structure was retained, while fitting additional variables including flow, diel patterns, and fish effects. For WPA, the barrier effect was also included because it represents obstruction of a primary route by which fish reach the Inner Delta. At TC, the model set was smaller because no barrier or 2011 effect was considered, and we fit models including flow, diel pattern, and fish effects.

All continuous covariates were standardized to have a mean of zero and unit standard deviation prior to modeling. A manual “drop 1” procedure was used on the full models to confirm the influence of each variable on fit. Additionally, we tested for collinearity among covariates by calculating the

variance inflation factor (VIF). Variables that resulted in VIFs > 3 were not considered together. Akaike's information criterion (AIC) was used to select the most parsimonious model at each location for inference (Burnham and Anderson 2002).

Goodness of model fit was evaluated by comparing the observed versus fitted prevalence (the numbers of fish in each state over time). Model residuals were examined for the presence of individual fish with outlier detection histories. For the best fit model, important covariates for each transition were identified by the slope coefficient estimates with 95% confidence intervals that did not include zero.

Given the best fit model in each area, the effects of covariates on transition rates were examined by the following: 1) using the sign and magnitude of the slope coefficients; 2) plotting the effect of each covariate on the 15-minute probability of transition when the remaining covariates were held at constant values; and 3) plotting example fish transition probabilities (i.e., the probability of transitioning from state  $r$  to state  $s$  over a period of time during which fish were present, given the time series of covariates that actually occurred). Conditional on a transition not having occurred by time  $t$ , the probability of transitioning from state  $r$  to state  $s$  from time  $t$  to time  $t + 1$  was calculated as Equation 2.

### Equation 2

$$P(t + 1|z(t)) = \exp\{Q(z(t))\}$$

where:

$P(t + 1 z(t))$	=	single-timestep transition probability matrix conditional on covariates $z(t)$
$\exp$	=	matrix exponential
$Q(z(t))$	=	transition rate matrix, which is constant over time $t$ to time $t + 1$ and depends on covariate $z(t)$

The elements of the transition probability matrix are  $p_{rs}$ , the probability of transitioning from states  $r$  to  $s$ , given the covariate values during timestep  $t$ . Then, to examine the effects of time-changing covariates over a longer period, the transition probability matrix can be calculated in a piecewise manner as Equation 3, where  $u$  is a time after  $t$  over which the transition rate matrix,  $Q$ , is not constant because of the time-changing covariates  $z(t)$ .

**Equation 3**

$$P(t, u) = P(t, t + 1)P(t + 1, t + 2) \cdots P(u - 1, u)$$

where:

$P(t, u)$  = transition probability matrix conditional on covariates  $z(t)$  which change on each 15-minute timestep

$t$  = an initial time

$u$  = a later time over which the transition rate matrix,  $Q$ , is not constant

## 3 Results

### 3.1 UnTRIM

#### 3.1.1 Correlation Analysis

Initially, the hydrodynamic variables extracted from the hydrodynamic model predictions at discrete locations were extracted at the cross-section centers (Figure 2-9) and at each of the individual hydrophones deployed in each year. There were multiple and, in some cases, many, individual hydrophones in an individual hydrophone array (Figure 2-9). Even when hydrophone arrays were installed in the same general location in multiple years, there were differences in the exact locations of individual hydrophones between years. This resulted in hundreds of individual discrete hydrophone locations. However, the individual hydrophones in a given hydrophone array were in close proximity to each other, relative to the spatial scales of change in salinity, water temperature, and percent source water in the Delta. Some of the individual hydrophones were also located in the UnTRIM Bay-Delta model grid cells that can become dry as a result of spatial averaging of the bathymetry in each model grid cell.

Because of the proximity of the individual hydrophones in each array and the tendency for some individual hydrophone locations to become dry in the hydrodynamic model, a correlation analysis was performed. This analysis was used to determine whether the cross-section center location associated with each hydrophone array was representative of the conditions surrounding the entire hydrophone array. The purpose of this correlation analysis was to evaluate whether the number of individual locations where hydrodynamic variables were extracted from the hydrodynamic model predictions could be reduced without losing information on the environmental conditions at the hydrophone arrays.

The correlation analysis consisted of evaluating the correlation coefficient ( $R$ ) of predicted salinity, water temperature, percent Sacramento River water, water depth, and current speed at each hydrophone within a given hydrophone array to the values at the cross-section center for that hydrophone array. Correlations were not calculated for individual hydrophone locations that were dry in the hydrodynamic model for more than 50% of the time. This correlation analysis was performed using the simulation year of 2016 and included the complete set of hydrophone arrays from all 6 years considered in this study. The year 2016 was used for the correlation analysis because it had many hydrophone arrays. The results of the correlation analysis were assumed to be representative of the spatial scales of change throughout the Delta and applicable to all 6 years considered in this study.

The correlation coefficient between water temperature at each hydrophone and the corresponding cross-section center was  $>0.99$  at all the hydrophone arrays. The correlation coefficient between

water depth at each hydrophone and the corresponding cross-section center was also  $>0.99$  at all the hydrophone arrays. However, the absolute values of the water depth at each hydrophone and the cross-section center varied based on the bathymetry at each location. This analysis demonstrates there was a high degree of correlation between water temperature and water depth at the individual hydrophone locations and at the center of the cross sections used in the analysis.

The correlation coefficient between salinity at each hydrophone and the corresponding cross-section center was  $>0.93$  for all but one of the hydrophone arrays. The minimum correlation coefficient between salinity at individual hydrophone locations and the cross-section center was 0.82 for the array near the radial gates and entrance to CCF. The minimum correlation coefficient was lower at this location because some of the individual hydrophones were on the opposite side of the radial gates than the cross-section center in the hydrodynamic model; thus, salinity diverged between the cross-section center and locations inside CCF when the radial gates were closed. The correlation coefficient increased to approximately 0.97 for the individual hydrophones on the same side of the radial gates as the cross-section center. This analysis demonstrates there was a high degree of correlation between salinity at the individual hydrophone locations and at the center of the cross sections used in the analysis.

The correlation coefficient between percent Sacramento River water at each hydrophone and the corresponding cross-section center was  $>0.87$  for all but one of the hydrophone arrays. The minimum correlation was lowest ( $r = 0.85$ ) at the location near the radial gates for the same reason described previously for salinity.

The correlation coefficient between depth-averaged current speed at each hydrophone and the corresponding cross-section center was  $>0.83$  for all but four of the hydrophone arrays. These four hydrophone arrays had minimum correlations ranging from 0.57 to 0.76. At each of these four locations, the next-lowest correlation between the individual hydrophones and the cross-section centers was approximately 0.85. This demonstrates that the depth-averaged current speed at the individual hydrophone locations was generally correlated with the values at the cross-section centers, but that the correlation was sensitive to a few of the exact locations of the individual hydrophones.

In summary, this analysis demonstrated a large amount of correlation between conditions at the individual hydrophones and the corresponding cross-section centers for salinity, water temperature, percent Sacramento River water, and water depth. As a result of this high correlation, these variables were extracted from the hydrodynamic model predictions at only the cross-section center locations for possible use in the fish transition models. For depth-averaged current speed, this analysis demonstrated a large amount of correlation between the individual hydrophones and the corresponding cross-section centers at many of the hydrophone arrays and relatively lower minimum correlation at other hydrophone arrays. In addition to the cross-section centers, depth-averaged current speed was also extracted near the center of the channel in the vicinity of a hydrophone array

to potentially provide more information for the fish transition models because of the overall slightly lower correlation between the individual hydrophone locations and cross-section centers.

### *3.1.2 Exports and Net Water Flow Through Turner Cut*

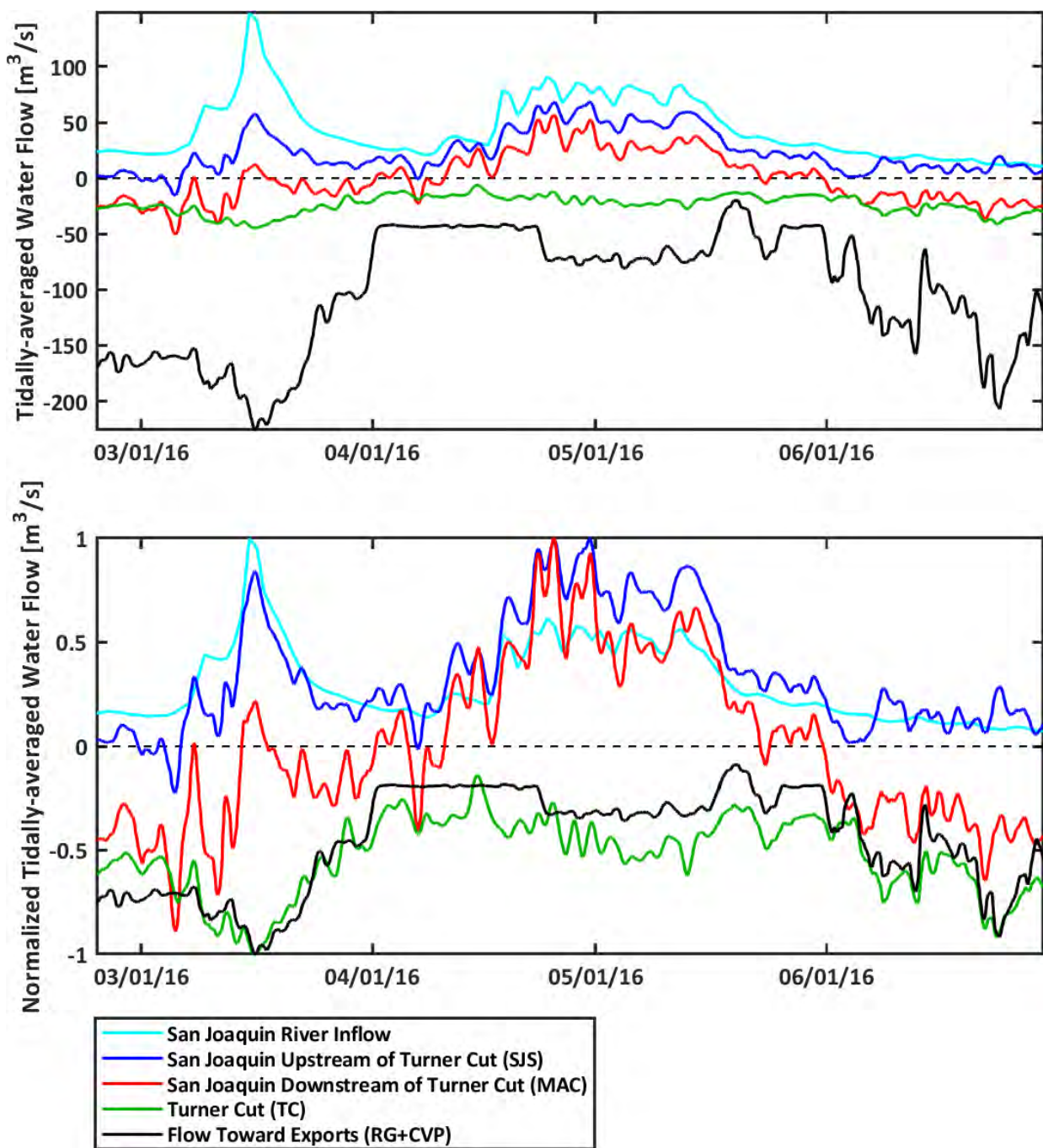
Net (tidal-averaged) water flow through TC was compared to net flow toward the SWP and CVP export facilities to evaluate whether there was a relationship between changes in exports and changes in net flow through TC. Years 2016 (Figure 3-1) and 2013 (Figure 3-2) are shown as representative time series of the flows used in this analysis.

The predicted net flow through the SJR upstream of TC was nearly always downstream (positive), but the predicted net flow downstream of TC was both downstream and upstream (negative). The predicted net flow through TC was nearly always away from the SJR into TC (negative). The normalized predicted net flows suggest a strong relationship between the predicted flow toward the export facilities and predicted net flow through TC. An increase in predicted net flow toward the export facilities corresponded to an increase in the net flow down TC.

The relationship between an increase in predicted flow toward the export facilities and an increase in net flow down TC is maintained when all 6 years are considered together (Figure 3-3). The relationship between net flow toward the export facilities and net flow through TC was significant ( $p < 0.001$ ) for each of the 6 years individually and when all 6 years were considered together ( $R_s = 0.84$ ). Figure 3-3 shows the trend is an increase in net flow from the SJR down TC (negative) as the net flow toward the export facilities increases (negative). There is some variation around the trend line, most notably in 2011. Additional work would be needed to determine the cause of this variation.

A similar relationship was seen in the data-based flows, in which changes in daily exports corresponded to changes in data-based daily-averaged flow through TC (Figures 3-4 and 3-5). This relationship was significant ( $p < 0.001$ ,  $R_s = 0.79$ ; Figure 3-6). Similar to the predicted net flows, there is a period during 2011 when the relationship is not as strong, and additional work could be conducted to determine the cause.

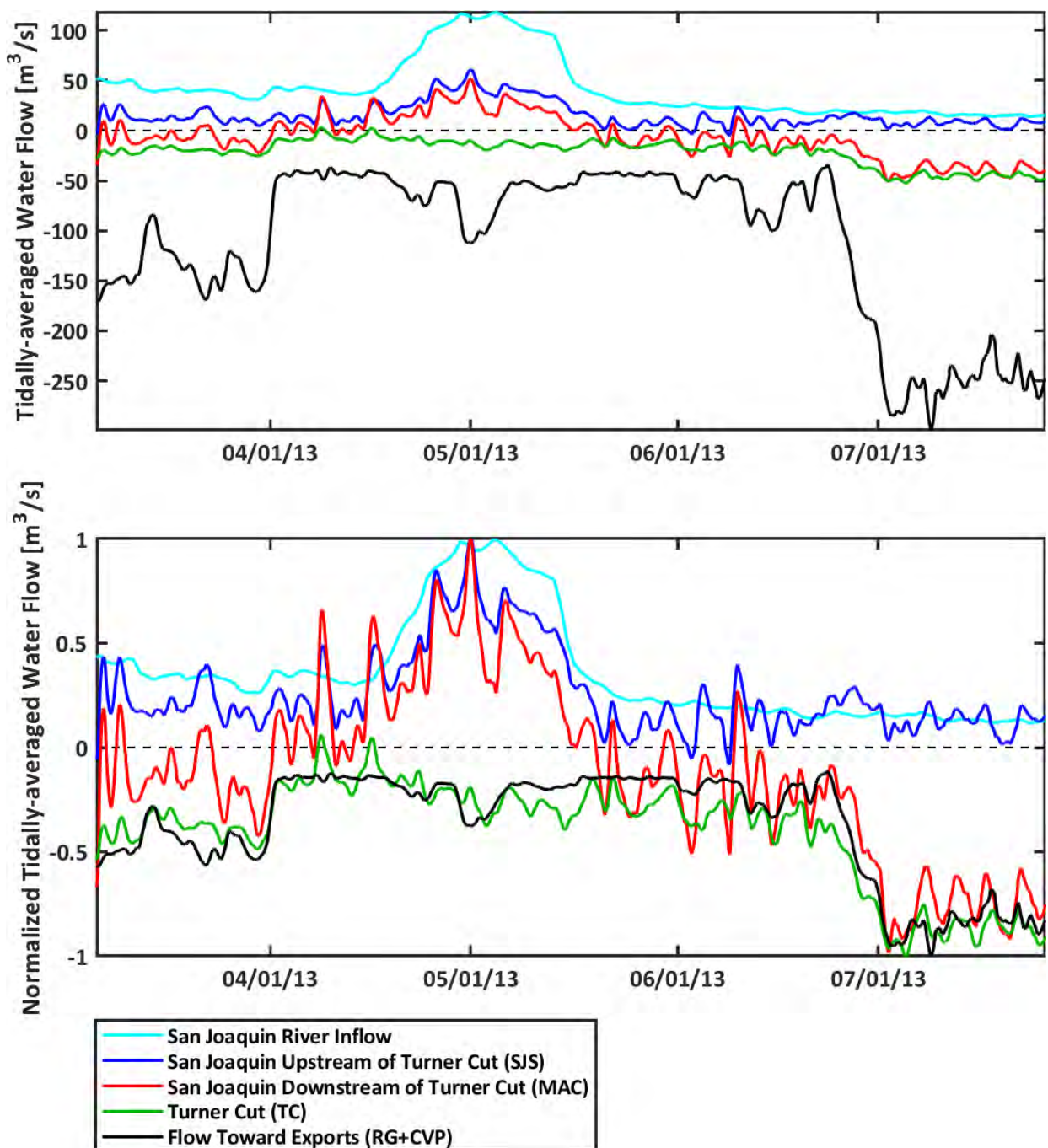
**Figure 3-1**  
**Predicted Net Flow During 2016**



Note:

(Parens) Parenthetical abbreviations note the hydrophone arrays from which predicted water flow was extracted from the hydrodynamic model.

**Figure 3-2**  
**Predicted Net Flow During 2013**



Note:

(Parens) Parenthetical abbreviations note the hydrophone arrays from which predicted water flow was extracted from the hydrodynamic model.

**Figure 3-3**

**Relationship Between Predicted Net Flow Through Turner Cut and Toward the Export Facilities**

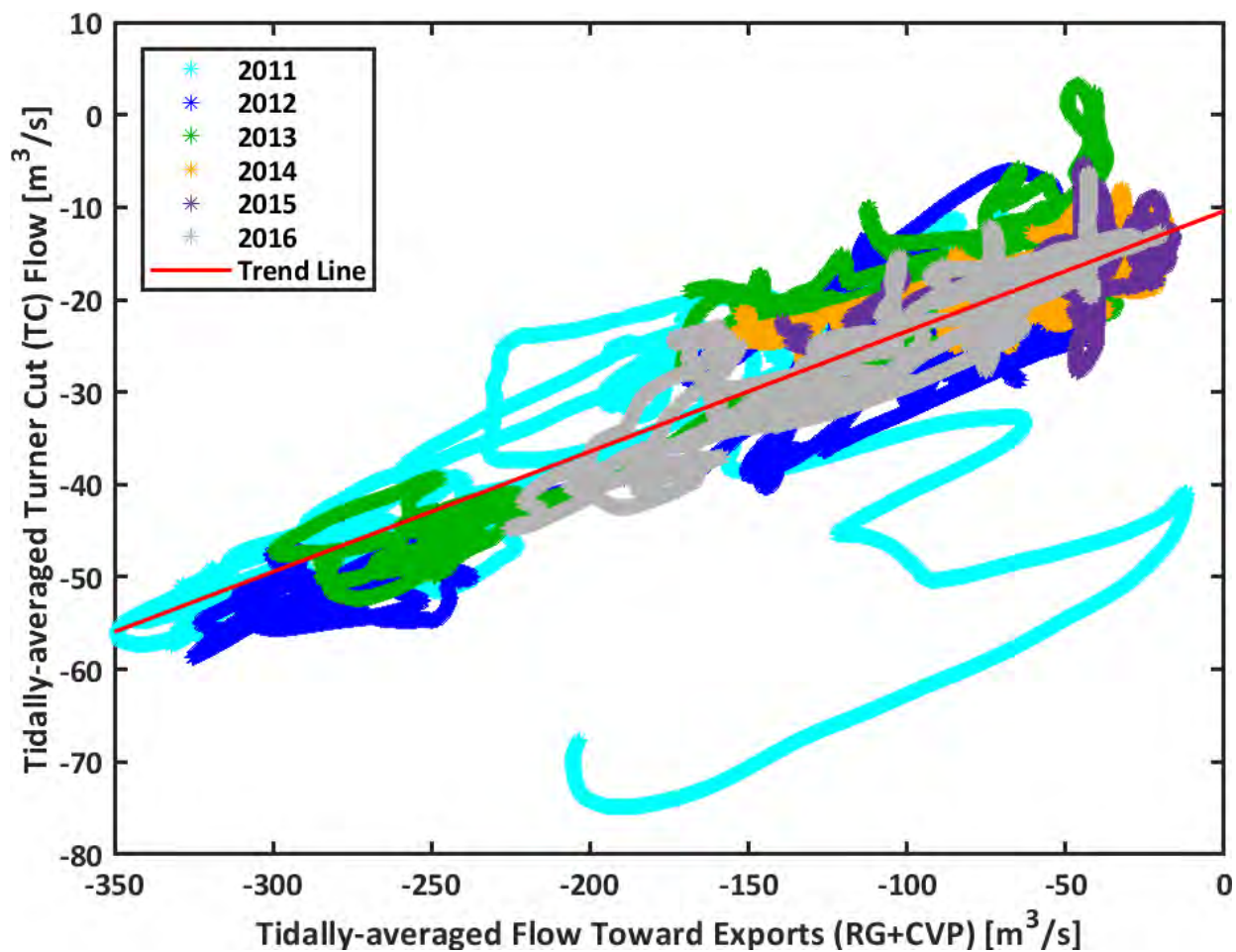
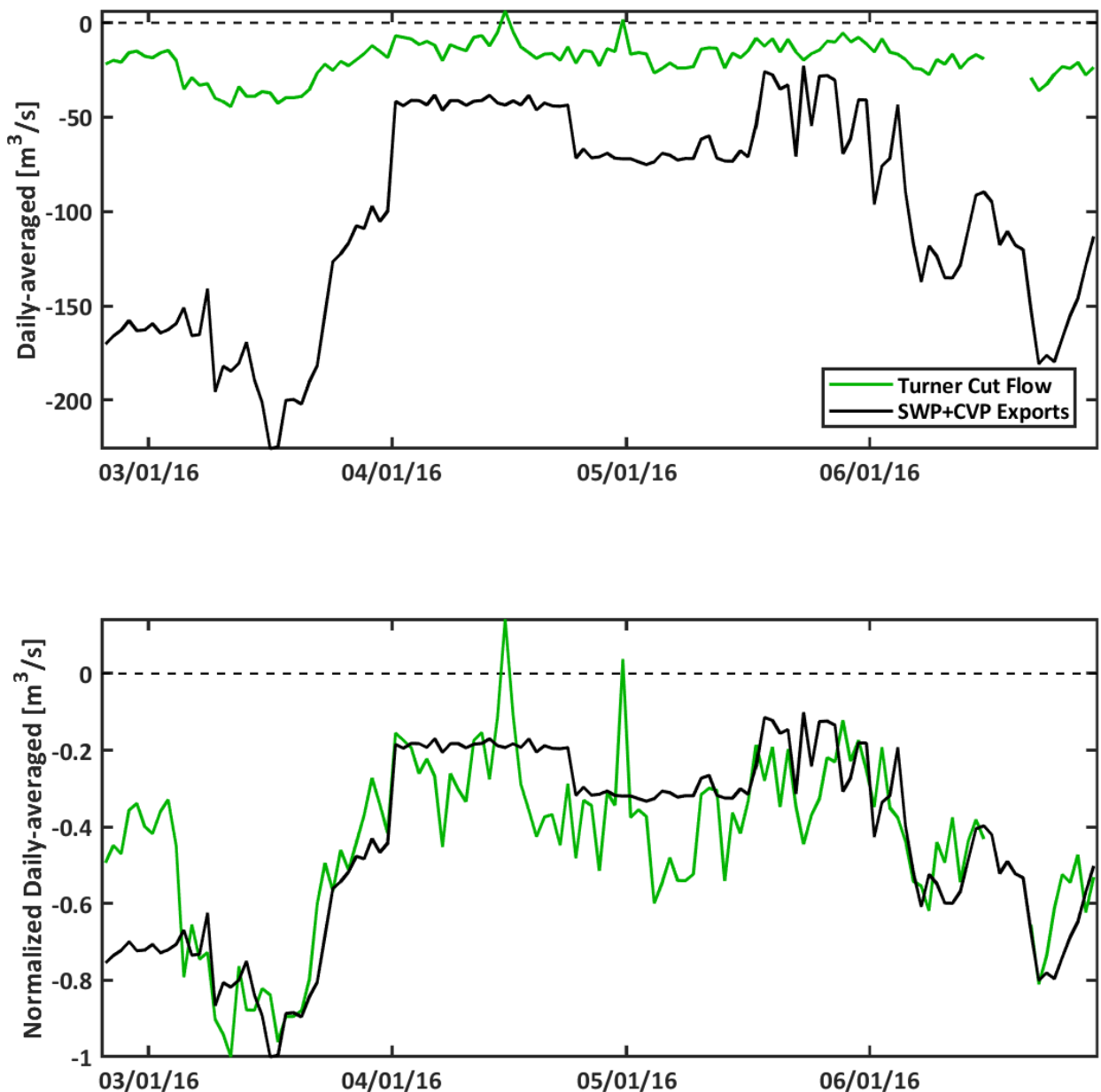
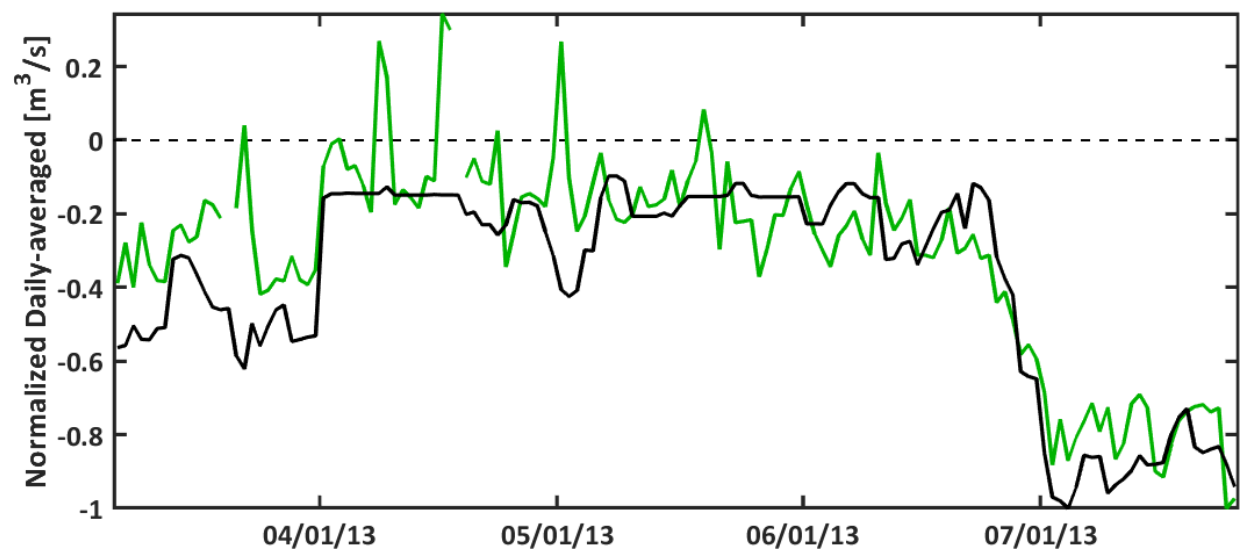
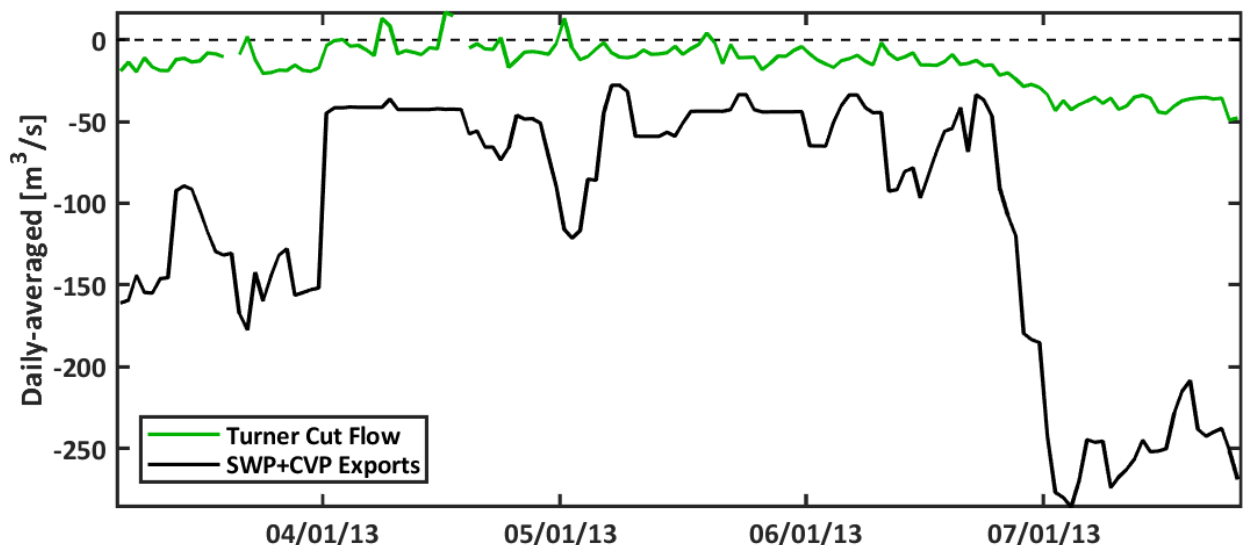


**Figure 3-4**  
**Data-Based Net Flow During 2016**



Note:  
 Missing sections of the TC flow line indicate missing data.

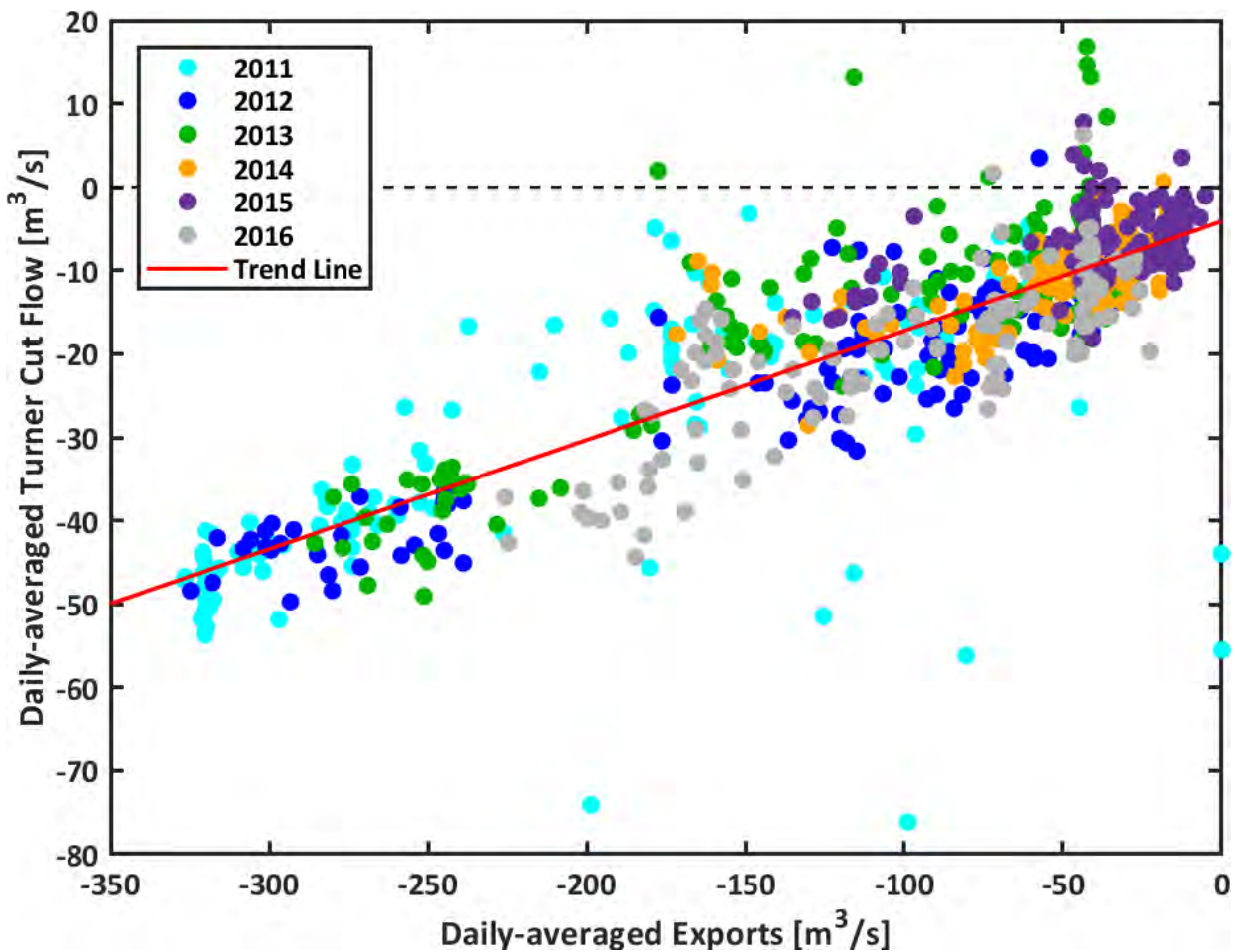
**Figure 3-5**  
**Data-Based Net Flow During 2013**



Note:  
 Missing sections of the TC flow line indicate missing data.

**Figure 3-6**

**Relationship Between Data-Based Flow Through Turner Cut and Water Exports**



### 3.2 Head of Old River

A total of 4,580 tagged juvenile steelhead were detected in the HOR junction between 2011 and 2016 (Appendix D, Table D.1-1). Fork lengths ranged from 106 to 396 mm, and average fork lengths ranged from 215 to 280 mm. There were 3,298 observed fish transitions between states at the HOR made by 1,910 smolts when the barrier was installed and 3,217 observed transitions made by 2,695 smolts when the barrier was not installed (Appendix D, Figure D.1-1).

The distribution of state-to-state transitions was different when the barrier was installed versus when it was not ( $\chi^2 = 2988.4$ ,  $P < 2.2 \cdot 10^{-16}$ ; Figure 3-7). During all periods (both when the barrier was and was not installed), approximately twice as many transitions (53% of total transitions) were made from the upstream state (state U) to the downstream state on the mainstem (state D) than from the upstream state to the distributary state on Old River (state T; 28% of total transitions). Fewer transitions (12%)

were fish moving from downstream to upstream on the mainstem or even fewer (5%) from downstream on the mainstem into the distributary. It was uncommon for fish to move from the distributary either upstream (0.6%) or downstream (0.4%) on the mainstem. The distribution of transitions was quite different with and without the barrier installed; the upstream to downstream transition accounted for 74% of the transitions when the barrier was installed but only 32% of the transitions when the barrier was not installed. When the barrier was not installed, the upstream to tributary transition accounted for 54% of the transitions, compared with only 3% of the transitions when the barrier was installed. Additionally, there was more variability in the percentage of fish classified as active migrators when the barrier was installed (24% to 97%) compared to when it was not installed (73% to 91%).

**Figure 3-7**  
**Distribution of HOR Junction Observed State-to-State Transitions with and Without the Barrier Installed**

	<i>U</i>	<i>D</i>	<i>T</i>		<i>U</i>	<i>D</i>	<i>T</i>
<i>U</i>	—	53%	28%	<i>U</i>	—	32%	54%
<i>D</i>	12%	—	5%	<i>D</i>	2%	—	10%
<i>T</i>	1%	0.4%	—	<i>T</i>	1.1%	0.8%	—

	<i>U</i>	<i>D</i>	<i>T</i>		<i>U</i>	<i>D</i>	<i>T</i>
<i>U</i>	—	74%	3%	<i>U</i>	—	32%	54%
<i>D</i>	22%	—	0%	<i>D</i>	2%	—	10%
<i>T</i>	0%	0.1%	—	<i>T</i>	1.1%	0.8%	—

Barrier Installed
Barrier Not Installed

### 3.2.1 Model Selection

The model identified as providing the best fit to the data using AIC contained one interaction and four covariates: an interaction between barrier presence (Barrier) and daytime (Day), the net and tidal components of flow (Net and Tide), migrator status, and the tidal component of flow in the distributary (Tide<sub>T</sub>). The indicator variable for alternate upstream hydrophone placement in 2011 was not carried forward in the model because it had a high VIF (approximately 5) with net flow, as 2011 was also the only wet water year. VIFs for all covariate main effects in the best fit model were <2.0,

and the VIF for the interaction between Barrier and Day was 2.6, indicating that multicollinearity (i.e., the occurrence of high intercorrelations among two or more independent variables in a multiple regression model) was not an issue (Zuur et al. 2009). The remaining models in the model set had AIC values more than 78 points higher than that of the best fit model (Table 3-1).

**Table 3-1**  
**Head of Old River Junction Model Selection Results**

Model	k	Dev	AIC	ΔAIC
Barrier × Day + Net + Tide + Migrator + Tide <sub>T</sub>	34	28414.5	28482.5	0.0
Barrier + Day + Net + Tide + Migrator + Tide <sub>T</sub>	30	28501.3	28561.3	78.8
Barrier × Day + Net + Tide + Migrator	30	28633.2	28693.2	210.7
Barrier + Net + Tide + Migrator + Tide <sub>T</sub>	26	28672.15	28724.15	241.62
Barrier + Net + Tide + Migrator × Day	30	28699.2	28759.2	276.6
Barrier + Net + Tide + Migrator	22	28896.6	28940.6	458.0
Barrier + Net + Tide + Tide <sub>T</sub>	22	32540.4	32584.4	4101.9
Barrier + Net + Tide + Day	22	32609.9	32653.9	4171.4
Barrier + Net + Tide + Temp <sub>Avg</sub>	22	32743.8	32787.8	4305.3
Barrier + 2011 + Tide	18	33371.0	33407.0	4924.5
Barrier + 2011 + Net	18	33879.3	33915.3	5432.8
Barrier + Net + Tide	18	32781.1	32817.1	4334.6
Barrier + 2011 + Day	18	34675.5	34711.5	6229.0
Barrier + 2011	14	34722.1	34750.1	6267.6
No covariates	6	39201.0	39213.0	10730.5

Notes:

ΔAIC: the difference in AIC value between the given model and the model with the lowest AIC value

2011: indicator variable for year 2011 effects

Barrier: indicates whether the barrier is installed

Day: day/night indicator

Dev: deviance

k: number of parameters

Migrator: actively migrating fish (fish that spend one complete tidal cycle [24.8 hours] or less at the junction)

Net: net flow on the mainstem

Temp<sub>Avg</sub>: daily running-average water temperature

Tide: tidal component of flow on the mainstem

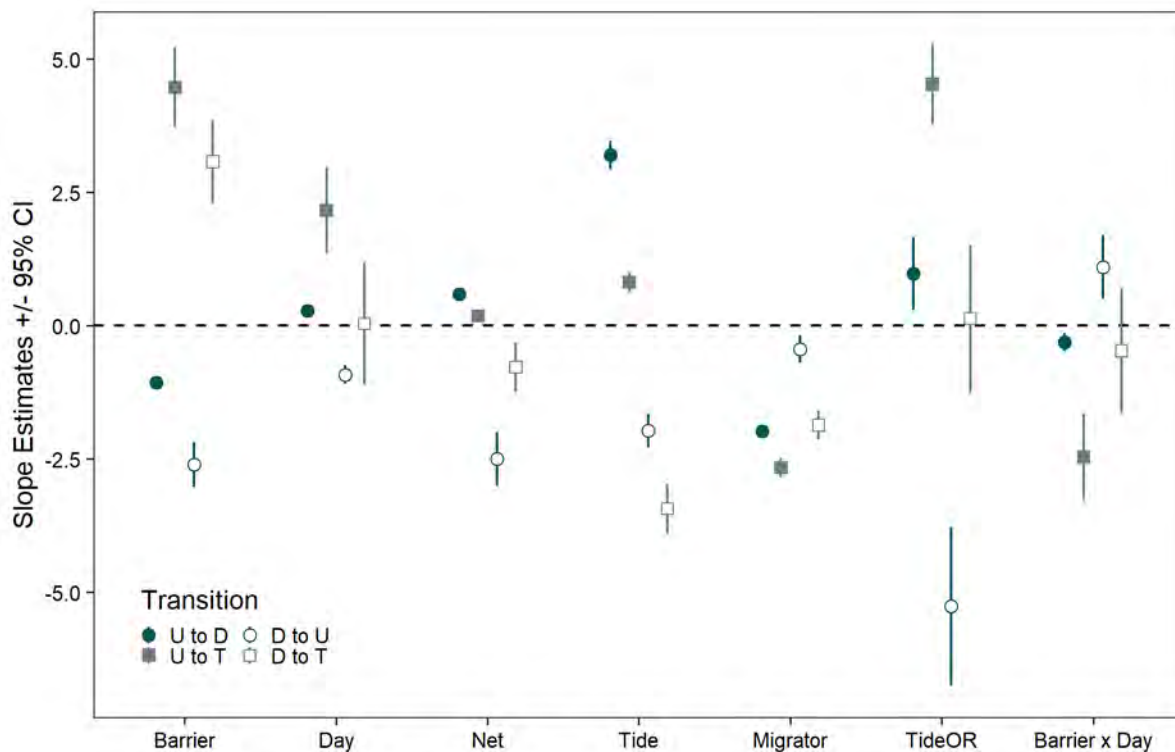
Tide<sub>T</sub>: tidal component of flow on Old River distributary

Slope coefficient estimate and 95% confidence intervals for the best fit model are presented in Table 3-2 and Figure 3-8. Only slope coefficients identified as important (i.e., their 95% confidence interval did not include zero) are discussed in the text. An important consideration for interpreting slope coefficients in the HOR is to define the baseline state for categorical variables because the slope coefficient shows the response to a change from that baseline state. There are three categorical variables in the best fit model: Barrier, Day, and Migrator. The baseline states for these

are that the Barrier is installed (versus not installed), the time of day is Day (versus night), and that fish are Migrators (versus non-migrators). Therefore, a positive coefficient for a categorical variable is interpreted as increasing the transition rate when not in the baseline state (i.e., a large positive coefficient for Barrier means transition rates increase when the barrier is not installed). Additionally, the sign convention for positive flow is downstream on the mainstem and into the distributary (Figure 2-5).

The best fit model showed upstream to downstream transition rates ( $q_{UD}$ ) were lower when the barrier was not installed. Tide was the strongest predictor for this transition. Upstream to downstream transition rates were higher when the tide was ebbing (increasing downstream) on the mainstem (Figure 3-8). The next-strongest predictor was migrator status; the upstream to downstream transition rates were lower when fish were classified as non-migrators. The slope coefficient for the distributary tidal component of flow was small but positive, which showed that downstream transition rates increased with an ebbing tide. There was a similar positive relationship, although smaller in magnitude, for downstream transitions at night and with increasing net flow. The interaction of Barrier  $\times$  Day was less influential on this transition, but there was a negative relationship (i.e., lower transition rates) at night when the barrier was not installed.

**Figure 3-8**  
**Head of Old River Junction Best Fit Model Covariate Slope Coefficient Estimates**



Note: Line ranges show the 95% confidence interval for slope coefficient estimates.

The strongest positive predictors of upstream to distributary transition rates ( $q_{UT}$ ) were when the barrier was not installed and when distributary tide was ebbing (Table 3-2 and Figure 3-8). The slope coefficient for the tidal component of mainstem flow was positive, which showed upstream to distributary transition rates also increased with an ebbing mainstem tide. There was a negative relationship (i.e., lower transition rates) for distributary transitions for the interaction of Barrier and Day (i.e., when the barrier was not installed and at night) and for being a non-migrator. Upstream to distributary transition rates were higher at night but only when the barrier was installed (i.e., for the few fish that entered the barrier culverts). Net flow was a positive predictor but less influential on the upstream to distributary transition rate.

The strongest predictor of increasing downstream to upstream transition rates ( $q_{DU}$ ) was when the tide was flooding (reverse tide flow) on both the distributary and mainstem (Figure 3-8). This transition rate was lower when the barrier was not installed and with increasing net flow. Downstream to upstream transition rates were lower at night when the barrier was installed. However, this transition rate decreased at night when the barrier was not installed. Migrator status was a negative but less influential predictor of the downstream to upstream transition rate.

The strongest predictors of downstream to distributary transition rate ( $q_{DT}$ ) were the barrier indicator and mainstem tide flow (Figure 3-8). This transition rate increased when the barrier was out and with reverse mainstem tide flow. Downstream to distributary transition rate was lower for non-migrants and decreased with increasing net flow.

**Table 3-2**  
**Best Fit Head of Old River Model Parameter Estimates**

Transition Rate ( $q_{rs}$ )	Covariate	Slope Coefficient Estimate ( $\beta_{rs}$ )
$q_{UD}$	Baseline	1.763 (1.643, 1.891)
	Barrier	<b>-1.064 (-1.179, -0.949)</b>
	Day	<b>0.274 (0.179, 0.37)</b>
	Net	<b>0.588 (0.513, 0.663)</b>
	Tide	<b>3.201 (2.938, 3.465)</b>
	Migrator	<b>-1.983 (-2.065, -1.901)</b>
	Tide <sub>T</sub>	<b>0.976 (0.288, 1.663)</b>
	Barrier × Day	<b>-0.304 (-0.473, -0.135)</b>
$q_{UT}$	Baseline	0.2 (0.153, 0.262)
	Barrier	<b>4.475 (3.733, 5.216)</b>
	Day	<b>2.162 (1.354, 2.971)</b>
	Net	<b>0.184 (0.112, 0.255)</b>
	Tide	<b>0.814 (0.623, 1.004)</b>
	Migrator	<b>-2.666 (-2.847, -2.485)</b>
	Tide <sub>T</sub>	<b>4.529 (3.768, 5.289)</b>
	Barrier × Day	<b>-2.467 (-3.283, -1.652)</b>
$q_{DU}$	Baseline	0.278 (0.225, 0.343)
	Barrier	<b>-2.604 (-3.022, -2.186)</b>
	Day	<b>-0.919 (-1.092, -0.746)</b>
	Net	<b>-2.498 (-2.998, -1.998)</b>
	Tide	<b>-1.971 (-2.286, -1.655)</b>
	Migrator	<b>-0.436 (-0.698, -0.174)</b>
	Tide <sub>T</sub>	<b>-5.263 (-6.754, -3.772)</b>
	Barrier × Day	<b>1.101 (0.503, 1.698)</b>
$q_{DT}$	Baseline	0.055 (0.038, 0.08)
	Barrier	<b>3.074 (2.3, 3.848)</b>
	Day	0.042 (-1.1, 1.184)
	Net	<b>-0.78 (-1.243, -0.318)</b>
	Tide	<b>-3.437 (-3.91, -2.963)</b>
	Migrator	<b>-1.868 (-2.136, -1.599)</b>
	Tide <sub>T</sub>	0.133 (-1.253, 1.52)
	Barrier × Day	-0.473 (-1.641, 0.695)
$q_{TU}$	Baseline	0.407 (0.321, 0.515)
$q_{TD}$	Baseline	0.135 (0.086, 0.213)

Notes:

**Bold** values indicate covariates identified as important (i.e., their 95% confidence intervals did not overlap zero).

Slope coefficient estimates ( $\beta_{rs}$ ) are shown with 95% confidence intervals in parentheses.

$q_{rs}$ : transition rate from state  $r$  to state  $s$ , where (at HOR)  $r$  and  $s$  can be upstream (U), downstream (D), or distributary (T)

Barrier: indicates whether the barrier is installed

Day: day/night indicator

Migrator: actively migrating fish (fish that spend one complete tidal cycle [24.8 hours] or less at the junction)

Net: net flow on the mainstem

Tide: tidal component of flow on the mainstem

Tide<sub>T</sub>: tidal component of flow on Old River distributary

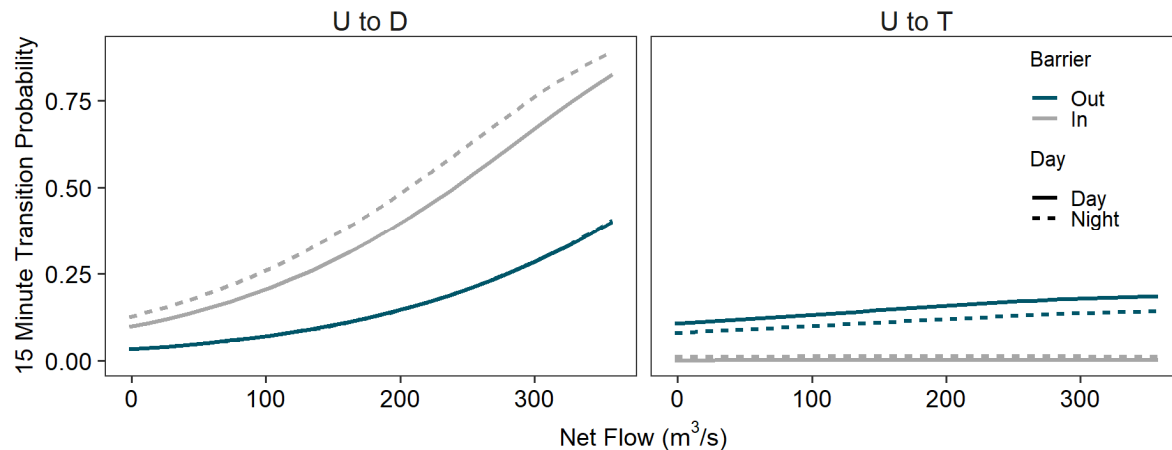
### 3.2.2 Fifteen-Minute Transitions

Fifteen-minute transitions are the probability that a fish detected at one state will be detected at another state or at the same state after one timestep of the model (15 minutes). Fifteen-minute transitions are plotted over the range of continuous variables to show the full range of effects, while categorical effects are shown as offsets from their baseline.

The probability that fish would transition from upstream to downstream was strongly influenced by increasing mainstem net flow (Figure 3-9, left panel), while the probability of transitioning from upstream to the distributary was relatively invariant to mainstem net flow (Figure 3-9, right panel). The influence of time of day on transition probability depended on transition (e.g., upstream to downstream or upstream to distributary) and whether the barrier was in or out. For example, fish had a higher probability of transitioning upstream to downstream at night when the barrier was installed. When the barrier was not installed, and fish were more easily able to transition to the distributary, this was more likely to happen during the day. Net flow increased the upstream to downstream transition probability for active migrators more than for non-migrators, especially when the barrier was in (Figure 3-10, left panel).

**Figure 3-9**

**Net Flow Effect on the 15-Minute Transition Probability of Actively Migrating Smolts from HOR (State U)**

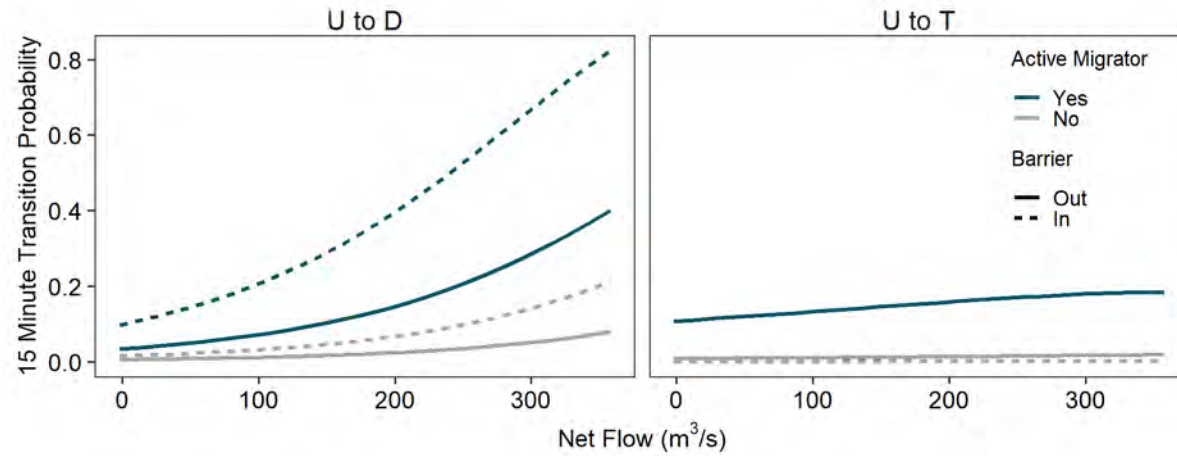


Note:

Moving from upstream to downstream (state U to D) or upstream to distributary (state U to T)

**Figure 3-10**

**Net Flow and Barrier Effect on 15-Minute Transition Probabilities for Active Migrators and Non-Migrants**



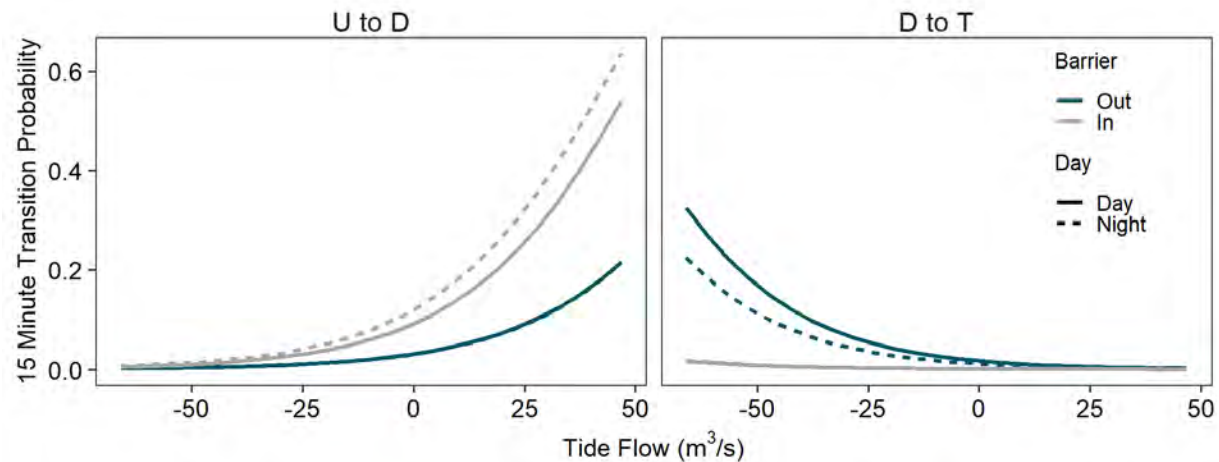
Note:

Moving from upstream to downstream (state U to D) or upstream to distributary (state D to T)

Upstream to downstream transition probability was also increased by increasing tide flow (ebb tides; Figure 3-11, left panel), while flood tide flow increased the probability that fish would backtrack from downstream on the mainstem into the distributary (Figure 3-11, right panel). The influence of tide flow on both transition probabilities was stronger for fish designated as active migrants (Figure 3-12, right and left panels). However, the influence of flood tides on downstream to upstream transition probabilities for all fish was higher when the barrier was in place (Figure 3-12, middle panel).

**Figure 3-11**

**Tide Flow Effect on the 15-Minute Transition Probability of Actively Migrating Smolts**

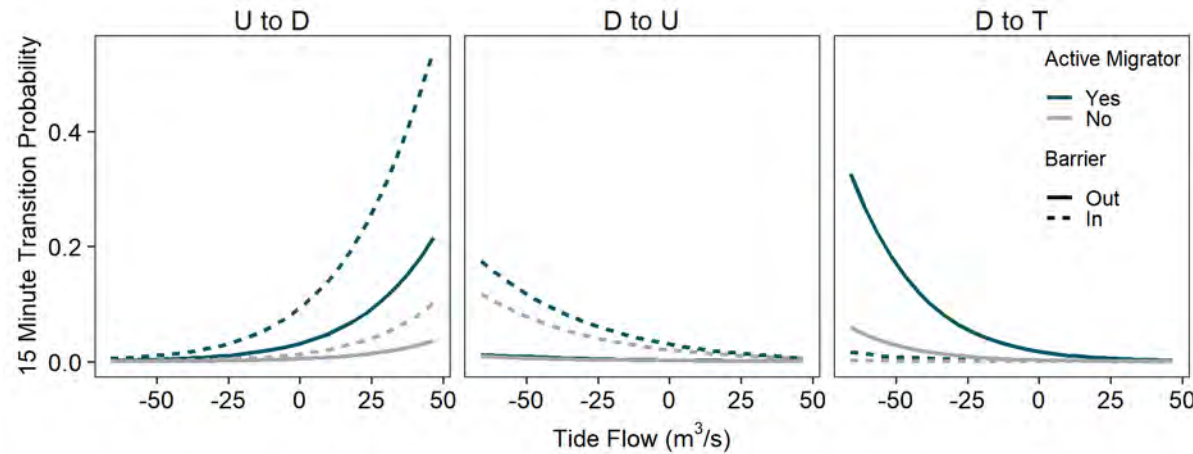


Note:

Moving from upstream to downstream (state U to D) or downstream to distributary (state D to T)

**Figure 3-12**

**Tide Flow and Barrier Effect on 15-Minute Transition Probabilities for Active Migrators and Non-Migrators**



Note:

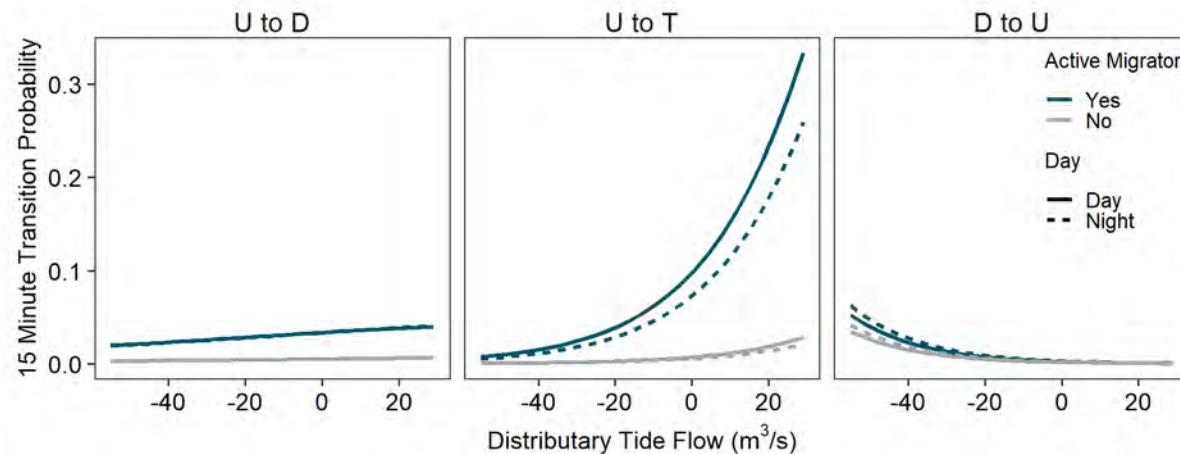
Moving from upstream to downstream (state U to D), upstream to distributary (state U to T), downstream to upstream (state D to U), or downstream to distributary (state D to T)

For distributary tide flow, only periods when the barrier was not installed are shown in Figure 3-13. The range of distributary tide flow when the barrier was not installed was often within  $\pm 10$  m³/s or less and may not have acted directly on fish. Actively migrating fish had a high probability of

transitioning upstream to distributary with increasing distributary tide flow during the day (ebb tide; Figure 3-13, middle panel).

**Figure 3-13**

**Distributary Tide Flow Effect on the 15-Minute Transition Probability of Actively Migrating Smolts with No Barrier**



Note:

Moving upstream to downstream (state U to D), upstream to distributary (state U to T), or downstream to upstream (state D to U)

### 3.2.3 Example Period Transition Probabilities

Transition probabilities for HOR represent the probability that a fish in one state will be in another state or the same state over an example 3-day period, given the hydrodynamic and physical conditions that actually occurred. At HOR, the majority of fish were detected during the following two general types of scenarios:

- Low flow with the barrier installed as occurred for release groups 1, 2, and 3 in 2012 and release groups 2 and 3 in 2014 and 2015 (e.g., May 22 to May 24, 2012)
- High flow with the barrier not installed as occurred in 2011 and for release groups 1 and 2 in 2016 (e.g., March 17 to March 19, 2016)

When net flow was high and the barrier was installed, fish had the highest probability of transitioning from upstream to downstream on the mainstem, and the chance of them entering the distributary from either upstream or downstream was very low (Figure 3-14). During the period from May 22 to May 24, 2012, the barrier was out, and net flow was relatively low, ranging between 43 and 48 m<sup>3</sup>/s (Figure 3-15). The probability of fish moving upstream to downstream (state U to D) or downstream to upstream (state D to U) fluctuated with tide flow and time of day (Figure 3-14). The main difference for fish classified as active migrators was that the probability of transitioning downstream increased 80% after only 3 hours.

Non-migrators also had a high chance of moving downstream over time, but that probability did not exceed 75% until approximately 1.5 days after entering the HOR junction (Figure 3-14, right panel). Non-migrators also had a higher probability of transitioning back upstream over time.

**Figure 3-14**  
**Example Transition Probabilities over a 3-Day Period: May 22 to May 24, 2012**

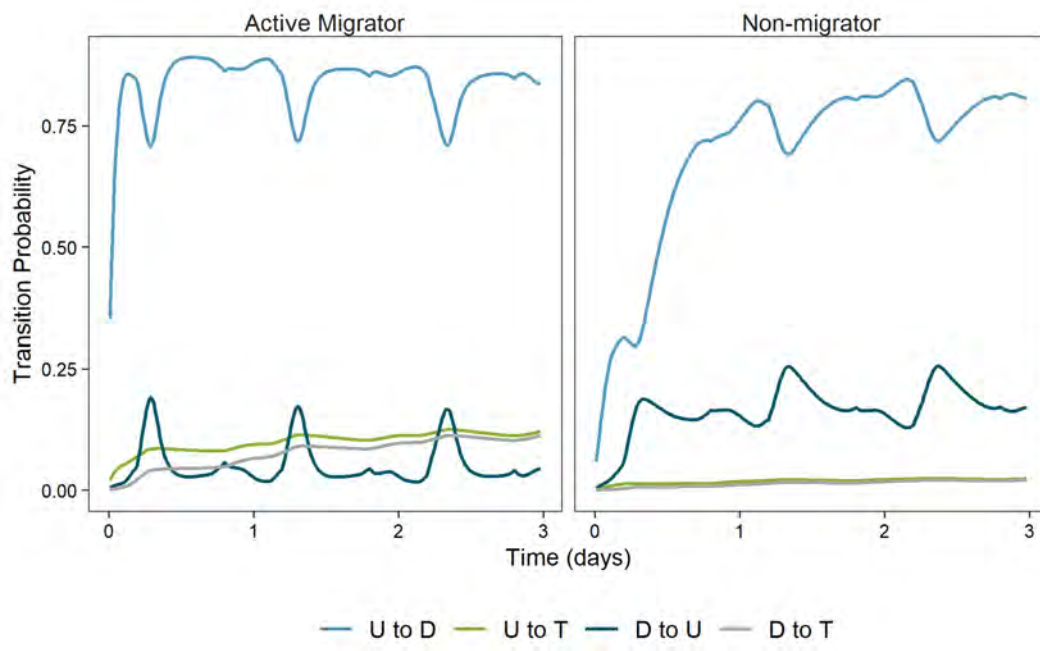
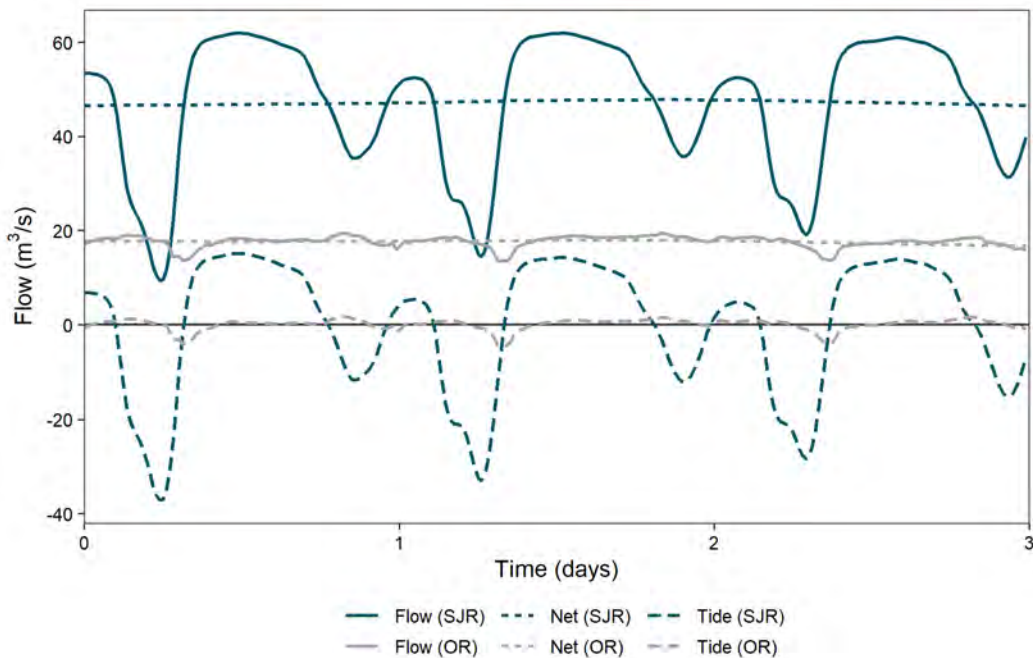


**Figure 3-15**  
**Flow Conditions at HOR over a 3-Day Period: May 22 to May 24, 2012**



When the barrier was not installed, there was a high probability that actively migrating fish would transition either directly to the distributary from the mainstem or backtrack from downstream on the mainstem into the distributary (Figure 3-16). During the period from March 17 to March 19, 2016, the barrier was not installed, and net flow was high (Figure 3-17). There were also large tide flows on both the mainstem and distributary. For non-migrators, the probability of staying on the mainstem was higher than for active migrators. For all smolts, the probability of transitioning back upstream against the high net flow was low over the 3 days.

**Figure 3-16**

**Example Transition Probabilities over a 3-Day Period: March 17 to March 19, 2016**

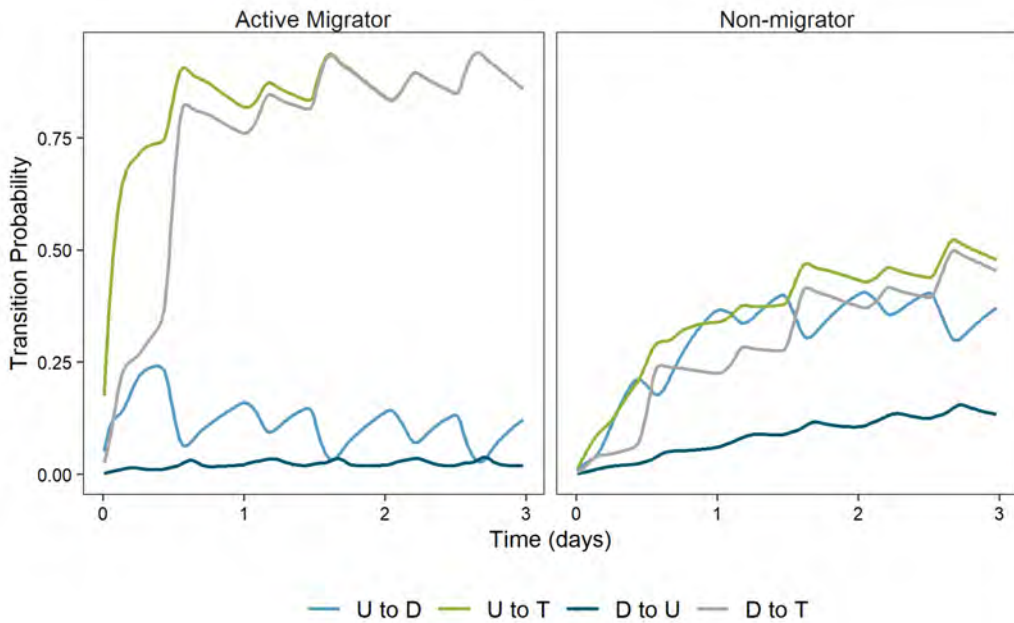
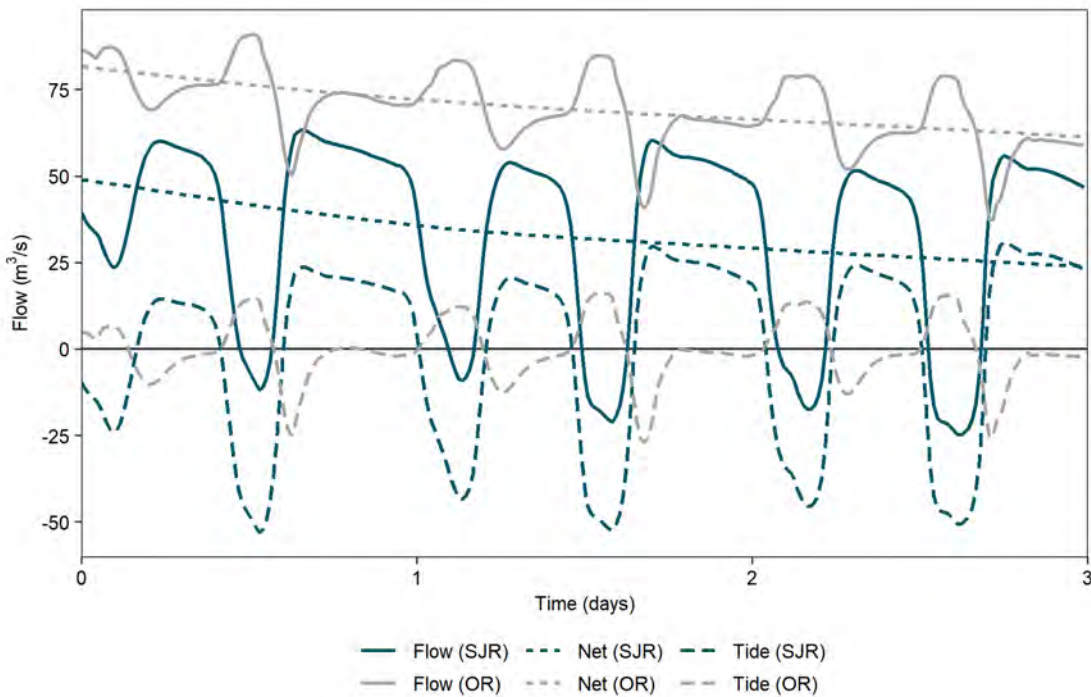


**Figure 3-17**

**Flow Conditions over a 3-Day Period: March 17 to March 19, 2016**



### 3.3 Turner Cut

A total of 576 tagged juvenile steelhead were detected at the TC junction in 2013, 2015, and 2016 (Appendix D, Table D.1-2). Fork lengths ranged from 180 to 292 mm, and average fork lengths were 221, 246, and 255 mm in 2013, 2015, and 2016, respectively. The median amount of time spent at TC ranged from 7.9 hours in 2013 to 9.6 hours in 2016. In the 3 years, 90% of fish spent 1.3 days or less in this area.

Study fish made a total of 893 observed transitions between states at the TC junction (Appendix D, Figure D.1-2). The highest number of transitions (64%) were made from upstream to downstream (state U to D) on the mainstem, showing that this was the predominant transition direction (Figure 3-18). Fifteen percent of transitions were downstream to upstream (state D to U) on the mainstem, and 15% of transitions were from upstream into the TC distributary (state U to T). Fewer transitions (approximately 3% each) were for fish moving from downstream on the mainstem into the distributary (state D to T) or out of the distributary back upstream (state T to U). The fewest number of transitions (0.6%) were from the TC distributary to downstream on the mainstem (state T to D).

**Figure 3-18**

**Distribution of Turner Cut Junction Observed State-to-State Transitions**

	<i>U</i>	<i>D</i>	<i>T</i>
<i>U</i>	—	64%	15%
<i>D</i>	15%	—	3%
<i>T</i>	2%	1%	—

#### 3.3.1 Model Selection

The model identified as providing the best fit to the data using AIC included four covariates: the net and tidal components of flow (Net and Tide), daytime (Day), and the tidal component of flow in the distributary (Tide<sub>T</sub>). VIFs for all covariate main effects in the best fit model were <2.0, indicating there was not a problem with multicollinearity (Zuur et al. 2009). The remaining models in the model set had AIC values more than 86 points higher than that of the best fit model (Table 3-3).

**Table 3-3**  
**Turner Cut Junction Model Selection Results**

Model	k	Dev	AIC	ΔAIC
Net + Tide + Tide <sub>T</sub> + Day	18	4086.7	4122.7	0.0
Net + Tide + Tide <sub>T</sub>	15	4178.9	4208.9	86.2
Net + Tide + PSJW <sub>Tide</sub>	15	4228.0	4228.0	105.3
Net + Tide + PMW <sub>Tide</sub>	15	4212.7	4242.7	119.9
Net + Tide + Temp <sub>Avg</sub>	15	4239.7	4269.7	147.0
Net + Tide + Temp <sub>Dev</sub>	15	4239.7	4269.7	147.0
Net + Tide + PSJW <sub>Avg</sub>	15	4247.5	4277.5	154.8
Net + Tide	12	4258.7	4282.7	160.0
Net + Tide + Net <sub>T</sub>	15	4253.1	4283.1	160.3
Baseline (no covariates)	6	4966.9	4978.9	856.1

Notes:

Day: day/night indicator

Net: net flow on the mainstem

PMW<sub>Tide</sub>: tidal component of percent Mokelumne River water

PSJW<sub>Avg</sub>: average component of percent SJR water

PSJW<sub>Tide</sub>: tidal component of percent SJR water

Temp<sub>Avg</sub>: daily average water temperature

Temp<sub>Dev</sub>: water temperature deviations from the daily average

Tide: tidal component of flow on the mainstem

Tide<sub>T</sub>: tidal component of flow on Turner Cut distributary

Slope coefficient estimate and 95% confidence intervals for the best fit model are presented in Table 3-4 and Figure 3-19. Only slope coefficients identified as important (i.e., their 95% confidence interval did not include zero) are discussed in the text. An important consideration for interpreting slope coefficients at the TC junction is that the assumed positive direction of flow in the distributary is out of TC and into the mainstem. Similar to HOR, the baseline state for the variable "Day" is daytime (versus nighttime). Therefore, a negative coefficient would be interpreted as decreasing the transition rate at night relative to during the day.

**Table 3-4**  
**Best Fit Turner Cut Model Parameter Estimates**

Transition Rate ( $q_{rs}$ )	Covariate	Slope Coefficient Estimate ( $\beta_{rs}$ )
$q_{UD}$	Baseline	2.2 (1.836, 2.635)
	Net	<b>2.338 (0.596, 4.081)</b>
	Tide	<b>1.056 (0.85, 1.262)</b>
	$Tide_T$	<b>0.36 (0.209, 0.512)</b>
	Day	<b>-0.831 (-1.084, -0.578)</b>
$q_{UT}$	Baseline	0.83 (0.618, 1.115)
	Net	-0.653 (-3.44, 2.133)
	Tide	0.146 (-0.102, 0.395)
	$Tide_T$	<b>-1.108 (-1.427, -0.789)</b>
	Day	<b>-1.276 (-1.692, -0.861)</b>
$q_{DU}$	Baseline	0.401 (0.241, 0.668)
	Net	0.065 (-2.635, 2.764)
	Tide	<b>-1.525 (-1.967, -1.083)</b>
	$Tide_T$	-0.074 (-0.314, 0.166)
	Day	-0.01 (-0.342, 0.322)
$q_{DT}$	Baseline	0.012 (0, 3.413)
$q_{TU}$	Baseline	2.903 (2.127, 3.963)
$q_{TD}$	Baseline	0.039 (0, 8.273)

Notes:

**Bold** values indicate covariates identified as important (i.e., their 95% confidence intervals did not overlap zero).

Slope coefficient estimates ( $\beta_{rs}$ ) are shown with 95% confidence intervals in parentheses.

$q_{rs}$ : transition rate from state  $r$  to state  $s$ , where (at TC) possible states are upstream (U), downstream (D), and distributary (T).

Day: day/night indicator

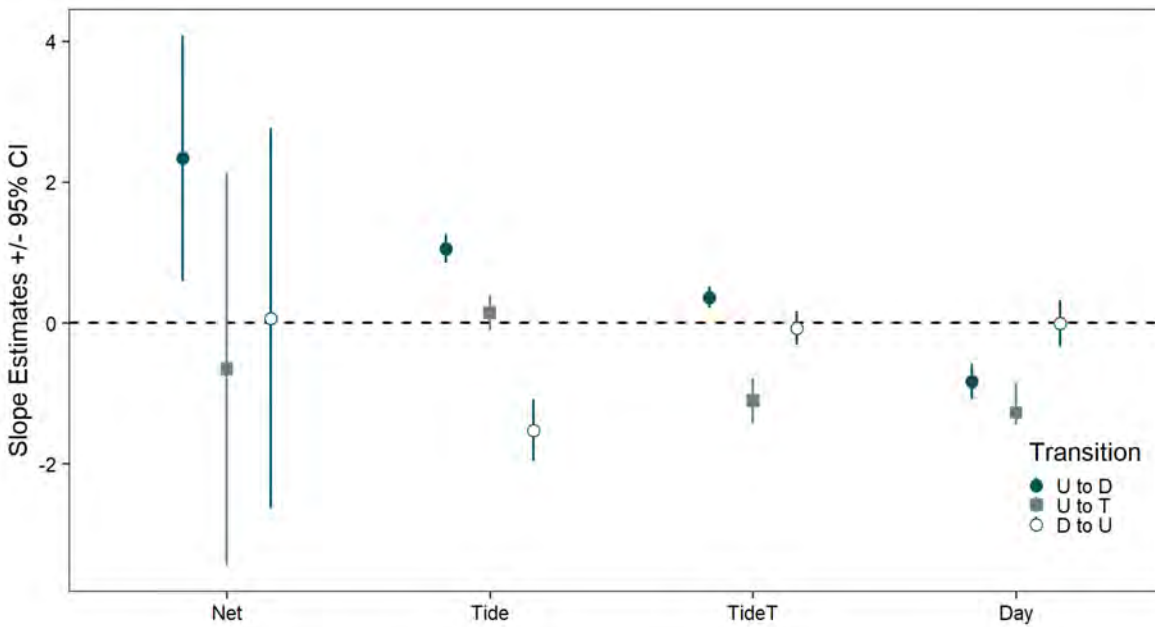
Net: net flow on the mainstem

Tide: tidal component of flow on the mainstem

$Tide_T$ : tidal component of flow on Turner Cut distributary

**Figure 3-19**

**Turner Cut Junction Best Fit Model Covariate Slope Coefficient Estimates**



Note:

Line ranges show the 95% confidence interval (CI) for slope coefficient estimates.

Rates of transition from upstream to downstream ( $q_{UD}$ ) increased with increasing net flow (Net) and tide flow (Tide) on the mainstem, and with increasing tide flow out of the distributary ( $Tide_T$ ). Upstream to downstream transition rates were also lower at night.

The baseline transition rate for  $q_{UT}$  (upstream to distributary) was lower than that of  $q_{UD}$  (0.83 versus 2.2), and  $q_{UT}$  was further decreased by increased outflow (ebb tide) from the TC distributary and at night. The baseline transition rate for upstream transitions on the mainstem ( $q_{DU}$ ) was lower than the rates for either downstream transition ( $q_{UD}$ ,  $q_{UT}$ ) and was further decreased by increasing downstream tide flow (ebb tide).

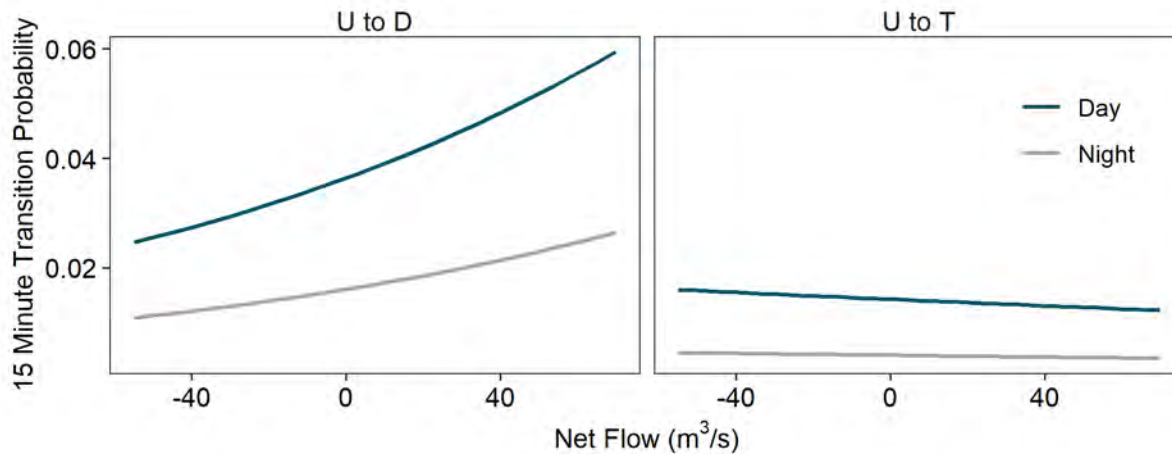
The baseline rate of transition from distributary to upstream ( $q_{TU} = 2.9$ ) was much higher than the rate of transition from distributary to downstream ( $q_{TD} = 0.039$ ). Since there were few transitions out of the distributary, no covariates were fit to either transition.

### 3.3.2 Fifteen-Minute Transitions

Fifteen-minute transitions are the probability that a fish detected at one state will be detected at another state, or at the same state, after one timestep of the model (15 minutes). At the TC junction, the probabilities of being in another state after 15 minutes were generally lower than at HOR. Net

flow was the strongest predictor of upstream to downstream transition, but the range of net flows was much lower than at HOR (-55 m<sup>3</sup>/s to 72 m<sup>3</sup>/s; Figure 3-20).

**Figure 3-20**  
**Net Flow Effect on 15-Minute Transition Probabilities**

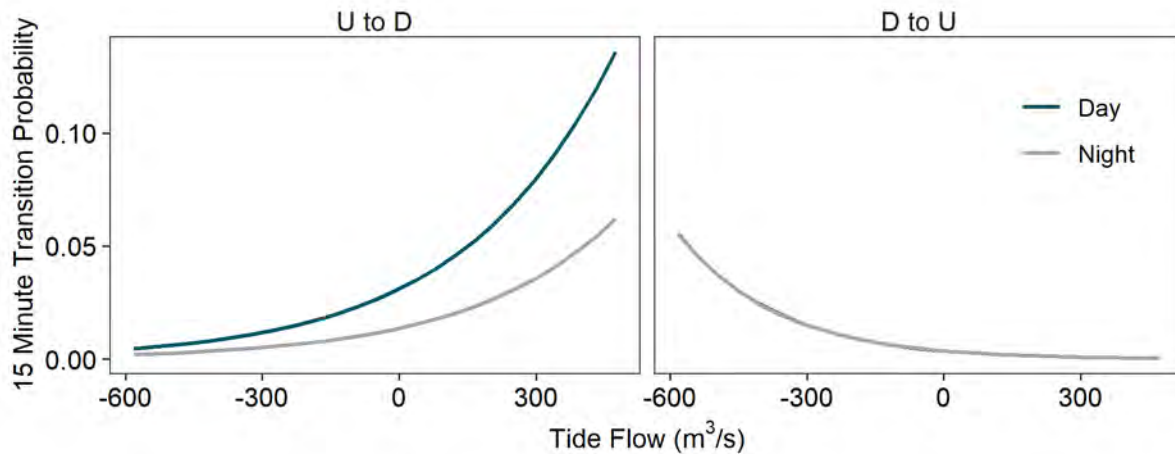


Note:

Transitions from upstream to downstream (state U to D) and upstream to distributary (state U to T)

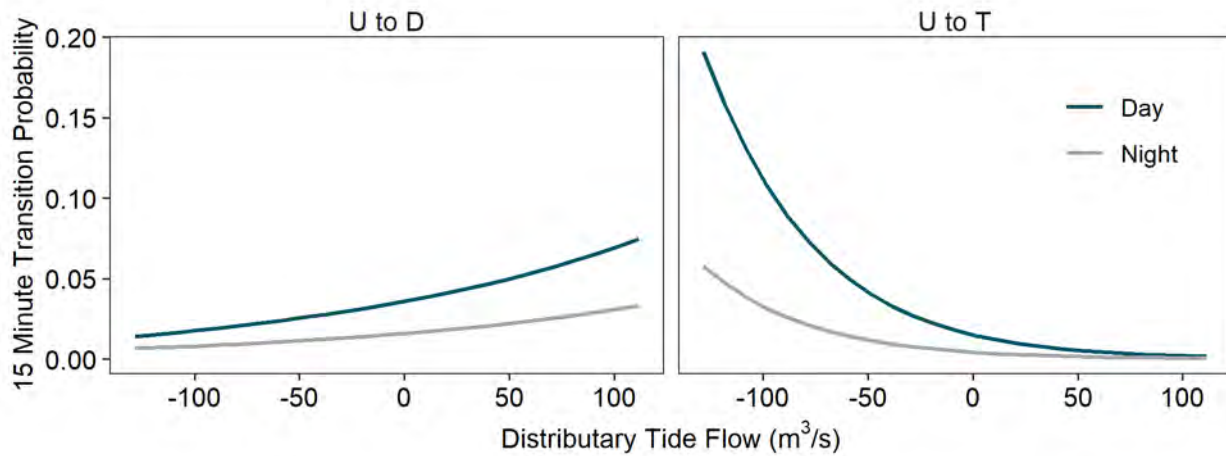
The probability of transitioning upstream to downstream increased during the ebb tide (Figure 3-21, left panel), while the probability of upstream transition increased during the flood tide (Figure 3-21, right panel). Reverse tide flow in the TC distributary (flood tide) increased the probability of transitioning into the distributary (Figure 3-21, right panel), while downstream tide flow (ebb tide) in the distributary increased the probability of fish moving downstream on the mainstream (Figure 3-22, left panel).

**Figure 3-21**  
**Tide Flow Effect on 15-Minute Transition Probabilities**



Note:  
Transitions from upstream to downstream (state U to D) and downstream to upstream (state D to U)

**Figure 3-22**  
**Distributary Tide Flow Effect on 15-Minute Transition Probabilities**



Note:  
Transitions from upstream to downstream (state U to D) and upstream to distributary (state U to T)

### 3.3.3 Example Period Transition Probabilities

Transition probabilities for TC represent the probability that a fish in one state will be in another state or the same state over an example 3-day period, given the hydrodynamic and physical conditions that actually occurred. For the period from May 2 to May 4, 2016, the probability of fish detected upstream transitioning to downstream increased to approximately 60% after approximately 16 hours but then varied between 45% and 82% with daily tide flow (Figure 3-23). The probability of transitioning from upstream into the distributary remained at 14% or lower over time but varied with distributary tide flow and time of day.

On average, the probability of smolts moving upstream on the mainstem was lower than the probability they would move downstream. However, during periods of high reverse tide flow (flood tide just after the start of days 1 and 2; Figure 3-24), the probability of upstream or downstream transition on the mainstem was approximately equal for short periods of time. An interesting feature of the water flow is bimodal peaks in flow rate at the peak and trough of each tidal cycle, the cause of which was discussed but not definitively identified. They do not appear to be aligned with water project operations but may reflect differences in tidal timing from multiple channels in the Delta. The bimodal peaks in flow rate were not reflected in the example period transition probabilities.

**Figure 3-23**  
**Example Period Transition Probabilities over a 3-Day Period: May 2 to May 4, 2016**

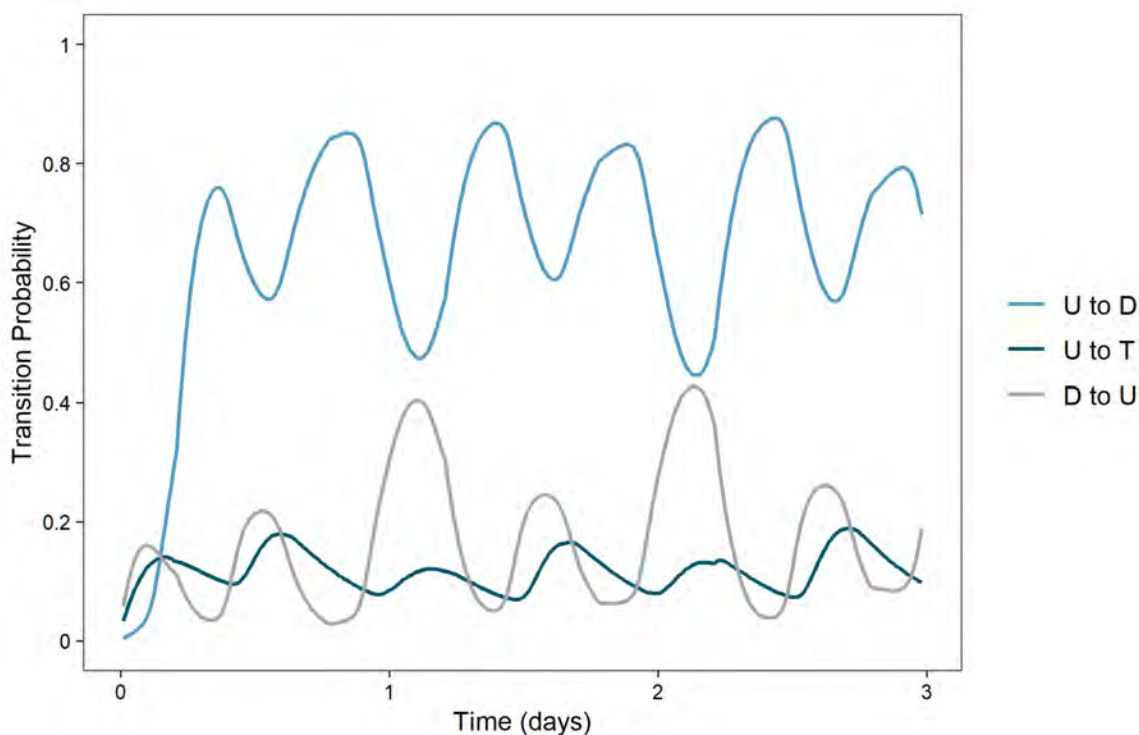
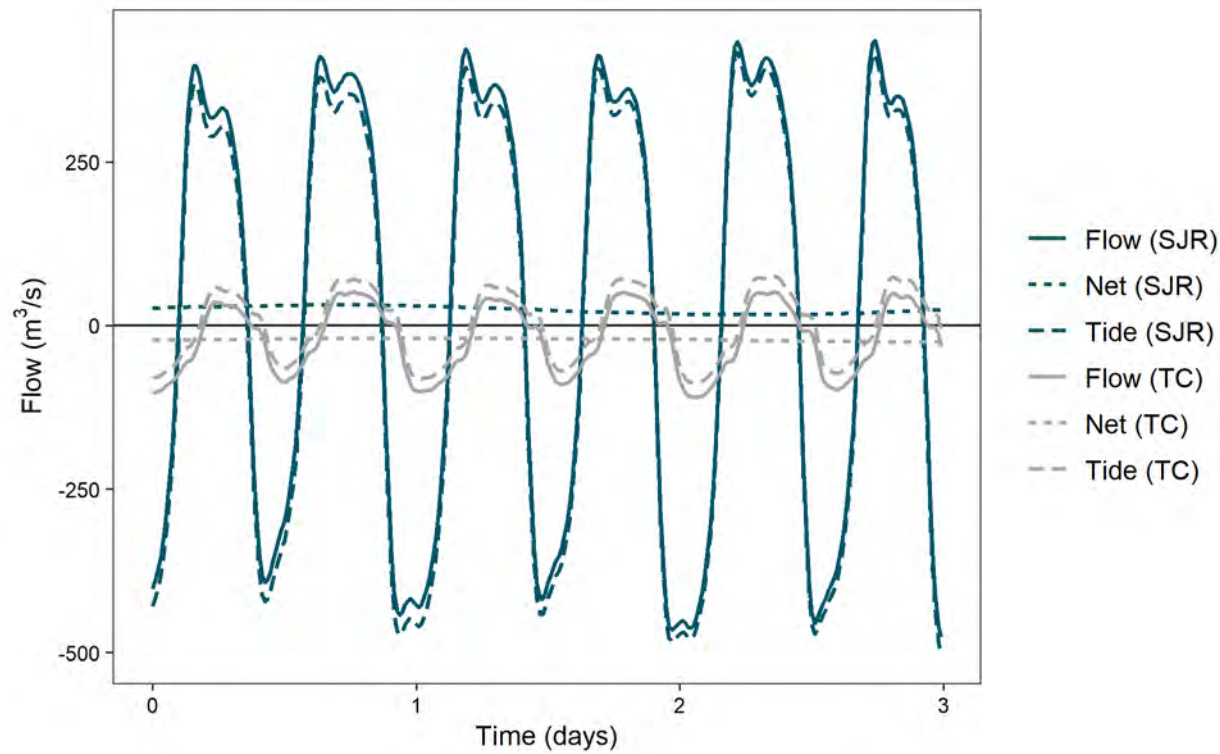


**Figure 3-24**  
**Flow Conditions over a 3-Day Period: May 2 to May 4, 2016**



### 3.4 Water Project Area

A total of 790 tagged juvenile steelhead were detected in the WPA from 2014 through 2016 (Appendix D; Table D.1-3). Fork lengths ranged from 148 to 281 mm, and average fork lengths were 241, 236, and 248 mm in 2014, 2015, and 2016, respectively. The median amount of time spent in the WPA ranged from 11.4 hours in 2016 to 29.4 hours in 2015. Over the 3 years, 90% of fish spent 6.5 days or less in this area, which was much longer than the time fish spent at the mainstem junctions (HOR and TC).

Study fish made a total of 1,273 observed transitions between states in the WPA (Appendix D, Figure D.1-3). A similar number of transitions (18% to 20% of total transitions) were made from West Canal (state W) to the radial gate entrance to CCF (state R), from the radial gates to back to West Canal, or from the radial gates to CVP (state C; Figure 3-25). Fewer transitions (9%) were for fish moving from downstream in West Canal to upstream at CVP. Though fish must pass the inlet leading to the CCF entrance to move from West Canal to CVP, the chance that fish in the main West Canal channel would be detected by acoustic receivers located at the CCF radial gate is low (Figure 2-1; Appendix A). Fish may also transition between downstream and upstream locations via alternate

routes that did not have hydrophone coverage, such as by staying in Old River where it branches from West Canal around a small island.

**Figure 3-25**

**Distribution of Water Project Area Observed State-to-State Transitions**

	C	R	W	V
C	—	9%	6%	19%
R	18%	—	20%	0%
W	9%	19%	—	0%
V	0%	0%	0%	—

There were also many transitions where fish were repeatedly detected in the upstream state (Figure 3-25), meaning that fish were detected at CVP and then returned to CVP sometime later without having been detected at other sites (states in the multistate model) in the WPA. This could indicate fish left the vicinity or were simply blocked from detection by islands, docks, and other nearby structures. Once detected at CVP, approximately 9% of interstate transitions were to radial gates, and 6% were to West Canal. More transitions (20%) were fish moving from CVP to CVP salvage tanks (state V). Since the salvage tanks represent an absorbing state from which fish cannot return, each of these 243 transitions corresponds to a single fish, indicating that 243 of 790 (or 30.7%) of fish detected in the WPA were detected at the CVP salvage tank.

### 3.4.1 Model Selection

The model identified as providing the best fit to the data using AIC contained four covariates: the net and tidal components of flow in West Canal (Netw and Tidew), release day (standardized) as a continuous covariate, and temperature deviations at CVP (Tempc\_Dev). VIFs for all covariates in the best fit model were <1.3, indicating that multicollinearity was not an issue (Zuur et al. 2009). The remaining models in the model set had AIC values more than 7 points higher than that of the best fit model (Table 3-5).

**Table 3-5**  
**Water Project Area Model Selection Results**

Model	k	Dev	AIC	ΔAIC
Net <sub>W</sub> + Tide <sub>W</sub> + ReleaseDay + Temp <sub>C_Dev</sub>	35	10463.1	10533.1	0.0
Net <sub>W</sub> + Tide <sub>W</sub> + PSJW <sub>C_Avg</sub> + Temp <sub>C_Dev</sub>	35	10470.8	10540.8	7.7
Net <sub>W</sub> + Tide <sub>W</sub> + ReleaseDay + PSJW <sub>C_Avg</sub>	35	10475.0	10545.0	11.9
Net <sub>W</sub> + Tide <sub>W</sub> + Temp <sub>C_Avg</sub> + Temp <sub>C_Dev</sub>	35	10479.3	10549.3	16.2
Net <sub>W</sub> + Tide <sub>W</sub> + RG <sub>IND</sub> + Temp <sub>C_Dev</sub>	35	10488.2	10558.2	25.1
Net <sub>W</sub> + Tide <sub>W</sub> + Temp <sub>C_Avg</sub> + PSJW <sub>C_Avg</sub>	35	10507.4	10577.4	44.3
Net <sub>W</sub> + Tide <sub>W</sub> + Temp <sub>C_Dev</sub>	28	10525.6	10581.6	48.5
Net <sub>W</sub> + Tide <sub>W</sub> + ReleaseDay	28	10534.5	10590.5	57.4
Net <sub>W</sub> + Tide <sub>W</sub> + PSJW <sub>C_Avg</sub>	28	10542.8	10598.8	65.7
Net <sub>W</sub> + Tide <sub>W</sub> + Temp <sub>C_Avg</sub>	28	10548.9	10604.9	71.8
Net <sub>W</sub> + Tide <sub>W</sub> + RG <sub>IND</sub>	28	10553.0	10609.0	75.9
Net <sub>W</sub> + Tide <sub>W</sub> + Temp <sub>W_Dev</sub>	28	10556.3	10612.3	79.1
Net <sub>W</sub> + Tide <sub>W</sub> + Barrier	28	10568.0	10624.0	90.9
Net <sub>W</sub> + Tide <sub>W</sub>	21	10596.8	10638.8	105.6
Net <sub>C</sub> + Tide <sub>C</sub>	21	10949.9	10991.9	458.8
Net <sub>R</sub> + Tide <sub>R</sub>	21	11315.5	11357.5	824.3
No covariates	7	11661.6	11675.6	1142.5

Note:

Barrier: indicator for whether the rock barrier at HOR was installed

Net<sub>W, C, R</sub>: net flow in West Canal (W), at CVP (C) and at CCF radial gates (R)

PSJW<sub>C\_Avg</sub>: average percent SJR water at CVP

ReleaseDay: ordinal fish release day

RG<sub>IND</sub>: CCF radial gate open/closed indicator

Temp<sub>C\_Avg</sub>: average water temperature at CVP

Temp<sub>C\_Dev</sub>: water temperature deviation at CVP

Tide<sub>W, C, R</sub>: tide flow in West Canal (W), at CVP (C) and at CCF radial gates (R)

Slope coefficient estimates and 95% confidence intervals for the best fit model are presented in Table 3-6 and Figure 3-26. Only slope coefficients identified as important (i.e., their 95% confidence interval did not include zero) are discussed here. An important consideration for interpreting slope coefficients in the WPA is that Net<sub>W</sub> flow was upstream (reversed) for the entire study period, but the sign convention for positive downstream flow was retained. Net<sub>W</sub> ranged from -177 to -13 m<sup>3</sup>/s with median Net<sub>W\_med</sub> = -43 m<sup>3</sup>/s. Therefore, a positive coefficient that would generally be interpreted as "increasing downstream flow" can be thought of here as "decreasing reversed flow."

**Table 3-6**  
**Best Fit Water Project Area Model Parameter Estimates**

Transition Rate ( $q_{rs}$ )	Covariate	Slope Coefficient Estimate ( $\beta_{rs}$ )
$q_{CR}$	Baseline	0.105 (0.084, 0.132)
	$Net_W$	0.678 (-0.01, 1.366)
	$Tide_W$	<b>0.334 (0.106, 0.562)</b>
	ReleaseDay	0.067 (-0.107, 0.241)
	$Temp_{C\_Dev}$	<b>-3.296 (-5.373, -1.218)</b>
$q_{CW}$	Baseline	0.013 (0.005, 0.032)
	$Net_W$	<b>4.291 (2.565, 6.016)</b>
	$Tide_W$	<b>1.622 (0.936, 2.308)</b>
	ReleaseDay	<b>-0.35 (-0.644, -0.057)</b>
	$Temp_{C\_Dev}$	-0.638 (-3.671, 2.395)
$q_{CV}$	Baseline	0.105 (0.086, 0.127)
	$Net_W$	<b>-3.39 (-3.912, -2.868)</b>
	$Tide_W$	<b>-0.294 (-0.418, -0.17)</b>
	ReleaseDay	<b>0.198 (0.044, 0.352)</b>
	$Temp_{C\_Dev}$	<b>2.277 (1.5, 3.054)</b>
$q_{RC}$	Baseline	0.524 (0.423, 0.65)
	$Net_W$	<b>1.002 (0.502, 1.502)</b>
	$Tide_W$	<b>-0.975 (-1.158, -0.792)</b>
	ReleaseDay	<b>0.334 (0.2, 0.467)</b>
	$Temp_{C\_Dev}$	<b>2.648 (1.69, 3.606)</b>
$q_{RW}$	Baseline	1.053 (0.85, 1.305)
	$Net_W$	<b>1.506 (1.071, 1.94)</b>
	$Tide_W$	<b>0.958 (0.758, 1.157)</b>
	ReleaseDay	<b>0.255 (0.144, 0.367)</b>
	$Temp_{C\_Dev}$	-0.443 (-1.51, 0.623)
$q_{WC}$	Baseline	0.144 (0.077, 0.27)
	$Net_W$	<b>-1.79 (-2.735, -0.846)</b>
	$Tide_W$	<b>-1.884 (-2.386, -1.382)</b>
	ReleaseDay	0.235 (-0.089, 0.56)
	$Temp_{C\_Dev}$	0.236 (-1.684, 2.156)

Transition Rate ( $q_{rs}$ )	Covariate	Slope Coefficient Estimate ( $\beta_{rs}$ )
$q_{WR}$	Baseline	1.781 (1.451, 2.186)
	Net <sub>W</sub>	<b>-0.861 (-1.307, -0.415)</b>
	Tidew	<b>-1.047 (-1.239, -0.855)</b>
	ReleaseDay	0.091 (-0.043, 0.226)
	Temp <sub>C_Dev</sub>	-0.042 (-0.971, 0.887)

Notes:

**Bold** values indicate covariates identified as important (i.e., their 95% confidence intervals did not overlap zero).

Slope coefficient estimates ( $\beta_{rs}$ ) are shown with 95% confidence intervals in parentheses.

$q_{rs}$ : transition rate from state  $r$  to state  $s$ , where (at WPA) possible states are CVP (C), West Canal (W), CCF radial gates (R), and CVP salvage (V)

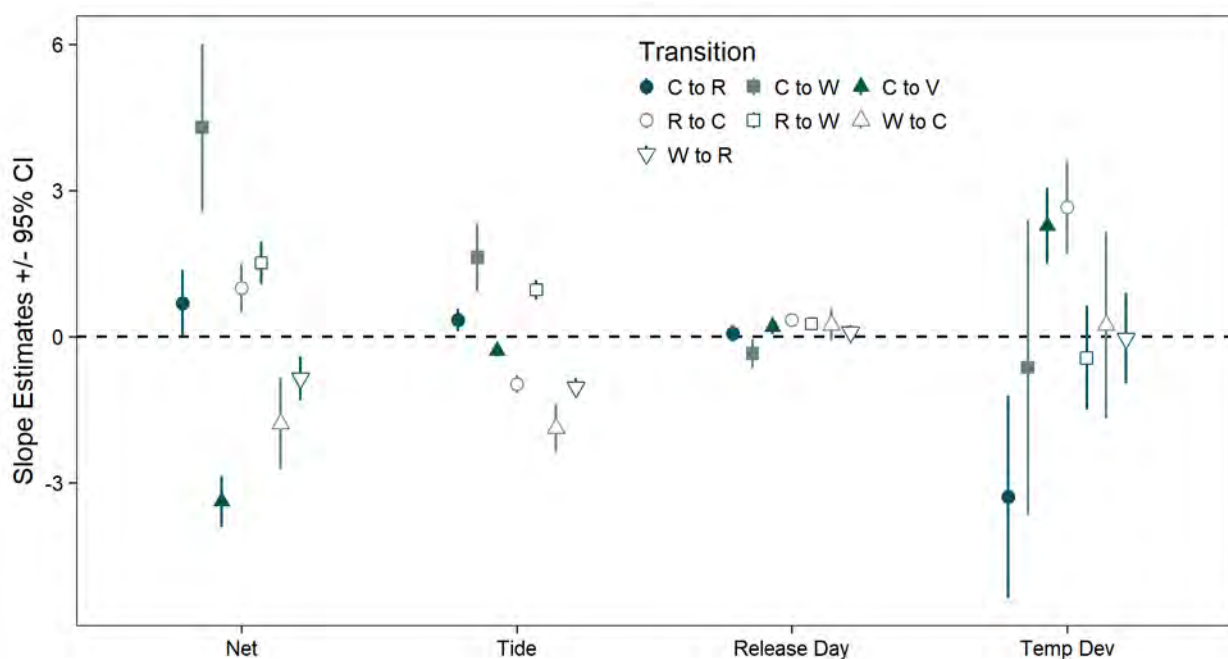
Net<sub>W</sub>: net flow in West Canal

ReleaseDay: ordinal fish release day

Temp<sub>C\_Dev</sub>: water temperature deviation at CVP

Tidew: tide flow in West Canal

**Figure 3-26**  
**Water Project Area Best Fit Model Covariate Slope Coefficient Estimates**



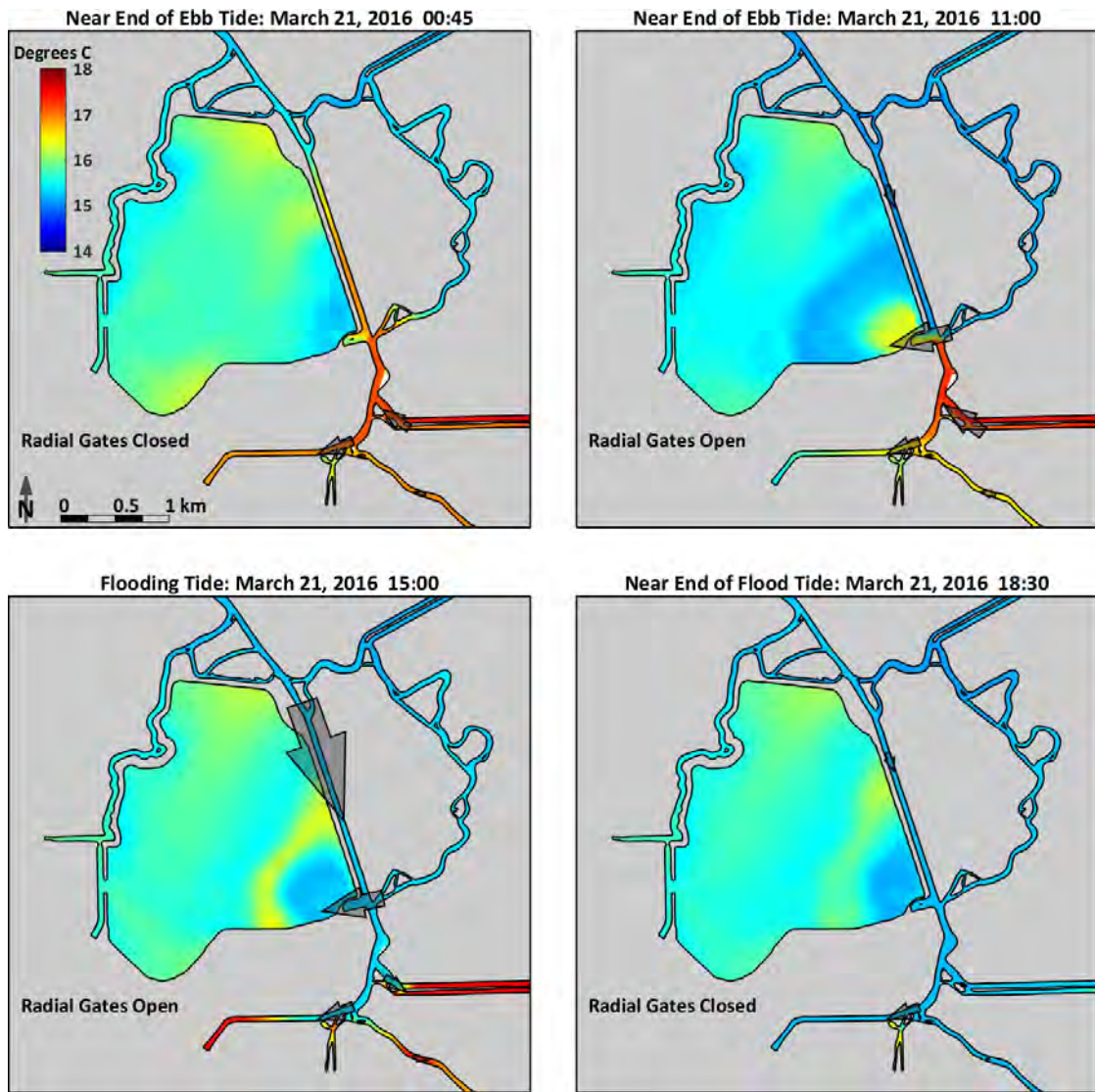
The best fit model showed that salvage rates ( $q_{cv}$ ) increased with increasing reverse Netw and Tidew flow, though Netw flow was a stronger predictor (Table 3-6). Increasing water temperature deviation at the entrance to CVP (Temp<sub>C\_Dev</sub>) was also a strong predictor of salvage, while later release day (ReleaseDay) was a smaller but positive predictor. In addition to expected daytime/nighttime

deviations in water temperature, increasing or decreasing water temperatures by 1°C to 2°C at CVP were sometimes driven by incoming water from the SJR (e.g., peaks in water temperature at night). An example of river water-driven temperature changes over time in the WPA is shown in Figure 3-27.

The rates of downstream transition from CVP to CCF radial gates and from CVP to West Canal ( $q_{CR}$  and  $q_{CW}$ ) increased with increasing downstream tidal flow in West Canal (i.e., on the ebb tide). Less reversed net flow also increased the rate of moving downstream from CVP to West Canal ( $q_{CW}$ ), while a later release day had the opposite effect. Increasing temperature deviations at CVP decreased the rate of downstream transition from CVP to CCF radial gates ( $q_{CR}$ ) and was the strongest predictor of this transition.

For fish at CCF radial gates, less reversed (i.e., slower moving) Netw increased the rate of moving both downstream ( $q_{RW}$ ) and upstream ( $q_{RC}$ ). It may seem counterintuitive that less reversed flow would correspond with upstream transitions; however, periods of lower Netw generally corresponded to longer periods when the CCF radial gates were closed, preventing fish from entering the forebay (Figure 3-28). Flood tides (increasing reverse Tidew flow) and increasing temperature deviation also increased the rate of upstream transition from CCF radial gates to CVP. Ebb tides (increasing downstream Tidew flow) increased the rate of downstream transitions from CCF radial gates to West Canal. There was also a small effect of later release day increasing the rate of transition away from CCF radial gates. When fish are in West Canal, upstream transition rates ( $q_{WC}$  and  $q_{WR}$ ) are increased by increasing reversed net and tidal flow.

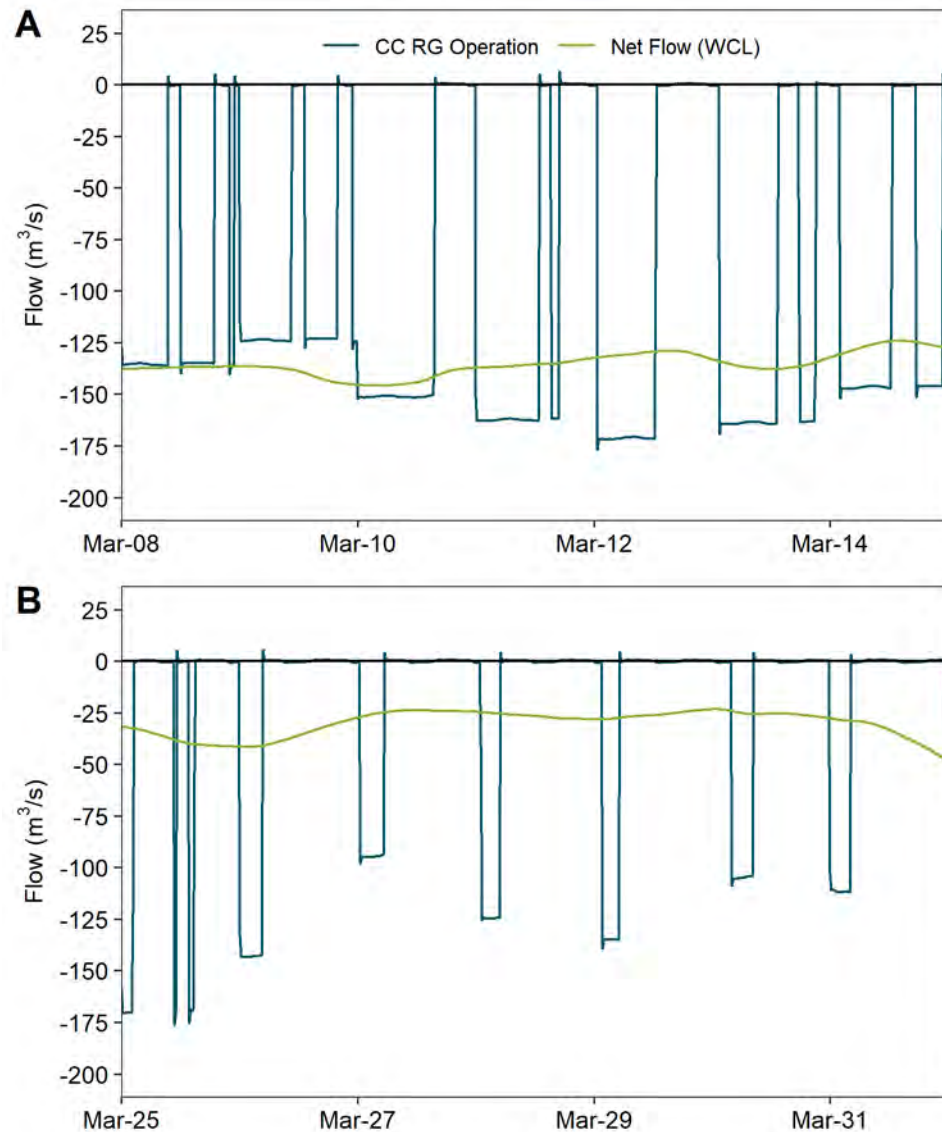
**Figure 3-27**  
**Predicted Depth-Averaged Water Temperature in the Water Project Area: March 21, 2016**



Note:

Arrows show the direction and relative magnitude of water flow through the channels.

**Figure 3-28**  
**Net Flow in West Canal and Corresponding Clifton Court Forebay Radial Gate Operation in March 2014**

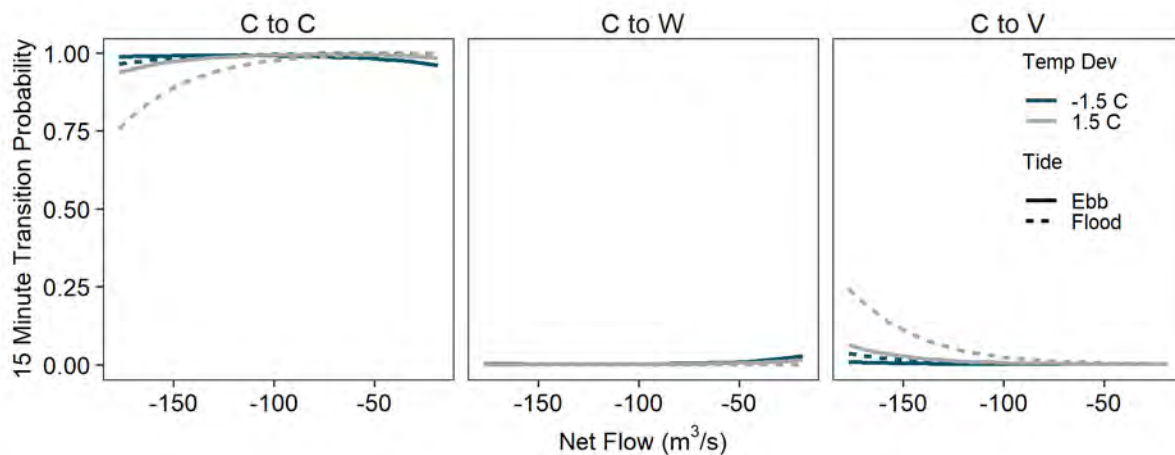


Notes: Panel A shows a period of higher reverse net flow in West Canal and longer periods when the CCF radial gates are open. Panel B shows a period with lower reverse net flow in West Canal and longer periods when the CCF forebay radial gates are closed (i.e., blue line equal to zero).

### 3.4.2 Fifteen-Minute Transitions

Fifteen-minute transitions are the probability that a fish detected at one state will be detected at another state, or at the same state, after one timestep of the model (15 minutes). Since study fish spent longer periods of time in the WPA, the probabilities of being in another state after 15 minutes were generally lower than at HOR. In particular, the baseline transition rates for fish moving away from CVP were low. Covariate effects considered relative to low baseline transition rates were also low. This means that for fish detected at CVP, the highest probability was that fish would again be detected at CVP 15 minutes later (Figure 3-29). This was true over a range of tide and net flows, though the probability of moving downstream to West Canal increased slightly on the ebb tide (high downstream tide flow), while the probability of being collected at Tracy Fish Facility and detected in the salvage tank increased slightly during flood tide if there was high reverse net flow. There was little change transition probability away from CVP because of increases or decreases in temperature.

**Figure 3-29**  
**Tide Flow Effect on 15-Minute Transition Probabilities from CVP (State C)**



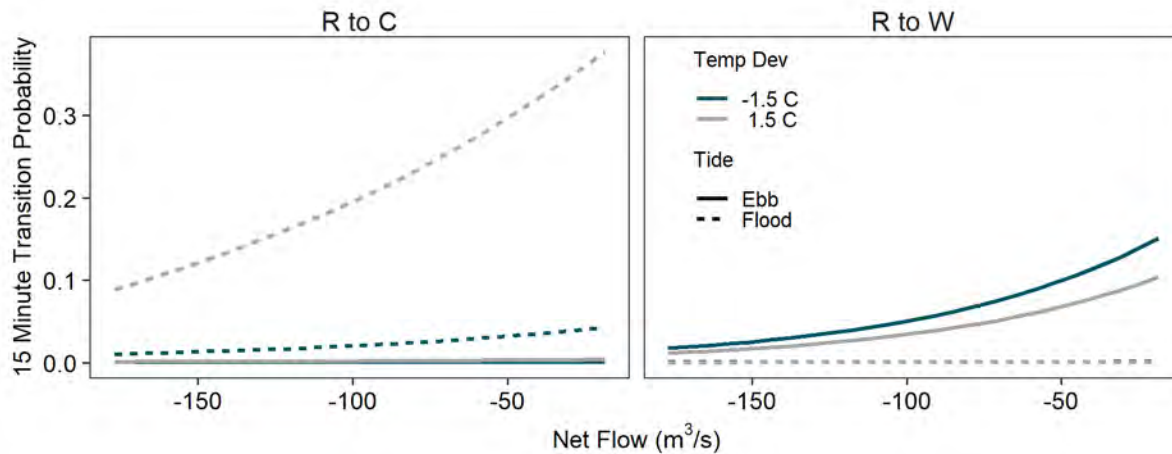
Note:

Transition probabilities are for fish released in mid-March and from CVP (state C) and returning to CVP or transitioning to West Canal (state W) or the CVP salvage tank (V).

For fish detected at the radial gates, the 15-minute probability of moving either upstream or downstream increased with lower net flow (Figure 3-30). As discussed in Section 3.4.1, lower net flow in West Canal corresponded to longer periods with the radial gates closed (Figure 3-28). The probability that fish would transition upstream from the radial gates was higher during the flood tide, while the probability that fish would transition downstream was higher during the ebb tide (Figure 3-31). Transition probability was also higher if water temperature warmed above the daily running average for both transitions away from the radial gates.

**Figure 3-30**

**Net Flow Effect on 15-Minute Transition Probabilities from CCF Radial Gates (State R)**

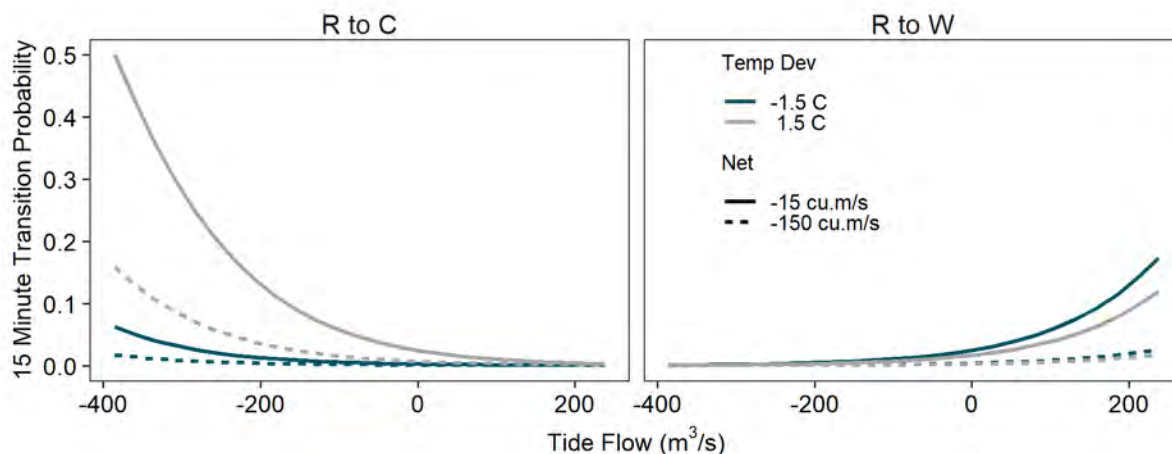


Note:

Transitions are from radial gates to CVP (state R to C) and radial gates to West Canal (state R to W) for fish released in mid-March.

**Figure 3-31**

**Tide Flow Effect on 15-Minute Transition Probabilities from CCF Radial Gate (State R)**



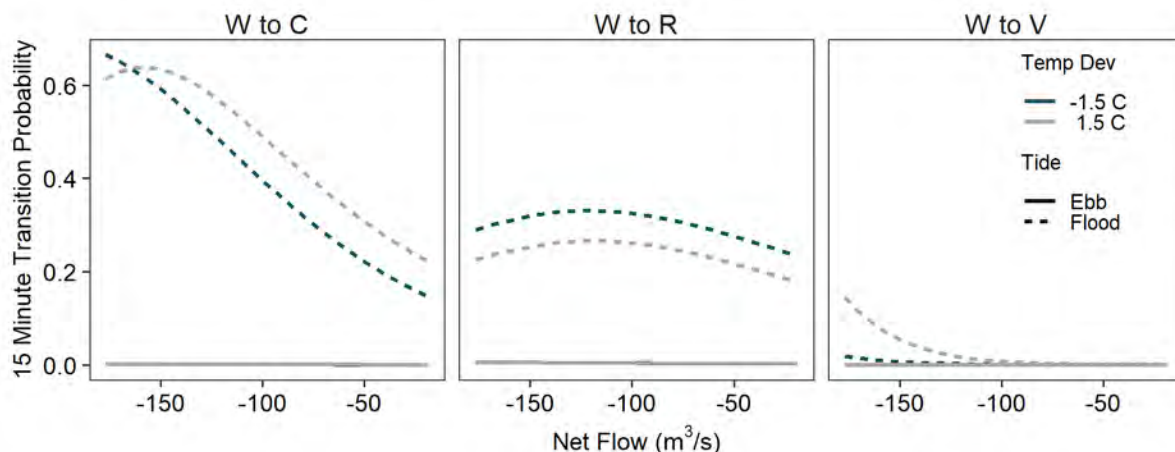
Note:

Transitions are from radial gates to CVP (state R to C) and radial gates to West Canal (state R to W) for fish released in mid-March.

The highest 15-minute transition probabilities in the WPA were fish moving from downstream in West Canal back upstream to CCF radial gates or to CVP (Figure 3-32 and Figure 3-33). The probability of transitioning from downstream to upstream increased with decreasing (more reversed)

net flow, but only if there was a flood tide. The probability of transitioning from downstream to the radial gates increased with decreasing (more reversed) net flow during flood tide but only up to approximately  $-120 \text{ m}^3/\text{s}$  (Figure 3-32, middle panel). At very reversed net flows, the chance of transitioning from West Canal to CVP salvage tanks increases slightly (Figure 3-32, right panel). Similar trends can be seen in response to changing tidal flows, with the highest upstream transition probabilities depending on amount of reversed net flow. When tide flow is reversed, and net flow is also highly reversed, the transition probability response for moving from downstream to radial gates is not monotonic but, instead, peaks at approximately  $-300 \text{ m}^3/\text{s}$ , after which the probability of transitioning to salvage also increases slightly (Figure 3-33, middle and right panels).

**Figure 3-32**  
**Net Flow Effect on 15-Minute Transition Probabilities from West Canal (State W)**

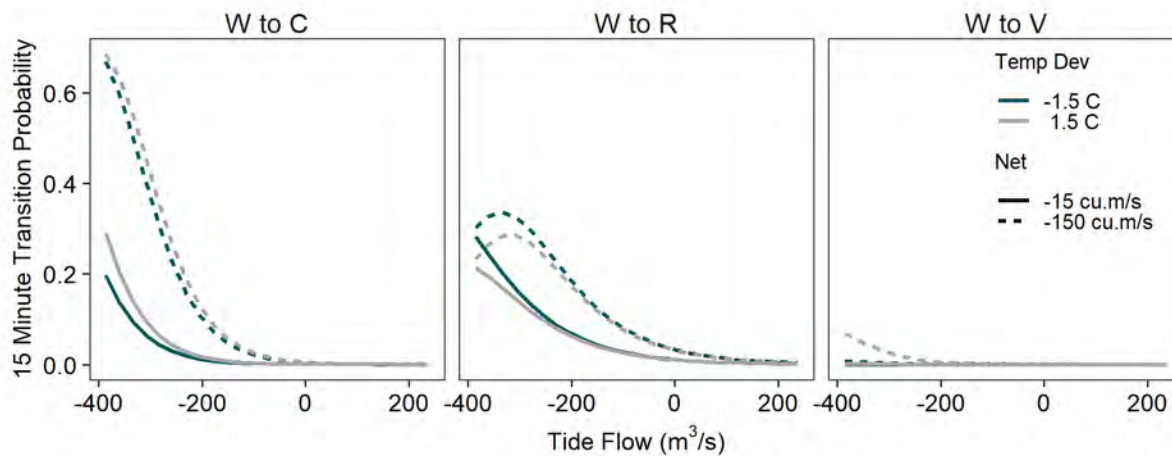


Note:

Transitions are from West Canal to CVP (state W to C), West Canal to radial gates (state W to R), and West Canal to salvage (state W to V) for fish released in mid-March.

**Figure 3-33**

**Tide Flow Effect on 15-Minute Transition Probabilities from West Canal (State W)**

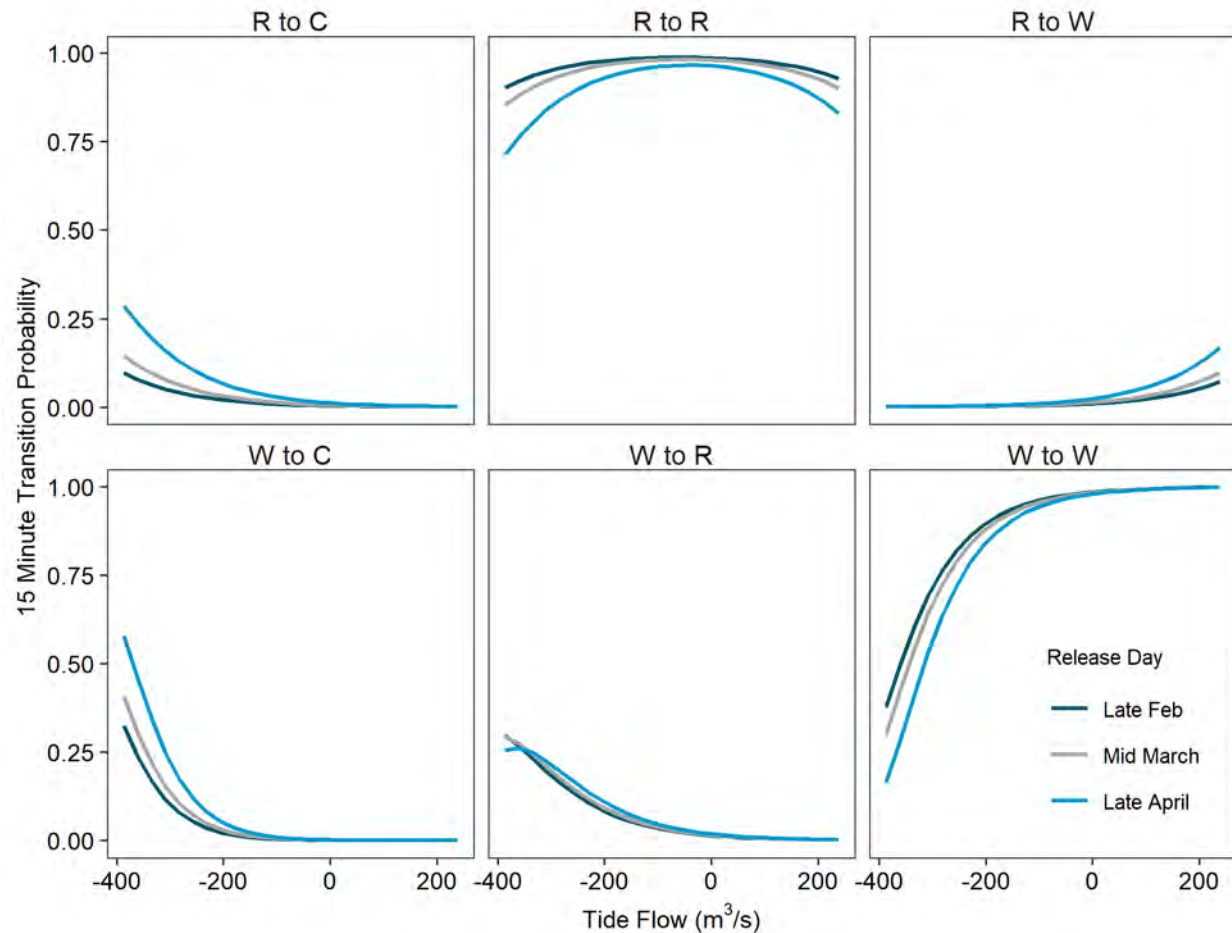


Note:

Transitions are from West Canal to CVP (state W to C), West Canal to radial gates (state W to R), and West Canal to salvage (state W to V) for fish released in mid-March.

In the WPA, a later release day increased the probability that fish would transition between states, rather than being detected at the same state over a single 15-minute timestep (Figure 3-34). Over a range of late February to late April release dates, the probability that fish would transition upstream from West Canal or CCF radial gates to CVP during the flood tide increased, while the probability that fish would transition downstream from CCF radial gates to West Canal during ebb tides also increased slightly.

**Figure 3-34**  
**Release Day Effect on 15-Minute Transition Probabilities in the WPA**



### 3.4.3 Example Period Transition Probabilities

Transition probabilities for WPA represent the probability that a fish in one state will be in another state or the same state over an example 5-day period, given the hydrodynamic and physical conditions that actually occurred. For fish detected upstream at CVP, the probability of transitioning to downstream in West Canal or to the radial gate entrance to CCF remained low over time but fluctuated with tide flow, net flow, and temperature conditions (Figure 3-35). The probability of being detected at CVP decreased slowly with time, corresponding to an increase in the probability of being detected in the fish facility salvage tanks.

Most fish present from April 17 to April 21, 2015 (the period shown in Figures 3-35, 3-36, 3-37, and 3-38) were released on days 84 to 87. Net flow during this period ranged between -37 and -28  $m^3/s$ , tide flow was between -177 and 170  $m^3/s$ , and temperature deviations were -1°C to 1.5°C.

(Figure 3-38). At this location, the bimodal peaks in flow rate shown in Figure 3-38 are likely a result of operations of the radial gates leading into CCF.

After being detected at CCF radial gates, juvenile steelhead had the highest probability of moving upstream over time (Figure 3-36). After 1.5 days, the probability of being detected at CVP was above 60% but then began to decline as the probability of being detected in the salvage tank increased. The probability of being detected downstream in West Canal peaked just below 40% after approximately 0.5 day but then declined over time (Figure 3-36). There were similar patterns in transition probability when fish were first detected downstream in West Canal (Figure 3-37). The probability of being detected at CCF radial gates peaked at 43% after 6 hours and then declined, while the probability of being detected upstream at CVP increased to above 60% after approximately 40 hours but then declined as the probability of detection in the salvage tank increased.

**Figure 3-35**  
**Example Transition Probabilities from CVP (State C): April 17 to April 23, 2015**

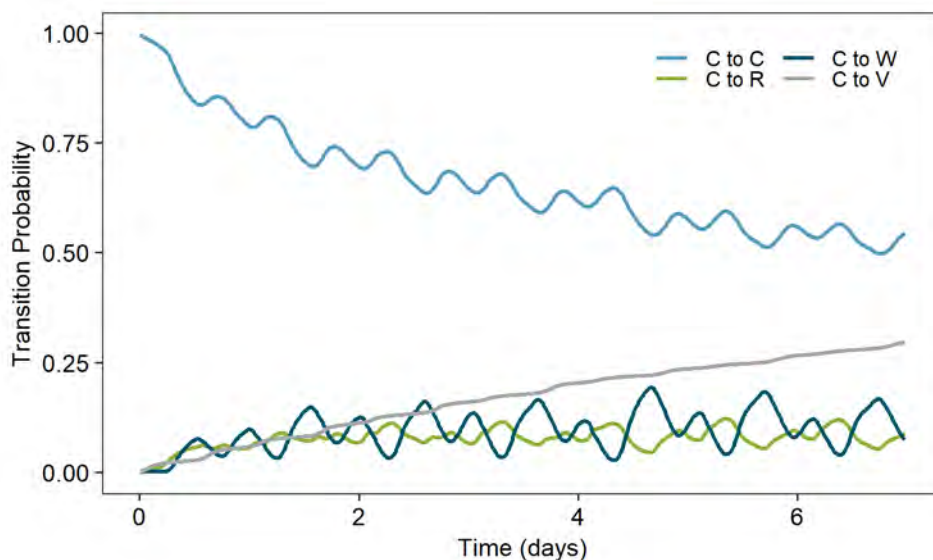


**Figure 3-36**

**Example Transition Probabilities from CCF Radial Gates (State R): April 17 to April 23, 2015**

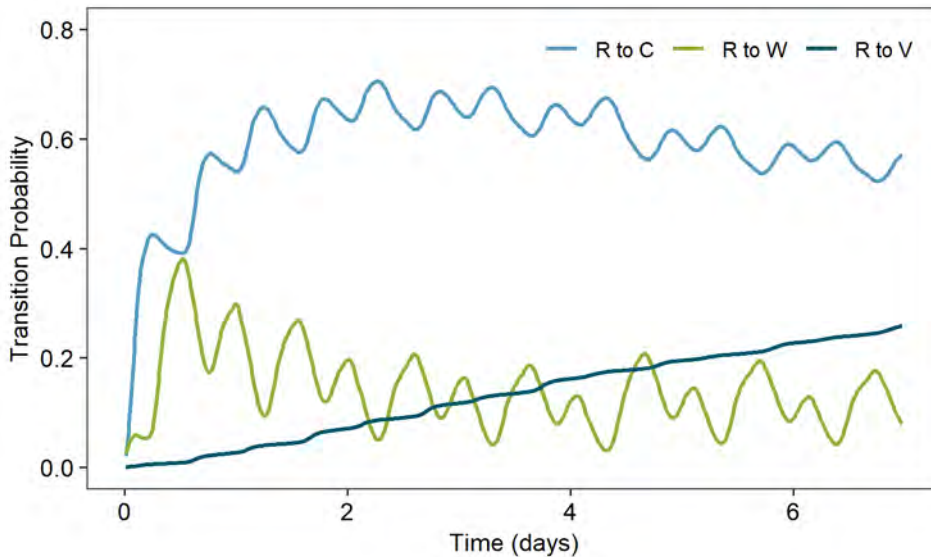


**Figure 3-37**

**Example Transition Probabilities from Downstream in West Canal (State D): April 17 to April 23, 2015**

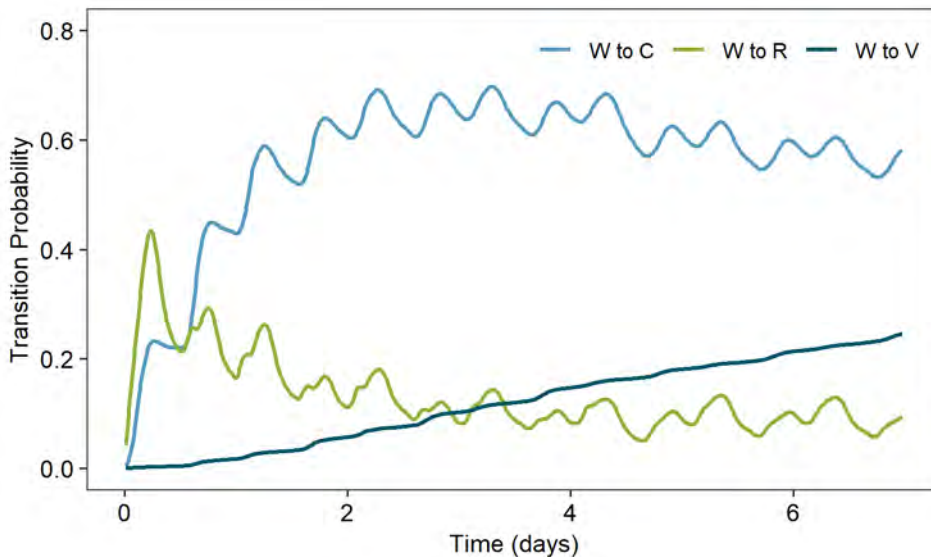
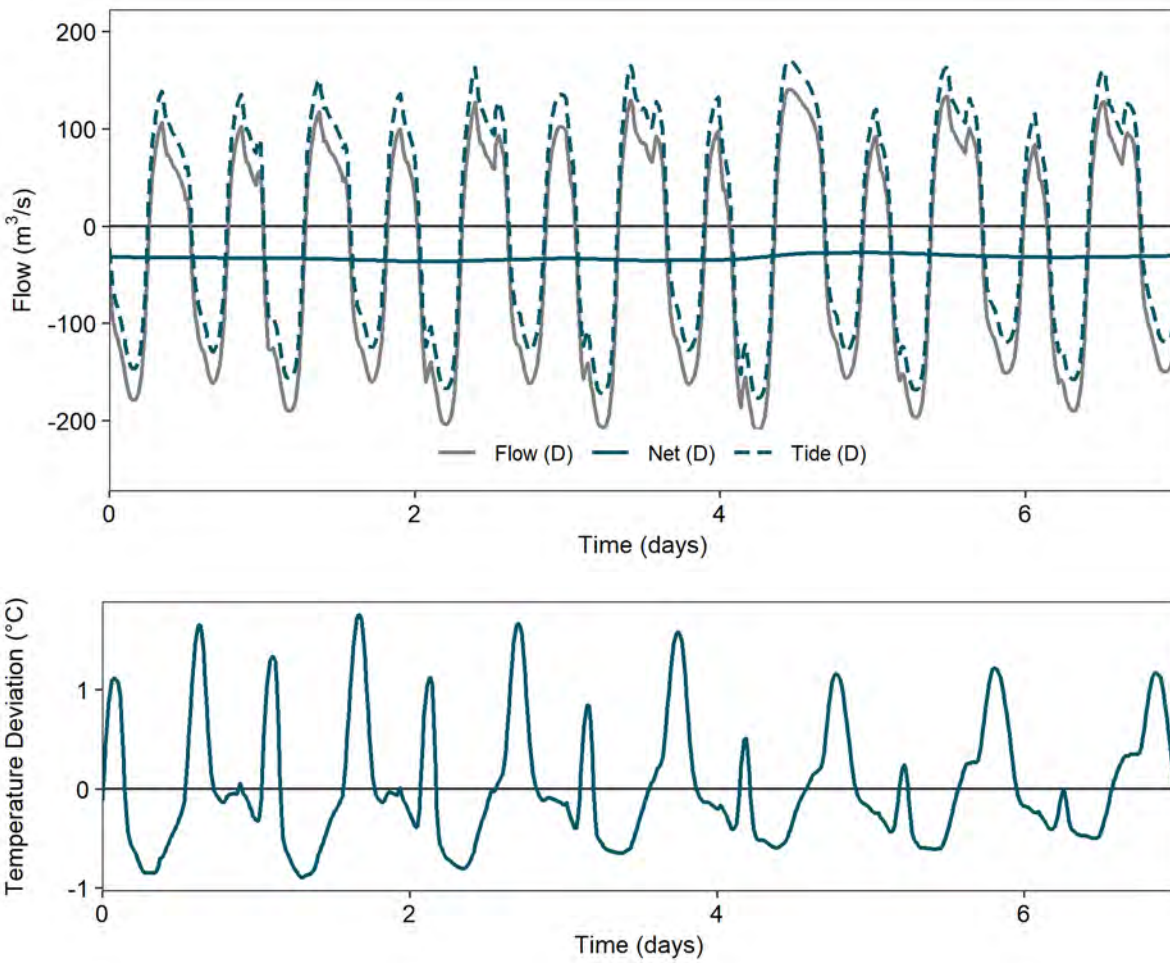


**Figure 3-38**  
**Flow and Temperature Conditions: April 17 to April 23, 2015**



Example period transition probabilities in the WPA were also found to vary in response to seasonal and annual hydrodynamic and environmental conditions (Figures 3-39, 3-40, and 3-41). The period from March 20 to March 26, 2016, was characterized by high reverse net flow ranging from -117 m<sup>3</sup>/s to -68 m<sup>3</sup>/s (Figure 3-42). Most fish detected during this period were released on days 76 to 79. Water temperatures varied by -1°C to 1.6°C.

The high reverse net flow meant that the probability of transitioning to the CVP salvage tank, after being at CVP, rose to more than 80% after approximately 2.5 days (Figure 3-39). The probability of fish later being detected downstream during this period was low (Figure 3-39). The probability of fish transitioning to the salvage tank after being at CCF radial gates or downstream in West Canal also increased to more than 70% after 4 days (Figures 3-40 and 3-41). The probability of fish transitioning

to West Canal from CCF radial gates peaked at 58% after approximately 4.6 hours but then declined as the probability of moving farther upstream to CVP and entering the salvage tank increased.

**Figure 3-39**  
**Example Period Transition Probabilities from Upstream at CVP (State C): March 20 to March 26, 2016**

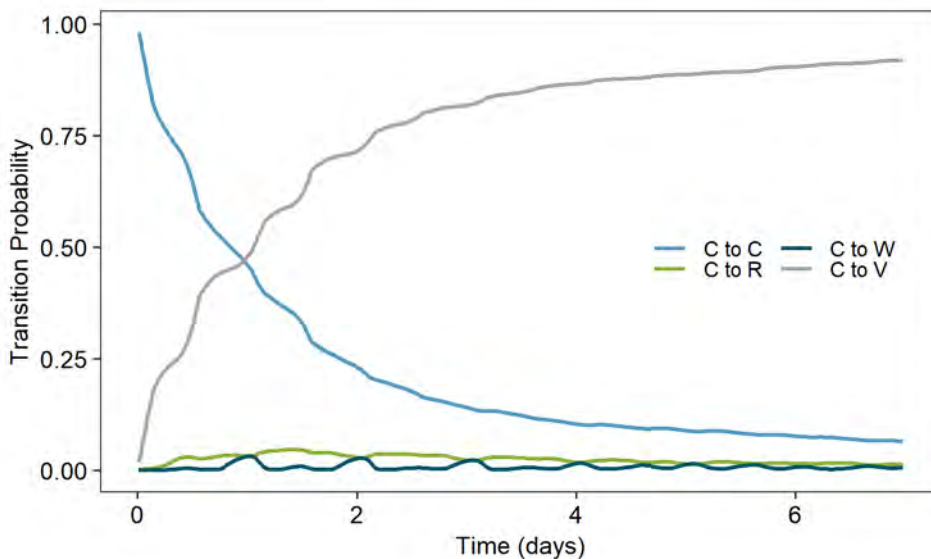


**Figure 3-40**  
**Example Period Transition Probabilities from CCF Radial Gate (State R): March 20 to March 26, 2016**

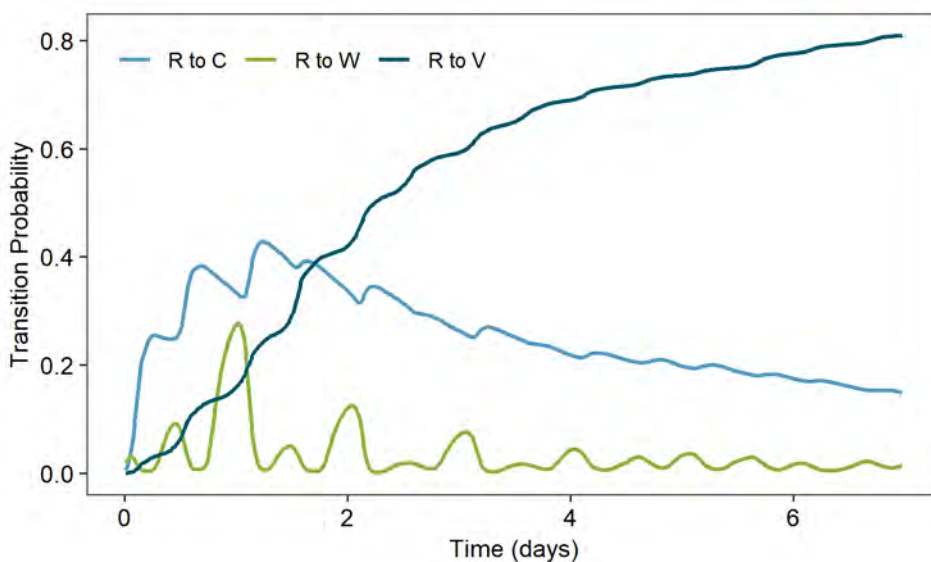


**Figure 3-41**

**Example Period Transition Probabilities from Downstream in West Canal (State W):  
March 20 to March 26, 2016**

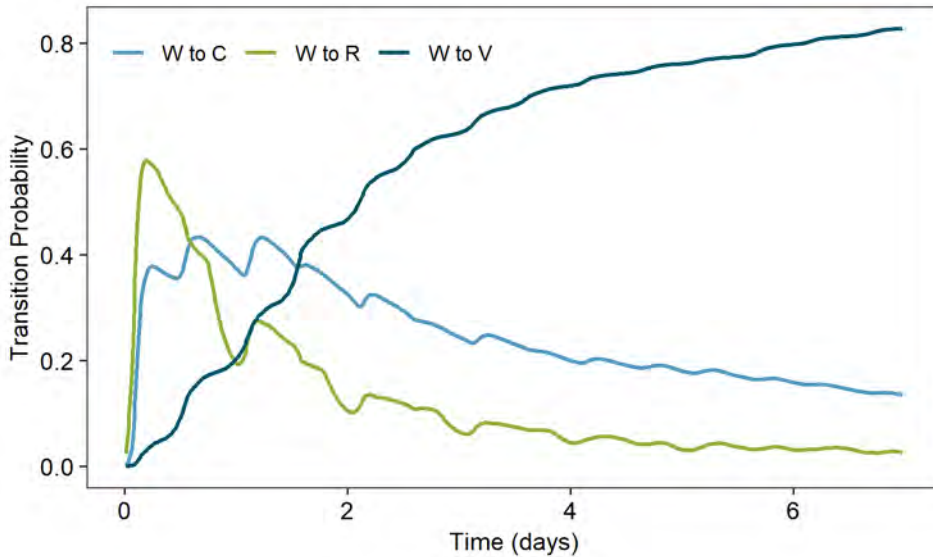
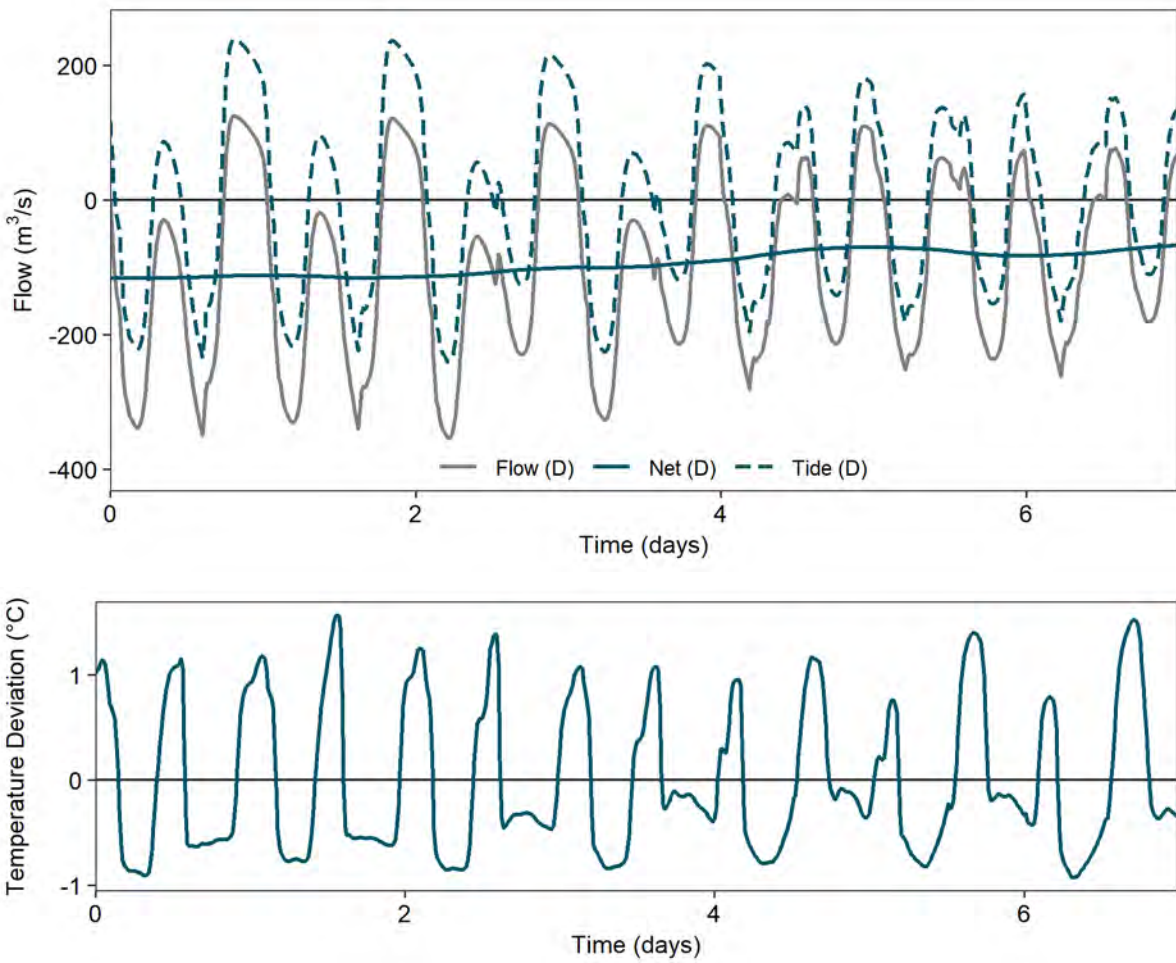


**Figure 3-42**  
**Flow and Temperature Conditions: March 20 to March 26, 2016**



## 4 Discussion

### 4.1 Steelhead Behavioral Responses

A central hypothesis for salmonid behavior in the Delta identified by the SST (SST 2017a) was that fish behavior is driven by flow. This was the main hypothesis evaluated in our study, and there was substantial support for the hypothesis at all three locations evaluated. This is based on both the net and tidal components of flow being in the best fit models for all three locations. In one sense this is not surprising given all that is known about juvenile salmonid smolt migrations from rearing habitats in freshwater to marine environments, and how outmigration timing evolved to take advantage of high flow conditions to increase smolt survival (Michel et al. 2015). However, the strength of the relationship between transition and flow was striking given how different the three locations evaluated in this study are hydrodynamically and the different behaviors observed at each location.

For example, fish spent a much longer time in the WPA (90% spent  $\leq 6.5$  days) compared to the mainstem junctions (90% of fish spent  $\leq 1.6$  days HOR and  $\leq 1.3$  days TC). At HOR, there were unique patterns of transition, indicating that some fish were actively migrating downstream while other fish were moving downstream more slowly, as well as evidence of interaction with the barrier. At the more tidally influenced TC junction, fish were more likely to transition downstream during the day.

Despite these differences, net flow was always an important predictor for upstream to downstream transitions on the mainstem, while reverse net flow in the WPA increased the chance of fish moving toward the state and federal water exports and ending up in CVP salvage. To the extent that net flow and SJR inflow are related, this finding is similar to that of Buchanan et al. (2021). They reported that “the relationship between San Joaquin River inflow and survival was particularly strong and, together with year, barrier status, and fork length, accounted for all the variation in survival that was associated with other environmental and operational covariates.”

The results also identify that it is common for juvenile steelhead to make multiple transitions through the study areas (see example fish detection histories in Appendix D.2). This was especially true of the WPA. As shown in Figure 3-25, the number of fish transitions from the CCF radial gates were similar in both upstream and downstream directions (18% to CVP and 20% to West Canal, respectively). Another 28% of total transitions at WPA were from West Canal to upstream hydrophone locations (CCR radial gates and CVP). The cause of this “milling” behavior deserves more investigation, potentially with a fine-scale telemetry study (e.g., with methods similar to Holleman et al. 2022), but our modeling results indicate that it could be related to the mixing of net flow, tide flow, and temperature signals in this area.

At TC, “backtracking” transitions from downstream to upstream were relatively common (15% of total transitions; Figure 3-23) and were strongly related to flood tide flow (Figure 3-21). Despite

higher downstream net flow at HOR, backtracking from downstream to upstream was common when the barrier was installed (22% of total transitions). When the barrier was not installed, backtracking transitions dropped by about 45%. This change in transition pattern could indicate that the presence or absence of the barrier not only influences the final route taken by fish but also their behavior while in the junction.

Juvenile steelhead behavior in each area, as described by the example period transition probabilities, depended on the specific hydrodynamic conditions that occurred when fish were present, as well as fish-specific and physical conditions, such as whether the fish was classified as actively migrating and whether the barrier was installed. For example, at the WPA, the chance of transitioning to the CVP salvage tank over a 6-day period was strongly related to higher reverse net flow (CVP to salvage transition in Figure 3-35 compared to Figure 3-39). Behavior at HOR was influenced by migrator status. Fish classified as non-migrators were slower to make all transitions, and when the barrier was not installed were about equally likely to transition downstream on the mainstem or Old River over a 3-day period (Figure 3-16). Fish classified as active migrators were much more likely to enter Old River when the barrier was not installed.

As discussed further in Section 4.2.3, Holleman et al. (2022) reported that lateral swimming behavior was common for the spring-run Chinook salmon at HOR when a partial barrier was installed, which they attributed to a searching behavior. The backtracking, milling, and non-migrator status behavior need further investigation and research on ways to reduce the behavior since it increases travel time and exposure to predation and likely has an effect on overall survival.

#### *4.1.1 Head of Old River*

The barrier had a strong influence on all transitions and changed the overall distribution of transitions at the junction. For instance, when the barrier was installed, 74% of transitions were upstream to downstream on the mainstem, and only 3% of transitions were to the distributary via the barrier culverts (Figure 3-7). When the barrier was not installed, only 32% of transitions were upstream to downstream on the mainstem, and 54% of transitions were from upstream into the Old River distributary. Additionally, when the barrier was installed, 22% of transitions were fish moving downstream to upstream on the mainstem. With the barrier not installed, smolts were more likely to "backtrack" from downstream into the distributary (10%) than downstream to upstream (2%).

Over short periods (15 minutes) and when the barrier was not installed, the probability of smolts transitioning upstream to downstream on the mainstem is estimated to increase from about 3% when mainstem net flow was near zero to 40% as net flow exceeded 300 m<sup>3</sup>/s. The probability of transitioning into Old River was relatively constant over that range, increasing only from about 10% when net flow was near zero to 14% to 18% (depending on time of day) when net flow exceeded 300 m<sup>3</sup>/s. However, these high flows only occurred in 2011. From 2012 to 2016, maximum mainstem

net flows at HOR junction ranged between 25 and 92 m<sup>3</sup>/s and the 15-minute probability of transitioning into the distributary was higher (10% to 13%) than staying in the mainstem (3% to 7%) over this lower range of flows when the barrier was not installed.

Given median net flows of approximately 10 m<sup>3</sup>/s, ebb tide flows of 40 to 50 m<sup>3</sup>/s in low flow years increased the 15-minute probability of transitioning upstream to downstream on the mainstem for active migrators to 20% if the barrier was not installed or to over 50% if the barrier was installed. Tide flow in Old River only interacted with fish when the barrier was not installed, but similarly could triple the chance of transitioning into the distributary from about 10% at slack tide to 30% at maximum ebb tide for active migrators. Flood tides similarly increased the 15-minute probability of “backtracking” transitions. However, when the barrier was installed, these transitions were downstream to upstream on the mainstem, while when the barrier was not installed, more transitions were from downstream to distributary.

The variation in 15-minute transition probabilities ultimately affects juvenile steelhead transition probabilities over time (e.g., 3-day period shown in Figures 3-14 and 3-16) depending on the specific conditions that occurred when smolts were present at the junction. During one period when the barrier was installed (May 2012), actively migrating fish had an 80% chance of transitioning downstream after only 3 hours, although this probability varied in response to changing tidal conditions (Figure 3-14). Non-migrators also had a high chance of moving downstream over time, but that probability did not exceed 80% until about 1.7 days after entering the HOR junction (Figure 3-14). Non-migrators also had a higher probability of making upstream transitions over time when the barrier was installed.

The physical presence of the barrier has been shown to be a primary factor that increases survival on the SJR route because of the way it diverts both fish and flow into the SJR (Buchanan et al. 2021). Our analysis shows that the barrier being installed creates a higher chance that actively migrating fish will backtrack upstream at HOR junction. There is also more variability in the percentage of fish classified as active migrators when the barrier is installed (24% to 97%) compared to when it is not installed (73% to 91%), potentially indicating that the barrier is affecting fish behavior.

There were also differences in behavior when the barrier was not installed. After about 1 day, actively migrating juvenile steelhead had a high probability of transitioning into Old River distributary (>90% during ebb tides) or of “backtracking” from downstream on the mainstem into Old River (>80% during ebb tides). The chance of making other transitions over time was low. In contrast, non-migrators had a much more even distribution of transitions over time: 34% chance of transitioning from upstream to downstream on the mainstem, 50% chance of transitioning from upstream into the distributary, and 50% chance of “backtracking” from downstream into the distributary after 3 days.

In general, fish classified as non-migrators had lower transition rates for all transitions, as well as different patterns of transition (e.g., higher probability of transitioning downstream on the mainstem). Though we refer to juvenile steelhead that were not moving quickly enough to be consistent with documented travel times for HOR to Chipps Island (1.4 to 34.9 days; Buchanan et al. 2021) as “non-migrators,” there is no way to know if fish are showing signs of extended rearing before eventual outmigration or residualization. Juvenile steelhead are known to make more upstream transitions and have longer travel times between telemetry detections compared to Chinook salmon in some parts of the Delta (ESA and AECOM 2018).

A recent detailed study of juvenile spring-run Chinook salmon at HOR found a wide variety of behaviors including foraging, holding, lateral swimming that varied with time of day, and swimming both with and against the direction of water flow (Hoellmann et al. 2022). Juvenile steelhead likely show a similar range of behaviors. For example, our finding of an interactive effect between Barrier and time of day (Day), where fish were more likely to make upstream to downstream transitions at night when the barrier was installed and more likely to make either upstream to distributary or downstream to distributary transitions during the day when the barrier was not installed (Figure 3-9 and 3-11), could indicate altered behavioral patterns such as foraging or predator avoidance because of the barrier. Transitions during the day are similar to findings that juvenile steelhead were more active during the day at TC where there is no barrier (Figure 3-20, 3-21, and 3-22). Because of this range of behaviors, McEwan (2001) recommended an integrated management strategy that treats all *O. mykiss* as a single population because all life histories are important for persistence of anadromous forms, as has been found in other California steelhead populations (Hodge et al. 2016).

#### 4.1.2 Turner Cut

At TC, the most common transition was upstream to downstream on the mainstem (64%; Figure 3-18). There were much fewer transitions from mainstem into TC distributary (18%), and even fewer transitions of fish leaving TC to either upstream or downstream on the mainstem (3%). One caveat is that this distribution of transitions only represents 3 of the 6 years of steelhead acoustic telemetry data (2013, 2015, and 2016). This is because the upstream array was not installed in other years. Over the 6 years of the juvenile steelhead acoustic telemetry study, Buchanan et al. (2021) found that 489 fish (25%) were detected entering TC, while 1,451 fish (75%) stayed in the SJR mainstem route. While transitions do not correspond to individual fish (i.e., one fish may make multiple transitions; Appendix D, Figure D.2-2), the representation of the overall behavior pattern is consistent between the two analyses.

Our finding of six times more transitions into TC than out of TC, coupled with the finding of Buchanan et al. (2021) of much lower survival from the TC junction to Chipps Island via interior Delta routes, supports the concerns about lower survival. Juvenile salmonids entering the lake-like habitats of the Inner Delta via TC are potentially exposed to high predation by non-native fishes (Nobriga and

Freyer 2007, Conrad et al. 2016). However, our findings also support the conclusion by Cavallo et al. (2015) that hydrodynamics at TC were not always conducive to fish entering the distributary because there were periods each day (ebb tides) when flows were not entering the distributary.

The rate of fish transitioning from upstream to downstream increased with increasing downstream net flow, tide flow, and distributary tide flow. Mainstem ebb tide flow was the largest in magnitude (up to 300 m<sup>3</sup>/s) and caused the greatest increase in 15-minute upstream to downstream transition probabilities. Distributary flood tide flow caused the greatest increase in the 15-minute transition probability from upstream into TC distributary, while mainstem flood tide flow caused the greatest increase in downstream to upstream 15-minute transition probability.

Both upstream to downstream and upstream to distributary transition rates were higher during the day. This is consistent with findings for Sacramento River released juvenile steelhead which, in contrast to juvenile Chinook salmon, showed a strong preference for daytime travel in the Delta (Chapman et al. 2013).

Most fish (90%) spent less than 1.3 days at TC junction, and 77% of fish that had previously been designated as actively migrating at HOR continued to move through TC junction at approximately the same rate. During the example period, the probability of fish transitioning from upstream to downstream increased to 75% by approximately 18 hours, but afterwards varied by nearly 40% with daily tide flow (Figure 3-23). During periods of high reverse tide flow, the probability of upstream or downstream transition on the mainstem was approximately equal for short periods. This could indicate more time spent in passive behaviors (i.e., moving exactly with the speed of the surrounding water, rather than actively swimming) as fish enter the more tidally dominated areas of the Delta at TC, or that lower net flow makes these behaviors more noticeable.

Buchanan et al. (2021) reported that influences on survival of steelhead varied in upstream versus downstream reaches. Survival in upstream reaches was associated with SJR inflow, while survival in downstream reaches was associated with migration route. Diel patterns of juvenile steelhead behavior have also been found to change with downstream migration, with fewer nighttime detections farther downstream (Chapman et al. 2013). Therefore, it is reasonable that juvenile steelhead could show different patterns of behavior at TC relative to HOR, related to both hydrodynamic and biological conditions.

The analysis using both predictions from the hydrodynamic model and data-based observed water flows demonstrated that there is a relationship between increasing exports and increasing net flow down TC (Sections 2.3.4 and 3.1.2). Previous studies have not documented this relationship of increasing exports corresponding to increasing net flow through TC (e.g., Cavallo et al. 2015, SST 2017a). However, Cavallo et al. (2015) evaluated the proportion of Delta Simulation Model 2 (DSM2)-predicted flow down the SJR that entered TC as exports were increased using steady inflow

and export conditions over 24 hours, while this study evaluated the magnitude of the flow through TC and unsteady conditions over many months.

The UnTRIM Bay-Delta model-predicted net flows were used to attempt an analysis similar to Cavallo et al. (2015) and that evaluated the proportion of flow down TC. However, the analysis was problematic because the proportion became infinite as predicted net flows upstream of TC neared zero. SST (2017a) found little effect of export levels on DSM2-predicted water velocity at TC over a tidal cycle. However, TC is strongly tidal and the magnitudes of net flows through TC shown in Figure 3-24 are only approximately 5% to 30% of the range in water flow magnitude over a tidal cycle (approximately 150 m<sup>3</sup>/s). Thus, it is not unexpected that although changes in exports more strongly affect net flows, these changes in exports have a relatively small effect on instantaneous flow and velocity at TC relative to tidally driven variations.

Additional work could be conducted to better understand similarities and differences between the findings from Cavallo et al. (2015) and the net flow through TC versus exports relationship described in this report. Additional model-based and data-based analyses could be conducted to further understand the relationship and any factors resulting in a stronger or weaker relationship between exports and net flow through TC. For example, evaluating a longer time period in 2011 in combination with evaluating any gate/barrier operations and other tributary inflows could improve the understanding of this relationship. Evaluating complete water years instead of approximately 4 months a year during spring and summer could also improve the understanding of the relationship between net flow through TC and exports.

#### *4.1.3 Water Project Area*

In the WPA, the results indicated long residence times combined with non-directional transition. Tagged steelhead displayed longer residence times compared to the mainstem junctions at HOR and TC. Ninety percent of fish spent 6.5 days or less, compared to 1.6 days or less at HOR and 1.3 days or less at TC. This was consistent with a previous finding that juvenile steelhead had much slower migration rates and longer travel times between detection sites in the Inner Delta, compared to juvenile Chinook salmon (ESA and AECOM 2018).

There was also a high number of fish detection events at CVP without intervening detections at other locations in the area. This could be because there were alternate routes in the WPA that lacked hydrophone coverage such that fish could avoid detection at CCF radial gates and West Canal. Fish could also swim back upstream on Old River where there are islands, docks, and other structures that may provide shade or refuge from predators. Another possibility is that some fish were eaten by predators that then "lurked" near CVP. Though we employed a predator filter, the filter is limited to using residence time to distinguish smolt-like behavior if fish do not transition between hydrophone

arrays. A previous analysis of acoustically tagged juvenile steelhead found a predator filter to be unreliable in the Inner Delta (ESA and AECOM 2018).

Also, at the WPA there was no single most common transition between locations, in contrast with state transitions observed at HOR and TC. Eighteen to 20% of transitions were from the CCF radial gates to CVP or to West Canal, from West Canal to CCF radial gates, or from CVP to the CVP salvage tank. An additional 6% to 9% of transitions were from CVP to CCF radial gates or West Canal, or from West Canal to CVP. The more even number of transitions allowed covariate effects to be examined for all transitions but also indicated a lack of directional transition.

Of the total number of fish detected in the WPA, 30.7% ended up in the CVP salvage tank. The long residence times in the area and a lack of directional transition may have contributed to this entrainment rate. Under high reverse net flow, the probability of transitioning to the CVP salvage tank, after being detected at CVP, rose to over 80% after about 2.5 days. Given the changing tidal flow, net flow, and temperature conditions in this area, the probability of transitioning to the CVP salvage tank after being at CCF radial gates or in West Canal increased to over 70% after about 4 days in the WPA.

Fish detected at CVP had a greater than 90% probability of being detected there 15 minutes later, and this translated to low probability of transitioning to CCF radial gates or West Canal. This pattern was the case over a range of tide and net flows, though high temperature deviations caused the probability of being detected again at CVP to drop to 75%, with a corresponding increase in transitions to salvage (Figure 3-29). The 15-minute probability of moving downstream to West Canal increased slightly on the ebb tide (high downstream tide flow), while the 15-minute probability of being collected at the CVP salvage tank increased slightly during flood tide if reverse net flow was high at this time. Over the longer term, when net flows were low, the probability of being at CVP slowly declined as fish were salvaged at CVP or left the WPA.

Net flow was upstream (reversed) for the entire study period. We found that fish were more likely to move away from the entrance to CCF when the magnitude of net flow in West Canal is low (Figure 3-30 and 3-31). This corresponded to longer periods when the radial gates were closed (Figure 3-28). This may indicate that when fish are unable to enter CCF, they leave the entrance inlet more rapidly (i.e., increased transition rate). Additionally, the 15-minute probability that fish would transition upstream from the radial gates was higher during the flood tide, while the probability that a fish would transition downstream was higher during the ebb tide (Figure 3-31). Overall, the highest 15-minute transition probabilities in the WPA were fish moving from West Canal back upstream to CCF radial gates or to CVP, which increased during flood tides.

Two other effects, release day and water temperature deviation, were found to be influential in the analysis of WPA. Throughout the study seasons, daily water temperature at CVP showed changes

typical of slightly cooler water at night and warmer water during the day. During some periods, which varied by year, water temperature changes at CVP indicated warmer or cooler incoming water from the SJR. These water temperature changes were sometimes as much as 3°C within 12 hours, creating a quickly changing habitat for fish. A temperature deviation of +1.5°C during a flood tide increased the 15-minute probability of transitioning from CCF radial gates to CVP to 40%, compared to about 5% when temperatures were lower (Figure 3-30). Increasing water temperature deviations also increased the transition rate from West Canal to CVP by approximately 10% over a range of net flows (Figure 3-32). This could perhaps indicate that fish are waiting for cooler flood tide flows before moving between locations (e.g., Figure 3-27).

Later release day had a small but increasing effect on transition rates away from CCF radial gates in either direction and from West Canal to CVP, as well as a decreasing effect on the transition rate away from CVP back downstream to West Canal. Approximately 11% of fish (89 of 790) that were detected in the WPA were released after the HOR barrier was installed (release groups 2 and 3 in 2014, and release group 3 in 2015 and 2016; Table B.1-3). These fish were more likely to have reached the WPA by a longer route than directly from HOR and were present in WPA in May and June. If these fish entered the Inner Delta from lower on the SJR, such as near TC, transitions from CCF radial gate or West Canal to CVP represent a continued southward progression.

## 4.2 Approach

The continuous-time multistate Markov modeling approach adopted here for the juvenile steelhead analysis has been applied to assess transitions and behaviors of river and marine-going fishes such as lamprey, cod, and salmon in other systems (Bravener and McLaughlin 2013; Lewandoski et al. 2018; Kock et al. 2016, 2018). The previous work provided the study team with an analytical foundation and source of literature to build from. Kock et al. (2016) used the same modeling approach to quantify the effects of covariates on adult steelhead hatchery return and angler harvest rates in the Cowlitz River, Washington, finding that both return rate and harvest rate were positively affected by river discharge and negatively affected by time since release. In a multiyear radiotelemetry study to evaluate behavior and transition patterns of hatchery- and natural-origin adult spring Chinook salmon after a trap-and-haul program was implemented around three dams on the Cowlitz River, Kock et al. (2018) used a multistate model to describe how origin (hatchery versus natural), sex, release site location, and discharge affected transition rates to riverine areas where spawning habitat was located. The application to assessing juvenile steelhead behavior in the Delta by integrating model-simulated hydrodynamic variables with existing acoustic telemetry data proved successful.

Though the UnTRIM model allows for hydrodynamic variables to be output at 90-second timesteps, we found that a 15-minute timestep was biologically relevant given the distance between hydrophone arrays and fish travel times. The use of simulated data has an advantage compared to

gage data because it provides the flexibility to decide which areas to analyze instead of limiting the areas based on available gage data (either spatially or temporally). Modeling efforts provided information on hydrodynamic influences (e.g., flow, water temperature), biological influences (e.g., time of day), and physical influences (e.g., barrier presence) on transitions and behavior at all three locations. The small spatial scale of the analysis identified unique patterns of juvenile steelhead behavior at each of the three locations evaluated.

Other modeling approaches have been taken to improve understanding of juvenile salmonid migration through the Delta. For example, the ePTM is an agent-based particle tracking model used to estimate juvenile salmon migration dynamics (Sridharan et al. 2018). In ePTM, migration mechanics define how “clouds” of juvenile salmon disperse through the entire Delta. To our knowledge, ePTM has so far focused on Chinook salmon only and not steelhead. Were ePTM to be applied to SJR-origin juvenile steelhead, it would provide a “bigger picture” and complementary perspective to our evaluation of key individual junctions and areas in the Delta.

The steelhead study benefitted from engagement with stakeholders following several key steps in the analytical process. Two meetings with CAMT’s newly formed SSC were conducted to discuss key hypotheses of interest and to identify study locations after previously identified hypotheses were collated and initial telemetry data exploration was completed. Importantly, in fall 2021, a 2-day workshop was attended by more than 25 participants representing a variety of agencies and interest groups each day. The methods and results for the locations analyzed were presented, followed by a discussion of the results. The workshop concluded with the study team identifying additional hydrodynamic and fish modeling to discuss and consider (Appendix A). The study team conducted the additional modeling where feasible and incorporated the results in the final findings presented here.

#### ***4.2.1 Data Limitations***

The analysis results reflect what could be evaluated given the hydrophone locations, fish detections, water operations, and inflows observed throughout the 6 years of study. The UnTRIM model proved to be highly applicable for this study, and no data limitations were identified for the hydrodynamic modeling and variables available in the model. This was because of its fine-scale grid structure, the spatial coverage of the Delta that included all three study locations, and the types of hydrodynamic data available in the model. The data limitations encountered were related to the acoustic telemetry data and hydrophone placements among years, and flow conditions that occurred during the 6-year study period. The following limitations of the data are noted and should be kept in mind when interpreting the results:

- The distance between hydrophone arrays was established to meet survival and routing study objectives. The arrays were not very close to the HOR and TC junctions.

- Few fish were detected on Middle River; therefore, the Old and Middle River junction could not be evaluated.
- The study years evaluated at TC and WPA did not include 2011, a wet water year (Figure 2-10).
- There were only two overlapping years of data for all three locations evaluated (2015 and 2016).
- Not all routes at WPA were covered by hydrophones; for example, tagged fish that stayed on Old River where it branches from West Canal around a small island could not be detected.
- Hydrophones were not placed at SWP salvage tanks; therefore, tagged fish salvaged at this facility could not be detected.

#### **4.2.2 SST Metrics**

The SST identified five metrics that could be developed and tested to potentially help refine water project operations to improve juvenile salmonid survival through the Delta: 1) Qwest; 2) hydraulic residence times; 3) percentage time flow is positive (i.e., in a downstream direction) in Old River, Middle River, and other South Delta locations; 4) proportion of CVP exports relative to total export level; and 5) the proportion of Sacramento River water arriving at the export facilities relative to the total volume of Sacramento River flow entering the Delta. As discussed in Section 2.4.3, several of the metrics were removed from consideration during initial data exploration. The metrics identified by the SST were incorporated in the multistate model as follows:

- Qwest: Although Qwest ( $m^3/s$ ) was calculated for a 90-second timestep and tidally averaged (Table 2-2), it was removed from the analysis due its high correlation with local flow conditions that were incorporated into the model; for example,  $R > 0.9$  for Qwest and mainstem flow at TC.
- Hydraulic residence times: Residence time was not explicitly included in the analysis.
- Percentage time flow is positive: This was considered in each model through the inclusion of net and tide flow components.
- Proportion of CVP exports: This was removed from the analysis because total export flow is calculated at a location more than 30 km away from HOR and TC and was highly correlated with net flow in West Canal in the WPA.
- Proportion of Sacramento River water: Depth-averaged percent Sacramento River water, percent SJR water, and percent Mokelumne River water were calculated every 3 minutes and tidally averaged. Both metrics were evaluated in each model. Feedback from the stakeholder workshop indicated that percent SJR water may be a more appropriate metric for assessment of SJR fish behavior.

### **4.2.3 Similar Analyses**

As discussed in Section 1, information on steelhead behavior and survival within and through the Delta is limited, and estimates of steelhead survival within and among years are highly variable. Buchanan et al. (2021) analyzed all 6 years of available steelhead telemetry data and provided the best summary of steelhead routing and survival through the Delta. The authors concluded that survival in upstream reaches was associated with river discharge, while survival through the lower reaches was associated with migration route. The results from our analysis of steelhead generally comport with this key conclusion in Buchanan et al. (2021), because the net and tidal components of flow were in the best model for all three locations evaluated.

Most Delta studies have focused on analysis of Chinook salmon behavior, routing, and survival, and many focus on fish originating in the Sacramento River. Given the large differences between the two species, we do not review all of those studies here. Rather, we identify information from the Chinook salmon studies and our analyses that seem instructive for fish originating from the SJR, starting with the most recently published information.

Dodrill et al. (In Press) applied continuous time multistate Markov models to examine the influence of tidal and riverine hydraulics, behavioral factors, and management actions on juvenile Chinook salmon transitions. Because USGS was also a member of this steelhead study team, the analytical approach they used was similar to ours. The main difference was that Dodrill et al. (In Press) evaluated Chinook salmon and DSM2, whereas our analysis focused on steelhead using the UnTRIM hydrodynamic model. Both study teams decomposed modeled flows into tidal and net flow signals to understand how each component influenced transitions into and out of distributary channels. For Chinook salmon, Dodrill et al. (In Press) found that increasing net flows generally increased transition rates, while flood tides decreased transition rates. Similarly, ebb tides increased downstream transitions as fish move with the flow. They found less support for diel transition behaviors compared to flow metrics. Installation of the HOR barrier decreased entrainment into the interior Delta. Our steelhead results comport with these findings for Chinook salmon.

Holleman et al. (2022) evaluated swimming behavior of spring-run Chinook salmon in 2018 at HOR when the barrier was partially installed (extended from the southern shoreline and blocked a portion of the channel). They combined 2D acoustic fish telemetry at HOR with a 3D hydrodynamic model to estimate in situ emigration swimming behavior. They developed a 3D model for the small study area and calibrated it using velocity data collected by a shipboard acoustic doppler current profiler. They found that although the tagged fish were emigrating toward the ocean, the most prominent behavior was positive rheotaxis. A positive rheotaxis in this case would be one in which the fish would turn to face into an oncoming current of water. Therefore, as fish migrated downstream, they were oriented such that their heads were pointed upstream. While this might seem counterintuitive, it is a common position for salmonid smolts to use since their most powerful fin is the caudal fin

(i.e., tail), which is used for locomotion and predator avoidance. In their study, positive rheotaxis was broadly observed, increased with water velocity, and was consistent with smolts moving through the area more slowly than the mean flow velocity. Diurnal variation in longitudinal swimming indicated greater positive rheotaxis or downward vertical migration during daylight hours. The authors also reported that lateral swimming was common and most prevalent during daylight hours, suggesting a searching behavior when predation risk was higher than at night. Lateral swimming was strongly related to time of day, with a clear diel pattern of faster lateral transition during daylight hours and a peak near 14:00 local time.

In our analysis of steelhead behavior, the second strongest predictor of transition in the best fit model was migrator status; the upstream to downstream transition rates were lower when fish were non-migrators. We interpreted this as a milling behavior in the HOR area, similar to what Holleman et al. (2022) reported for Chinook salmon in terms of lateral behavior.

Cavallo et al. (2015) assembled 41 estimates of juvenile Chinook salmon routing at six junctions throughout the Delta to test the ability of three hydrologic metrics to predict fish routing at distributary channels. The three metrics were 1) proportion of flow into the distributary channel, 2) the ratio of velocity in main channel to velocity in the distributary, and 3) the proportion of time that flow is entering the distributary channel. The proportion of flow entering the distributary channel was selected as the best predictor, and it explained 70% of observed variation in fish routing. They used their linear model to predict routing at nine junctions under various combinations of inflow and exports. Their results suggest that more fish entered distributaries at junctions with strong riverine influence, whereas entrainment was lower at tidally dominated junctions. River inflow had the largest effect on entrainment at two riverine-dominated junctions (Old River and Georgiana Slough). Exports had a smaller than expected effect but had the greatest effect at junctions directly connected to the channels with water diversions. Cavallo et al. (2015) concluded that flow proportion is an effective metric to predict fish routing.

Our findings generally agree with Cavallo et al. (2015). We also found that fish were much more likely to enter the distributary channel at HOR where there is stronger riverine influence than at the tidally influenced TC junction. However, we found that, besides barrier presence, tide flow into the distributary channel had the strongest influence on whether fish would enter the distributary. In contrast to Cavallo et al. (2015), we noted a relationship between increasing exports and increasing net flow down TC. However, there were differences in data structure that may explain these differing findings, as described in Section 4.1.2.

## 5 Conclusions

Overall, the pairing of a detailed hydrodynamic simulation model with acoustic telemetry data was successful. It was used to evaluate steelhead transitions in a multistate modeling framework where fish transitions among states (e.g., upstream to downstream) were evaluated at three different locations in the Delta: two distributary junctions from the mainstem SJR to the Inner and South Delta, and at the WPA.

Researchers have now developed this modeling approach for Chinook salmon (Dodrill et al., In Press) and steelhead. Given that the spatial domain of the UnTRIM hydrodynamic model covers the entire Delta, behavioral responses of fish can be evaluated for any location in the Delta that is deemed important for water management and fish routing and survival objectives if acoustic tag detections at the location of interest are robust enough to support the analysis. As discussed in Section 5.2, completing this significant analytical step provides the linkage between acoustic data and life cycle modeling needed to integrate observed fish behavior and water project alternatives in a quantitative framework to assess effects on fish at the population level.

The results from this study on local-scale transitions, in combination with results of routing and survival through the Delta (Buchanan et al. 2021), represent an extensive analysis of steelhead transitions in the Delta based on the 6-year acoustic dataset. As was stated in Buchanan et al. (2021): “Before now, there had been no direct information on Delta survival for this SJR steelhead population or how survival varies with environmental conditions and resource management operations. In the absence of such information, management decisions for this population have been based largely on juvenile Chinook salmon survival studies (McEwan 2001) and a series of untested hypotheses that Delta survival is higher for SJR steelhead when more water enters the Delta from upstream, when less water is extracted from the Delta for human use (“export”), and when fish remain in the mainstem migration route (NMFS 2009).” Now the behavior, routing, and survival information can be brought together to inform water management discussions, as described in Section 5.2.

The SST explicitly identified potential linkages between project operations, salmonid migration behavior, and survival through a conceptual model. The SST hypothesized that flow conditions influence fish behavior and thus routing and survival through Delta channels. Hydrodynamic conditions drive entrainment mortality and through-Delta survival to Chipps Island through behavior responses to migration cue linkages (Figure 2-2; SST 2017a). At all three locations, model results support the SST’s hypothesis. The net and tidal components of flow were in the best model for all three locations evaluated.

However, study results also clearly indicate that behavior was unique at all three sites in several ways. First, steelhead residence time in the WPA was substantially longer than the other locations (90% of fish spent ≤6.5 days, compared to ≤1.6 days at HOR and ≤1.3 days at TC). Second, state transitions

from upstream to downstream in mainstem channels were largely unidirectional at TC and at HOR when the barrier is in, and less directional at HOR with the barrier out and especially for fish classified as active migrants, which had a high probability of entering Old River. Transitions were non-directional at WPA where 30% of tagged fish end up being collected at CVP salvage facilities.

Third, the proportion of tagged fish going from upstream into the distributary channels varied greatly by location. A total of 54% versus 15% of the state transitions were upstream into the distributary channel at HOR (barrier out) and TC, respectively. This large difference potentially indicates there are differences in very localized hydraulic conditions at the two junctions that could not be informed with the existing hydrophone locations evaluated in our study (i.e., how fish behave very close to the distributary entrance).

Fourth, the number of tagged steelhead available for the analysis was substantially different between the upper study location (HOR, 4,580 tagged juvenile steelhead detected) and lower study location (576 and 790 fish detected at TC and WPA, respectively). This is partly a result of more study years being incorporated into the analysis for HOR (6 years) compared to the other locations (3 years at TC and WPA). It also likely results from mortality of tagged fish between the upper and lower locations, fish entering Old River when the barrier is not installed, and the partial hydrophone coverage of all potential fish migration routes at WPA. It suggests, however, that for any future studies the proximity of tagged fish release locations to the location(s) being evaluated needs to be considered in a study design to account for the reduction in detections with distance from release.

Important findings at the HOR location include the following:

- Fish generally stayed in the SJR when the barrier was installed and moved into Old River when the barrier was not installed.
- When the barrier was installed:
  - There was more variability in the percentage of fish classified as active migrants (range from 24% to 97%), compared to when it was not installed (range from 73% to 91%).
  - During one period (May 2012), active migrants had an 80% chance of moving downstream after 3 hours, while non-migrants did not reach an 80% chance of transitioning downstream until 1.7 days.
- Over short time periods, fish were more likely to move downstream on the SJR rather than into Old River when net flows were high (generally during high water years) on the SJR, even when the barrier was not installed.
- During low flow years, tidal flow had more influence on the probability of transitioning at the 15-minute timescale, with fish generally moving downstream with the ebb tide and “backtracking” on the flood tide. The Old River tidal flow was only a factor when the barrier was not installed.

- The interactive effect between barrier and time of day could indicate altered behavioral patterns because of the barrier, such as foraging or predator avoidance.

Important findings at the TC location include the following:

- Few fish entered TC, but those that did were more likely to enter during flood tide flow into TC. The tidal component of flow had the strongest influence on fish transitions in the TC junction among the three areas evaluated.
- Over three-quarters of fish that had previously been designated as actively migrating at HOR continued to move through the TC junction at approximately the same rate as was observed at HOR.
- Juvenile steelhead were generally more likely to move during the day.
- Although the range of mainstem net flow was limited (-55 to 72 m<sup>3</sup>/s), during the 3 years of telemetry data available at this location, net flow was the strongest predictor of upstream to downstream transition.
- The analyses evaluated total flow, net flow, and tidal flow at each location (where total = net + tidal). Water project exports influenced net flow through TC. This finding is in contrast with earlier findings by the SST and published results by other researchers that found little influence of water project operations on flow in TC. The magnitude of net flow in TC influenced how "reversed" the total flow became during flood tides, which in turn increased the chance of fish entering TC.

Important findings at the WPA location include the following:

- Fish in this area displayed longer residence time and a lack of directional transition, unlike the other two areas where one transition direction had a much higher rate. Additionally, fish had higher probabilities of transitioning in the direction of tidal flows.
- Of the total number of fish detected in the WPA, 30.7% ended up in the CVP salvage tank. The probability of this happening over time increased with high reverse net flow. Since net flow was reversed for the entire study period evaluated at this location (2014 to 2016), all fish experienced some level of reverse net flow.
- Fish were more likely to move away (either direction) from the entrance to CCF (i.e., radial gates) when net flow in West Canal was low, probably because the radial gates are generally closed when net flow is low.
- Temperature, source water, and tidal flows are highly dynamic in this area. Temperature fluctuations related to source water and tidal flow were influential in the model, but we were not able to isolate the effects on fish transition. Data were only available in critical or below normal water years (Table 2-1). The influence of these interacting variables requires further investigation.

- Fish released into the SJR after the HOR barrier was installed (i.e., later release day) were more likely to transition toward CVP in the WPA, potentially a result of taking a longer route down the SJR and generally moving in a southward direction through the Inner Delta.

Findings related to the SST Metrics include the following:

- Several were removed from consideration during initial data exploration due to high correlation with other covariates that were modeled, or due to the metrics not aligning with the scale needed for analyses of behaviors.
- Qwest was shown to have a high correlation with local flow conditions that were incorporated into the model in some areas (e.g.,  $R > 0.9$  for Qwest and mainstem flow at TC).
- Total export flows were highly correlated with net flow in West Canal ( $R > -0.95$ ).
- Depth-averaged percent Sacramento River water, percent SJR water, and percent Mokelumne River water were evaluated in the models, but they were not included in the best fit fish models for the three areas evaluated.

## 5.1 Management Implications

Management implications for the three study areas are discussed below.

### **Head of Old River**

Based on this analysis, the strategy of installing the barrier to prevent fish from taking the Old River migration route through the Delta is successful.

- **Basis:** Our analysis shows that the barrier being installed creates a high chance that actively migrating fish will not enter Old River, but also increases the chance that fish will backtrack from downstream to upstream on the mainstem SJR at the HOR junction. The observed proportion of transitions from upstream of the HOR junction into Old River increased from 3% when the barrier was installed to 54% when the barrier was not installed. There was more variability in the percentage of fish classified as active migrators (24% to 97%) when the barrier was installed compared to when it was not installed (73% to 91%), potentially indicating that the barrier is affecting fish behavior. The presence of the barrier has been shown to be a primary factor that increases survival on the SJR route because of the way it diverts both fish and flow into the mainstem SJR (Buchanan et al. 2021). However, the barrier could potentially lower survival if it delays fish migration. Additionally, the barrier appeared to alter diel transition patterns, with fish less likely to make downstream transitions during the day when the barrier was installed.

### **Turner Cut**

Adjust the timing of water project operations during daytime such that net flow during ebb tides is enhanced and exports do not coincide with flood tide flows at TC. This would increase the

proportion of fish staying on the mainstem SJR and not entering TC. This may also allow fish to move through the area more quickly (increase the probability of upstream fish transitioning to downstream). These changes would result in higher survival (Buchanan et al. 2021).

Alter the physical conditions at TC such that steelhead are less likely to enter TC on a flood tide. This could include altering the physical structure of the entrance to TC or installing some type of non-physical barrier that alters the behavior of juvenile steelhead and reduces the proportion of fish entering TC. If successful, these physical or non-physical changes would result in higher survival (Buchanan et al. 2021).

- **Basis:** UnTRIM modeling showed the net flow in TC and total tidally averaged export flow are highly correlated ( $R \sim 0.9$ ) for 2013, 2015, and 2016 (dry, critical, and below normal water years, respectively; Table 2-1). Fish modeling results show that flood tide flows increase the chance of fish entering TC, but when net flow is lower, flood tides are more likely to be reversed. We also observed a relationship between an increase in predicted flow toward the export facilities and an increase in net flow down TC when all 6 years of the study are considered together.

## Water Project Area

No direct management implications were identified, but information potentially of management interest includes the following:

- Fish have a longer residence time in this area than HOR or TC, and 31% of the fish detected here ended up in the CVP salvage tank. The SWP salvage tank was not outfitted with a hydrophone and the number of tagged fish ending up at this location is unknown. High reverse net flow increased the probability of transitioning from CVP to the CVP salvage tank to more than 80% after approximately 2.5 days. Long residence times in the area likely increase exposure to predation, but also the potential for being collected at salvage facilities.
- Fish were more likely to move away (either direction) from the entrance to CCF (i.e., radial gates) when net flow in West Canal was low.
- Fish generally displayed a lack of directional transition, but transitions appeared to be in the direction of tidal flows (ebb and flood).
- One notable observation that may warrant further investigation is that fish released after the HOR barrier was installed (i.e., later release day) were more likely to move toward the CVP. Buchanan et al. (2021) conducted a preliminary analysis showing that the salvage subroute may increase survival because it shortens route length. If trucking of salvaged fish has a higher route survival than other longer routes through the Inner Delta, this might be a positive factor.

## 5.2 Recommendations

The following recommendations are provided based on analysis of juvenile steelhead responses to hydrodynamic and environmental conditions in the Delta. The analyses evaluated conditions present at the three locations from fish releases made during 2011 to 2016 and water management metrics identified in regulatory documents or in SST reports (SST 2017a, 2017b). As discussed in Section 5, the pairing of hydrodynamic simulation model estimates with acoustic telemetry data was successful. Based on results of the analysis and the successful approach developed, the following recommendations are provided:

- 1. Conduct additional fine-scale, juvenile steelhead acoustic telemetry studies at HOR, TC, and WPA.** At a minimum we recommend evaluating a wet water year at all three sites. High inflows were experienced in 2011 and briefly in March 2016 (Figure 2-4). The only location with full hydrophone coverage in 2011 was HOR. The high inflows experienced in March 2016 were monitored at all three study locations, but very few acoustic tags were detected at WPA due to the barrier at HOR being installed (Figure 2-10). The study should be repeated using the same hydrophone array locations as the 6-year steelhead study at TC and HOR for comparability to the 2011 to 2016 data. However, due to the limited hydrophone coverage in WPA, additional hydrophone arrays should be added to the locations used in 2011 to 2016 to provide coverage in the missing channels, such as Old River where it branches from West Canal. A secondary recommendation would be to deploy the arrays in a low-outflow year, including the more comprehensive array deployment in WPA. To complete these evaluations, fish may need to be released closer to areas of interest to have sufficient and more equal sample sizes among treatment locations each year. For example, we evaluated TC in 2013, 2015, and 2016, but the majority of fish (80%) were detected in 2016.

One benefit of additional studies with the same hydrophone deployment is that data from the study could then be used to evaluate whether the existing multistate models have predictive power. The model could be used to predict transitions, and the predictions could be assessed based on the additional field data collected. If the multistate model performed adequately, it could be used to assess where fish would likely go if there was some management action to change the geometry or flow patterns at the junction, either by restoration actions or installation of a permanent gate. This would support Recommendations 3 and 4, below. If studies are repeated, hydrophone locations used in 2015 and 2016 should be considered because these were more extensive than some of the early years that did not have full coverage at important areas.

Replicating the study at the current locations as described above raises a logistical concern given the variable nature of the hydrograph, especially during wet water years which seem to be

episodic recently. To implement these studies, the study designs, contracting, equipment purchases, and fish allocations would have to be approved ahead of time and placed on hold until water year forecasts indicate the required conditions are likely to occur that year. An option would be to conduct another multiyear study that covers the sites identified in Recommendations 1 and 2 and assume that high and low flow conditions will be sampled during the study timeframe.

- 2. Conduct additional fine-scale, juvenile salmonid acoustic telemetry studies at additional important locations in the Delta.** Our study was limited by the low number of detections present at most locations throughout the Delta; we could only assess behavior at a few locations. This was a result of hydrophone arrays being placed in locations that supported through-Delta routing and survival study objectives, not fine-scale transition and behavior study objectives. Following our initial discussions with the SSC on key hypotheses and locations of interest, several areas of interest were investigated. However, telemetry data in these areas were sparse and insufficient to support the analysis. Examples include Columbia Cut junction, False River and Three Mile Slough junction, Old San Joaquin junction, and Montezuma Slough. Since the UnTRIM hydrodynamic model covers the entire Delta, the approach developed here could be applied to any location in the Delta deemed important from a fish routing or water management perspective once sufficient telemetry data are available from these locations in the future.

- 3. Integrate the multistate model results from this study with routing and final fate analysis conducted by others and water management strategies.** Integrating behavioral information from this study with routing and final fate analysis conducted by others is needed for three reasons. First, as was identified during the stakeholder workshop (Appendix A), relating the high-level summary of steelhead behavior to survival is key to evaluating whether any behavior mechanisms need further investigation.

Second, follow-on integration is needed to develop a more wholistic picture of the influence of fine-scale behaviors on the ultimate fate of fish. This step would take the behavior information at a junction or location and relate route-specific survival to the observed behavior. The behavior information would be related to survival using updated survival analyses such as those provided by Buchanan et al. (2018, 2021). For example, at TC the example period transition probabilities for May 2 to 4, 2016, indicated the probability of upstream fish transitioning to downstream increased to about 60% after approximately 16 hours, but then varied between 45% and 82% with daily tide flow. If fish transition down the mainstem or into TC, what does that mean in terms of overall survival? How sensitive is overall survival to the variability in transitions observed due to daily tidal flow fluctuations? As pointed out in a parallel study of Chinook salmon, flow conditions influence behavior and thus routing through Delta channels. Linking hydrodynamic simulation

models to statistical models of smolt transitions at the fine temporal resolution necessary to realistically capture ecological dynamics would provide critical information to inform management of threatened species in the Delta (Dodrill et al. In Press).

Third, the multistate modeling described here could be extended to allow managers to assess the impacts of inflow and alternative flow management regimes on estimated physical conditions at key junctions and to predict fish transitions. Buchanan et al. (2021) point out that during the 2011 to 2016 study period there was relatively low variability in export levels due to regulatory restrictions, making it difficult to detect potential survival effects, and that different survival patterns might be exhibited under unrestricted (i.e., higher) exports (especially in the Old River route which passes the entrances to the pumping facilities). Expanded conditions or alternative water management strategies could be developed and evaluated in a modeling framework using the integrated information (hydrodynamic model estimates, multistate modeling of transitions, and route-specific survival) to estimate effects on through-Delta survival without having to physically manipulate exports and Delta flows.

- 4. Incorporate results from the predictive multistate model, routing, and final fate analysis into life cycle models to assess population-level effects.** Results of various inflow levels and alternative flow management regimes evaluated through Recommendation 3 could be incorporated into existing life cycle models. If ePTM modeling was conducted on migrating steelhead, findings from multistate Markov modeling could help migration mechanics results. Rules currently applied to juvenile Chinook salmon indicating they migrate mostly at night, for example, may not apply to steelhead. Importantly, incorporating the results into a life cycle framework would allow effects from alternative water management alternatives on populations to be estimated.
- 5. Conduct additional flow-based analyses at TC.** This would include model-based and data-based analyses to further understand the relationship between exports and net flow through TC. Other studies could include flow modeling to investigate how a physical barrier at TC would change flows into downstream distributaries.
- 6. Conduct acoustic telemetry studies on wild juvenile steelhead of different age classes.** The analyses conducted were based on large, hatchery-origin steelhead with median fork lengths ranging between 215 mm and 280 mm. Similar information on natural-origin steelhead should also be collected based on steelhead smolts from different age classes captured and tagged at existing traps such as the Mossdale Kodiak trawl or tributary screw traps.

In summary, additional telemetry information should be collected to evaluate key hypotheses on juvenile steelhead behavior at locations of interest in the Delta. This should be done under various

inflow levels and export operations. Information should be analyzed by using the multistate modeling approach (Recommendations 1, 2, and 5); related to available information on routing and survival (Recommendation 3); and extended to population-level effects if possible (Recommendation 4). The analyses conducted were based on large, hatchery-origin steelhead. Similar information on natural-origin steelhead should also be collected based on steelhead smolts captured and tagged at existing traps (Recommendation 6). Additional telemetry information on Chinook salmon could be collected at the same time using the same hydrophone locations to develop additional information on fine-scale transitions and behavior of salmon.

## 6 References

- Anchor QEA (Anchor QEA, LLC), 2018a. *Evaluation of the Effects of Summer Operation of the Suisun Marsh Salinity Control Gates*. Prepared for the California Department of Water Resources. May 2018.
- Anchor QEA, 2018b. *FLoAT MAST – Physical Habitat Subteam: Hydrodynamic Modeling of Salinity, Temperature, and Turbidity*. Prepared for the California Department of Water Resources. December 2018.
- Anchor QEA, 2019a, *Evaluation of the Effects of Summer 2018 Suisun Marsh Salinity Control Gates Action*. Prepared for the California Department of Water Resources. May 2019.
- Anchor QEA, 2019b, *Evaluation of the Effect of Outflow on the Temperature of the Low Salinity Zone*. Prepared for U.S. Fish and Wildlife Service. November 2019.
- Bever, A.J., and M.L. MacWilliams, 2016. "Factors Influencing the Calculation of Periodic Secondary Circulation in a Tidal River: Numerical Modelling of the Lower Sacramento River, USA." *Hydrological Processes* 30:995–1016. Available at: <https://doi.org/10.1002/hyp.10690>.
- Bravener, G.A., and R.L. McLaughlin, 2013. "A Behavioural Framework for Trapping Success and its Application to Invasive Sea Lamprey." *Canadian Journal of Fisheries and Aquatic Sciences*, 70(10), pp.1438-1446.
- Buchanan, R.A., 2018a. *2014 Six-Year Acoustic Telemetry and Steelhead Study: Statistical Methods and Results*. Prepared for the U.S. Bureau of Reclamation. July 2018. Available at: <http://www.cbr.washington.edu/sites/default/files/papers/UW%206yr%20steelhead%20report%202014%20FINAL.PDF>.
- Buchanan, R.A., 2018b. *2015 Six-Year Acoustic Telemetry and Steelhead Study: Statistical Methods and Results*. Prepared for the U.S. Bureau of Reclamation. July 2018. Available at: <https://www.cbr.washington.edu/sites/default/files/papers/UW%206yr%20steelhead%20report%202015%20FINAL.pdf>.
- Buchanan, R.A., 2018c. *2016 Six-Year Acoustic Telemetry and Steelhead Study: Statistical Methods and Results*. Prepared for the U.S. Bureau of Reclamation. December 2018. Available at: <http://www.cbr.washington.edu/sites/default/files/papers/UW%206yr%20steelhead%20report%202016%20FINAL.pdf>.
- Buchanan, R.A., P.L. Brandes, and J.R. Skalski, 2018. "Survival of Juvenile Fall-Run Chinook Salmon Through the San Joaquin River Delta, California, 2010–2015." *North American Journal of Fisheries Management* 38(3):663–679. DOI:10.1002/nafm.10063.

- Buchanan, R.A., E. Buttermore, and J. Israel, 2021. "Outmigration Survival of a Threatened Steelhead Population Through a Tidal Estuary." *Canadian Journal of Fisheries and Aquatic Sciences* 78(12): 1869–1886.
- Cavallo, B., S. Zueg, and J. Melgo, 2015. "Predicting Juvenile Chinook Salmon Routing in Riverine and Tidal Channels of a Freshwater Estuary." *Environmental Biology of Fishes*. DOI: 10.1007/s10641-015-0383-7.
- CDFA (California Department of Food and Agriculture), 2020. *California Agricultural Statistics Review 2019–2020*. Available at: [https://www.cdfa.ca.gov/Statistics/PDFs/2020\\_Ag\\_Stats\\_Review.pdf](https://www.cdfa.ca.gov/Statistics/PDFs/2020_Ag_Stats_Review.pdf).
- Chapman, E.D., A.R. Hearn, C.J. Michel, A.J. Ammann, S.T. Lindley, M.J. Thomas, P.T. Sandstrom, G.P. Singer, M.L. Peterson, R.B. MacFarlane, and A.P. Klimley, 2013. "Diel movements of out-migrating Chinook salmon (*Oncorhynchus tshawytscha*) and steelhead trout (*Oncorhynchus mykiss*) smolts in the Sacramento/San Joaquin watershed." *Environmental Biology of Fishes*, 96(2), pp. 273-286.
- Conrad, J.L., A.J. Bibian, K.L. Weinersmith, D. De Carion, M.J. Young, P. Crain, E.L. Hestir, M.J. Santos, and A. Sih, 2016. "Novel species interactions in a highly modified estuary: association of Largemouth Bass with Brazilian waterweed *Egeria densa*." *Transactions of the American Fisheries Society*, 145(2), pp.249-263.
- Deltares, 2014. *Delft3D-FLOW: Simulation of Multi-Dimensional Hydrodynamic Flows and Transport Phenomena, Including Sediments, User Manual*. Delft, Netherlands: Deltares.
- Dodrill, M., R. Perry, A. Pope, and X. Wang (forthcoming). "Quantifying the Effects of Tides, River Flow, and Barriers on Movements of Chinook Salmon Smolts at Junctions in the Sacramento – San Joaquin River Delta Using Multistate Models." *Environmental Biology of Fishes*.
- DWR (California Department of Water Resources), 2018. "California Irrigation Management Information System (CIMIS) Website." Accessed January 15, 2018. Available at: <https://cimis.water.ca.gov/>.
- DWR, 2022. "Dayflow Program." Accessed March 1, 2022. Available at: <https://water.ca.gov/Programs/Environmental-Services/Compliance-Monitoring-And-Assessment/Dayflow-Data>.
- DWR CDEC (California Department of Water Resources California Data Exchange Center), 2020. "California Data Exchange Center Website." Accessed January 15, 2020. Available at: <http://cdec.water.ca.gov>.

- EDI (Environmental Data Initiative), 2022. EDI Data Portal. Available at:  
<https://doi.org/10.6073/pasta/f2579d5a59eb856a595ad07f531b2311>.
- Federal Register, 2006. *Endangered and Threatened Species: Final Listing Determinations for 10 Distinct Population Segments of West Coast Steelhead*. Final Rule. 71 FR 834, January 5, 2006.
- Federal Register, 2016. *Endangered and Threatened Species; 5-Year Reviews for 28 Listed Species of Pacific Salmon, Steelhead, and Eulachon*. Final Rule. 81 FR 33468, May 26, 2016.
- Gocic, M., and S. Trajkovic, 2013. "Analysis of Changes in Meteorological Variables Using Mann-Kendall and Sen's Slope Estimator Statistical Tests in Serbia." *Global and Planetary Change* 100: 172–182. Available at: <https://doi.org/10.1016/j.gloplacha.2012.10.014>.
- Gross, E.S., J. Korman, L.F. Grimaldo, M.L. MacWilliams, A.J. Bever, and P.E. Smith, 2021. "Modeling Delta Smelt Distribution for Hypothesized Swimming Behaviors." *San Francisco Estuary and Watershed Science* 19(1). Available at: <https://doi.org/10.15447/sfews.2021v19iss1art3>.
- Holleman, R.C., E.S. Gross, M.J. Thomas, A.L. Rypel, and N.A. Fangue, 2022. "Swimming Behavior of Emigrating Chinook Salmon Smolts." *PLOS One* 17(3).
- Jackson, C.H., 2011. "Multi-State Models for Panel Data: The msm Package for R." *Journal of Statistical Software* 38(8). Available at: <https://doi.org/10.18637/jss.v038.i08>.
- Jackson, C.H., 2019. Multi-state modelling with R: the msm package. Version 1.6.8. December 16, 2019. Available at: <https://cran.r-project.org/web/packages/msm/index.html>. Accessed on: October 7, 2020.
- Kock, T., R. Perry, C. Gleizes, W. Dammers, and T. Liedtke, 2016. "Angler Harvest, Hatchery Return, and Tributary Stray Rates of Recycled Adult Summer Steelhead *Oncorhynchus Mykiss* in the Cowlitz River, Washington." *River Research and Applications* 32: 1,790–1,799. DOI: 10.1002/rra.3023.
- Kock, T., R. Perry, A. Pope, J. Serl, M. Kohn and T. Liedtke, 2018. "Responses of Hatchery- and Natural-Origin Adult Spring Chinook Salmon to a Trap-and-Haul Reintroduction Program." *North American Journal of Fisheries Management* 38:1,004–1,016. DOI: 10.1002/nafm.10199.
- Lewandoski, S.A., M.A. Bishop, and M.K. McKinzie, 2018. "Evaluating Pacific Cod Migratory Behavior and Site Fidelity in a Fjord Environment Using Acoustic Telemetry." *Canadian Journal of Fisheries and Aquatic Sciences*, 75(11), pp. 2084–2095.

- Lindley, S.T., R.S. Schick, A. Agrawal, M. Goslin, T.E. Pearson, E. Mora, J.J. Anderson, B. May, S. Greene, C. Hanson, A. Low, D. McEwan, R.B. MacFarlane, C. Swanson, and J.G. Williams, 2006. "Historical Structure of Central Valley Steelhead and Its Alteration by Dams." *San Francisco Estuary and Watershed Science* 4(1). Available at: <https://escholarship.org/uc/item/1ss794fc>.
- Lund, J.R., E. Hanak, W. Fleenor, R. Howitt, J. Mount, and P. Moyle, 2007. *Envisioning Futures for the Sacramento-San Joaquin Delta* (p. 325). San Francisco: Public Policy Institute of California.
- Luoma, S.N., C.N Dahm, M. Healey, and J.N. Moore, 2015. "Challenges Facing the Sacramento-San Joaquin Delta: Complex, Chaotic, or Simply Cantankerous?" *San Francisco Estuary and Watershed Science* 13(3).
- MacWilliams, M.L., and R.T. Cheng, 2007. *Three-Dimensional Hydrodynamic Modeling of San Pablo Bay on an Unstructured Grid*. 7th International Conference on Hydroscience and Engineering (Philadelphia, Pennsylvania); September 2007.
- MacWilliams, M.L., and E.S. Gross, 2007. *UnTRIM San Francisco Bay-Delta Model Calibration Report, Delta Risk Management Study*. Prepared for the California Department of Water Resources. March 2007.
- MacWilliams, M.L., and E.S. Gross, 2010. *UnTRIM San Francisco Bay-Delta Model Sea Level Rise Scenario Modeling Report, Bay Delta Conservation Plan*. Final Report. Prepared for the Science Applications International Corporation and California Department of Water Resources. July 16, 2010.
- MacWilliams, M.L., and E. G. Gross, 2013. "Hydrodynamic Simulation of Circulation and Residence Time in Clifton Court Forebay." *San Francisco Estuary and Watershed Science*. 11(2). Available at: <https://doi.org/10.15447/sfews.2013v11iss2art1>.
- MacWilliams, M.L., E.S. Gross, J.F. DeGeorge, and R.R. Rachiele, 2007. *Three-Dimensional Hydrodynamic Modeling of the San Francisco Estuary on an Unstructured Grid*. 32nd Congress of the International Association of Hydro-Environment Engineering and Research (Venice, Italy); July 2007.
- MacWilliams, M.L., F.G. Salcedo, and E.S. Gross, 2008. *San Francisco Bay-Delta UnTRIM Model Calibration Report, POD 3-D Particle Tracking Modeling Study*. Prepared for the California Department of Water Resources. December 19, 2008.
- MacWilliams, M.L., F.G. Salcedo, and E.S. Gross, 2009. *San Francisco Bay-Delta UnTRIM Model Calibration Report, Sacramento and Stockton Deep Water Ship Channel 3-D Hydrodynamic and Salinity Modeling Study*. Prepared for the U.S. Army Corps of Engineers, San Francisco District. July 14, 2009.

MacWilliams, M.L., N.E. Kilham, and A.J. Bever, 2012. *South San Francisco Bay Long Wave Modeling Report*. Prepared for the U.S. Army Corps of Engineers, San Francisco District. 2012.

MacWilliams M.L., P.F. Sing, F. Wu, and N. Hedgecock, 2014. *Evaluation of the Potential Salinity Impacts Resulting from the Deepening of the San Francisco Bay to Stockton Navigation Improvement Project*. 33rd PIANC World Congress (San Francisco, California); June 2014.

MacWilliams, M.L., A.J. Bever, E.S. Gross, G.S. Ketefian, and W.J. Kimmerer, 2015. "Three-Dimensional Modeling of Hydrodynamics and Salinity in the San Francisco Estuary: An Evaluation of Model Accuracy, X2, and the Low Salinity Zone." *San Francisco Estuary and Watershed Science* 13(1). Available at: <http://escholarship.org/uc/item/7x65r0tf>.

MacWilliams, M.L., A.J. Bever, and E. Foresman, 2016. "3-D Simulations of the San Francisco Estuary with Subgrid Bathymetry to Explore Long-Term Trends in Salinity Distribution and Fish Abundance." *San Francisco Estuary and Watershed Science* 14(2). Available at: <http://escholarship.org/uc/item/5qj0k0m6>.

McEwan, D.R., 2001. "Central valley steelhead." *Fish Bulletin*, 179(1), pp.1-43. In Brown, R.L., 2001 (Editor). Contributions to the Biology of Central Valley Salmonids. Volumes 1 and 2.

Michel, C.J., Henderson, M.J., Loomis, C.M., Smith, J.M., Demetras, N.J., Iglesias, I.S., Lehman, B.M. and Huff, D.D., 2020. "Fish predation on a landscape scale." *Ecosphere*, 11(6), p.e03168.

Nichols, F.H., J.E. Cloern, S.N. Luoma, and D.H. Peterson, 1986. "The Modification of an Estuary." *Science* 231(4,738):567–573.

NOAA, 2005. *Endangered and Threatened Species; Designation of Critical Habitat for Seven Evolutionarily Significant Units of Pacific Salmon and Steelhead in California*. Final Rule. Docket No. 041123329–5202–02; I.D. No.110904F. 50 CFR Part 226. September 2, 2005.

NOAA, 2009. *Biological Opinion on Long-Term Operations of the Central Valley Project and State Water Project*. June 4, 2009. National Marine Fisheries Service, Southwest Region, Long Beach, California. Available at: <https://nrm.dfg.ca.gov/FileHandler.ashx?DocumentID=21473>.

NOAA NARR (National Oceanic and Atmospheric Administration North American Regional Reanalysis), 2018. "NCEP North American Regional Reanalysis." *NOAA Physical Sciences Laboratory*. Accessed January 15, 2018. Available at: <https://www.esrl.noaa.gov/psd/data/gridded/data.narr.html>.

Nobriga, M.L. and F. Freyer, 2007. "Shallow-water piscivore-prey dynamics in California's Sacramento-San Joaquin Delta." *San Francisco Estuary and Watershed Science*, 5(2).

Octavio, K.A.H., G.H. Jirka, and D.R.F. Harleman, 1977. *Vertical Heat Transport Mechanisms in Lakes and Reservoirs*. Technical Report 227. Cambridge, Massachusetts: Massachusetts Institute of Technology.

Perry, R.W., J.R. Skalski, P.L. Brandes, P.T. Sandstrom, A.P. Klimley, A. Ammann, and B. MacFarlane, 2010. "Estimating Survival and Migration Route Probabilities of Juvenile Chinook Salmon in the Sacramento–San Joaquin River Delta." *North American Journal of Fisheries Management* 30(1):142–156.

Perry, R.W., P.L. Brandes, J.R. Burau, A.P. Klimley, B. MacFarlane, C. Michel, and J.R. Skalski, 2013. "Sensitivity of Survival to Migration Routes Used by Juvenile Chinook Salmon to Negotiate the Sacramento-San Joaquin River Delta." *Environmental Biology of Fishes*, 96(2):381–392.

Perry, R.W., R.A. Buchanan, P.L. Brandes, J.R. Burau, and J.A. Israel, 2016. "Anadromous Salmonids in the Delta: New Science 2006–2016." *San Francisco Estuary and Watershed Science* 14(2).

R Core Team (2021). "The R Project for Statistical Computing." Available at: <https://www.R-project.org/>.

SCCOOS (Southern California Coastal Ocean Observing System), 2020. "SIO Manual Shore Stations Program, SE Farallon Island Shore Station." Accessed January 15, 2020. Available at: <http://www.sccoos.org>.

Sridharan, V.K, D. Jackson, A.M. Hein, E.M. Danner, and S.T. Lindley, 2018. "Abstracting Micro-Scale Fish Movements into a System-Scale Migration Model for an Engineered Urban Estuary." *Poster Abstracts, Integrative and Comparative Biology*, 58(suppl\_1):e265–e458.

SST (Salmon Scoping Team), 2017a. *Effects of Water Project Operations on Juvenile Salmonid Migration and Survival in the South Delta. Volume 1: Findings and Recommendations*. Prepared for the Collaborative Adaptive Management Team. January 2017.

SST, 2017b. *Effects of Water Project Operations on Juvenile Salmonid Migration and Survival in the South Delta. Volume 2: Responses to Management Questions*. Prepared for the Collaborative Adaptive Management Team. January 2017.

Sen, P.K. 1968. "Estimates of the Regression Coefficient Based on Kendall's Tau." *Journal of the American Statistical Association* 63(324): 1379–1389. Available at: <http://dx.doi.org/10.2307/2285891>.

Smith, C.D., Plumb, J.M., Adams, N.S. and Wyatt, G.J., 2020. "Predator and prey events at the entrance of a surface-oriented fish collector at North Fork Dam, Oregon." *Fisheries Management and Ecology*, 28(2), pp.172–182.

- Theil, H. 1950. "A Rank-invariant Method of Linear and Polynomial Regression Analysis. Part 3." *Proceedings of Koninklijke Nederlandse Akademie van Wetenschappen A* 53: 1397–1412.
- Thieurmel and Elmarhraoui (Benoit Thieurmel and Achraf Elmarhraoui), 2019. suncalc: Compute Sun Position, Sunlight Phases, Moon Position, and Lunar Phase. R package version 0.5.0. <https://CRAN.R-project.org/package=suncalc>.
- USBR (U.S. Bureau of Reclamation), 2018a. *NMFS Biological Opinion RPA IV.2.2: 2011 Six-Year Acoustic Telemetry Steelhead Study*. Bay-Delta Office, Mid-Pacific Region, Sacramento, California: May 14, 2018.
- USBR, 2018b. *NMFS Biological Opinion RPA IV.2.2: 2012 Six-Year Acoustic Telemetry Steelhead Study*. Bay-Delta Office, Mid-Pacific Region, Sacramento, California: May 16, 2018.
- USBR. 2018c. *NMFS Biological Opinion RPA IV.2.2: 2013 Six-Year Acoustic Telemetry Steelhead Study*. Bay-Delta Office, Mid-Pacific Region, Sacramento, California: June 2018.
- USGS (U.S. Geological Survey), 2020. "USGS Water Data for California." *National Water Information System*. Accessed January 15, 2020. Available at: <http://waterdata.usgs.gov/ca/nwis/>.
- Yoshiyama R.M., E.R. Gerstung, F.W. Fisher, and P.B. Moyle, 1996. "Historical and Present Distribution of Chinook Salmon in the Central Valley Drainage of California." *Sierra Nevada Ecosystem Project: Final Report to Congress, Volume III*. Centers for Water and Wildland Resources, University of California, Davis. Davis, California: pp. 309–361.
- Yue, S., P. Pilon, and G. Cavadias, 2002. "Power of the Mann-Kendall and Spearman's rho Tests for Detecting Monotonic Trends in Hydrological Series. *Journal of Hydrology* 259: 254–271. Available at: [http://dx.doi.org/10.1016/S0022-1694\(01\)00594-7](http://dx.doi.org/10.1016/S0022-1694(01)00594-7).
- Zuur, A.F., E.N. Ieno, N.J. Walker, A.A. Saveliev, and G.M. Smith, 2009. *Mixed effects models and extensions in ecology with R* (Vol. 574). New York: Springer.

## Appendix A

### Stakeholder Workshop

---



## A.1 Workshop Agenda



# Workshop Agenda

## Stakeholder Workshop

---

Evaluating Juvenile Salmonid Behavioral Responses to Hydrodynamic Conditions in the Sacramento-San Joaquin Delta

November 17, 2021, 9:00-12:00 pm PT, Virtual / WebEx

Click the "Join Meeting" link in the Outlook invite, or click here:

<https://aq.webex.com/aq/j.php?MTID=m427093ffd852b45dc8fe299ebb1d07e3>

WebEx: 1-877-309-3457; Access Code: 2469-870-2617

---

### Day 1

- 9:00-9:15 – Introduction (Michelle)
- 9:15-9:30 – Project Overview and Workshop Objectives (John)
- 9:30-10:00 – Methods (Aaron and Sydney)
  - UnTRIM Hydrodynamic Model
  - Multi-State Model
  - Questions?
- 10:00-10:05 – BREAK
- 10:05-11:20 – Model Results – Water Project Area (Sydney)
  - Available fish data
  - Fish Behavior
  - Best Fit Model
  - Model Interpretations
- 11:20-11:30 – BREAK
- 11:30-11:50 – Workshop Discussion (John)
  - Are there any additional elements that should be included in the model?
  - Is there anything we're missing on the interpretation?
  - How should we present the information so that it's usable by managers?
- 11:50-12:00 – Wrap Up (Michelle)

---

## Evaluating Juvenile Salmonid Behavioral Responses to Hydrodynamic Conditions in the Sacramento-San Joaquin Delta

November 18, 2021, 9:00-12:00 pm PT, Virtual / WebEx

Click the "Join Meeting" link in the Outlook invite, or click here:

<https://aq.webex.com/aq/j.php?MTID=m2ffdbeec247604e3098c9dd36eb36e2c> X

WebEx: 1-877-309-3457; Access Code: 2456-389-6173

---

## Day 2

- 9:00-9:15 – Introduction/Summary of Day 1 (Michelle)
- 9:15-10:15 – Model Results – Head of Old River (Sydney)
  - Available fish data
  - Fish Behavior
  - Best Fit Model
  - Model Interpretations
  - Participant discussion
- 10:15-10:30 – BREAK
- 10:30-11:30 – Model Results – Turner Cut (Sydney)
  - Available fish data
  - Fish Behavior
  - Best Fit Model
  - Model Interpretations
  - Participant discussion
- 11:30-11:50 – Workshop Discussion (John)
  - Are there any additional elements that should be included in the model?
  - Is there anything we're missing on the interpretation?
  - How should we present the information so that it's usable by managers?
- 11:50-12:00 – Next Steps (Michelle)

## A.2 Technical Memorandum

---



# Memorandum

November 11, 2021

To: Workshop Participants  
From: John Ferguson, Michael MacWilliams, Sydney Gonsalves, Aaron Bever, Michelle Havey  
cc: John Plumb, Russell Perry, Mike Dodrill, Darcy Austin, Linda Standlee, Ben Geske, Alison Collins

**Re: Evaluating Juvenile Salmonid Behavioral Responses to Hydrodynamic Conditions in the Sacramento-San Joaquin Delta – Stakeholder Workshop Summary**

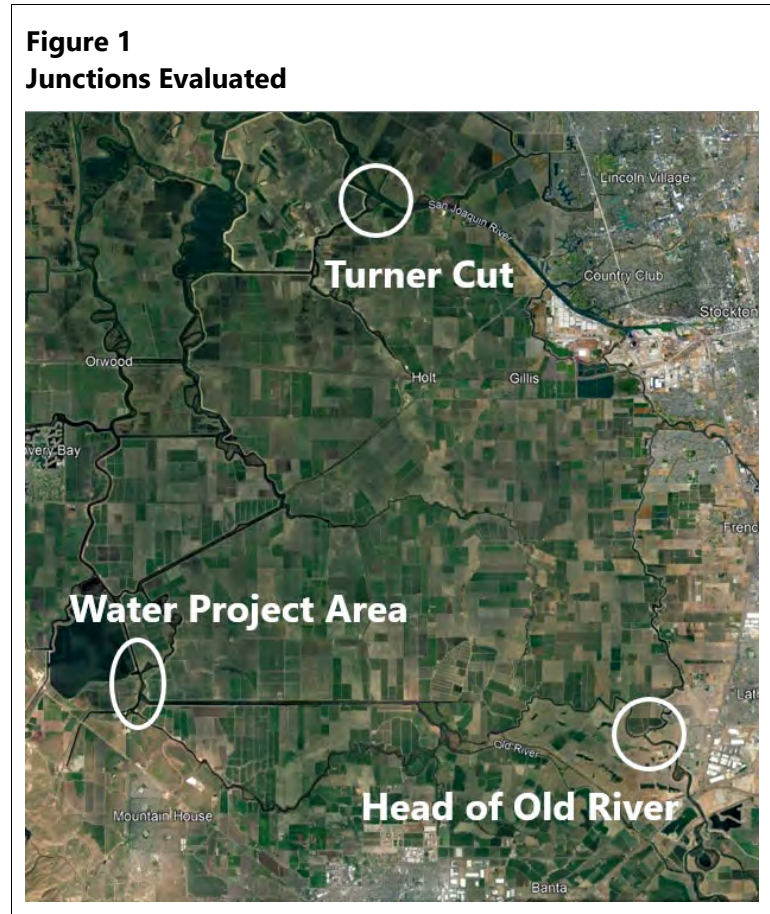
## Introduction

Anchor QEA, LLC, and the U.S. Geological Survey have been working with Delta Stewardship Council, State Water Contractors, and Metropolitan Water District of Southern California on a steelhead behavioral study as part of a Delta Science Proposal Prop 1 Watershed and Delta Ecosystem Restoration Grant. The study uses the 6-year acoustic telemetry dataset collected between 2011 and 2016 and the UnTRIM 3D hydrodynamic model to evaluate fine-scale behavioral responses of steelhead to hydrodynamic conditions. Combining these data to develop a multistate fish movement model has provided insight into how different hydrodynamic variables are correlated with behavior and the routes that salmonids take through the Delta, and how these hydrodynamic variables are likely to influence their route choice at select individual junctions and in the vicinity of water project pump intakes.

## Areas of Interest

We met with the CAMT Salmon Subcommittee (SSC) on October 29, 2020, to discuss initial hypotheses and proposed locations for detailed analyses based on hydrophone placement and number of detections available each year. Telemetry data for all 6 years were compiled, and a previously developed predator filter (Buchanan 2018a, 2018b, 2018c) was applied prior to analysis. The areas included in this evaluation were selected based on several factors, including: 1) the area was identified as an area of interest by stakeholders (e.g., Salmon Scoping Team and SSC) and addressed hypotheses developed by the Salmon Scoping Team (2017) and South Delta Research Collaborative (Anchor QEA 2014); 2) hydrophone arrays were located close enough to evaluate route selection; 3) a sufficient number of fish detections was available to support model analysis; and 4) the deployment of hydrophone arrays was sufficiently close to the area and in the same locations across multiple years. Based on discussions with SSC and a subsequent review of additional locations, the available hydrophone locations, and number of fish detected each year, three sites were selected for detailed analysis using a multistate model: Water Project Area, Head of Old River, and Turner Cut

(Figure 1). Once the areas and years were selected, the UnTRIM model produced all hydrodynamic outputs at a center point or cross-section corresponding with each hydrophone array in the model.



Most analyses have been completed, and the purpose of this workshop is threefold: 1) present and discuss the methods and preliminary findings of the study with a technical group of resource managers, fisheries biologists, modelers, and other stakeholders; 2) solicit input and suggestions on interpretation of the project findings; and 3) identify any additional analyses that should be implemented. This memorandum provides a high-level summary of what will be presented and discussed in detail during the workshop to orient participants to the modeling approach and initial findings.

## Approach

A multistate Markov model for fish movement analysis was chosen because it allows individual fish to make any number of movements, or “transitions,” between states and allows for evaluation of fish-specific and time-dependent covariates. State transitions can be modeled with the same or different covariates, which allows for a more detailed analysis of the influence that localized

hydrodynamics have on fish movements. The model outputs are transition probabilities, or the likelihood of a fish transitioning from one state to another.

Hydrophone detections were analyzed using the multistate model to estimate transition rates of acoustic-tagged steelhead at each area of interest in response to important covariates. Covariates considered during model fitting included river flow, current speed (center channel and side of channel), water temperature, percentage of Sacramento River water, salinity, total exports, time of day, release day, and fish length. It is commonly hypothesized that river flow or current speed would be the most important cue for fish transitions (CAMT 2018); therefore, baseline models included either flow or velocity. Flow-based models were determined to be more informative for managers and are presented below.

Hydrodynamic variables were considered as either instantaneous (at a 15-minute timestep) or as tidally averaged. Because the variables of interest vary widely in units and magnitude, all data were standardized (centered on the mean and scaled on the standard deviation) before being used for model fitting. At each area of interest, covariates were only fit to state transitions with adequate representation (i.e., greater than 20 transitions per covariate). Determination of whether hydrodynamic variables should be included together in the model was based on pairwise plots, correlation coefficients ( $R \leq 0.6$ ), and variance inflation factors (VIFs;  $VIF \leq 3$ ), with final determination based on VIFs (Zuur et al. 2009).

The best fit fish movement model(s) was selected for each area of interest by adding single variables to the baseline flow model. The best single variables were used to build a full model. Model selection was based on Akaike information criterion (AIC), a commonly used criterion for selecting the best predictive model (Ding et al. 2009). Model fit was also assessed by comparing model-predicted versus observed data. The fitted model slope coefficients were used to interpret how the individual covariates influenced transition probabilities.

Using this analytical approach, preliminary results and interpretations of the data for the three areas evaluated are outlined in the following sections.

## Water Project Area

The Water Project Area includes three hydrophone arrays: Central Valley Project (CVP), State Water Project radial gates (RG), and West Canal (WCL) (Figure 2). A total of 789 fish were detected over 3 years, including 117 in 2014, 218 in 2015, and 454 in 2016. The median time fish spent in the Water Project Area was 15.6 hours, and 90% of fish spent less than 6.5 days here. A summary of the data and model findings are included in the following sections.

**Figure 2**  
**Water Project Area**



White arrows indicate positive direction of flow.

## Data Summary

- Fish spent a longer time near water projects than the other two areas evaluated, and the chance of remaining at CVP was high.
- Flow in West Canal was reversed (i.e., flow was in the upstream direction) 63% of the time, but 80% of fish experienced at least some downstream flow when at the West Canal array.
- Fish did not show a predominant direction of movement.
- Percentage of Sacramento River water is variable throughout the season and from year to year (20% to 80%); it was generally highest at West Canal and lowest at CVP.

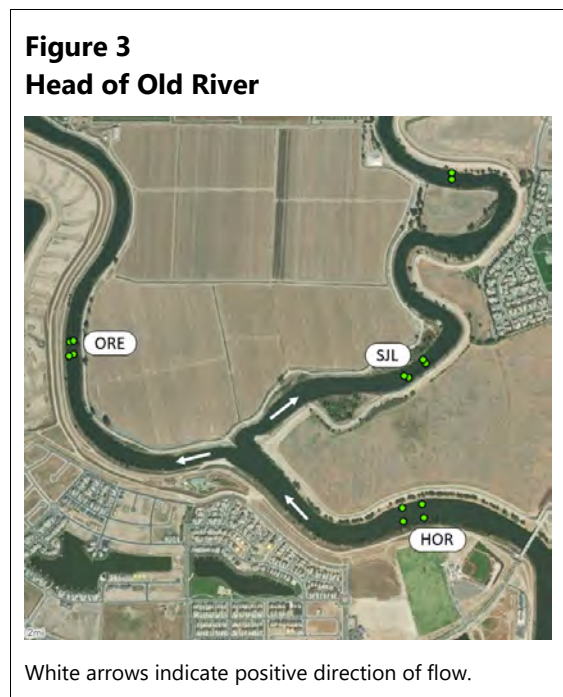
## Model Findings

- Key variables included in the best fit fish movement model were instantaneous flow at West Canal, difference in percentage of Sacramento River water between West Canal and CVP, and fish release date.
- The chance of fish moving downstream (toward West Canal) was increased by increasing downstream flow (or decreasing reverse flow) in West Canal.
- The chance of fish moving upstream (toward water projects) was increased by decreasing downstream flow (or increasing reverse flow).
- Increasing the difference in the percentage of Sacramento River water between WCL and CVP and later release date increased the chance of both upstream and downstream movements. This may indicate nondirectional movement and exploratory behavior.
- The cumulative probability of a fish remaining at CVP once detected there was high.

- The cumulative probability of a fish detected at West Canal (WCL) or radial gates (RG) transitioning to CVP increased to approximately 70% after 6 days.

## Head of Old River

The Head of Old River junction includes three hydrophone arrays: Head of Old River on the mainstem (HOR), San Joaquin River downstream on the mainstem (SJL), and Old River (ORE) (Figure 3). This junction was evaluated only during periods when the HOR barrier was out, as the intent was to assess variables influencing fish behavior and route selection. A total of 1,934 fish were detected over 5 years, including 17 in 2012, 917 in 2013, 144 in 2014, 274 in 2015, and 582 in 2016. The median time fish spent at this junction was 2.6 hours, and 90% of fish spent less than 1.1 days here. A summary of the data and model findings are included in the following sections.



## Data Summary

- The most common direction of fish movement was from Head of Old River onto Old River (i.e., downstream). The second most common was moving downstream on the mainstem.
- There were also a substantial number of movements from downstream on the mainstem to Old River (i.e., "backtracking").
- Movements upstream out of Old River were uncommon.
- Flow on the mainstem was reversed about 40% of the time, while flow on Old River was only reversed about 22% of the time.

- Most fish moved through this area quickly (approximately 1 day; i.e., "migrators") but a subset of fish did not (i.e., "nonmigrators").

## Model Findings

- Key variables in the best fit fish movement model were Old River flow, San Joaquin River flow, water depth, and being classified as a migrator.
- The chance of staying on the mainstem (HOR to SJL) was increased by the following:
  - Increasing downstream mainstem flow (strongest influence)
  - Decreasing downstream flow on Old River (lesser influence)
- The chance of leaving the mainstem (HOR to ORE) was increased by the following:
  - Increasing downstream mainstem flow
  - Increasing downstream flow on Old River
- The chance of moving downstream on either route was reduced by increasing water depth and by being classified as a nonmigrant.
- As flow on the mainstream increased, the chance of backtracking decreased (SJL to ORE, SJL to HOR).
- As flow on Old River increased, the chance moving upstream out of Old River decreased.
- Migrator status had the greatest influence on cumulative transition probability for moving downstream to SJL or ORE, and for backtracking from SJL to ORE compared to flow and water depth.

## Turner Cut

The Turner Cut junction includes three hydrophone arrays: San Joaquin Shipping Channel (SJS), San Joaquin River at MacDonald Island (MAC), and Turner Cut (TC) (Figure 4). A total of 576 fish were detected over 3 years, including 29 in 2013, 91 in 2015, and 456 in 2016. The median time fish spent at this junction was 9.4 hours, and 90% of fish spent less than 1.3 days here. A summary of the data and model findings are included in the following sections.

**Figure 4**  
**Turner Cut**



White arrows indicate positive direction of flow.

## Data Summary

- Most of fish spent a similar amount of time near Turner Cut as at the Head of Old River junction. There were very few "lingering" fish.
- Most of the transitions (64%) were fish continuing downstream on the mainstem (SJS to MAC).
- Only about 15% of transitions were fish entering Turner Cut from upstream (SJS to TC). Similarly, 15% of transitions were fish backtracking on the mainstem (MAC to SJS).
- There were very few transitions out of Turner Cut (3%; TC to MAC or TC to SJS) or backtracking into Turner Cut (3%; MAC to TC).

## Model Findings

- Key variables in the best fit fish movement model were flow on the San Joaquin River, flow in Turner Cut, percentage of Sacramento River water, and time of day.
- The chance of downstream transition on the mainstem (SJS to MAC) was increased by the following:
  - Increasing downstream mainstem flow
  - Presence during the morning to evening (5 a.m. to 8 p.m.) timeframe, relative to night (8 p.m. to 5 a.m.)
- The chance of returning upstream on the mainstem (MAC to SJS) was:
  - Increased by decreasing downstream mainstem flow

- Decreased by presence in the evening (4 p.m. to 8 p.m.), relative to night (8 p.m. to 5 a.m.)
- The chance of entering Turner Cut from upstream on the mainstem (SJS to TC) was increased by the following:
  - Presence during the morning to evening (5 a.m. to 8 p.m.) timeframe, relative to night (8 p.m. to 5 a.m.)
  - Decreasing downstream flow out of Turner Cut (into the San Joaquin River)
- The chance of backtracking into Turner Cut from downstream on the mainstem (MAC to TC) was increased by decreasing downstream mainstem flow.
- The chance of leaving Turner Cut and returning to the mainstem (TC to SJS) was increased by increasing downstream flow on Turner Cut.
- Cumulative transition probabilities are strongly driven by tidal fluctuations.

## **Workshop Participation Feedback and Discussion**

This memorandum was intended to provide a high-level summary of the content that will be presented and discussed in more detail during the workshop. We have dedicated time on both days for discussion with workshop participants, and we would like to solicit input on the following questions:

- Are there any additional elements that should be included in the model?
- Is there anything we're missing on the interpretation?
- How should we present the information so that it is most useful to managers?

## A.3 Stakeholder Meeting Presentation

---



# Evaluation of Juvenile Steelhead Behavioral Responses to Hydrodynamic Conditions in the Sacramento-San Joaquin Delta

Presented by  
Anchor QEA and USGS  
November 17-18, 2021



17306074771\_22cac6d7a7\_o.jpg by formulalone  
is licensed under Creative Commons BY-SA 2.0

# Introduction

- Acknowledge SWC, MWD, DSC
- Introduction to the team
  - John Ferguson and Michael MacWilliams, principal investigators
  - Sydney Gonsalves, lead analyst, with support from John Plumb, Russ Perry, Mike Dodrill, and Adam Pope (USGS)
  - Aaron Bever, hydrodynamic modeler, UnTRIM
  - Michelle Havey, project manager
- Workshop format and agenda
- WebEx tools
  - Audio
  - Q&A versus chat

# Project Overview

- Developed out of SST-identified need for more detailed analysis of fish behavior
- Combine detailed 3D hydrodynamic model predictions with steelhead telemetry data
- Compliments other recent Sacramento-San Joaquin Delta work on salmonid behavior and survival in the delta
- Methods consistent with USGS (partner) Chinook Salmon analysis

# Project Timeline

- Fall 2020 – CAMT Salmon Subcommittee presentation
  - Preliminary methods
  - Areas of interest
- Fall 2021 – Stakeholder workshop
- Spring 2022 – Final report

# Workshop Objective

Report on work completed:

- Available information
- Methods
- Preliminary findings

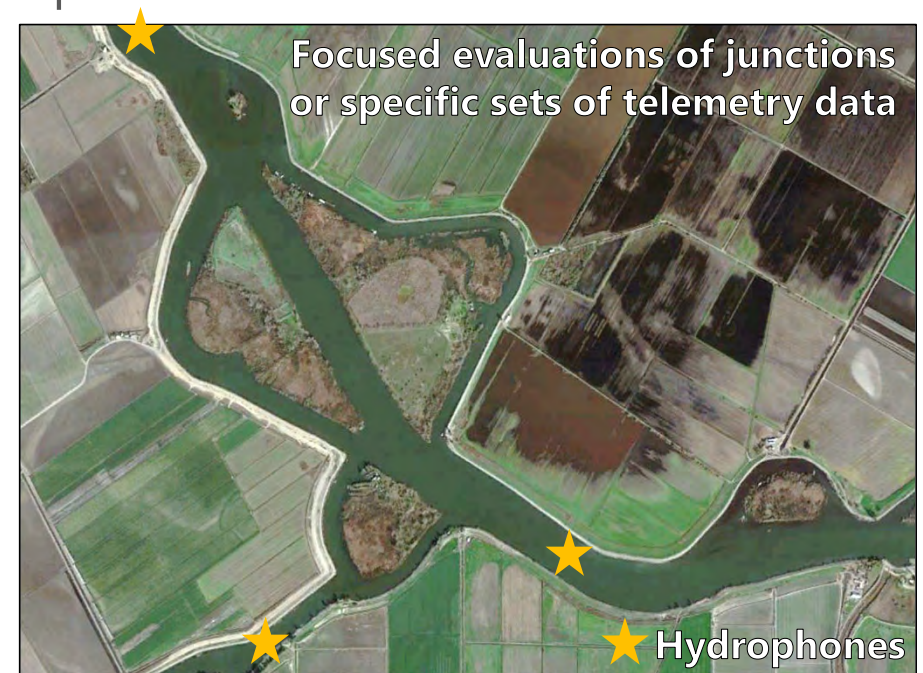
Participants:

- Input and suggestions on interpretation
- Identify additional analyses or interpretations
  - Within scope of current methods and areas considered

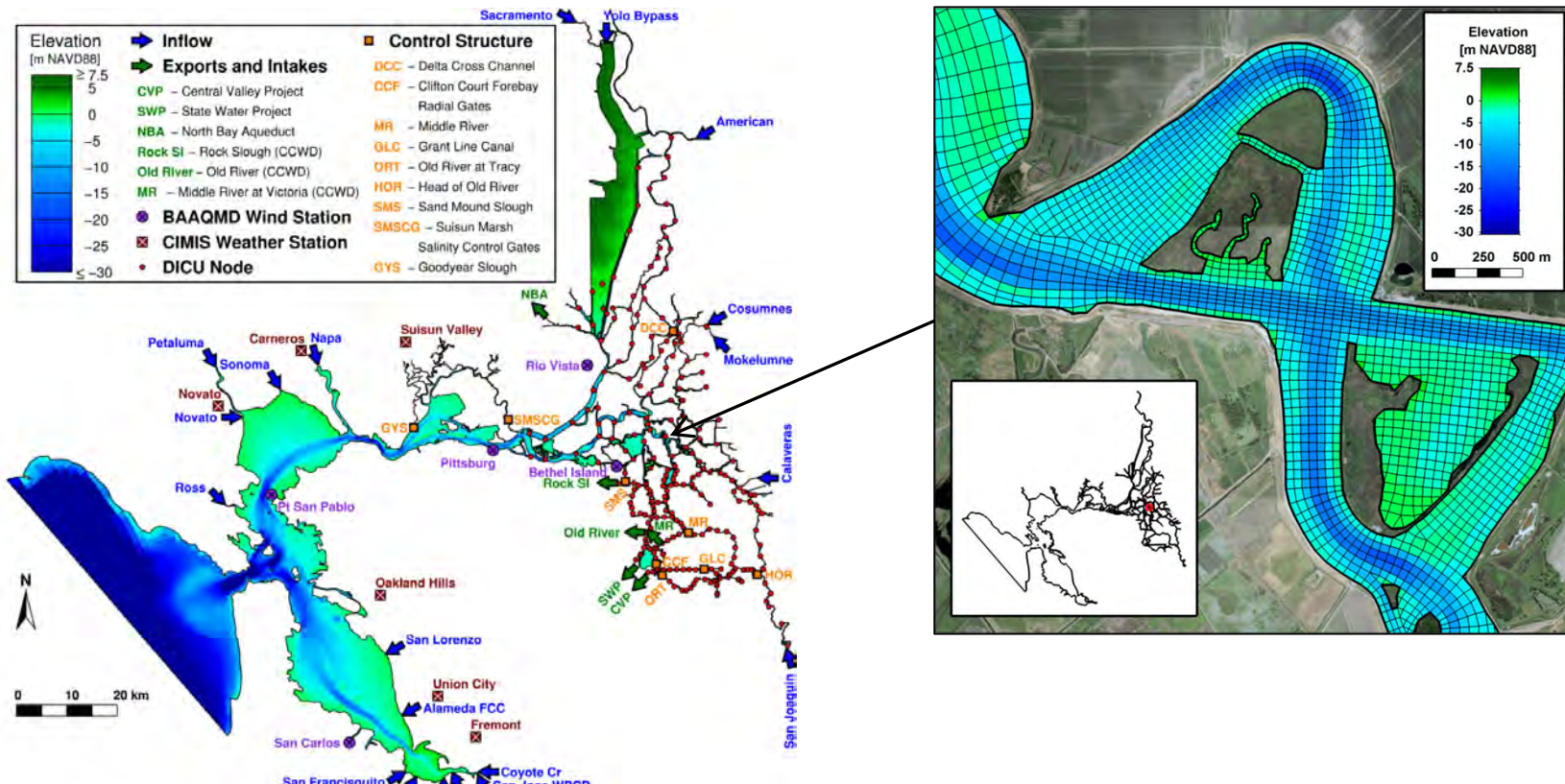
# Methods Overview

# Hydrodynamic Modeling

- Use 3D UnTRIM Bay-Delta Model to predict environmental conditions throughout the Delta down to a 90s timestep
- Extract environmental variables from hydrodynamic model
  - Predictions of what a fish would have experienced at a given time and location
  - Modeled environmental variables available at finer temporal and/or spatial scales than observation data



# UnTRIM Bay-Delta Model



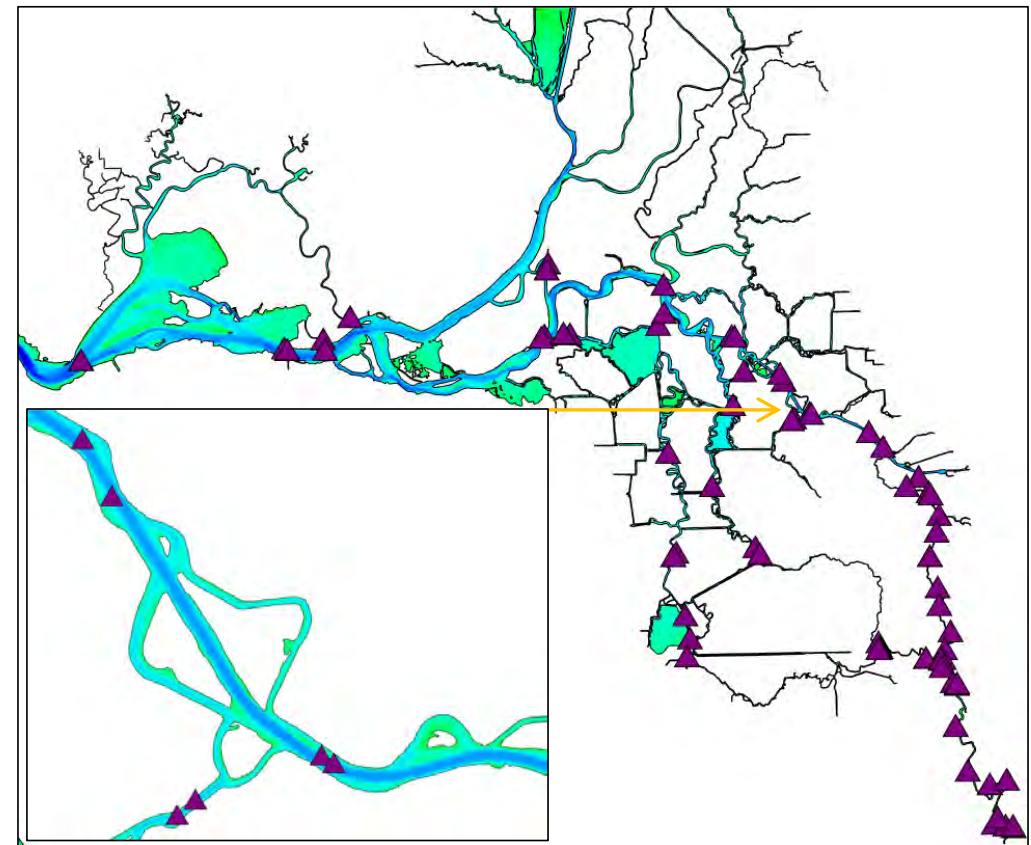
# Hydrodynamic Modeling

- Simulated the periods of telemetry data collection
  - 2011, 2012, 2013, 2014, 2015, 2016
- Tagged Sacramento River water with a tracer to predict the percent of Sacramento River water at hydrophone array locations
- Extracted predictions of 8 environmental variables directly from the hydrodynamic model
- Calculated another 6 variables from model predictions
- Instantaneous, tidally averaged, and daily variables

# Environmental Variables from Hydrodynamic Model

Directly Extracted From Model

Variable	Frequency
Cross-sectional water flow	90 seconds
Depth-averaged salinity	
Depth-averaged temperature	
Water level	
Water depth	
Depth-averaged percent Sacramento River water	3 minutes
Depth-averaged current speed	
Depth-averaged velocity (including direction of flow)	



10 Variables also calculated as tidally averaged

Current speed and velocity also extracted at channel center and side

# Environmental Variables from Hydrodynamic Model

## Calculated From Model Output

Variable	Frequency	Summary
OMR flow	90 seconds	Combined Old and Middle River water flow
Qwest		Water flow past Jersey Point
Delta outflow		Water flow from the Delta to the Bay
Flow toward SWP and CVP exports		Water flow toward the largest exports
Delta tributary inflows	Daily	Water inflows to the Delta
IE ratio		Ratio of San Joaquin River inflow to combined CVP and SWP exports

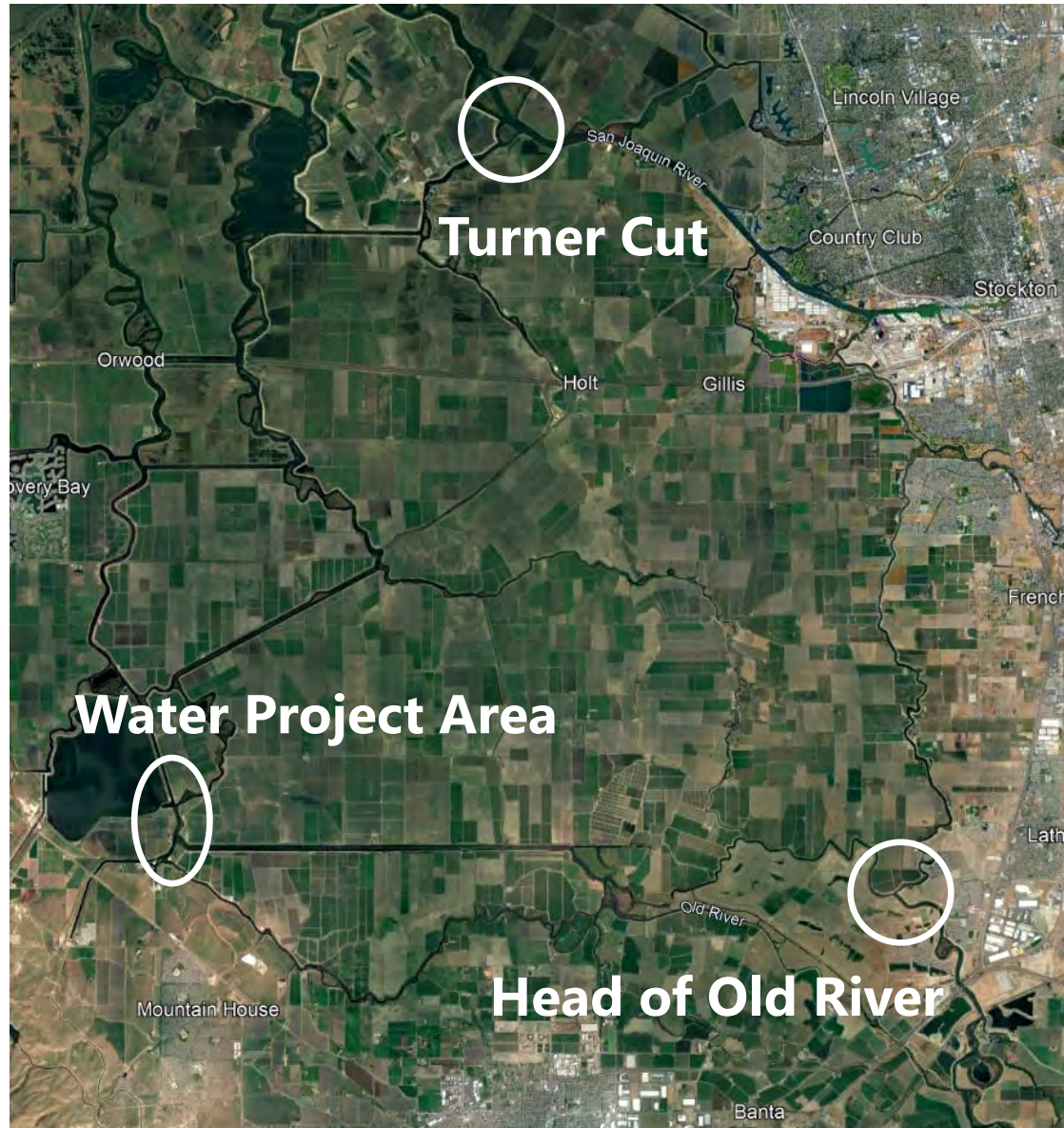
Variables on 90 second frequency also calculated as tidally averaged

# Juvenile Steelhead Telemetry Data Background

- Study fish were obtained from the Mokelumne River Fish Hatchery (MRFH)
- From 2011 to 2016, 958 to 2,196 fish were surgically implanted with acoustic transmitters and released in the San Joaquin River at Durham Ferry
- The raw acoustic tag detection data were processed into detection events for each tag by the USGS lab in Cook, Washington (2011) or Sacramento, California (2012–2016).
- A predator filter based on assumed behavioral differences between juvenile steelhead and resident predatory fish such as juvenile and subadult bass was applied by Rebecca Buchanan at University of Washington, Seattle, Washington.
- Described in more detail in Buchanan et al. 2020, Buchanan 2018a, 2018b, 2018c, and U.S. Bureau of Reclamation (USBR) 2018a, 2018b, 2018c.

## Areas of Interest

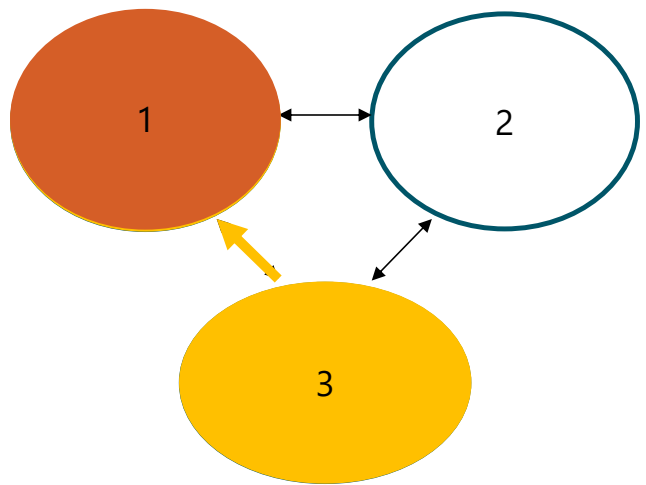
- Water Project Area
- Head of Old River
- Turner Cut



# Fish Model Overview

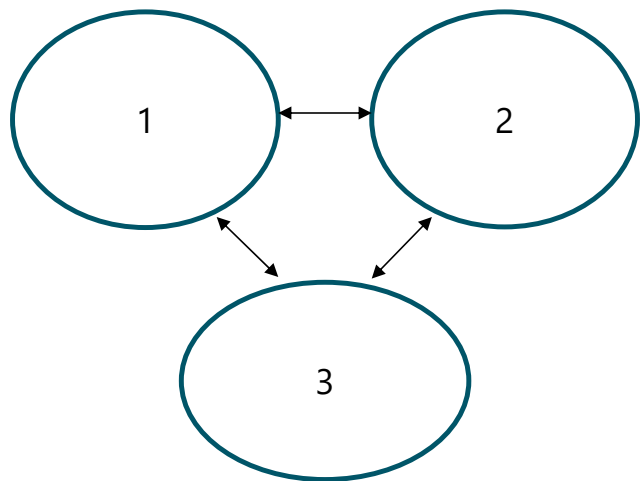
- Continuous time multistate Markov model
- Each location is a state fish can visit or “transition” to one or more times
- Allows for fish-specific and time-dependent covariates
  - 15-minute timestep
- Each transition can be modeled with the same or different covariates
- Outputs are transition probabilities

# Model Structure



$$Q = \begin{bmatrix} q_{11} & q_{12} & q_{13} \\ q_{21} & q_{22} & q_{23} \\ q_{31} & q_{32} & q_{33} \end{bmatrix}$$

# Model Structure



- With covariates

$$q_{rs}(z(t)) = q_{rs}^{(0)} \exp(\beta_{rs}^T z(t))$$

- Solve for transition probabilities

$$P(t) = \exp(tQ)$$

- Cumulative chance of transition
  - Depends on changing covariates

$$P(t_1, t_n) = P(t_1, t_2) P(t_2, t_3) \dots P(t_{n-1}, t_n)$$

# Modeling Methods

- Hypothesized that river flow or velocity would be the most important cue for fish transitions
  - All models included either flow or water velocity
- Other covariates
  - Fish specific (fork length, release day, release group, migrator status)
  - Other hydrodynamic variables and management metrics
  - Time of day, HOR barrier presence
- Many of the hydrodynamic variables were correlated
  - Inclusion based on correlation coefficients and variance inflation factors (VIFs)

# Modeling Process

- Single variables were added to the baseline flow model
- Best single variables were used to build the full model
- A manual drop 1 procedure was used on the full model to confirm the influence of each variable on fit
- Model selection using Akaike Information Criteria (AIC)
- Collinearity between predictors was checked using VIFs
- Residuals from individuals on maximum likelihood checked
- Evaluated by comparing observed data to model-predicted values

# Questions?

# Model Results

## Water Project Area

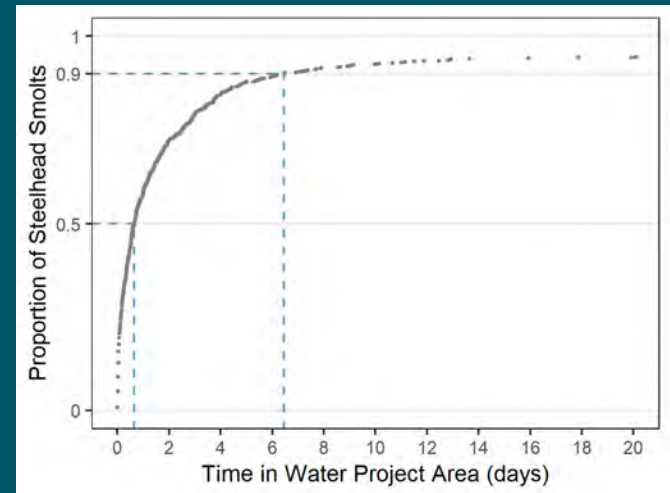
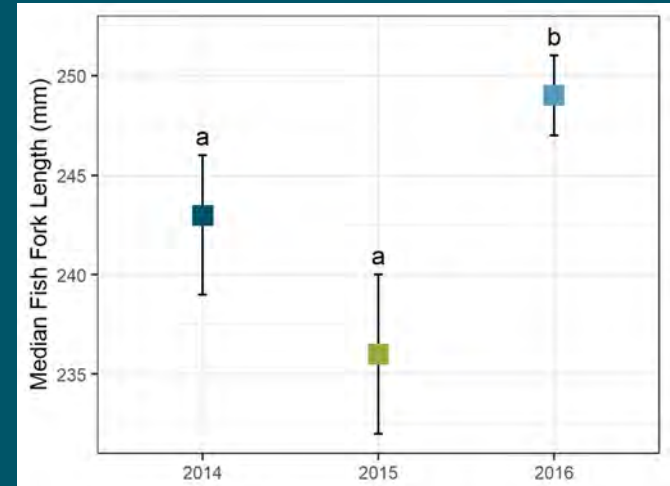


# Overview

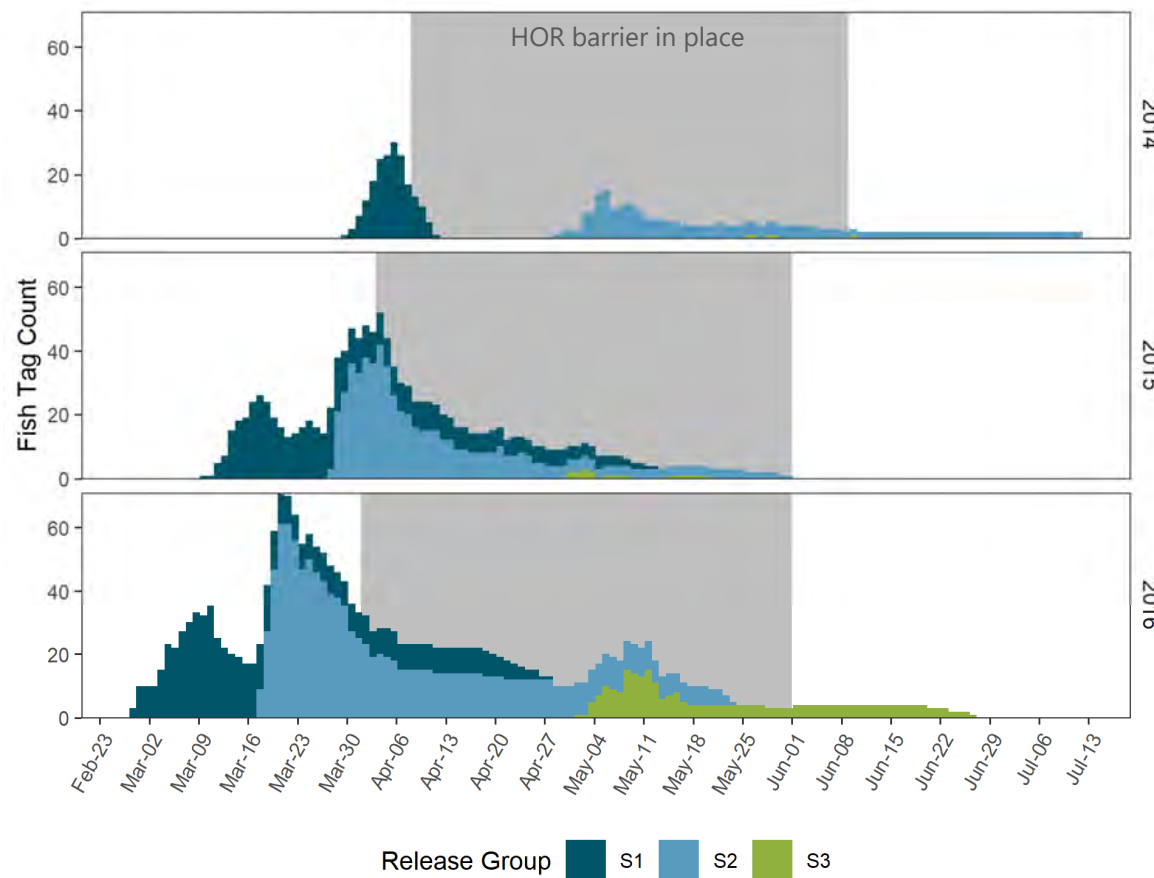
1. Fish data
2. Key hydrodynamic conditions
3. Model results
  - a. Model fit
  - b. Influence of covariates
  - c. Transition probabilities
4. Summary

## Fish Data

- 789 fish detected
  - 117 in 2014
  - 218 in 2015
  - 454 in 2016
- Median fork length greater in 2016
- Median time spent in Water Project Area was 15.6 hours (0.65 day)
- 90% of fish spent  $\leq 6.5$  days
- Predator filter applied (Buchanan 2018a, 2018b, 2018c)
- Fish censored after 20 days

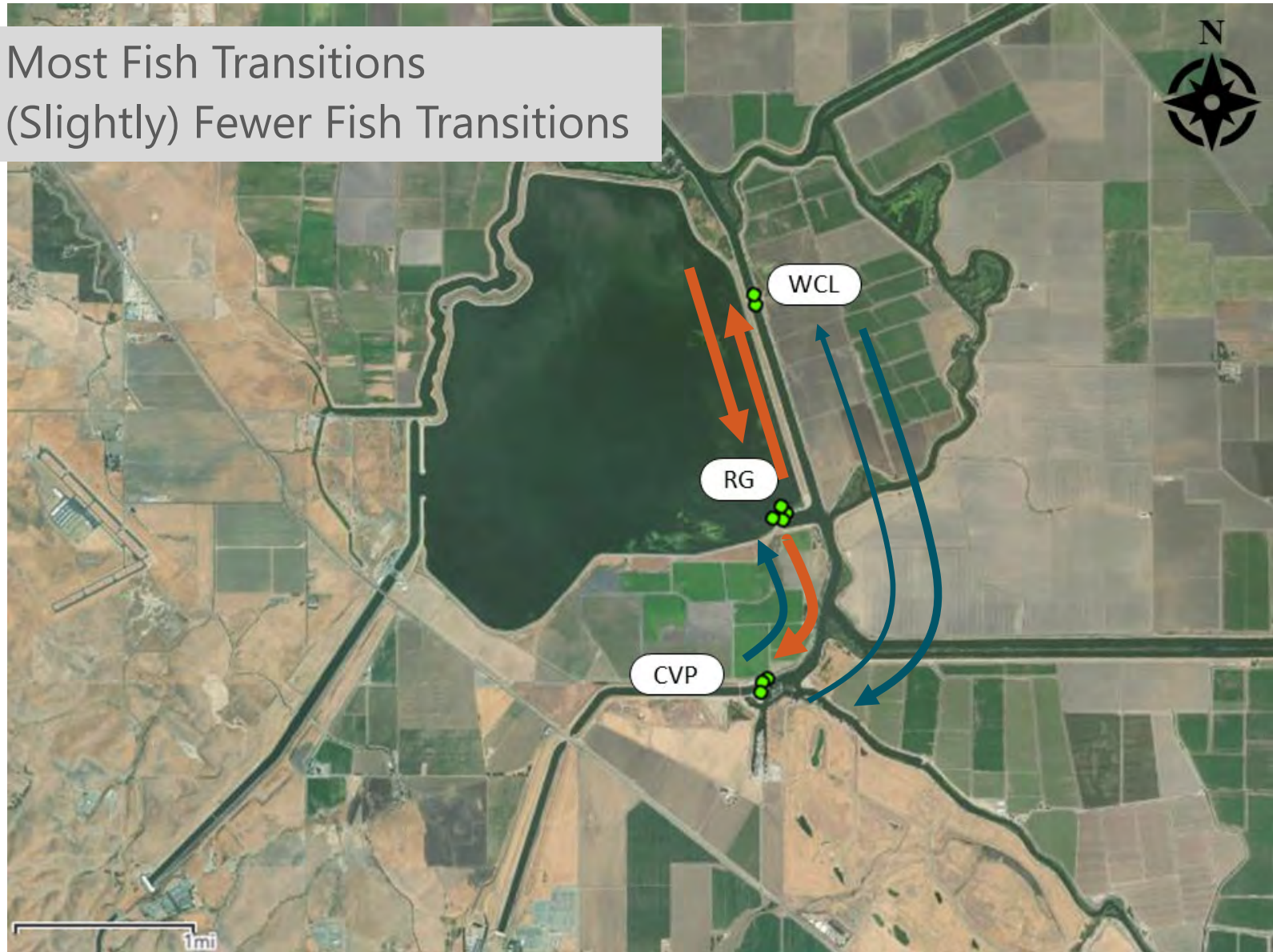


# Steelhead Timing in Water Project Area

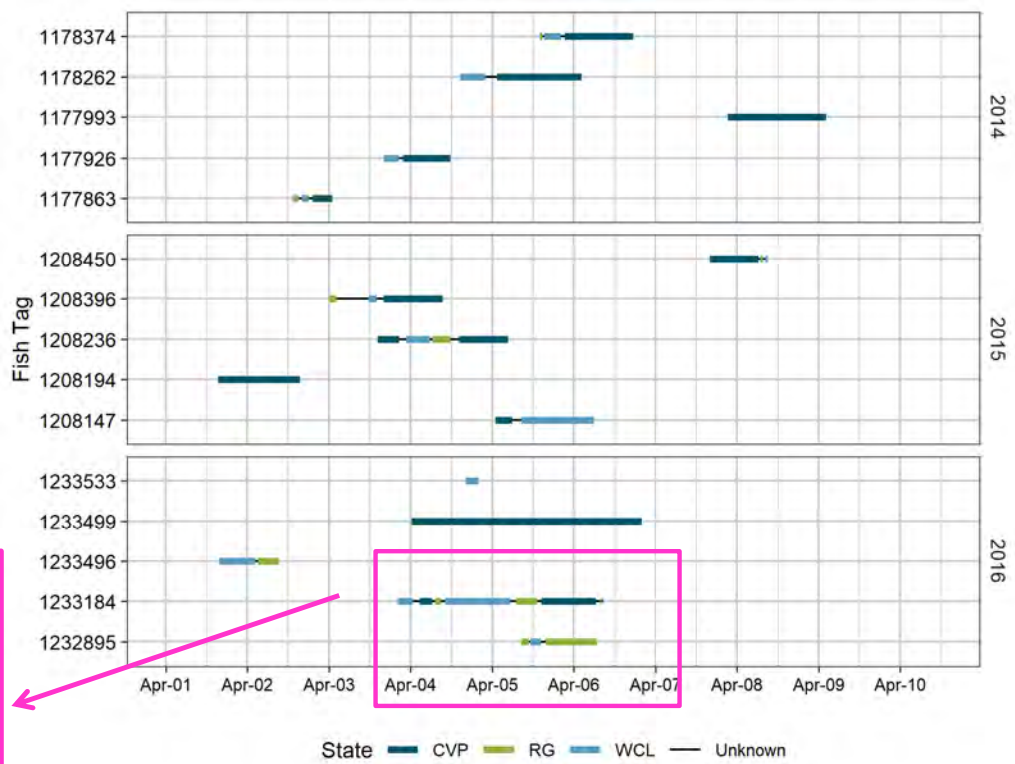
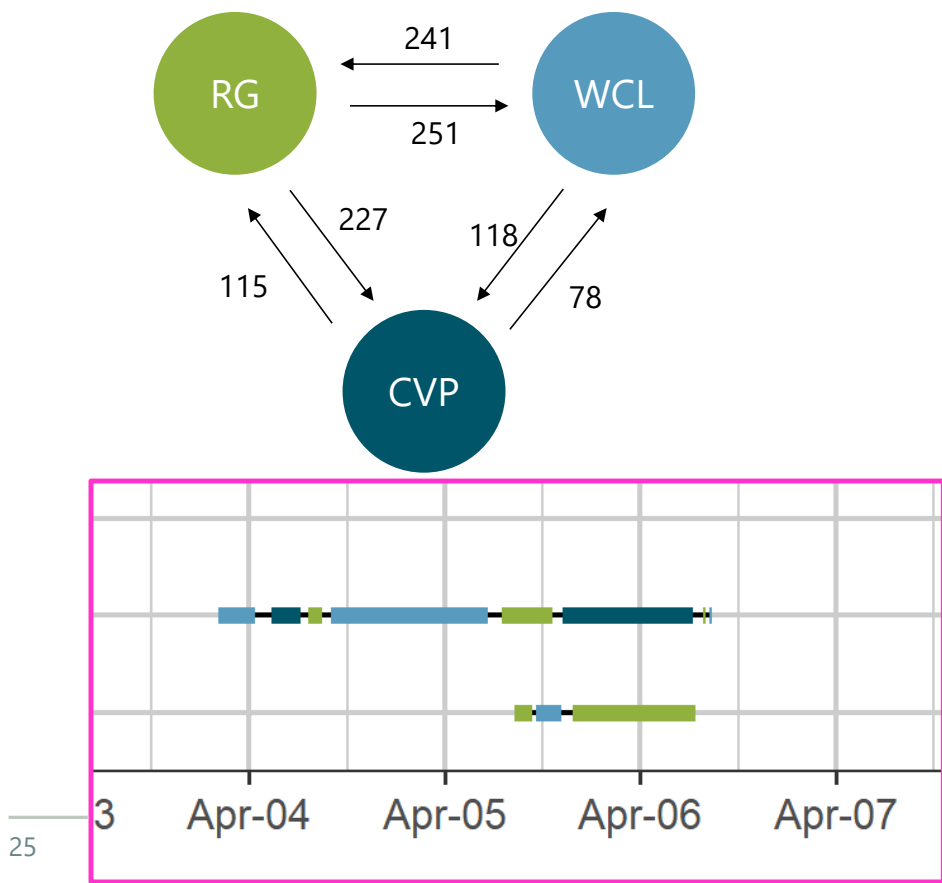


→ = Most Fish Transitions

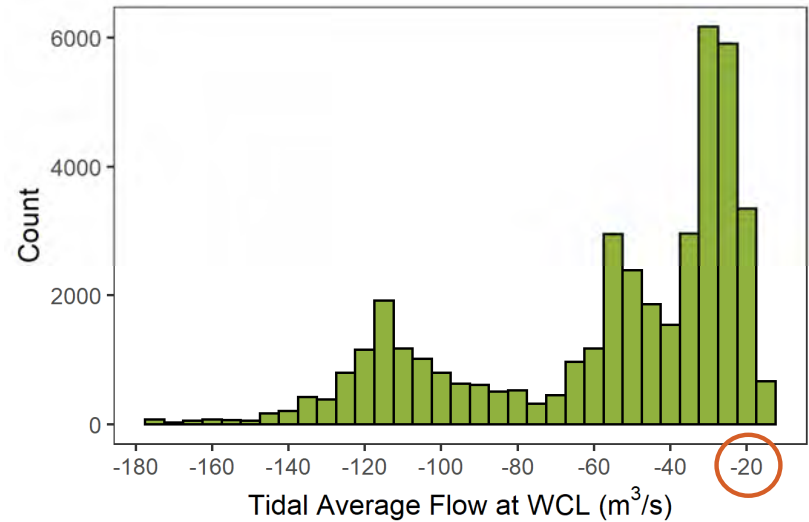
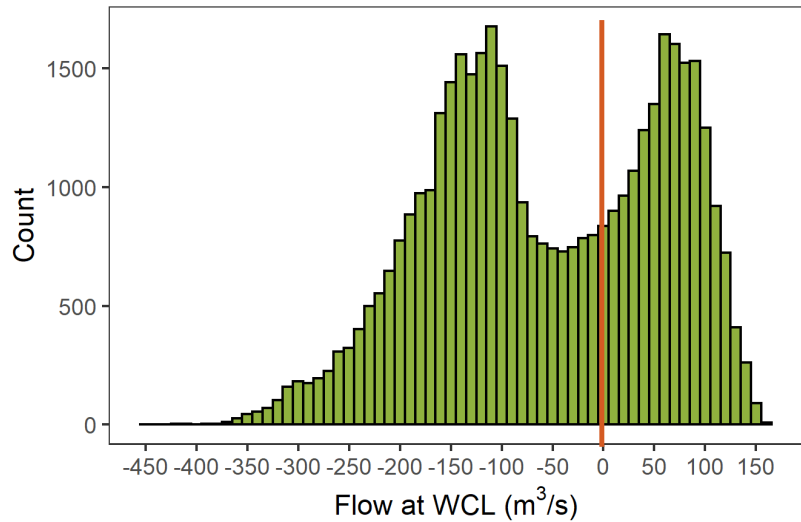
→ = (Slightly) Fewer Fish Transitions



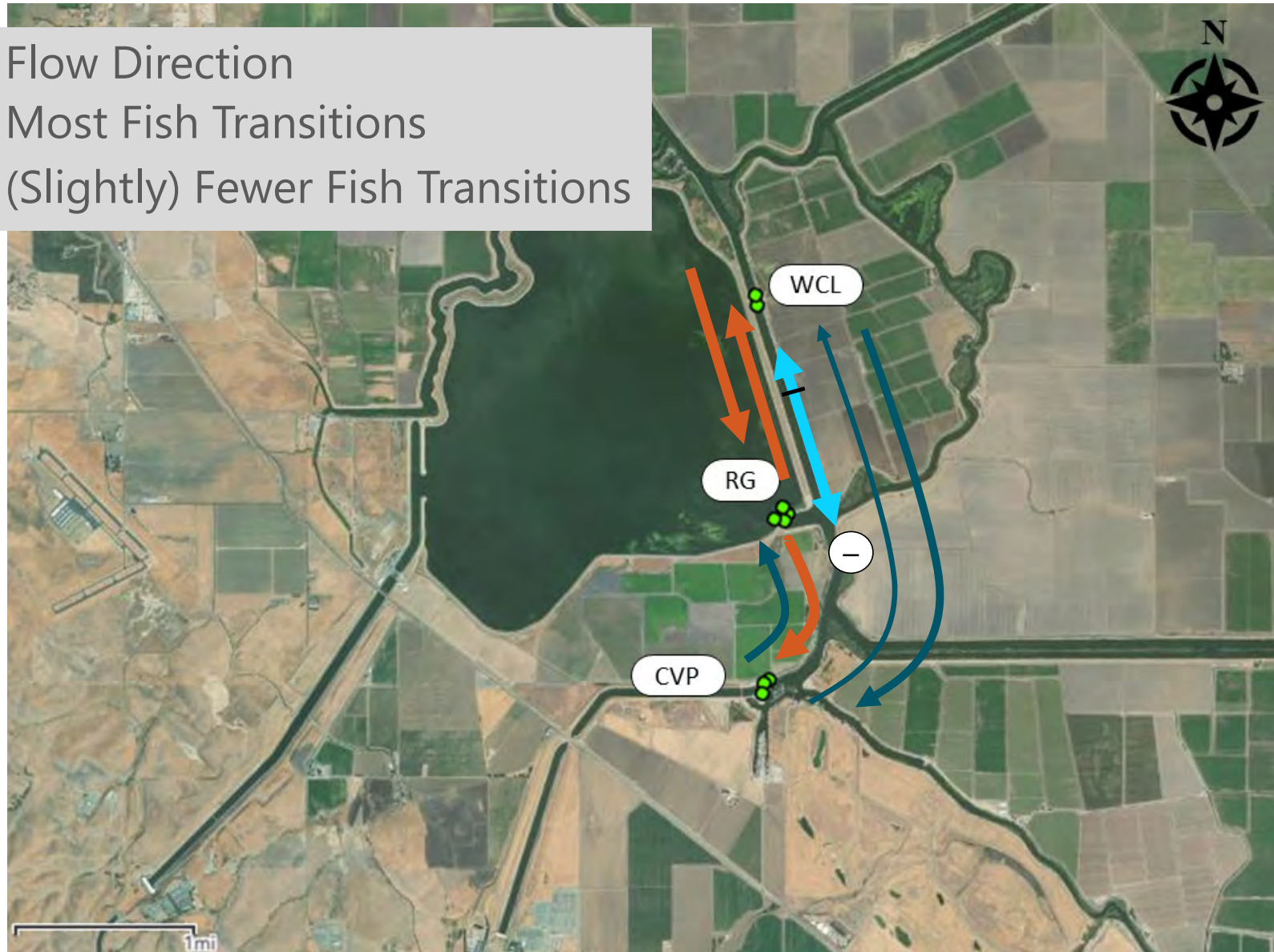
# Fish Behavior



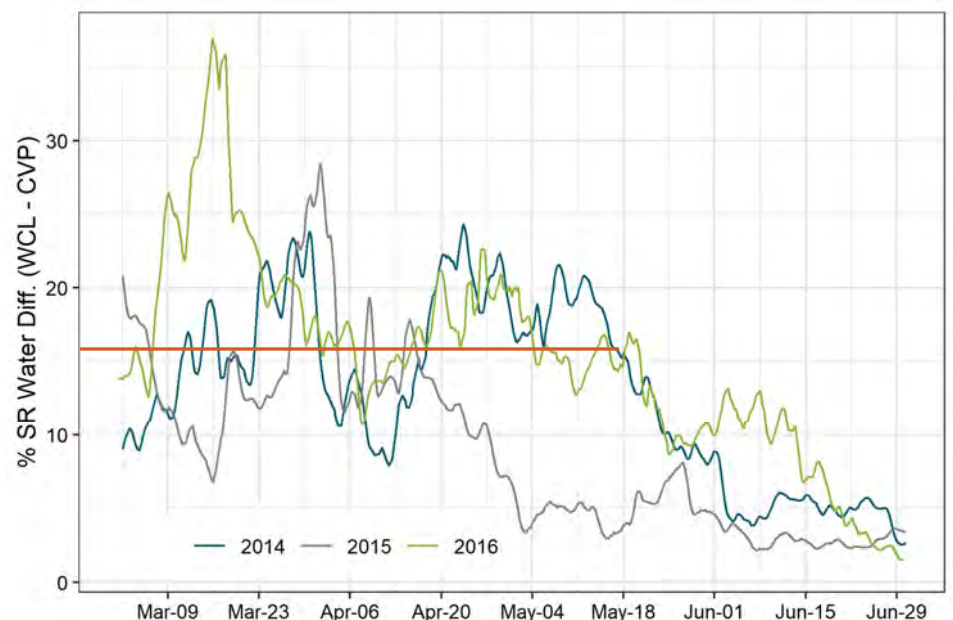
# Key Hydrodynamic Conditions: Flow



- = Flow Direction
- = Most Fish Transitions
- = (Slightly) Fewer Fish Transitions

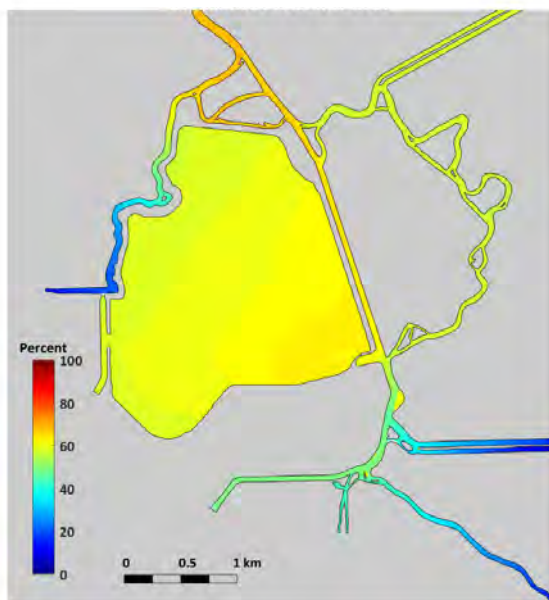


# Key Hydrodynamic Conditions: Percent of Sacramento River Water

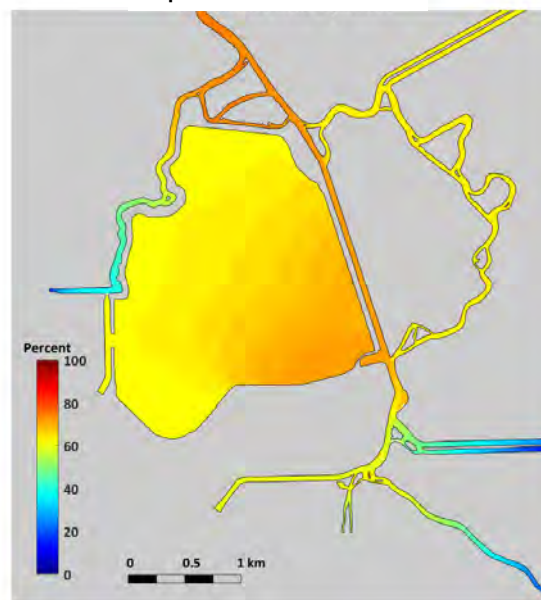


# Key Hydrodynamic Conditions: Percent of Sacramento River Water

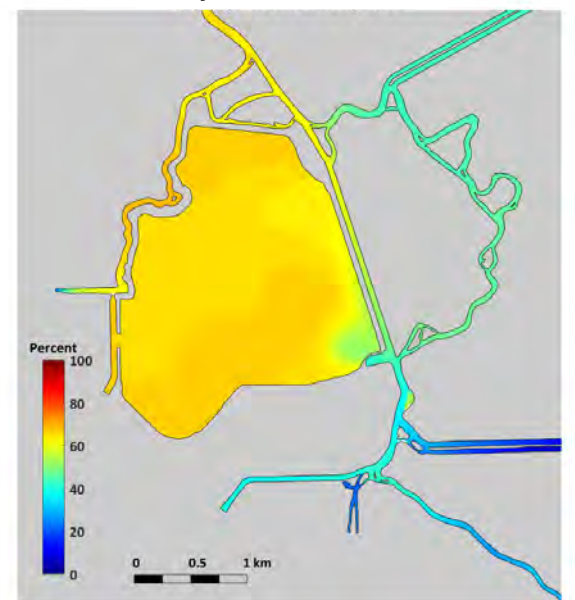
March 16 to 22, 2014



April 3 to 9, 2014

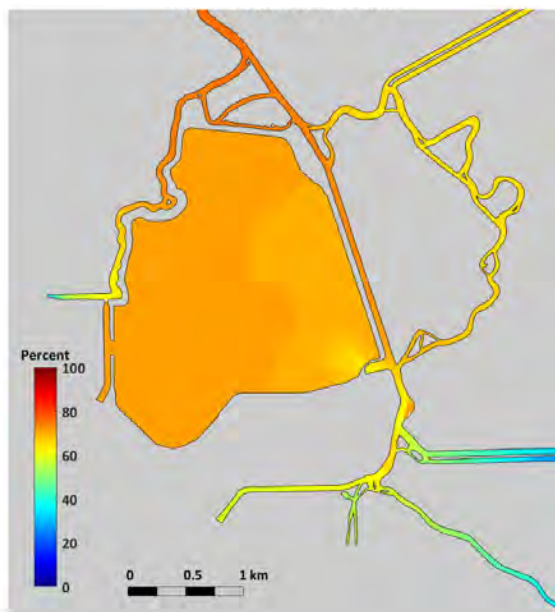


May 4 to 10, 2014

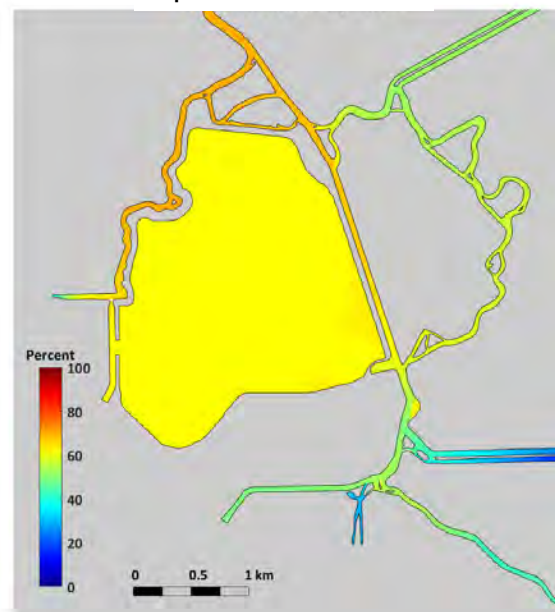


# Key Hydrodynamic Conditions: Percent of Sacramento River Water

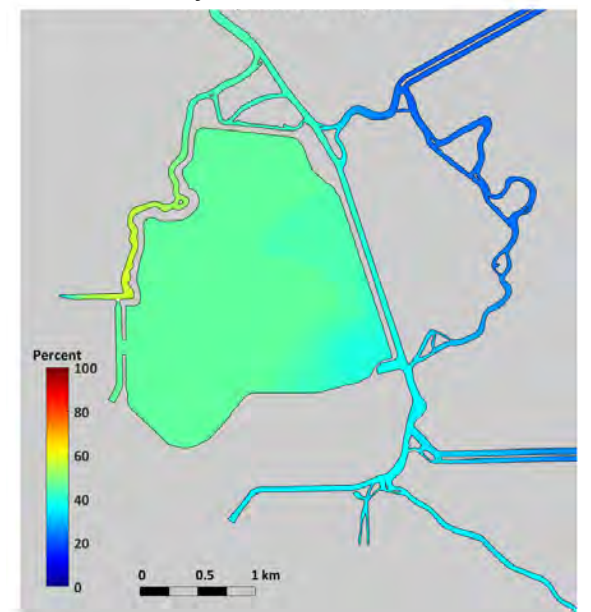
March 16 to 22, 2015



April 3 to 9, 2015

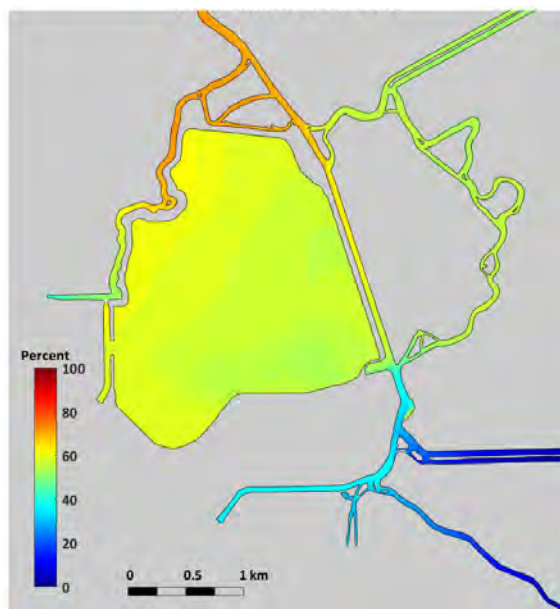


May 4 to 10, 2015

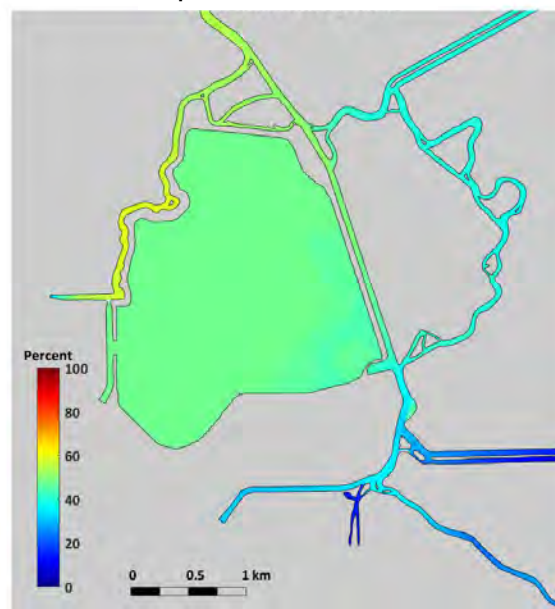


# Key Hydrodynamic Conditions: Percent of Sacramento River Water

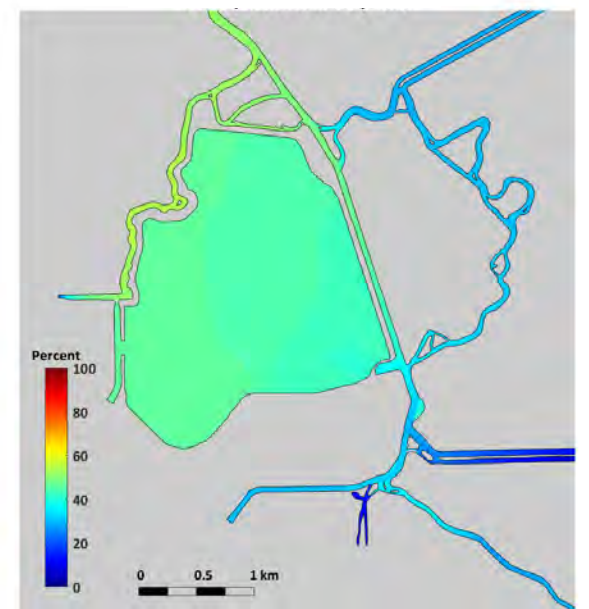
March 16 to 22, 2016



April 3 to 9, 2016



May 4 to 10, 2016



# Modeling Methods Reminder

- Single variables were added to the baseline flow model
- Best single variables were used to build the full model
- Checked influence of each individual variable on fit
- Model selection with AIC

Model	K	Deviance	AIC	ΔAIC
$Q_{WCL} + dPSW_{CVP-WCL,AT} + RD$	24	8257.0	8305.0	0.0
$Q_{WCL} + PSW_{WCL,AT} + RD$	24	8281.0	8329.0	24.0
$Q_{WCL} + PSW_{WCL} + RD$	24	8281.7	8329.7	24.7
$Q_{WCL} + TE + RD$	24	8313.3	8361.3	56.3
•	•	•	•	•
•	•	•	•	•
•	•	•	•	•
$Q_{WCL} + FL$	18	8409.8	8445.9	140.9
$Q_{WCL}$	12	8429.8	8453.8	148.7
$Q_{CVP}$	12	9041.9	9065.9	760.9
$TE$	12	9101.9	9125.9	820.8
no covariates	6	9206.5	9218.5	913.5

# Water Project Area

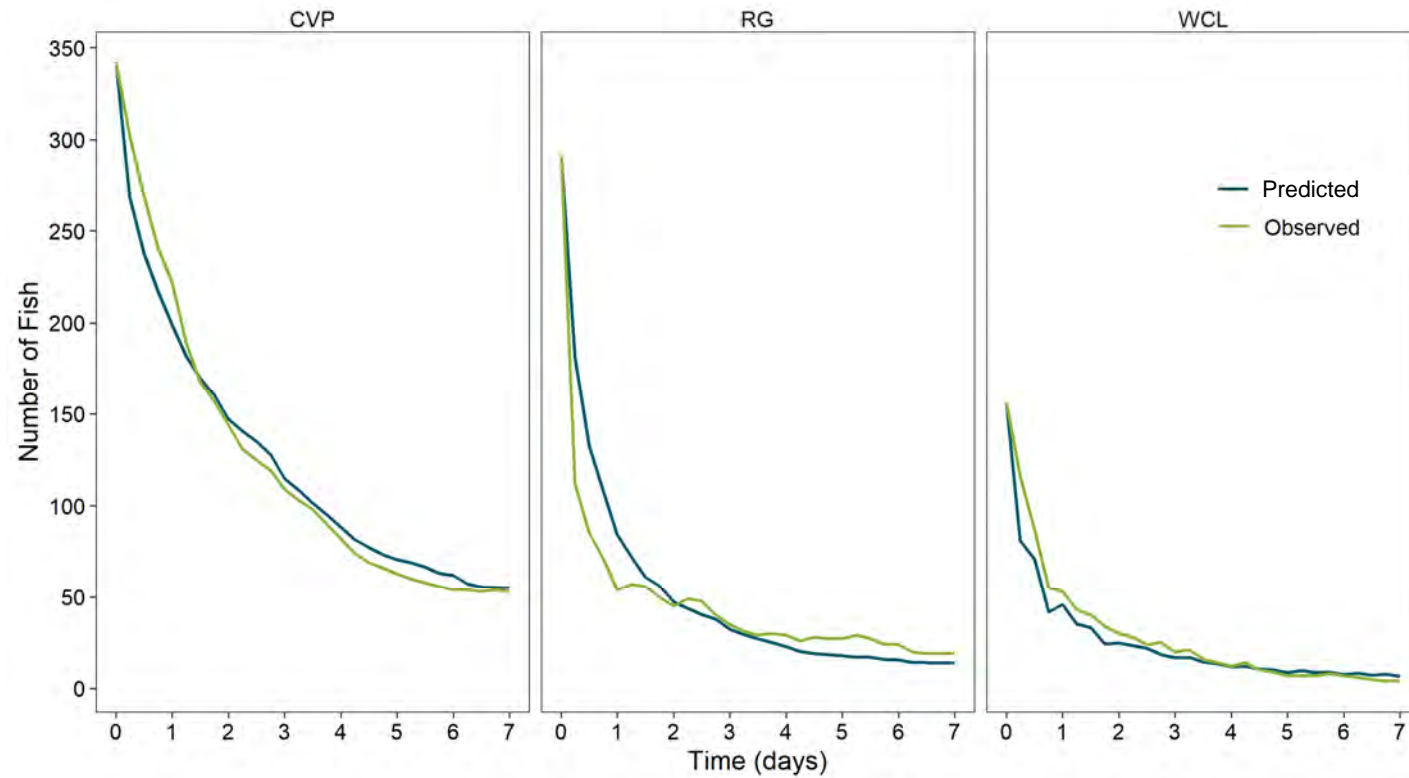
## Best Fit Model

$$\left\{ \begin{array}{l} CVP \rightarrow RG \\ CVP \rightarrow WCL \\ RG \rightarrow CVP \\ RG \rightarrow WCL \\ WCL \rightarrow CVP \\ WCL \rightarrow RG \end{array} \right. \sim Q_{WCL} + dPSW_{CVP-WCL,AT} + RD$$

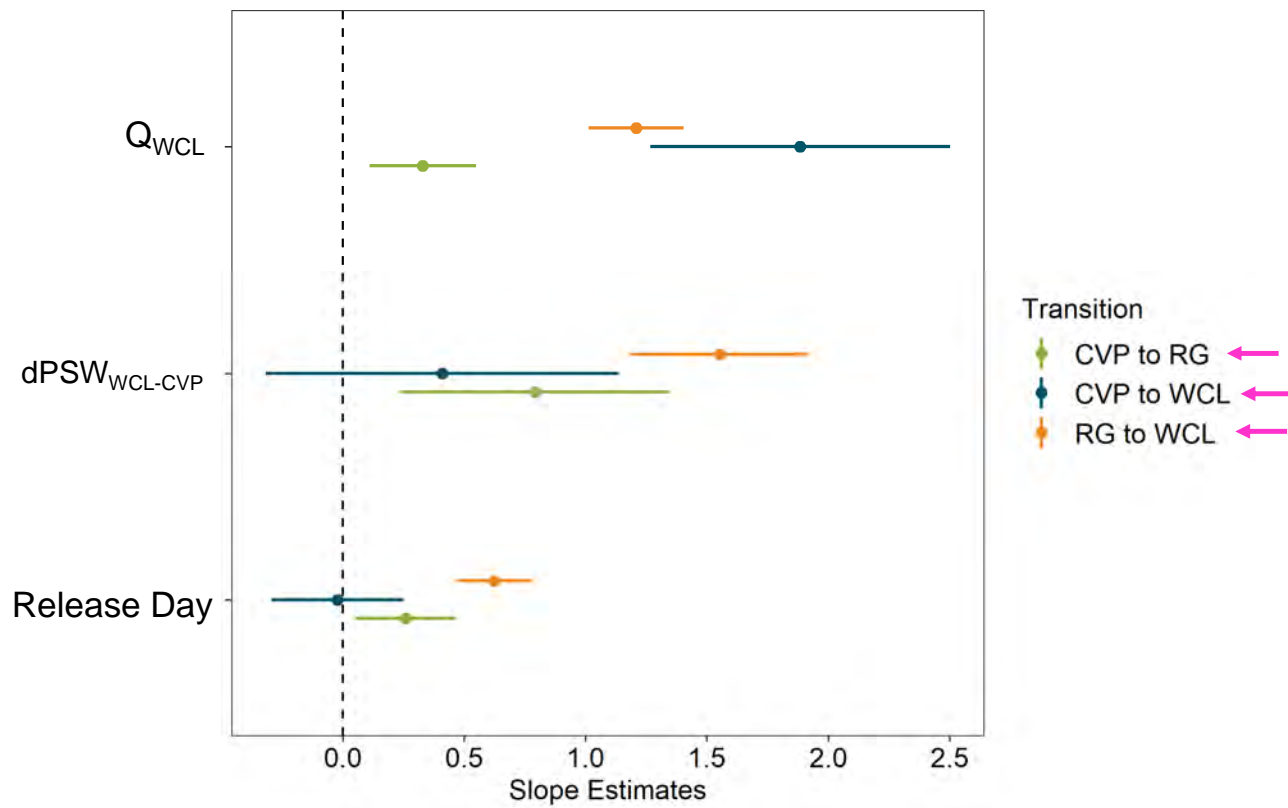


Model	K	Deviance	AIC	$\Delta AIC$
$Q_{WCL} + dPSW_{CVP-WCL,AT} + RD$	24	8257.0	8305.0	0.0
$Q_{WCL} + PSW_{WCL,AT} + RD$	24	8281.0	8329.0	24.0
$Q_{WCL} + PSW_{WCL} + RD$	24	8281.7	8329.7	24.7
$Q_{WCL} + TE + RD$	24	8313.3	8361.3	56.3
.	.	.	.	.
.	.	.	.	.
.	.	.	.	.
$Q_{WCL} + FL$	18	8409.8	8445.9	140.9
$Q_{WCL}$	12	8429.8	8453.8	148.7
$Q_{CVP}$	12	9041.9	9065.9	760.9
$TE$	12	9101.9	9125.9	820.8
no covariates	6	9206.5	9218.5	913.5

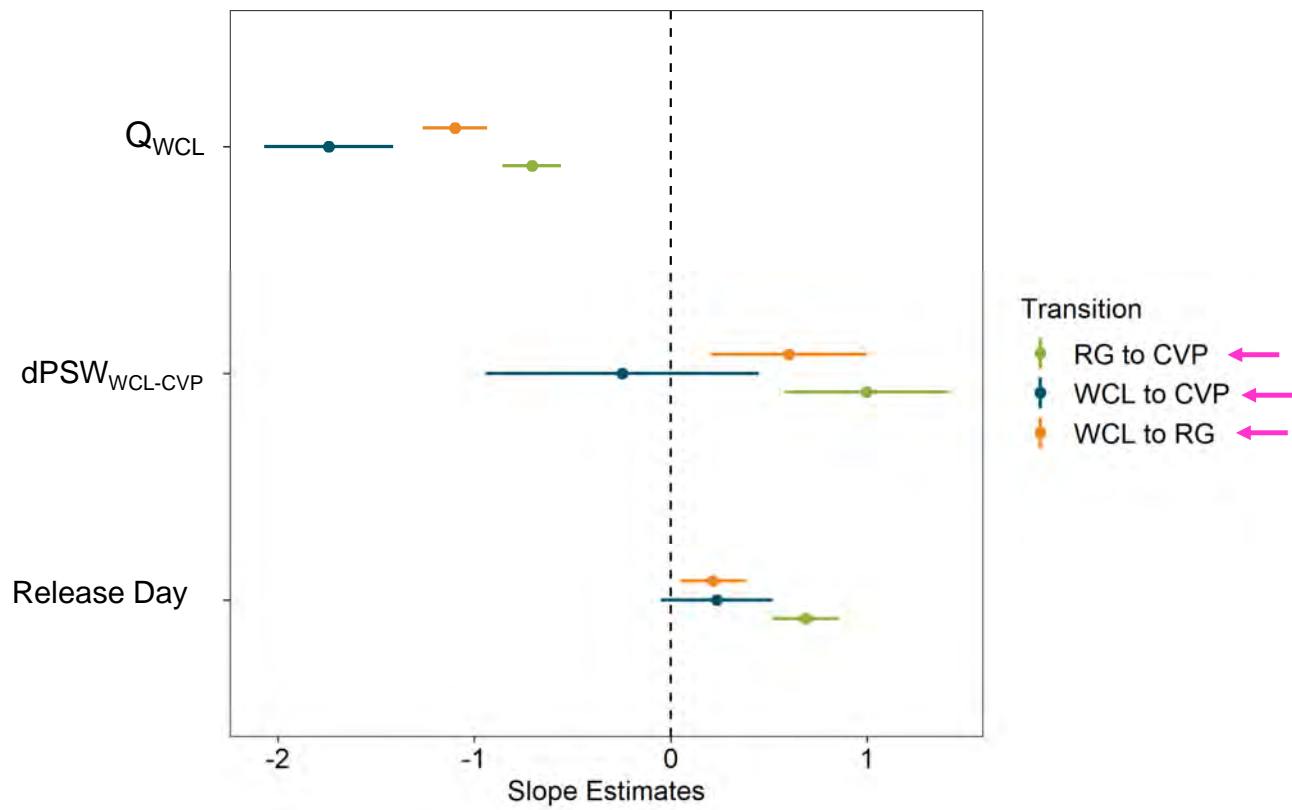
# Model Evaluation



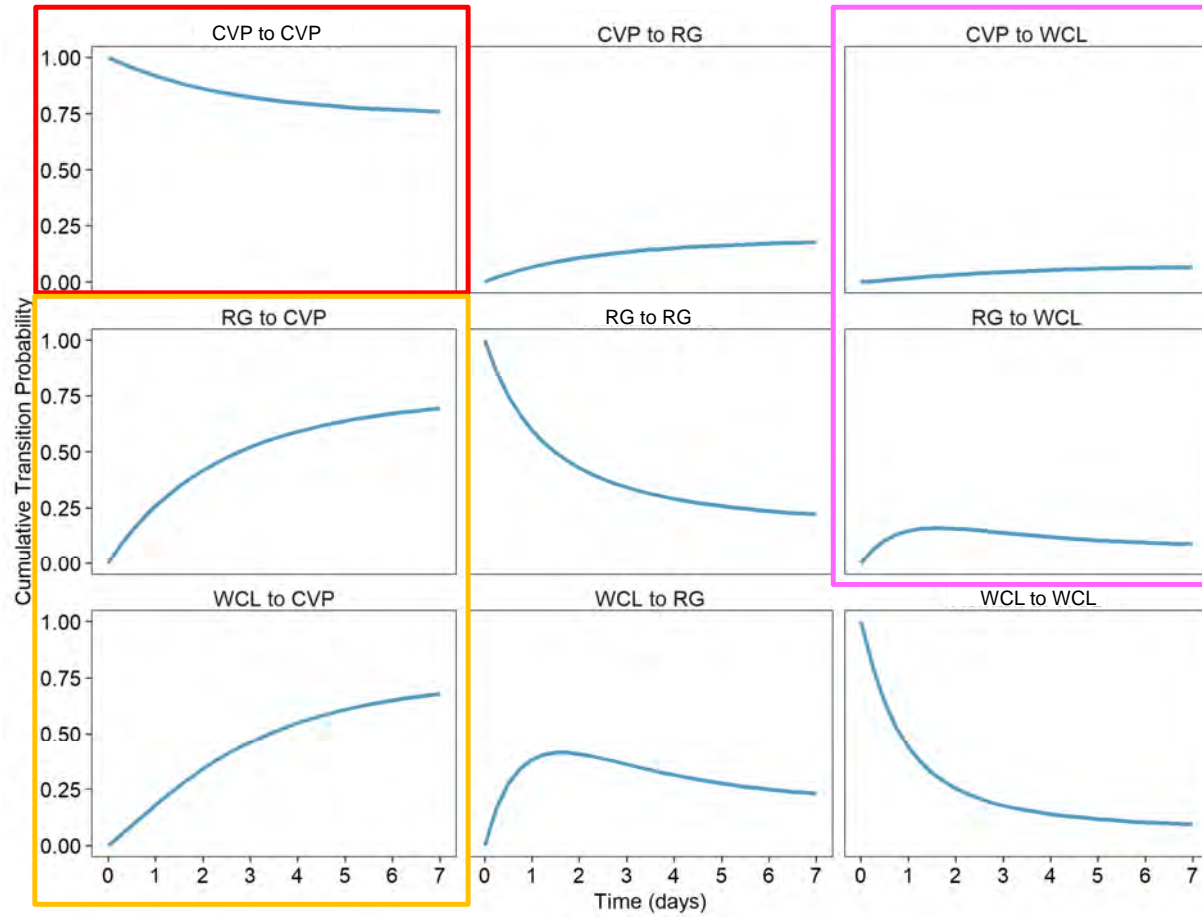
# Slope Estimates: Downstream Transition



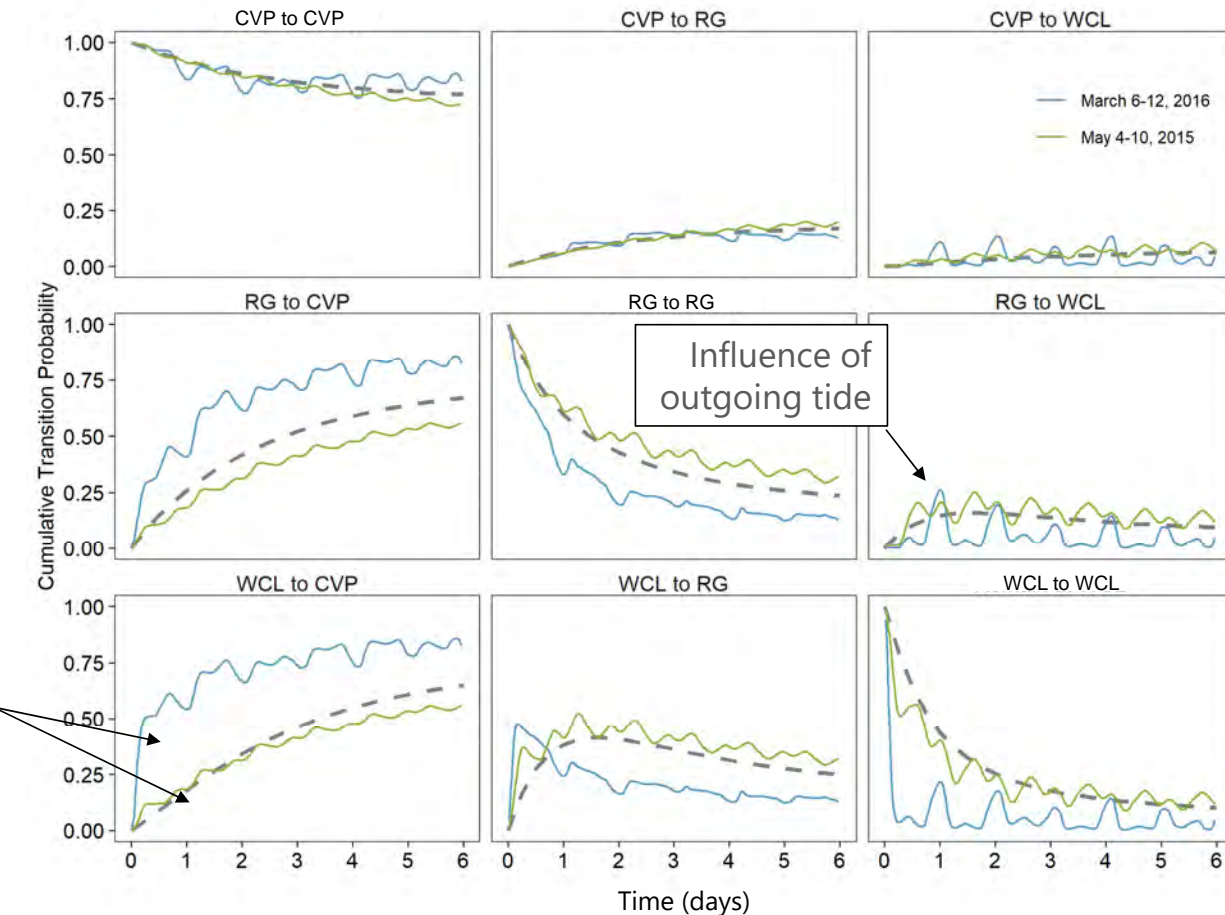
# Slope Estimates: Upstream Transition



# Cumulative Transitions: Covariate Averages



# Cumulative Transitions: Time-Varying Covariates



Averages not sufficient to fully describe variability in transition probabilities

# Summary

- Fish spent a longer time near water projects than other areas evaluated
  - The chance of remaining at CVP is high
- 80% of fish experienced some downstream flow, however flow in west canal was reversed about 63% of the time
- No predominant direction of movement
- Sacramento River water is variable throughout the season, between years (20% to 80%), and across the area

# Model Findings

- Key variables in best fit fish movement model
  - Instantaneous flow at west canal, difference in % SR water between WCL and CVP, fish release date
- Chance of fish moving downstream (toward West Canal) is increased by
  - **Increasing** downstream flow (or decreasing reverse flow) in west canal
- Chance of fish moving upstream (toward water projects) is increased by
  - **Decreasing** downstream flow (or increasing reverse flow)
- Increasing difference in percent of Sacramento River water and later release date increased the chance of both upstream and downstream movements
  - Does this suggest non-directional movement and exploratory behavior by fish?

# Model Findings

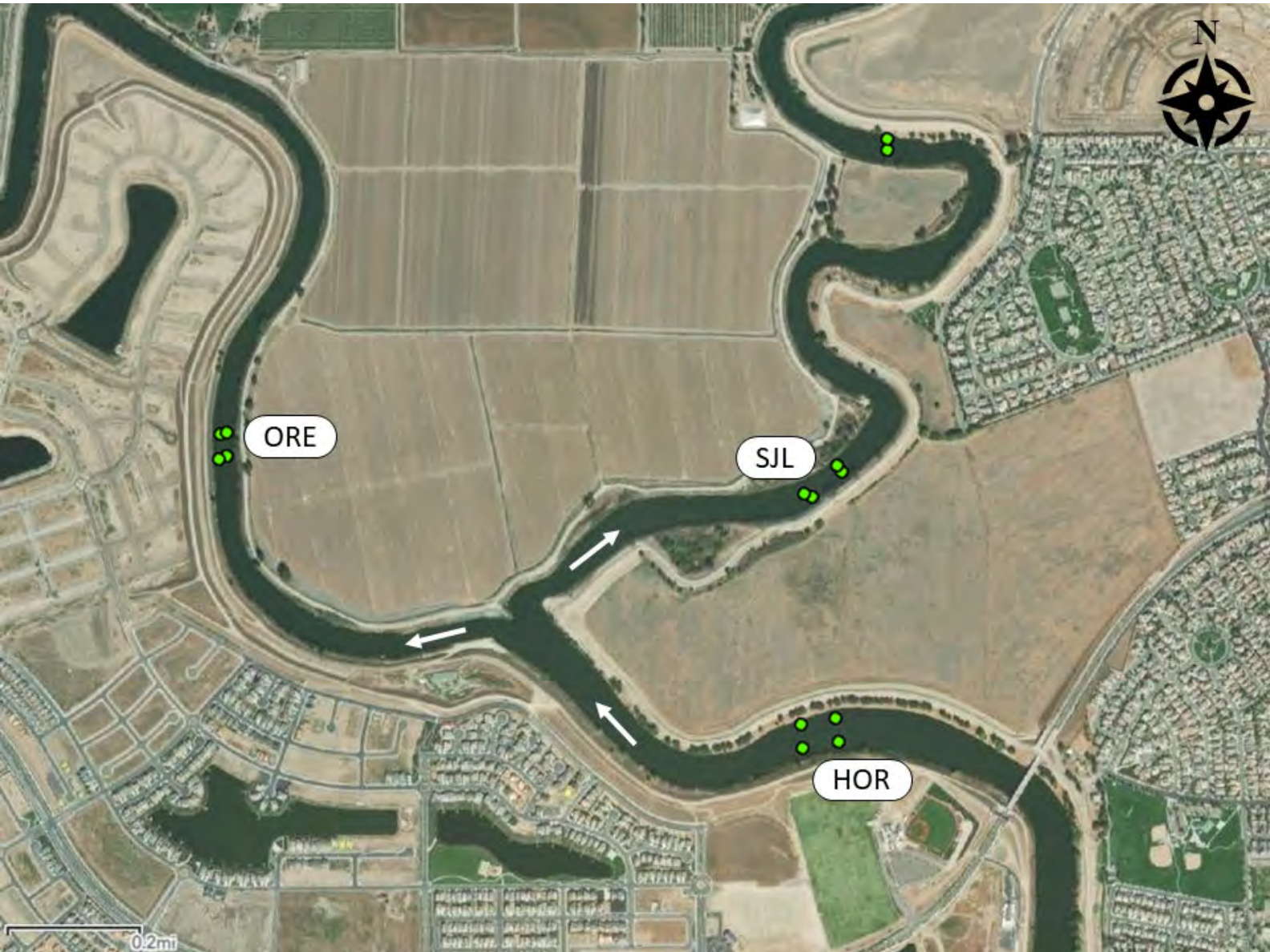
- The average cumulative probability of a fish remaining at CVP once detected there was high
- The average cumulative probability of a fish detected at WCL or RG transitioning to CVP increased to approximately 70% after 6 days
- Cumulative transitions considering time-varying covariates show that average conditions are not sufficient to fully describe variability in transition probabilities

# Discussion

- Are there any additional elements that should be included in the model?
- Is there anything missing in the interpretation?
- How should this information be presented so it is most useful to managers?

# Model Results

## Head of Old River

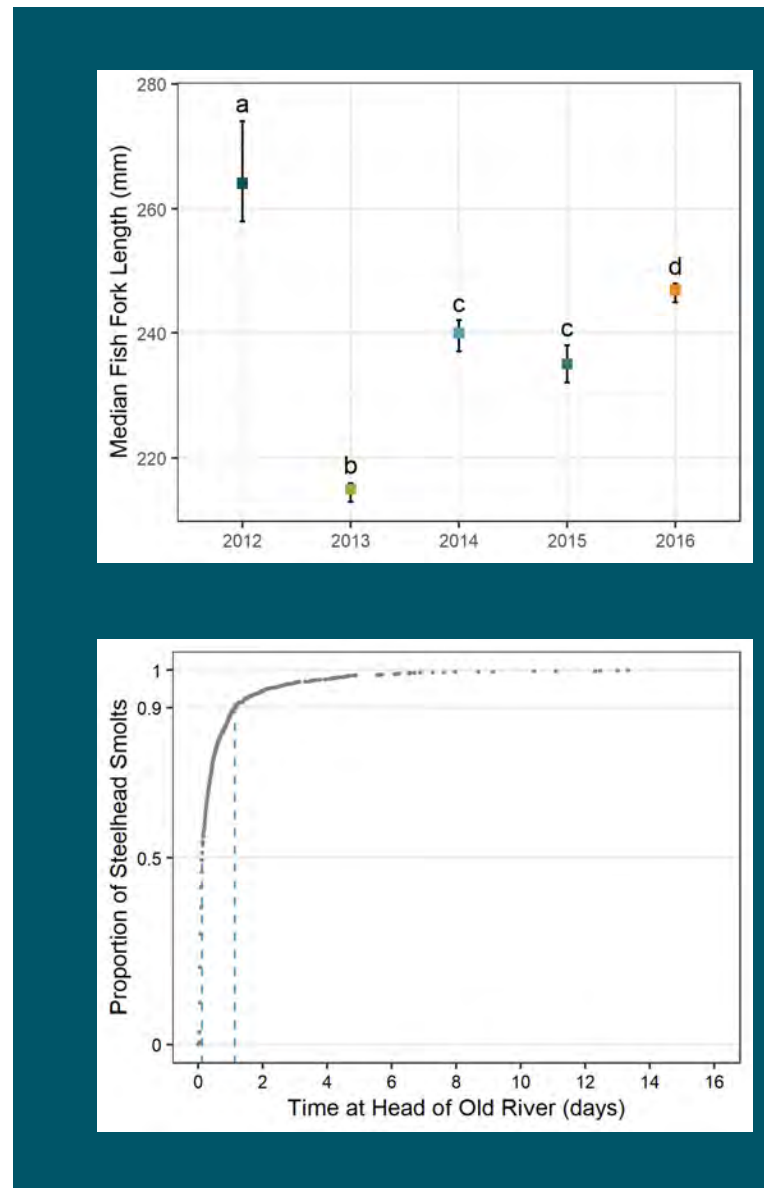


# Overview

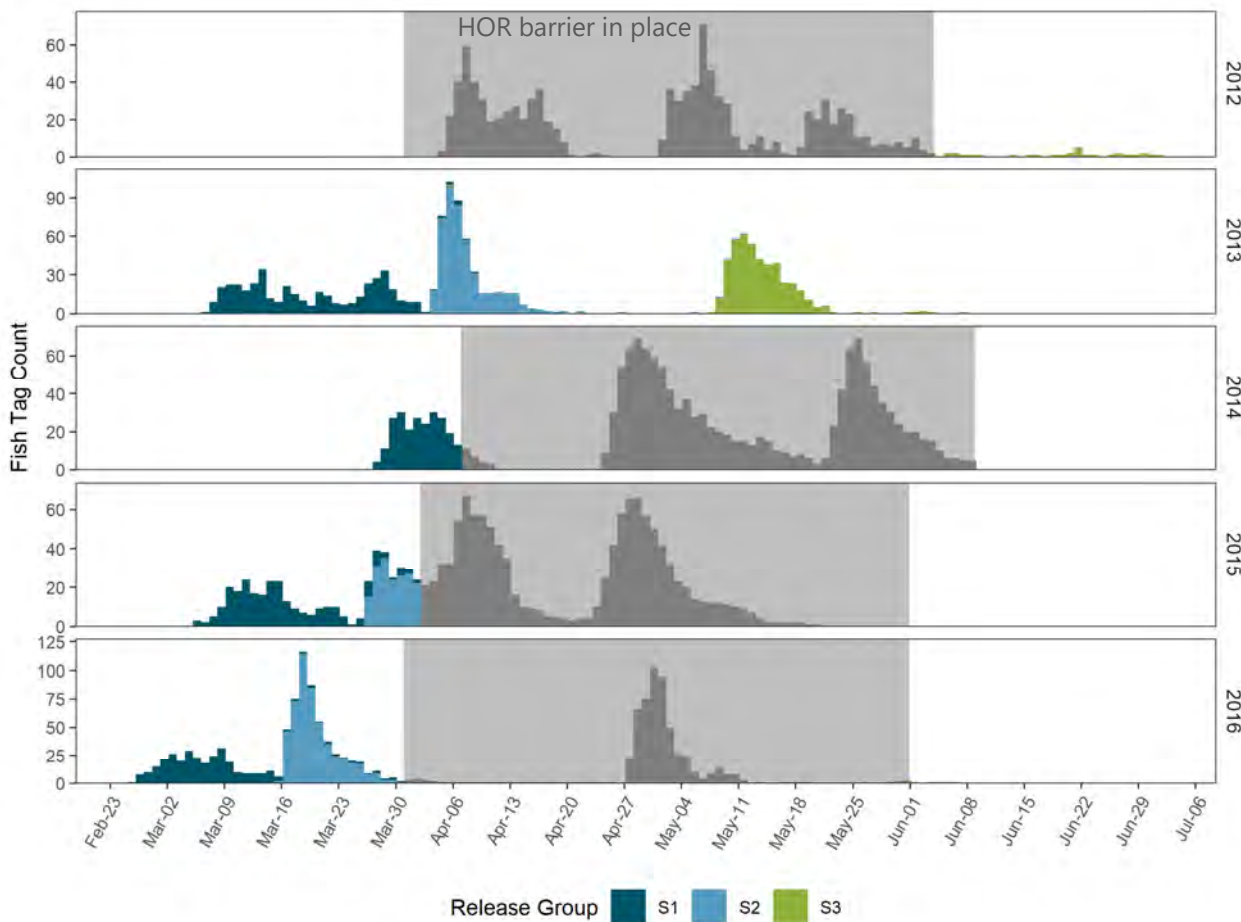
1. Fish data
2. Key hydrodynamic conditions
3. Model results
  - a. Model fit
  - b. Influence of covariates
  - c. Transition probabilities
4. Summary

# Fish Data

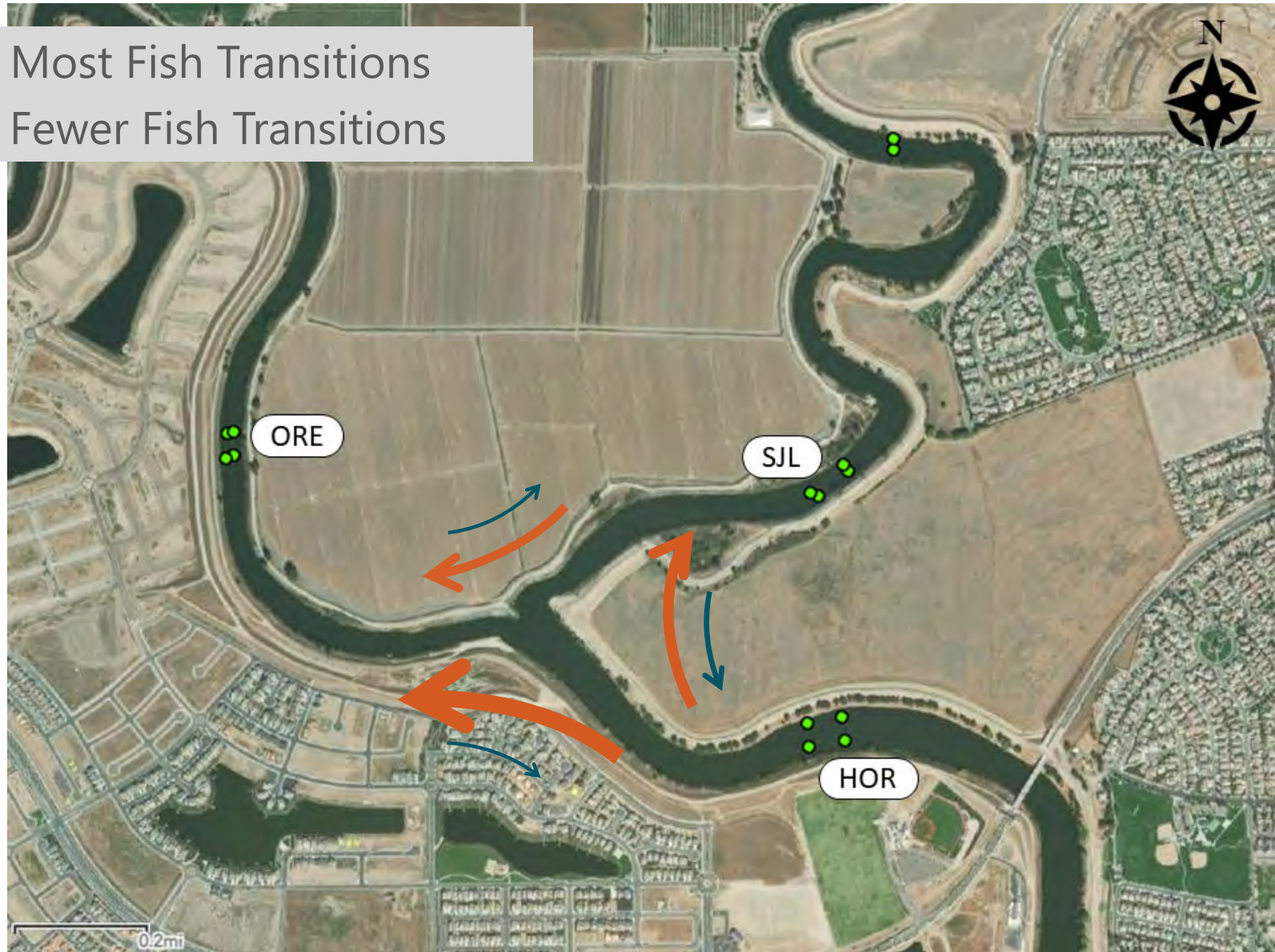
- 1,934 fish detected, HOR barrier out only
  - 17 in 2012
  - 917 in 2013
  - 144 in 2014
  - 274 in 2015
  - 582 in 2016
- Median fork length different each year, except 2014 and 2015
- Median time spent at HOR was 2.64 hours (0.11 day)
- 90% of fish spent  $\leq 1.13$  days at HOR
- Predator filter applied
- Censored after 25 days



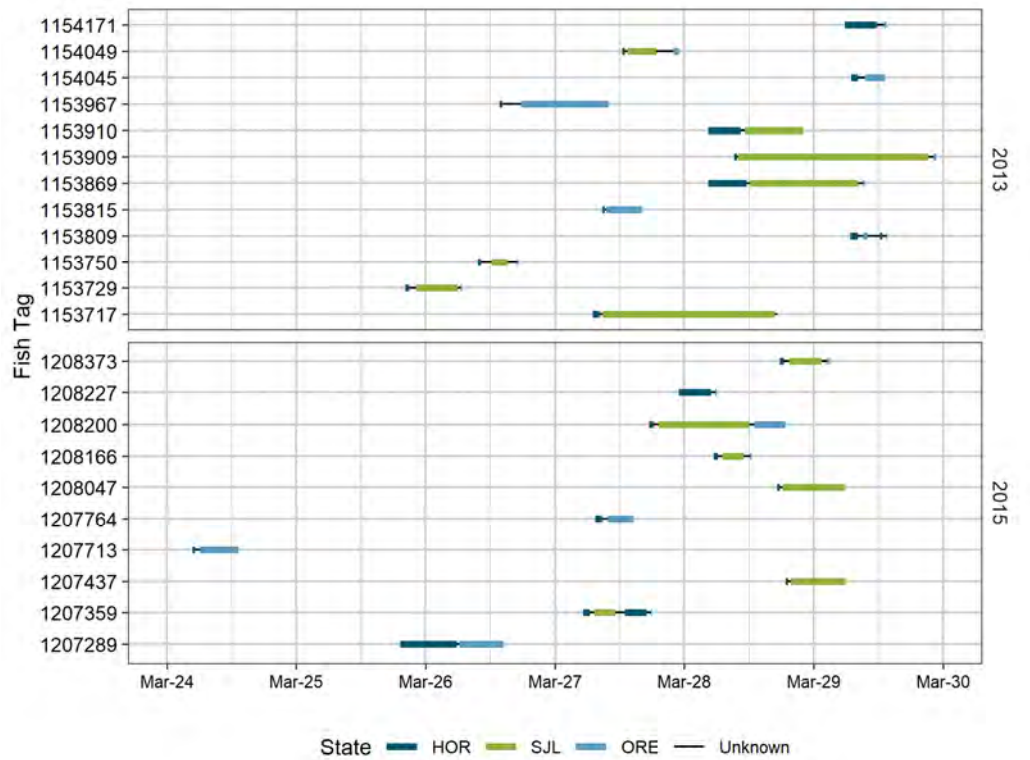
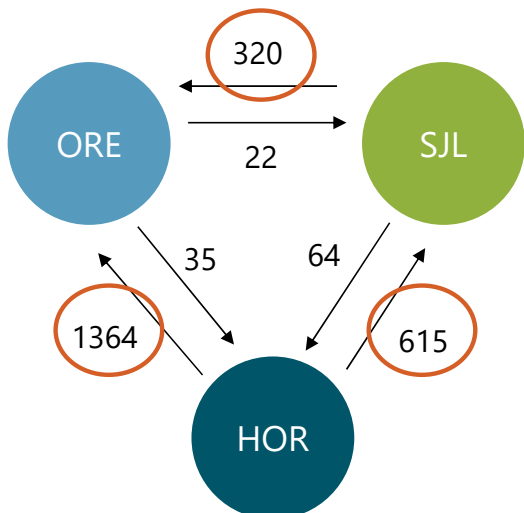
# Steelhead Timing at Head of Old River



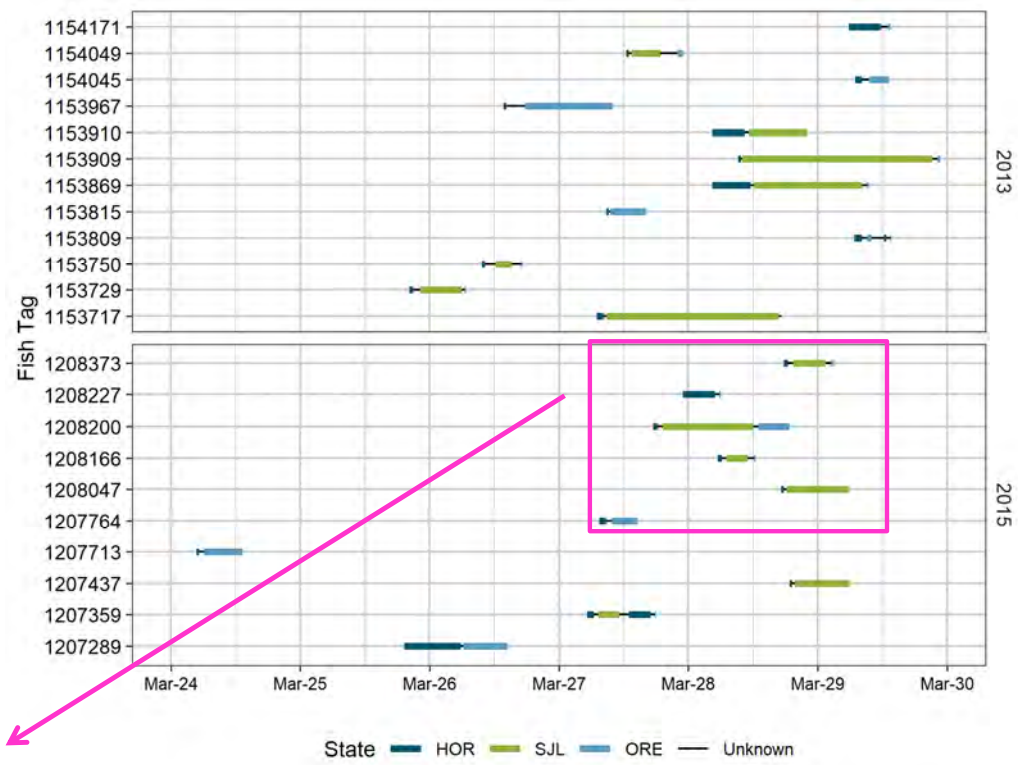
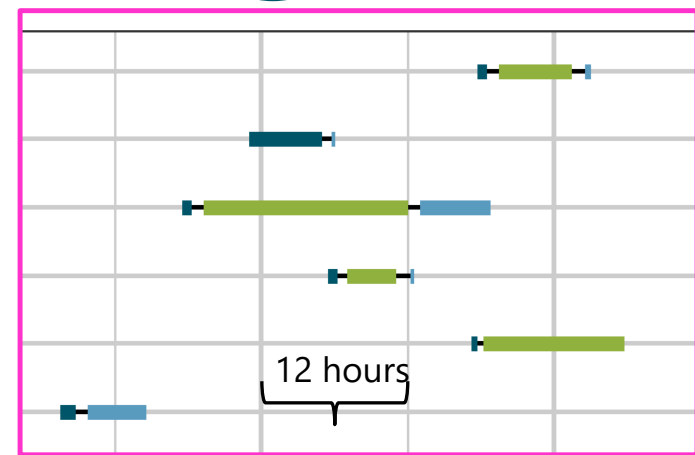
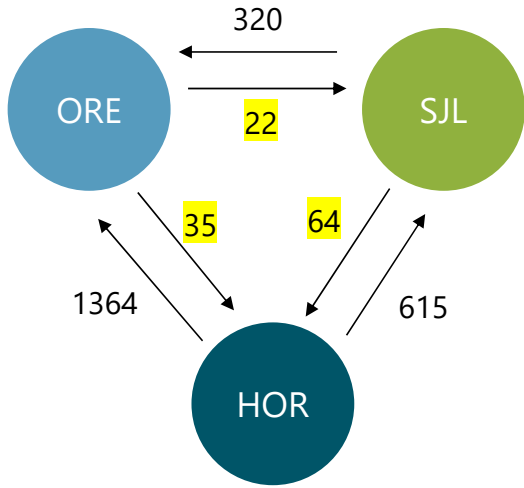
→ = Most Fish Transitions  
← = Fewer Fish Transitions



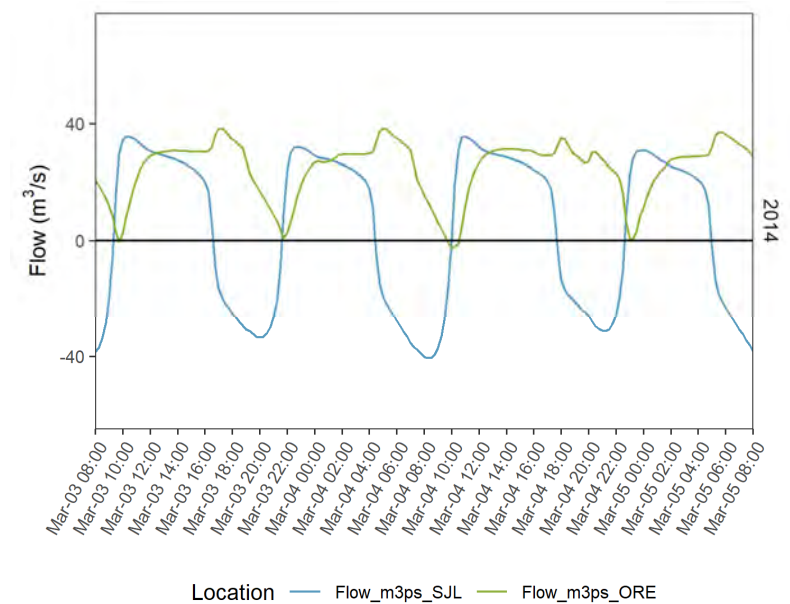
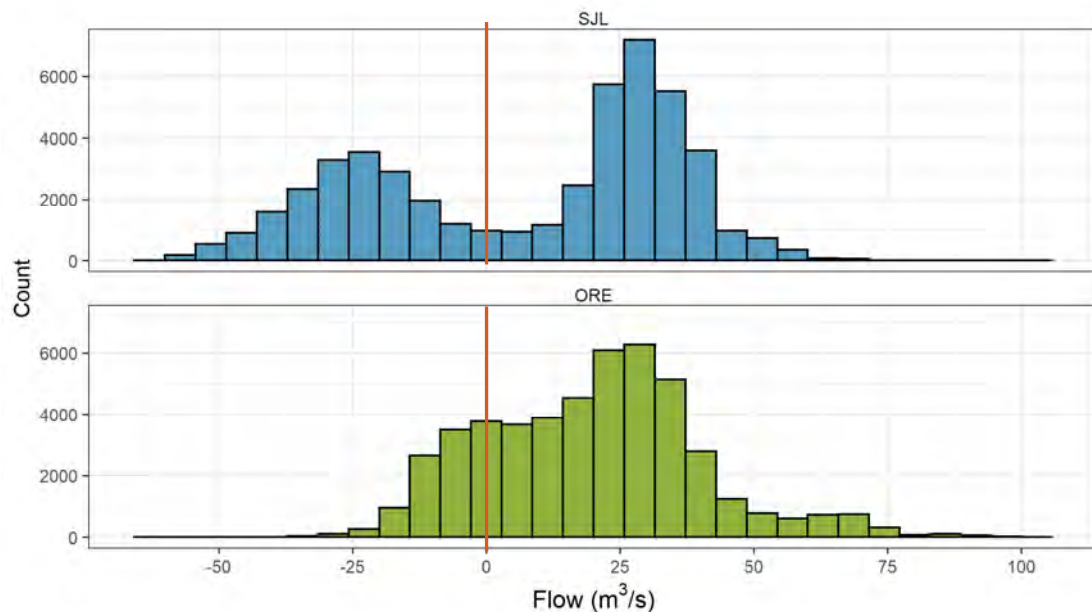
# Fish Behavior

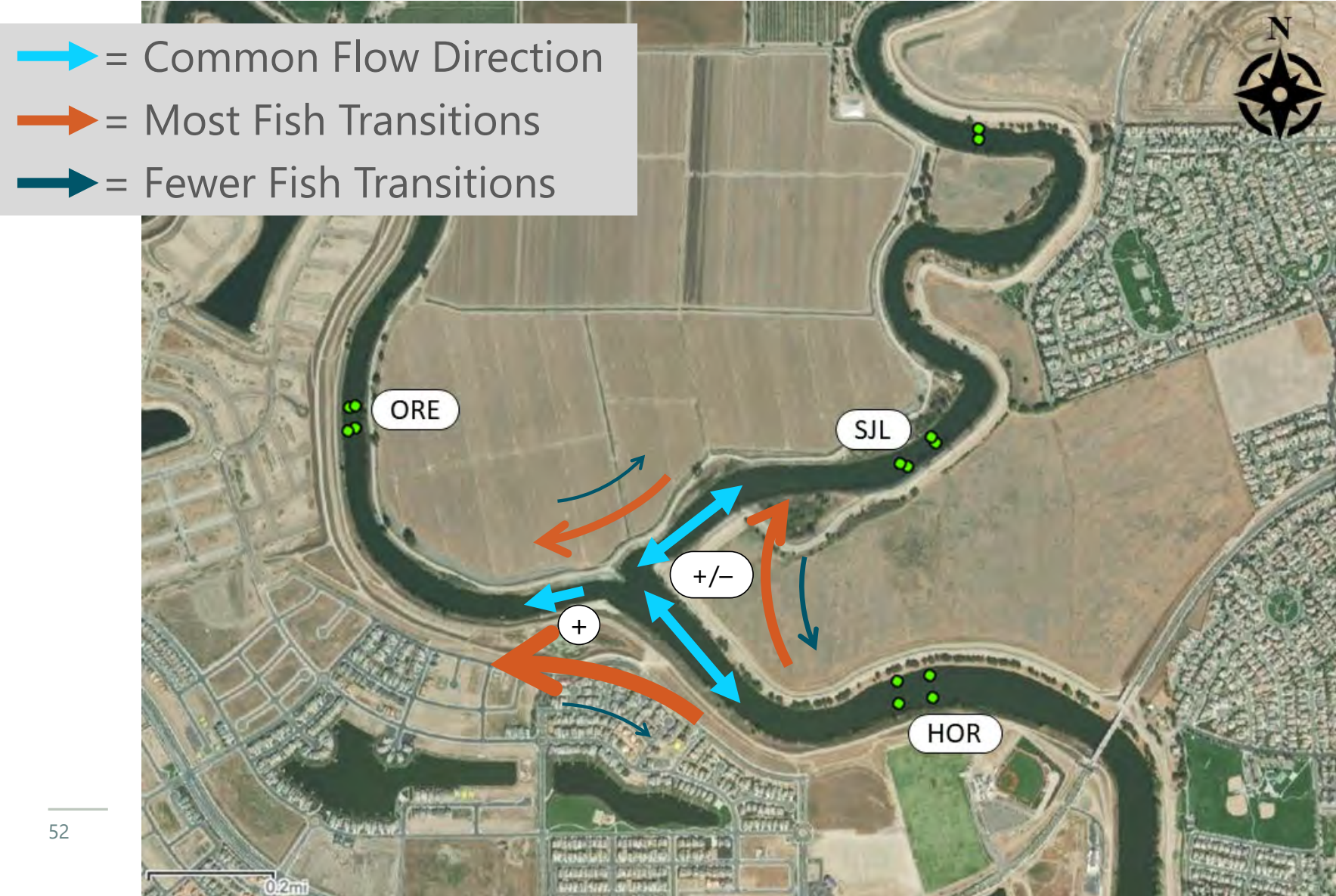


# Fish Behavior



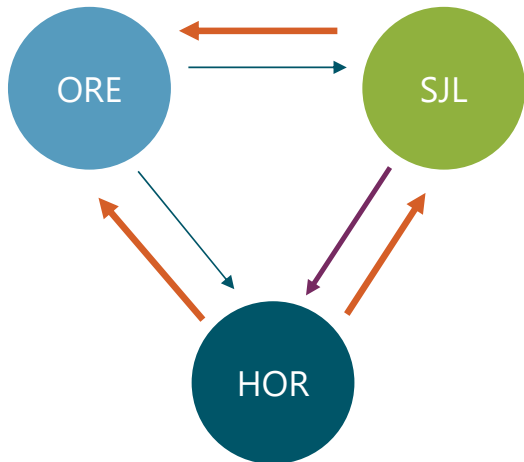
# Key Hydrodynamic Conditions: Flow





# Modeling Methods Reminder

- Fewer covariates can be fitted to individual transitions, depending on representation in the data



Model		<i>K</i>	Deviance	AIC	ΔAIC
Transition	Covariates				
$\begin{cases} HOR \rightarrow SJL \\ HOR \rightarrow ORE \\ SJL \rightarrow ORE \end{cases}$	$Q_{SJL} + Q_{ORE} + WD_{SJL} + Ind_{MGR}$	21	12184.1	12228.1	0.0
$\begin{cases} SJL \rightarrow HOR \\ ORE \rightarrow HOR \\ ORE \rightarrow SJL \end{cases}$	$Q_{SJL} + Ind_{MGR}$ $Q_{ORE}$				
$\begin{cases} HOR \rightarrow SJL \\ HOR \rightarrow ORE \\ SJL \rightarrow ORE \end{cases}$	$Q_{SJL} + Q_{ORE} + WD_{SJL} + Ind_{MGR}$	21	12207.6	12249.6	24.5
$\begin{cases} SJL \rightarrow HOR \\ ORE \rightarrow HOR \\ ORE \rightarrow SJL \end{cases}$	$Q_{SJL}$ $Q_{ORE}$				
$\begin{cases} HOR \rightarrow SJL \\ HOR \rightarrow ORE \\ SJL \rightarrow ORE \end{cases}$	$Q_{SJL} + Q_{ORE} + WD_{SJL} + WT$	21	14068.3	14110.3	1882.1
$\begin{cases} SJL \rightarrow HOR \\ ORE \rightarrow HOR \\ ORE \rightarrow SJL \end{cases}$	$Q_{SJL}$ $Q_{ORE}$				
•	•	•	•	•	•
•	•	•	•	•	•
•	•	•	•	•	•
All	$Q_{SJL}$	12	14694.6	14718.6	2490.5
All	$Q_{ORE}$	12	15322.9	15346.9	3118.8
no covariates		6	15605.3	15617.3	3389.1

# Head of Old River Best Fit Model

$$\begin{cases} HOR \rightarrow SJL \\ HOR \rightarrow ORE \sim Q_{SJL} + Q_{ORE} + WD_{SJL} + Ind_{MGR} \\ SJL \rightarrow ORE \end{cases}$$

$$\{ SJL \rightarrow HOR \sim Q_{SJL} + Ind_{MGR}$$

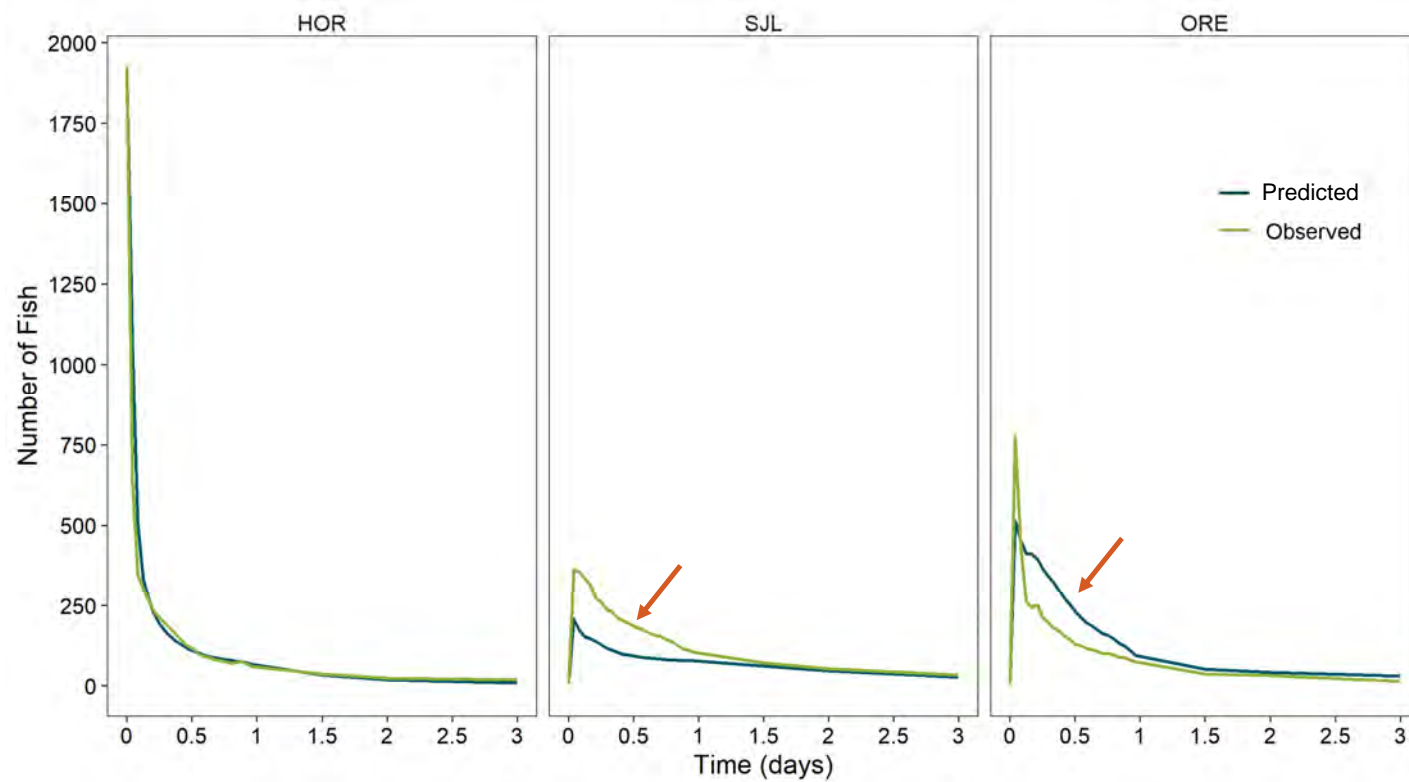
$$\begin{cases} ORE \rightarrow HOR \\ ORE \rightarrow SJL \end{cases} \sim Q_{ORE}$$

- VIFs < 1.1
- 2 individuals having greater influence on model residuals

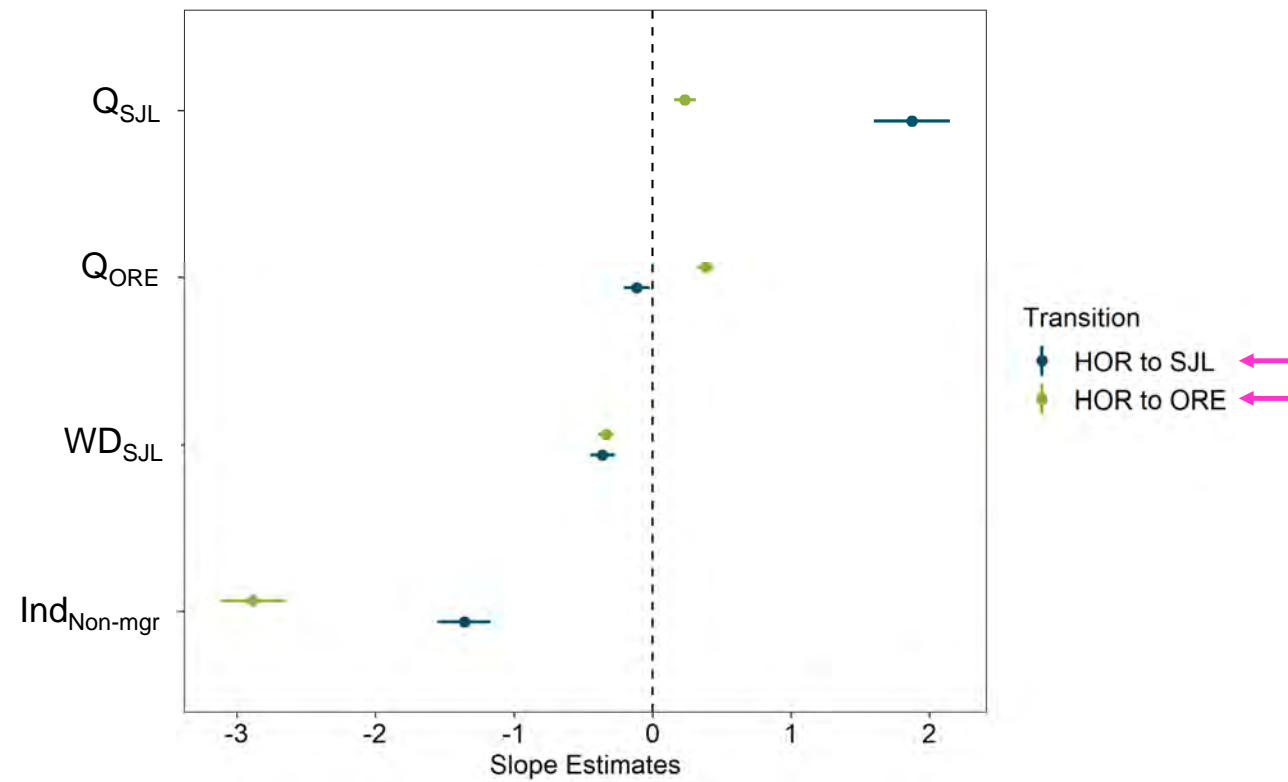


Model		K	Deviance	AIC	$\Delta AIC$
Transition	Covariates				
$\begin{cases} HOR \rightarrow SJL \\ HOR \rightarrow ORE \\ SJL \rightarrow ORE \end{cases}$	$Q_{SJL} + Q_{ORE} + WD_{SJL} + Ind_{MGR}$	21	12184.1	12228.1	0.0
$\begin{cases} SJL \rightarrow HOR \\ ORE \rightarrow HOR \\ ORE \rightarrow SJL \end{cases}$	$Q_{SJL} + Ind_{MGR}$				
$\begin{cases} HOR \rightarrow SJL \\ HOR \rightarrow ORE \\ SJL \rightarrow ORE \end{cases}$	$Q_{SJL} + Q_{ORE} + WD_{SJL} + Ind_{MGR}$	21	12207.6	12249.6	24.5
$\begin{cases} SJL \rightarrow HOR \\ ORE \rightarrow HOR \\ ORE \rightarrow SJL \end{cases}$	$Q_{SJL}$				
$\begin{cases} HOR \rightarrow SJL \\ HOR \rightarrow ORE \\ SJL \rightarrow ORE \end{cases}$	$Q_{SJL} + Q_{ORE} + WD_{SJL} + WT$	21	14068.3	14110.3	1882.1
$\begin{cases} SJL \rightarrow HOR \\ ORE \rightarrow HOR \\ ORE \rightarrow SJL \end{cases}$	$Q_{SJL}$				
$\begin{cases} HOR \rightarrow SJL \\ HOR \rightarrow ORE \\ SJL \rightarrow ORE \end{cases}$	$Q_{SJL} + Q_{ORE} + WD_{SJL} + WT$	21	14694.6	14718.6	2490.5
$\begin{cases} SJL \rightarrow HOR \\ ORE \rightarrow HOR \\ ORE \rightarrow SJL \end{cases}$	$Q_{ORE}$				
All	$Q_{SJL}$	12	15322.9	15346.9	3118.8
All	$Q_{ORE}$	12	15605.3	15617.3	3389.1
no covariates		6			

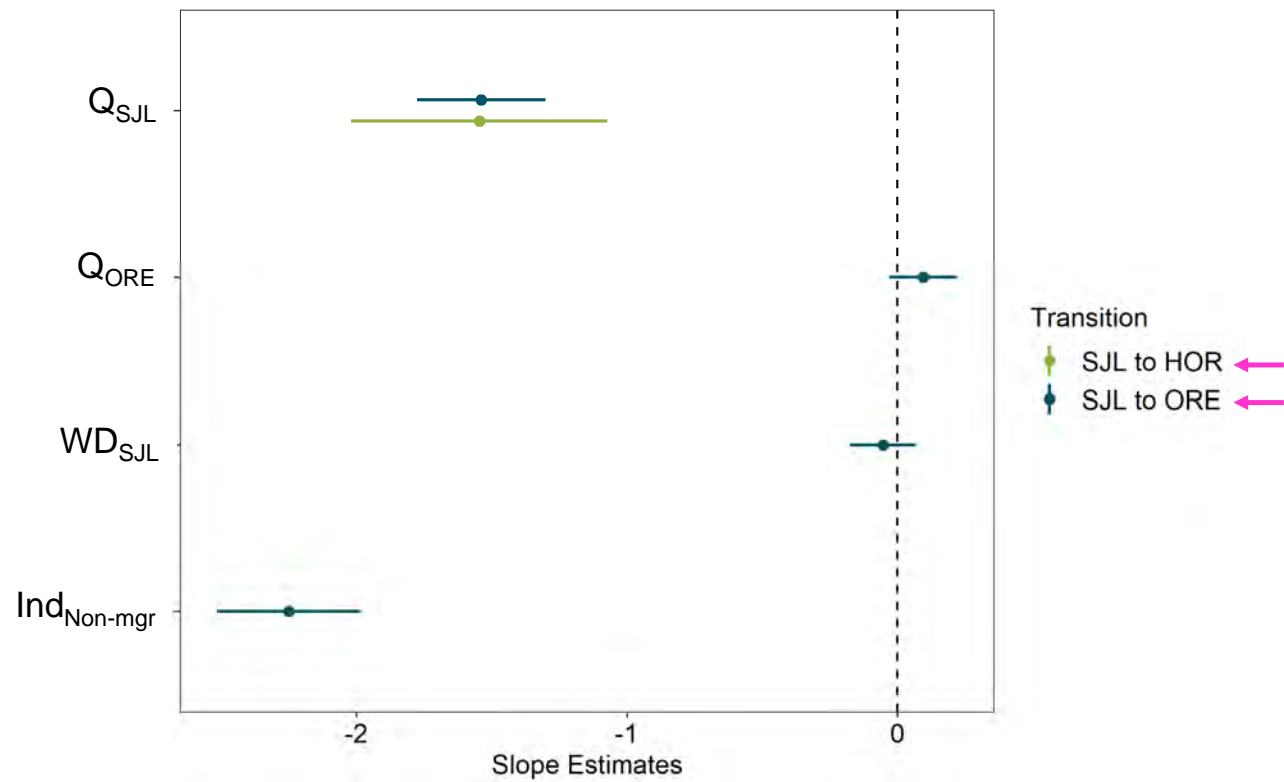
# Model Evaluation



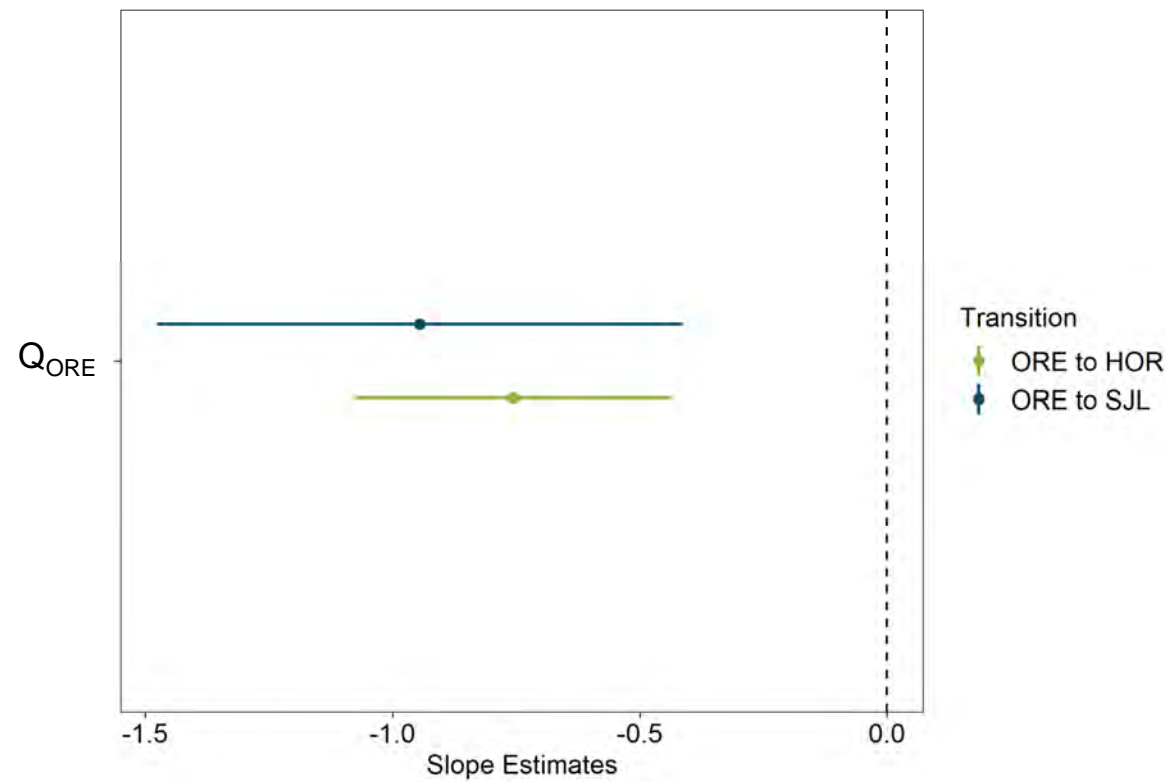
# Slope Estimates: Downstream Route Choice



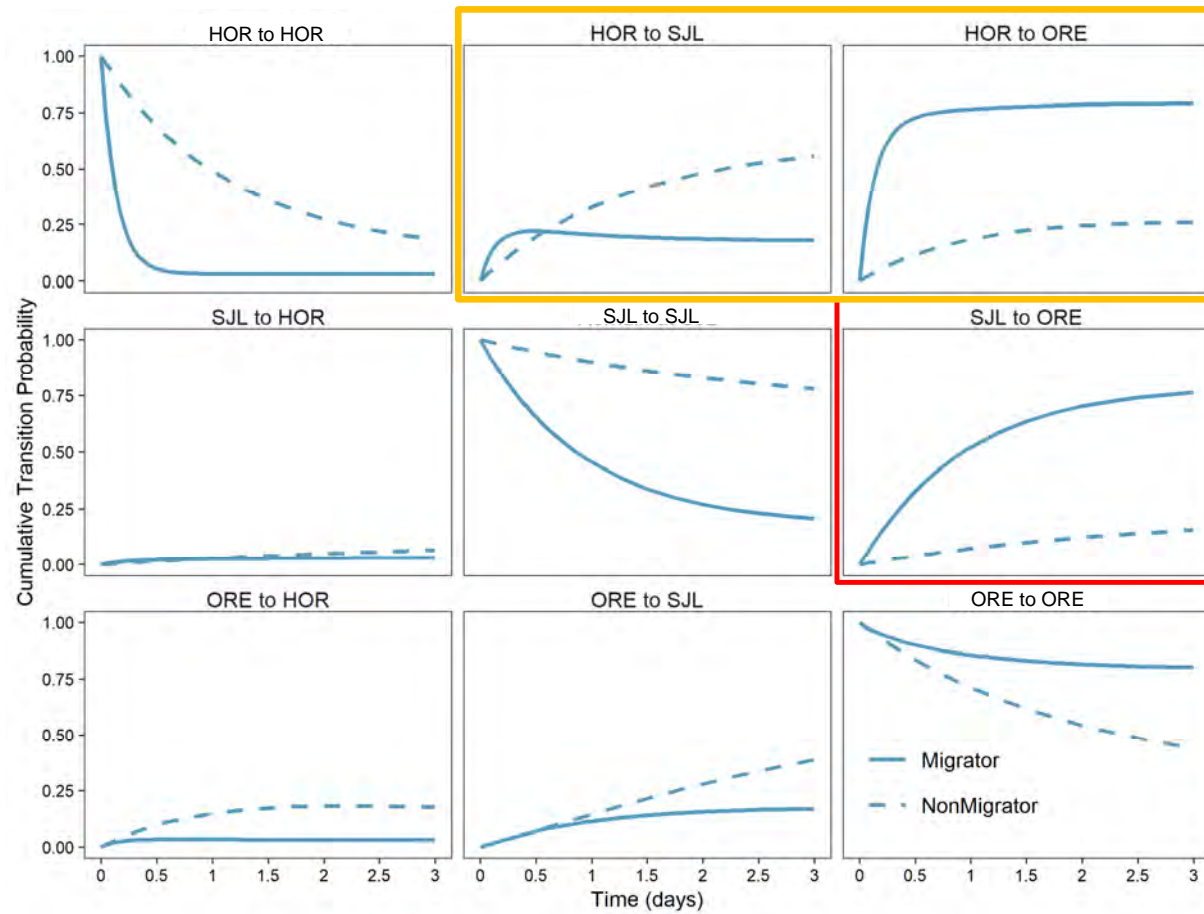
# Slope Estimates: Backtracking or Upstream Movements



# Slope Estimates: Leaving Old River

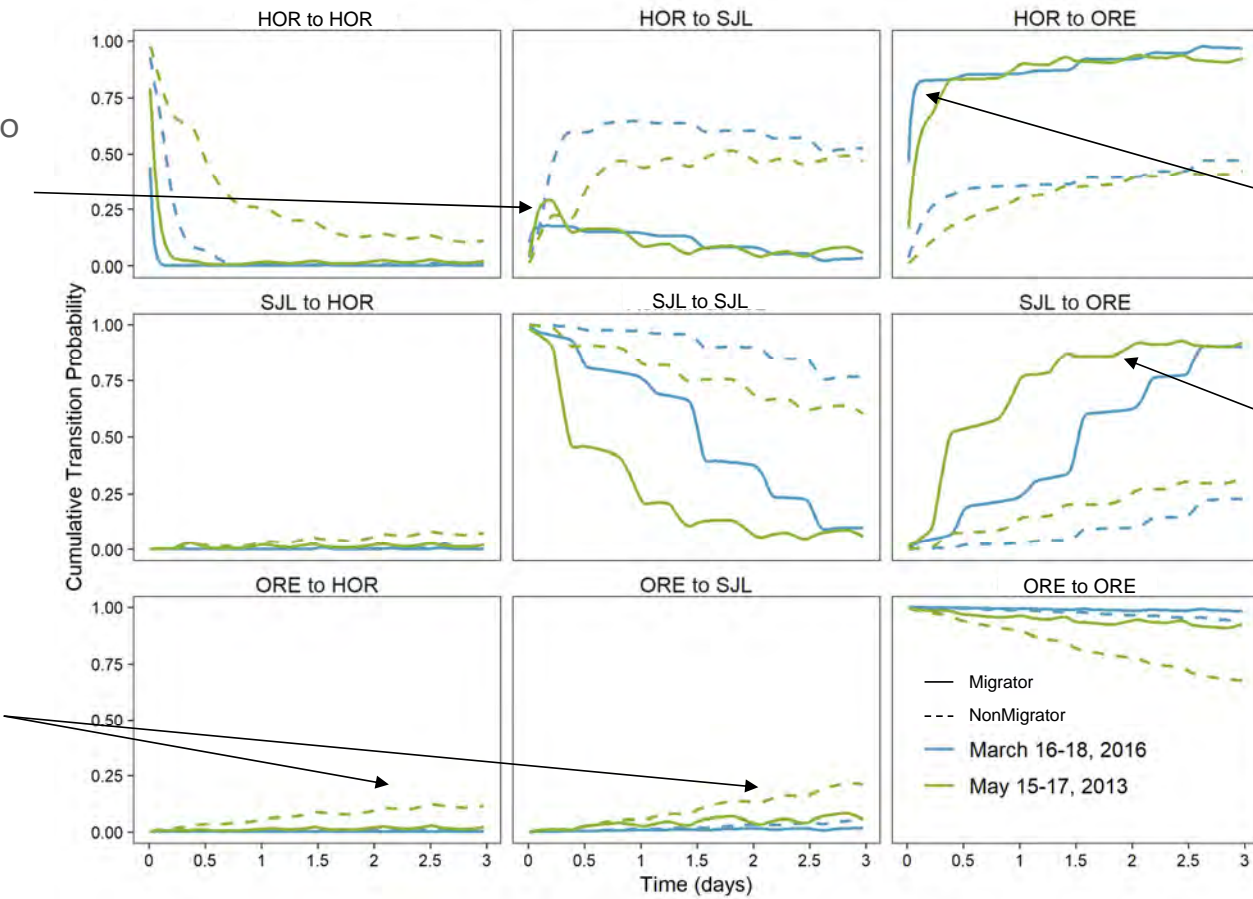


# Cumulative Transitions: Covariate Averages



# Cumulative Transitions: Time-Varying Covariates

Similar flow into both channels, WD dropping



# Summary

- The most common direction of movement was from head of Old River onto Old River (i.e., downstream)
  - Second most common was moving downstream on the mainstem
- There were also a substantial number of movements from downstream on the mainstem to Old River (i.e., “backtracking”)
- Movements upstream out of Old River were uncommon
- Flow on the mainstem was reversed about 40% of the time, while flow on Old River was reversed about 22% of the time
- Most fish moved through this area quickly (approximately 1 day; i.e., “migrants”), but a subset of fish did not (i.e., “nonmigrants”)

# Model Findings

- Key variable in best fit fish movement model
  - Flow on both Old River and San Joaquin River, water depth, and being classified as a “migrator”
- The chance of staying on the mainstem (HOR to SJL) was increased by
  - **Increasing** downstream mainstem flow (strongest influence)
  - **Decreasing** downstream flow on Old River (smaller influence)
- The chance of leaving the mainstem (HOR to ORE) was increased by
  - **Increasing** downstream mainstem flow
  - **Increasing** downstream flow on Old River
- Chance of moving downstream on either route is reduced by increasing water depth and by being a “nonmigrator”

# Model Findings

- As flow on the mainstem increases, the chance of “backtracking” decreases (SJL to ORE, SJL to HOR)
- As flow on Old River increases, the chance moving upstream out of Old River decreases
- Migrator status has the greatest influence on cumulative transition probability for most common transitions (HOR to ORE, HOR to SJL, SJL to ORE) compared to flow and water depth
  - Less common transitions (ORE to SJL, ORE to HOR) more influenced by hydrodynamic conditions

# Discussion

- Are there any additional elements that should be included in the model?
- Is there anything missing in the interpretation?
- How should this information be presented so that it is most useful to managers?

# Model Results

Turner Cut

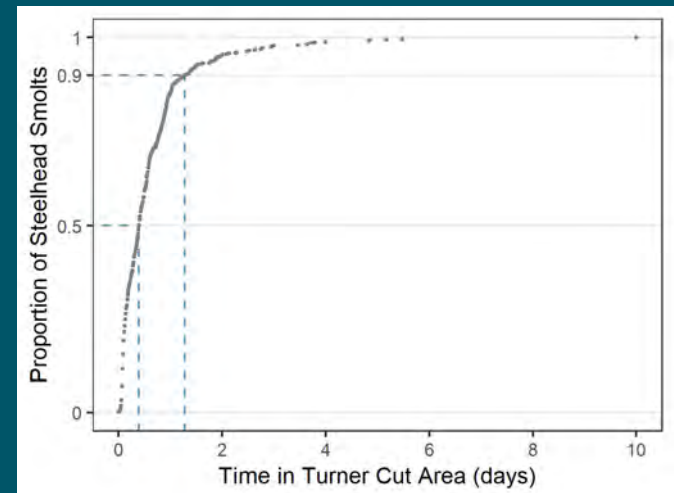
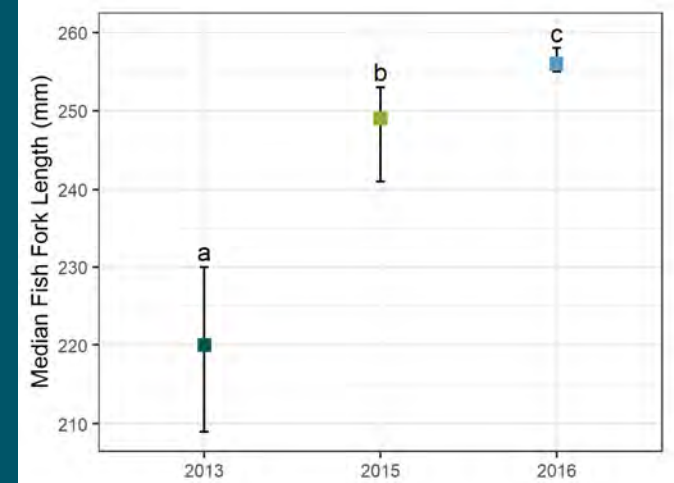


# Overview

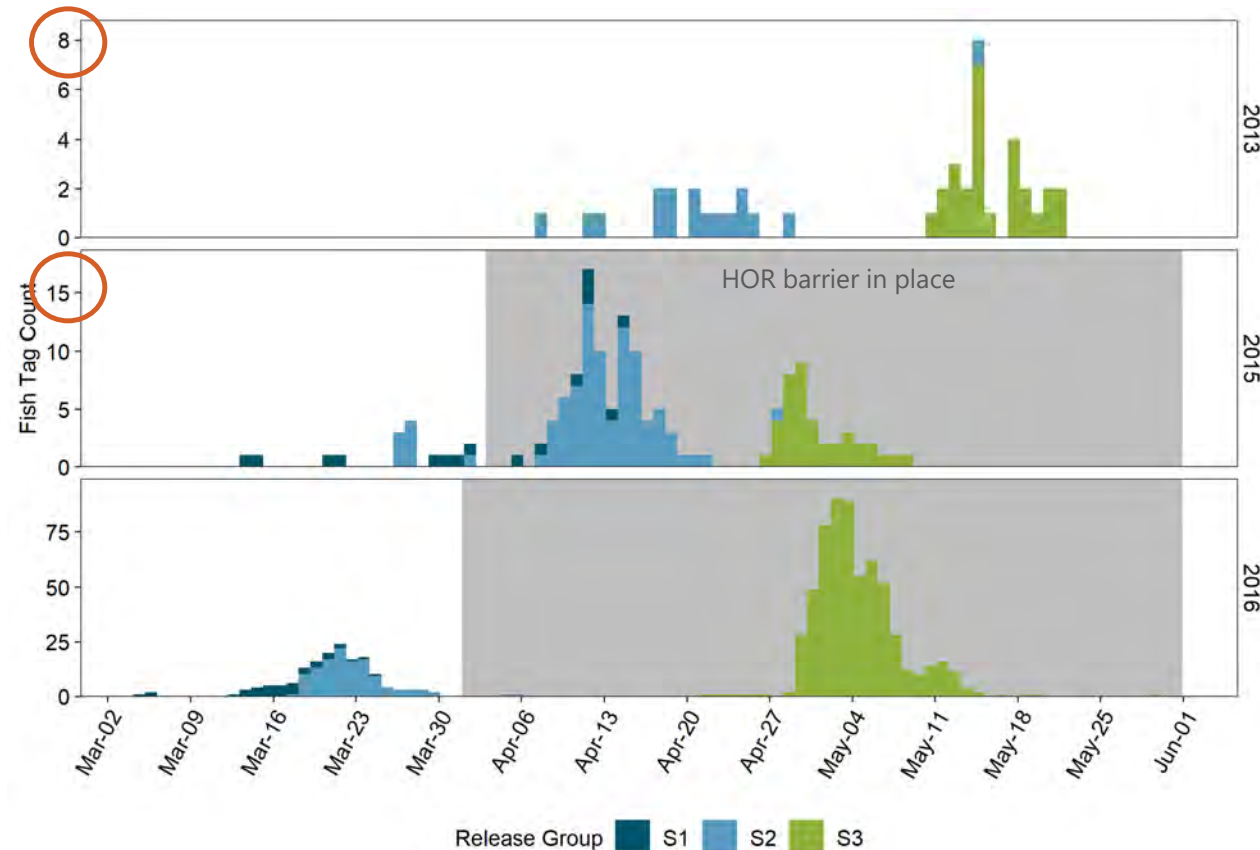
1. Fish data
2. Key hydrodynamic conditions
3. Model results
  - a. Model fit
  - b. Influence of covariates
  - c. Transition probabilities
4. Summary

# Fish Data

- 576 fish detected
  - 29 in 2013
  - 91 in 2015
  - 456 in 2016
- Median fork length different each year
- Median time spent in Turner Cut was 9.4 hours (0.39 days)
- 90% of fish spent  $\leq 1.3$  days in Turner Cut area
- Predator filter applied
- Censored after 10 days

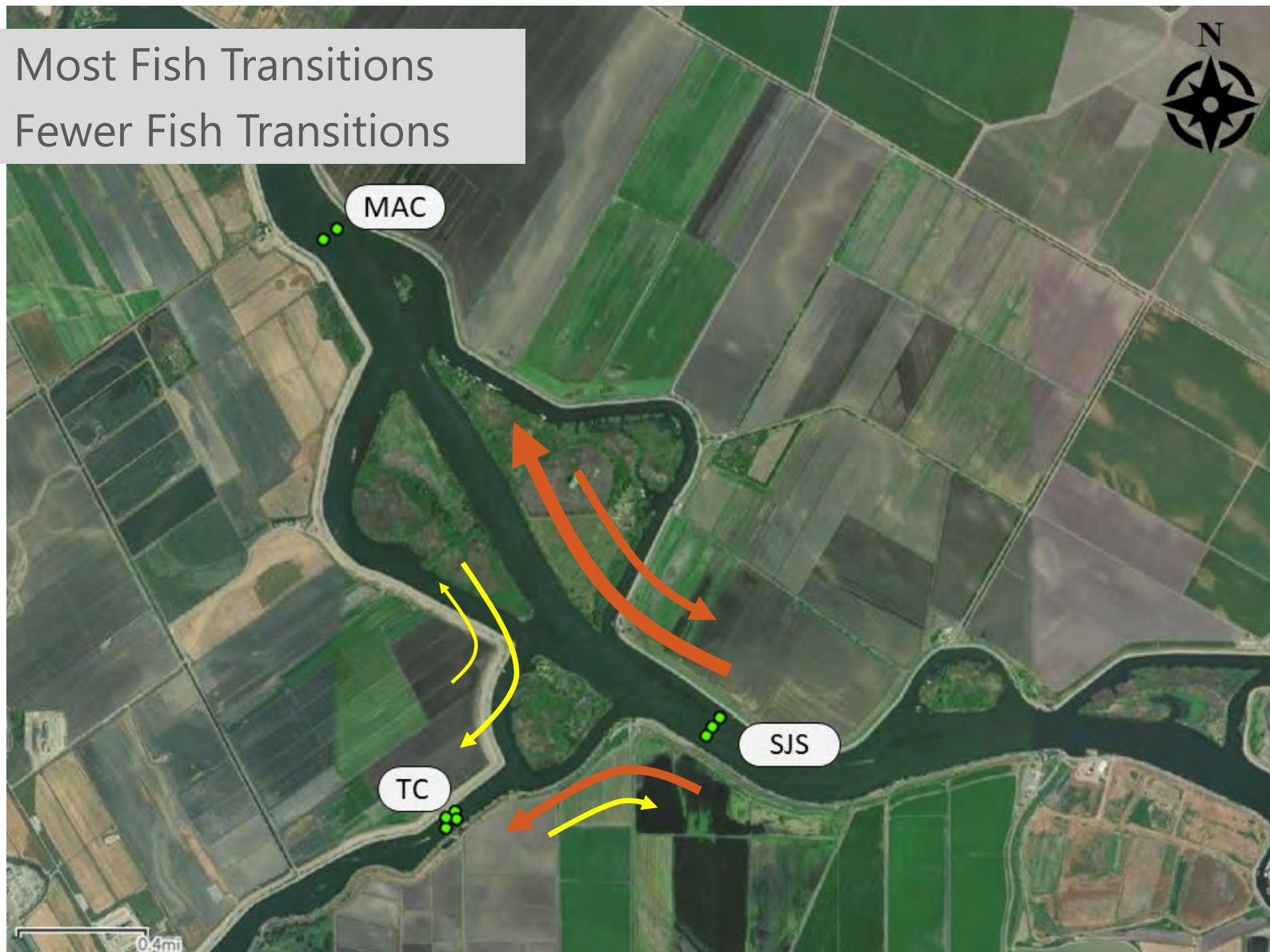


# Steelhead Timing in Turner Cut

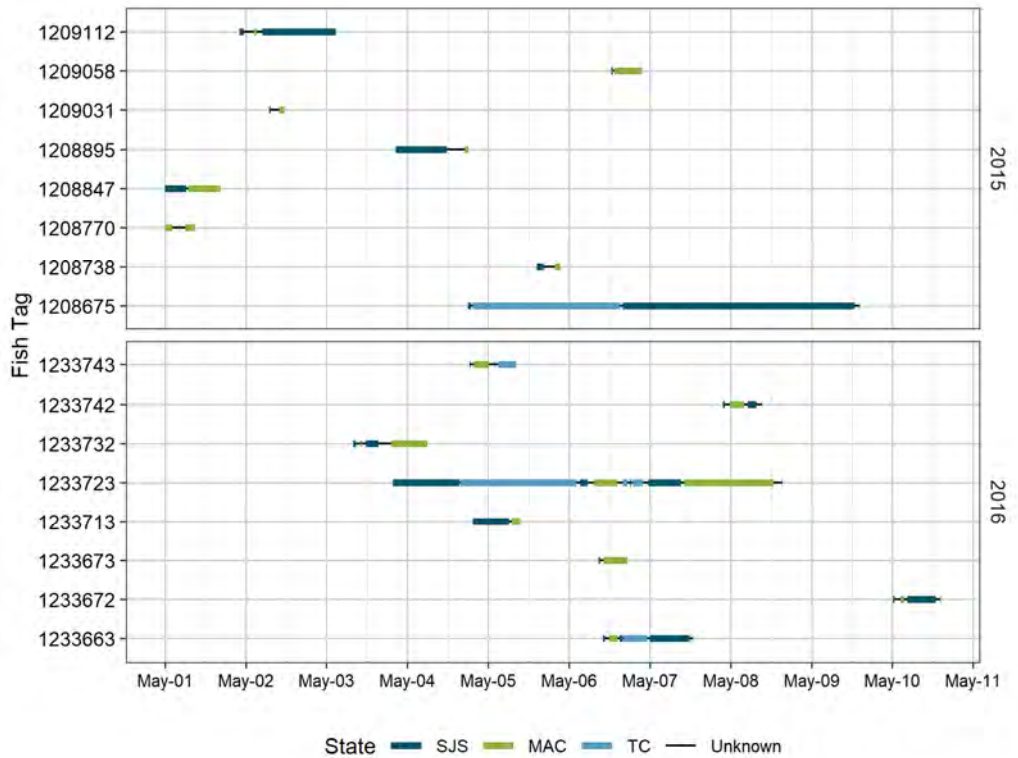
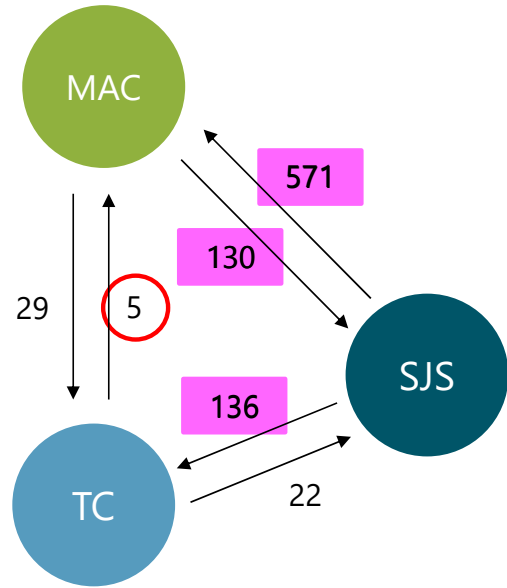


Between 84-92% of juvenile steelhead took Old River Route in 2013 (Buchanan 2015)

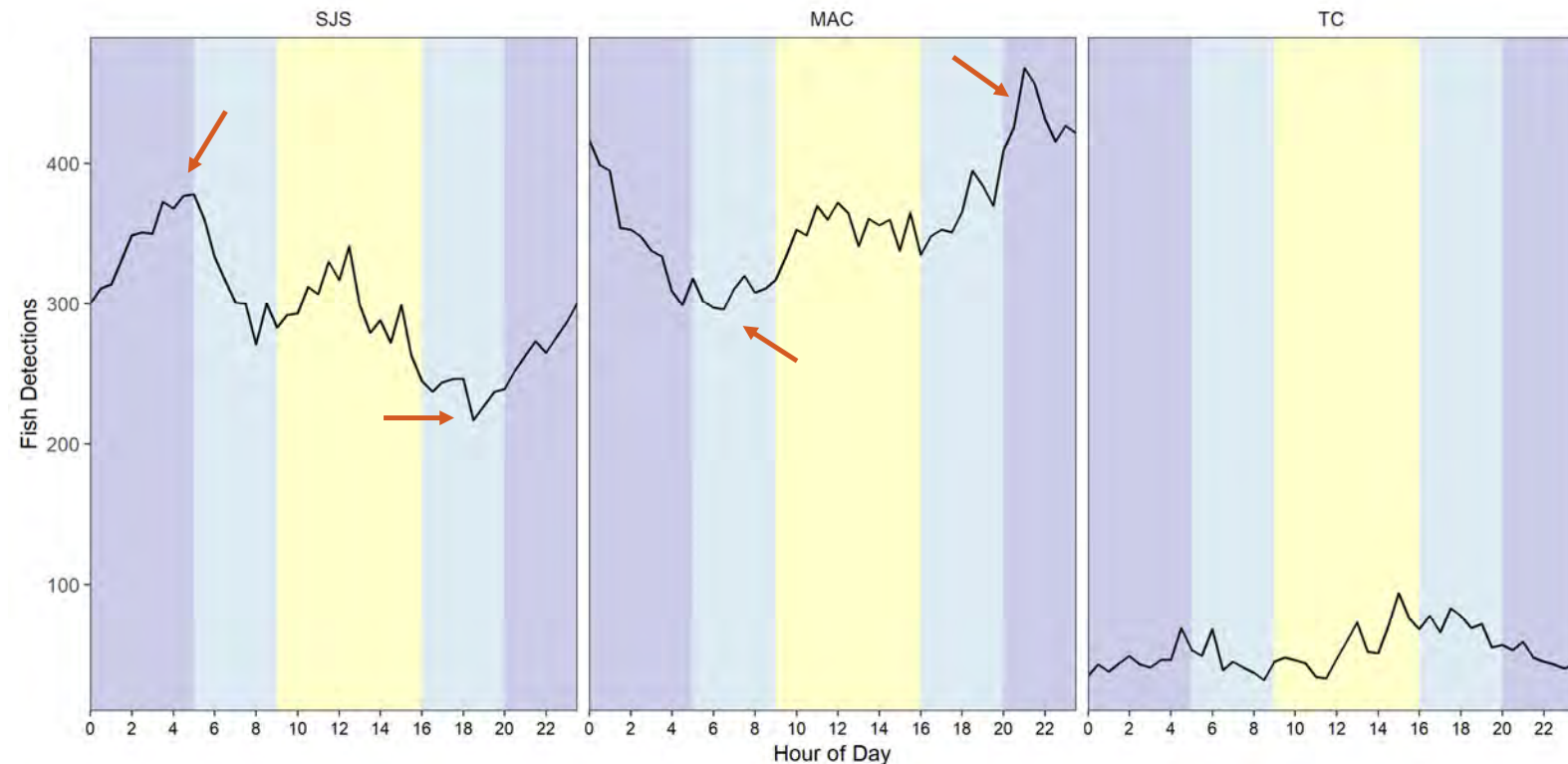
→ = Most Fish Transitions  
→ = Fewer Fish Transitions



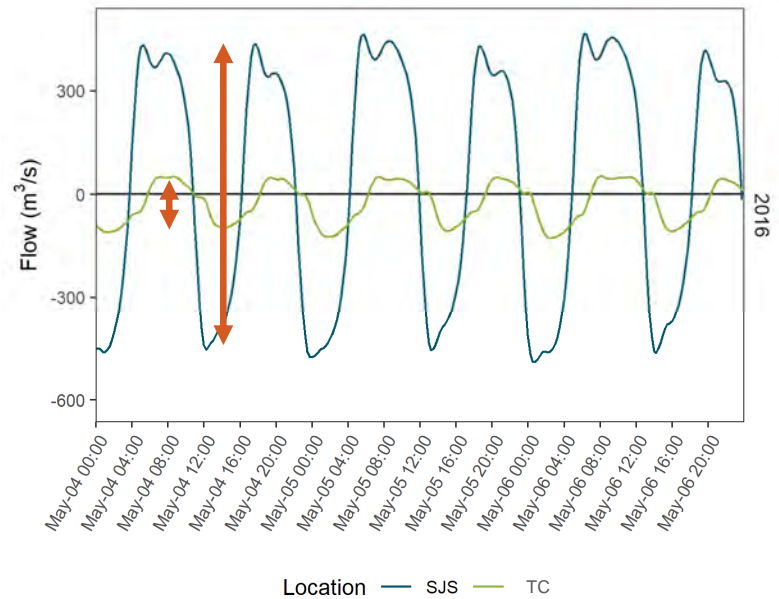
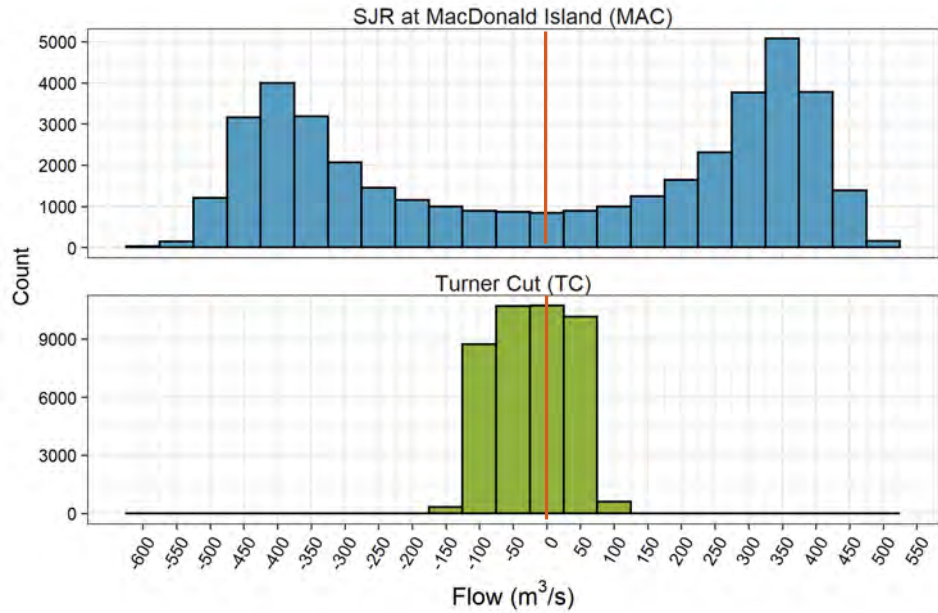
# Fish Behavior

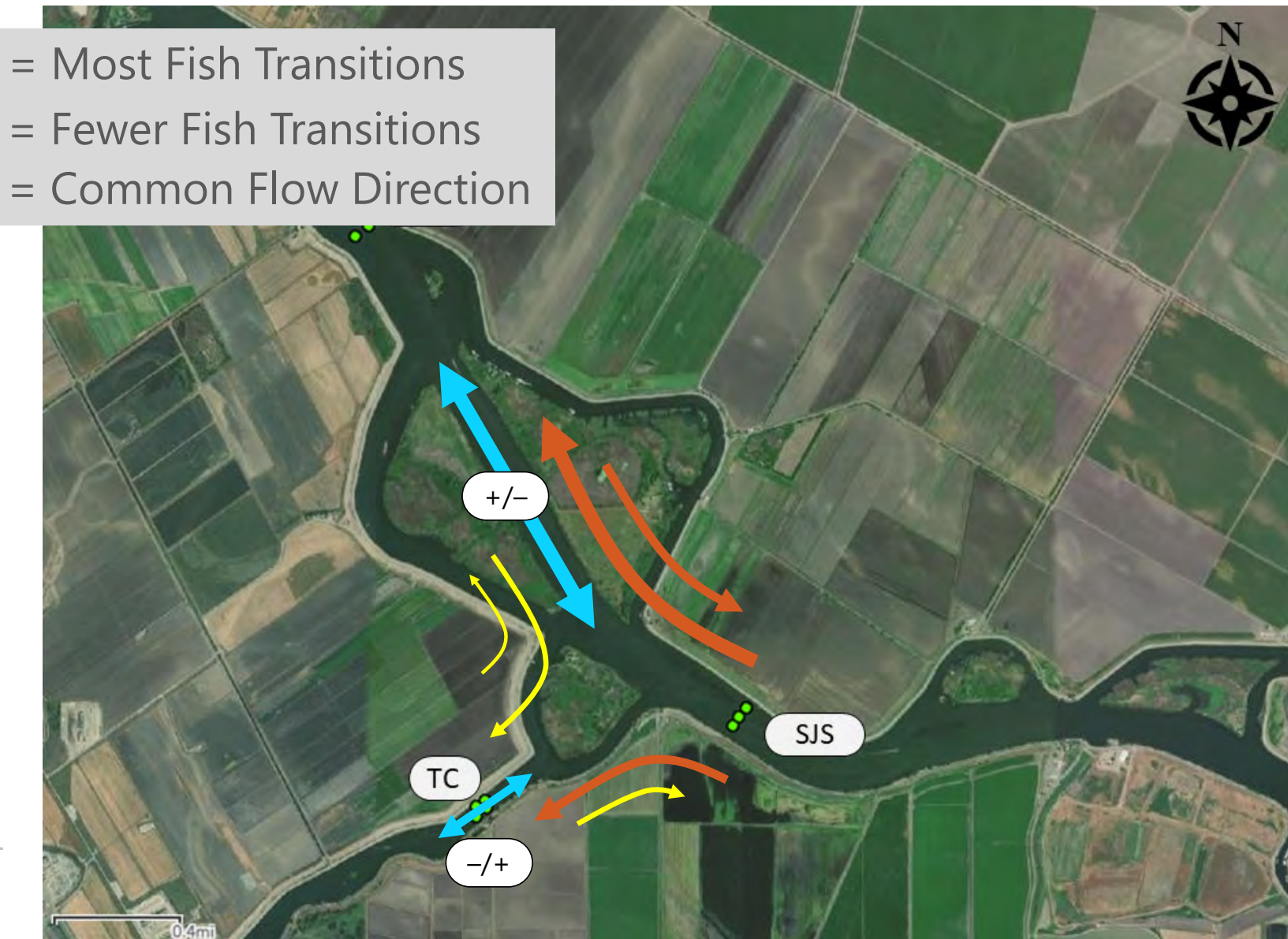


# Steelhead Activity in Turner Cut Area



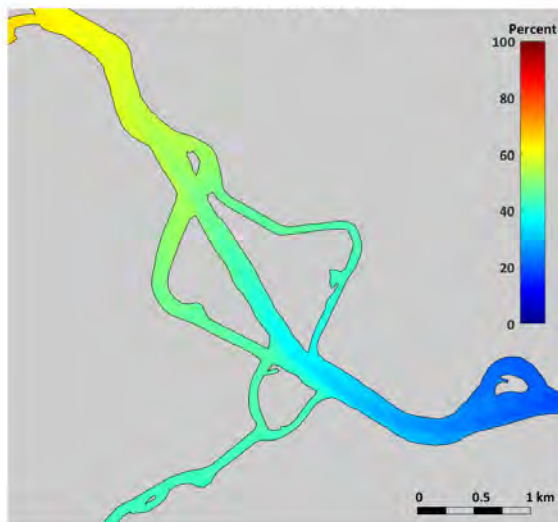
# Key Hydrodynamic Conditions: Flow



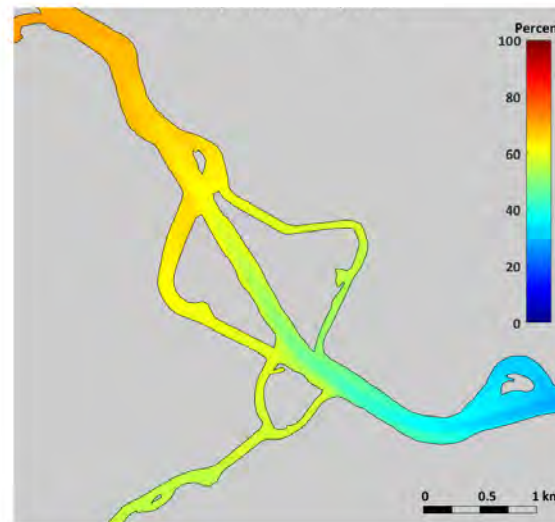


# Key Hydrodynamic Conditions: Percent Sacramento River Water

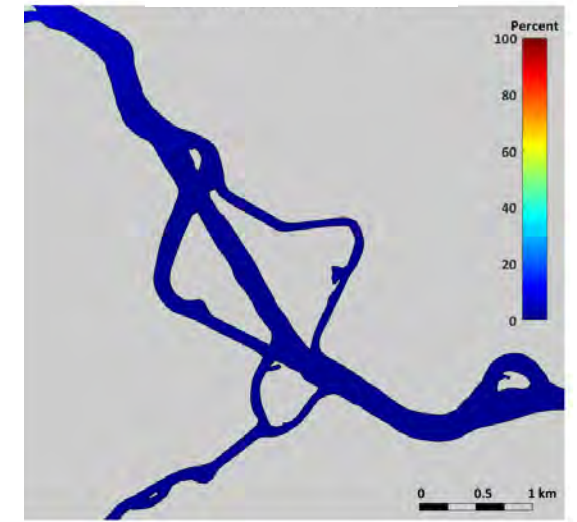
March 16 to 22, 2013



April 3 to 9, 2013

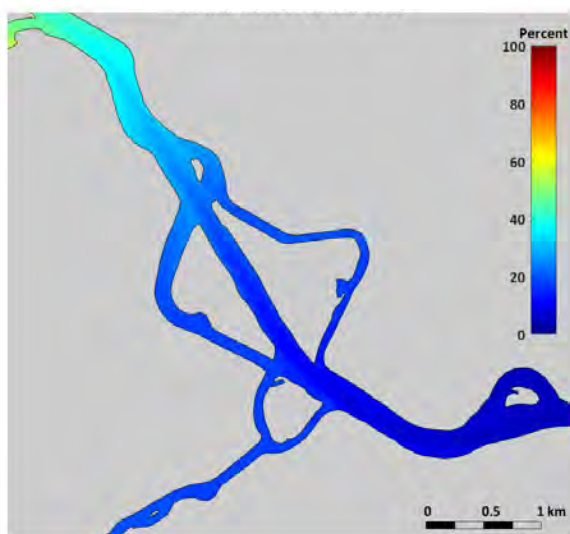


May 4 to 10, 2013

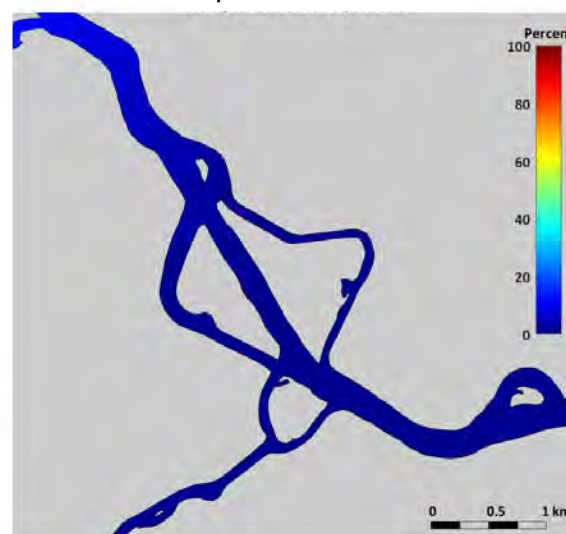


# Key Hydrodynamic Conditions: Percent Sacramento River Water

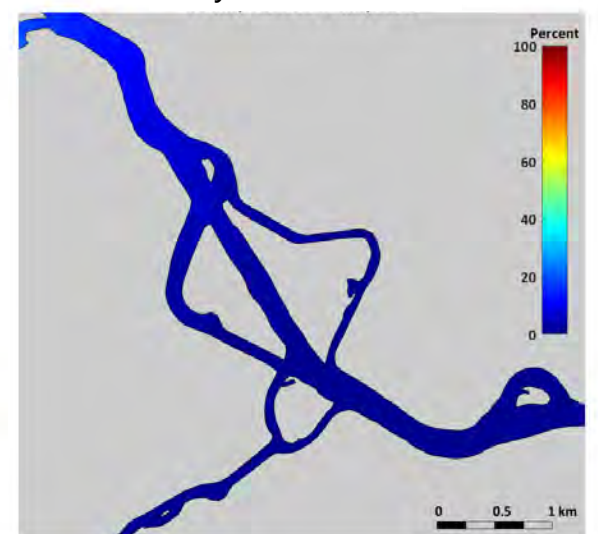
March 16 to 22, 2015



April 3 to 9, 2015

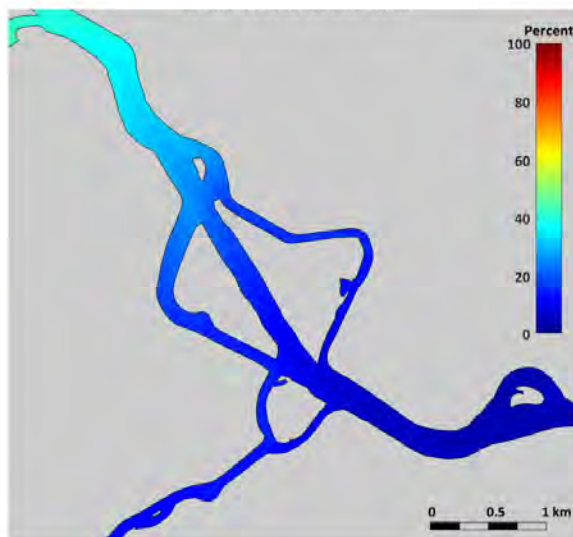


May 4 to 10, 2015

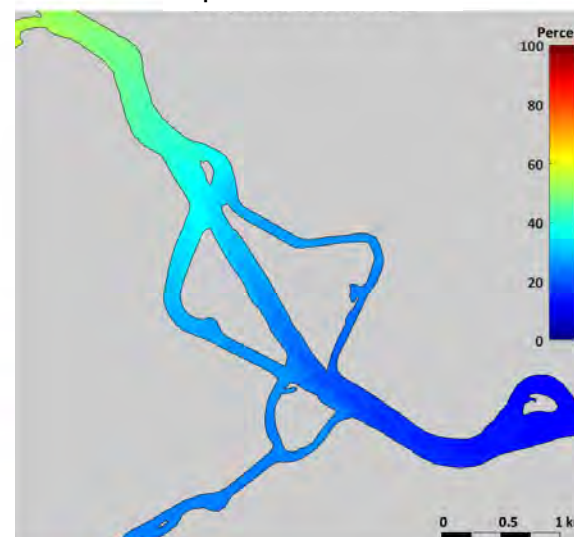


# Key Hydrodynamic Conditions: Percent Sacramento River Water

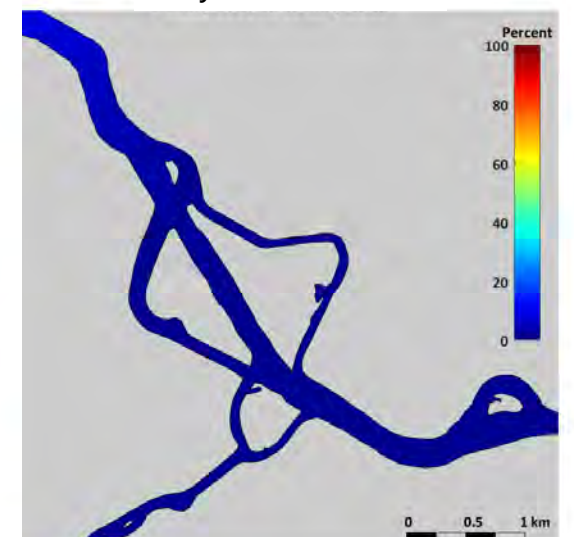
March 16 to 22, 2016



April 3 to 9, 2016



May 4 to 10, 2016



# Modeling Methods Reminder

- Single variables were added to the baseline flow model
- Best single variables were used to build the full model
- Fewer covariates can be fitted to individual transitions, depending on representation in the data
- Checked influence of each individual variable on fit
- Model selection with AIC

Model		<i>K</i>	Deviance	AIC	$\Delta AIC$
Transition	Covariates				
{SJS → MAC {MAC → SJS	$Q_{MAC} + PSW_{MAC} + TOD$				
{SJS → TC	$Q_{TC} + PSW_{MAC} + TOD$	23	4327.3	4373.3	0
{TC → SJS	$Q_{TC}$				
{MAC → TC	$Q_{MAC}$				
{SJS → MAC {MAC → SJS	$Q_{MAC} + TOD$				
SJS → TC	$Q_{TC} + TOD$	20	4334.8	4374.8	6.2
TC → SJS	$Q_{TC}$				
MAC → TC	$Q_{MAC}$				
{SJS → MAC {MAC → SJS	$Q_{MAC} \times Day + PSW_{MAC}$				
SJS → TC	$Q_{TC} \times Day + PSW_{MAC}$	20	4351.3	4391.3	22.7
TC → SJS	$Q_{TC}$				
MAC → TC	$Q_{MAC}$				
{SJS → MAC {MAC → SJS	$Q_{MAC} + PSW_{MAC} + TOD$	21	4437.6	4479.6	106.3
{SJS → TC	$Q_{TC} + PSW_{MAC} + TOD$				
.	.	.	.	.	.
.	.	.	.	.	.
.	.	.	.	.	.

All	$Q_{MAC}$	9	4644.3	4668.3	295.0
All	$Q_{TC}$	9	4849.2	4873.2	499.9
no covariates		6	5322.1	5334.1	960.8

# Turner Cut Best Fit Model

$$\begin{cases} SJS \rightarrow MAC \\ MAC \rightarrow SJS \end{cases} \sim Q_{MAC} + PSW_{MAC} + TOD$$

$$SJS \rightarrow TC \sim Q_{TC} + PSW_{MAC} + TOD$$

$$TC \rightarrow SJS \sim Q_{TC}$$

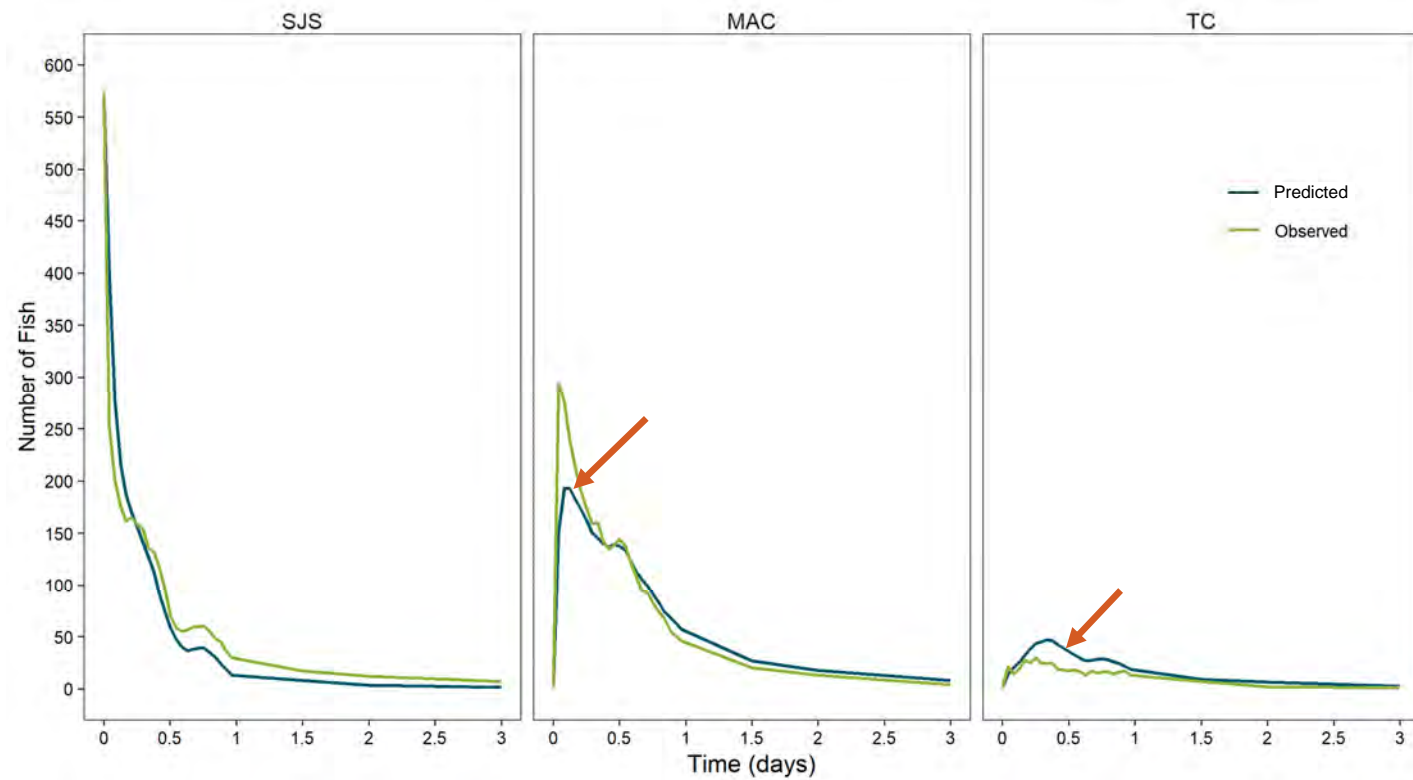
$$MAC \rightarrow TC \sim Q_{MAC}$$

- VIFs <1.2
- 2 individuals having greater influence on model residuals

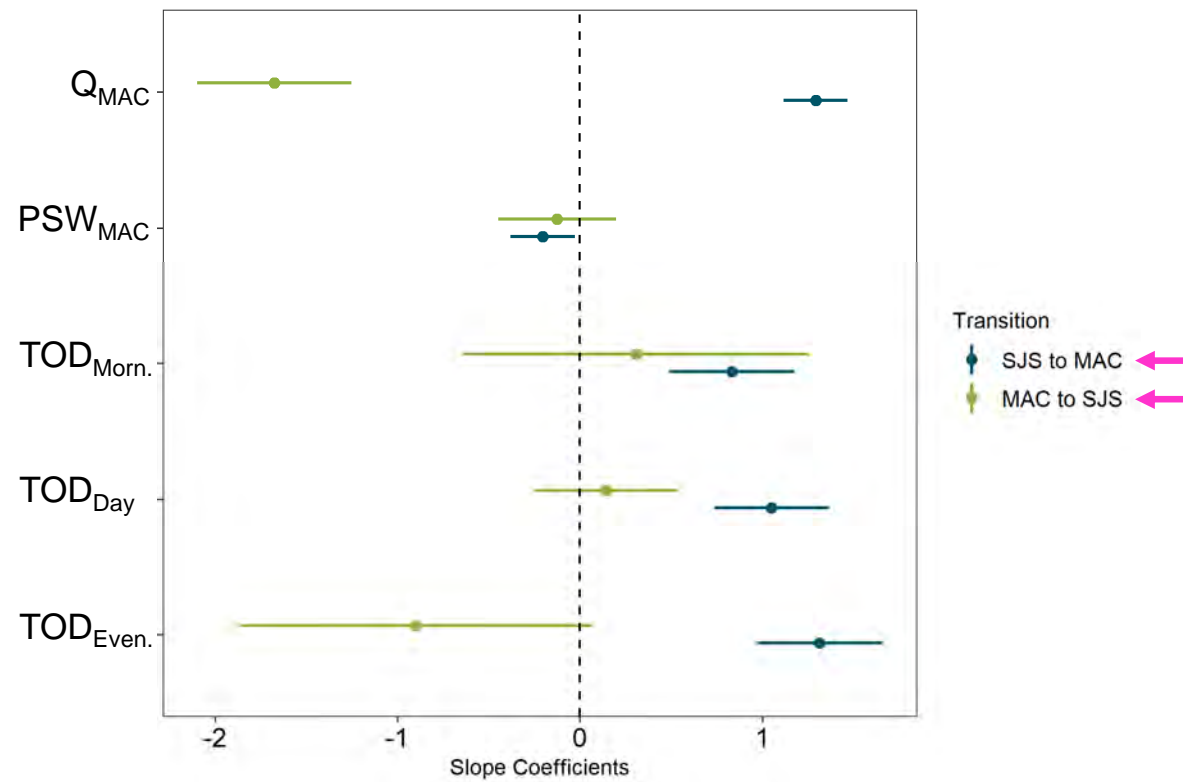
Model		<i>K</i>	Deviance	AIC	$\Delta AIC$
Transition	Covariates				
$\{SJS \rightarrow MAC\}$	$Q_{MAC} + PSW_{MAC} + TOD$	23	4327.3	4373.3	0
$\{MAC \rightarrow SJS\}$	$Q_{TC} + PSW_{MAC} + TOD$				
$\{SJS \rightarrow TC\}$	$Q_{TC}$	20	4334.8	4374.8	6.2
$\{TC \rightarrow SJS\}$	$Q_{MAC}$				
$\{MAC \rightarrow TC\}$					
$\{SJS \rightarrow MAC\}$	$Q_{MAC} + PSW_{MAC}$	20	4351.3	4391.3	22.7
$\{MAC \rightarrow SJS\}$	$Q_{TC} + PSW_{MAC}$				
$SJS \rightarrow TC$	$Q_{TC}$				
$TC \rightarrow SJS$	$Q_{MAC}$				
$MAC \rightarrow TC$					
$\{SJS \rightarrow MAC\}$	$Q_{MAC} + PSW_{MAC} + TOD$	21	4437.6	4479.6	106.3
$\{MAC \rightarrow SJS\}$	$Q_{TC} + PSW_{MAC} + TOD$				
$\{SJS \rightarrow TC\}$					
•	•	•	•	•	•
•	•	•	•	•	•
•	•	•	•	•	•
•	•	•	•	•	•

All	$Q_{MAC}$	9	4644.3	4668.3	295.0
All	$Q_{TC}$	9	4849.2	4873.2	499.9
no covariates		6	5322.1	5334.1	960.8

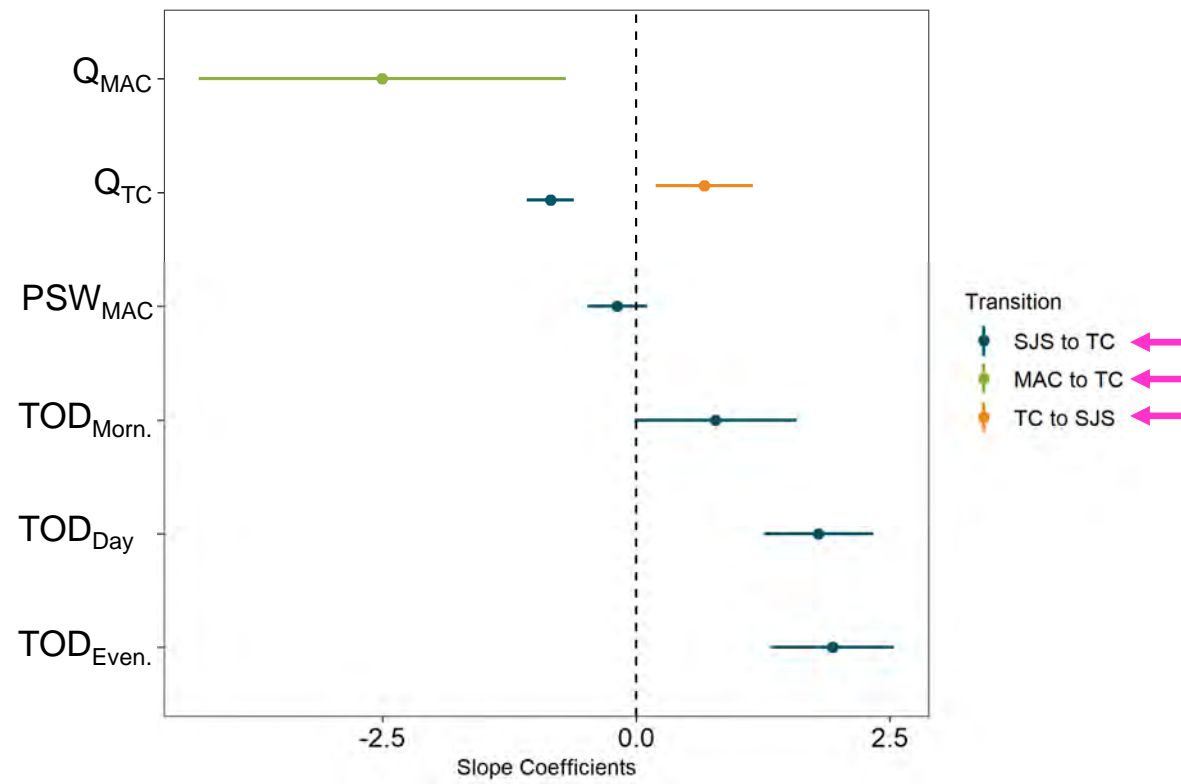
# Model Evaluation



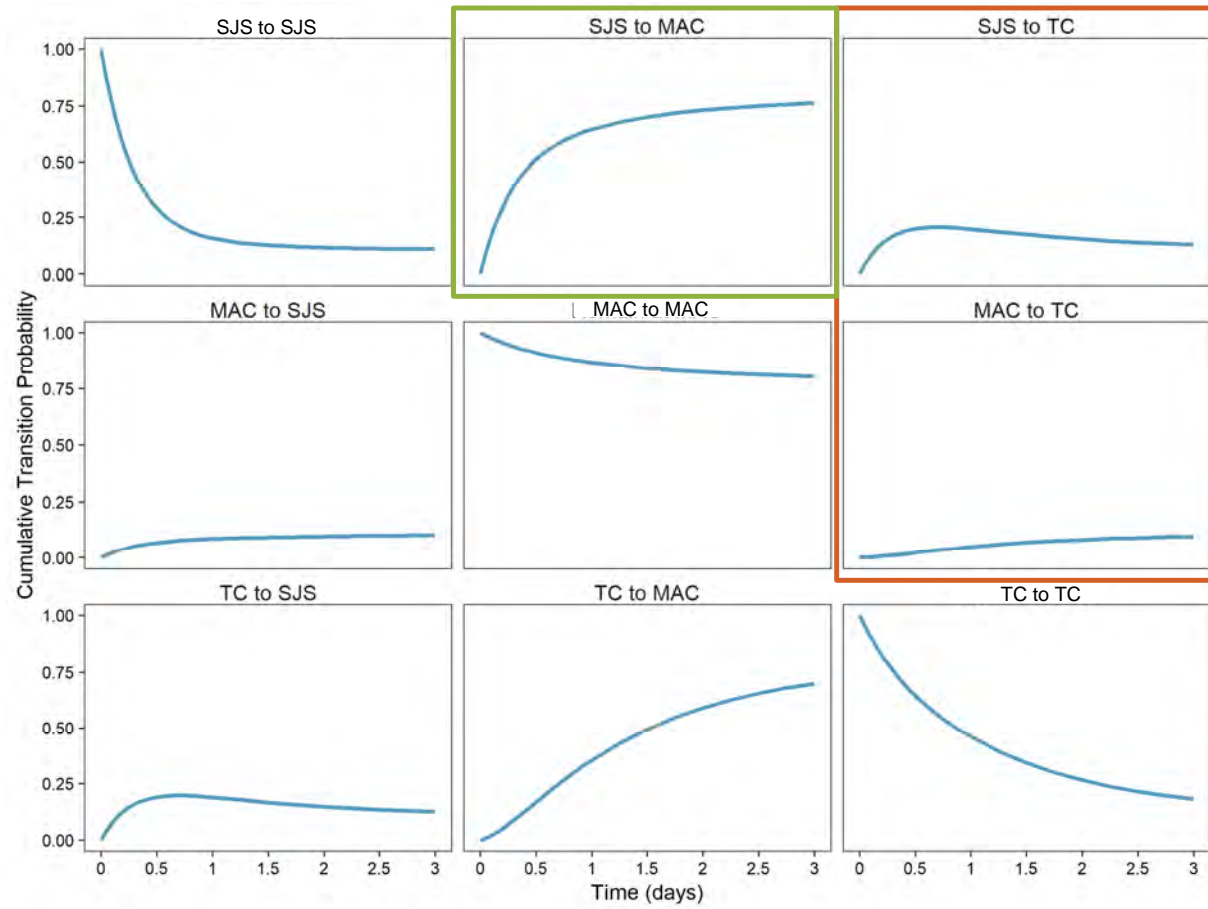
# Slope Estimates: Mainstem



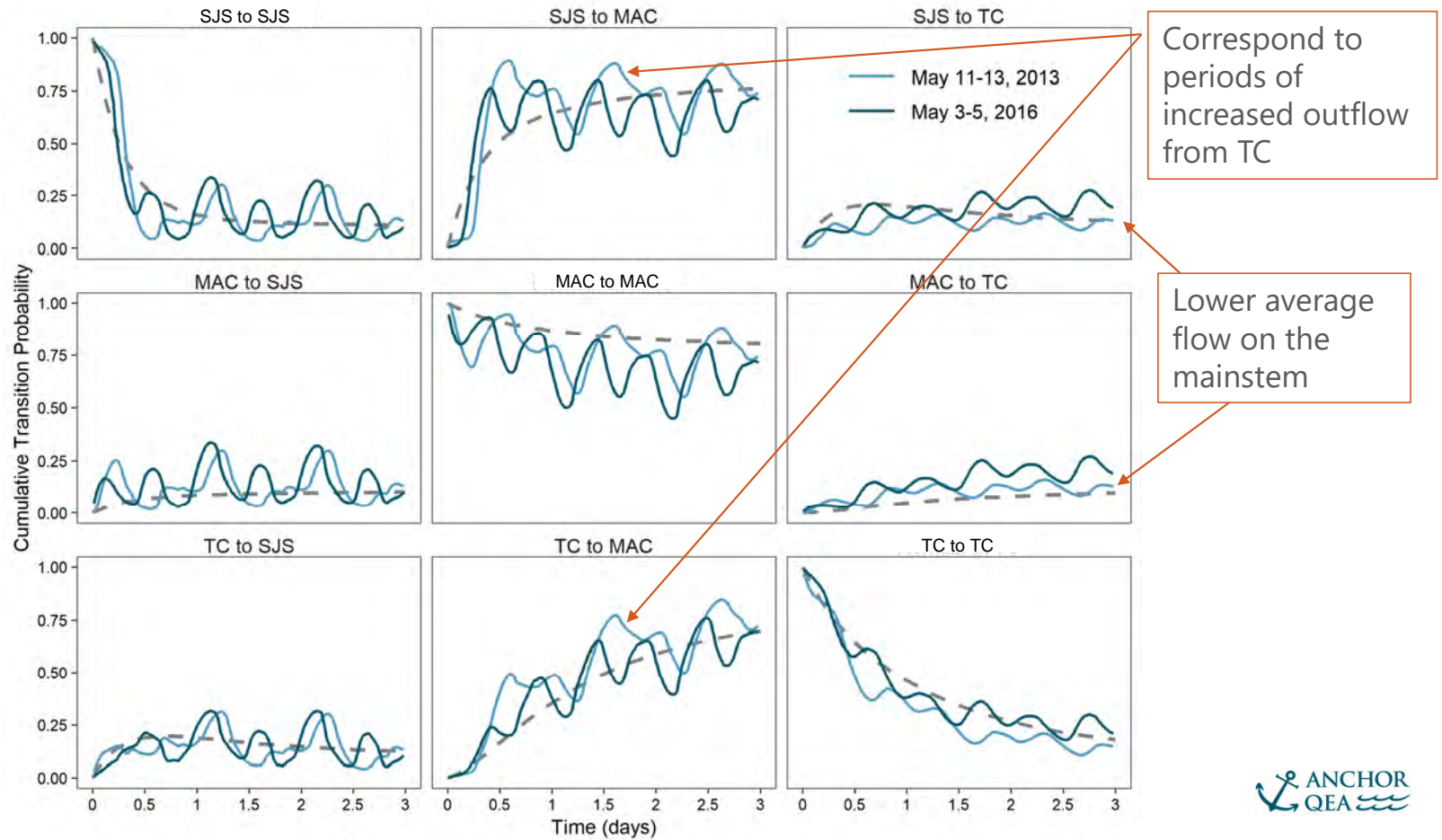
# Slope Estimates: Turner Cut



# Cumulative Transitions: Covariate Averages



# Cumulative Transitions: Time-Varying Covariates



# Summary

- Most of fish spent similar amount of time near Turner Cut (approximately 1 day) as at head of Old River junction
- Majority of transitions (64%) were fish continuing downstream on the mainstem (SJS to MAC)
- About 15% of transitions were fish entering Turner Cut from upstream (SJS to TC) and 3% of transition were fish backtracking from MacDonald Island into Turner Cut (MAC to TC)
- Similarly, 15% of transitions were fish backtracking on the mainstem (MAC to SJS)
- Very few transitions out of Turner Cut (3%)

# Model Findings

- Key variables in best fit fish movement model
  - Flow on San Joaquin River, flow in Turner Cut, percent Sacramento River water, and time of day
- The chance of downstream transition on the mainstem (SJS to MAC) was increased by
  - **Increasing** downstream mainstem flow
  - Presence during the **morning to evening (5 a.m. to 8 p.m.) time**, relative to night (8 p.m. to 5 a.m.)
- The chance of returning upstream on the mainstem (MAC to SJS) was
  - Increased by **decreasing** downstream mainstem flow

# Model Findings

- The chance of entering Turner Cut from San Joaquin Shipping was increased by
  - Presence during **morning to evening (5 a.m. to 8 p.m.)**, relative to night (8 p.m. to 5 a.m.)
  - **Decreasing** outflow from Turner Cut
- The chance of backtracking into Turner Cut from MacDonald Island was increased by **decreasing** downstream mainstem flow
- The chance of leaving Turner Cut and returning to the mainstem (TC to SJS) was increased by **increasing** outflow from Turner Cut
- Cumulative transitions are strongly driven by tidal fluctuations

# Discussion

- Are there any additional elements that should be included in the model?
- Is there anything missing in the interpretation?
- How should this information be presented so that it is most useful to managers?

# Bigger Picture Findings

# High-Level Summary

- Confirmed hypothesis that flow has a large influence on behavior at all three locations
- Water Project Area
  - Fish residence time is much higher than the other areas
    - Chance of remaining at CVP is high once detected there
  - No predominant direction of fish movement
  - Increasing difference in % Sacramento River water across this area increased the chance of all transitions
- Head of Old River
  - Increased mainstem flow increases chance of both downstream transitions
  - Increased Old River flow increases chance of transition onto Old River, but decreases chance of transition downstream on the mainstem
  - Non-migrators are important to model fit
  - Some effect not captured by model (less good fit early in time)

# High-Level Summary

- Turner Cut
  - Most fish are moving quickly downstream on the mainstem
    - Few transitions into Turner Cut
    - Very few transitions out of Turner Cut
  - Daily patterns to movements



What questions  
do you have?

## A.4 Webinar Workshop Meeting Minutes





# Meeting Minutes

## Stakeholder Meeting

---

Evaluation of Juvenile Steelhead Behavioral Response to Hydrodynamic Conditions in the Sacramento-San Joaquin Delta

November 17 and 18, 2021

---

### Webinar Notes: Day 1

#### Attendees

John Ferguson	Anchor QEA, LLC
Michael MacWilliams	Anchor QEA
Sydney Gonsalves	Anchor QEA
Aaron Bever	Anchor QEA
Michelle Havey	Anchor QEA
Makenna Brown	Anchor QEA
Russell Perry	U.S. Geological Survey (USGS)
John Plumb	USGS
Mike Dodrill	USGS
Ben Geske	Delta Stewardship Council (DSC)
Darcy Austin	State Water Contractors (SWC)
Alison Collins	Metropolitan Water District of Southern California (MWD)
Gabe Singer	California Department of Fish and Wildlife (CDFW)
Colby Hause	CDFW
Deanna Sereno	Contra Costa Water District (CCWATER)
Pascale Goertler	DSC
Brett Harvey	California Department of Water Resources (DWR)
Kevin Clark	DWR
Cathy Marcinkevage	National Marine Fisheries Service (NMFS)
Kate Spear	NMFS
Brian Ellrott	NMFS
Barbara Byrne	NMFS
Rene Henry	Trout Unlimited (TU)
Rebecca Buchanan	University of Washington (UW)
Josh Israel	U.S. Bureau of Reclamation (USBR)
Suzanne Manugian	USBR
Matthew Dekar	U.S. Fish and Wildlife Service (USFWS)
Steve Zeug	Cramer Fish Sciences

## **Opening Remarks (Michelle Havey, Anchor QEA)**

Anchor QEA, LLC, opened the meeting by thanking everyone for joining and stated that this project is a collaboration between Anchor QEA and U.S. Geological Survey (USGS). Michelle Havey (Anchor QEA) then introduced the team of investigators and their roles, which consisted of John Ferguson (Anchor QEA), Michael MacWilliams (Anchor QEA), Sydney Gonsalves (Anchor QEA), John Plumb (USGS), Russell Perry (USGS), Mike Dodrill (USGS), Adam Pope (USGS), Aaron Bever (Anchor QEA), and Michelle Havey. Michelle also acknowledged State Water Contractors (SWC), Metropolitan Water District of Southern California (MWD), and Delta Stewardship Council (DSC) for their contributions.

Michelle asked everyone to please sign in to Webex with their name to track the flow of conversation more easily.

### **1. Meeting Objectives, Agenda, and Format**

- Michelle Havey went over the objectives of today's workshop, which are to provide updates to, discuss, and receive input on the following topics:
  - Available information
  - Modeling methods
  - Preliminary findings of the model in the Water Project Area (WPA), Head of Old River (HOR), and Turner Cut (TC)
- Michelle Havey noted that the workshop format would be to provide brief presentations on each of the topics followed by open floor questions and dialogue before moving on to the next topic.
- This was followed by introductions—each person introduced themselves as well as their affiliation (see list of participants on page 1).

### **2. Project Overview (John Ferguson, Anchor QEA)**

- When a Request for Proposals regarding the uncertainty of fish behavior at channel junctions came out, John Ferguson called Michael MacWilliams.
- The project developed out of a Salmon Scoping Team (SST)-identified need for more detailed analysis of fish behavior. Analysis combined detailed 3D hydrodynamic model predictions with steelhead telemetry data and used methods consistent with USGS Chinook Salmon analysis.
- An overview of the timeline is as follows:
  - Fall 2020
    - Reviewed documents about what was going on with salmonids in the south Sacramento-San Joaquin Delta (Delta).
    - Gathered hypotheses.
    - The Collaborative Adaptive Management Team (CAMT) Salmon Subcommittee replaced SST.

- A meeting was held to discuss hypotheses, what data was available, and adjusted future plans.
- December 2020
  - Gathered more thoughts and perspectives before launching into the analysis that is being presented today.
- Fall 2021
  - Stakeholder workshop to go through methods and results as a check-in before a more formal interpretation of the model commences. Participants are urged to give their input, make suggestions, and identify additional analyses or interpretations.
- Spring 2022
  - Draft and final contract reports and a draft manuscript for publication are due.

### 3. Methods Overview

#### *Hydrodynamic Modeling (Aaron Bever, Anchor QEA)*

- The goal was to predict environmental conditions that are collocated with telemetry data at a fine temporal and spatial scale to describe what the environmental conditions at a particular junction/hydrophone array would have been using the UnTRIM Bay-Delta Model. The model includes major inflows, exports, and intakes and spatially varying precipitation, wind, and evaporation rates. The model also includes Delta Island Consumptive Use (DICU) and temporary gates and barriers. It can accurately predict many variables, including flow, salinity, and water temperature, throughout the Delta.
- The model was used to simulate 6 years of hydrodynamic conditions corresponding to the time periods with the telemetry data collection.
- Sacramento River (SR) water was tagged with tracer to predict the percentage of SR water at hydrophone array locations.
- From the model, eight variables were extracted (cross-sectional water flow, depth-averaged salinity, depth-averaged temperature, water level, water depth, depth-averaged percentage of SR water, depth-averaged current and speed, and depth-averaged velocity), and an additional six variables were calculated using model output (Old and Middle River [OMR] flow, Qwest, Delta outflow, flow towards State Water Project (SWP) and Central Valley Project (CVP) exports, Delta tributary inflows, and inflow-to-export [I:E ratio]). These variables were calculated at a very large number of locations corresponding to all of the locations where telemetry data were collected, channel center and edge locations at each cross-section, and at numerous other locations throughout the Delta. Some variables, such as percentage of SR water, were calculated at every model grid cell to allow for spatial visualization at both Delta-wide and junction-specific scales.

### *Preliminary Juvenile Steelhead Telemetry Data Background (Sydney Gonsalves, Anchor QEA)*

- From 2011 to 2016, fish were surgically implanted with acoustic transmitters and released into the San Joaquin River (SJR). A USGS laboratory processed the acoustic tag detection data into detection events. Rebecca Buchanan (UW) applied a predator filet based on assumed behavioral differences between juvenile steelhead and resident predator fish.

### *Choosing Smaller-Scale Areas for Analysis Was Based On the Following*

- Stakeholder feedback
- What areas were of interest/needed additional analysis
- Initial evaluation of the telemetry data to see if the areas of that were of interest had enough coverage in terms of hydrophone arrays being in close enough proximity to each other and enough fish detections in those areas.
- Based on that process, three areas were determined for further analysis: WPA, HOR, and TC.

### *Type of Model Implemented*

- The model structure was that fish can move back and forth from any of the states (hydrophone arrays) and the transitions can be modeled with the same or different covariates. The outputs are transition probabilities.
- To develop hypotheses, the team went through research hypotheses to find what people think are important for fish behavior. Based on this, the hypothesis was developed that water flow or water velocity would be the most important cue for fish transitions. Other covariates included were fish specific data, other hydrodynamic variables, time of day, and HOR barrier presence.
- Sydney Gonsalves then described the modeling process and asked if there were any questions. Two participants commented that thus far the presented information was clear.

## **4. Model Results: Water Project Area (Sydney Gonsalves, Anchor QEA)**

- Unfortunately, in this area, all three hydrophone arrays were only operational from 2014 to 2016, so the analysis is limited to those years. The hydrophones were located in West Canal (WCL), near the Radial Gates (RG), and near the CVP.
- Over the course of those 3 years, 789 fish were detected with a median time spent in the WPA of 15.6 hours. Additionally, fish release groups that were released after the HOR barrier was in place were less likely to show up later in the WPA. Sydney Gonsalves noted that there was not a strong directional trend of fish movement transitions, although there were slightly more transitions from RG to both WCL and CVP and from WCL to RG. This could also be because fish that transitioned from WCL to CVP may have been detected at RG.
- Based on the UnTRIM model, there is not one predominant direction of flow in the WPA.

### *Key Hydrodynamic Conditions*

- In West Canal there is both upstream and downstream flow (indicated by negative and positive values), although more of the distribution of flow was negative (upstream), towards RG and CVP. Tidal average flow was generally negative over the tidal cycle.
- There is a large range over both the different years as well as the seasons in terms of percentage of SR water. The difference of percentages of SR water from WCL to CVP: There was an average difference of about 16%.
- Question (Josh Israel, USBR): Do we know if the difference between percentage of SR water between West Canal and CVP is consumed in the Delta or if it moves west and out of the Delta?
  - Response (Brett Harvey, DWR): It may also be dilution due to the SJR water coming from the east.
  - Michael MacWilliams: During periods of high SJR flow, water ending up at CVP is usually coming from the SJR via Grant Line Canal and the southern part of Old River. Water that's ending up at RG is primarily coming down from the north much of the time. Also, the source of the water to the CVP depends on SJR flow—when it's strong, then it goes across the south Delta and reaches the CVP; when it's weak, more SR water goes into the CVP.
  - Josh Israel: Said he was misinterpreting the area, he thought it was 20 miles further north (Frank's track). He agrees that it makes more sense why you have predominant water on Grant line; he thought it was railroad cut.
- For the six transitions in the WPA, the same three covariates were used in the model. Those covariates were instantaneous flow in the West Canal, the difference in percentage of SR water between CVP and WCL, and release day (RD). The predicted compared to observed data was a good fit.

### *Slope Coefficient Estimates: Downstream Transitions (Towards Ocean; Central Valley Project to Radial Gates, Central Valley Project to West Canal, and Radial Gates to West Canal)*

- Sydney Gonsalves used a dot-whisker plot to illustrate that as flow increases, as differences of percentages of SR water between WCL and CVP increases ( $dPSW_{WCL-CVP}$ ), and as RD increases, the likelihood of downstream transitions increases, with the exception of CVP to WCL for the latter two metrics. Michelle Havey then asked to pause to allow participants to digest information, ask questions, and provide input.
- Question (Barbara Byrne, NMFS): Regarding the  $dPSW_{WCL-CVP}$ , I think it could happen if the inflow from the Vernalis and the SR to the Delta were the same, then the percentage differential could change if exports change. For example, if exports go up, then that may draw in more SR water and increases that SR percentage when inflows are constant. But is it also correct that if exports were constant and if SR inflows increased, it would also increase the  $dPSW_{WCL-CVP}$ ? Can Anchor QEA comment on that?

- Response (Michael MacWilliams): The main drivers of the  $dPSW_{WCL-CVP}$  are what the exports are individually and combined, the SR inflow, and the SJR inflow. The SR water percentage is relatively low if the SJR inflows can meet the export demand. When the SJR inflow is smaller, then the exports tend to pull more SR water. Still, it looks like CVP is primarily going to get the first gulp of SJR water, the deficit gets pulled from SR down through the Delta, and the first gulp of water goes to the SWP.
  - Barbara Byrne: What is the independent mechanism of the  $dPSW_{WCL-CVP}$ ? For a given  $Q_{WCL}$ , how does the  $dPSW_{WCL-CVP}$  independently impact the increased likelihood to go downstream?
- Michael MacWilliams: Given that it's an important variable at this location, I think we need to do more analysis to find what it is correlated to and how it fits together with SJR exports. This is a conceptually new covariate that not many people have looked at, so it's interesting that it has become predictive.
- Question (John Ferguson): Why would an increased  $dPSW_{WCL-CVP}$  cause fish to move more downstream? Different increases cause them to move further downstream?
  - Response (Sydney Gonsalves): That's a good question, and I think looking at the upstream transitions may further scramble the thought process.
  - Michelle Havey: We have two more questions; let's answer those before moving on to upstream transitions.
  - Comment (Deanna Sereno, CCWATER): We have done a lot of fingerprinting analysis in the Delta and it does vary significantly with HOR and Delta cross-channel operations. The way they're looking at this doesn't consider the residence time of the water; some of the SR water may have come in 2 months ago. I think if we're going to use it as a variable here, we need to better understand the mechanism driving these transitions. I'm hoping to learn a little more about the water quality variables you looked at as well.
- Question (Deanna Sereno): The  $Q_{WCL}$  on the graph is the tidal flow not the tidally averaged, correct?
  - Response (Sydney Gonsalves): Yes, that's the instantaneous flow.
- Question (Brett Harvey): It seems like you have mainly SR water on one side and SJR water on the other side, and the flow in West Canal would be a dominant driver of the  $dPSW_{WCL-CVP}$ . It seems like there would be some correlation between the flow and the differential. In this analysis, was the variability caused by the  $Q_{WCL}$  removed from the  $dPSW_{WCL-CVP}$ ? Does the slope represent the independent influence of the differential?
  - Response (Sydney Gonsalves): No, this is the fitted slope coefficient for the whole model, so they are not partial slope coefficients.
  - Brett Harvey: If the influence of flow was removed, then one potential mechanism for the effect of the differential would be an olfactory cue, but it would be difficult to disentangle it from the influence of flow in the West Canal.

- Question (Brian Ellrott, NMFS): Can I look take a look at the percentage of SR water maps again, and specifically the portion of Old River that connects Middle River to the RG area? I'm trying to see the difference between WCL and that stretch there.
  - Barbara Byrne: Can we highlight the WCL hydrophones and the CVP hydrophones on that map to illustrate where the  $dPSW_{WCL-CVP}$  comes from?
  - Sydney Gonsalves: The UnTRIM model generated the percentage of SR water at each of those locations for those dates. When I saw these figures, I calculated the difference between WCL and CVP because I wondered if it was more the difference than the actual point value, and it did end up improving the fit of the model. We're excited to talk to the participants about the interpretation.
  - Deanna Sereno: These maps are just meant to be snapshot examples; it would be good to look at how it varies in different years.
  - Sydney Gonsalves: We have maps for all 3 years that we can add.

*Slope Estimates: Upstream Transitions (Radial Gates to Central Valley Project, West Canal to Central Valley Project, and West Canal to Radial Gates)*

- Looking at the  $Q_{WCL}$ , we see what we would intuitively expect, which is that as downstream flow decreases, the chance of making these upstream transitions increases. However, increases in the other two variables ( $dPSW_{WCL-CVP}$  and RD) still lead to increases in upstream transitions. Sydney Gonsalves notes that this is making it difficult to interpret the model.
- Question (Barbara Byrne): On the map with the blue and orange arrows to show the directionality of flow, the arrow off of Old River into the CVP facility where the arrow was pointing from export facilities out to Old River was counterintuitive. Is that maybe why this differential is different than what we would expect?
  - Sydney Gonsalves: No, the upstream transitions are just the nomenclature from WCL or RG to CVP. The only flow that we have here is the flow in WCL. It would affect the results if the flow into CVP was one of the variables included in the model, but because the only flow direction is WCL, it is based only on flow at that position.
- Note (Sydney Gonsalves): I heard someone ask about water quality variables, and we had temperature and salinity that were generated from the UnTRIM model, but temperature was pretty much the same across the whole area, as was salinity. During the modeling process those variables weren't influential on the transition. But it is true that we didn't have a whole range of water quality variables to consider.
- Question (Deanna Sereno): Did you ground-truth your model to actual salinity observations?
  - Response (Aaron Bever): Yes, we ran an assortment of model validations for each of the years, and they all looked the same as we expected.

- Deanna Sereno: There was 1 year where the salinity jumped up high late in the season but there weren't fish left at that point. It was a bromide problem on Old River at Highway 4 that they saw at both banks, but we didn't see it just a couple miles to the north.

### *Cumulative Transitions: Covariate Averages*

- The figure shows that the covariates held to their averages, which is unrealistic but at the same time a good summary. The x-axis shows the time in days, and the y-axis shows the cumulative transition probability over time. Fish were mostly in the area for 6.5 days and show only until 7 days.
  - Once a fish is detected at CVP, the chance of remaining there never drops below 75%.
  - Upstream transition probabilities (being detected at RG or WCL and then later at CVP) increased over time.
  - Downstream transition probabilities (CVP to WCL or RG to WCL) remains low over time.
- Comment (Alison Collins, MWD): It could help if in the figure it was easily color-coded for transitions between upstream and downstream.
- One participant asked for clarification on what the panels meant, and Sydney Gonsalves clarified that the graphs illustrate the transition probabilities rather than what fish did between two places—it's about the chance of ultimately moving in a certain direction.
- Question (Brett Harvey): Where are the WCL telemetry points? Are they between the CVP and RG or are they downstream of RG?
  - This question spurred a discussion of whether or not the receivers at RG would detect fish just passing through the WCL. The discussion included Sydney Gonsalves, Brett Harvey, Kevin Clark (DWR), Rebecca Buchanan, and unidentified participants.
  - Response (Sydney Gonsalves): Downstream of RG. This area is not a true junction like the other areas, but we needed to work with what we had.
  - Brett Harvey: What's the difference between WCL to CVP versus RG to CVP? RG to CVP means that they're actually going into Clifton Court or just passing the gates.
  - Sydney Gonsalves: Fish could potentially just pass by RG, be detected there, and then continue towards CVP.
  - Brett Harvey: So they don't have to actually be inside the RG?
- Question (Kevin Clark): Which receivers did you use at RG for analysis? The two that are inside should not be able to hear out to WCL, but the outside two should.
  - Response (Sydney Gonsalves): We used all four.
  - Kevin Clark: Maybe you should only use the ones on the inside, so that detections would indicate that they were inside RG, since the receivers outside might only tell you that they were passing by.
  - Rebecca Buchanan: The outside receivers would be able to detect fish in the entrance channel but not actually detect fish just passing by in the canal. Furthermore, if the gates

have been opened for a while, the receivers inside the gates can also "hear" the entrance channel.

- Kevin Clark: Does fish that are denoted as remaining at RG mean that they're detected twice or that they just weren't detected elsewhere?
- Brett Harvey: Bear in mind that they might have gone into Clifton Court, but we don't know.
- Kevin Clark: It may not even indicate the inlet channel, which is the tricky part.
- Brett Harvey: Reflect on fish movement and behavior; it seems like once they move into these facilities, fish are not experiencing flows or the SR differential.
- John Ferguson: I suggest that we look at all three variations of the receivers—using all four, using just the two inside, and using just the two outside.
- Sydney Gonsalves: We can also find out where fish ended up, which won't affect results of this model, but we'll be able to say this many fish generated this many transitions and of those this number or percentage had they're last detection there.
- Part of the point of this study was to see how far the available information could be pushed to answer questions and those questions that could not be answered; as a result, we could then recommend additional studies to be conducted.
- Michelle Havey: The document that we sent out on Friday does have little inset maps to keep yourself oriented to the hydrophone array. We will send out the slides after the discussion today so that tomorrow you can have your slides open.
- Question (Deanna Sereno): The discussion with Kevin helped her quite a bit since her expertise is in hydrodynamics rather than biology. When it says that a fish remained at the CVP for so many days, does that mean that it stayed there or that it wasn't detected? Because it seems that a fish may pass by RG, get detected, and then get salvaged but be counted as "remaining at RG."
  - Response (Sydney Gonsalves): When looking at the transition probabilities it's the chance that a fish is detected at one state and then is detected at another state in the future. It doesn't say anything about the detection history of the fish. The terminology "remaining at CVP" means that if a fish is detected there, then the fish's chance of remaining there is high. Even if it stays there for a while its chance of remaining is still high. But at RG, over time, the chance of a fish still being there is low is the interpretation. Same with WCL, it's not some place where the fish are staying.
    - Note correction to participants on November 17: terminology "remaining at CVP" should correctly be "CVP to CVP". Meaning is the same as stated earlier for other transitions: it's the probability of being detected at CVP at some time (t) and then being detected at CVP some later time (t + u). It does not indicate whether the fish was present at CVP the entire time.
  - John Ferguson, Anchor QEA: Does "remaining" mean they don't make another transition?

- Michael MacWilliams: I think the question is, do you need another detection or just an absence of a detection somewhere else to be counted as "remaining?"
- Sydney Gonsalves: Capturing distribution of all individuals in the study.
- Deanna Sereno: It seems like fish that get salvaged get counted as "remaining." She arrived at this conclusion by adding probabilities.
- Sydney Gonsalves cautioned against adding the rates of transition probabilities because we're looking at the cumulative transition probabilities and not the instantaneous rates, they don't necessarily sum to equal the other.
- Comment (Russell Perry): These are calculated just as the average covariate values. You can use the model if you have a timeseries of covariates for a particular timeseries to say what's the cumulative probability of transition to every state. Over time that should give you the stationary state distribution, which would eventually be the final proportions of fish in each state. That's the way he's used it before. That must consider an entire timeseries of the covariates for the given starting point in time when exposure starts. It can be used to look at expected distribution last transitioning to a state after a certain about of time.

### *Cumulative Transitions: Time-Varying Covariates*

- The gray dotted line is still the transition probabilities over the covariate averages but can also look at when covariates are changing. The blue is from March 6 to 12, 2016, and the green line is from May 4 to 10, 2015. This figure illustrates that specific hydrodynamic conditions affect transition probabilities. For example, a quick jump up on the WCL to CVP panel happened during a period of relatively high reverse flow in March 2016. You can also see the effect of incoming tide on the RG to WCL panel. The averages fail to describe the variability in the transition probabilities.
- Blue line is from March 6 to 12, 2016; fish were released between February 24 and 27, 2016; range of flow in WCL was -400 square meters per second ( $m^3/s$ ) to +120  $m^3/s$ , and the  $dPSW_{WCL-CVP}$  was about 23%.
  - Green line is from May 4 to 10, 2015; there was a wider range of release groups present (early, late March and in April), median flow was much lower reverse flow (25  $m^3/s$ ), and  $dPSW_{WCL-CVP}$  was 5%.
- In general, cumulative transition probability sort of comes to an asymptote; you can see periods of high flow and tidal influence.
- Question (Barbara Byrne): On that panel where you have the influence of outgoing tide, are those bumps fish going in and out of the RG?
  - Response (Sydney Gonsalves): Those are showing periods during which the transition probability is higher (of RG to WCL) because there's more downstream flow. It's a piecewise transition probability, so it's showing what the probability was over a 15-minute period and the covariates are changing, and we take the product of that, and that gives

you the probability of transition of every time up until that point. As more periods of time are added, it cumulatively adds transition probability.

- Question (Steve Zeug, Cramer Fish Sciences): On the bottom left panel there's this period of relatively high reverse flow, and so the transition probability is much higher than the average. But on the next panel the transition is going the same direction, but the arch is lower. Why would that blue line flip?
  - Response (Sydney Gonsalves): The high reverse tide is only in the first half of that day. And you do get that on both the bottom left panels (WCL to CVP and WCL to RG). And another interpretation would be that they went by RG. In any case though we get a peak and then a drop-off.
  - Steve Zeug: Does the bottom middle panel mean that they went past RG and that wasn't their destination?
  - Sydney Gonsalves: The model is only saying that early on the chance of transition from WCL to RG was high and then the chance of ultimately ending up to RG was lower.
  - Michael MacWilliams: Both are ultimately being detected at CVP whether they are detected at RG or not.
  - Rebecca Buchanan: Not all fish that passed the entrance to the RG were detected at RG.
  - Steve Zeug: Kevin's question needs to be resolved: What does RG mean? Are the RG are a state? Did they enter that state?
  - Rebecca Buchanan: They did try so that receivers at RG did not reach WCL. They lowered the gain of those receivers.
  - Michelle Havey confirmed that the receivers don't see in the main canal.

## *Summary*

- Fish spent a longer time near water projects than other areas evaluated.
  - The chance of being detected at CVP and later being detected again at CVP is high.
- 80% of fish experienced some downstream flow; however, flow in West Canal was reversed about 63% of the time.
- There was no predominant direction of movement.
- SR water is variable throughout the season, between years (20% to 80%), and across the area.

## *Model Findings*

- Key variables were instantaneous flow,  $dPSW_{WCL-CVP}$ , and fish release date.
- Chance of fish moving downstream (toward WCL) is increased by increasing downstream flow (or decreasing reverse flow) in WCL.
- Chance of fish moving upstream (toward water projects) is increased by decreasing downstream flow (or increasing reverse flow).

- Increasing difference in percentage of SR water and later release date increased the chance of both upstream and downstream movements.
- Does this suggest nondirectional movement and exploratory behavior by fish?
- The average cumulative probability of a fish remaining at CVP once detected there was high.
- The average cumulative probability of a fish detected at WCL or RG transitioning to CVP increased to approximately 70% after 6 days.
- Cumulative transitions considering time-varying covariates show that average conditions are not sufficient to fully describe variability in transition probabilities

## 5. Discussion

- John Ferguson asked the participants to comment, point out what was missed, and offer ideas for interpretation and how it can be presented so the information is useful and applicable.
- Question (Rebecca Buchanan): Did you consider the route fish took to get to WPA? Was it via Grant/SJR via TC or Columbia Cut? There may be some difference in how they're responding to hydrodynamic conditions in that area based on where they came from.
  - Response (Sydney Gonsalves): We haven't done an in-depth analysis on that yet but have tried release group, RD, etc. Of those that were released before the HOR barrier was in place, more came directly to the WPA. After the HOR barrier was in place, a lot fewer of the fish made it to the WPA in the first place, likely because they had to take a more circuitous route to that area. She will keep trying to figure out for each fish what route they took.
- Was there much data from Columbia Cut?
  - Sydney Gonsalves: In order to look at a junction need there needs to be three places near each other with hydrophone arrays. Columbia Cut only had sufficient hydrophone arrays installed in 2 years, 2015 and 2016, so given the time limitations, we decided to focus on other areas.
- Comment (Steve Zeug): In terms of how to present this to managers, he suggested that it could be useful to put into the framework of how operations is affecting behavior. That might include things like OMR thresholds and how fish are responding to those thresholds, especially if they ever move north again. He also suggested potentially looking at the preferential operations of CVP versus the SWP, and how drawing water from one facility is affecting behavior at all relative to the other. And finally, it would be interesting to look at the final fate of these fish—when they arrive under a particular set of conditions, are they found alive elsewhere in the data? What are the survival and behavioral outcomes?
- Question: (Alison Collins): Of the fish that remain near the CVP, are they entrained?
  - Response: Sydney Gonsalves did not know that answer off the top of her head.
- Comment: (Brett Harvey): It might be good to reflect on unanswered questions from the CAMT report and discuss what this model can inform in terms of decisions and what it can't. How does a change in cumulative flow, average flow, and instantaneous flow influence the movement of

fish one direction or other? This could reflect on fish anywhere in the Old River corridor. Since the model looks at how fish respond to changes in velocities and flows, it could potentially be used for other channels as well. We don't understand how fish respond to other cues: olfactory with the differential or fingerprint. It might also be interesting to look at the influence of olfactory cues (in terms of the SR differential), and this could also be used at other locations. How fish experience that gradient is something to think about, and hopefully the model can help answer questions without setting up a separate experiment. Since the model is still not super certain, it would be good to dive in with a targeted study. What happens to fish once they get around the facilities? These are big fish that are on their way out (older juvenile salmon).

- John Ferguson noted that it is just as interesting to see what variables are not in the model as what are. The model only has three variables, but many were looked at.
- Comment (Deanna Sereno): Fish movement is affected by operation of gates. One of the strategies (Priority 1) to operate the gates is to close them during a flood tide and then open on ebb tide. She suggested looking at different groups and seeing if those strategies affected their movement. Changing the gate operations is a strong driver of currents in that area. She also wanted to mention that the percentage of SJR water is not 1 minus the percentage of SR water, since a lot of water is diverted from agriculture. Because of this, knowing the percentage of SJR water would allow you to be more mechanistic about why you're seeing what you're seeing.
  - Michael MacWilliams: Regarding the Clifton Court gate strategy, the hydrodynamic model used the exact time of opening and closing of the gates, but noted that we haven't looked at how different gate operations strategies affect the behavioral decisions yet, but that it is a good suggestion.
- John Ferguson asked Michael MacWilliams and Aaron Bever if percentage of SJR water could be calculated.
  - Michael MacWilliams responded that it could be done but would require rerunning all the model simulations. He also noted that there are many additional inputs (from other rivers and agricultural diversions). We will look into adding percentage of SJR water into the analysis.
- Comment (Josh Israel): Trying to explain something that we do not understand (like the finding of percentage of SR water increasing the chance of transition) will confuse managers. He also noted that he liked Deanna Sereno's idea of looking at SJR water since we're working with SJR detections, and it might show nondirectional or exploratory behavior. Additionally, the finding of the traditional covariates not being useful is still an important finding to managers. We did show that the instantaneous flow variable is important and is mechanistically explanatory; it makes sense to him that if you have a positive or negative flow, you have an increasing or decreasing probability of transitioning. He suggests that one way to explore the percentage of SR water difference would be to look at another location where you see differences in SR water that look like the differences close to the facility space, and you may be able to see similar exploratory

behavior to support the findings of the model. This would be important because he is worried that people will jump to the conclusion that something is going on with the facilities, but that's not what we showed. It's also not clear to him whether transition to the CVP is good or bad. He hasn't really thought too much about management response being about increasing or decreasing transitions. We've tended to have the goal be to improve survivability rather than just transitions.

- Michael MacWilliams agrees that there are other junctions with similar percentage of SR water differences. And we could further investigate the olfactory idea.
  - Josh Israel: The area between Columbia Cut to Frank's Track is tricky for looking at fish routes since there are so many possible routes, and we also see low survival.
  - Rebecca Buchanan: We have the potential to see what was going on with the steelhead in the later years when we did have receivers at Columbia Cut and at the mouth of Old River and further upstream at TC.
  - John Ferguson: We're looking at behavior at junctions on short spatial and temporal scales, but he thinks that it is interesting OMR is not included in any of the models for any of the locations.
- Comment (Barbara Byrne): Regarding the SR water differential, she has been thinking that the metric may be something that fish are not responding to mechanistically but may still be informative. So it might be interesting to look at how the percentage of SR or SJR water differential relates to the underlying velocity distributions. Maybe it's a useful proxy for what underlying velocity distribution looks like, and may explain a sort of "escape from Alcatraz" scenario.
- Comment (Steve Zeug): Since we found that the instantaneous flow is one of the controlling factors, it might be interesting to look at same value of OMR but different arrangements of SJR flow and exports, and see how that affects the probabilities. The flows that are affecting things around the facilities are not necessarily strongly influenced by the SJR. He suggested that drilling down into the components of OMR and I:E might reveal some better metrics to manage the system.
- Comment (Russell Perry): One idea is if the receiver is on the inside of the gate and we believe that's a one-way street for fish, that can be coded as an absorbing state. Then you can see how those movements are affecting transitions to Clifton Court, which is a state that a fish can't return from.
  - Steve Zeug: Based on some data he has been working on, it's definitely not a one-way street into Clifton Court for big fish.
- Comment (Deanna Sereno): One of the problems with only doing a tracer on SR water rather than all inflow points is that when you have areas that are less than 10% SR water, the water could have come from SR before the model simulation started or could have come from so many different inflows. It may make more sense to do the tracer from the SJR because then you can be

sure what you're measuring as SJR comes from SJR while you're releasing the dye. But the SR has long residence times and so some of the water may have come from before the tracer was released.

### *Closing Remarks for Day 1*

Michelle Havey reminded folks to briefly review the slides for tomorrow's presentation so they can preview of TC and HOR. She asked if there were any last thoughts before closing out the meeting.

## Webinar Notes: Day 2

### Attendees

John Ferguson	Anchor QEA
Michael MacWilliams	Anchor QEA
Sydney Gonsalves	Anchor QEA
Aaron Bever	Anchor QEA
Michelle Havey	Anchor QEA
Theresa Bersin	Anchor QEA
Russell Perry	USGS
John Plumb	USGS
Mike Dodrill	USGS
Ben Geske	DSC
Alison Collins	MWD
Gabe Singer	CDFW
Colby Hause	CDFW
Deanna Sereno	CCWATER
Steve Zeug	Cramer Fish Sciences
Brett Harvey	DWR
Kevin Clark	DWR
Kate Spear	NMFS
Krisin Begun	NMFS
Brian Ellrott	NMFS
Barbara Byrne	NMFS
Arnold Ammann	NMFS
Rene Henry	TU
Cyril Michel	University of California Santa Cruz (UCSC)/NMFS
Rebecca Buchanan	UW
Josh Israel	USBR
Matthew Dekar	USFWS

### 1. Review of Yesterday's Workshop

John Ferguson (Anchor QEA) opened the meeting with a summary of yesterday's workshop. After the workshop, the Anchor QEA team talked through model structure with Mike Dodrill (USGS) and held an email conversation with Rebecca Buchanan (UW) regarding the predator filter. John Ferguson presented some takeaways from the after-meeting discussion:

- UnTRIM model and residence time: Deanna Sereno (CCWATER) had raised the point that SR water could have come in much earlier. When Michael MacWilliams (Anchor QEA) and Aaron Bever (Anchor QEA) run the UnTRIM model, they start the model run several months before the actual period of interest, which would allow residence time to factor in.

- Could we compare the percentage of SR water at water projects and at TC? Sydney Gonsalves (Anchor QEA) pointed out that the differentials at TC are much lower, so comparison would not work, but that we can keep in mind those types of comparisons moving forward.
- Analyzing percentage of SJR water: Would have to re-run the UnTRIM model for all years, which would take approximately 8 days of running time.
- Brett Harvey (DWR) had a comment on disentangling variables and looking at each variable separately, which would work in a linear regression, but Sydney Gonsalves pointed out that we can't really do this in a multistate model.
- Discussed looking at the ultimate fate of individual tagged fish—this is something we will work on.
- RG: Four hydrophones are present there, providing detectability of fish on the inside versus outside. We will look at separating those; we'll separate the four hydrophones into sets of two and run the model with just inside, just outside, and combined to detect influence.
- Russell Perry (USGS) pointed out that there is a hydrophone in the CVP salvage tank. We may want to look at which fish end up in this absorbing state and are therefore removed from further analysis.
- Rebecca Buchanan pointed out that the predator filter is not perfect. The Anchor QEA team is talking to her about communicating clearly how the filter was applied in the model. We will potentially look at sensitivity by turning the filter off and rerunning the model. The filter flag would be a covariate and would allow us to see how sensitive it is.
- Correction to Slide 74 showing the 3 years of data at TC. The years should be 2013 (not 2014), 2015, and 2016.
- Discussion of the term "Remain at" for cumulative state plots. We decided that the term "remain at" should be replaced by "CVP to CVP". Sydney will clarify this when presenting the HOR results.

John Ferguson concluded yesterday's summary. Michelle Havey (Anchor QEA) then moderated chat questions before the start of the presentation.

### *Chat Questions Before Start of Meeting*

- Question (Barbara Byrne, NMFS): Approximately what percentage of the fish were removed with the predator filter?
  - Response (Sydney Gonsalves): I don't know the number of fish with predator-like detection at this time. It wasn't that an individual fish was removed, it was when the predator filter flag goes on, all subsequent detections are removed.
- Comment (Kevin Clark, DWR): The steelhead used in these studies were raised at the Mokelumne River (MR) Hatchery, tagged, and then transported and released in the SJR. Is it possible that the percentage of SR water is really just acting as a surrogate for the percentage of MR water?
  - Response (John Ferguson): It's possible, as a lot of SR water comes down through the same pathway. Where are we putting the tracer in?

- Michael MacWilliams: The tracer goes in at Knight's Landing.
  - Deanna Sereno: Percentage of SR water is likely not acting as a surrogate for percentage of MR water based on other work in which tracers do not correlate.
  - Deanna Sereno can send other fingerprinting results that show how MR water is one of the main reasons SJR is not 1 minus percentage of SR water. She believes that the SR tracer is not ideal for this exercise.
  - John Ferguson: Do we have these for 2014, 2015, and 2016?
  - Deanna Sereno: Yes, for 2015.
  - MR water tracer is quite relevant for these fish—what are they looking for in MR water?
  - Deanna Sereno: Need to start the tracer about 5 to 6 months early as that is how long a good proportion of that water needs to reach this project.
  - Michael MacWilliams: UnTRIM generally starts at least 3 months early (should be 3 to 5 months).
- Question (Brian Ellrott, NMFS): Fish are trying to get away from the MR water; is there a reason why we think they would be attracted to MR water? Fish are trying to leave MR and get to the ocean, is there support for fish trying to get back to the MR?
    - Response (John Ferguson): Fish are released in the SJR, get to WPA, experience a different source of water, and show a stopping movement. He believes it's an olfactory cue more than a hydrodynamic cue. Based on work in the Columbia River, we see that when fish come down and experience a different environment, (e.g., steelhead encounter a structure), the resulting behavior often involves looking around and interrogating the area. That said, he acknowledges that this could be conjecture.
    - Michael MacWilliams: There are also pretty big hydrodynamic differences in the Delta when you have a big gradient between the SR water and exports. Generally, when SJR flow is high, net flows are across the south Delta from the HOR to the exports.
    - There are confounding olfactory and hydrodynamic differences that could be related to this.
  - Question (Steve Zeug, Cramer Fish Sciences): Olfactory issue is very interesting and needs to be investigated further. He would caution against teasing it out with these data, as we don't currently have a working hypothesis as to the potential mechanism. These data could be leading to the development of a potential mechanism in the future. Also, it's important to report out variables that are not important; if variables are not affecting transitions, reporting these negative results should be highlighted.
    - Response: Michael MacWilliams agrees. After looking at all the metrics and how they were correlated with management metrics, understanding the relationship between the most predictive variables and those used to inform management.
    - Steve Zeug: True, but it's also important to keep in mind the danger of using a correlation if we don't understand the mechanistic relationship. Operational decisions should ideally

be based on variables that are as mechanistic as possible or as directly related to the fish as possible.

Michelle Havey holds roll call of all meeting attendees: Name and associated agency.

## 2. Model Results: Head of Old River (Sydney Gonsalves, Anchor QEA)

- Question (John Plumb, USGS): Is it not possible to estimate the effect of the barrier in the model?
  - Response (Sydney Gonsalves): It is possible, but based on previous analyses, it was pretty strong; the effect the barrier was having on fish was pretty clear. We thought that the effect was clear and wanted to focus on the effect of other variables. Eighty percent to 90% of fish take the Old River route if the barrier is in place. If the barrier is not in place, they stay on the mainstem route. We thought that effect was clear and wanted to focus our efforts on the effects of other variables.

### *Fish Behavior*

- Question (Barbara Byrne): What does the number 1,364 that went from HOR to Old River East include? Does that refer just to fish that moved directly HOR to ORE and does not include fish that moved HOR to San Joaquin River downstream on the mainstem (SJL) back to ORE? Is 320 the backtracking number? Are these completely unique fish in these counts?
  - Response (Sydney Gonsalves): No, these are not completely unique fish; a single fish could have made these transitions more than once. These numbers are not 1:1 representations of fish.
  - John Ferguson: Fish are individually tagged, but these are not necessarily individual fish. Numbers reflect transitions. The 320 fish are not included in 1,364.
  - Sydney Gonsalves: The number 320 just represents transitions directly from SJL to ORE.

### *Model Evaluations*

- Question (Deanna Sereno): Could you elaborate more on your migratory indicator? Is it just the speed the fish is moving at, or what do you think it represents?
  - Response (Sydney Gonsalves): Most fish stay at this junction for about a day, but those fish staying longer than that were assigned nonmigrator status. Assigning migrator status improved the fit of the model, but we want to dig into it more.
  - Michelle Havey: There was a clear break point of a large group of fish moving through the area quickly and a smaller subset of fish that seems to be confusing the model results somewhat. We were trying to distinguish a threshold as to what was causing a smaller group of fish to stay around longer and not move through the junction as quickly.
  - Barbara Byrne: Could these fish have been predated on at this time or would the predator filter capture this?

- Sydney Gonsalves: This relates to Rebecca Buchanan's comment yesterday; the predator filter is not perfect but represents her best professional judgement. We could potentially include "predators" in the model and use these as a covariate.
  - Rebecca Buchanan: That region tends to have high predation, and in some of these study years, some of those sites were among the top sites with predator instance. We saw quite a bit of overlap in the behavior seen in the steelhead tags and the behavior expected from predators, so it was difficult to distinguish between steelhead and predators using a behavior filter. The predator filter did include a residence time criterion on different spatial scales.
- Question (Barbara Byrne): Are there any spatial assumptions about how fish approach? Is there any cross-channel distribution or approach behavior going on? Does the model account for cross-channel fish distribution?
  - Response (Sydney Gonsalves): Telemetry detections don't tell us anything about fish location in channel (at which side fish are present), so we couldn't tease that out.
  - Michael MacWilliams: We looked at this in a lot of detail, because we did save model results at every hydrophone location. The problem in using the hydrophone dataset is that there is no way to tease out where the fish is traveling through. If we used 2D tracking instead of binary tracking, we could potentially understand more.
  - Brett Harvey: Some folks have pondered buying that land (with the horn that sticks out) and using it as an attractive habitat to get fish on other side of the critical line. That could be another possible hypothesis for the deviation between the predicted and the observed. Brett supports Michael MacWilliam's recommendations for putting that into the model.
  - John Ferguson: Would including that point capture complex hydrodynamic conditions? Any recent studies? John supports including this in recommendations for our report.
  - Steve Zeug: Ed Gross just published a paper at University of California, Davis, on that topic:
    - [https://urldefense.proofpoint.com/v2/url?u=https-3A\\_.www.mdpi.com\\_2073-2D4441\\_13\\_20\\_2904&d=DwMFAg&c=euGZstcaTDllvimEN8b7jXrwqOf-v5A\\_CdpgnVfiiMM&r=yTFpIDFkuiNkP0a95f9Rf0CHUICOBYS1wpg-De78GE&m=UUn5mQhWpVaVDmGgZTfedAomUx87hSD7tqexdjn\\_hwo&s=NxJV9PyblcOu2JvQUFWqVOwt1aH0L9-q6pMCnfjzMw&e=](https://urldefense.proofpoint.com/v2/url?u=https-3A_.www.mdpi.com_2073-2D4441_13_20_2904&d=DwMFAg&c=euGZstcaTDllvimEN8b7jXrwqOf-v5A_CdpgnVfiiMM&r=yTFpIDFkuiNkP0a95f9Rf0CHUICOBYS1wpg-De78GE&m=UUn5mQhWpVaVDmGgZTfedAomUx87hSD7tqexdjn_hwo&s=NxJV9PyblcOu2JvQUFWqVOwt1aH0L9-q6pMCnfjzMw&e=)
- Question (Steve Zeug): Are the flow covariates averaged over a certain time period or is it the value observed when a fish is detected at a location?
  - Response (Sydney Gonsalves): It is the value observed when the fish was detected.
- Question (Deanna Sereno): Concerning the overprediction and underprediction of fish at those locations, have you looked at the barrier at Old River near Tracy? It would be interesting to see how it impacts flow data. The barriers are typically installed during this time period, but may not have been during some release groups. If the model correctly captures the barriers (present or

absent), then it should have correctly captured flows, but Deanna happens to know that other models do not.

- John Ferguson: Where is this barrier?
- Deanna: The barrier is at the HOR near the CVP export facility.
- Comment (Russell Perry) The covariates aren't just linked to fish at the time of detection, but the model is using the entire 15-minute timeseries. The model used the entire 15-minute timeseries' worth of information and is integrating over that to estimate how those varying conditions influence the transition probability. Russell believes that this is one of the key strengths of this modeling approach, in that you don't have to average over a transition time, and the model is using all of this information for each individual.

### *Slope Estimates: Downstream Route Choice*

- Sydney Gonsalves and Michelle Havey: Being classified as a nonmigrator greatly reduced the chance of making a downstream transition: 0 = migrator, 1 = nonmigrator.

### *Slope Estimates for Leaving ORE*

- Slope estimates and transitions were negative in both directions (both leaving Old River and returning upstream to HOR and leaving Old River in downstream direction). As the flow on Old River would increase in the downstream direction, those transitions became less likely.

### *Cumulative Transitions: Time-Varying Covariates*

- Question (Deanna Sereno): What is the difference between the dashed and the solid lines in the Cumulative Transition Probability figure?
  - Response (Sydney Gonsalves): Dashed lines represent the migrants, and solid lines represent nonmigrating fish. It was shown in this way so we could visualize the difference between the behavior of the two migrator statuses and could also see the effects of the continuous covariates.
- Sydney Gonsalves: The two bottom left panels show transitions out of ORE. Resultant fish leaving ORE was a combined difference between migrator status and conditions that occurred.
- Sydney Gonsalves addresses the diagonal panels and mentioned that after yesterday's comments, the labels were changed from "Remain at" to "HOR to HOR" to better represent a fish being detected at HOR, then also being detected there sometime later. This applies to all panels.
  - John Ferguson pointed out that we don't necessarily know where the fish are between detections and are not implying that fish remain at those locations.
  - Sydney Gonsalves: Yes, and that same interpretation applies to all panels. A reminder from yesterday, "HOR to HOR" does not describe where fish go during intervening period between detections.

- Question (Steve Zeug): It seems like flow magnitude in this area would be related to flow direction (e.g., more backtracking on a flood tide). Was flow direction examined as an effect on backtracking?
  - Response (Sydney Gonsalves): Yes, flow direction was included in the model covariate. When flow direction is a negative, this includes reverse flow.

## *Discussion*

- Question (Barbara Byrne): How do you see the water depth variable as mechanistically affecting what fish do? Seems likely that water depth is correlated with flow, would guess that with more flow, water is deeper. Is there an independent depth mechanism occurring?
  - Response (Brett Harvey): Tide will change water depths.
  - John Ferguson was wondering the same thing and observed that flow and depth seem highly correlated. He mentioned that an incoming tide could change the depth and decrease downstream flow; however, mechanistically there is no good connection there yet.
  - Sydney Gonsalves: The correlations were moderate. Nothing mechanistic right now. In this model, temperature was one of variables dropped out because it only marginally increased the fit of the model, and there was very little gain for including that additional variable. This was the only area in which temperature was in the running as an explanatory variable.
  - Barbara Byrne: Did the water depth term increase the likelihood of staying in the SJR?
  - Unknown Participant: No, it was the opposite.
  - Barbara Byrne: Jeff Stewart had looked at some work during the drought showing that the tides came in very high on the SJR side, so the tidal prism coming in may have pressured fish into Old River. Wondering if it was a tidal excursion proxy? If that is true, it would seem to keep fish out of Old River, and it looks like the pattern is different.
  - Sydney Gonsalves: Increasing water depth decreased the chance of fish making either downstream transition. We used instantaneous water depth, not tidal average.
- Question (Steve Zeug): Regarding the nonmigrator variable, it would be interesting to see if there are hydrodynamic conditions that are changing a migrator status to a nonmigrator status (e.g., a flow pulse encouraging fish to migrate out of or push out of the Delta). To see if we could affect behavior of individuals and induce migration by some type of condition. Plug for the fate analysis; it would be interesting to see if decisions made affect mortality (e.g., do fish going downstream in HOR suffer more mortality than on the mainstem?).
- Question (Mike Dodrill): It's interesting to see the results at HOR, especially for USGS folks, who have done similar analysis for Chinook at HOR. Ideas of things that might be helpful to include things that were that were done for Chinook. During same time period, USGS included 2011 data by setting 2011 as an offset. This allowed USGS to include transitions for the high-water year by providing more contrast in the flow variables and to set 2011 as an offset; it allowed us to

include transitions for the high-water year. Another thing that might be helpful that was done for the Chinook analysis: decompose flows into: 1) a net flow; and 2) a tidal signal, and compare Akaike Information Criterion (AIC) scores. The decomposed net flows and tidal signal were more highly supported than the flows alone. This may help to aid in the interpretation of net flow effect versus tidal effect.

- Response (Sydney Gonsalves): We did decompose them, and included either net flow or tidal signal, but can try including both going forward.
- Question (Brett Harvey): Regarding the predation filter, how did you tease apart nonmigrator fish from a predicated fish? And how confident are you in that designation?
  - Response (Sydney Gonsalves): The predator filter was not developed by Anchor QEA (who used Rebecca Buchanan's predator filter and applied it to the dataset). We removed the predator-like detection prior to starting the analysis and were only working with the smolt-like detections. But we know that the predator filter is not perfect, and it was more difficult to detect differences in behavior between steelhead and predators than for Chinook. This made applying the predator filter more difficult, as did the fact that this area is one in which more conversions to predator occur. So, we don't know for sure exactly how good the predator filter is. But for the analysis, we only looked at the smolt-like detections, and migrator and nonmigrator status was assigned based on total time spent in this junction.
- Question (Barbara Byrne): Steve Zeug had mentioned the migrator versus nonmigrator distinction. The question was posed to those who have observed steelhead releases or worked with these studies directly. Draftees from the hatchery are smolt-sized but may not be inclined to migrate, and may be inclined to residualize. Are their behaviors inherently different? Could there be a way to do a preliminary migrator versus nonmigrator assignment even upon release (maybe looking at smoltification characteristics)?
  - Response (Cyril Michel, UCSC/NMFS): Cyril has performed tagging of these fish and noted that even in the raceway, fish exhibit variability in size and coloration (e.g., some fish distinctly rainbow versus steelhead in appearance already). He proposed using a condition factor.
  - Steve Zeug: We release Nimbus steelhead (these are an out of basin stock). We also performed mobile tracking in the American River and in the SR below the city and saw very few residualizations. Nimbus stock all seemed to be migrators.
- John Ferguson: We didn't see this behavior at Old River, where the turn is sharp. What is going on at the junction hydrodynamically? It may be confusing to the fish. What is really going on there? Maybe UC Davis study will elucidate further?

Meeting adjourned for a 10-minute break.

Michelle Havey poses one last call for questions on HOR before moving to TC.

## Model Results: Turner Cut

Three hydrophone arrays used for this analysis: San Joaquin Shipping Channel (SJS), San Joaquin River at MacDonald Island (MAC), and Turner Cut (TC). Years evaluated were 2013, 2015, and 2016 based on the presence of San Joaquin shipping hydrophone array. White arrows show assumed direction of positive flow.

### *Key Hydrodynamic Conditions: Flow*

- Barbara Byrne was surprised by how different SJS and MAC flows are in the figure.
  - Deanna Sereno asks if the label flow incorrect on graph.
  - Sydney Gonsalves: Yes, that is a typo. The green color is TC, and we will fix in slides going forward (green line in figure should be TC).

### *Key Hydrodynamic Conditions: Percentage of Sacramento River Water*

- Michelle Havey: Figures that show all 3 years are actually 2013 graphics; we will fix before sending slides out.
- Sydney Gonsalves: In the 2013 graphics there are three periods, time averaged for March, April, and May 2013 and the percentage of SR water.
  - Subsequent slides show 2015 and 2016 percentage of SR water.
  - We directly included the percentage of SR water in the model, but didn't calculate a differential between SJS and MAC because the percentage of SR water was so low at SJS most of the time that it would have been analogous to subtracting 0.

### *Slop Estimates: Mainstem*

- Question (Barbara Byrne): What are the diel patterns saying? The charts show that one of mainstem locations saw a peak in early morning and at other location saw a peak in the evening. If it's really a diel pattern of fish behavior, why would it be opposite? Time of day seems strange if it's really a diel pattern of fish behavior at different locations if only a mile apart.
  - Response (Sydney Gonsalves): What we are saying is that relative to nighttime, downstream transitions are more likely to occur at other times of day. We did try other time of day patterns to look at (e.g., day versus night, sunrise versus sunset), but we are not completely sure why these discrepancies occur
  - Barbara Byrne: During times at which fish were transitioning, was peak flood going? Could it be partly tied to when tidal things were happening (e.g., nighttime versus daytime when fish were passing through this junction).
  - Sydney Gonsalves: Yes, that could be the case. We looked at some flood flow plots with time of day superimposed. It didn't necessarily stand out because tidal cycles are moving relative to time of day.

- Michelle Havey: We are looking at a fairly short window. It might be worth looking at the full season to see if there is a tidal effect.
  - Sydney Gonsalves: Relative to nighttime, the downstream is transition more prevalent during the day.
- Comment (Josh Israel, USBR): Consider how model use would inform management. Yesterday's presentation talked about using environmental variables, and the subsequent discussion involved incorporating underlying behavioral and biological variables. In all cases, the best model included biological variables (e.g., release date and time of day) that may provide some explanatory power. He would encourage including the biological variables to help tie together results from all three areas and help to inform model development and selection. Josh then had to log off, but thanked everyone for the TC information.
- Michelle Havey: Looping back to Barbara Byrne's comment, we did look at time of day and flood flows, but may not have looked at the full timescale of when fish were there. The timescale may be too tight for the signal; it might be worth looking at full season to see if there is a tidal effect.
  - Sydney Gonsalves: Including continuous versus categorical variables in model: she likes to include continuous, but temperature was not useful in the model.
- Question (John Ferguson): What are your thoughts on percentage of SR water affecting transitions seen on figure showing slope estimates for time of day? Looking at the three lower plots, and at the difference between upstream and downstream movements, is the effect of percentage of SR water higher at MAC than at SJS?
  - Response (Sydney Gonsalves): Percentage of SR water was generally higher at Macdonald Island but was not having an effect on the upstream transition and only had a slight effect on the downstream transition.
- Question (Josh Israel): Did you also look at the time of day for the other junctions, for RD for HOR, or for individual facilities at TC? Did you look at migrator versus nonmigrator at water projects or at TC?
  - Response (Sydney Gonsalves): We included time of day and other variables to describe release timing (RD, month, group, etc.) at all three junctions.
  - John Ferguson: We didn't see the bifurcation in the data to evaluate migrator versus nonmigrator at TC or water projections, so we didn't see the need to evaluate migrator status there.
- Matthew Dekar (USFWS; in chat) noted that he will have to drop off the call.
- Question: (Barbara Byrne): Time of day theory: When you release the fish, might time of day be influenced by arrival times?
  - Response (Sydney Gonsalves): Yes, we can look at the tagging data. We know we have the release date, but it would be worth checking to see if release time was included.
  - John Ferguson: It is approximately 25 kilometers from the release point to HOR, so it seems like fish would be pretty well dispersed.

- Rebecca Buchanan: It might be worth looking at the release location. In some release years, some fish may have been released at Durham or Stockton.
- Russell Perry: In our analysis of Chinook, we looked at time of day. It is important to determine that there is no aliasing between time of day and tides. He suggests that steelhead are more active during the day than at night. Diel patterns are highly plastic in terms of foraging and risk. He has seen other work in which steelhead are more active during the day than at night.
- Rebecca Buchanan: We have seen steelhead activity differ at HOR during the day versus at night—it appears they can see the barrier during the day and are less likely to try to pass.
- Josh Israel had to drop off the call.

### *Discussion*

- Comment (Russell Perry): The 15% transitions into TC was a lower number than he was expecting. He mentioned that at least for Chinook, when fish get into the interior Delta, they don't tend to survive very well.
  - Sydney Gonsalves: The transitions into TC were more representative of a single fish. Even though there was a lower percentage, there was more movement back and forth on the mainstem: 165 transitions in, representing 138 fish. Of those 138 fish, 53 experienced final fate at TC. Some fish did end up back at the water projects. Fate discussion is an area we would like to continue to explore.
- Barbara Byrne: Mainstem flow results make sense. In patterns that some of the transitions are affected by flow on TC, is there a management tool to increase flow out of TC to the mainstem?
  - Steve: It's likely that the false river barrier is responsible.
- Questions (Steve Zeug): In terms of what is important to managers: It seems that flow on the mainstem is important for keeping fish on the mainstem, but is also driven by tidal dynamics. Key question: How much can inflow affect the tidal dynamics? It would be interesting to see how tidally averaged flow relates to those tidal dynamics.
  - Response (Sydney Gonsalves): We looked at the flows as both instantaneous and as tidal average. It may be interesting to decompose net flow and tidal signal instead of just including the combined total.
  - Steve Zeug thought that the flow variable was instantaneous, so how is the tidal average included?
  - Sydney Gonsalves: Tidal average flow is a continuous variable, but it is a rolling average. Both types of flow were considered in the modeling process but were less explanatory than instantaneous flow.
- Question (Barbara Byrne): Might the percentage of SR water on the mainstem SJR be a proxy for tidal extent? She would imagine that the greater percentage of SR water is correlated with the upstream extent of the tides, as the tides could bring in some of that SR water.

- Response (Sydney Gonsalves): Yes, we did see that, and also saw that daily pattern with the oscillating percentage.

### *High-Level Summary*

- Comment (Kevin Clark): Relating the high-level summary to survival is key to evaluate which behavior mechanisms we need to investigate further.
  - Michelle Havey: We've talked about survival a number of times throughout the analysis process and we've tried to be very careful in directing our analysis and in focusing on the fine-scale behaviors because there has been survival work already done and we didn't want to replicate that.
  - John Ferguson: Good thought—we need to think about how to bring survival into the discussion in the paper. We have talked with USGS about a synthesis paper directed to managers to pull together everything on both species.
- Comment (Steve Zeug): I like the summary idea. However, consider instantaneous flow versus tidally averaged flow when presenting to managers. Managers will think in terms of tidally averaged flow, so it's important to make it clear that the volume of the tidal movement is represented by tidally averaged flow. It would also be interesting to look at the migratory status of fish when the barrier is in versus out. Hydrologic conditions created by the barrier may create multiple routes and limit migrants.
  - John Ferguson: Good thought. At the HOR there is something that is causing nonpredator tagged fish to not migrate in that area for a while.
  - (Kevin Clark agrees in chat): Good thought, Steve.
  - Steve Zeug thanks the Anchor QEA team for their efforts.

Michelle Havey thanks everyone for their time and describes next steps.

- We will send out final slides and links to recordings for yesterday and today. Both will be sent out early next week; we'll also be developing a workshop summary.
- We will finalize the analysis and finish modeling. We will include recommendations in the report for future consideration. Coming out of the workshop, we will draft a report and finalize by the end of April.
- Comment (Barbara Byrne): She wanted to be clear that the expert advice on Clifton Court was not to set it as an absorbing boundary.
  - Michelle Havey: We discussed this with Mike Dodrill after the meeting yesterday. We will consider the tank at CVP as an absorbing state, but not RGs. RGs will be evaluated for effects of interior versus exterior hydrophones.
  - Barbara Byrne: "Remain at CVP" issue: if a hydrophone is in a tank and not detected, how are you evaluating presence of hydrophones in a tank?

- Sydney Gonsalves: Right now, we are only using external hydrophones (not tank) hydrophones.
- Michelle: This would be adding a fourth state to the model (an absorbing state).
- John Ferguson: We will look at RG and analyze the two inside versus two outside hydrophones.
- Michelle Havey: During yesterday's discussion, we discussed that if fish hit an internal hydrophone, they can go back out, so it would not be treated as an absorbing state.

John Ferguson thanks everyone for their input.

## Internal Debrief and Next Steps

### *Hydrodynamic To-Do Items*

- Rerun UnTRIM with additional tracers to track water from additional inputs (e.g., from the SJR). Tracked water will include the following:
  - SR (down mainstem or over Fremont weir) + American River
  - SJR
  - MR
  - All other Delta inflows
  - All other DICU flows (agricultural returns)
- Old River at Tracy barrier near Tracy—closer to CVP.
  - This is already in the model but we aren't really using it as a flag for anything.

### *Telemetry To-Do Items*

- Final fate
  - Final fate does not incorporate instantaneous behavior, which was the focus of this work.
  - Final fate is better addressed by others' work and will be referenced, but not analyzed, in the final report.
- Add 2011? And barrier in?
  - 2011 data and data when the barrier is in will be added to the analysis.
  - This will improve the estimates of the transitions on the SJR and will better align the steelhead analysis with the Chinook analysis recently completed by USGS.
- Is barrier out-affecting classification as migrator versus nonmigrator?
  - With the addition of all data, the criterion for determining migrator status will be re-evaluated.
- Predator filter: Using it as a variable instead of removing the detections from analysis?
  - Turning off the filter to test the sensitivity would result in certain inclusion of predator-like detections. Assessing the impact of applying the predator filter is not the focus of this analysis.

- There is precedent for using this filter, so the predator filter application will remain as-is for this analysis.
  - The filter was applied consistent with others' work.
  - There will be a discussion included in the report to identify limitations and uncertainties with the filter.
- Is there a correlation between tidal flow and time of day?
  - This will be evaluated.
- Decomposing tidal from net?
  - This will be evaluated.
- Adding an absorbing state to CVP.
  - Adding more states to the multistate model can cause issues, but it will be evaluated to determine if it provides any clarity on model interpretations.
- RG (inside or outside)
  - This analysis uses the array in the same way that others have.
  - No new analysis will be completed.
- Double-check release location.
  - The release locations for all steelhead used in the analysis will be confirmed.
- Reporting the negative findings (variables that weren't important in the model) will be important.
  - Negative findings will be included in the final report.



# Appendix B

## Hydrodynamic Model Output

### Memorandum

---



# Memorandum

April 27, 2022

To: Users of Hydrodynamic Model Output

From: Aaron Bever, Sydney Gonsalves, and Michael MacWilliams, Anchor QEA, LLC

cc: Michelle Havey and John Ferguson, Anchor QEA, LLC  
Linda Standlee and Darcy Austin, State Water Contractors  
Ben Geske, Delta Stewardship Council

**Re: Hydrodynamic Model Output Used to Evaluate Responses of Juvenile Steelhead to Hydrodynamic Conditions in the Sacramento-San Joaquin Delta**

## Overview

This memorandum details the output variables extracted from the UnTRIM Bay-Delta hydrodynamic model (hydrodynamic model) for use in evaluating the effects of hydrodynamics on the behavior of acoustically tagged juvenile steelhead in the Sacramento-San Joaquin Delta. Work was funded by Proposition 1 and completed by Anchor QEA, LLC, and U.S. Geological Survey for the State Water Contractors under a Proposition 1 Grant (*Evaluating Juvenile Salmonid Behavioral Responses to Hydrodynamic Conditions in the Sacramento-San Joaquin Delta*), contracted by Delta Stewardship Council. The details of the hydrodynamic model and the model simulations are presented in the final project report (Anchor QEA 2022). The hydrodynamic model output is available on the Environmental Data Initiative data portal (EDI 2022).

Not all the hydrodynamic model output variables in the output provided with this memorandum were used in the final fish models to analyze steelhead responses. Model outputs for additional variables and locations were included for completeness and to make these output files more broadly useful to researchers interested in other locations or variables in the Sacramento-San Joaquin Delta. This memorandum summarizes the hydrodynamic model output variables that were included in the Environmental Data Initiative data portal distribution—and the locations where hydrodynamic model output variables were extracted from the model—and describes the file formats. Hydrodynamic model simulations were conducted for 2011, 2012, 2013, 2014, 2015, and 2016, with hydrodynamic model output variables provided at the same locations for each period simulated. The model simulation for each year spanned the full period of steelhead detections in the telemetry data collected during that year. Table 1 provides the date range over which the model output was provided for each of the 6 years simulated.

**Table 1**

**Date Ranges of Provided Hydrodynamic Model Output for Each Year**

Year	Date Ranges of Steelhead Detections at Hydrophones	Date Ranges of Provided Hydrodynamic Model Output
2011	March 22, 2011, to July 27, 2011	March 1, 2011, to August 1, 2011
2012	March 27, 2012, to August 3, 2012	March 1, 2012, to August 6, 2012
2013	March 6, 2013, to July 26, 2013	March 1, 2013, to August 1, 2013
2014	March 26, 2014, to August 8, 2014	March 1, 2014, to August 10, 2014
2015	March 4, 2015, to July 1, 2015	March 1, 2015, to July 4, 2015
2016	February 24, 2016, to June 29, 2016	February 1, 2016, to July 1, 2016

**Description of Hydrodynamic Model Output Variables**

A range of variables representative of the conditions at each of the hydrophone arrays were output from the hydrodynamic model predictions for use in analyzing steelhead telemetry data. Some of the hydrodynamic model output variables were extracted directly from the hydrodynamic model predictions, and some were variables calculated from other hydrodynamic model output variables. Eight hydrodynamic model output variables were extracted directly from the hydrodynamic model predictions, and four variables were calculated from other variables in the model (Table 2). This section provides a summary of the hydrodynamic model output variables and the frequency with which they were provided.

**Table 2**

**Hydrodynamic Model Output Variables Provided**

Type	Variable (Units)	Frequency
Directly Extracted from Model	Cross-sectional water flow (m <sup>3</sup> /s)	90 seconds and tidally-averaged
	Depth-averaged salinity (PSU)	
	Depth-averaged water temperature (°C)	
	Water depth (m)	
	Depth-averaged current speed (m/s)	
	Depth-averaged percent Sacramento River Water (%)	
	Depth-averaged percent San Joaquin River Water (%)	
	Depth-averaged percent Mokelumne River Water (%)	
Calculated	OMR flow (m <sup>3</sup> /s)	90 seconds and tidally-averaged
	Qwest (m <sup>3</sup> /s)	
	Flow toward SWP and CVP exports (m <sup>3</sup> /s)	
	I:E Ratio (unitless)	Daily

Notes:

CVP: Central Valley Project

I:E: inflow:exports

m: meter

OMR: Old River and Middle River

PSU: practical salinity unit

s: second

SWP: State Water Project

### *Output Variables Extracted Directly from Hydrodynamic Model*

Water flow in the study area was provided as the total cross-sectional water flow. Cross-sectional water flow is the predicted rate of water flow through a cross section across a channel. The provided cross-sectional flows correspond to the flows past sets of hydrophones (hydrophone arrays). The direction of water flow is indicated by the sign of the flow. The sign convention used is that positive flow is downstream toward San Francisco Bay (Bay) and the Pacific Ocean, while negative flow is upstream. Cross-sectional water flow at the hydrophone array locations leading to the State Water Project (SWP) and Central Valley Project (CVP) export facilities are positive when flow is directed east away from the CVP and away from Clifton Court Forebay. These locations are FSHL\_SH\_RG (SWP near the radial gates [RG]) and FSHL\_SH\_CVP (CVP). The location naming convention was based on the original hydrophone array naming convention in the telemetry data and is described in the Locations of Hydrodynamic Model Output Variables section of this memorandum.

Depth-averaged salinity, depth-averaged water temperature, water depth, and depth-averaged current speed were extracted from the hydrodynamic model at discrete locations in the vicinity of each hydrophone array. Depth-averaged percent Sacramento River water, depth-averaged percent San Joaquin River water, and depth-averaged percent Mokelumne River water were also extracted from the hydrodynamic model at discrete locations in the vicinity of each hydrophone array. These hydrodynamic model output variables were provided as time series of modeled environmental conditions at individual locations. If a location went dry, the values were set to -999. Some locations may be periodically dry, depending on the bathymetry in the hydrodynamic model grid cell associated with the individual location and the time-varying water levels.

Water flow was extracted from the hydrodynamic model every 90 seconds, and both the 90-second instantaneous values and the tidally-averaged (24.8-hour average) values were provided. The tidally-averaged water flow is representative of the net flow over a 24.8-hour tidal period.

Hydrodynamic model output variables provided at discrete locations were extracted from the hydrodynamic model every 3 minutes, and the tidally-averaged values were also provided every 3 minutes. The tidally-averaged values are representative of the average over a tidal period.

### *Output Variables Calculated from Multiple Hydrodynamic Model Variables*

Four variables were calculated from the hydrodynamic model predictions for evaluation in the steelhead transition models. This section summarizes how those variables were calculated.

The OMR flow is the combined cross-sectional water flow through Old River and Middle River and is positive toward the Bay (north) and negative toward the exports (south). OMR flow was calculated as the sum of the predicted water flow at the Old River at Bacon Island and the Middle River at Middle River locations in the Delta. These locations are nearest to the OLD and MRE hydrophone arrays. The OMR flow was calculated from the hydrodynamic model every 90 seconds, and both the instantaneous values and the tidally-averaged values were provided every 90 seconds.

Qwest is the cross-sectional flow past Jersey Point in the San Joaquin River. Qwest in the provided variables was calculated as the predicted flow past Jersey Point from the instantaneous hydrodynamic model output, not using the daily water balance method used by California Department of Water Resources. Qwest was calculated from the hydrodynamic model predictions every 90 seconds, and both the instantaneous values and the tidally-averaged values were provided every 90 seconds.

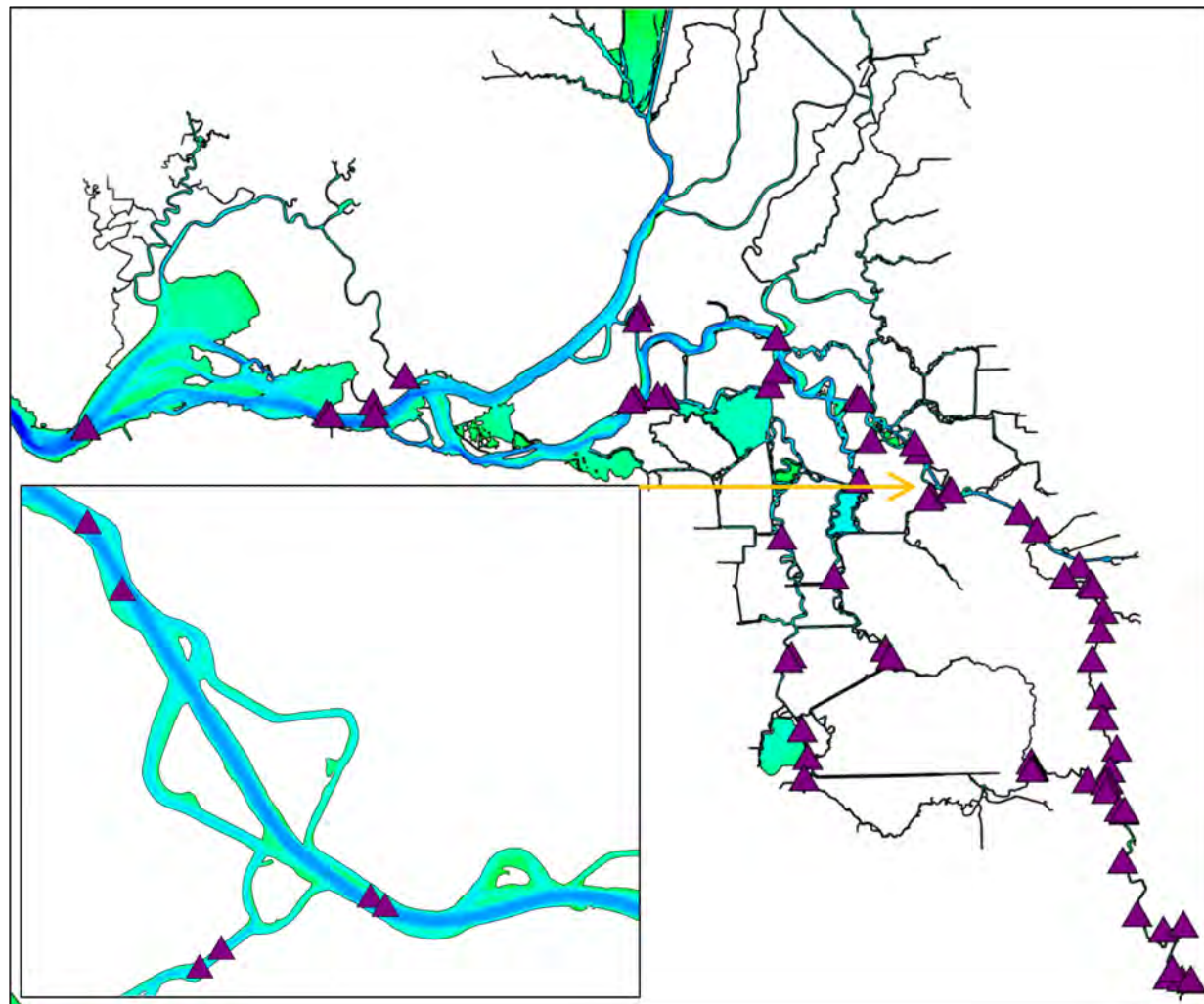
Flow toward SWP and CVP export facilities is the water flow toward these major export facilities. This flow was calculated as the water flow at model cross sections near the radial gates and entrance to Clifton Court Forebay (location FSHL\_SH\_RG) and in the channel leading to the CVP Bill Jones Pumping Plant (location FSHL\_SH\_CVP). The sign convention used is that positive flow is toward the export facilities and negative flow is away from the facilities. Note that the sign convention for this calculated variable is the opposite of the sign convention used for the instantaneous flow at these cross sections described previously. As such, this calculated variable is representative of the predicted flow toward the facilities. Flow toward the export facilities was calculated from the hydrodynamic model every 90 seconds, and both the instantaneous values and the tidally-averaged values were provided every 90 seconds.

The I:E ratio is the ratio of San Joaquin River inflow (I) to combined exports from the CVP and SWP (E). The IE ratio is calculated as I divided by E. The inflow was daily inflow from the San Joaquin River, and the flow exported from the SWP and CVP was the daily flow toward the export facilities. As such, the I:E ratio was calculated as a daily value. The I:E ratio becomes infinite and then undefined if the flow toward the facilities ever approaches zero or then equals zero, respectively, limiting the usefulness of the IE ratio on short timescales.

## Locations of Hydrodynamic Model Output Variables

Cross-sectional water flow and the hydrodynamic model output variables provided at discrete locations were extracted from the hydrodynamic model in the vicinity of each hydrophone array. Cross sections for water flow were specified to run approximately through the center of the hydrophone arrays and the variables extracted at discrete locations (except for current speed) were extracted at the center of the cross sections (Figure 1). An analysis was done to evaluate the correlation of the values extracted at each of the individual hydrophone locations to those extracted at the center of the cross sections. The values at the individual hydrophone locations were highly correlated to the values at the center of the cross sections (Anchor QEA 2022). Because of this high correlation, only the values at the center of the cross sections were evaluated in the steelhead models and are provided in this dataset. The depth-averaged current speed was extracted at the center of the water flow cross sections and at a location near the deepest model grid cell at the center of the channel. Current speed varies laterally across the channel, so these predicted current speeds should not be interpreted to represent the current speed across the entire channel.

**Figure 1**  
**Locations of Cross Section Centers**



Notes: Purple triangles represent the locations of the cross section centers for each hydrophone array. The background is the hydrodynamic model bathymetry.

In the output files provided, the header line lists the name of each water flow cross section or discrete location. The names were based on the original naming convention of hydrophones in the telemetry data. For example, FSHL\_SH\_RG is a location near the radial gates leading to Clifton Court Forebay. In these names, the prefix FSHL\_SH denotes that the point is a water Flow Section Hydrodynamic Location (FSHL) associated with a Steelhead Hydrophone (SH) array. These represent the center of the water flow cross sections. The prefix SHV denotes the Steelhead Hydrophone Velocity (provided as current speed) locations near the center of the channel. The easting (X) and northing (Y) locations in Universal Transverse Mercator Zone 10 of these points are provided in the "Prop1\_CrossSectionCenter\_VelocityPoint\_locations\_20220218.txt" file.

Although most hydrophone arrays were in consistent locations most years, hydrophone arrays were placed in slightly different locations during some years, and not all hydrophone array locations were reoccupied in every year. For hydrophone arrays placed in different locations from the other years or for extra hydrophone arrays, the specific year is noted in the name of the cross sections (and associated cross section center points). For example, cross section FSHL\_SH\_MOS\_2011 should be used with the 2011 telemetry data because it has the “\_2011” suffix that notes it is for the 2011 data. For 2013, cross section FSHL\_SH\_MOS\_2013 should be used with the telemetry data, and for the remaining years FSHL\_SH\_MOS should be used with the telemetry data. The same complete set of cross section and velocity point locations were included in the provided files for each year, to make the columns in the provided files consistent between all the years.

## Format of Provided Files

The hydrodynamic model output variables were provided in comma-separated values (CSV) text files. The rows in each file are individual dates/times. The first four columns of each CSV file provide the date/time for each row, and are the year, month, day, and decimal hour, respectively. The remaining columns are the values of the hydrodynamic model output variables at each location. A header line provides information specific to each of the columns in each file. The naming convention for each of the files is provided in Table 3.

**Table 3**  
**Naming Convention for Provided Files**

Variable (Units)	File Name <sup>1,2</sup>
Cross-sectional water flow (m <sup>3</sup> /s)	Prop1_YYYY_FLOW_m3ps_20220218.csv
Depth-averaged salinity (PSU)	Prop1_YYYY_DepthAvg_SAL_psu_20220218.csv
Depth-averaged water temperature (°C)	Prop1_YYYY_DepthAvg_WTEMP_DegC_20220218.csv
Water depth (m)	Prop1_YYYY_WDEPTH_m_20220218.csv
Depth-averaged current speed (m/s)	Prop1_YYYY_DepthAvg_CS_mps_20220218.csv
Depth-averaged percent Sacramento River Water (%)	Prop1_YYYY_DepthAvg_PercentSacramentoWater_20220218.csv
Depth-averaged percent San Joaquin River Water (%)	Prop1_YYYY_DepthAvg_PercentSanJoaquinWater_20220218.csv
Depth-averaged percent Mokelumne River Water (%)	Prop1_YYYY_DepthAvg_PercentMokelumneWater_20220218.csv
OMR flow (m <sup>3</sup> /s)	Prop1_YYYY_OMR_flow_m3ps_20220218.csv
Qwest (m <sup>3</sup> /s)	Prop1_YYYY_Qwest_m3ps_20220218.csv
Flow toward SWP and CVP exports (m <sup>3</sup> /s)	Prop1_YYYY_flow_toward_exports_m3ps_20220218.csv
IE Ratio (unitless)	Prop1_YYYY_IERatio_daily_20220218.csv

Notes:

1. “Prop1” signifies the Proposition 1-funded study *Evaluating Juvenile Salmonid Behavioral Responses to Hydrodynamic Conditions in the Sacramento-San Joaquin Delta*.
2. “YYYY” is replaced with the specific year in the file names of the provided files.

## References

Anchor QEA (Anchor QEA, LLC), 2022. *Synthesis of Juvenile Steelhead Responses to Hydrodynamic Conditions in the Sacramento-San Joaquin Delta*. April 2022.

EDI (Environmental Data Initiative), 2022. EDI Data Portal. Available at:

<https://doi.org/10.6073/pasta/f2579d5a59eb856a595ad07f531b2311>.



## Appendix C

### Hydrodynamic Model Validation

---



## C. Hydrodynamic Model Validation

### C.1 Summary

The UnTRIM Bay-Delta model has been extensively validated for water flow, salinity, water temperature, and water level (Anchor QEA 2018a, 2018b; MacWilliams et al. 2007, 2008, 2009, 2015, and 2016). MacWilliams et al. (2015) provide an extensive validation of the high-resolution model. Because the model has already been extensively validated, this appendix provides abbreviated model validations for water flow, salinity, and water temperature at a set of locations spanning from the Sacramento River through the central Delta and south Delta. The flow, salinity, and water temperature were validated using continuous-monitoring time-series data at fixed locations. Validations were conducted for each of the six simulated years over time periods that completely spanned the telemetry data.

### C.2 Statistics Used for Model Validation

Following the approach used by MacWilliams et al. (2015), model skill and target diagrams were used to provide quantitative metrics for evaluating model accuracy. Willmott (1981) defined the predictive skill of a model based on the quantitative agreement between observations ( $O$ ) and model predictions ( $M$ ) as shown in Equation C1.

#### Equation C1

$$Skill = 1 - \left[ \sum_{i=1}^N |X_{Mi} - X_{Oi}|^2 \right] / \left[ \sum_{i=1}^N \left( |X_{Mi} - \bar{X}_o| + |X_{Oi} - \bar{X}_o| \right)^2 \right]$$

where:

- |           |   |   |
|-----------|---|---|
| $X$       | = | the variable being compared                           |
| $\bar{X}$ | = | time average of $X$                                   |
| $M_i$     | = | model value at time $i$ of $N$ total comparison times |
| $O_i$     | = | observation at time $i$                               |

Perfect agreement between model results and observations yields a skill of 1. Although the Willmott (1981) model skill metric has some shortcomings (Ralston et al. 2010), it has nevertheless been used for comparing model predictions to observed data in numerous hydrodynamic modeling studies (e.g., Warner et al. 2005; Haidvogel et al. 2008; MacWilliams and Gross 2013; MacWilliams et al. 2015).

Jolliff et al. (2009) and Hofmann et al. (2011) provide detailed descriptions of target diagrams and their use in assessing model skill. This approach uses the *bias* and the unbiased root-mean-square difference (*ubRMSD*) to assess the accuracy of the model predictions. The *bias* of the model estimates is calculated as shown in Equation C2.

**Equation C2**

$$bias = \frac{1}{N} \sum_{i=1}^N X_{Mi} - \frac{1}{N} \sum_{i=1}^N X_{oi}$$

The *ubRMSD* is calculated as shown in Equation C3.

**Equation C3**

$$ubRMSD = \left( \frac{1}{N} \sum_{i=1}^N [(X_{Mi} - \bar{X}_M) - (X_{oi} - \bar{X}_o)]^2 \right)^{0.5}$$

To indicate whether the modeled variability is greater than or less than the observed variability, the *ubRMSD* is multiplied by the sign of the difference in the modeled and observed standard deviations, as shown in Equation C4.

**Equation C4**

$$ubRMSD_2 = ubRMSD (\sigma_M - \sigma_o) / |\sigma_M - \sigma_o|$$

where:

- |            |   |                             |
|------------|---|-----------------------------|
| $\sigma_M$ | = | modeled standard deviation  |
| $\sigma_o$ | = | observed standard deviation |

The *bias* and the *ubRMSD<sub>2</sub>* are normalized (denoted by subscript *N*) by the observed standard deviation to make their absolute values comparable among different variables and different sets of observed data, as shown in Equation C5 and Equation C6.

**Equation C5**

$$bias_N = bias/\sigma_0$$

**Equation C6**

$$ubRMSD_N = ubRMSD_2/\sigma_0$$

On each target diagram, the *bias<sub>N</sub>* between modeled and observed values is plotted on the Y-axis, and the *ubRMSD<sub>N</sub>* is plotted on the X-axis. The radial distance from the origin to each data point is the normalized root-mean-square difference (*RMSD<sub>N</sub>*).

MacWilliams et al. (2015) provide a more detailed description of the model validation methods and suggest thresholds for the validation metrics that indicate model accuracy. These target diagram thresholds were adopted in this report to classify the model accuracy. Very accurate predictions are classified as those with an *RMSD<sub>N</sub>* of less than 0.25, and accurate predictions an *RMSD<sub>N</sub>* less than 0.5. Acceptable predictions are indicated by an *RMSD<sub>N</sub>* of less than 1.0, and an *RMSD<sub>N</sub>* of greater than 1.0 indicates poor agreement between the observations and predictions and that the model would benefit from further calibration.

### C.3 Validation of Flow, Salinity, and Temperature

Water flow, salinity, and water temperature were validated at twelve fixed locations throughout the Delta using continuous-monitoring time-series data (Figures C-1 and C-2). These locations were selected for model validation because they span from the Sacramento River through the south Delta and also are concentrated around the three regions focused on for the fish transition model development. Data were not available at every station for every one of the simulated years. For example, flow data was only available at the West Canal at Clifton Court Intake (WCI) station for 2011 and 2012, but that location was relevant to the fish transition model for the water project area. Because of the limited flow data and the more complete data at surrounding locations, the West Canal at Clifton Court Intake location was only used to validate water flow in 2011 and 2012.

Using the thresholds for model accuracy from MacWilliams et al. (2015), water flow was nearly always very accurately or accurately predicted; 60 of the 63 comparisons made during the 6 years simulated indicated that flows were accurately or very accurately predicted (Tables C-1 through C-7, Figures C-3 through C-65). Water flow was acceptably predicted at two locations in 2011 and one location in 2012. Water flow was never poorly predicted. The time series validation demonstrates that the model predictions capture the tidal and non-tidal water flow throughout the Delta. For example, Figures C-21 and C-43 show accurate prediction of the tidal flows on the top panels and also the large changes in tidally-averaged (non-tidal) flows on the bottom left panels.

Using the thresholds for model accuracy from MacWilliams et al. (2015), salinity was accurately or acceptably predicted in 41 of the 60 comparisons made during the 6 years simulated (Tables C-1 and C-8 through C-13, Figures C-66 through C-126). Predicted salinity was very accurate at three locations in 2016. Salinity was classified as poorly predicted at 1 location in 2011, 4 locations in each of 2013 and 2014, 6 locations in 2015, and 1 location in 2016. However, the locations used in this model validation were at locations with very low average salinity. These stations tend to have very small seasonal cycles, which results in very challenging statistical comparisons, even if the absolute value of the mismatch between the observed and predicted values is small. For example, predicted salinity at Old River at Highway 4 in 2013 was classified as poor agreement between the model and data (Figure C-89), yet the observed and predicted average salinity were within 0.003 psu and the largest instantaneous error in the predicted salinity was only 0.14 psu. The time series validation demonstrates that the model predictions capture the tidal timescale and longer term (tidally averaged) salinity throughout the Delta. For example, Figures C-101 and C-123 show accurate prediction of complex tidal time-scale salinity variability.

Using the thresholds for model accuracy from MacWilliams et al. (2015), water temperature was very accurately or accurately predicted in 55 of the 63 comparisons made during the 6 years simulated (Tables C-1 and C-14 through C-19, Figures C-127 through C-190). Temperature was acceptably predicted at 1 location in 2014, 6 locations in 2015, and 1 location in 2016. The time series validation demonstrates that the model predictions capture the seasonal cycle of lower temperature in the winter and increasing throughout the simulation period and also the impact of shorter-term weather on the water temperature. For example, Figures C-135 and C-186 show that the predicted water temperature accurately captured the seasonal cycle and the shorter term (daily to weekly) changes in temperature in the observed data.

These time series validations of flow, salinity, and water temperature demonstrate that the model predictions were sufficiently accurate for use with the telemetry data to develop fish transition models and better understand fish movement at junctions in the Delta.

## References

- Anchor QEA (Anchor QEA, LLC), 2018a. *Evaluation of the Effects of Summer Operation of the Suisun Marsh Salinity Control Gates*. Prepared for the California Department of Water Resources. May 2018.
- Anchor QEA, 2018b. *FLoAT MAST – Physical Habitat Subteam: Hydrodynamic Modeling of Salinity, Temperature, and Turbidity*. Prepared for the California Department of Water Resources. December 2018.
- Haidvogel, D.B., H. Arango, W.P. Budgell, B.D. Coruelle, E. Curshitser, E.D. Lorenzo, K. Fennel, W.R. Geyer, A.J. Hermann, L. Lanerolle, J. Levin, J.C. McWilliams, A.J. Miller, A.M. Moore, T.M. Powell, A.F. Schepetkin, C.R. Sherwood, R.P. Signell, J.C. Warner, and J. Wilkin, 2008. "Regional Ocean Forecasting in Terrain-Following Coordinates: Model Formulation and Skill Assessment." *Journal of Computational Physics* 227:3,595–3,624.  
Available at: <https://doi.org/10.1016/j.jcp.2007.06.016>.
- Hofmann, E.E., B. Cahill, B., K. Fennel, M.A.M. Friedrichs, K. Hyde, C. Lee, A. Mannino, R.G. Najjar, J.E. O'Reilly, J. Wilkin, and J. Xue, 2011. "Modeling the Dynamics of Continental Shelf Carbon." *Annual Review of Marine Science* 3:93–122. Available at: <https://doi.org/10.1146/annurev-marine-120709-142740>.
- Jolliff, J.K., J.C. Kindle, I. Shulman, B. Penta, M.A.M. Friedrichs, R. Helber, and R.A. Arnone, 2009. "Summary Diagrams for Coupled Hydrodynamic-Ecosystem Model Skill Assessment." *Journal of Marine Systems* 76:64–82. Available at: <https://doi.org/10.1016/j.jmarsys.2008.05.014>.
- MacWilliams, M.L., and E. G. Gross, 2013. "Hydrodynamic Simulation of Circulation and Residence Time in Clifton Court Forebay." *San Francisco Estuary and Watershed Science*. 11(2). Available at: <https://doi.org/10.15447/sfews.2013v11iss2art1>.
- MacWilliams, M.L., E.S. Gross, J.F. DeGeorge, and R.R. Rachiele, 2007. *Three-Dimensional Hydrodynamic Modeling of the San Francisco Estuary on an Unstructured Grid*. 32nd Congress of the International Association of Hydro-Environment Engineering and Research (Venice, Italy); July 2007.
- MacWilliams, M.L., F.G. Salcedo, and E.S. Gross, 2008. *San Francisco Bay-Delta UnTRIM Model Calibration Report, POD 3-D Particle Tracking Modeling Study*. Prepared for the California Department of Water Resources. December 19, 2008.

MacWilliams, M.L., F.G. Salcedo, and E.S. Gross, 2009. *San Francisco Bay-Delta UnTRIM Model Calibration Report, Sacramento and Stockton Deep Water Ship Channel 3-D Hydrodynamic and Salinity Modeling Study*. Prepared for the U.S. Army Corps of Engineers, San Francisco District. July 14, 2009.

MacWilliams, M.L., A.J. Bever, E.S. Gross, G.S. Ketefian, and W.J. Kimmerer, 2015. "Three-Dimensional Modeling of Hydrodynamics and Salinity in the San Francisco Estuary: An Evaluation of Model Accuracy, X2, and the Low Salinity Zone." *San Francisco Estuary and Watershed Science* 13(1). Available at: <http://escholarship.org/uc/item/7x65r0tf>.

MacWilliams, M.L., A.J. Bever, and E. Foresman, 2016. "3-D Simulations of the San Francisco Estuary with Subgrid Bathymetry to Explore Long-Term Trends in Salinity Distribution and Fish Abundance." *San Francisco Estuary and Watershed Science* 14(2). Available at: <http://escholarship.org/uc/item/5qj0k0m6>.

Ralston, D.K., W.R. Geyer, and J.A. Lerczak, 2010. "Structure, Variability, and Salt Flux in a Strongly Forced Salt Wedge Estuary." *Journal of Geophysical Research* 115 (C6). Available at: <http://dx.doi.org/10.1029/2009JC005806>.

Warner, J. C., W.R. Geyer, and J.A. Lerczak, 2005. "Numerical Modeling of an Estuary: A Comprehensive Skill Assessment." *Journal of Geophysical Research* 110. Available at: <http://dx.doi.org/10.1029/2004JC002691>.

Willmott, C.J., 1981. "On the Validation of Models." *Physical Geography* 2:184–194.

## Tables

---



**Table C-1**  
**Number of Locations Within Each Accuracy Classification During all Six Years for Flow, Salinity, and Temperature**

Variable	Year	Number of Locations in Accuracy Classification			
		Very Accurate	Accurate	Acceptable	Poor
Flow	2011	1	9	2	0
	2012	2	8	1	0
	2013	4	7	0	0
	2014	4	6	0	0
	2015	4	5	0	0
	2016	2	8	0	0
Salinity	2011	0	4	4	1
	2012	0	4	4	0
	2013	0	3	3	4
	2014	0	4	3	4
	2015	0	1	4	6
	2016	3	0	7	1
Temperature	2011	10	0	0	0
	2012	5	5	0	0
	2013	3	7	0	0
	2014	2	8	1	0
	2015	0	5	6	0
	2016	4	6	1	0

**Table C-2**

**Predicted and Observed Flow, Cross-Correlation Statistics, Model Skill, and Target Diagram Statistics for Flow Continuous Monitoring Stations for the 2011 Simulation**

Station	Mean Flow		Cross Correlation		$r^2$	Skill	Target Diagram		
	Observed (m <sup>3</sup> /s)	Predicted (m <sup>3</sup> /s)	Amp Ratio	Lag (min)			bias <sub>N</sub>	ubRMSD <sub>N</sub>	RMSD <sub>N</sub>
SRV, Sacramento River at Rio Vista	1115.99	1165.90	1.023	-10	0.987	0.996	0.024	0.118	0.120
SJJ, San Joaquin River at Jersey Point	514.19	517.46	0.767	-10	0.984	0.980	0.001	-0.252	0.252
TRN, Turner Cut near Holt	-32.52	-38.54	0.810	-28	0.923	0.970	-0.097	-0.301	0.316
OBI, Old River at Bacon Island	-1.59	10.56	0.722	-25	0.966	0.967	0.046	-0.310	0.313
MDM, Middle River at Middle River	-9.79	-8.37	0.725	-22	0.936	0.963	0.005	-0.334	0.334
OH4, Old River at Highway 4	-1.80	2.77	0.848	-24	0.898	0.970	0.025	-0.324	0.325
VCU, Victoria Canal near Byron	-10.40	-20.15	0.603	-24	0.825	0.910	-0.084	-0.485	0.492
WCI, West Canal at Clifton Court Intake	-5.26	-12.68	0.809	16	0.834	0.951	-0.040	-0.408	0.410
GLC, Grant Line Canal near Clifton Court Ferry	207.11	166.82	0.702	-28	0.924	0.930	-0.293	-0.359	0.463
OH1, Old River at Head	176.99	230.59	1.560	-29	0.954	0.864	0.744	0.656	0.992
SJL, San Joaquin River below Old River near Lathrop	131.84	126.32	1.086	-5	0.851	0.950	-0.137	0.462	0.482
MSD, San Joaquin River at Mossdale	353.40	405.29	1.289	NA	0.926	0.939	0.343	0.465	0.578

Note:

The cross correlation did not find a maximum  $r^2$  within a lag of  $\pm 60$  minutes (indicated as NA for not applicable).

**Table C-3**

**Predicted and Observed Flow, Cross-Correlation Statistics, Model Skill, and Target Diagram Statistics for Flow Continuous Monitoring Stations for the 2012 Simulation**

Station	Mean Flow		Cross Correlation		$r^2$	Skill	Target Diagram		
	Observed (m <sup>3</sup> /s)	Predicted (m <sup>3</sup> /s)	Amp Ratio	Lag (min)			$bias_N$	ubRMSD <sub>N</sub>	RMSD <sub>N</sub>
SRV, Sacramento River at Rio Vista	354.55	366.08	0.911	-10	0.992	0.996	0.005	-0.120	0.120
SJJ, San Joaquin River at Jersey Point	9.86	100.35	0.778	-9	0.988	0.982	0.027	-0.238	0.240
TRN, Turner Cut near Holt	-22.59	-29.01	0.820	-26	0.955	0.978	-0.102	-0.253	0.273
OBI, Old River at Bacon Island	-55.30	-47.23	0.716	-19	0.980	0.969	0.031	-0.302	0.304
MDM, Middle River at Middle River	-75.29	-80.82	0.711	-17	0.966	0.966	-0.019	-0.318	0.319
OH4, Old River at Highway 4	-78.75	-78.98	0.859	-23	0.941	0.981	-0.001	-0.258	0.258
VCU, Victoria Canal near Byron	-42.05	-48.05	0.772	-20	0.862	0.953	-0.071	-0.384	0.391
WCI, West Canal at Clifton Court Intake	-91.88	-100.75	0.861	2	0.869	0.962	-0.064	-0.362	0.368
GLC, Grant Line Canal near Clifton Court Ferry	11.45	10.89	0.875	-16	0.883	0.968	-0.007	-0.342	0.342
OH1, Old River at Head	23.26	22.69	0.712	1	0.704	0.907	-0.041	-0.544	0.546
MSD, San Joaquin River at Mossdale	56.17	49.87	0.856	7	0.972	0.976	-0.204	-0.205	0.289

**Table C-4**

**Predicted and Observed Flow, Cross-Correlation Statistics, Model Skill, and Target Diagram Statistics for Flow Continuous Monitoring Stations for the 2013 Simulation**

Station	Mean Flow		Cross Correlation		$r^2$	Skill	Target Diagram		
	Observed (m <sup>3</sup> /s)	Predicted (m <sup>3</sup> /s)	Amp Ratio	Lag (min)			$bias_N$	ubRMSD <sub>N</sub>	RMSD <sub>N</sub>
SRV, Sacramento River at Rio Vista	251.95	238.12	0.956	-9	0.994	0.998	-0.006	-0.089	0.089
SJJ, San Joaquin River at Jersey Point	32.80	75.48	0.920	-8	0.992	0.996	0.015	-0.116	0.117
TRN, Turner Cut near Holt	-15.96	-22.22	0.871	-25	0.957	0.983	-0.105	-0.226	0.249
OBI, Old River at Bacon Island	-39.36	-40.01	0.747	-17	0.984	0.976	-0.003	-0.270	0.270
MDM, Middle River at Middle River	-63.31	-65.22	0.721	-16	0.974	0.969	-0.006	-0.303	0.303
OH4, Old River at Highway 4	-61.16	-65.12	0.916	-21	0.953	0.987	-0.025	-0.219	0.220
VCU, Victoria Canal near Byron	-34.79	-39.92	0.754	-21	0.883	0.956	-0.058	-0.369	0.374
WCI, West Canal at Clifton Court Intake	-85.36	-90.27	0.790	1	0.945	0.975	-0.036	-0.284	0.286
GLC, Grant Line Canal near Clifton Court Ferry	20.46	18.94	0.837	-27	0.896	0.969	-0.016	-0.329	0.329
OH1, Old River at Head	30.98	26.42	0.892	-1	0.898	0.962	-0.202	-0.320	0.378
MSD, San Joaquin River at Mossdale	36.13	38.63	0.954	1	0.885	0.968	0.078	0.347	0.356

**Table C-5**

**Predicted and Observed Flow, Cross-Correlation Statistics, Model Skill, and Target Diagram Statistics for Flow Continuous Monitoring Stations for the 2014 Simulation**

Station	Mean Flow		Cross Correlation		$r^2$	Skill	Target Diagram		
	Observed (m <sup>3</sup> /s)	Predicted (m <sup>3</sup> /s)	Amp Ratio	Lag (min)			$bias_N$	ubRMSD <sub>N</sub>	RMSD <sub>N</sub>
SRV, Sacramento River at Rio Vista	192.50	162.39	0.952	-10	0.994	0.998	-0.013	-0.086	0.087
SJJ, San Joaquin River at Jersey Point	56.45	73.52	0.929	-9	0.993	0.997	0.006	-0.107	0.107
TRN, Turner Cut near Holt	-11.12	-17.76	0.876	-26	0.964	0.984	-0.113	-0.209	0.238
OBI, Old River at Bacon Island	-32.45	-27.58	0.735	-22	0.985	0.974	0.019	-0.281	0.282
MDM, Middle River at Middle River	-43.46	-45.32	0.718	-18	0.982	0.970	-0.006	-0.298	0.298
OH4, Old River at Highway 4	-40.00	-44.09	0.942	-24	0.960	0.989	-0.029	-0.201	0.203
VCU, Victoria Canal near Byron	-23.33	-26.85	0.735	-24	0.921	0.961	-0.044	-0.342	0.345
GLC, Grant Line Canal near Clifton Court Ferry	5.42	6.91	0.872	-27	0.930	0.979	0.016	-0.271	0.271
OH1, Old River at Head	11.10	9.39	0.851	-10	0.810	0.943	-0.121	-0.439	0.455
MSD, San Joaquin River at Mossdale	23.22	22.79	0.795	-9	0.962	0.979	-0.012	-0.259	0.259

**Table C-6**

**Predicted and Observed Flow, Cross-Correlation Statistics, Model Skill, and Target Diagram Statistics for Flow Continuous Monitoring Stations for the 2015 Simulation**

Station	Mean Flow		Cross Correlation		$r^2$	Skill	Target Diagram		
	Observed (m <sup>3</sup> /s)	Predicted (m <sup>3</sup> /s)	Amp Ratio	Lag (min)			$bias_N$	ubRMSD <sub>N</sub>	RMSD <sub>N</sub>
SRV, Sacramento River at Rio Vista	120.25	113.51	0.975	-9	0.995	0.999	-0.003	-0.076	0.076
SJJ, San Joaquin River at Jersey Point	70.57	94.45	0.882	-8	0.993	0.995	0.008	-0.139	0.139
TRN, Turner Cut near Holt	-6.90	-16.44	0.853	-24	0.974	0.983	-0.139	-0.202	0.245
OBI, Old River at Bacon Island	-22.08	-18.22	0.712	-19	0.984	0.969	0.015	-0.302	0.302
MDM, Middle River at Middle River	-27.68	-31.64	0.756	-16	0.989	0.978	-0.014	-0.257	0.257
VCU, Victoria Canal near Byron	-14.81	-18.13	0.755	-20	0.963	0.973	-0.041	-0.287	0.290
GLC, Grant Line Canal near Clifton Court Ferry	-0.79	4.45	0.930	-21	0.966	0.990	0.054	-0.187	0.195
OH1, Old River at Head	6.24	6.75	0.738	-16	0.863	0.950	0.033	-0.394	0.395
MSD, San Joaquin River at Mossdale	7.76	11.32	0.718	-6	0.944	0.958	0.122	-0.332	0.354

**Table C-7**

**Predicted and Observed Flow, Cross-Correlation Statistics, Model Skill, and Target Diagram Statistics for Flow Continuous Monitoring Stations for the 2016 Simulation**

Station	Mean Flow		Cross Correlation		$r^2$	Skill	Target Diagram		
	Observed (m <sup>3</sup> /s)	Predicted (m <sup>3</sup> /s)	Amp Ratio	Lag (min)			$bias_N$	ubRMSD <sub>N</sub>	RMSD <sub>N</sub>
SRV, Sacramento River at Rio Vista	583.01	591.86	0.973	-9	0.992	0.998	0.004	-0.093	0.093
SJJ, San Joaquin River at Jersey Point	102.99	161.60	0.858	-8	0.991	0.992	0.019	-0.164	0.165
TRN, Turner Cut near Holt	-18.97	-23.46	0.834	-27	0.947	0.979	-0.074	-0.257	0.267
OBI, Old River at Bacon Island	-38.77	-33.29	0.721	-18	0.974	0.969	0.021	-0.302	0.303
MDM, Middle River at Middle River	-62.59	-59.74	0.713	-16	0.967	0.966	0.010	-0.316	0.316
OH4, Old River at Highway 4	-54.16	-58.84	0.885	-22	0.914	0.976	-0.031	-0.294	0.296
VCU, Victoria Canal near Byron	-34.27	-36.66	0.689	-21	0.863	0.942	-0.027	-0.415	0.416
GLC, Grant Line Canal near Clifton Court Ferry	16.11	18.90	0.870	-16	0.913	0.975	0.028	-0.298	0.299
OH1, Old River at Head	23.47	21.51	0.841	-1	0.831	0.950	-0.104	-0.411	0.424
MSD, San Joaquin River at Mossdale	46.87	40.30	0.785	-2	0.944	0.965	-0.177	-0.287	0.337

**Table C-8**

**Predicted and Observed Salinity, Cross-Correlation Statistics, Model Skill, and Target Diagram Statistics for Salinity Continuous Monitoring Stations for the 2011 Simulation**

Station	Mean Salinity		Cross Correlation		$r^2$	Skill	Target Diagram		
	Observed (psu)	Predicted (psu)	Amp Ratio	Lag (min)			$bias_N$	$ubRMSD_N$	$RMSD_N$
SRV, Sacramento River at Rio Vista	0.07	0.06	0.406	-21	0.544	0.652	-0.770	-0.701	1.041
SJJ, San Joaquin River at Jersey Point	0.08	0.08	0.835	-47	0.798	0.942	0.062	-0.452	0.456
TRN, Turner Cut near Holt	0.10	0.10	1.029	NA	0.580	0.846	0.121	0.876	0.884
OBI, Old River at Bacon Island	0.10	0.09	0.791	NA	0.670	0.898	-0.132	-0.593	0.608
MDM, Middle River at Middle River	0.10	0.10	1.033	NA	0.678	0.892	0.007	0.713	0.713
VCU, Victoria Canal near Byron	0.11	0.10	0.913	29	0.855	0.934	-0.336	-0.385	0.511
GLC, Grant Line Canal near Clifton Court Ferry	0.09	0.09	0.773	-27	0.891	0.946	-0.226	-0.353	0.419
SJL, San Joaquin River below Old River near Lathrop	0.10	0.09	0.866	NA	0.925	0.936	-0.402	-0.281	0.490
MSD, San Joaquin River at Mossdale	0.09	0.09	0.783	NA	0.948	0.969	-0.137	-0.284	0.315

Note:

The cross correlation did not find a maximum  $r^2$  within a lag of  $\pm 60$  minutes (indicated as NA for not applicable).

**Table C-9**

**Predicted and Observed Salinity, Cross-Correlation Statistics, Model Skill, and Target Diagram Statistics for Salinity Continuous Monitoring Stations for the 2012 Simulation**

Station	Mean Salinity		Cross Correlation		$r^2$	Skill	Target Diagram		
	Observed (psu)	Predicted (psu)	Amp Ratio	Lag (min)			$bias_N$	$ubRMSD_N$	$RMSD_N$
SRV, Sacramento River at Rio Vista	0.08	0.07	0.613	-17	0.515	0.821	-0.313	-0.709	0.775
TRN, Turner Cut near Holt	0.23	0.22	0.979	-38	0.921	0.978	-0.077	0.288	0.298
OBI, Old River at Bacon Island	0.15	0.15	1.513	-54	0.814	0.885	0.049	0.887	0.888
MDM, Middle River at Middle River	0.17	0.19	1.370		0.874	0.882	0.572	0.637	0.856
VCU, Victoria Canal near Byron	0.19	0.20	1.256	NA	0.918	0.955	0.173	0.455	0.487
GLC, Grant Line Canal near Clifton Court Ferry	0.26	0.22	0.835	-43	0.734	0.888	-0.415	-0.529	0.672
SJL, San Joaquin River below Old River near Lathrop	0.28	0.26	0.956	NA	0.985	0.983	-0.227	-0.128	0.261
MSD, San Joaquin River at Mossdale	0.28	0.26	0.915	NA	0.980	0.978	-0.242	-0.155	0.287

Note:

The cross correlation did not find a maximum  $r^2$  within a lag of  $\pm 60$  minutes (indicated as NA for not applicable).

**Table C-10**

**Predicted and Observed Salinity, Cross-Correlation Statistics, Model Skill, and Target Diagram Statistics for Salinity Continuous Monitoring Stations for the 2013 Simulation**

Station	Mean Salinity		Cross Correlation		$r^2$	Skill	Target Diagram		
	Observed (psu)	Predicted (psu)	Amp Ratio	Lag (min)			$bias_N$	$ubRMSD_N$	$RMSD_N$
SRV, Sacramento River at Rio Vista	0.09	0.08	0.418	-14	0.612	0.742	-0.486	-0.671	0.829
SJJ, San Joaquin River at Jersey Point	0.22	0.15	0.626	-22	0.911	0.876	-0.434	-0.422	0.605
TRN, Turner Cut near Holt	0.20	0.21	1.019	-59	0.857	0.947	0.236	0.416	0.478
OBI, Old River at Bacon Island	0.16	0.14	0.134	24	0.147	0.455	-0.428	-0.924	1.018
MDM, Middle River at Middle River	0.15	0.18	1.755	NA	0.707	0.679	1.297	1.360	1.879
OH4, Old River at Highway 4	0.17	0.17	0.218	7	0.038	0.514	-0.091	1.344	1.347
VCU, Victoria Canal near Byron	0.17	0.19	1.513	-14	0.791	0.851	0.453	0.930	1.034
GLC, Grant Line Canal near Clifton Court Ferry	0.26	0.22	0.769	-41	0.679	0.875	-0.383	-0.577	0.693
SJL, San Joaquin River below Old River near Lathrop	0.31	0.29	0.892	NA	0.945	0.968	-0.250	-0.241	0.347
MSD, San Joaquin River at Mossdale	0.31	0.28	0.901	NA	0.957	0.972	-0.242	-0.215	0.324

Note:

The cross correlation did not find a maximum  $r^2$  within a lag of  $\pm 60$  minutes (indicated as NA for not applicable).

**Table C-11**

**Predicted and Observed Salinity, Cross-Correlation Statistics, Model Skill, and Target Diagram Statistics for Salinity Continuous Monitoring Stations for the 2014 Simulation**

Station	Mean Salinity		Cross Correlation		$r^2$	Skill	Target Diagram		
	Observed (psu)	Predicted (psu)	Amp Ratio	Lag (min)			$bias_N$	$ubRMSD_N$	$RMSD_N$
SRV, Sacramento River at Rio Vista	0.17	0.15	0.808	-8	0.805	0.939	-0.121	-0.442	0.458
SJJ, San Joaquin River at Jersey Point	0.51	0.36	0.619	-13	0.881	0.877	-0.394	-0.444	0.594
TRN, Turner Cut near Holt	0.24	0.21	0.917	-8	0.863	0.923	-0.412	-0.375	0.557
OBI, Old River at Bacon Island	0.28	0.22	0.487	NA	0.414	0.689	-0.772	-0.774	1.093
MDM, Middle River at Middle River	0.23	0.20	1.149	42	0.240	0.573	-0.720	2.049	2.172
OH4, Old River at Highway 4	0.27	0.23	0.648	NA	0.264	0.660	-0.811	1.139	1.398
VCU, Victoria Canal near Byron	0.25	0.22	1.725	-30	0.456	0.617	-1.059	2.019	2.280
GLC, Grant Line Canal near Clifton Court Ferry	0.30	0.24	1.051	-49	0.711	0.835	-0.680	0.673	0.957
OH1, Old River at Head	0.29	0.27	1.002	25	0.936	0.977	-0.160	0.261	0.306
SJL, San Joaquin River below Old River near Lathrop	0.28	0.27	1.027	-1	0.947	0.983	-0.104	0.243	0.264
MSD, San Joaquin River at Mossdale	0.29	0.27	1.018	NA	0.951	0.982	-0.142	0.232	0.272

Note:

The cross correlation did not find a maximum  $r^2$  within a lag of  $\pm 60$  minutes (indicated as NA for not applicable).

**Table C-12**

**Predicted and Observed Salinity, Cross-Correlation Statistics, Model Skill, and Target Diagram Statistics for Salinity Continuous Monitoring Stations for the 2015 Simulation**

Station	Mean Salinity		Cross Correlation		$r^2$	Skill	Target Diagram		
	Observed (psu)	Predicted (psu)	Amp Ratio	Lag (min)			$bias_N$	$ubRMSD_N$	$RMSD_N$
SRV, Sacramento River at Rio Vista	0.25	0.14	0.359	-5	0.862	0.721	-0.414	-0.657	0.777
SJJ, San Joaquin River at Jersey Point	0.66	0.26	0.281	-5	0.893	0.560	-0.957	-0.726	1.201
TRN, Turner Cut near Holt	0.29	0.25	-0.030	NA	0.017	0.389	-0.718	-0.996	1.228
OBI, Old River at Bacon Island	0.31	0.18	0.272	NA	0.914	0.559	-1.385	-0.733	1.567
MDM, Middle River at Middle River	0.25	0.21	0.246	NA	0.502	0.635	-0.590	-0.793	0.988
OH4, Old River at Highway 4	0.30	0.20	0.306	-22	0.783	0.603	-1.167	-0.713	1.368
VCU, Victoria Canal near Byron	0.27	0.22	0.281	NA	0.570	0.641	-0.800	-0.759	1.103
GLC, Grant Line Canal near Clifton Court Ferry	0.33	0.23	0.487	-38	0.526	0.652	-1.142	-0.690	1.334
OH1, Old River at Head	0.34	0.29	0.603	NA	0.691	0.855	-0.363	-0.566	0.672
SJL, San Joaquin River below Old River near Lathrop	0.34	0.29	0.642	-29	0.786	0.883	-0.346	-0.490	0.600
MSD, San Joaquin River at Mossdale	0.33	0.29	0.738	NA	0.878	0.925	-0.316	-0.380	0.494

Note:

The cross correlation did not find a maximum  $r^2$  within a lag of  $\pm 60$  minutes (indicated as NA for not applicable).

**Table C-13**

**Predicted and Observed Salinity, Cross-Correlation Statistics, Model Skill, and Target Diagram Statistics for Salinity Continuous Monitoring Stations for the 2016 Simulation**

Station	Mean Salinity		Cross Correlation		$r^2$	Skill	Target Diagram		
	Observed (psu)	Predicted (psu)	Amp Ratio	Lag (min)			$bias_N$	$ubRMSD_N$	$RMSD_N$
SRV, Sacramento River at Rio Vista	0.08	0.07	0.632	-24	0.653	0.801	-0.603	-0.589	0.843
SJJ, San Joaquin River at Jersey Point	0.12	0.09	0.238	-19	0.558	0.566	-0.635	-0.791	1.014
TRN, Turner Cut near Holt	0.20	0.20	0.744	26	0.598	0.876	-0.011	-0.662	0.662
OBI, Old River at Bacon Island	0.13	0.11	1.069	NA	0.825	0.830	-0.832	0.497	0.969
MDM, Middle River at Middle River	0.16	0.17	1.137	NA	0.717	0.876	0.356	0.728	0.810
OH4, Old River at Highway 4	0.16	0.15	1.204	-14	0.792	0.899	-0.370	0.650	0.748
VCU, Victoria Canal near Byron	0.18	0.18	1.191	29	0.791	0.916	-0.193	0.641	0.669
GLC, Grant Line Canal near Clifton Court Ferry	0.25	0.22	0.949	-38	0.822	0.929	-0.316	0.444	0.545
OH1, Old River at Head	0.31	0.30	0.907	NA	0.957	0.985	-0.094	-0.213	0.233
SJL, San Joaquin River below Old River near Lathrop	0.31	0.30	0.943	-23	0.962	0.988	-0.088	-0.195	0.214
MSD, San Joaquin River at Mossdale	0.31	0.30	0.912	NA	0.962	0.987	-0.086	-0.201	0.219

Note:

The cross correlation did not find a maximum  $r^2$  within a lag of  $\pm 60$  minutes (indicated as NA for not applicable).

**Table C-14**

**Predicted and Observed Temperature, Cross-Correlation Statistics, Model Skill, and Target Diagram Statistics for Temperature Continuous Monitoring Stations for the 2011 Simulation**

Station	Mean Temperature		Cross Correlation		$r^2$	Skill	Target Diagram		
	Observed (°C)	Predicted (°C)	Amp Ratio	Lag (min)			$bias_N$	$ubRMSD_N$	$RMSD_N$
SRV, Sacramento River at Rio Vista	15.86	15.66	0.956	-11	0.980	0.994	-0.057	-0.142	0.153
SJJ, San Joaquin River at Jersey Point	17.20	16.93	0.998	25	0.981	0.994	-0.071	0.139	0.156
TRN, Turner Cut near Holt	17.37	17.30	0.966	-30	0.983	0.995	-0.020	-0.131	0.133
OBI, Old River at Bacon Island	18.24	17.69	0.949	NA	0.970	0.988	-0.130	-0.175	0.218
MDM, Middle River at Middle River	18.21	17.63	0.923	-16	0.978	0.988	-0.138	-0.158	0.210
OH4, Old River at Highway 4	18.01	17.42	0.903	-5	0.977	0.987	-0.131	-0.169	0.214
VCU, Victoria Canal near Byron	18.03	17.67	0.921	-30	0.973	0.990	-0.085	-0.173	0.193
GLC, Grant Line Canal near Clifton Court Ferry	16.82	16.89	0.978	-5	0.981	0.995	0.023	-0.137	0.139
SJL, San Joaquin River below Old River near Lathrop	16.49	16.61	0.987	43	0.986	0.996	0.039	-0.119	0.125
MSD, San Joaquin River at Mossdale	16.52	16.43	0.974	-22	0.985	0.996	-0.030	-0.124	0.128

Note:

The cross correlation did not find a maximum  $r^2$  within a lag of  $\pm 60$  minutes (indicated as NA for not applicable).

**Table C-15**

**Predicted and Observed Temperature, Cross-Correlation Statistics, Model Skill, and Target Diagram Statistics for Temperature Continuous Monitoring Stations for the 2012 Simulation**

Station	Mean Temperature		Cross Correlation		$r^2$	Skill	Target Diagram		
	Observed (°C)	Predicted (°C)	Amp Ratio	Lag (min)			$bias_N$	$ubRMSD_N$	$RMSD_N$
SRV, Sacramento River at Rio Vista	17.86	17.82	0.922	NA	0.968	0.991	-0.012	-0.185	0.185
SJJ, San Joaquin River at Jersey Point	18.19	18.14	0.993	53	0.982	0.996	-0.015	0.133	0.134
TRN, Turner Cut near Holt	19.60	18.57	0.912	-18	0.975	0.976	-0.249	-0.169	0.301
OBI, Old River at Bacon Island	19.36	18.72	0.949	-36	0.976	0.987	-0.153	-0.157	0.219
MDM, Middle River at Middle River	19.57	18.55	0.907	16	0.978	0.977	-0.238	-0.166	0.290
OH4, Old River at Highway 4	19.73	18.72	0.919	2	0.975	0.978	-0.236	-0.168	0.290
VCU, Victoria Canal near Byron	19.75	18.71	0.904	21	0.971	0.975	-0.242	-0.182	0.303
GLC, Grant Line Canal near Clifton Court Ferry	19.85	18.88	0.933	-32	0.956	0.974	-0.238	-0.211	0.318
SJL, San Joaquin River below Old River near Lathrop	19.65	19.05	0.943	8	0.965	0.985	-0.146	-0.188	0.238
MSD, San Joaquin River at Mossdale	19.75	19.05	0.968	17	0.974	0.986	-0.172	-0.162	0.236

Note:

The cross correlation did not find a maximum  $r^2$  within a lag of  $\pm 60$  minutes (indicated as NA for not applicable).

**Table C-16**

**Predicted and Observed Temperature, Cross-Correlation Statistics, Model Skill, and Target Diagram Statistics for Temperature Continuous Monitoring Stations for the 2013 Simulation**

Station	Mean Temperature		Cross Correlation		$r^2$	Skill	Target Diagram		
	Observed (°C)	Predicted (°C)	Amp Ratio	Lag (min)			$bias_N$	$ubRMSD_N$	$RMSD_N$
SRV, Sacramento River at Rio Vista	19.01	18.90	0.952	-7	0.972	0.992	-0.032	-0.167	0.170
SJJ, San Joaquin River at Jersey Point	18.82	19.04	1.012	29	0.974	0.992	0.070	0.167	0.181
TRN, Turner Cut near Holt	20.24	19.27	0.845	-15	0.966	0.967	-0.256	-0.222	0.339
OBI, Old River at Bacon Island	20.00	19.64	0.922	-12	0.957	0.985	-0.102	-0.211	0.234
MDM, Middle River at Middle River	20.34	19.47	0.861	25	0.958	0.971	-0.230	-0.227	0.323
OH4, Old River at Highway 4	20.42	19.67	0.870	2	0.957	0.975	-0.199	-0.226	0.301
VCU, Victoria Canal near Byron	20.45	19.63	0.831	21	0.937	0.965	-0.211	-0.275	0.347
GLC, Grant Line Canal near Clifton Court Ferry	20.43	19.68	0.800	-28	0.916	0.958	-0.200	-0.314	0.372
SJL, San Joaquin River below Old River near Lathrop	20.81	19.97	0.745	NA	0.927	0.953	-0.196	-0.330	0.384
MSD, San Joaquin River at Mossdale	20.97	20.04	0.763	-13	0.944	0.956	-0.220	-0.301	0.373

Note:

The cross correlation did not find a maximum  $r^2$  within a lag of  $\pm 60$  minutes (indicated as NA for not applicable).

**Table C-17**

**Predicted and Observed Temperature, Cross-Correlation Statistics, Model Skill, and Target Diagram Statistics for Temperature Continuous Monitoring Stations for the 2014 Simulation**

Station	Mean Temperature		Cross Correlation		$r^2$	Skill	Target Diagram		
	Observed (°C)	Predicted (°C)	Amp Ratio	Lag (min)			$bias_N$	$ubRMSD_N$	$RMSD_N$
SRV, Sacramento River at Rio Vista	19.80	19.51	0.925	19	0.978	0.991	-0.087	-0.157	0.179
SJJ, San Joaquin River at Jersey Point	19.64	19.53	1.006	44	0.985	0.996	-0.039	0.122	0.128
TRN, Turner Cut near Holt	20.93	19.65	0.844	9	0.977	0.955	-0.345	-0.203	0.400
OBI, Old River at Bacon Island	20.76	20.03	0.910	31	0.980	0.982	-0.207	-0.158	0.260
MDM, Middle River at Middle River	21.07	19.84	0.862	38	0.981	0.960	-0.334	-0.182	0.380
OH4, Old River at Highway 4	21.24	20.03	0.840	29	0.968	0.957	-0.317	-0.221	0.386
VCU, Victoria Canal near Byron	20.99	19.91	0.835	18	0.939	0.956	-0.283	-0.270	0.391
GLC, Grant Line Canal near Clifton Court Ferry	21.10	20.04	0.862	-38	0.928	0.955	-0.292	-0.276	0.402
OH1, Old River at Head	21.17	19.91	0.789	-1	0.939	0.948	-0.296	-0.292	0.416
SJL, San Joaquin River below Old River near Lathrop	21.95	19.97	0.749	NA	0.940	0.912	-0.440	-0.314	0.541
MSD, San Joaquin River at Mossdale	21.31	20.01	0.791	-14	0.952	0.951	-0.298	-0.275	0.405

Note:

The cross correlation did not find a maximum  $r^2$  within a lag of  $\pm 60$  minutes (indicated as NA for not applicable).

**Table C-18**

**Predicted and Observed Temperature, Cross-Correlation Statistics, Model Skill, and Target Diagram Statistics for Temperature Continuous Monitoring Stations for the 2015 Simulation**

Station	Mean Temperature		Cross Correlation		$r^2$	Skill	Target Diagram		
	Observed (°C)	Predicted (°C)	Amp Ratio	Lag (min)			$bias_N$	$ubRMSD_N$	$RMSD_N$
SRV, Sacramento River at Rio Vista	19.03	18.43	0.948	29	0.959	0.975	-0.235	-0.202	0.310
SJJ, San Joaquin River at Jersey Point	18.75	18.46	0.935	38	0.942	0.981	-0.113	-0.241	0.266
TRN, Turner Cut near Holt	20.16	18.00	0.904	0	0.899	0.868	-0.683	-0.318	0.753
OBI, Old River at Bacon Island	19.90	18.36	0.708	25	0.719	0.849	-0.506	-0.530	0.733
MDM, Middle River at Middle River	20.20	18.34	0.717	24	0.811	0.850	-0.580	-0.447	0.732
OH4, Old River at Highway 4	20.22	18.20	0.643	9	0.690	0.803	-0.598	-0.560	0.819
VCU, Victoria Canal near Byron	20.06	18.64	0.758	48	0.885	0.908	-0.425	-0.365	0.560
GLC, Grant Line Canal near Clifton Court Ferry	20.03	18.66	0.786	58	0.857	0.905	-0.432	-0.386	0.579
OH1, Old River at Head	20.63	19.57	0.909	0	0.954	0.961	-0.318	-0.219	0.386
SJL, San Joaquin River below Old River near Lathrop	20.63	19.55	0.891	NA	0.952	0.958	-0.321	-0.228	0.394
MSD, San Joaquin River at Mossdale	20.89	19.61	0.871	-23	0.957	0.950	-0.363	-0.225	0.427

Note:

The cross correlation did not find a maximum  $r^2$  within a lag of  $\pm 60$  minutes (indicated as NA for not applicable).

**Table C-19**

**Predicted and Observed Temperature, Cross-Correlation Statistics, Model Skill, and Target Diagram Statistics for Temperature Continuous Monitoring Stations for the 2016 Simulation**

Station	Mean Temperature		Cross Correlation		$r^2$	Skill	Target Diagram		
	Observed (°C)	Predicted (°C)	Amp Ratio	Lag (min)			$bias_N$	$ubRMSD_N$	$RMSD_N$
SRV, Sacramento River at Rio Vista	16.66	16.32	0.981	-38	0.984	0.994	-0.091	-0.128	0.157
SJJ, San Joaquin River at Jersey Point	17.43	17.10	1.058	26	0.989	0.994	-0.098	0.126	0.160
TRN, Turner Cut near Holt	18.33	17.28	0.954	-1	0.989	0.978	-0.275	-0.110	0.296
OBI, Old River at Bacon Island	18.03	17.52	0.977	3	0.987	0.992	-0.133	-0.114	0.175
MDM, Middle River at Middle River	19.46	17.35	1.099	13	0.988	0.915	-0.625	0.156	0.644
OH4, Old River at Highway 4	18.47	17.54	0.935	23	0.991	0.982	-0.234	-0.111	0.259
VCU, Victoria Canal near Byron	18.23	17.30	0.951	27	0.986	0.981	-0.241	-0.124	0.271
GLC, Grant Line Canal near Clifton Court Ferry	18.56	17.73	0.967	-28	0.975	0.981	-0.222	-0.158	0.272
OH1, Old River at Head	18.47	17.91	0.906	26	0.961	0.983	-0.147	-0.205	0.252
SJL, San Joaquin River below Old River near Lathrop	18.42	17.87	0.912	NA	0.957	0.982	-0.145	-0.212	0.257
MSD, San Joaquin River at Mossdale	18.41	17.89	0.913	-22	0.965	0.985	-0.139	-0.193	0.238

Note:

The cross correlation did not find a maximum  $r^2$  within a lag of  $\pm 60$  minutes (indicated as NA for not applicable).



## Figures

---



**Figure C-1**  
**Continuous Monitoring Stations in the Central Delta Used for Model Validation**

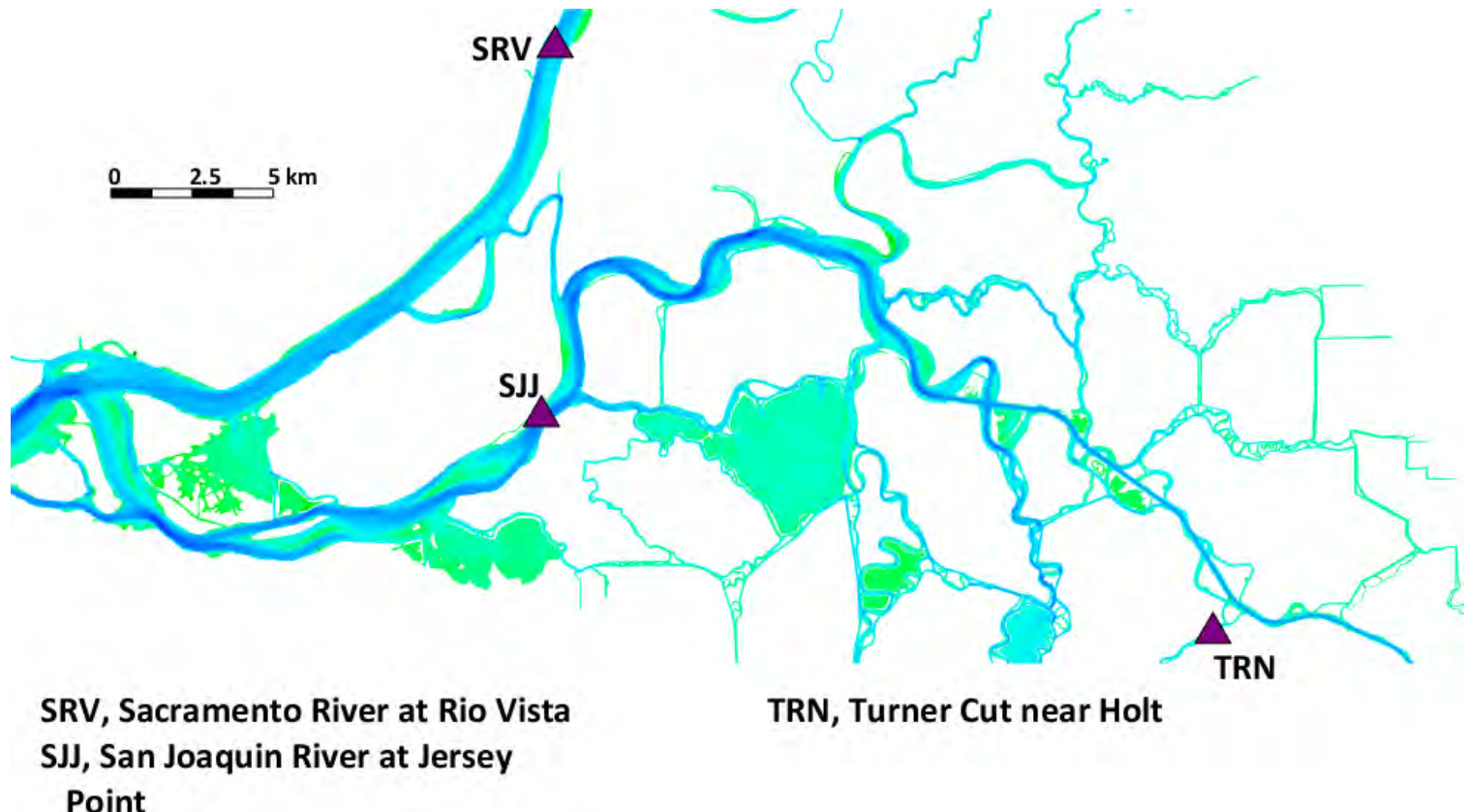


**Figure C-2**  
**Continuous Monitoring Stations in the South Delta Used for Model Validation**

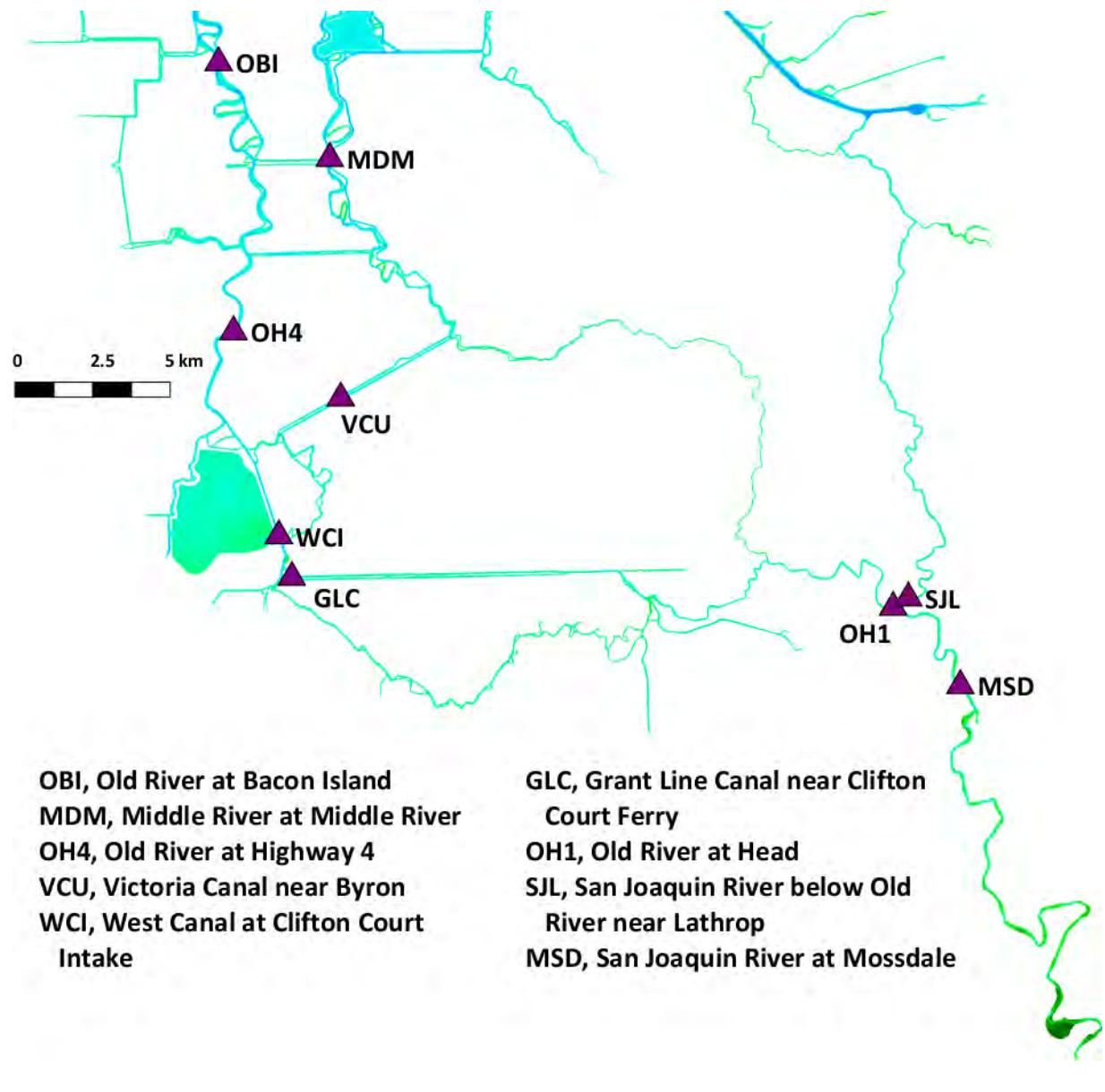


**Figure C-3**

**Target Diagrams Showing the Model Validation Using the Time Series Water Flow for the Six Years**

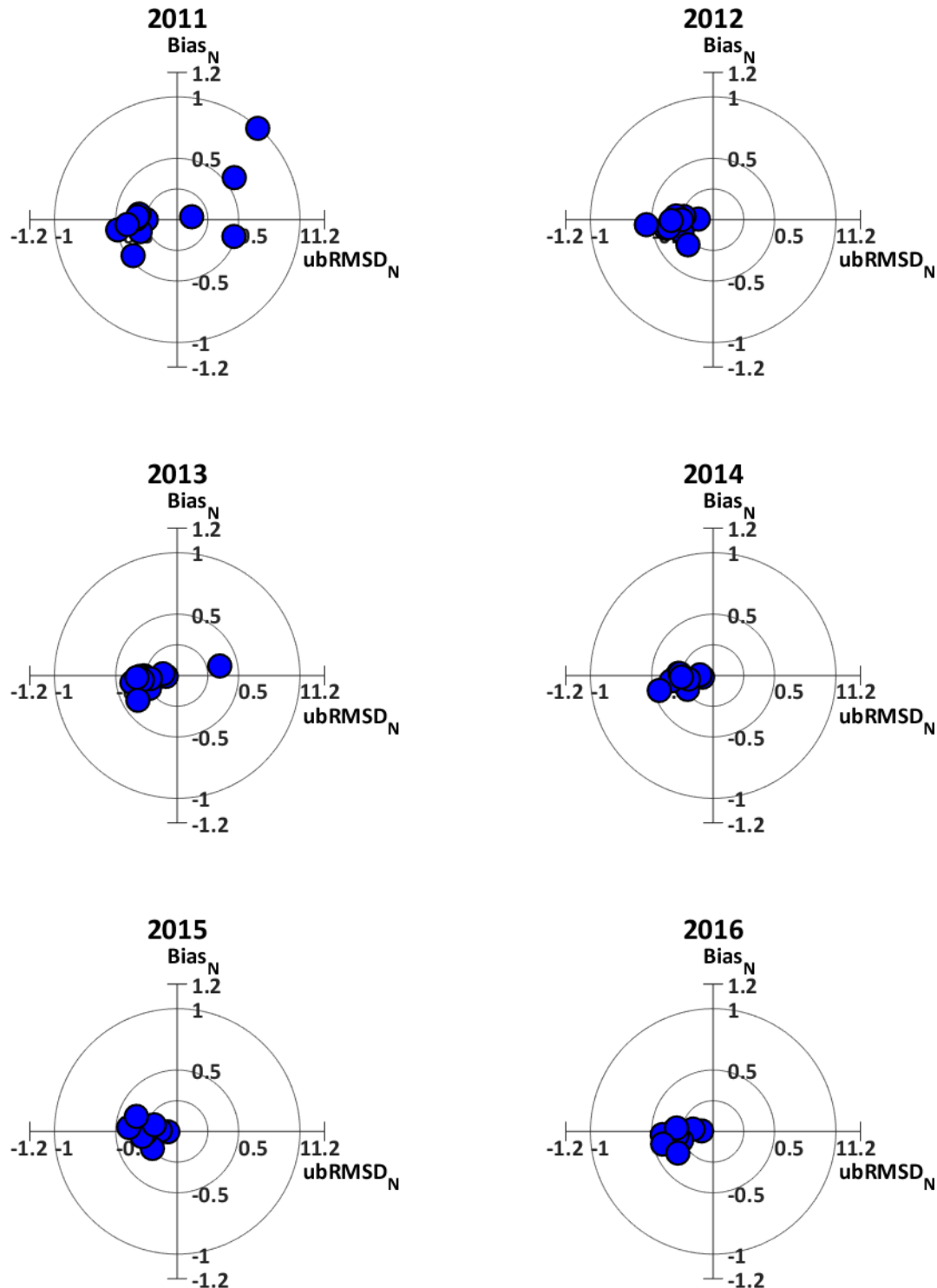


**Figure C-4**

**Observed and Predicted Water Flow at Sacramento River at Rio Vista (SRV) During 2011**

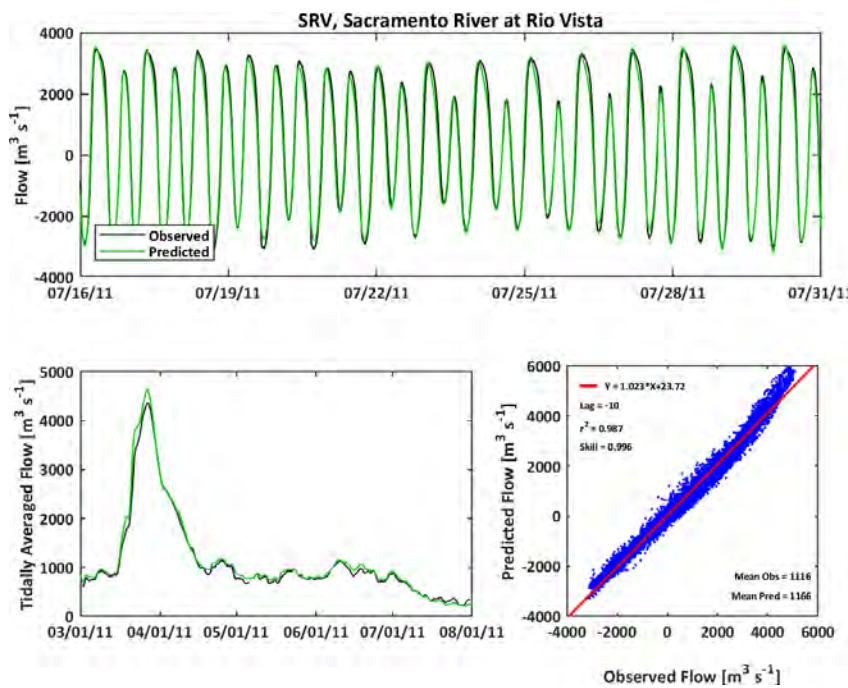


**Figure C-5**

**Observed and Predicted Water Flow at San Joaquin River at Jersey Point (SJJ) During 2011**

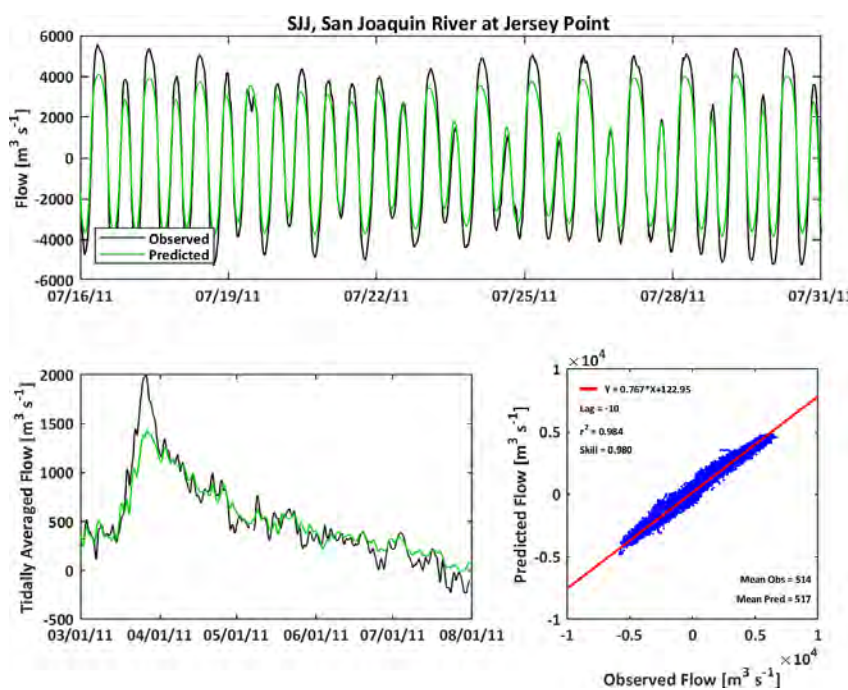


**Figure C-6**

**Observed and Predicted Water Flow at Turner Cut near Holt (TRN) During 2011**

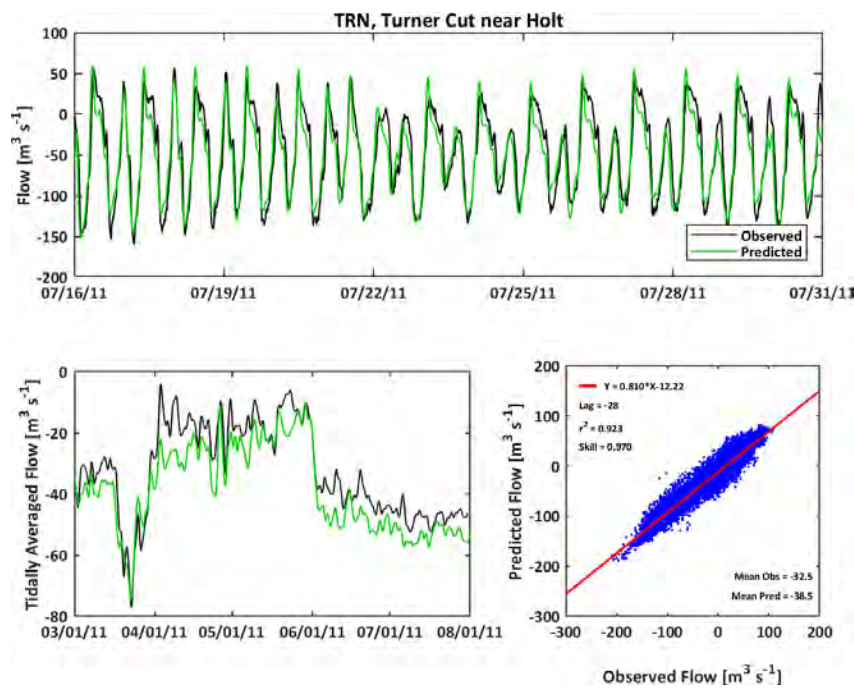


**Figure C-7**

**Observed and Predicted Water Flow at Old River at Bacon Island (OBI) During 2011**

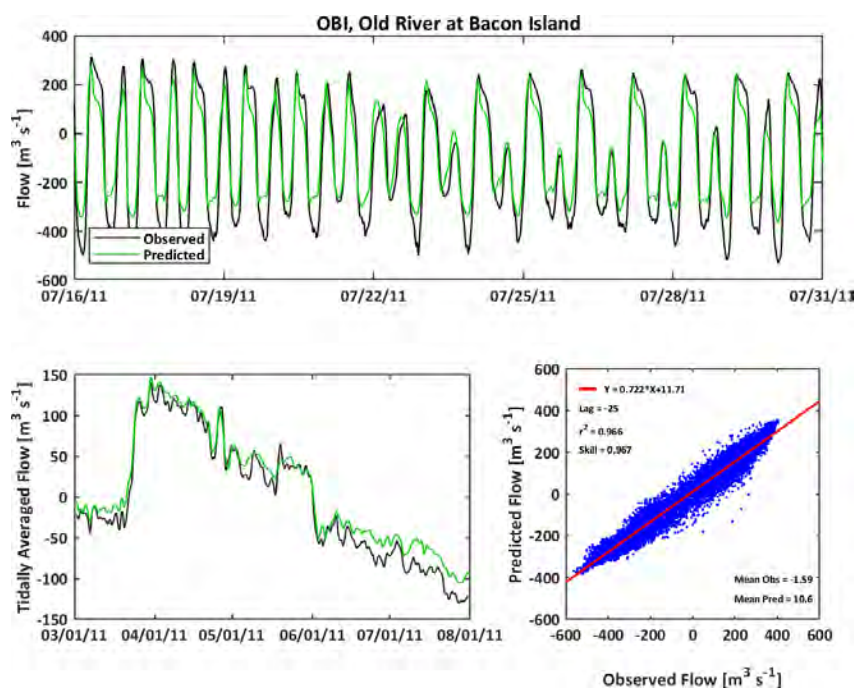


**Figure C-8**

**Observed and Predicted Water Flow at Middle River at Middle River (MDM) During 2011**

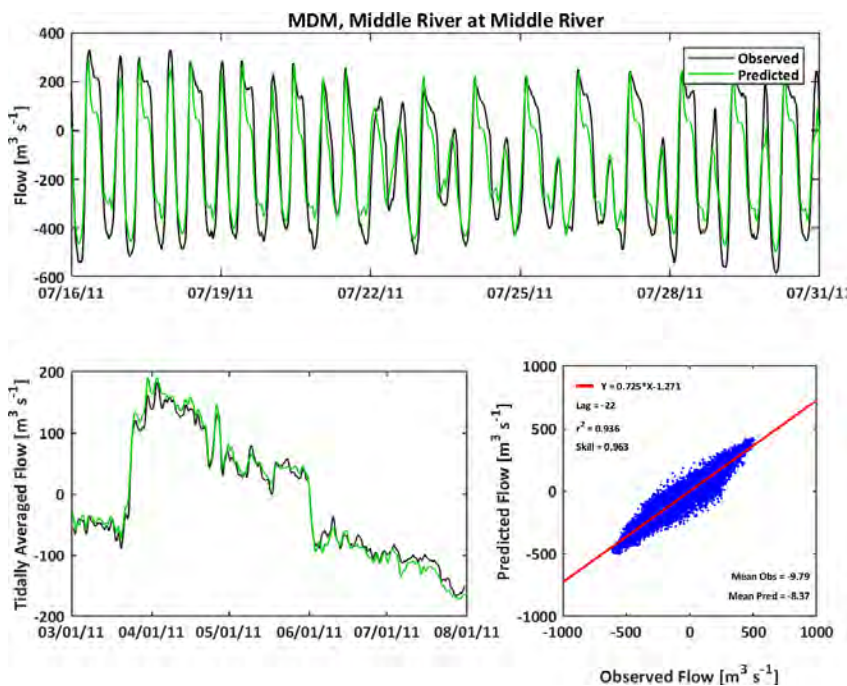


**Figure C-9**

**Observed and Predicted Water Flow at Old River at Highway 4 (OH4) During 2011**

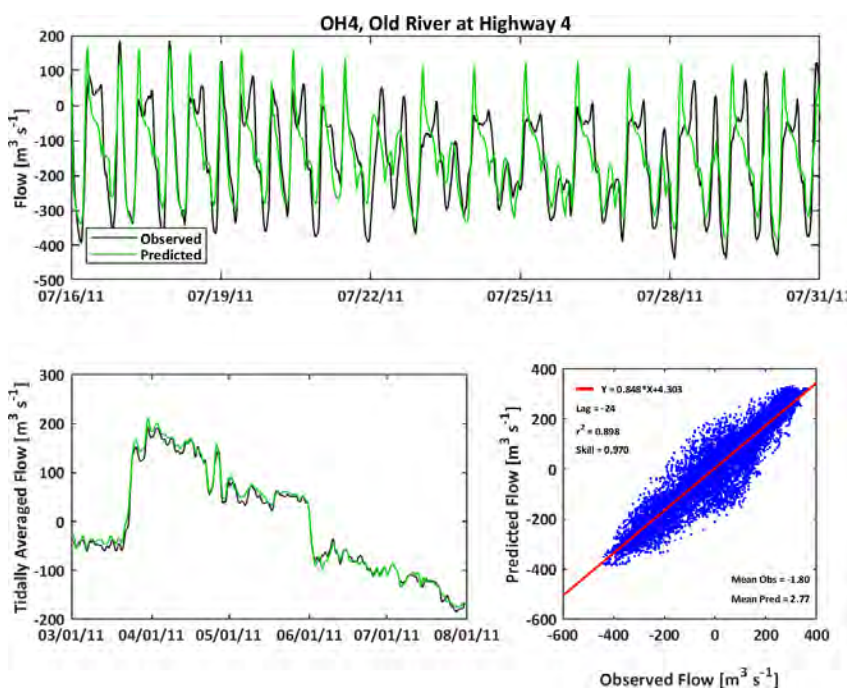


**Figure C-10**

**Observed and Predicted Water Flow at Victoria Canal near Byron (VCU) During 2011**

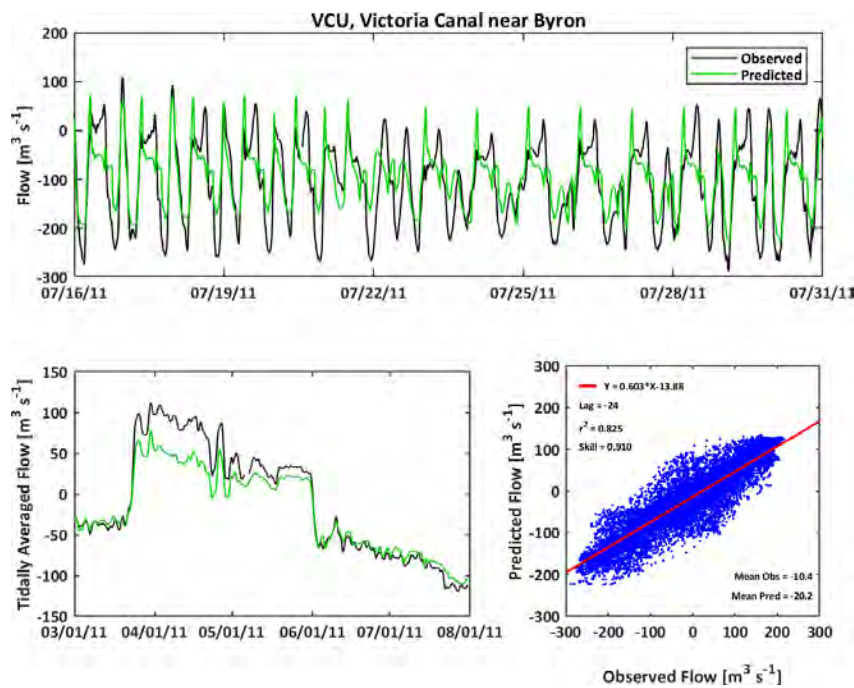


**Figure C-11**

**Observed and Predicted Water Flow at West Canal at Clifton Court Intake (WCI) During 2011**

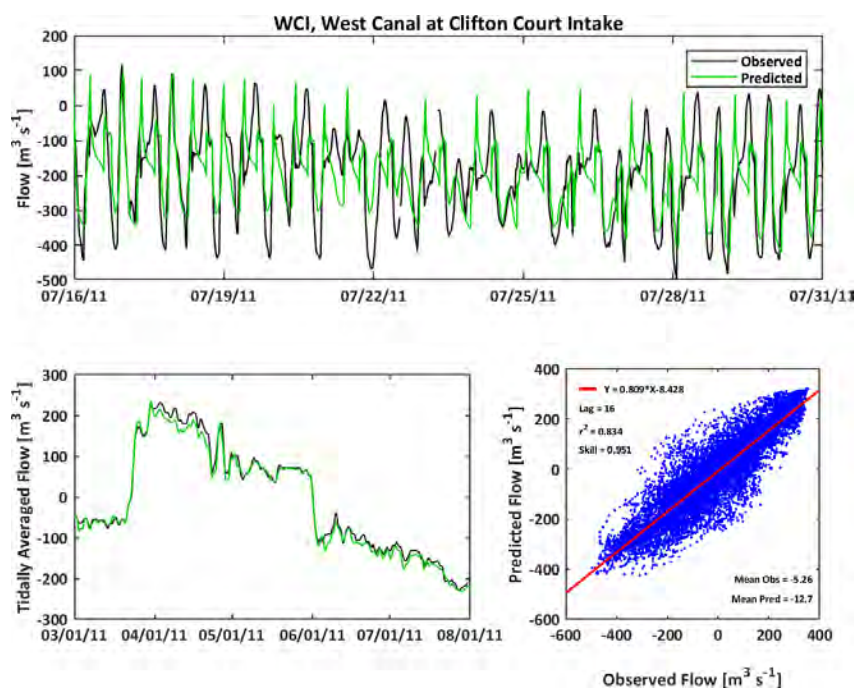


**Figure C-12**

**Observed and Predicted Water Flow at Grant Line Canal near Clifton Court Ferry (GLC) During 2011**

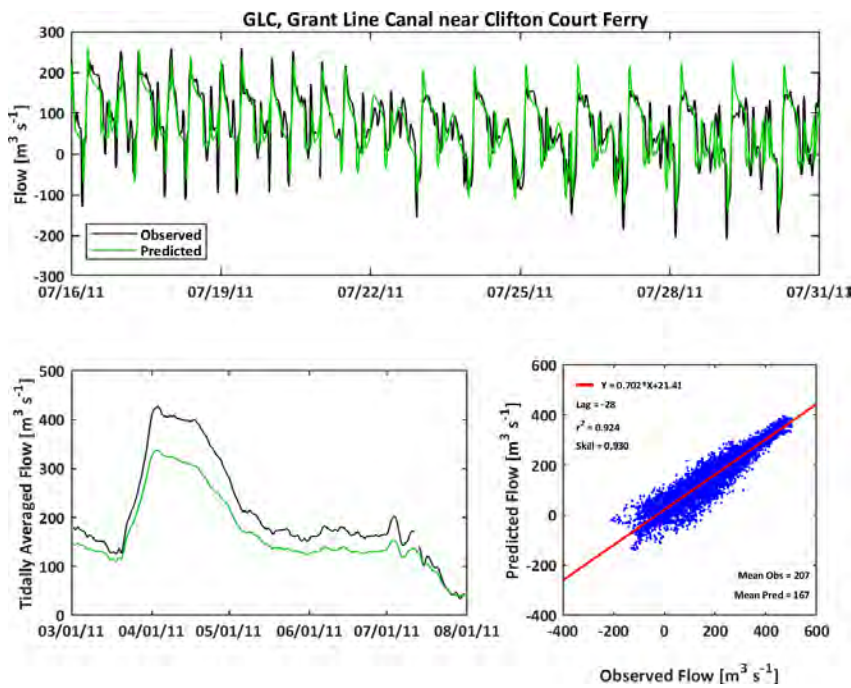


**Figure C-13**

**Observed and Predicted Water Flow at Old River at Head (OH1) During 2011**

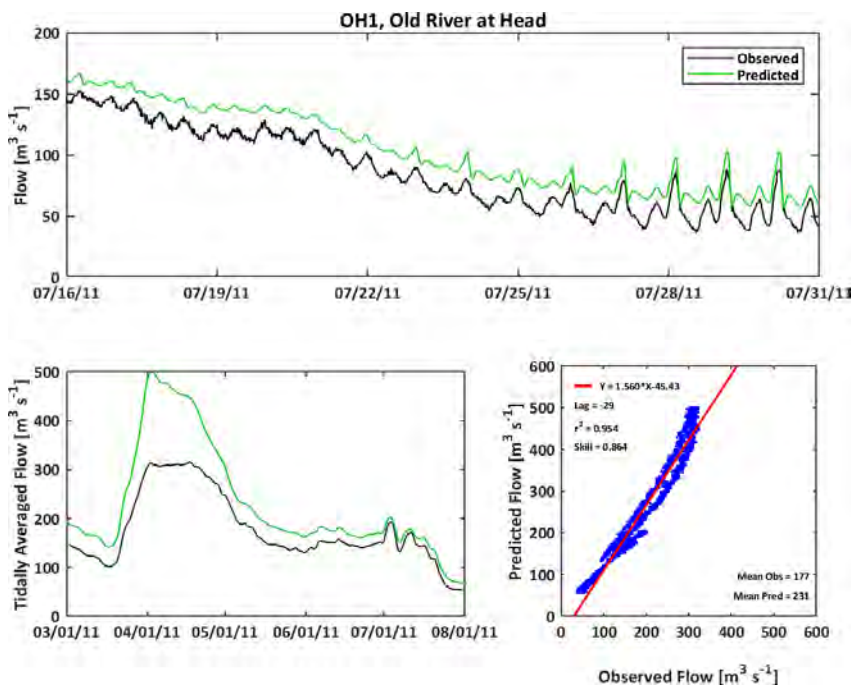


**Figure C-14**

**Observed and Predicted Water Flow at San Joaquin River below Old River near Lathrop (SJL) During 2011**

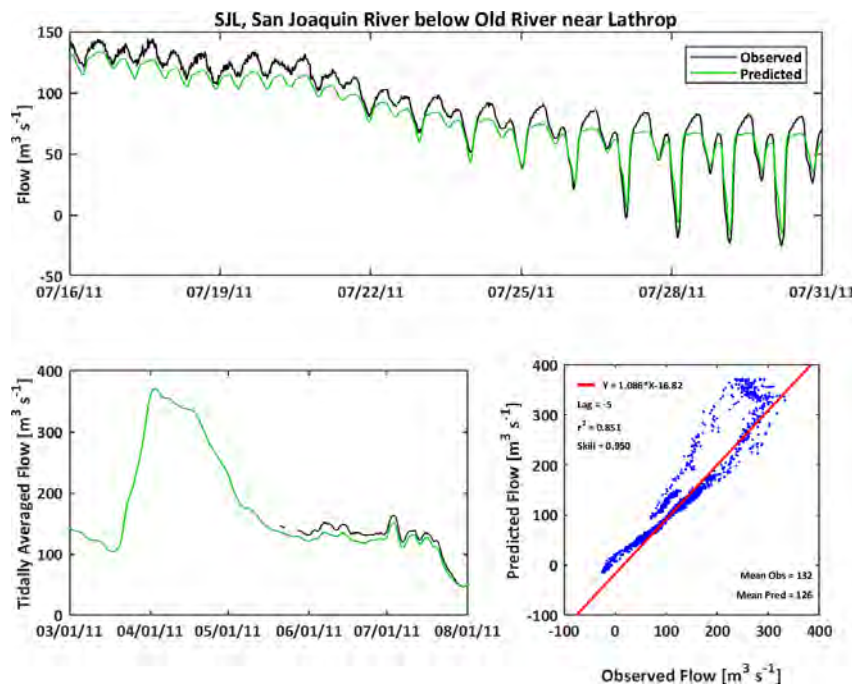


**Figure C-15**

**Observed and Predicted Water Flow at San Joaquin River at Mossdale (MSD) During 2011**

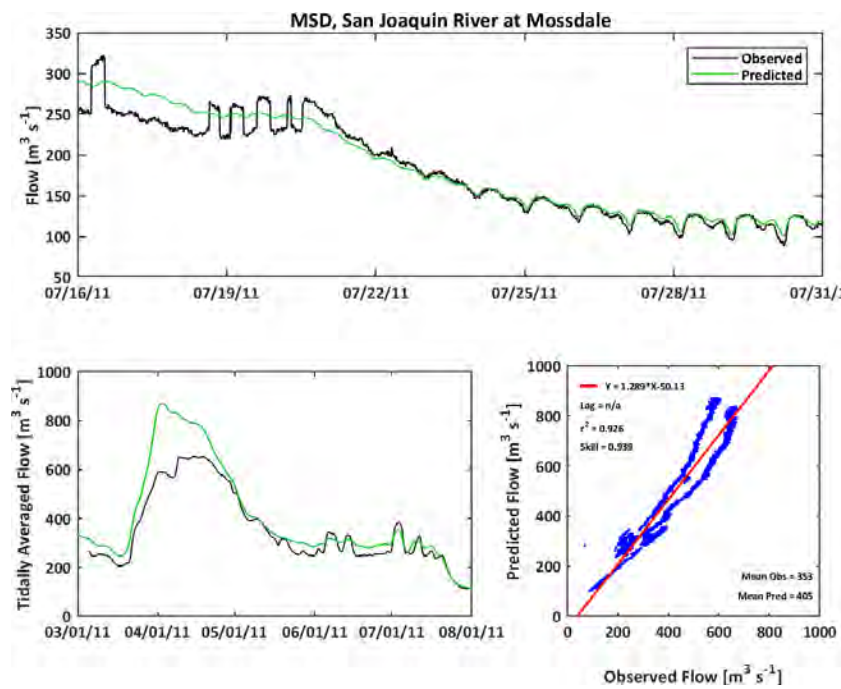


**Figure C-16**

**Observed and Predicted Water Flow at Sacramento River at Rio Vista (SRV) During 2012**

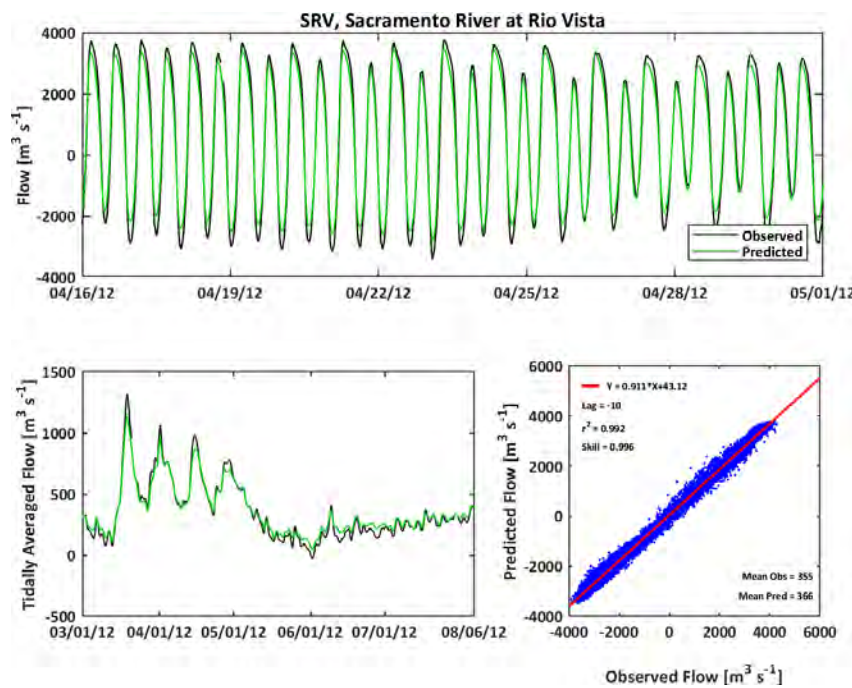


**Figure C-17**

**Observed and Predicted Water Flow at San Joaquin River at Jersey Point (SJJ) During 2012**

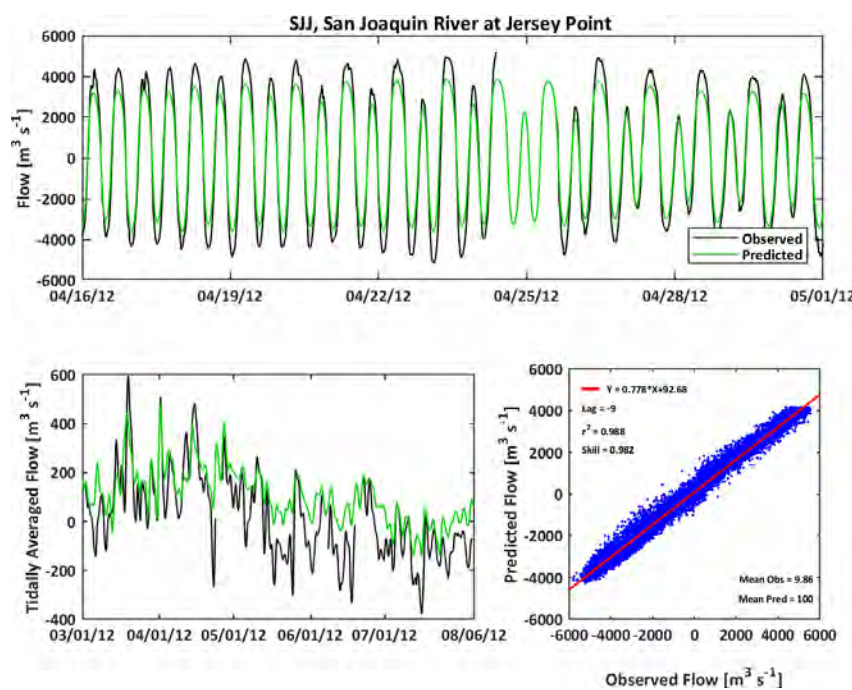


**Figure C-18**  
**Observed and Predicted Water Flow at Turner Cut near Holt (TRN) During 2012**

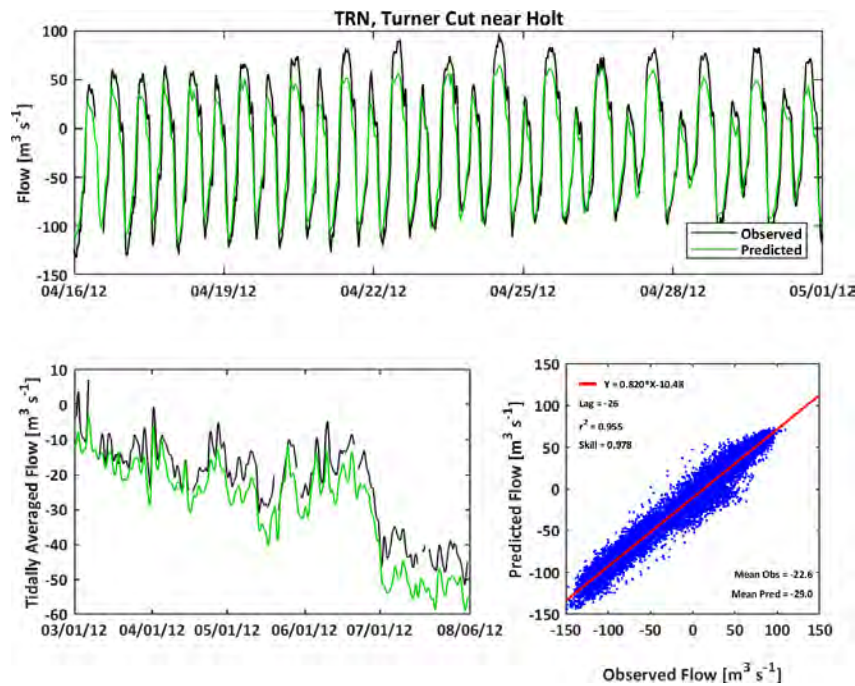


**Figure C-19**  
**Observed and Predicted Water Flow at Old River at Bacon Island (OBI) During 2012**

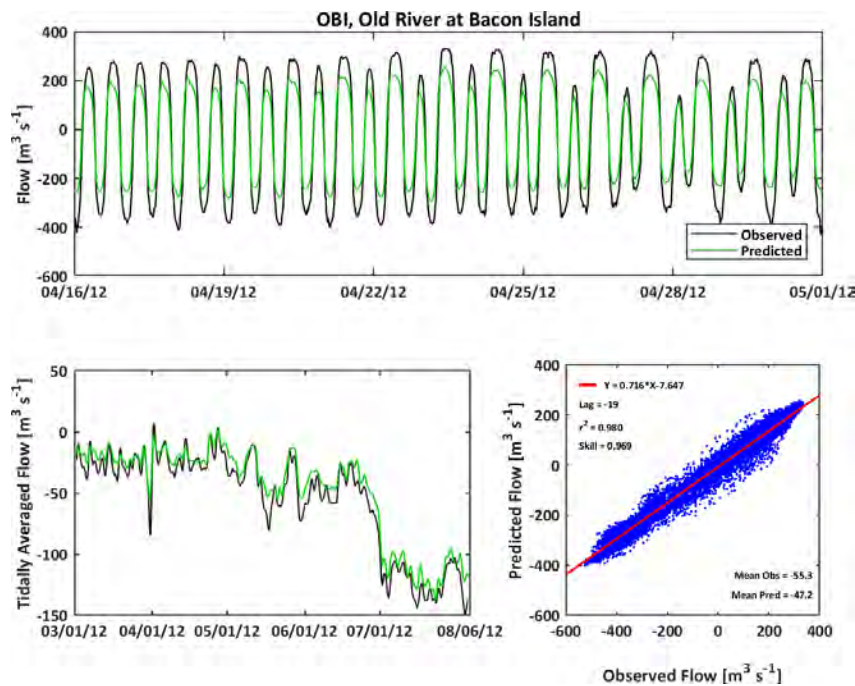


**Figure C-20**

**Observed and Predicted Water Flow at Middle River at Middle River (MDM) During 2012**

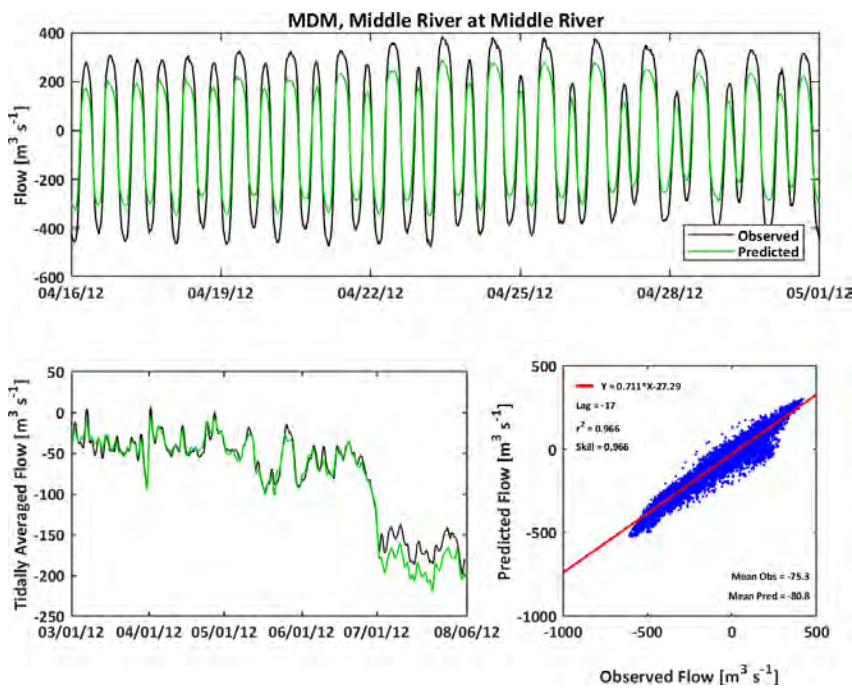


**Figure C-21**

**Observed and Predicted Water Flow at Old River at Highway 4 (OH4) During 2012**

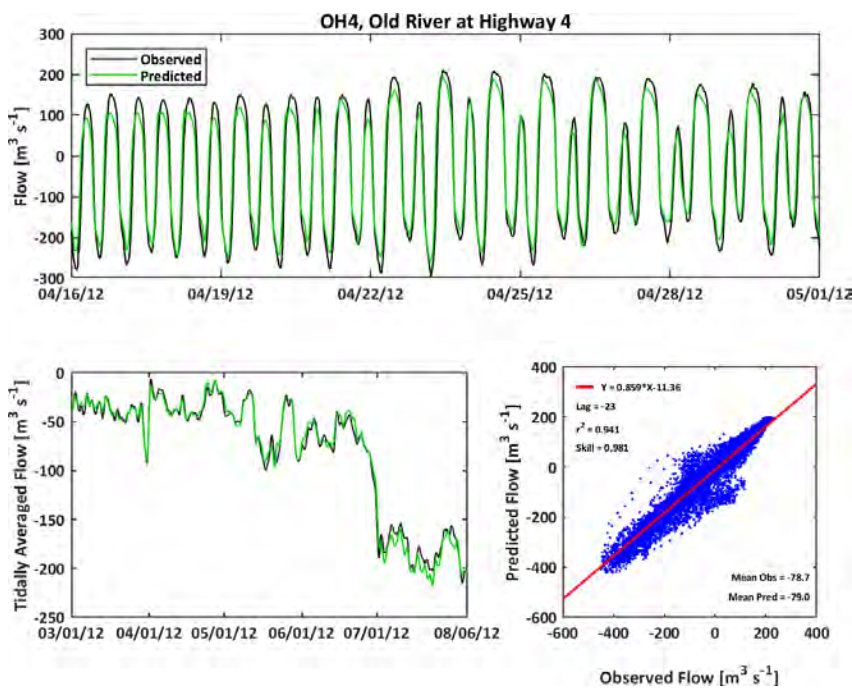


**Figure C-22**

**Observed and Predicted Water Flow at Victoria Canal near Byron (VCU) During 2012**

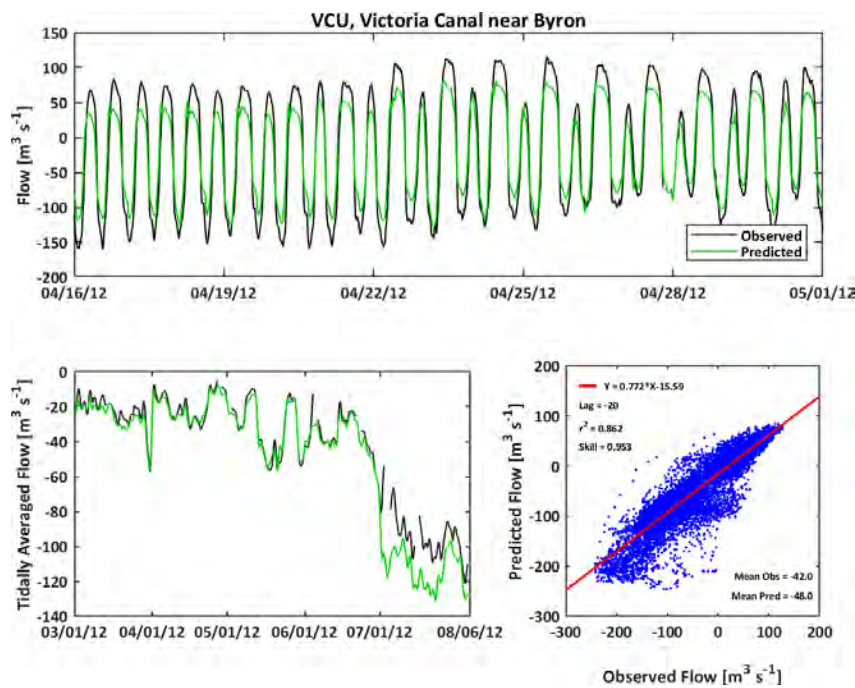


**Figure C-23**

**Observed and Predicted Water Flow at West Canal at Clifton Court Intake (WCI) During 2012**

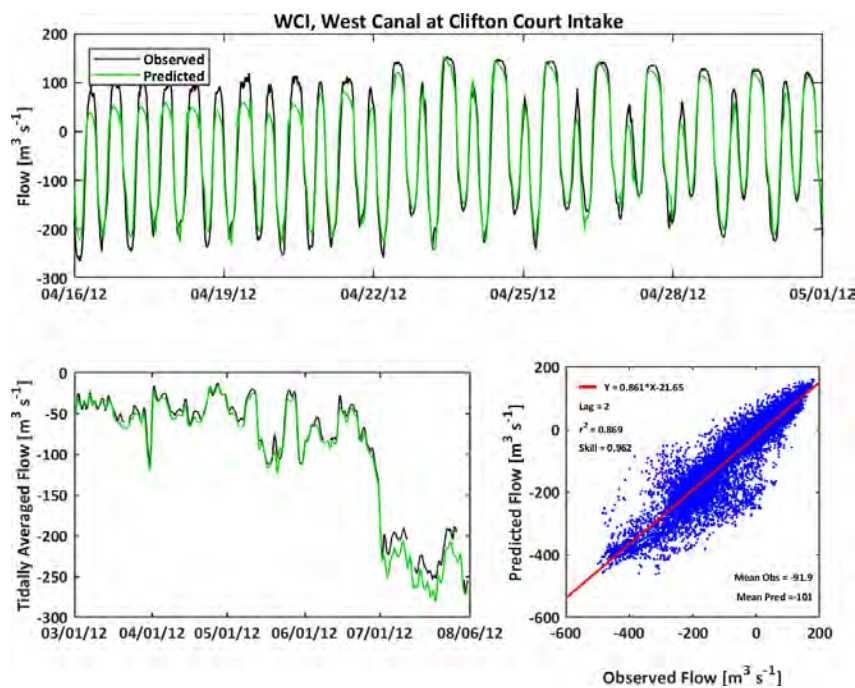


**Figure C-24**

**Observed and Predicted Water Flow at Grant Line Canal near Clifton Court Ferry (GLC) During 2012**

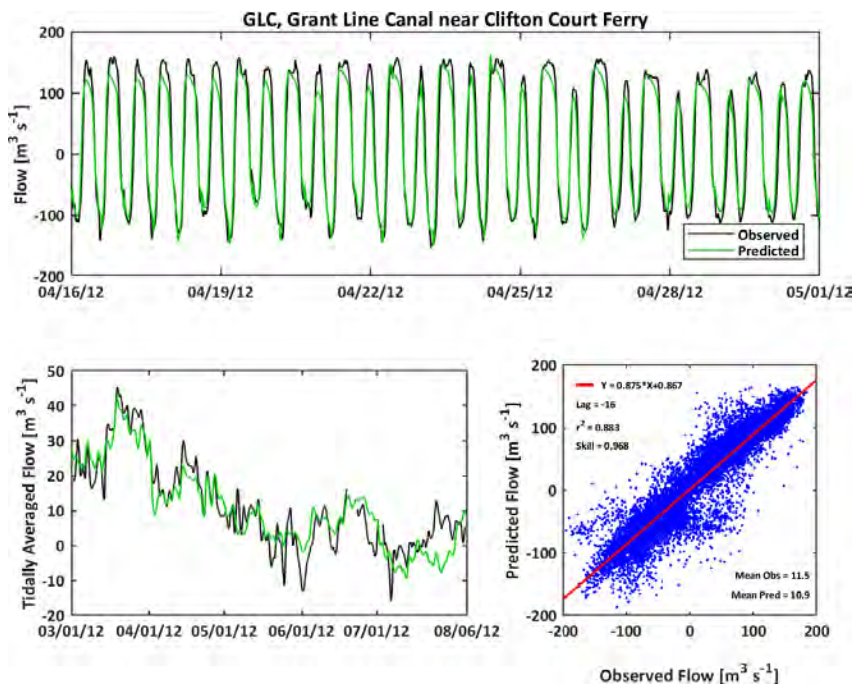


**Figure C-25**

**Observed and Predicted Water Flow at Old River at Head (OH1) During 2012**

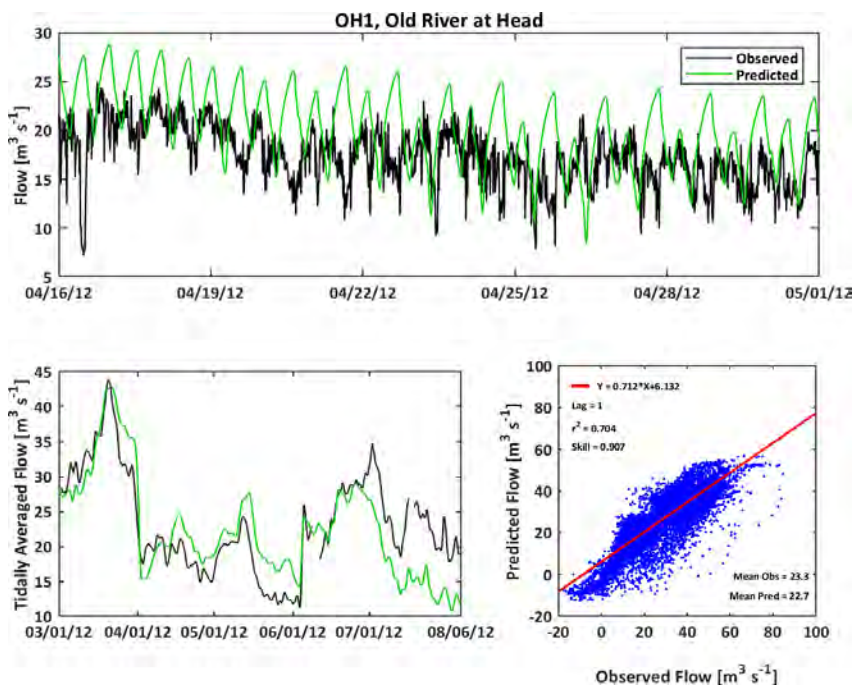


**Figure C-26**

**Observed and Predicted Water Flow at San Joaquin River at Mossdale (MSD) During 2012**

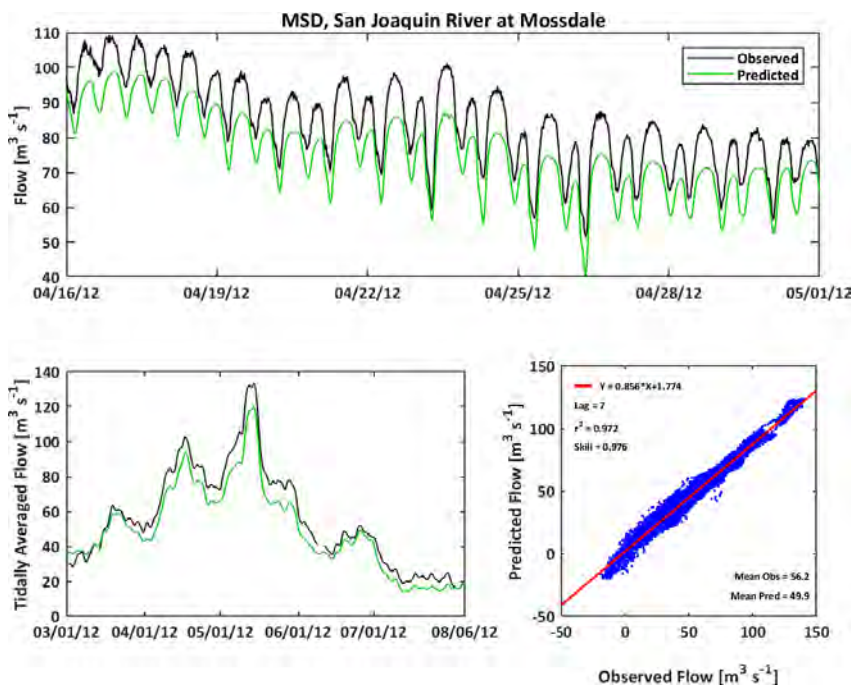


**Figure C-27**

**Observed and Predicted Water Flow at Sacramento River at Rio Vista (SRV) During 2013**

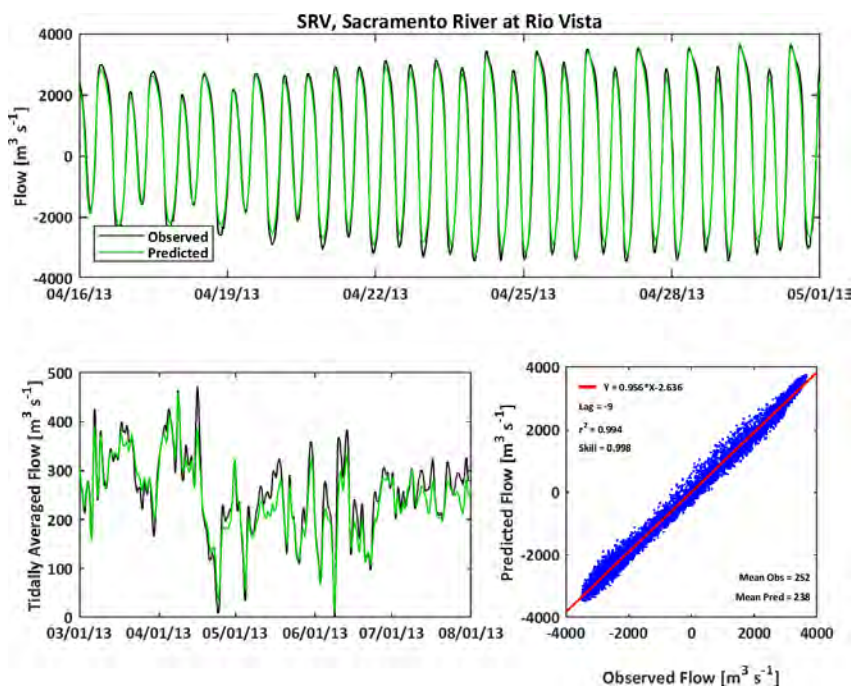


**Figure C-28**

**Observed and Predicted Water Flow at San Joaquin River at Jersey Point (SJJ) During 2013**

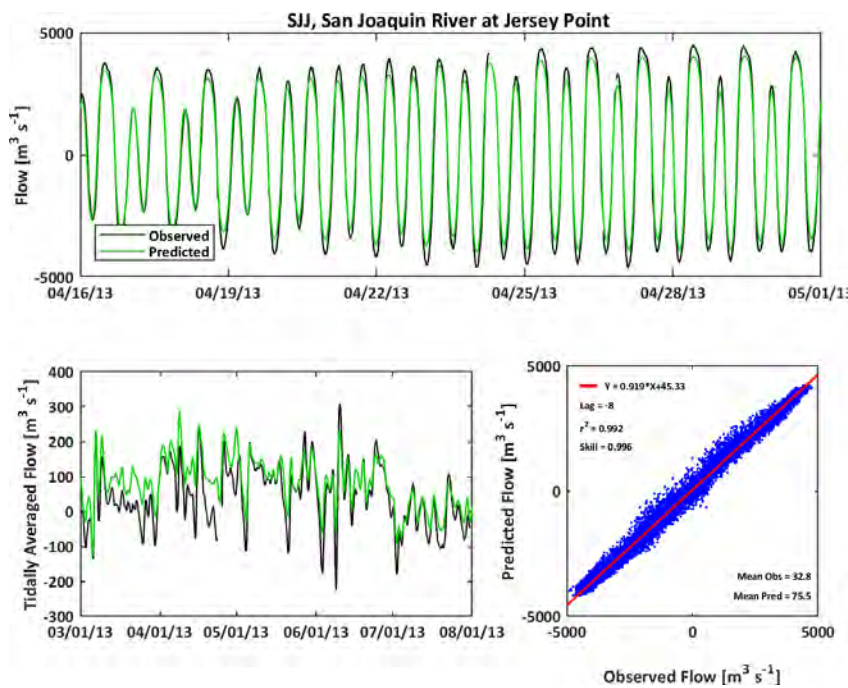


**Figure C-29**

**Observed and Predicted Water Flow at Turner Cut near Holt (TRN) During 2013**

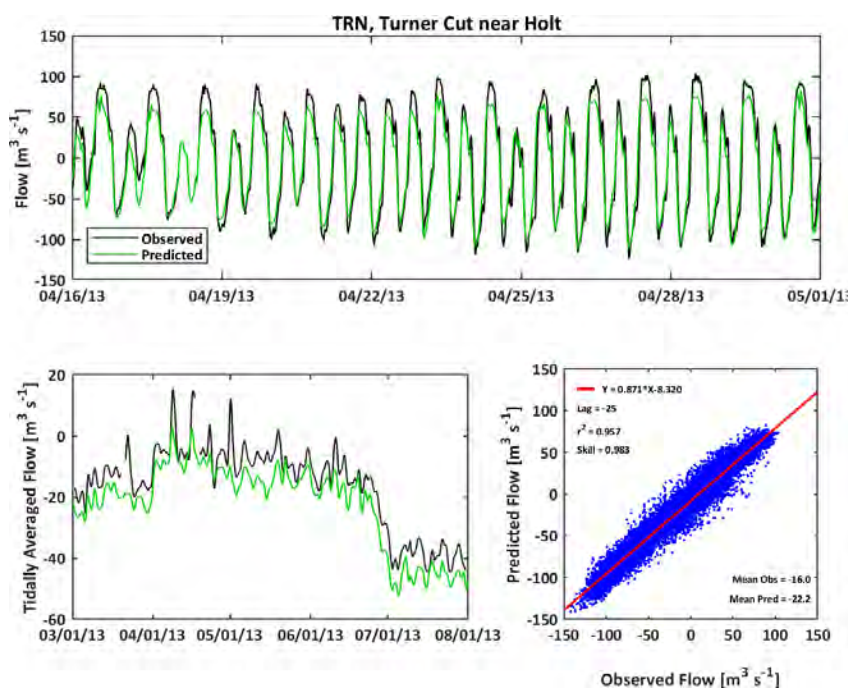


**Figure C-30**

**Observed and Predicted Water Flow at Old River at Bacon Island (OBI) During 2013**

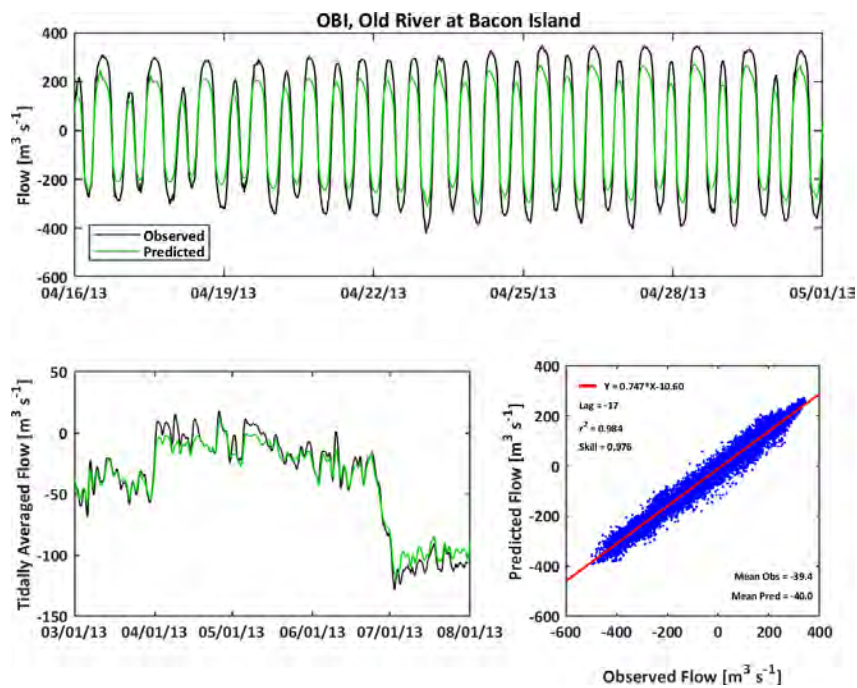


**Figure C-31**

**Observed and Predicted Water Flow at Middle River at Middle River (MDM) During 2013**

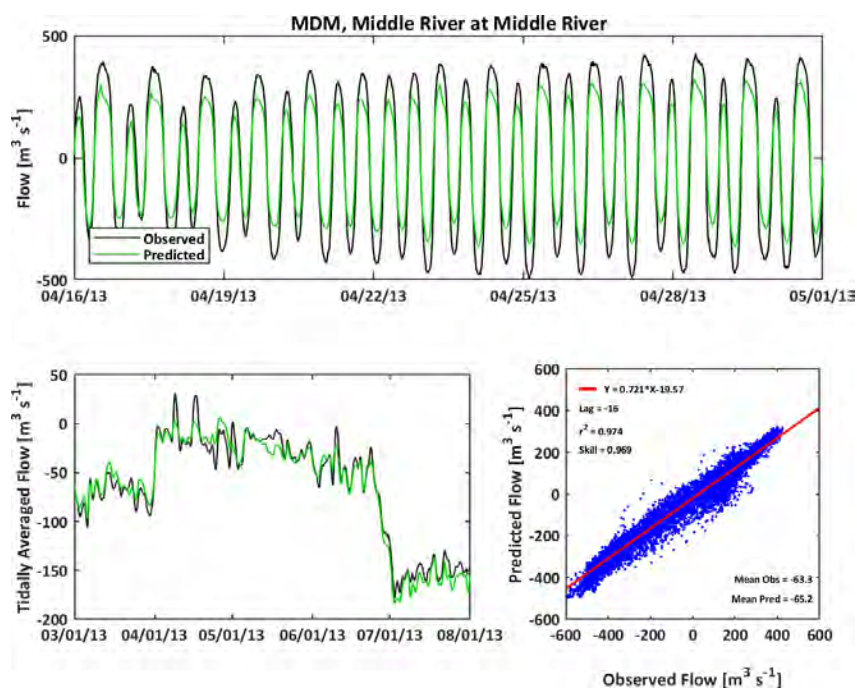


**Figure C-32**

**Observed and Predicted Water Flow at Old River at Highway 4 (OH4) During 2013**

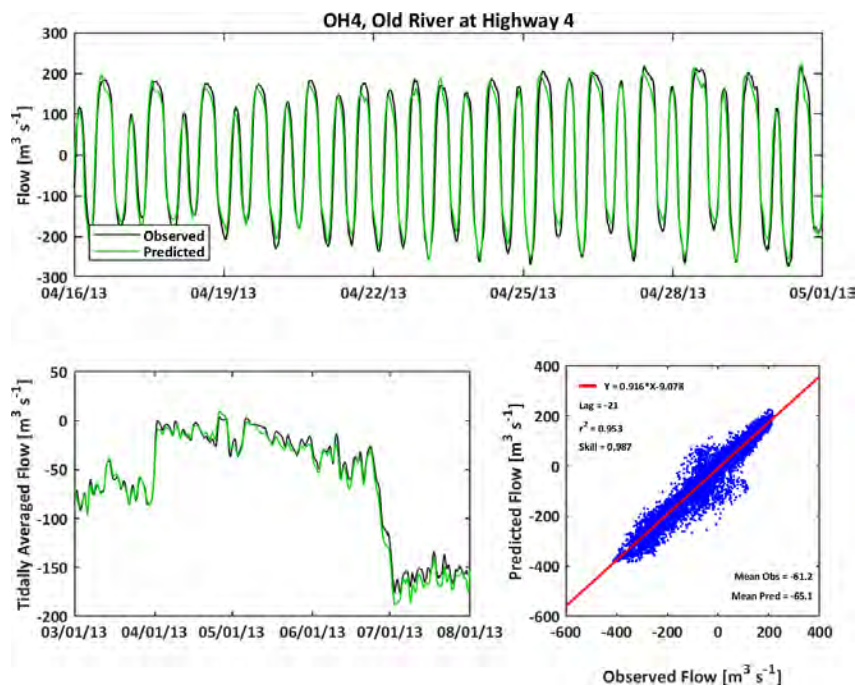


**Figure C-33**

**Observed and Predicted Water Flow at Victoria Canal near Byron (VCU) During 2013**

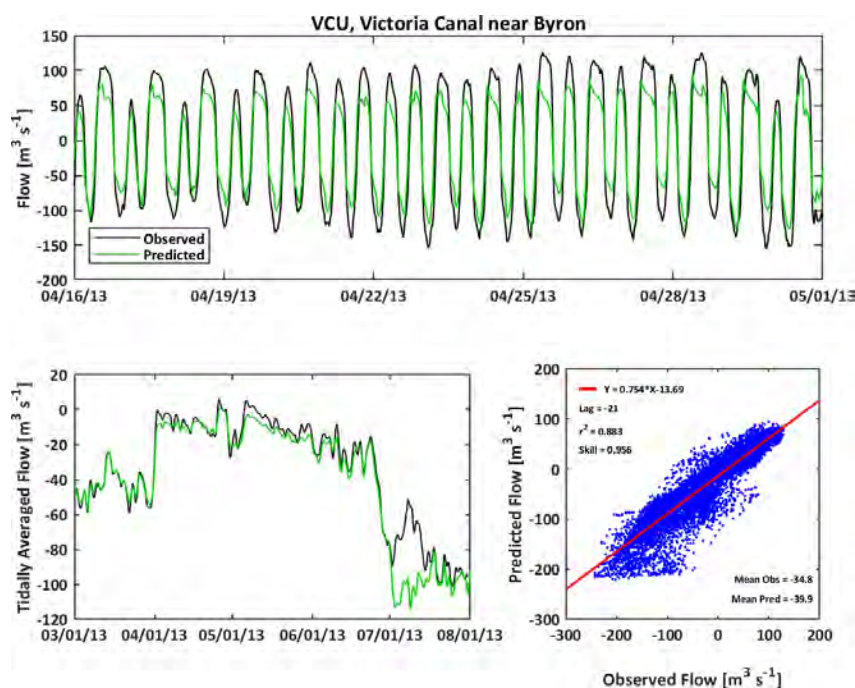


**Figure C-34**

**Observed and Predicted Water Flow at Grant Line Canal near Clifton Court Ferry (GLC) During 2013**

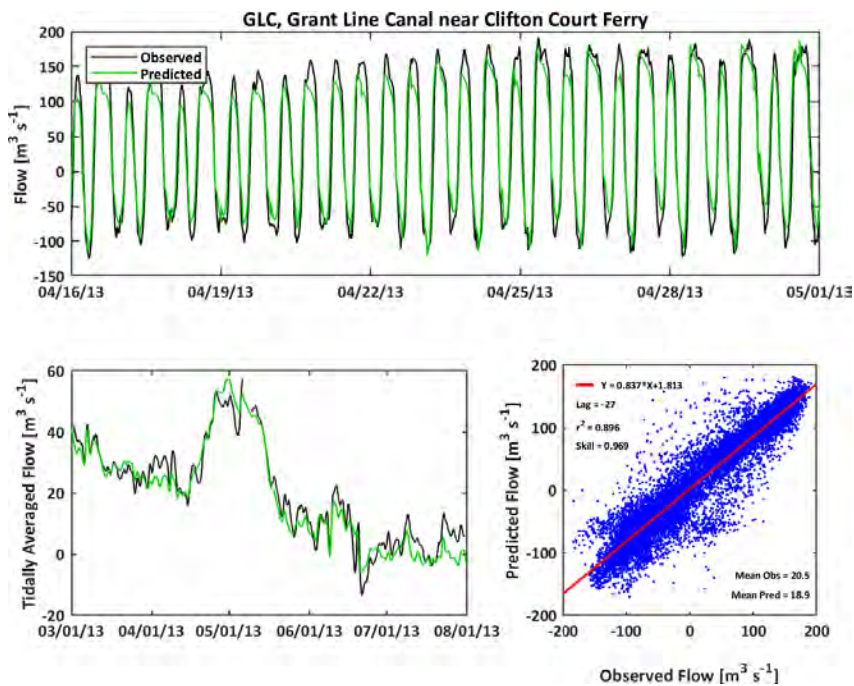


**Figure C-35**

**Observed and Predicted Water Flow at Old River at Head (OH1) During 2013**

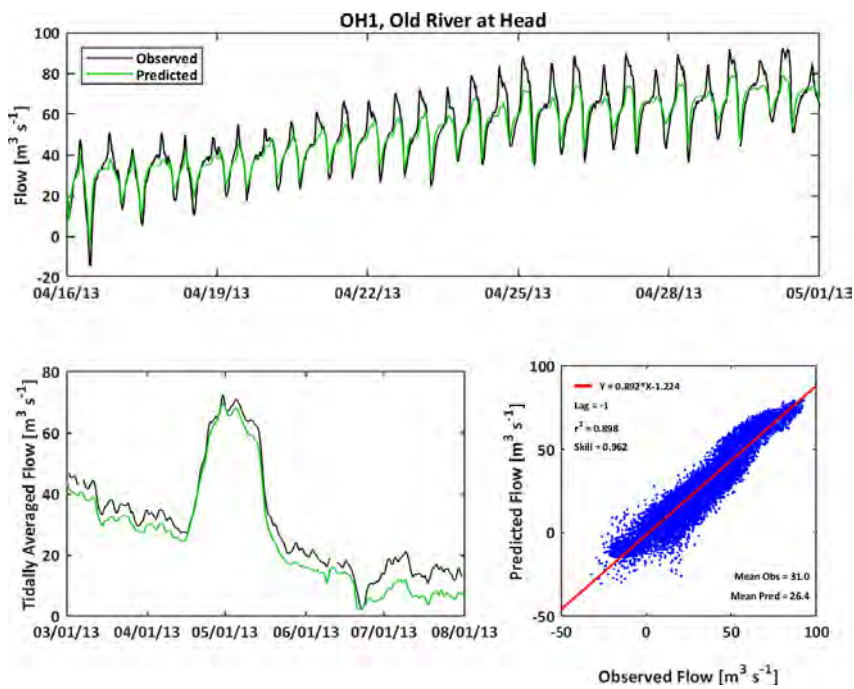


**Figure C-36**

**Observed and Predicted Water Flow at San Joaquin River at Mossdale (MSD) During 2013**

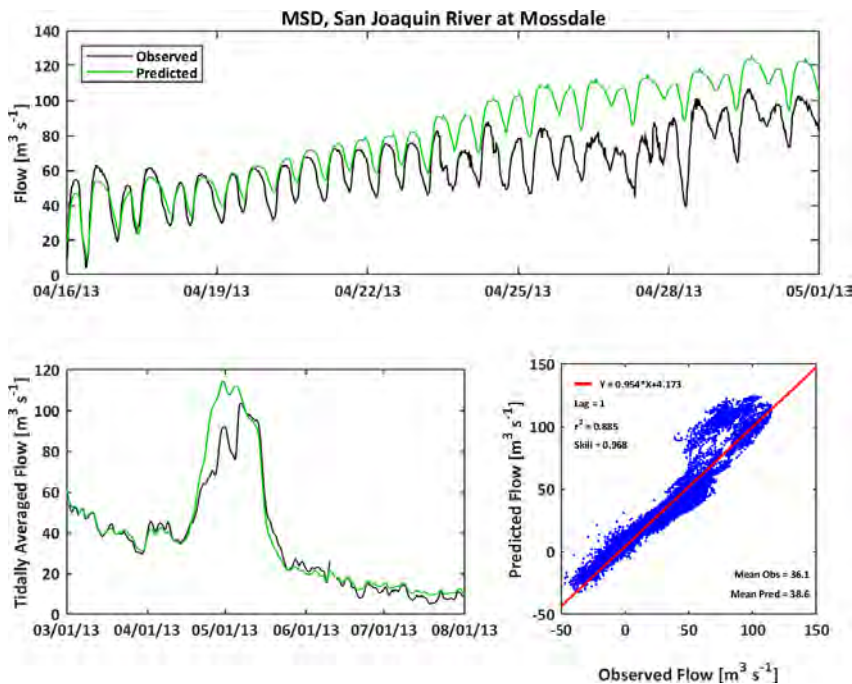


**Figure C-37**

**Observed and Predicted Water Flow at Sacramento River at Rio Vista (SRV) During 2014**

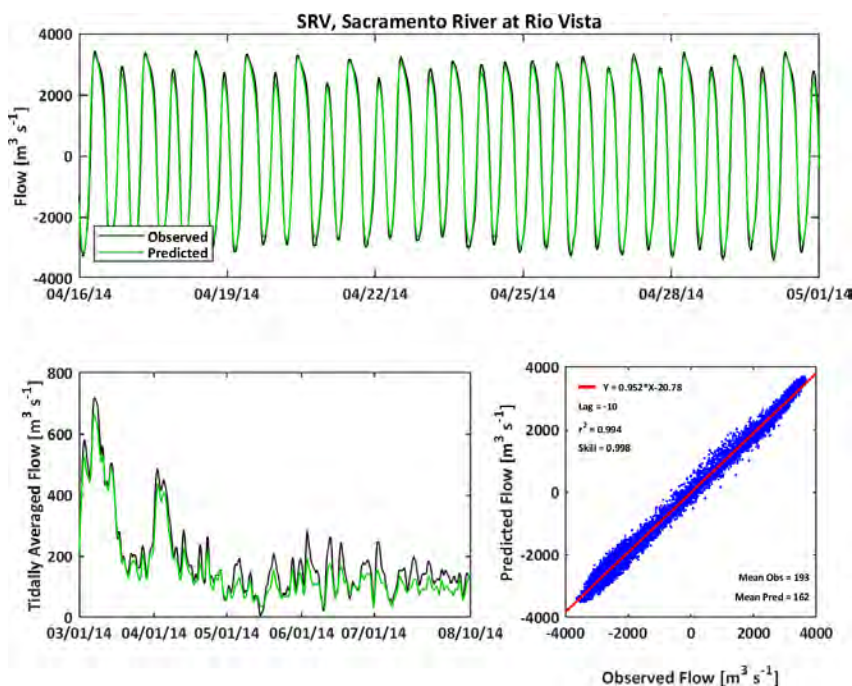


**Figure C-38**

**Observed and Predicted Water Flow at San Joaquin River at Jersey Point (SJJ) During 2014**

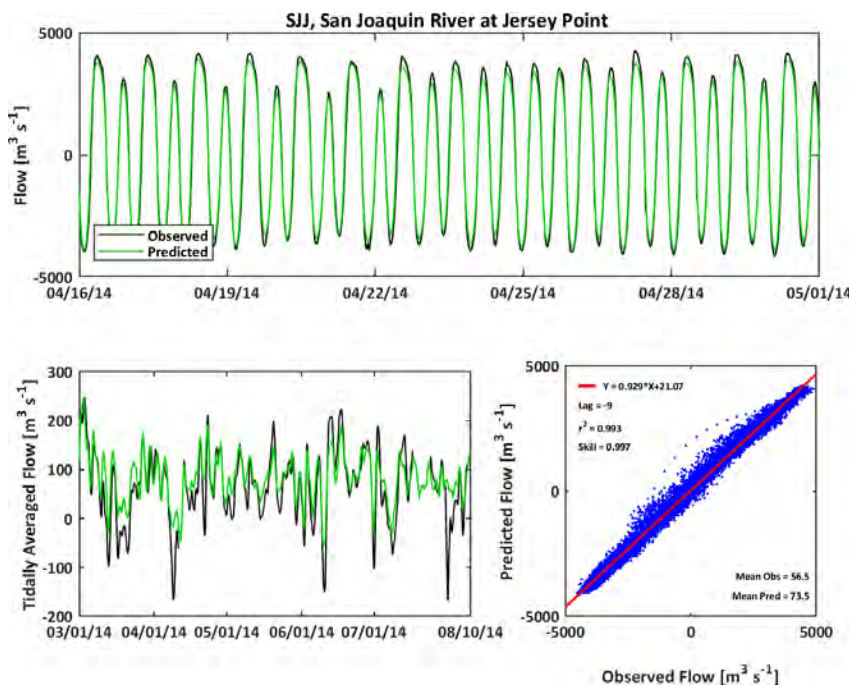


**Figure C-39**

**Observed and Predicted Water Flow at Turner Cut near Holt (TRN) During 2014**

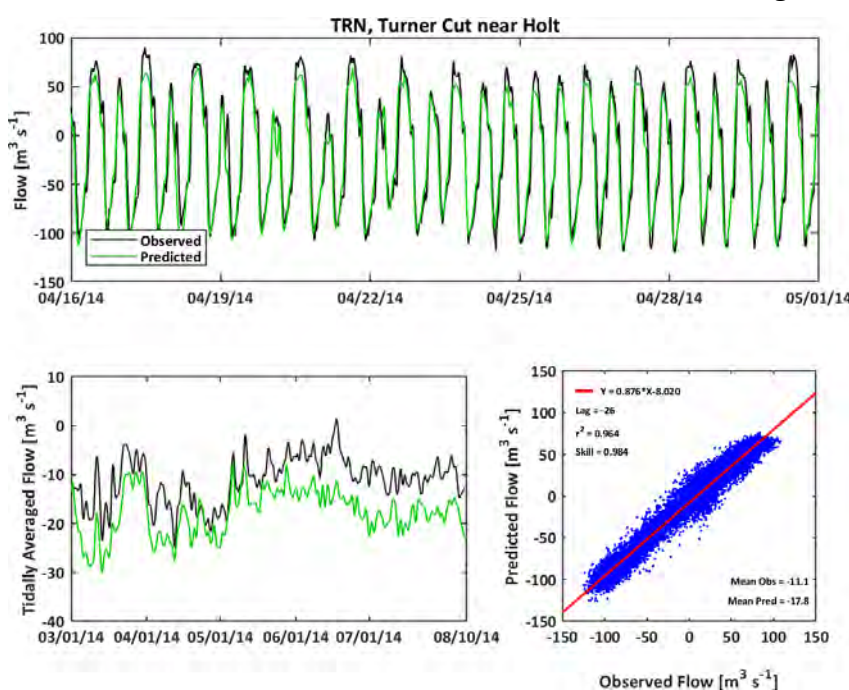


**Figure C-40**

**Observed and Predicted Water Flow at Old River at Bacon Island (OBI) During 2014**

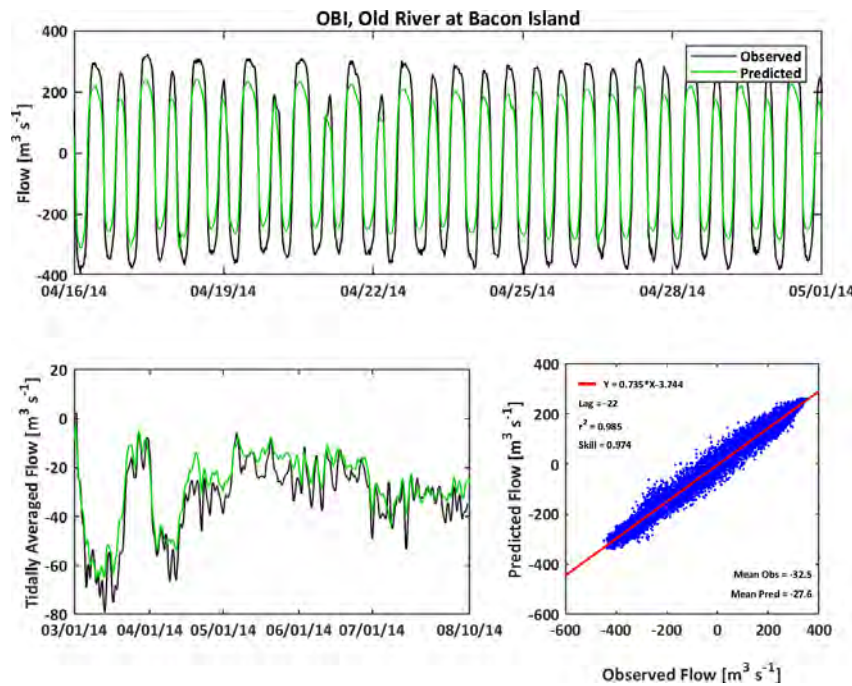


**Figure C-41**

**Observed and Predicted Water Flow at Middle River at Middle River (MDM) During 2014**

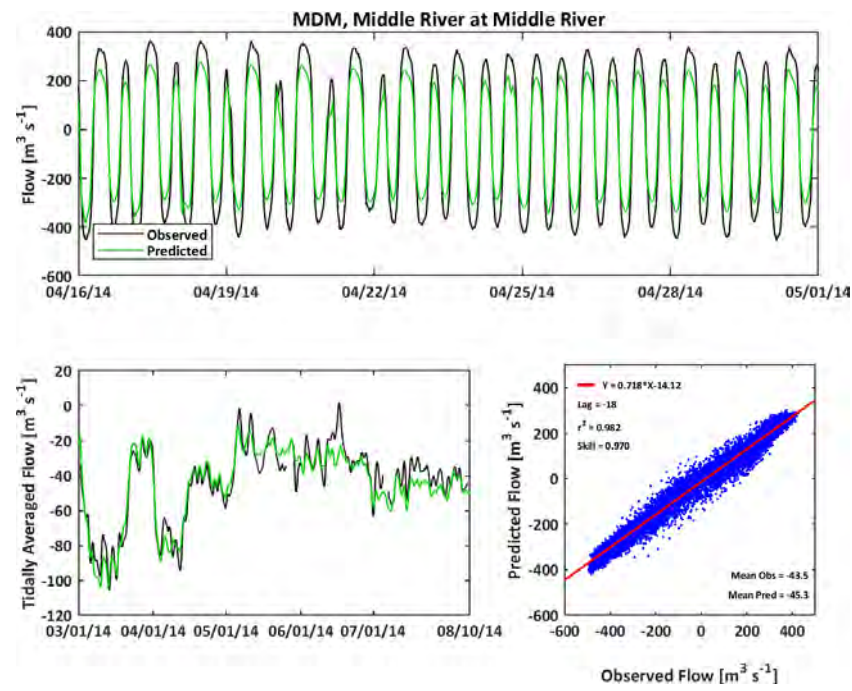


**Figure C-42**

**Observed and Predicted Water Flow at Old River at Highway 4 (OH4) During 2014**

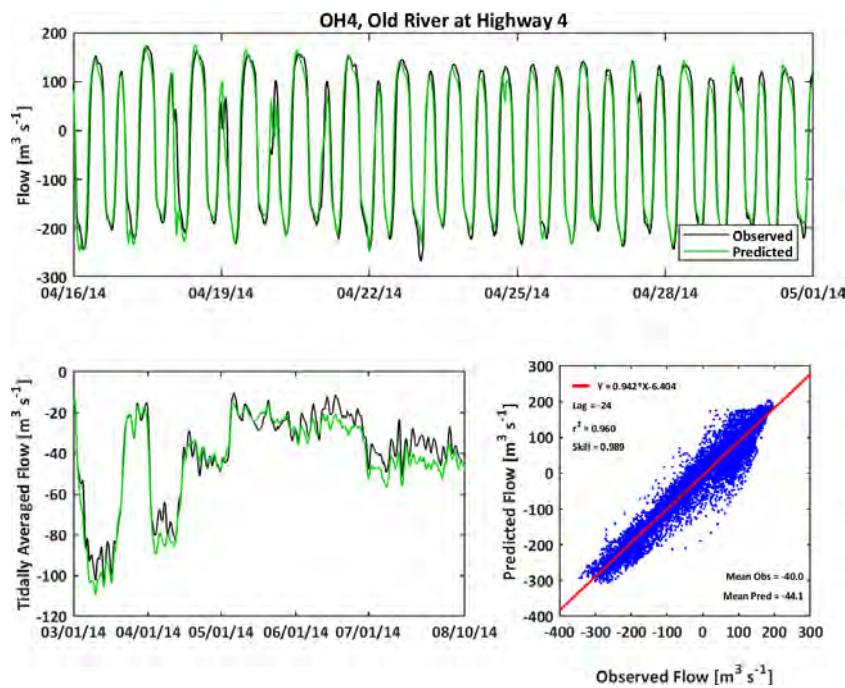


**Figure C-43**

**Observed and Predicted Water Flow at Victoria Canal near Byron (VCU) During 2014**

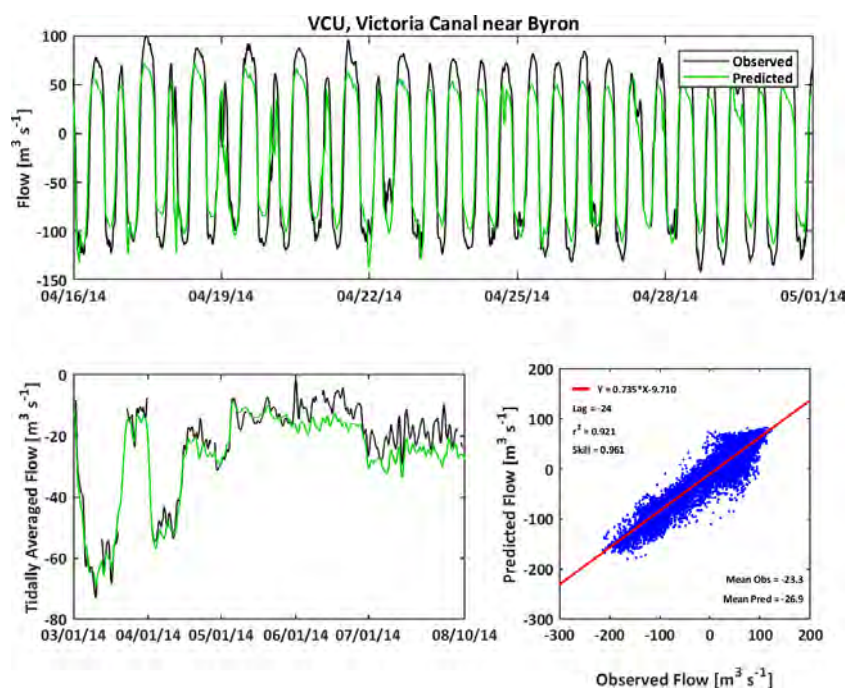


**Figure C-44**

**Observed and Predicted Water Flow at Grant Line Canal near Clifton Court Ferry (GLC) During 2014**

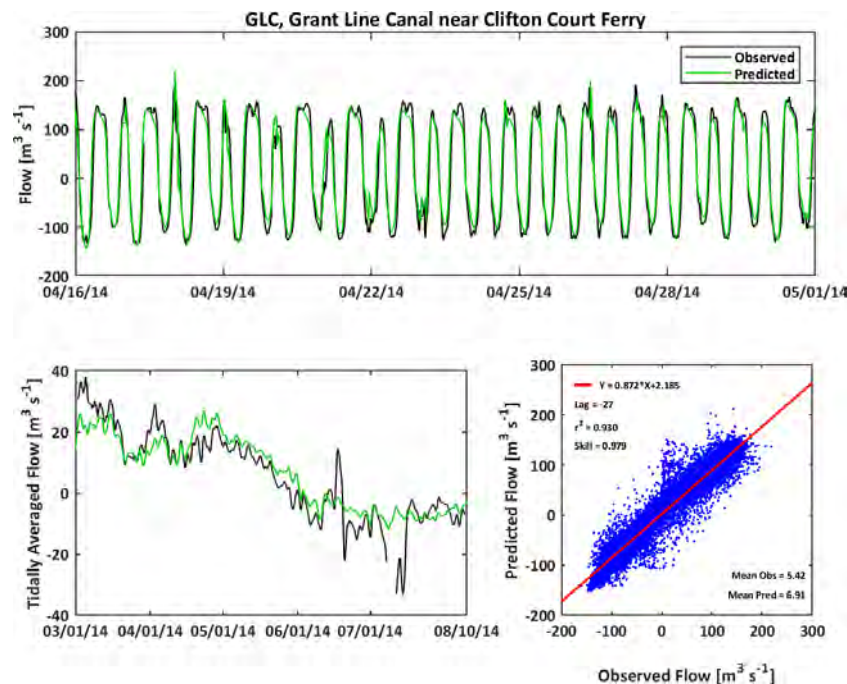


**Figure C-45**

**Observed and Predicted Water Flow at Old River at Head (OH1) During 2014**

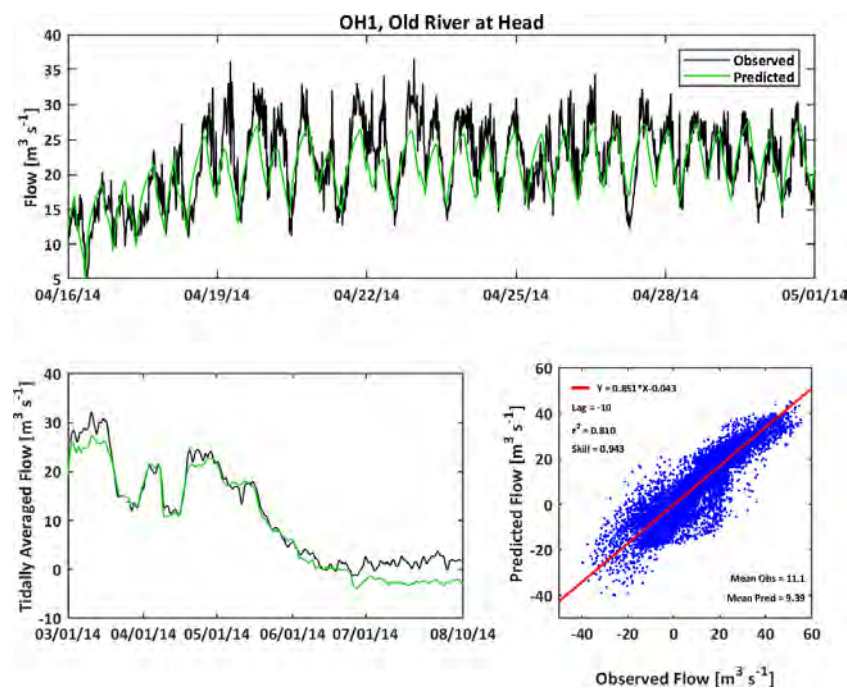


**Figure C-46**

**Observed and Predicted Water Flow at San Joaquin River at Mossdale (MSD) During 2014**

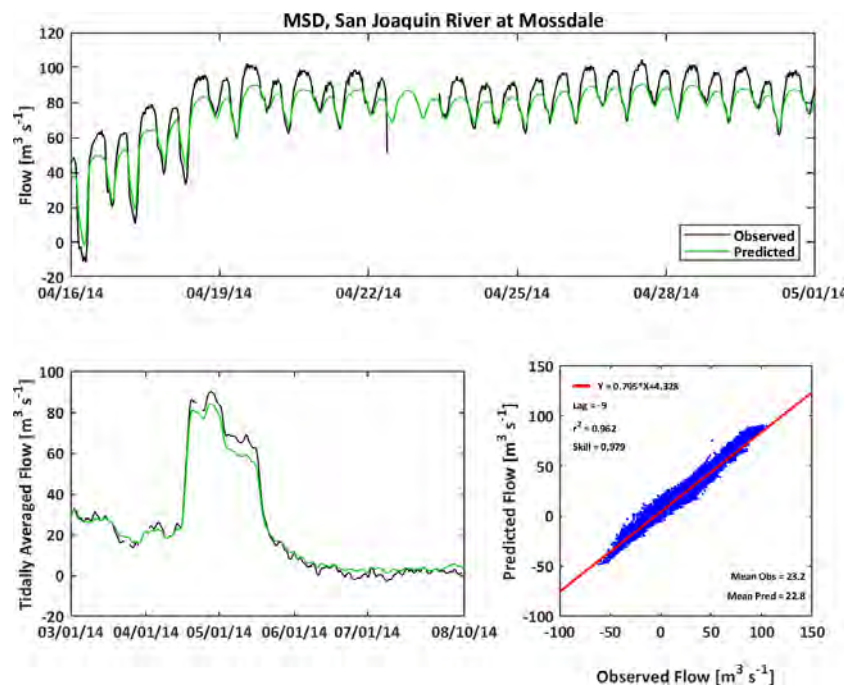


**Figure C-47**

**Observed and Predicted Water Flow at Sacramento River at Rio Vista (SRV) During 2015**

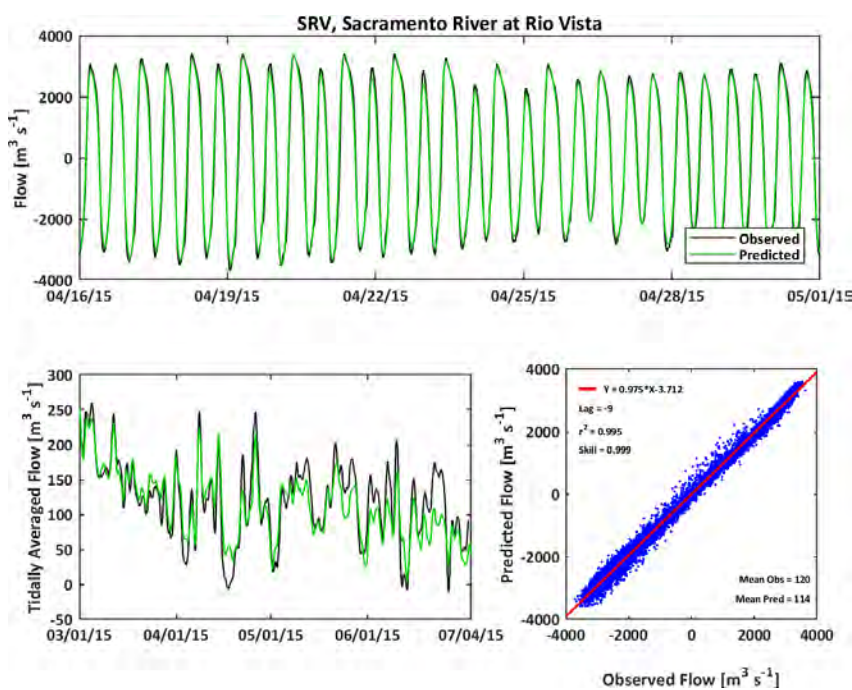


**Figure C-48**

**Observed and Predicted Water Flow at San Joaquin River at Jersey Point (SJJ) During 2015**

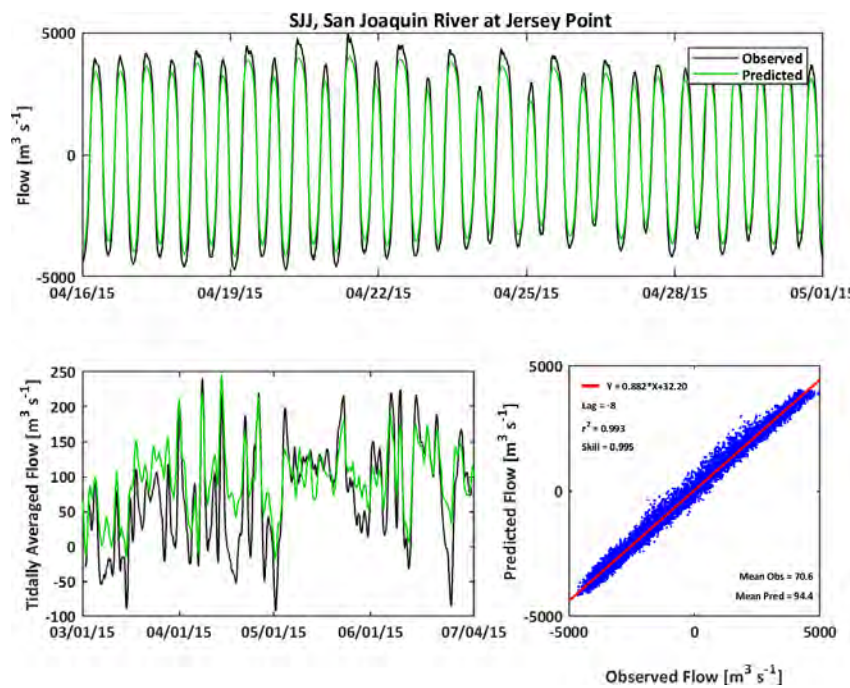


**Figure C-49**

**Observed and Predicted Water Flow at Turner Cut near Holt (TRN) During 2015**

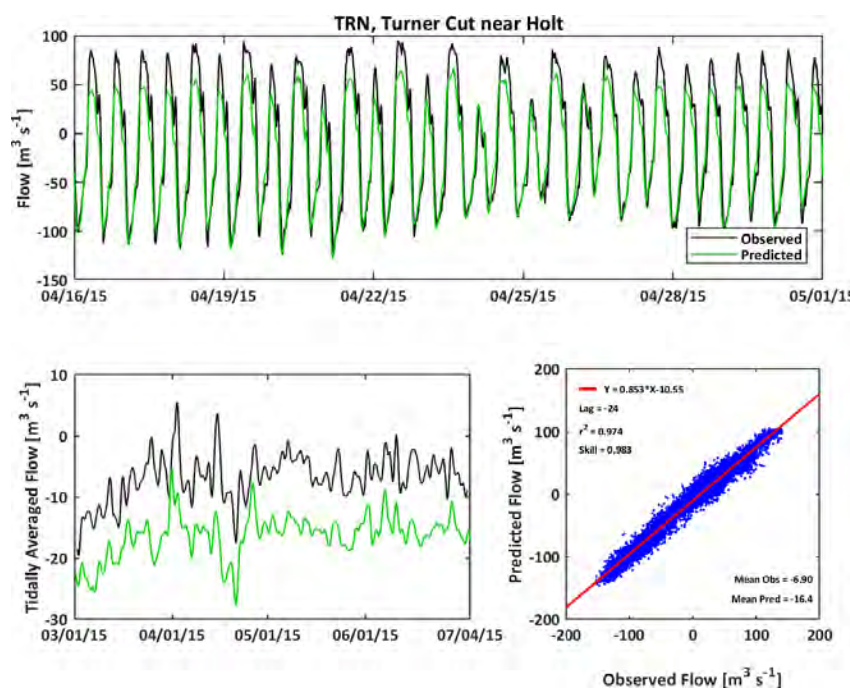


**Figure C-50**

**Observed and Predicted Water Flow at Old River at Bacon Island (OBI) During 2015**

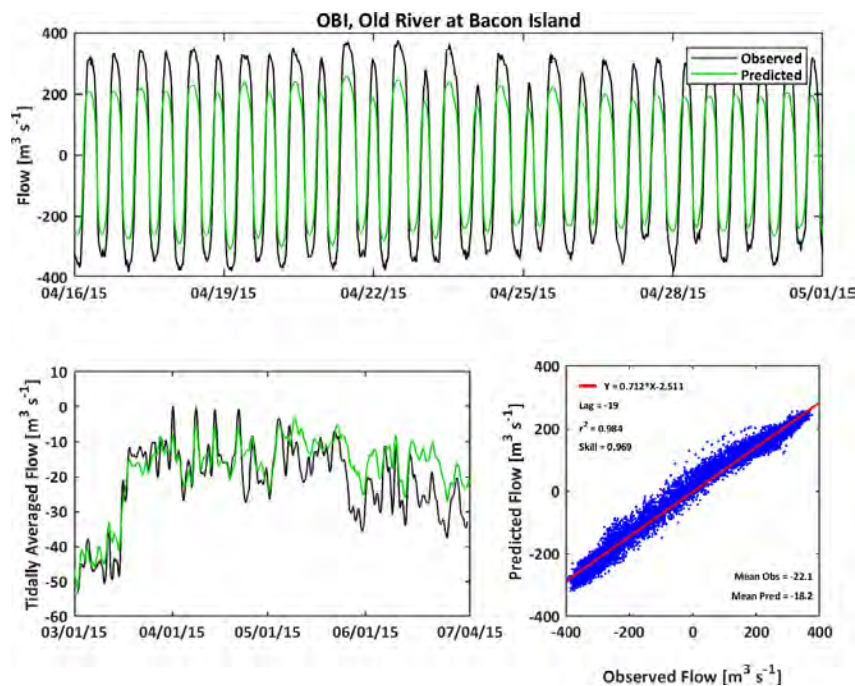


**Figure C-51**

**Observed and Predicted Water Flow at Middle River at Middle River (MDM) During 2015**

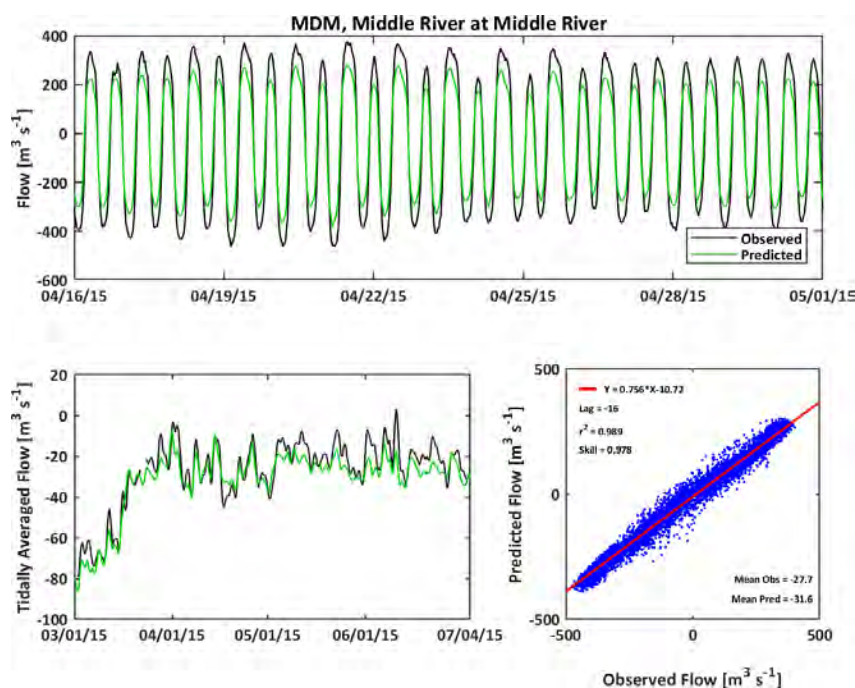


**Figure C-52**

**Observed and Predicted Water Flow at Victoria Canal near Byron (VCU) During 2015**

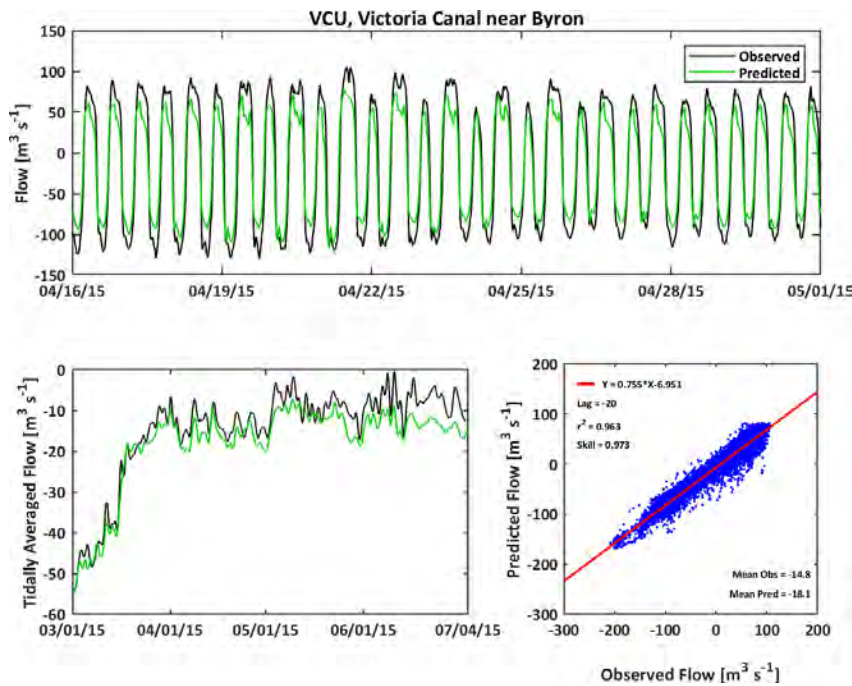


**Figure C-53**

**Observed and Predicted Water Flow at Grant Line Canal near Clifton Court Ferry (GLC) During 2015**

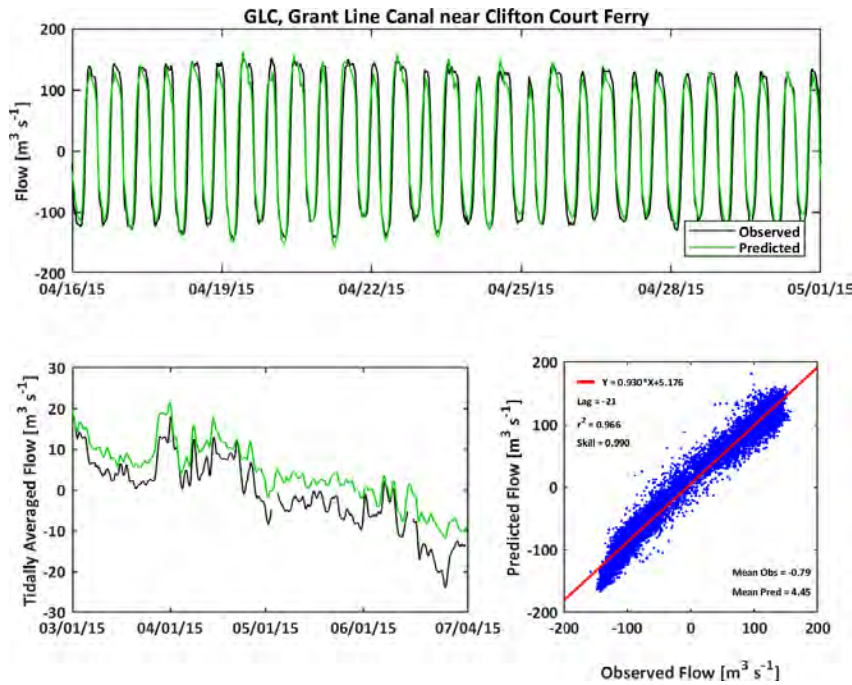


**Figure C-54**  
**Observed and Predicted Water Flow at Old River at Head (OH1) During 2015**

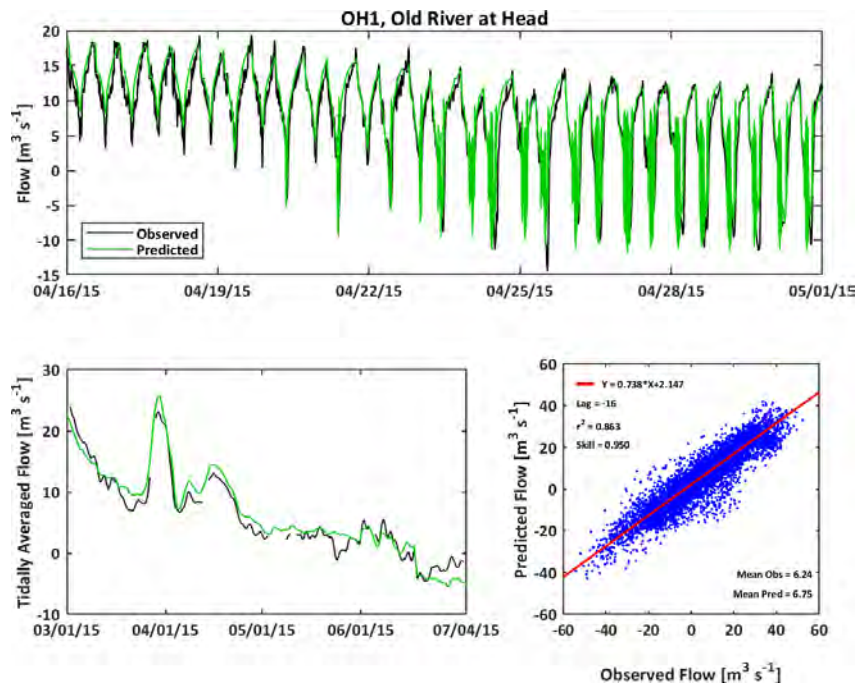


**Figure C-55**  
**Observed and Predicted Water Flow at San Joaquin River at Mossdale (MSD) During 2015**

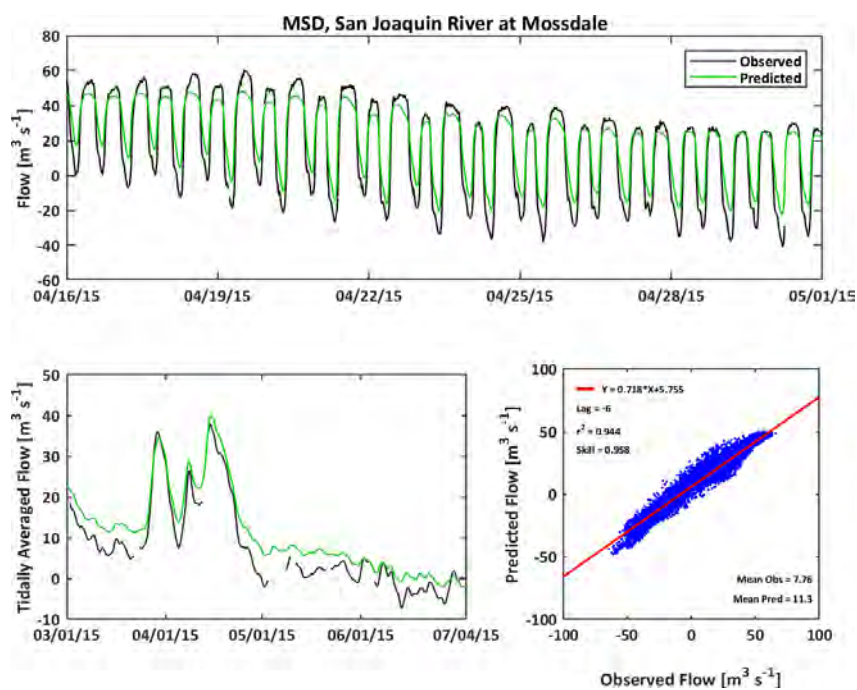


**Figure C-56**

**Observed and Predicted Water Flow at Sacramento River at Rio Vista (SRV) During 2016**

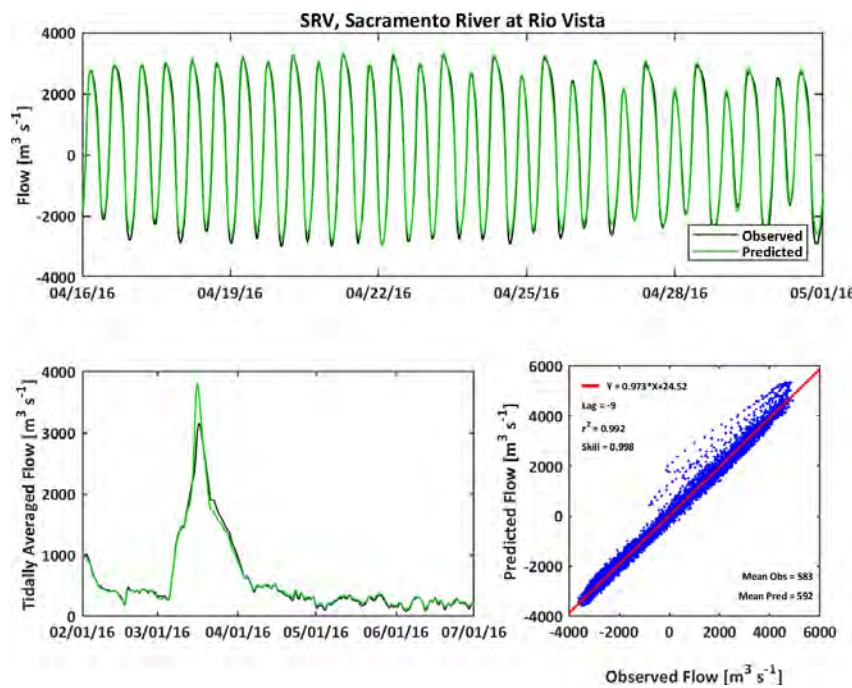


**Figure C-57**

**Observed and Predicted Water Flow at San Joaquin River at Jersey Point (SJJ) During 2016**

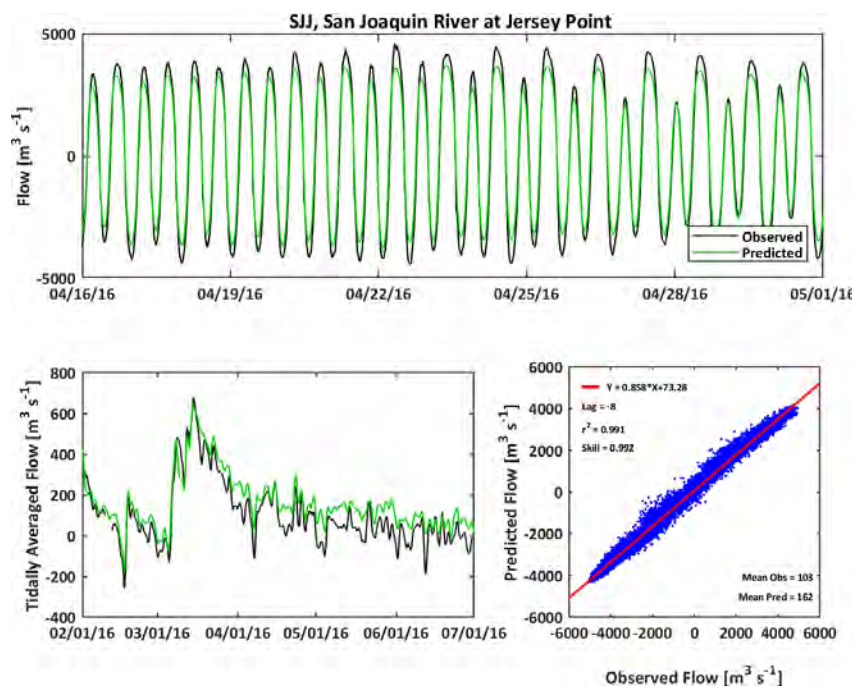


**Figure C-58**

**Observed and Predicted Water Flow at Turner Cut near Holt (TRN) During 2016**

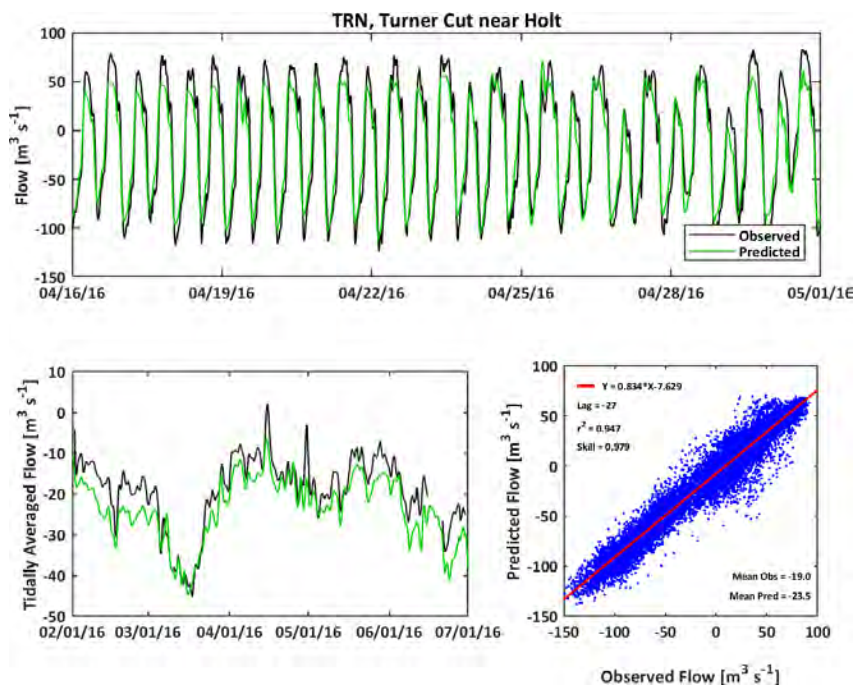


**Figure C-59**

**Observed and Predicted Water Flow at Old River at Bacon Island (OBI) During 2016**

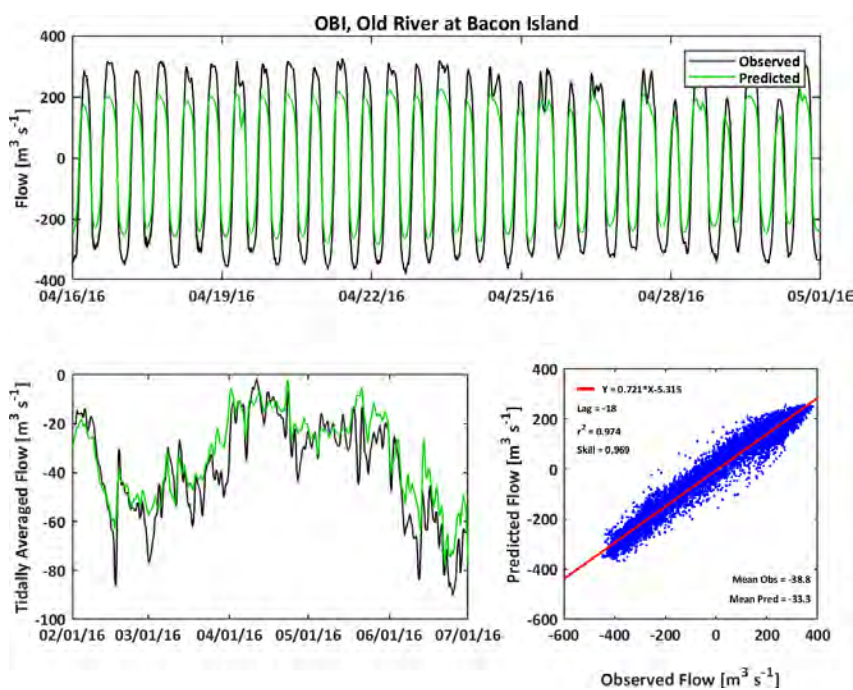


**Figure C-60**

**Observed and Predicted Water Flow at Middle River at Middle River (MDM) During 2016**

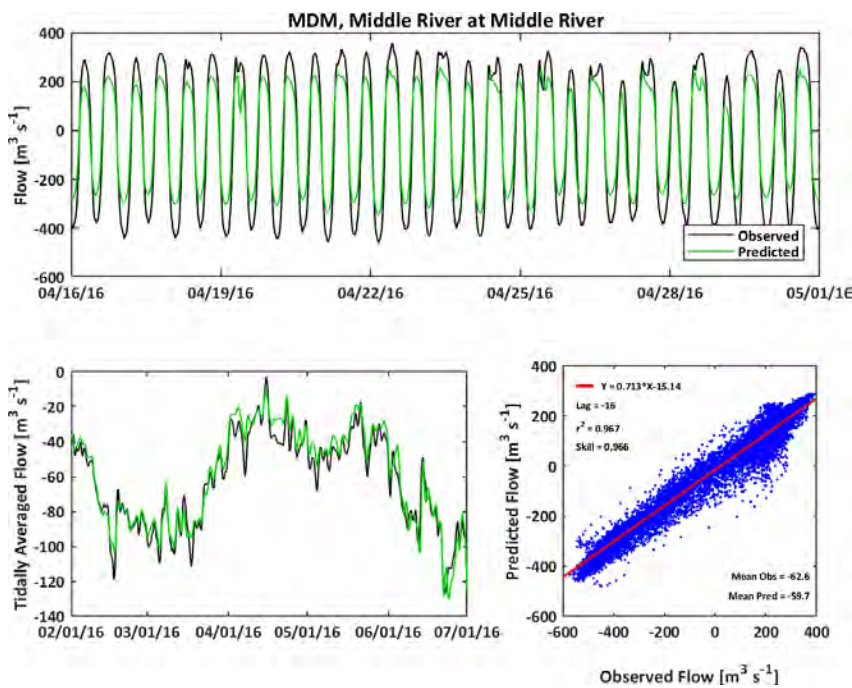


**Figure C-61**

**Observed and Predicted Water Flow at Old River at Highway 4 (OH4) During 2016**

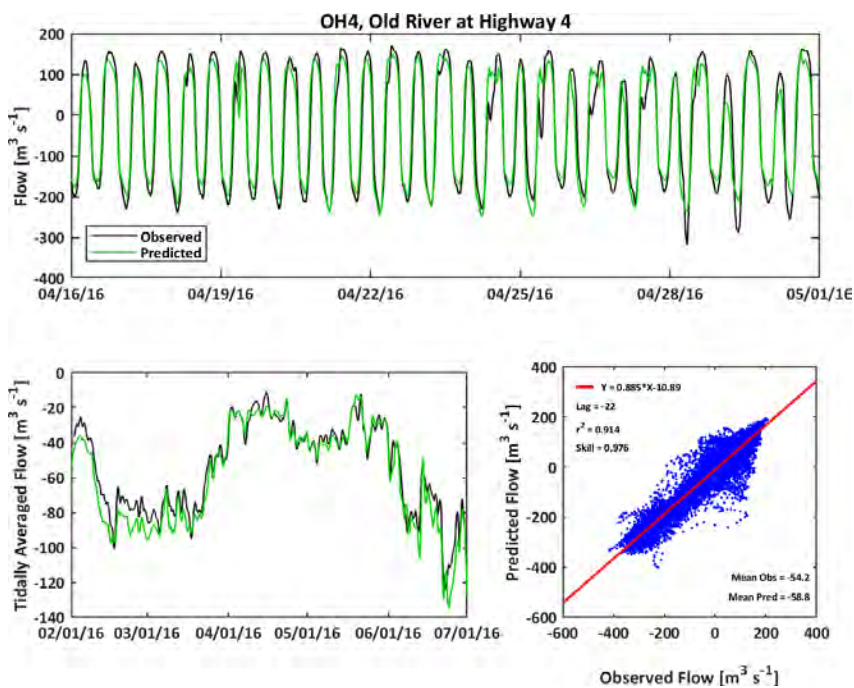


**Figure C-62**

**Observed and Predicted Water Flow at Victoria Canal near Byron (VCU) During 2016**

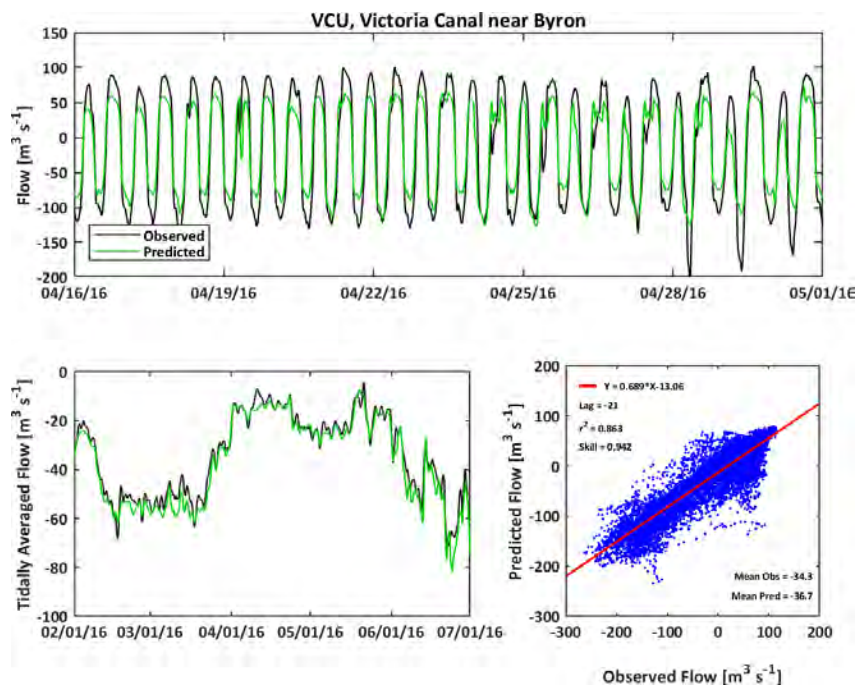


**Figure C-63**

**Observed and Predicted Water Flow at Grant Line Canal near Clifton Court Ferry (GLC) During 2016**

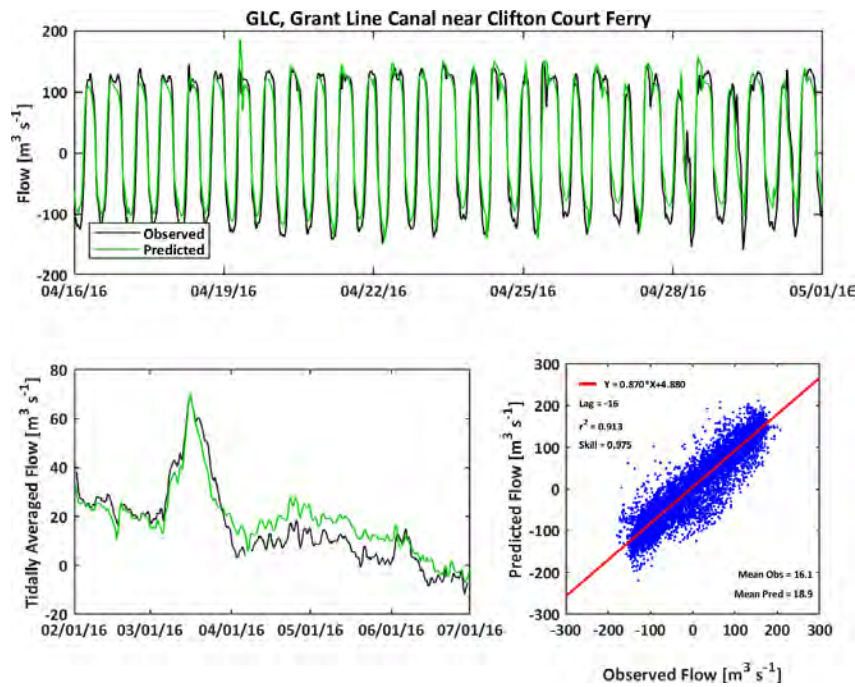


**Figure C-64**  
**Observed and Predicted Water Flow at Old River at Head (OH1) During 2016**

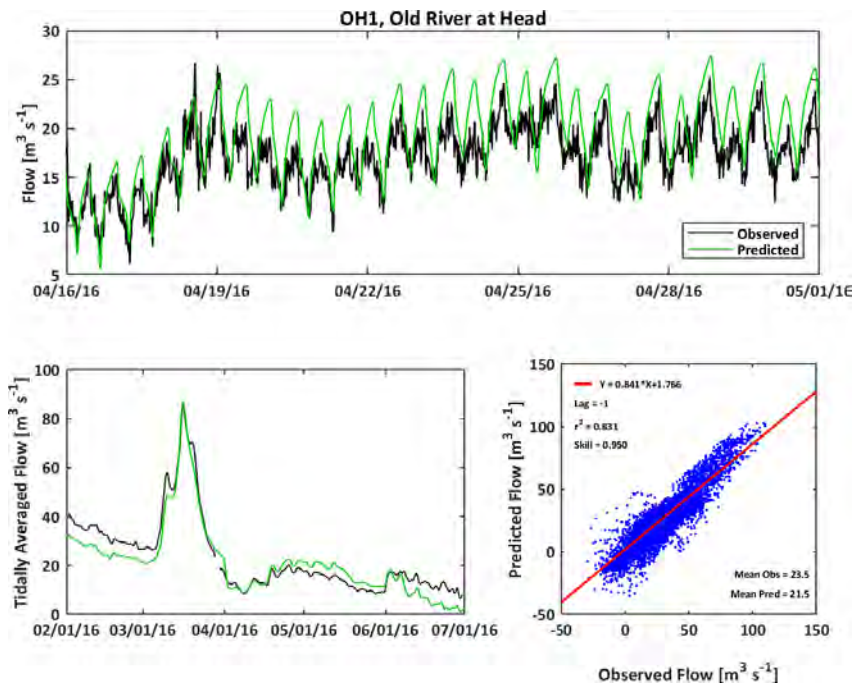


**Figure C-65**  
**Observed and Predicted Water Flow at San Joaquin River at Mossdale (MSD) During 2016**

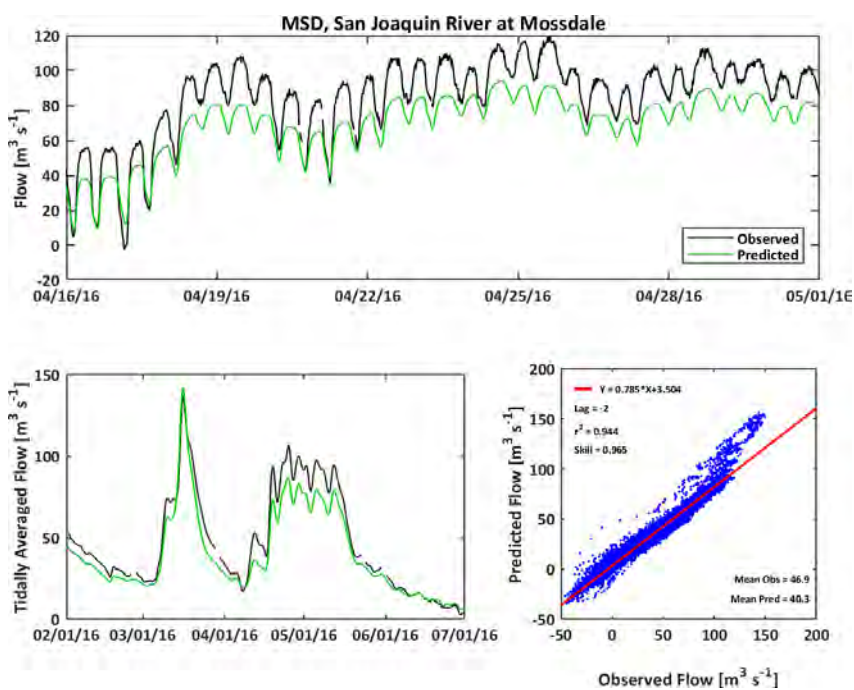


**Figure C-66**

**Target Diagrams Showing the Model Validation Using the Time Series Salinity for the Six Years**

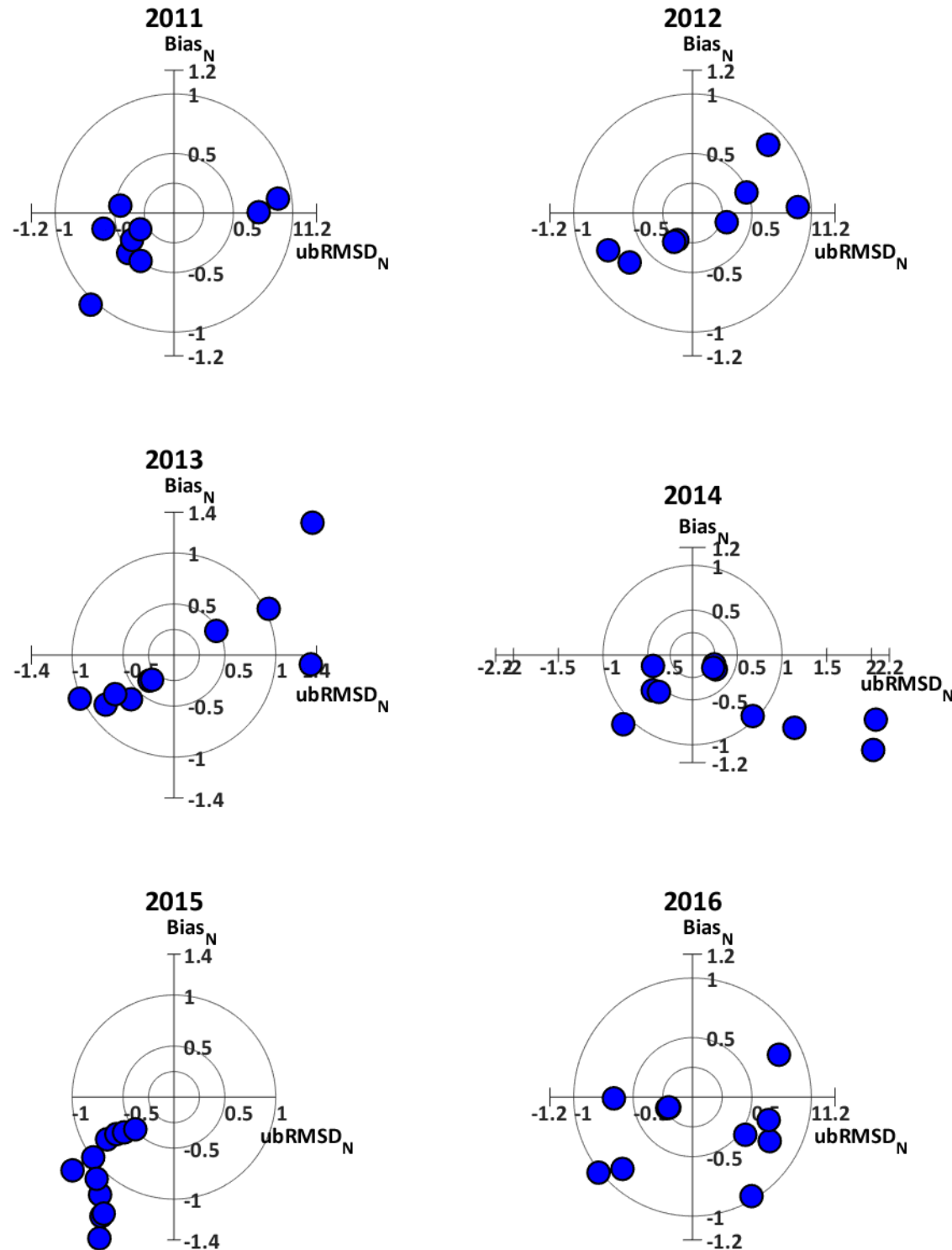


**Figure C-67**

**Observed and Predicted Salinity at Sacramento River at Rio Vista (SRV) During 2011**

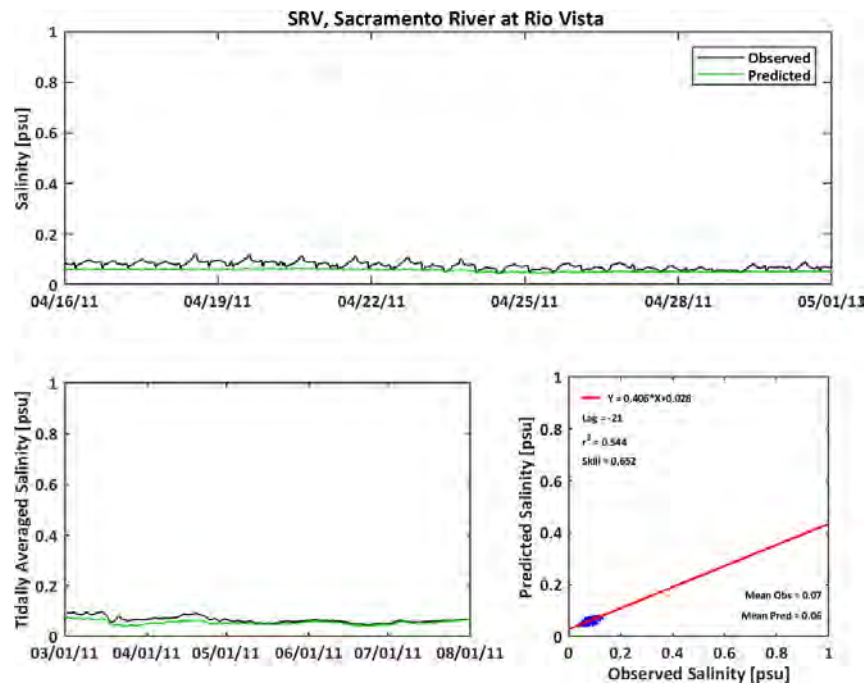


**Figure C-68**

**Observed and Predicted Salinity at San Joaquin River at Jersey Point (SJJ) During 2011**

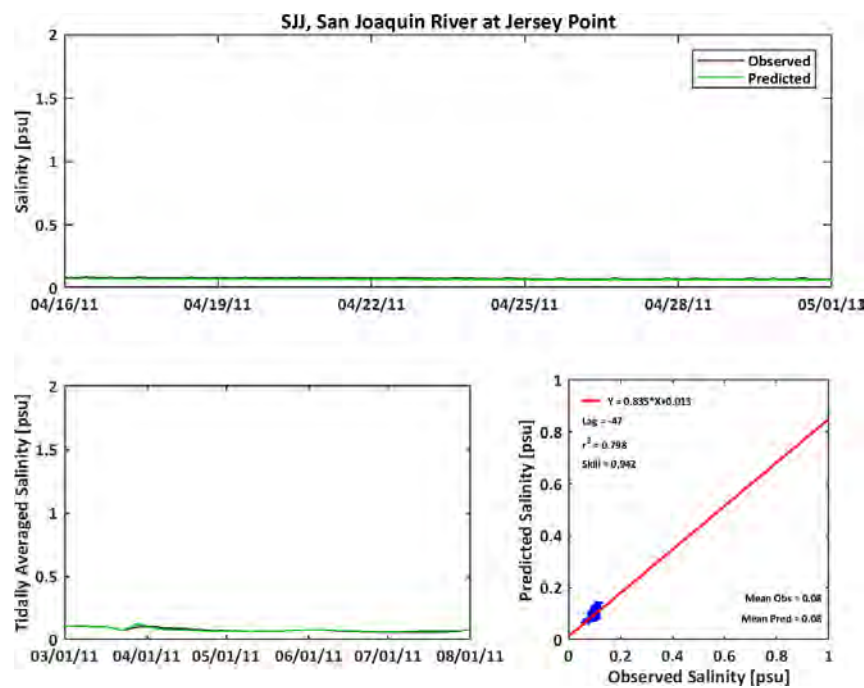


**Figure C-69**  
**Observed and Predicted Salinity at Turner Cut near Holt (TRN) During 2011**

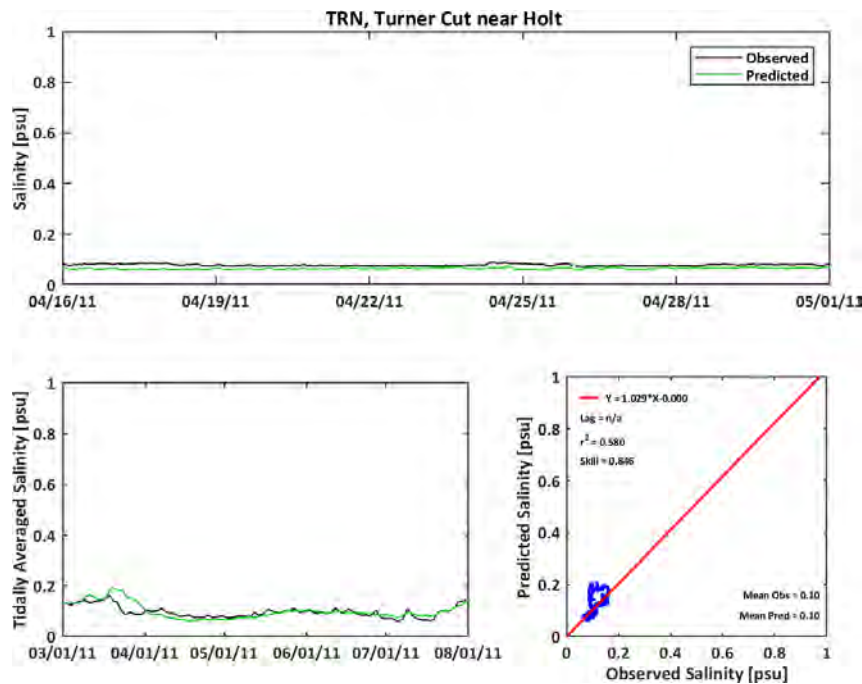


**Figure C-70**  
**Observed and Predicted Salinity at Old River at Bacon Island (OBI) During 2011**

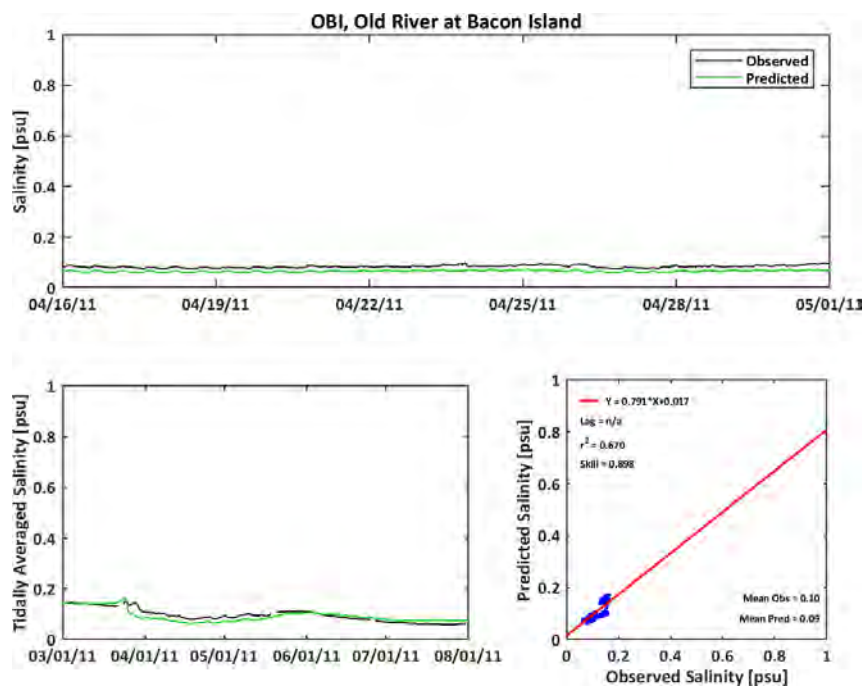


**Figure C-71**

**Observed and Predicted Salinity at Middle River at Middle River (MDM) During 2011**

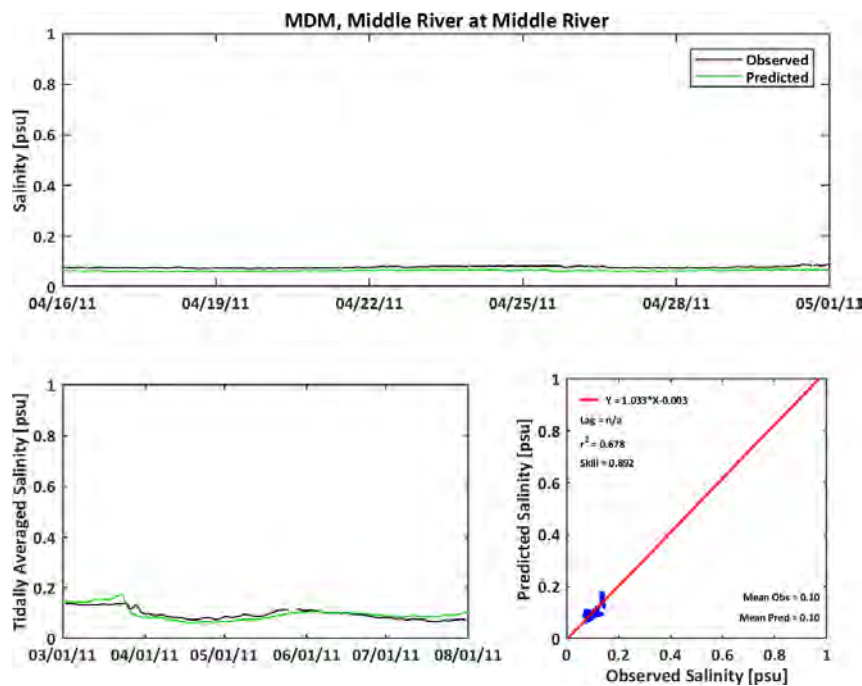


**Figure C-72**

**Observed and Predicted Salinity at Victoria Canal near Byron (VCU) During 2011**

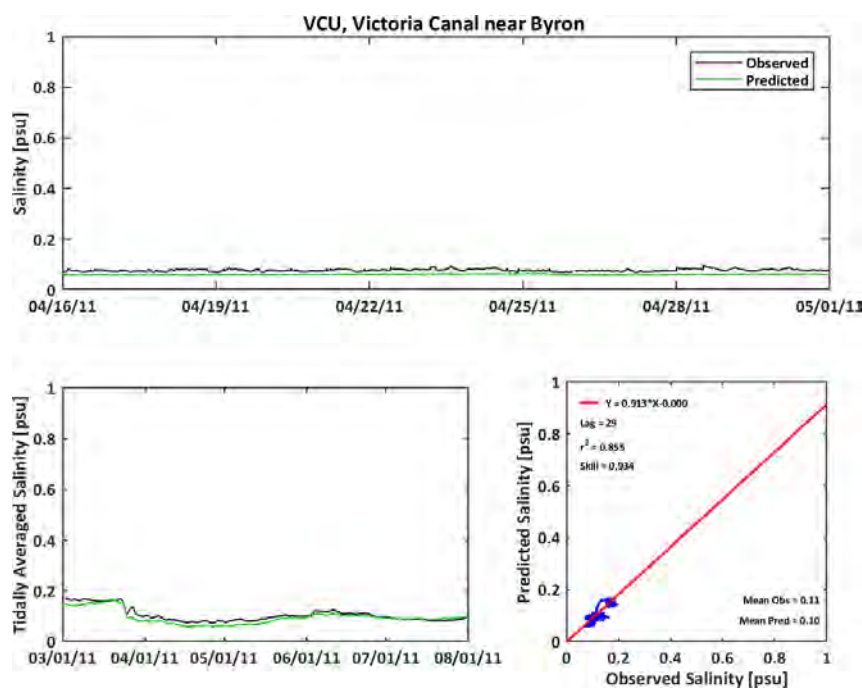


**Figure C-73**

**Observed and Predicted Salinity at Grant Line Canal near Clifton Court Ferry (GLC) During 2011**

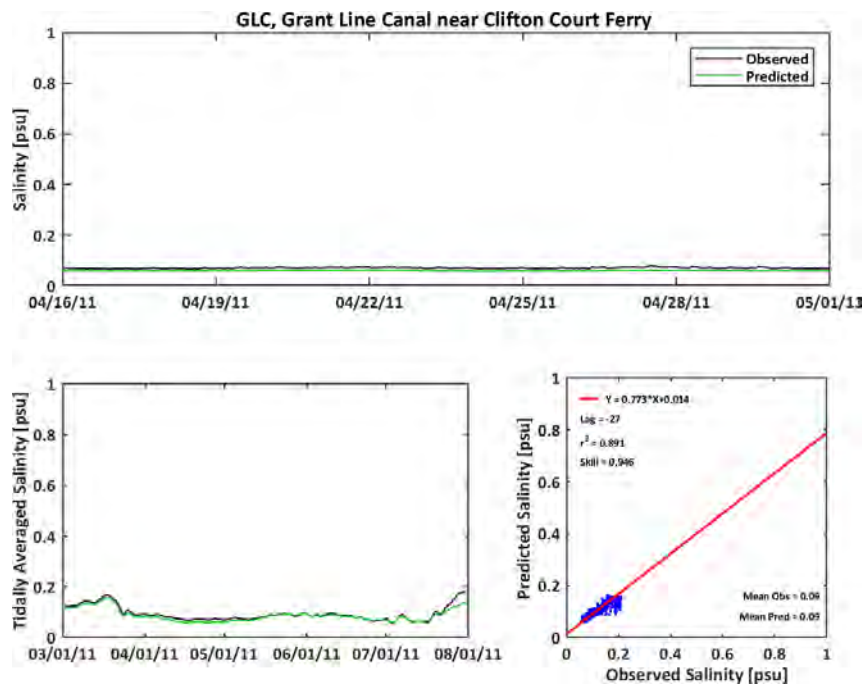


**Figure C-74**

**Observed and Predicted Salinity at San Joaquin River below Old River near Lathrop (SJL) During 2011**

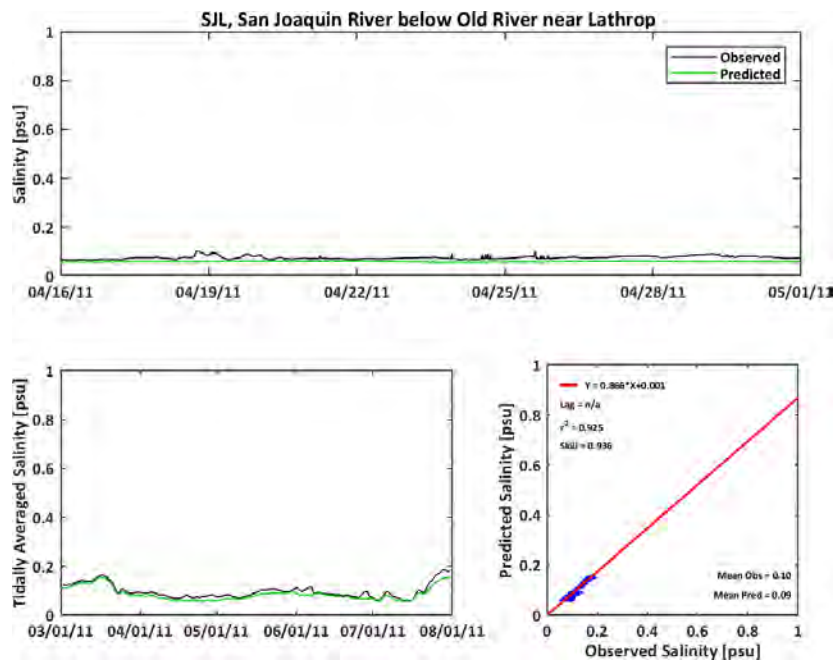


**Figure C-75**

**Observed and Predicted Salinity at San Joaquin River at Mossdale (MSD) During 2011**

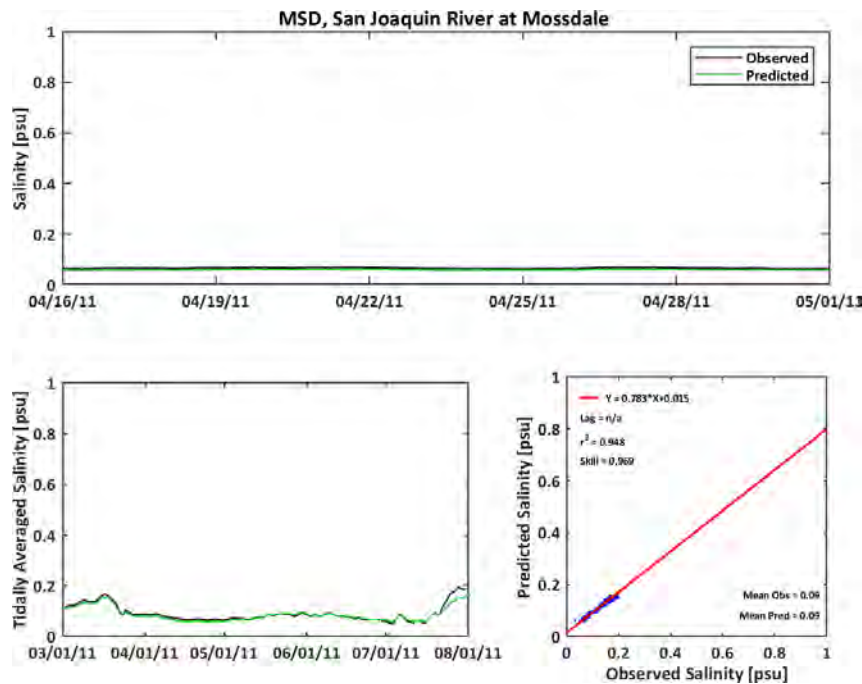


**Figure C-76**

**Observed and Predicted Salinity at Sacramento River at Rio Vista (SRV) During 2012**

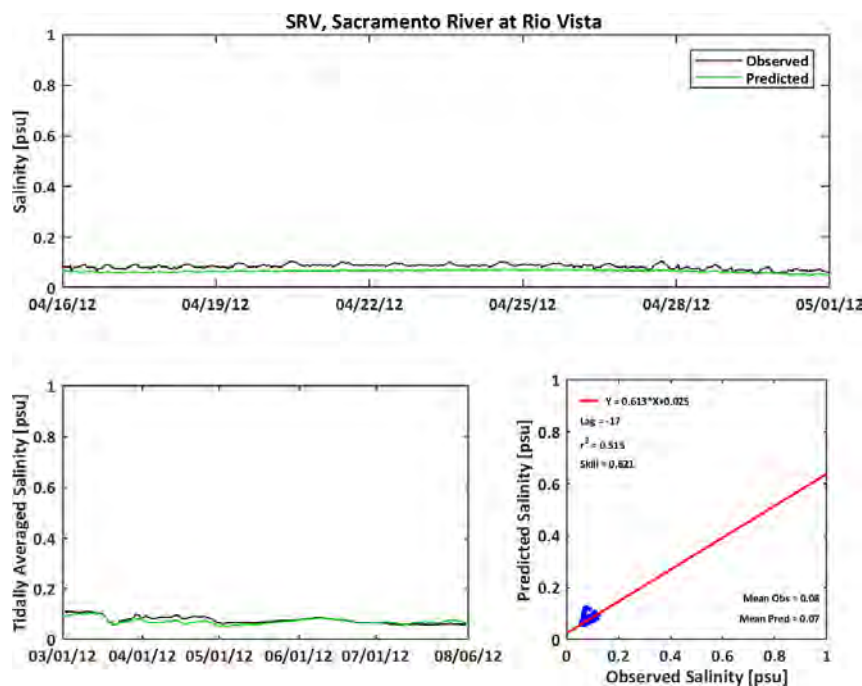


**Figure C-77**  
**Observed and Predicted Salinity at Turner Cut near Holt (TRN) During 2012**

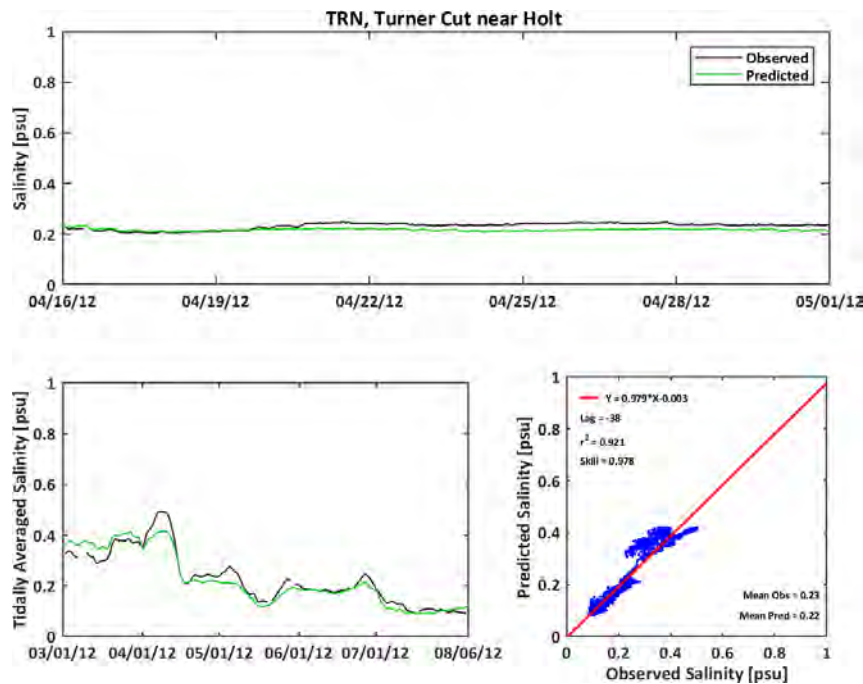


**Figure C-78**  
**Observed and Predicted Salinity at Old River at Bacon Island (OBI) During 2012**

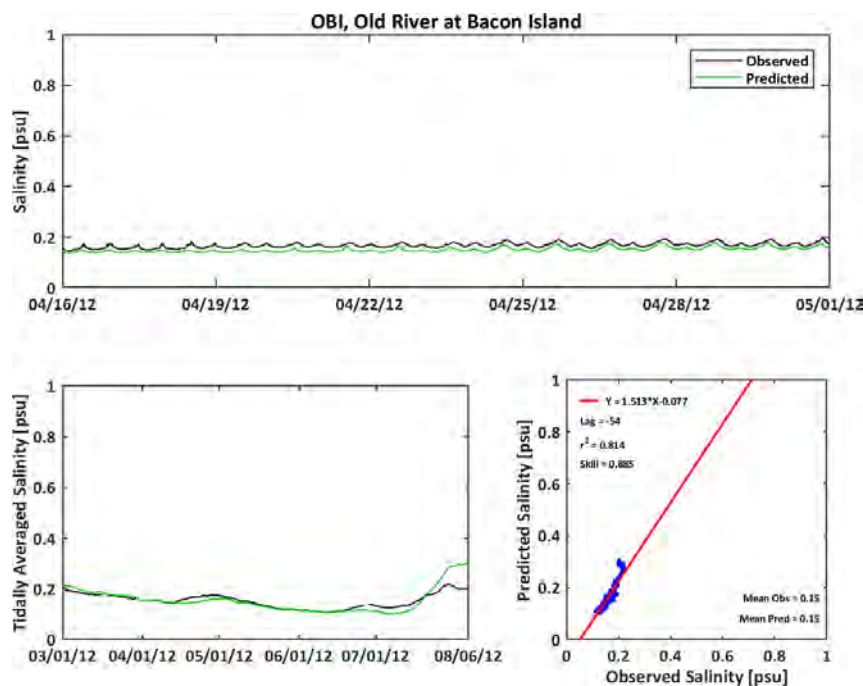


**Figure C-79**

**Observed and Predicted Salinity at Middle River at Middle River (MDM) During 2012**

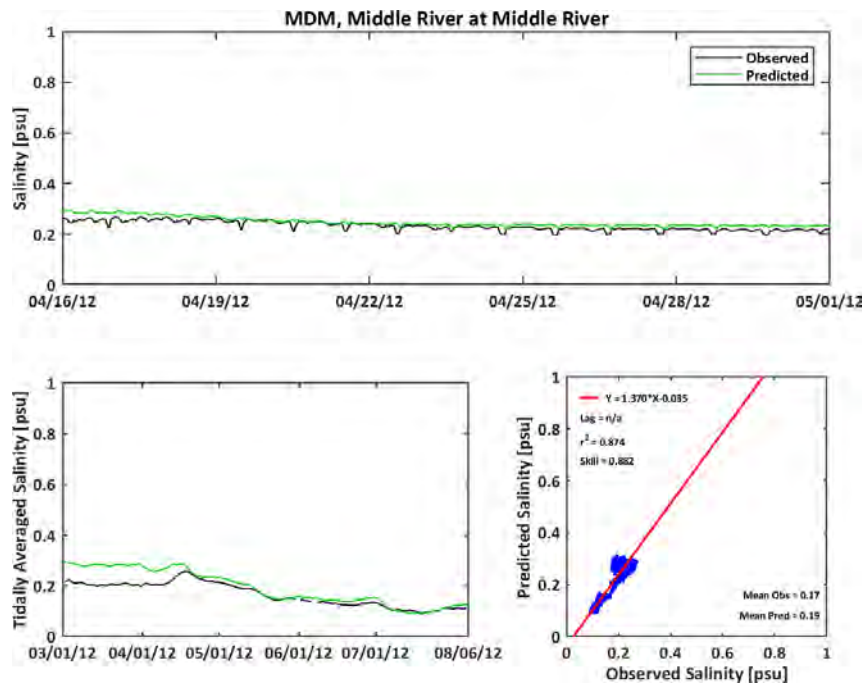


**Figure C-80**

**Observed and Predicted Salinity at Victoria Canal near Byron (VCU) During 2012**

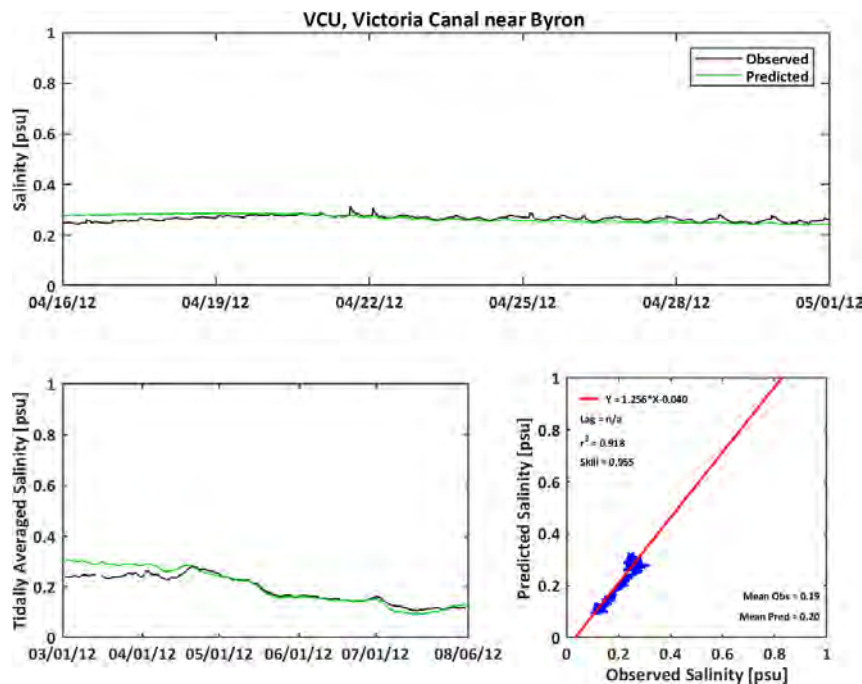


**Figure C-81**

**Observed and Predicted Salinity at Grant Line Canal near Clifton Court Ferry (GLC) During 2012**

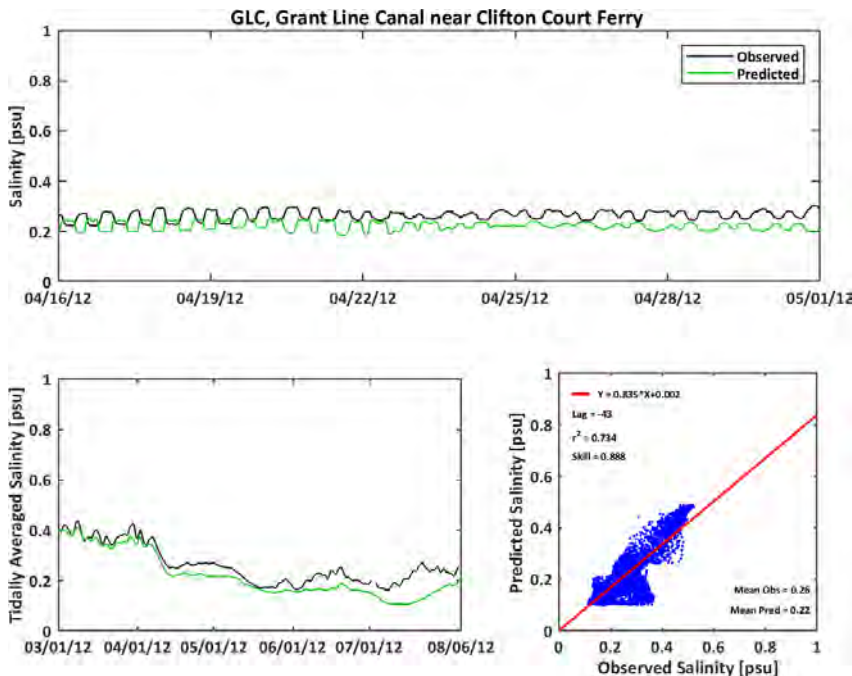


**Figure C-82**

**Observed and Predicted Salinity at San Joaquin River below Old River near Lathrop (SJL) During 2012**

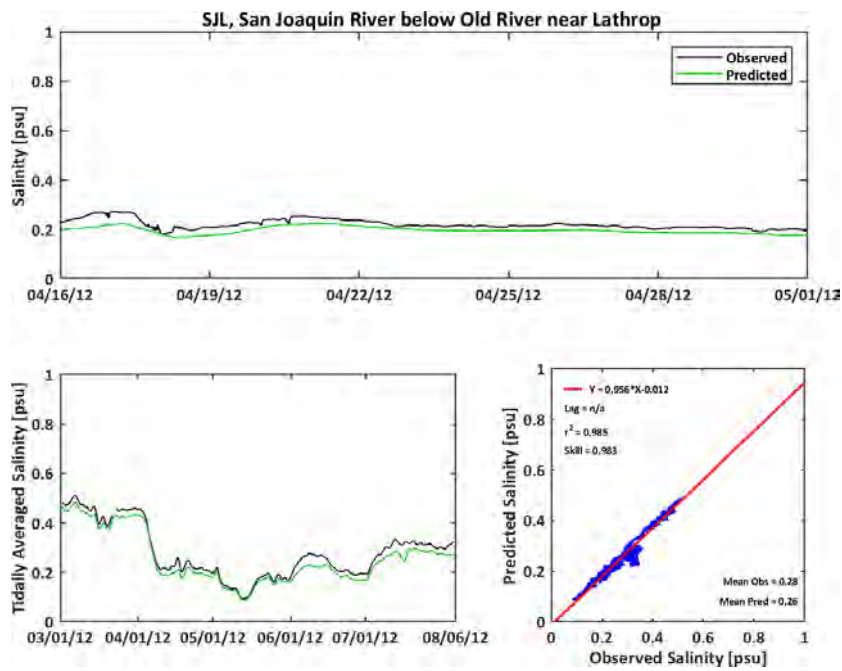


**Figure C-83**

**Observed and Predicted Salinity at San Joaquin River at Mossdale (MSD) During 2012**

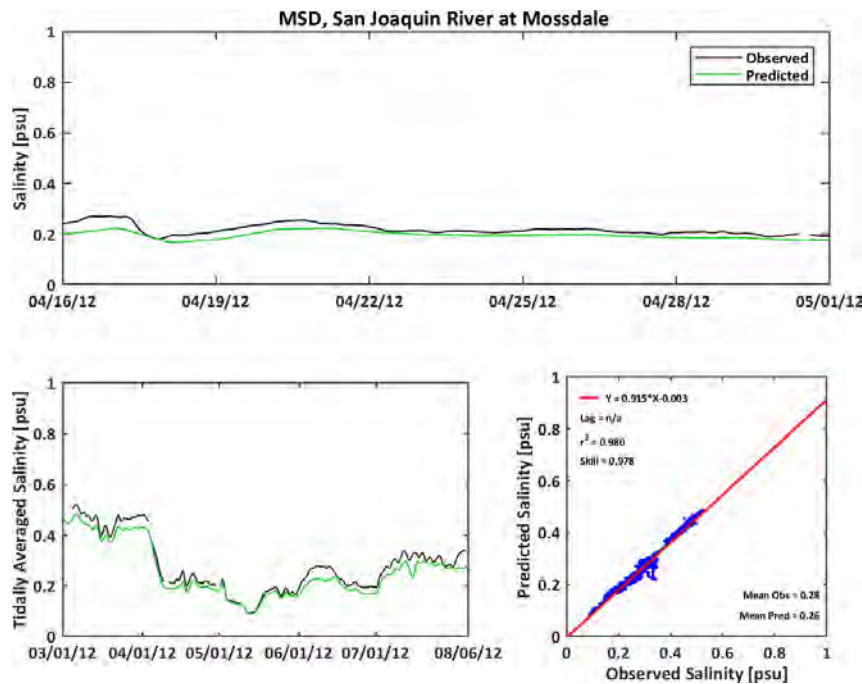


**Figure C-84**

**Observed and Predicted Salinity at Sacramento River at Rio Vista (SRV) During 2013**

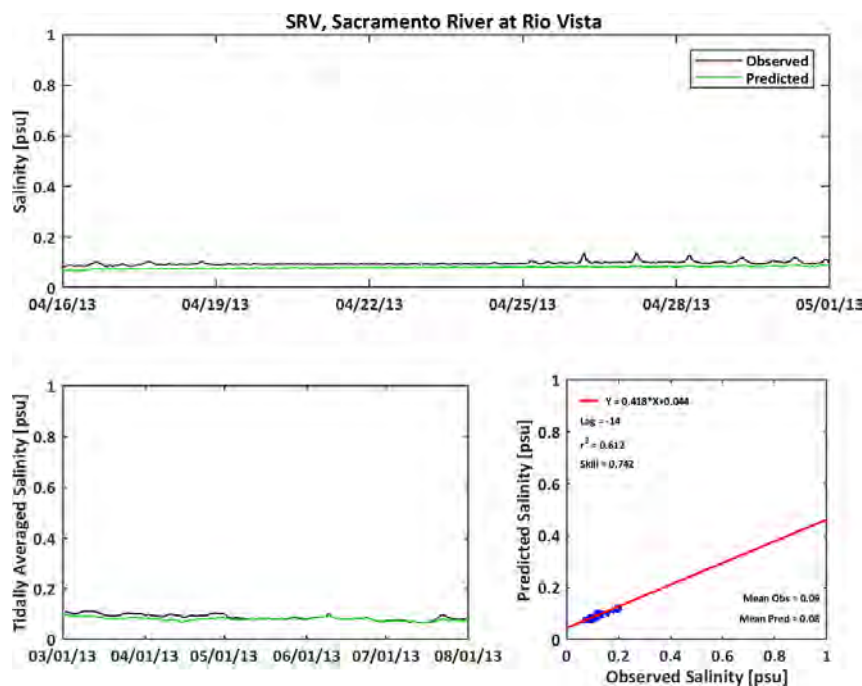


**Figure C-85**

**Observed and Predicted Salinity at San Joaquin River at Jersey Point (SJJ) During 2013**

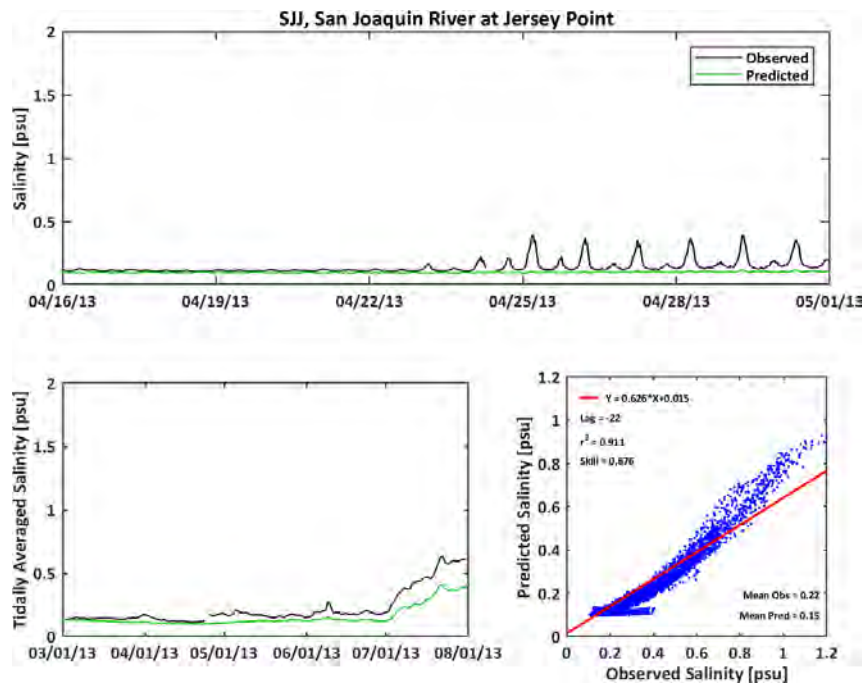


**Figure C-86**

**Observed and Predicted Salinity at Turner Cut near Holt (TRN) During 2013**

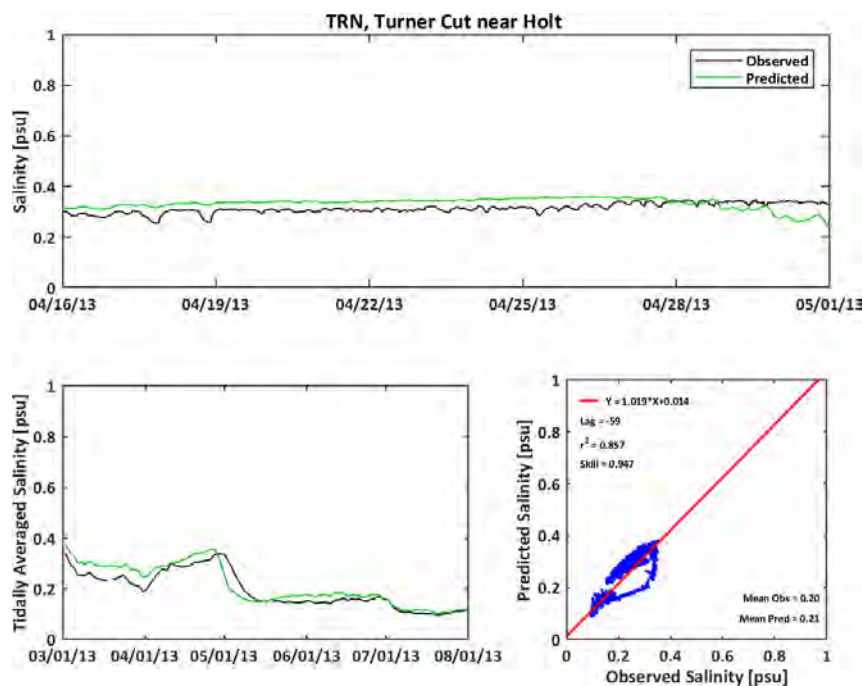


**Figure C-87**  
**Observed and Predicted Salinity at Old River at Bacon Island (OBI) During 2013**

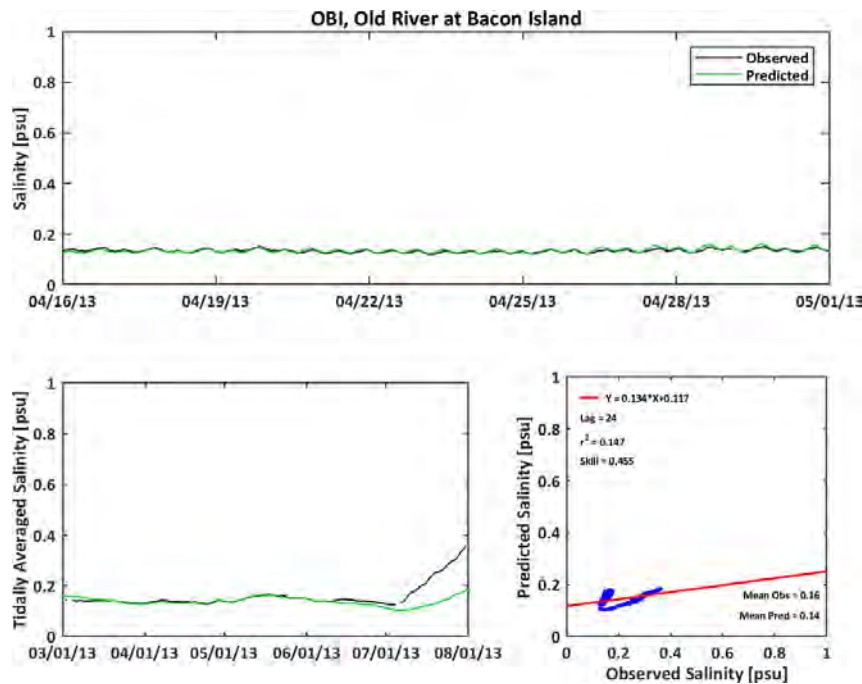


**Figure C-88**  
**Observed and Predicted Salinity at Middle River at Middle River (MDM) During 2013**

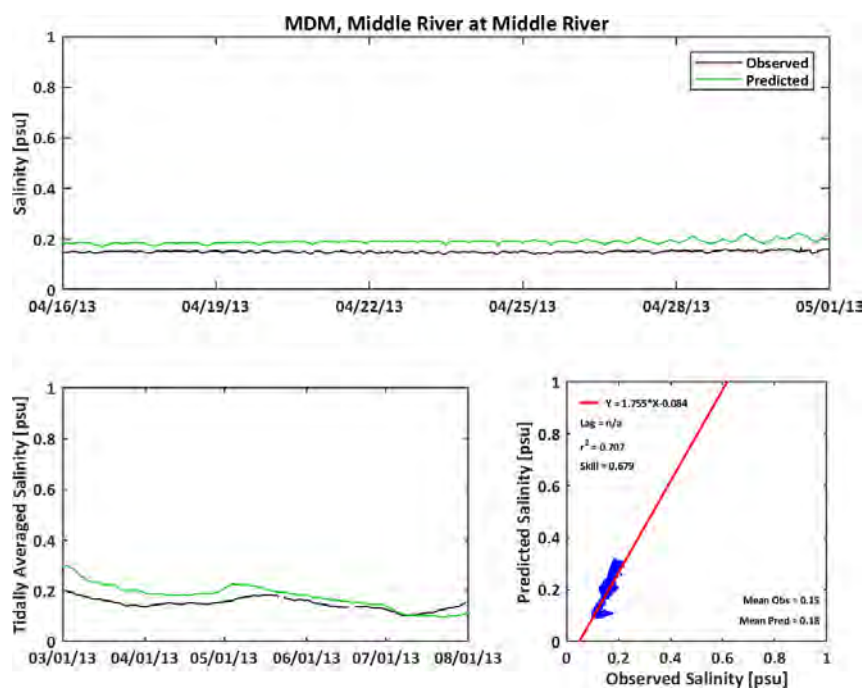


**Figure C-89**

**Observed and Predicted Salinity at Old River at Highway 4 (OH4) During 2013**

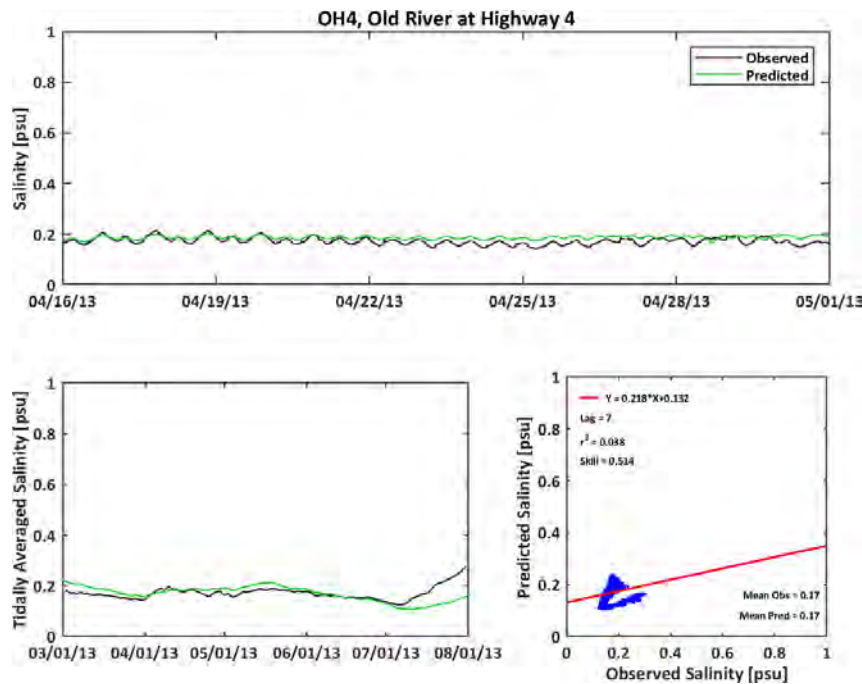


**Figure C-90**

**Observed and Predicted Salinity at Victoria Canal near Byron (VCU) During 2013**

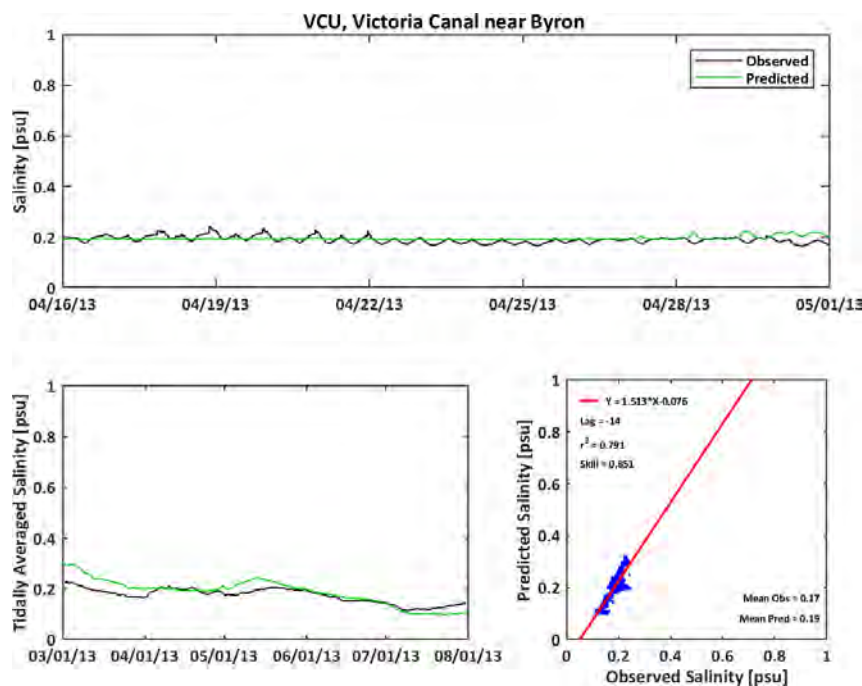


**Figure C-91**

**Observed and Predicted Salinity at Grant Line Canal near Clifton Court Ferry (GLC) During 2013**

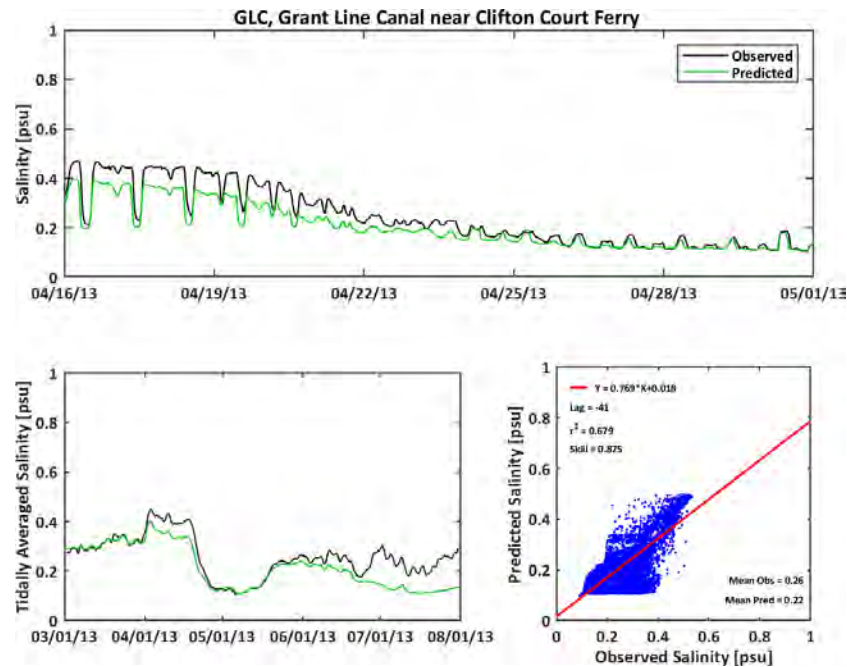


**Figure C-92**

**Observed and Predicted Salinity at San Joaquin River below Old River near Lathrop (SJI) During 2013**

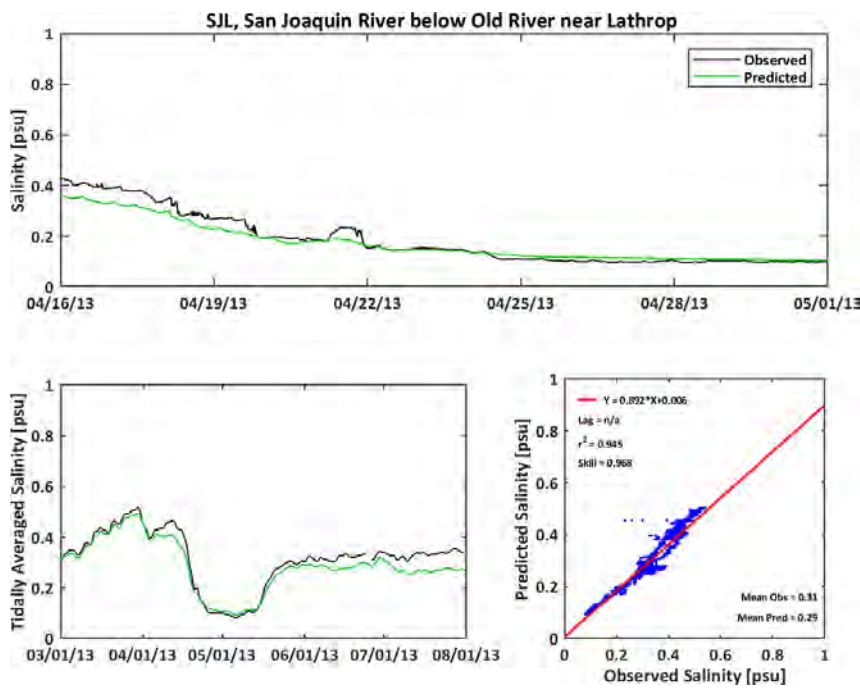


**Figure C-93**

**Observed and Predicted Salinity at San Joaquin River at Mossdale (MSD) During 2013**

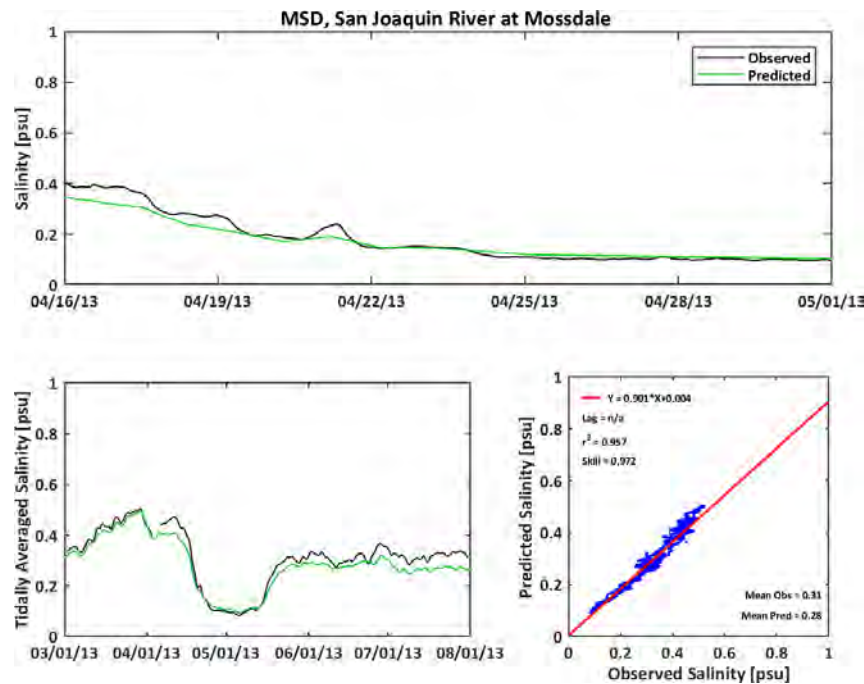


**Figure C-94**

**Observed and Predicted Salinity at Sacramento River at Rio Vista (SRV) During 2014**

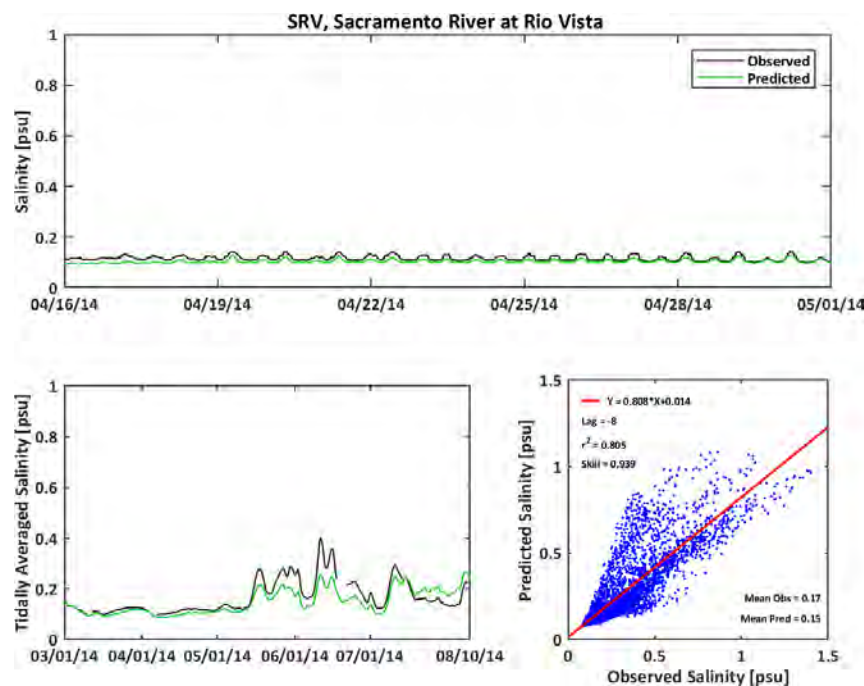


**Figure C-95**

**Observed and Predicted Salinity at San Joaquin River at Jersey Point (SJJ) During 2014**

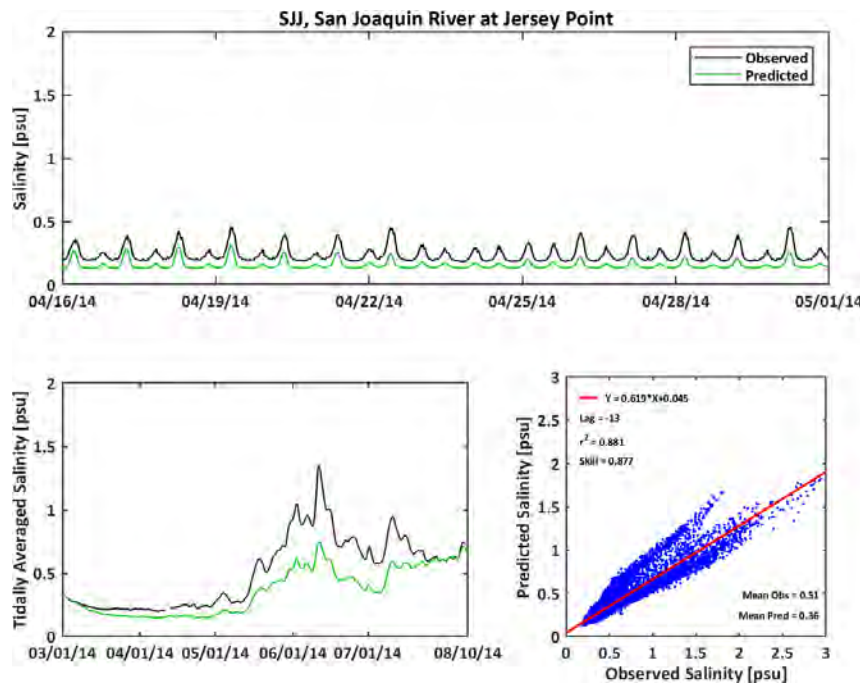


**Figure C-96**

**Observed and Predicted Salinity at Turner Cut near Holt (TRN) During 2014**

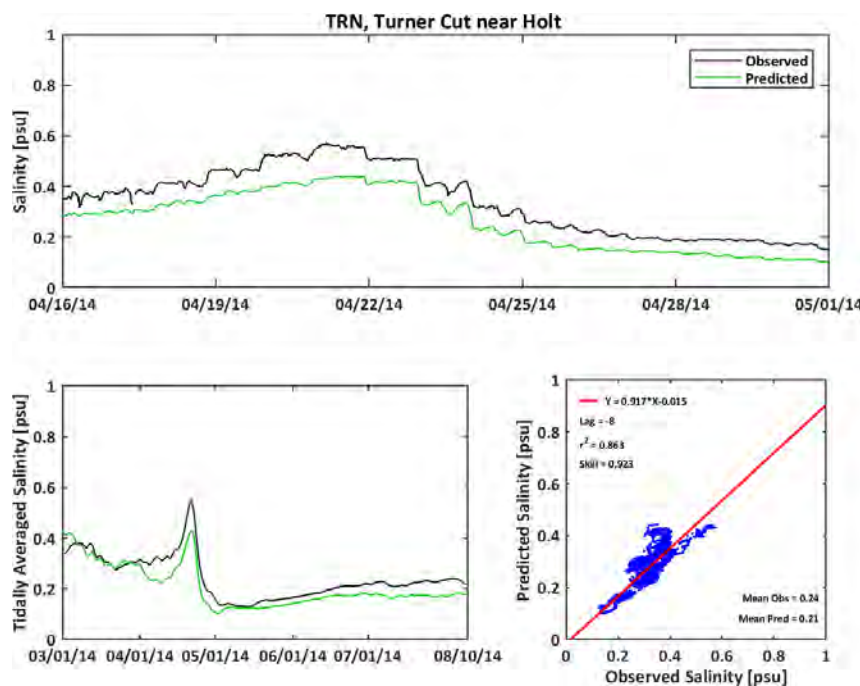


**Figure C-97**  
**Observed and Predicted Salinity at Old River at Bacon Island (OBI) During 2014**

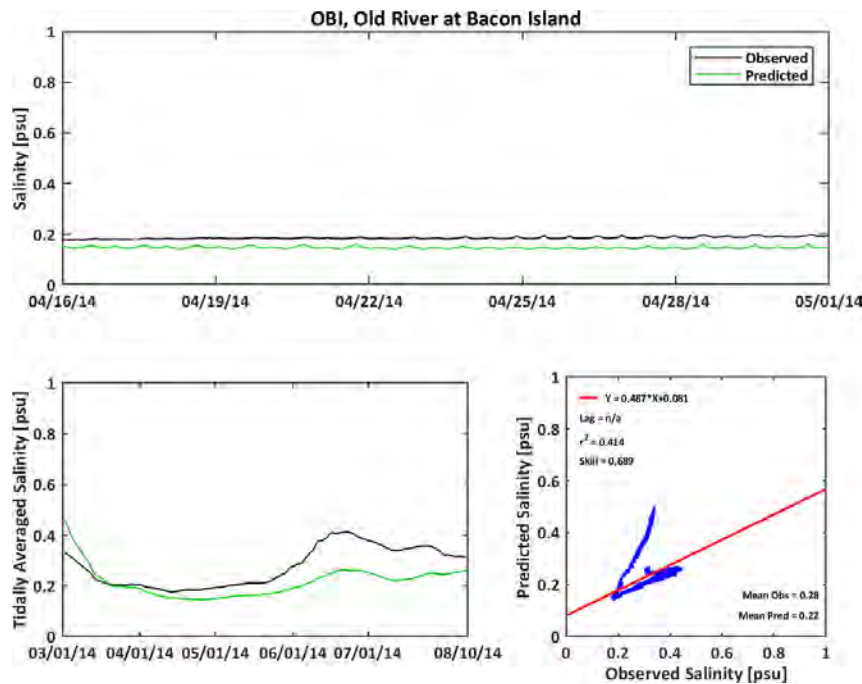


**Figure C-98**  
**Observed and Predicted Salinity at Middle River at Middle River (MDM) During 2014**

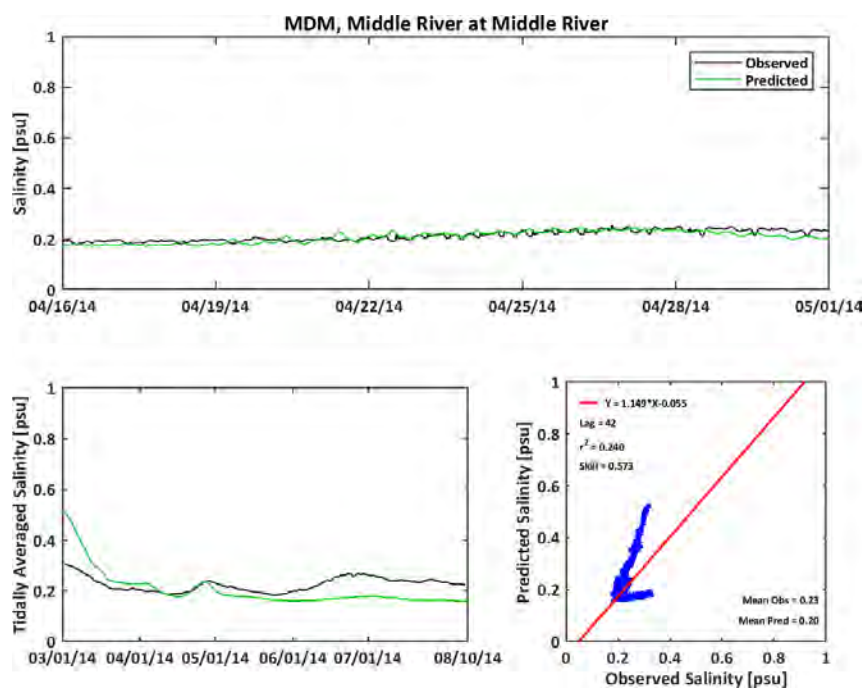


**Figure C-99**  
**Observed and Predicted Salinity at Old River at Highway 4 (OH4) During 2014**

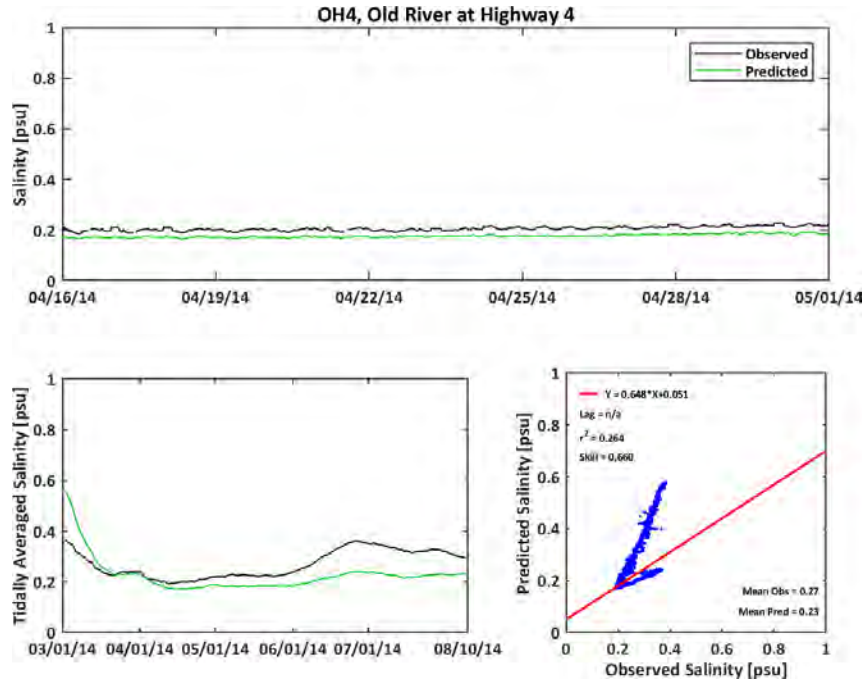


**Figure C-100**  
**Observed and Predicted Salinity at Victoria Canal near Byron (VCU) During 2014**

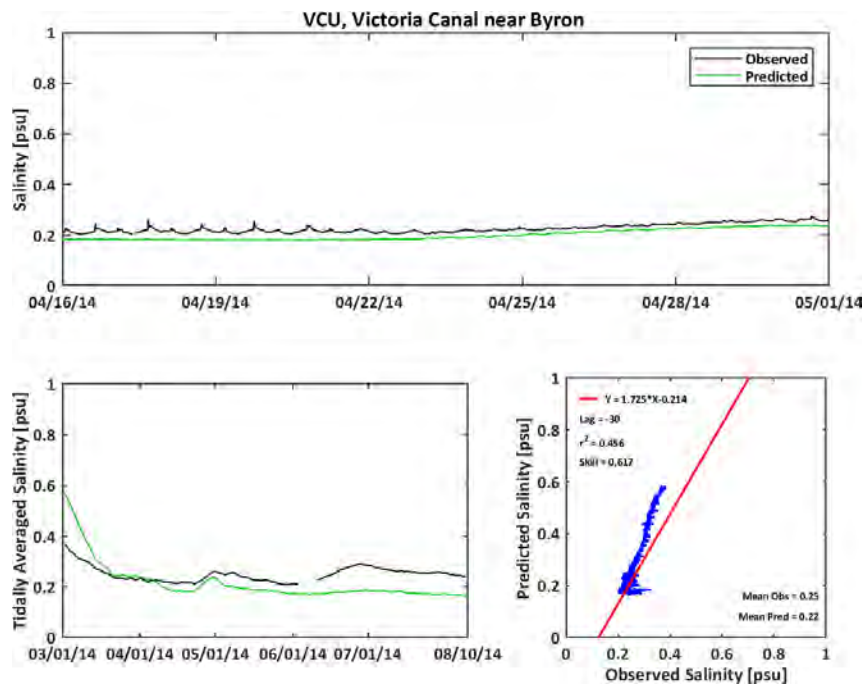


**Figure C-101**

**Observed and Predicted Salinity at Grant Line Canal near Clifton Court Ferry (GLC) During 2014**

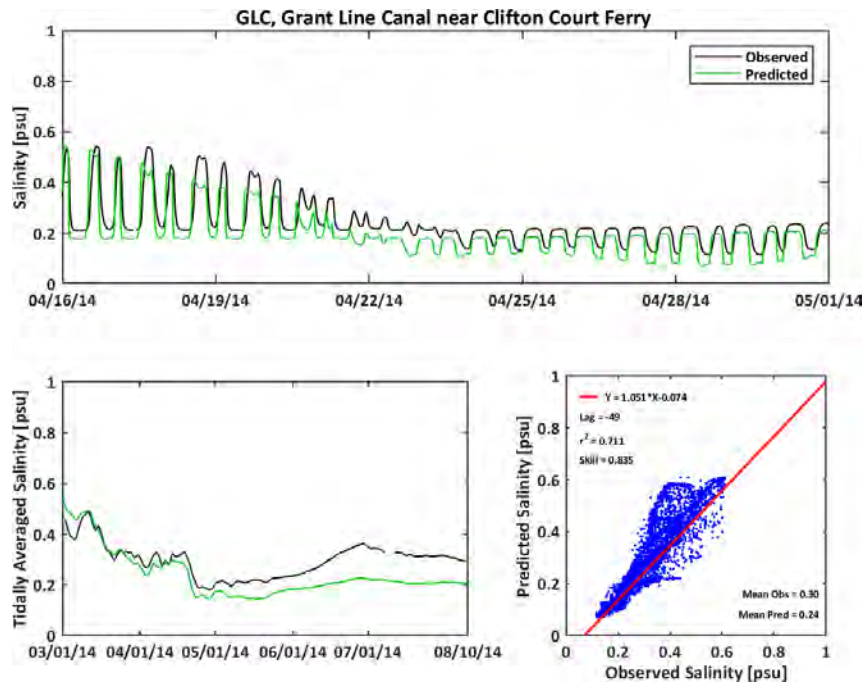


**Figure C-102**

**Observed and Predicted Salinity at Old River at Head (OH1) During 2014**

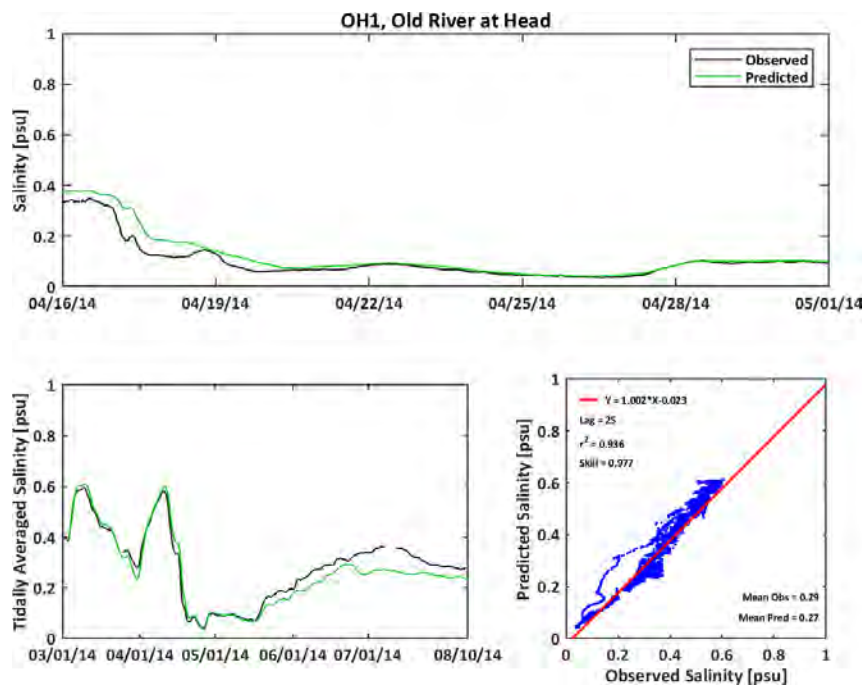


**Figure C-103**

**Observed and Predicted Salinity at San Joaquin River below Old River near Lathrop (SJL) During 2014**

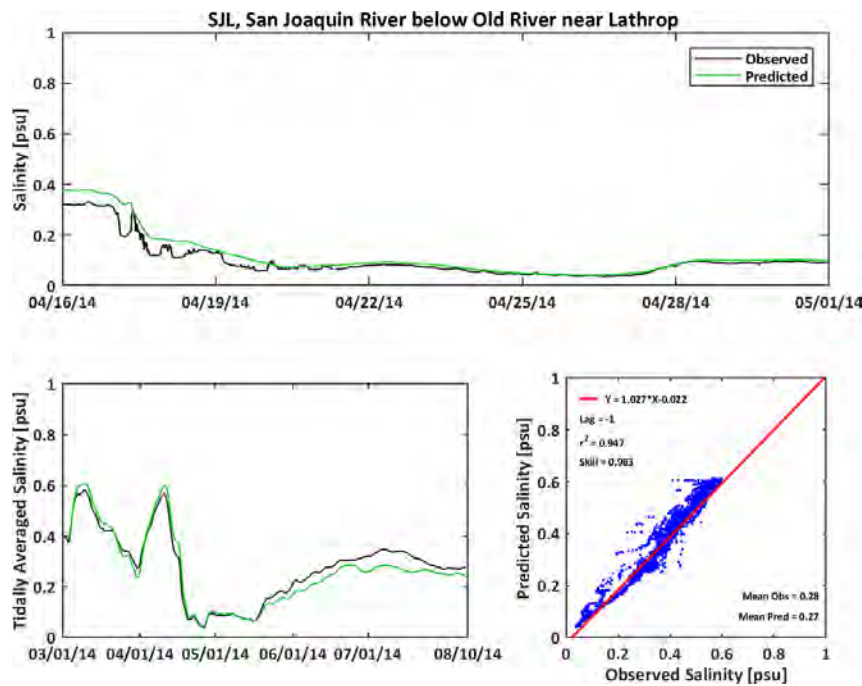


**Figure C-104**

**Observed and Predicted Salinity at San Joaquin River at Mossdale (MSD) During 2014**

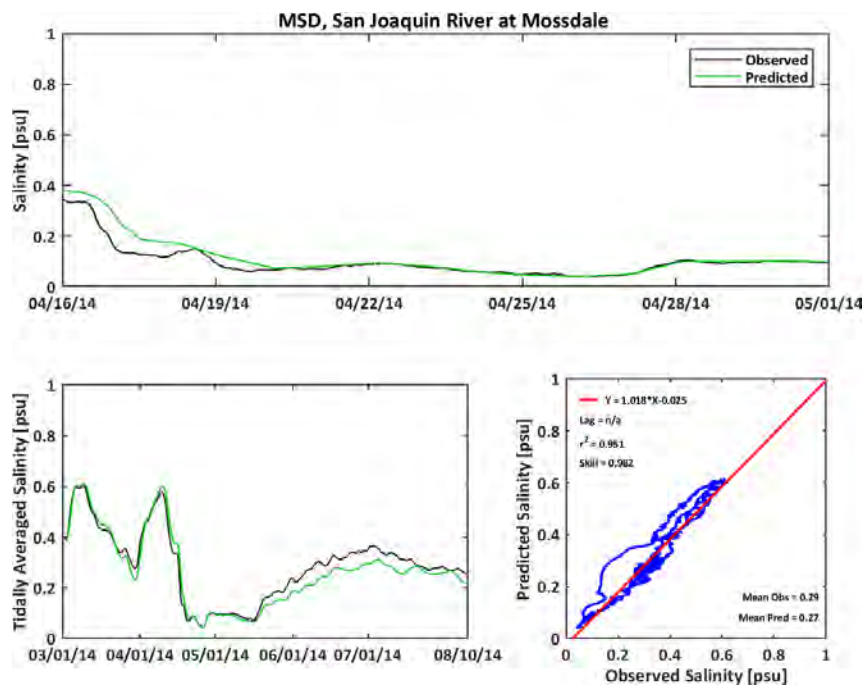


**Figure C-105**

**Observed and Predicted Salinity at Sacramento River at Rio Vista (SRV) During 2015**

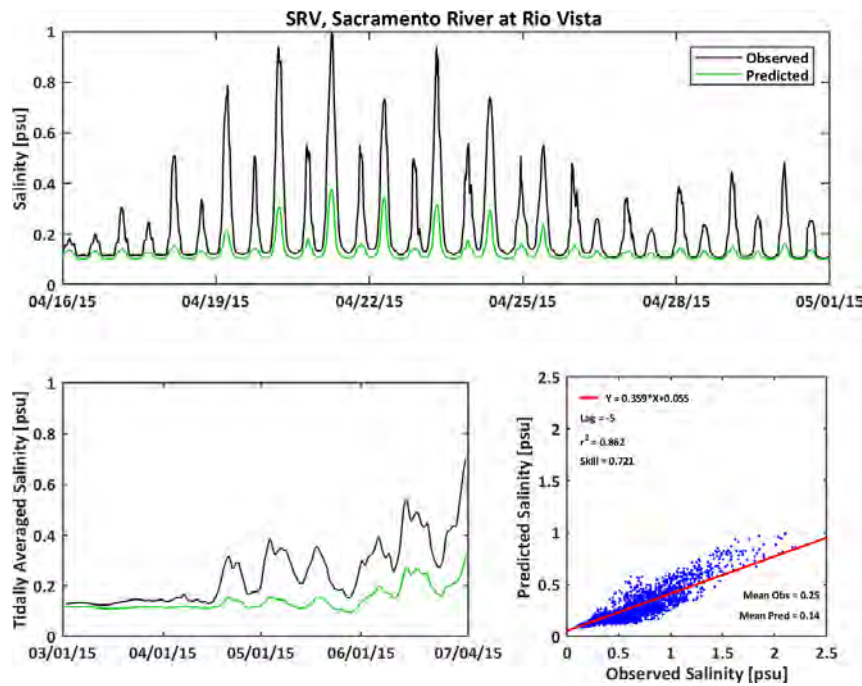


**Figure C-106**

**Observed and Predicted Salinity at San Joaquin River at Jersey Point (SJJ) During 2015**

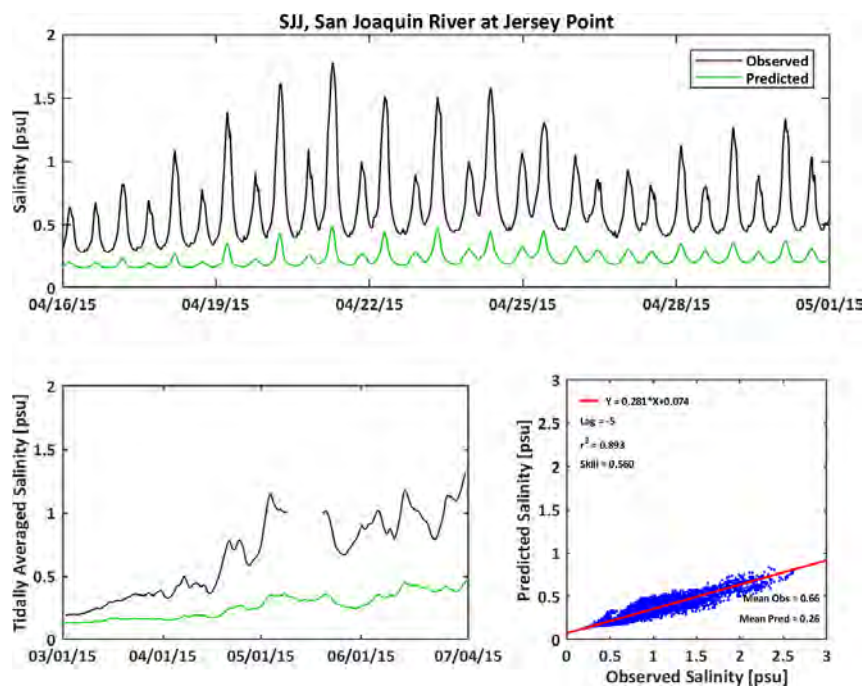


**Figure C-107**  
**Observed and Predicted Salinity at Turner Cut near Holt (TRN) During 2015**

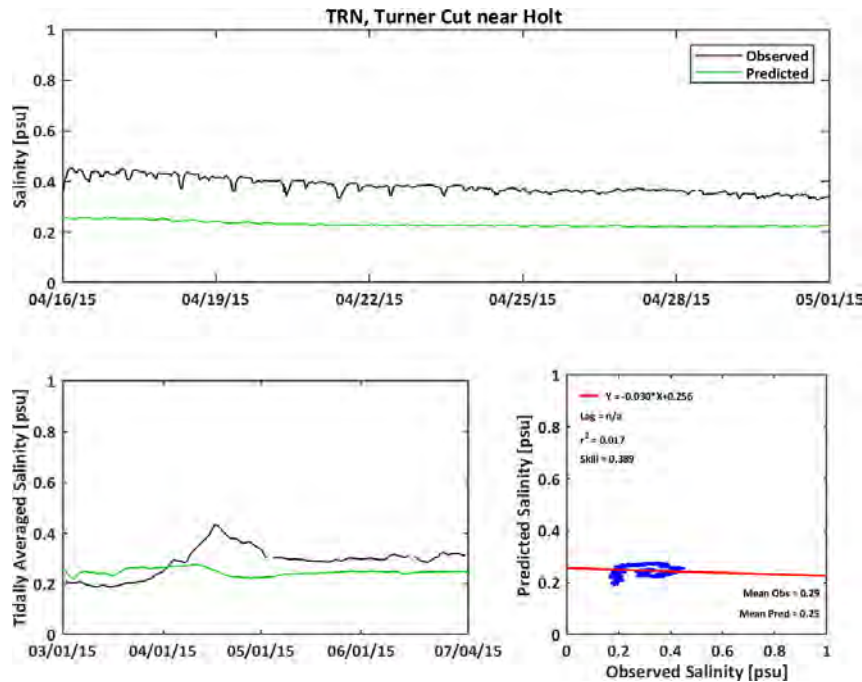


**Figure C-108**  
**Observed and Predicted Salinity at Old River at Bacon Island (OBI) During 2015**

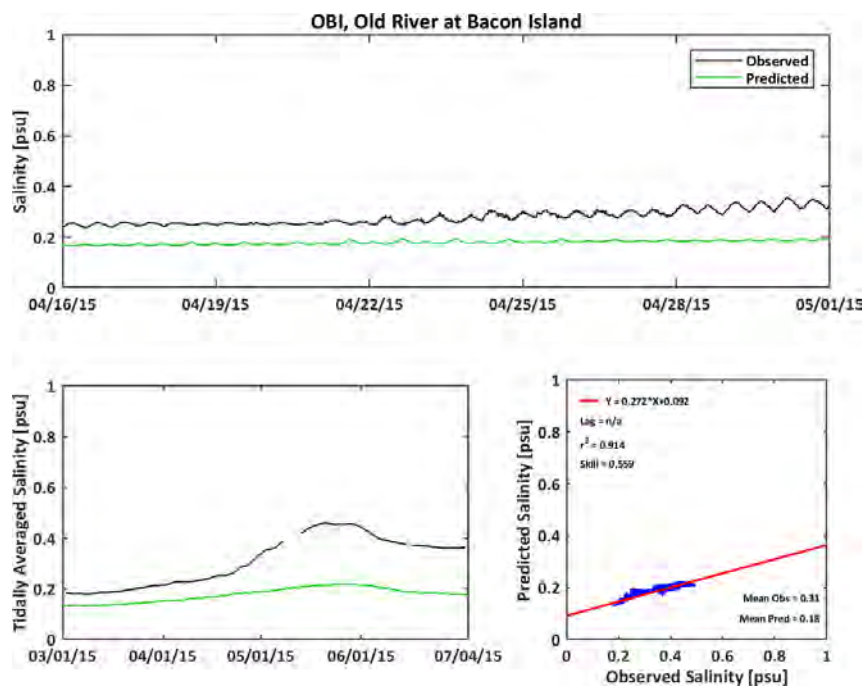


**Figure C-109**

**Observed and Predicted Salinity at Middle River at Middle River (MDM) During 2015**

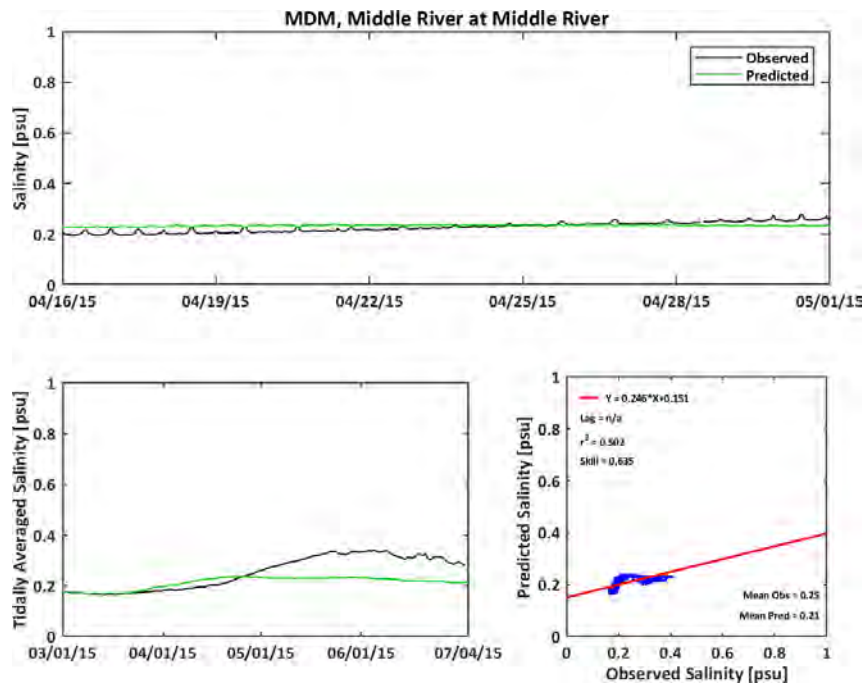


**Figure C-110**

**Observed and Predicted Salinity at Old River at Highway 4 (OH4) During 2015**

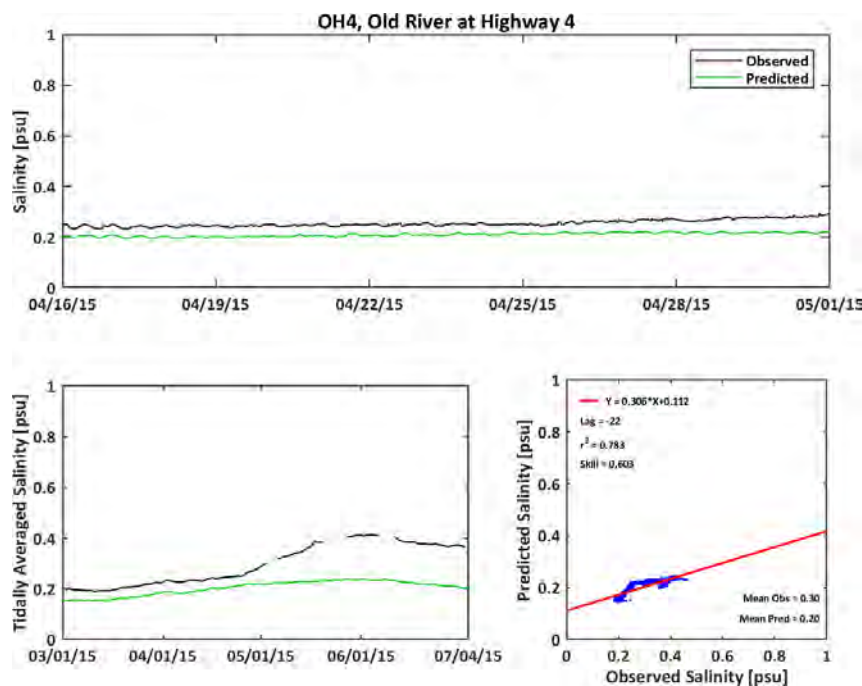


**Figure C-111**  
**Observed and Predicted Salinity at Victoria Canal near Byron (VCU) During 2015**

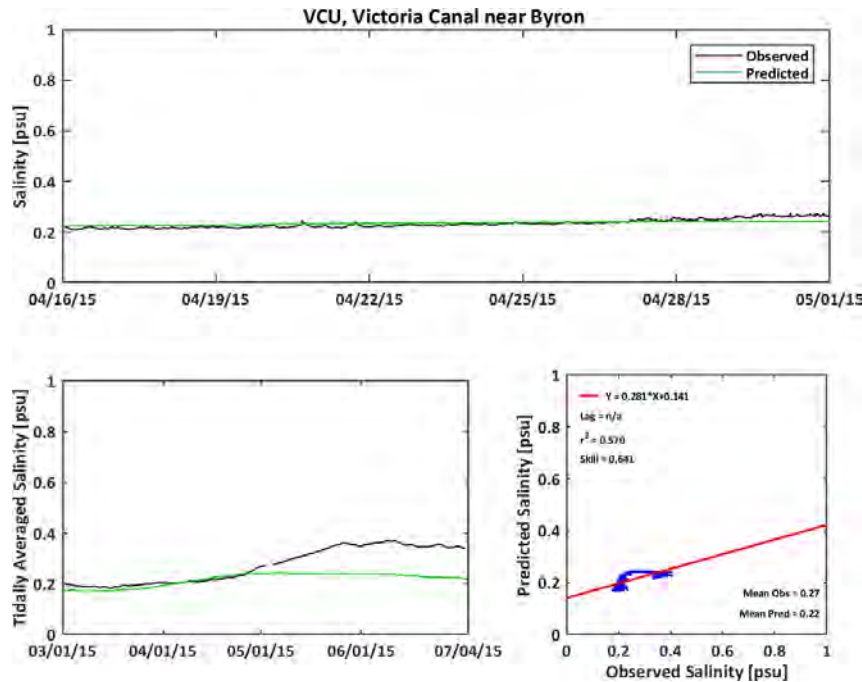


**Figure C-112**  
**Observed and Predicted Salinity at Grant Line Canal near Clifton Court Ferry (GLC) During 2015**

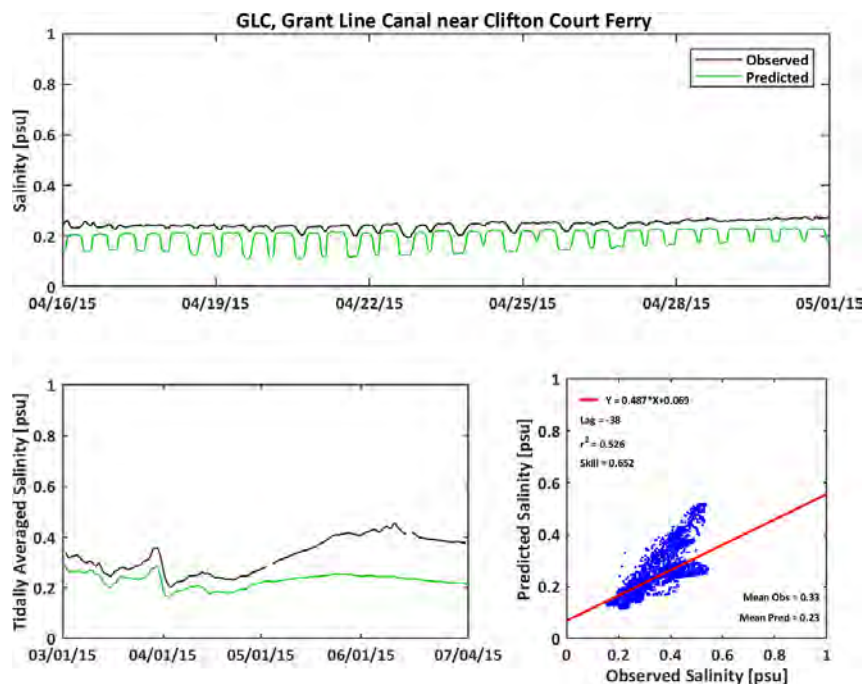


**Figure C-113**  
**Observed and Predicted Salinity at Old River at Head (OH1) During 2015**

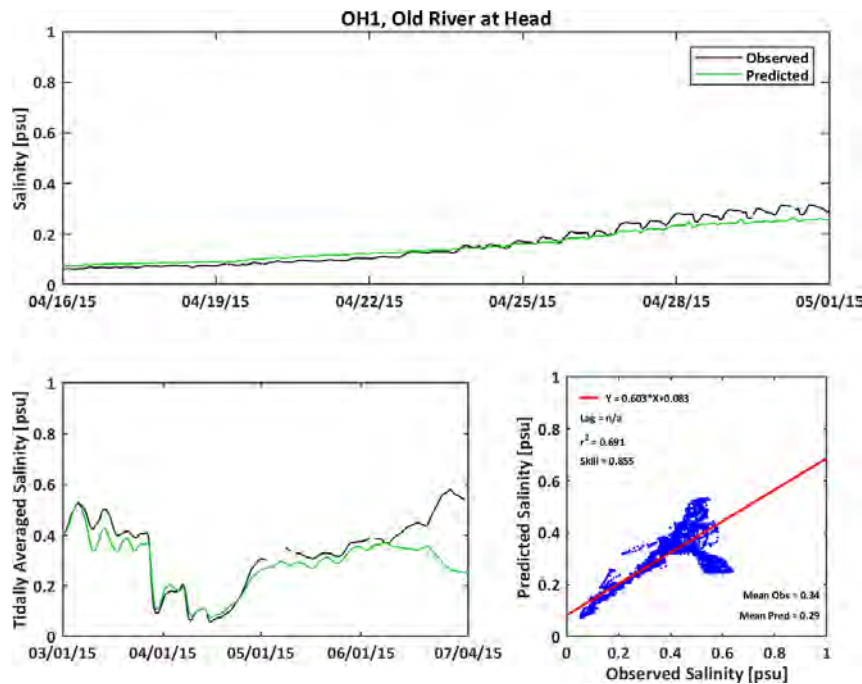


**Figure C-114**  
**Observed and Predicted Salinity at San Joaquin River below Old River near Lathrop (SJL)**  
**During 2015**

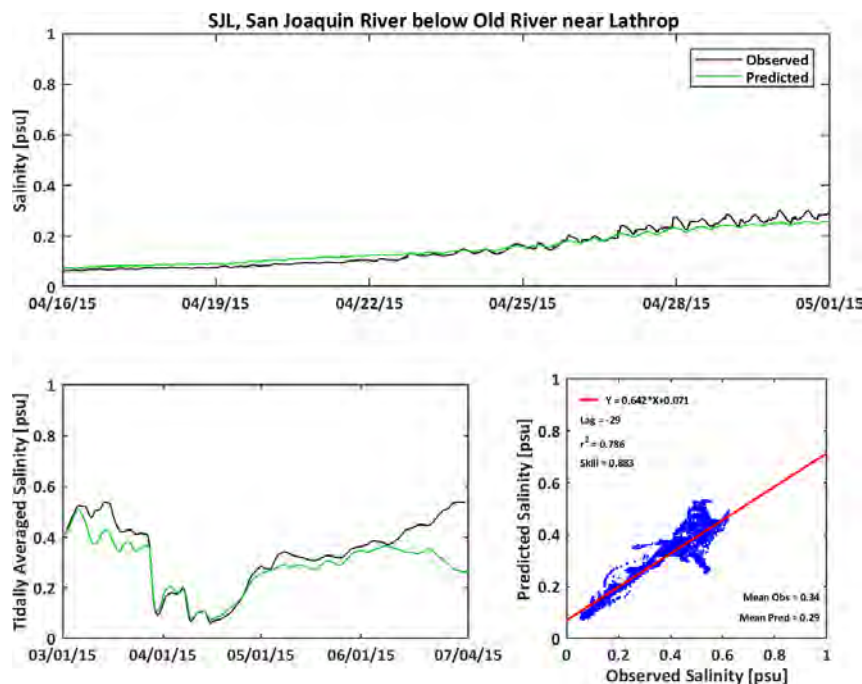


**Figure C-115**

**Observed and Predicted Salinity at San Joaquin River at Mossdale (MSD) During 2015**

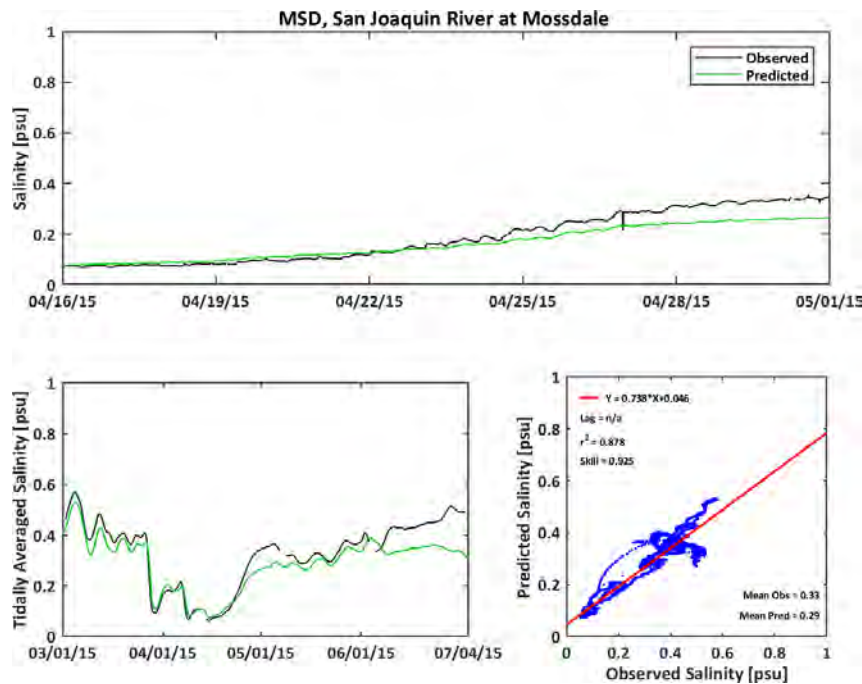


**Figure C-116**

**Observed and Predicted Salinity at Sacramento River at Rio Vista (SRV) During 2016**

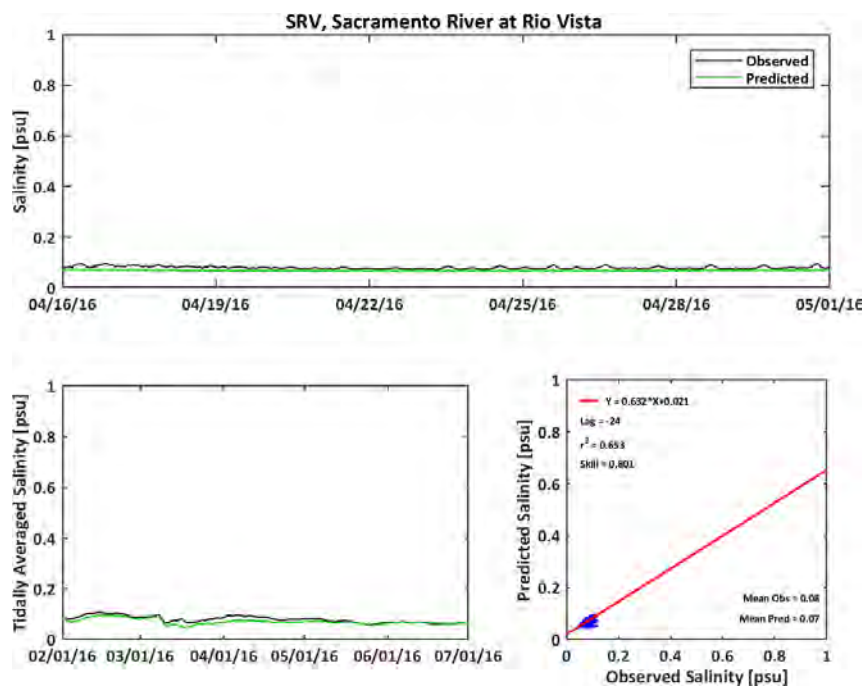


**Figure C-117**

**Observed and Predicted Salinity at San Joaquin River at Jersey Point (SJJ) During 2016**

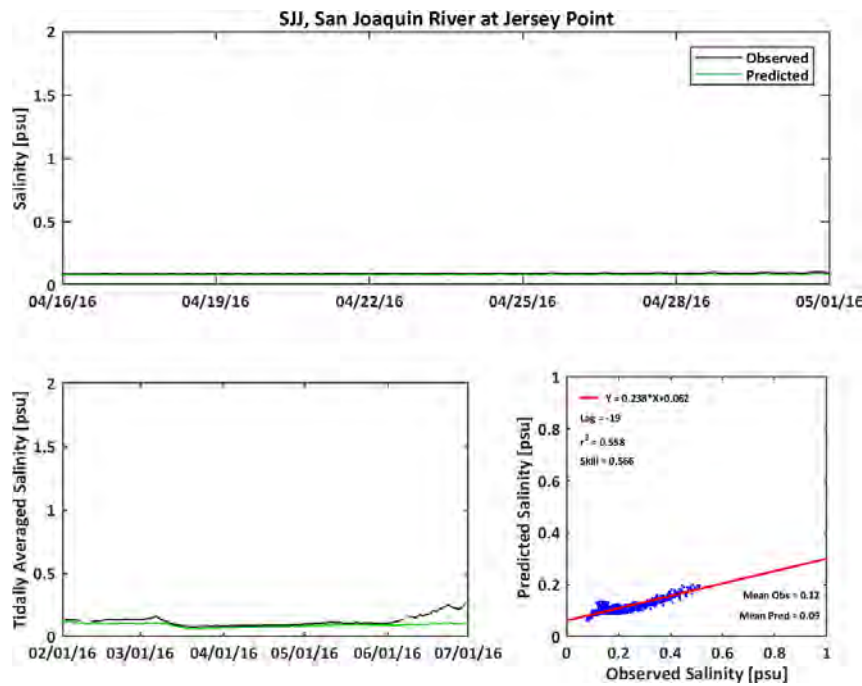


**Figure C-118**

**Observed and Predicted Salinity at Turner Cut near Holt (TRN) During 2016**

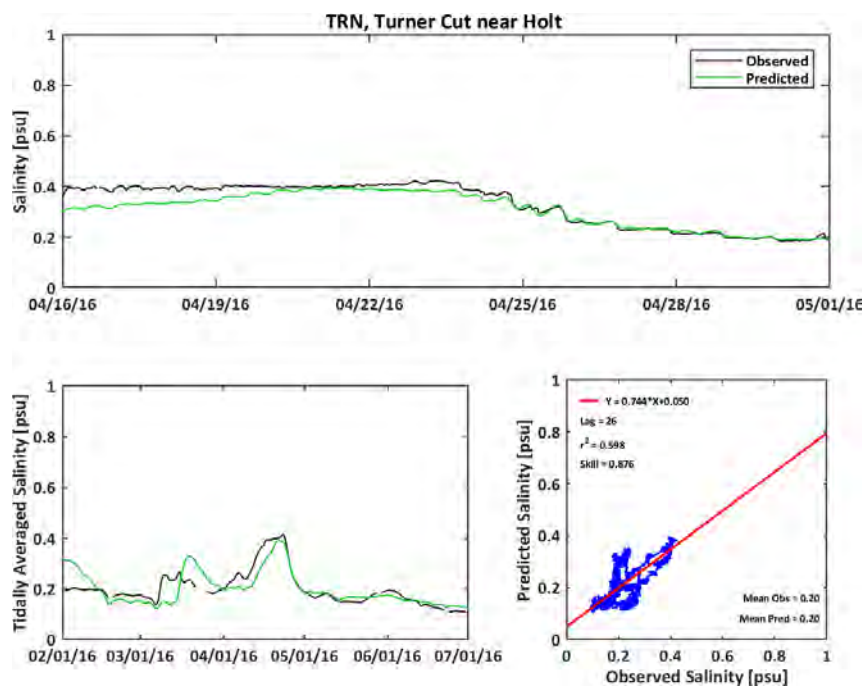


**Figure C-119**

**Observed and Predicted Salinity at Old River at Bacon Island (OBI) During 2016**

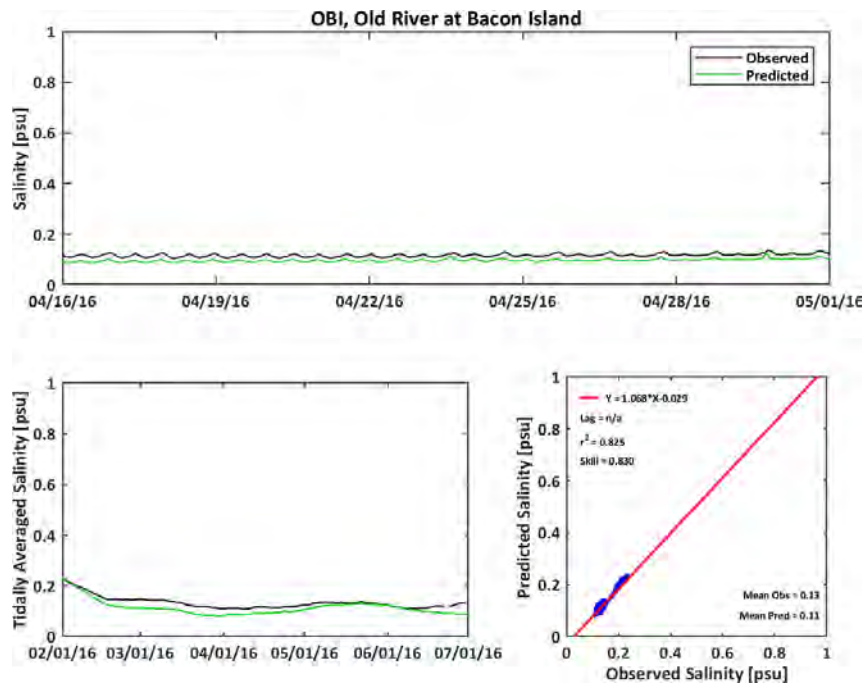


**Figure C-120**

**Observed and Predicted Salinity at Middle River at Middle River (MDM) During 2016**

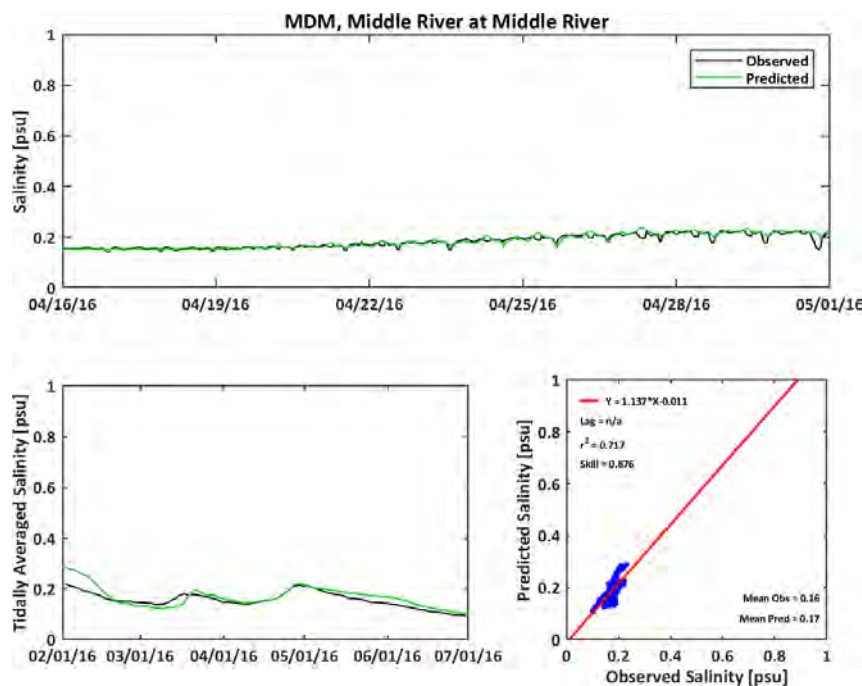


**Figure C-121**

**Observed and Predicted Salinity at Old River at Highway 4 (OH4) During 2016**

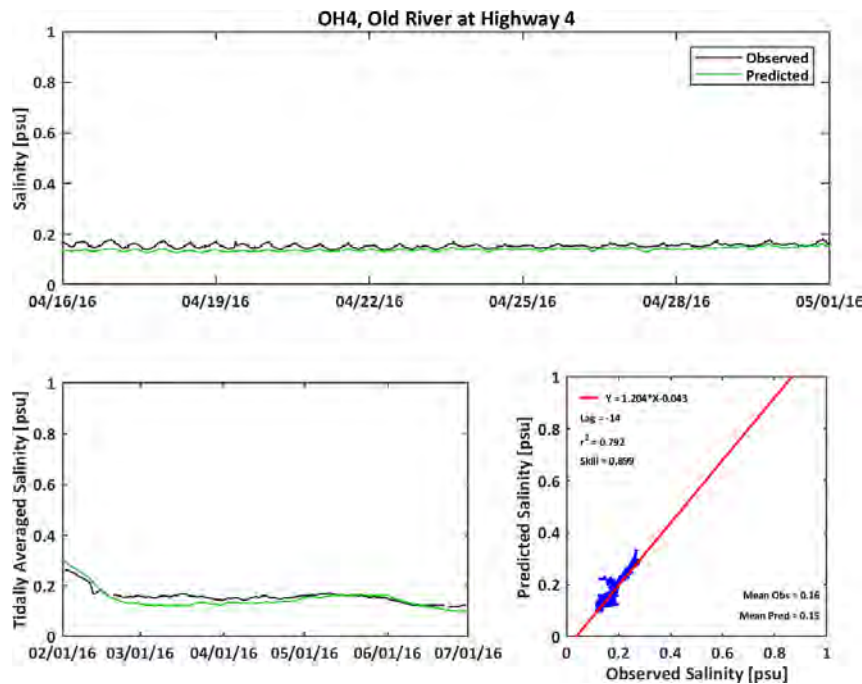


**Figure C-122**

**Observed and Predicted Salinity at Victoria Canal near Byron (VCU) During 2016**

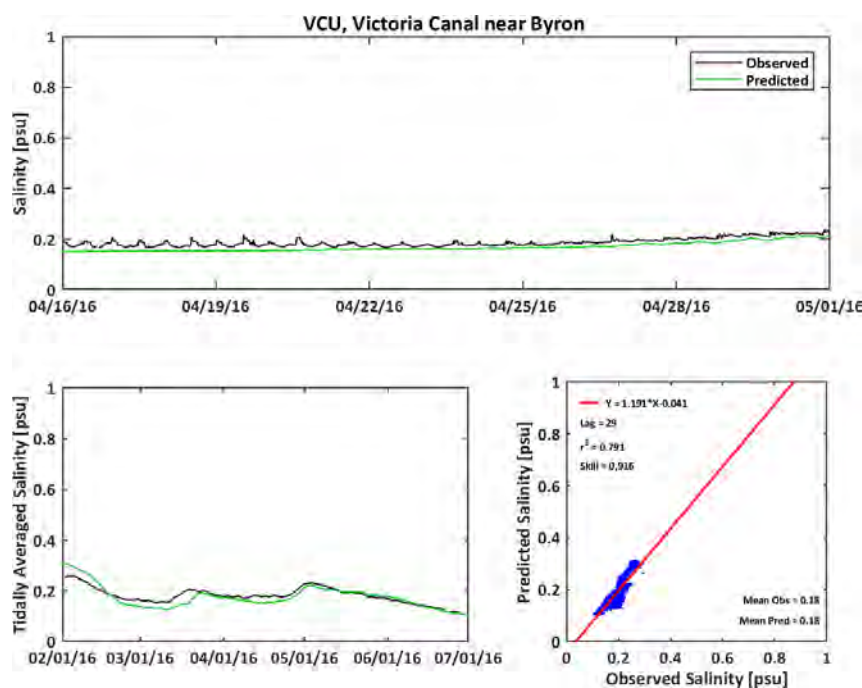


**Figure C-123**

**Observed and Predicted Salinity at Grant Line Canal near Clifton Court Ferry (GLC) During 2016**

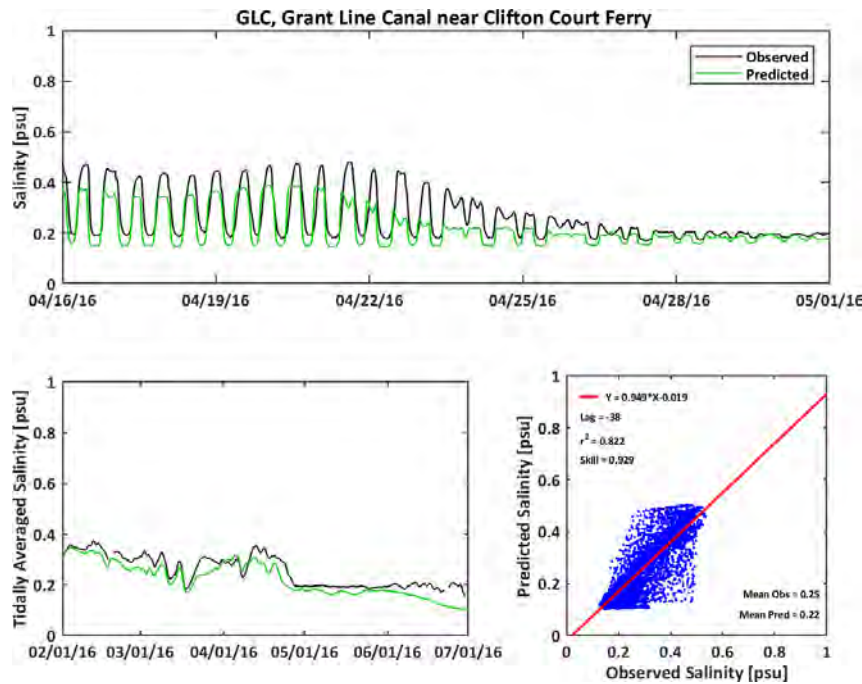


**Figure C-124**

**Observed and Predicted Salinity at Old River at Head (OH1) During 2016**

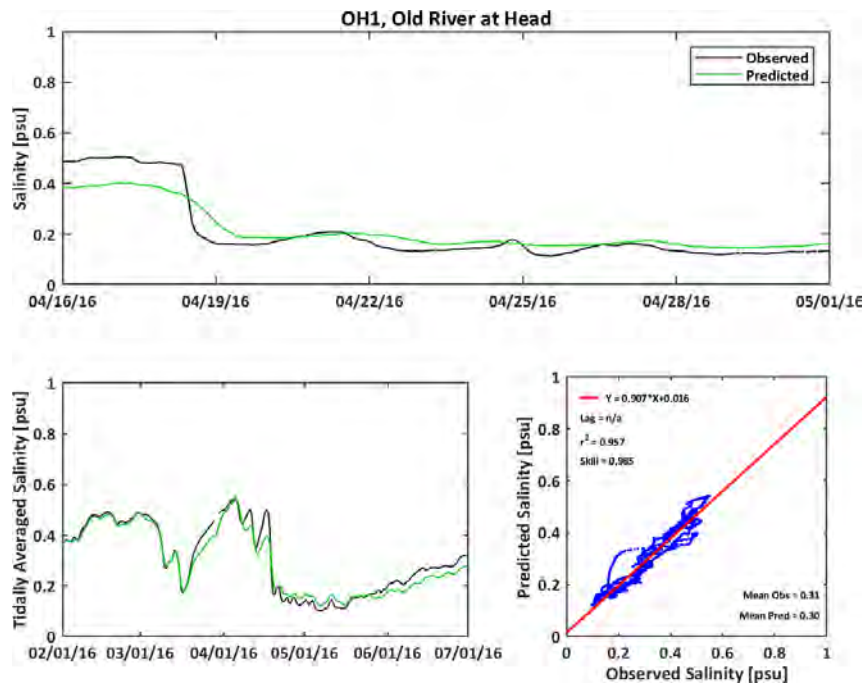


**Figure C-125**

**Observed and Predicted Salinity at San Joaquin River below Old River near Lathrop (SJL) During 2016**

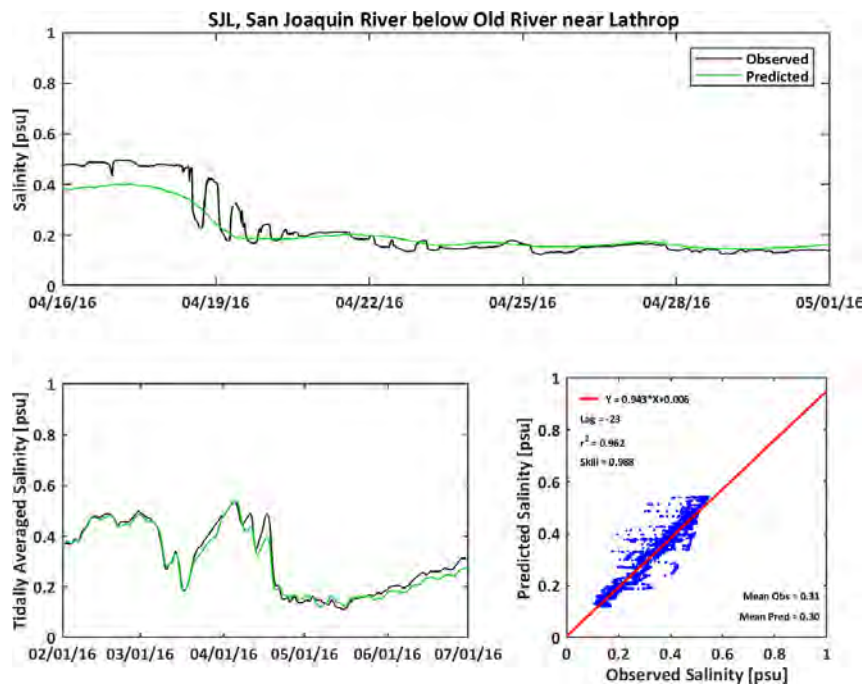


**Figure C-126**

**Observed and Predicted Salinity at San Joaquin River at Mossdale (MSD) During 2016**

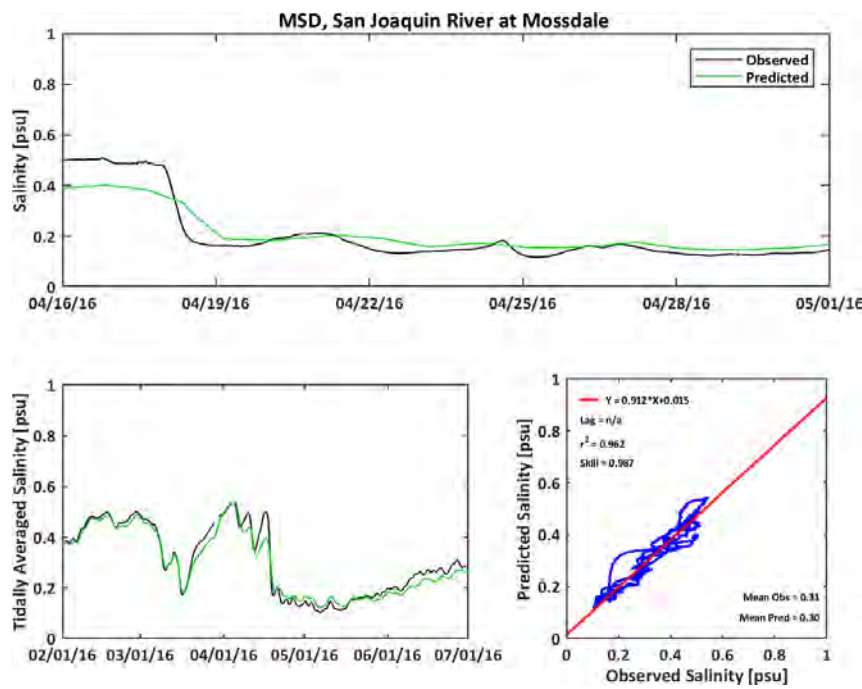


**Figure C-127**

**Target Diagrams Showing the Model Validation Using the Time Series Temperature for the Six Years**

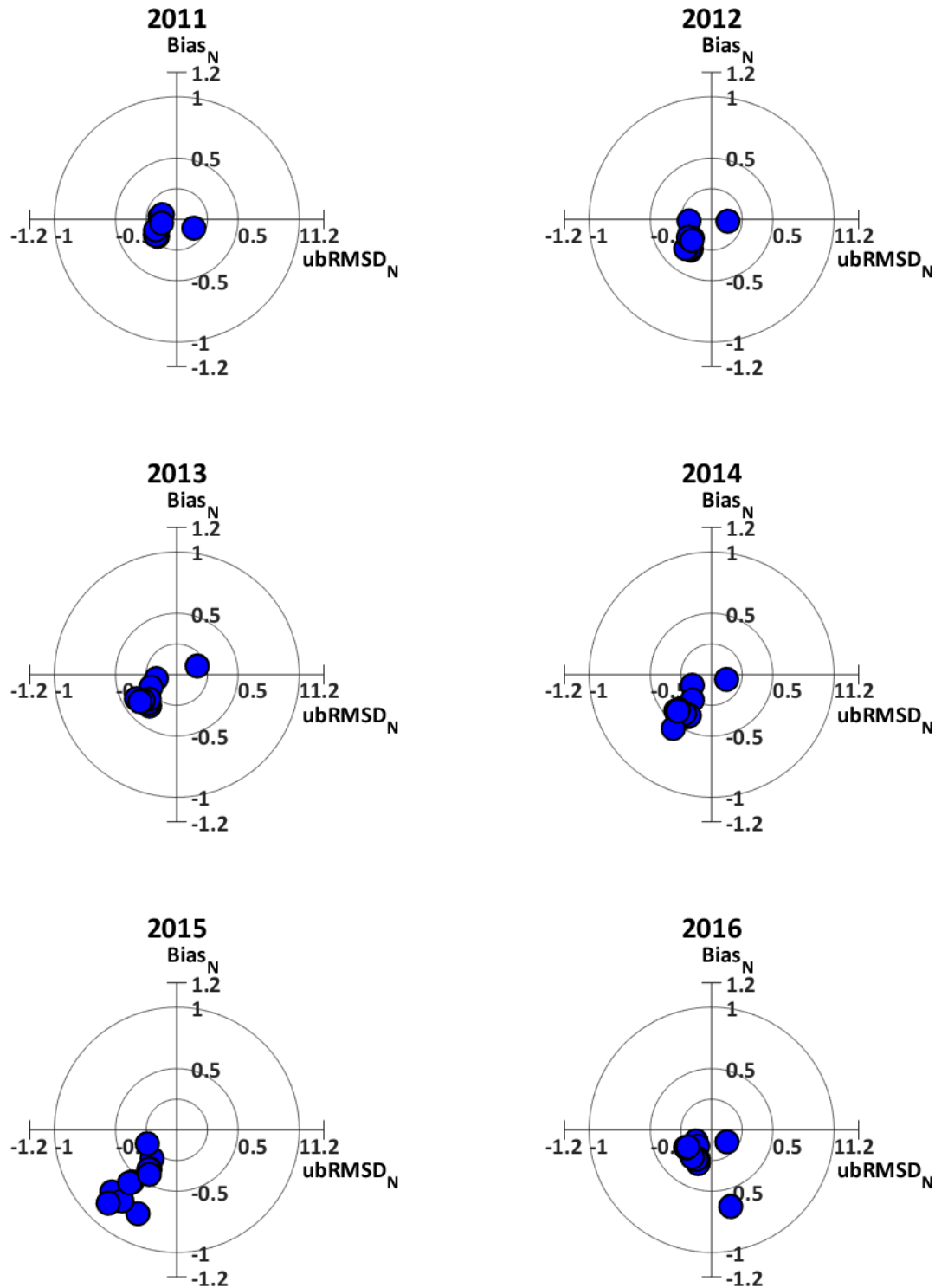


**Figure C-128**

**Observed and Predicted Temperature at Sacramento River at Rio Vista (SRV) During 2011**

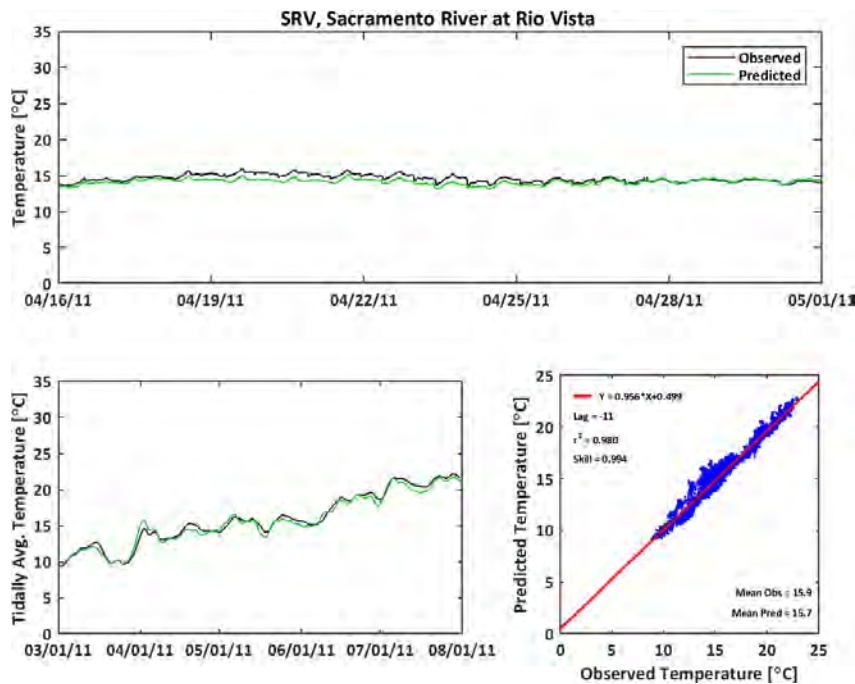


**Figure C-129**

**Observed and Predicted Temperature at San Joaquin River at Jersey Point (SJJ) During 2011**

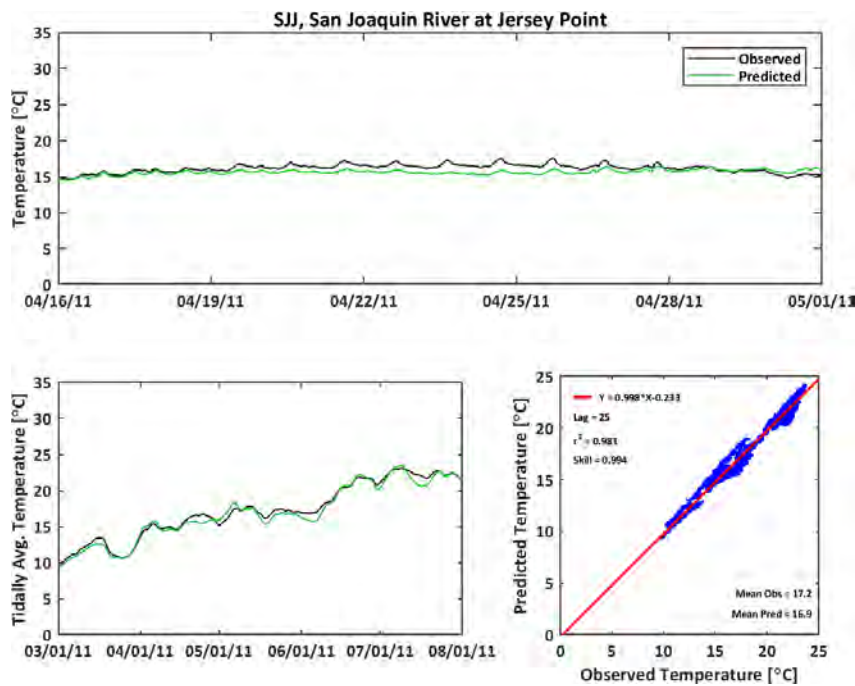


**Figure C-130**

**Observed and Predicted Temperature at Turner Cut near Holt (TRN) During 2011**

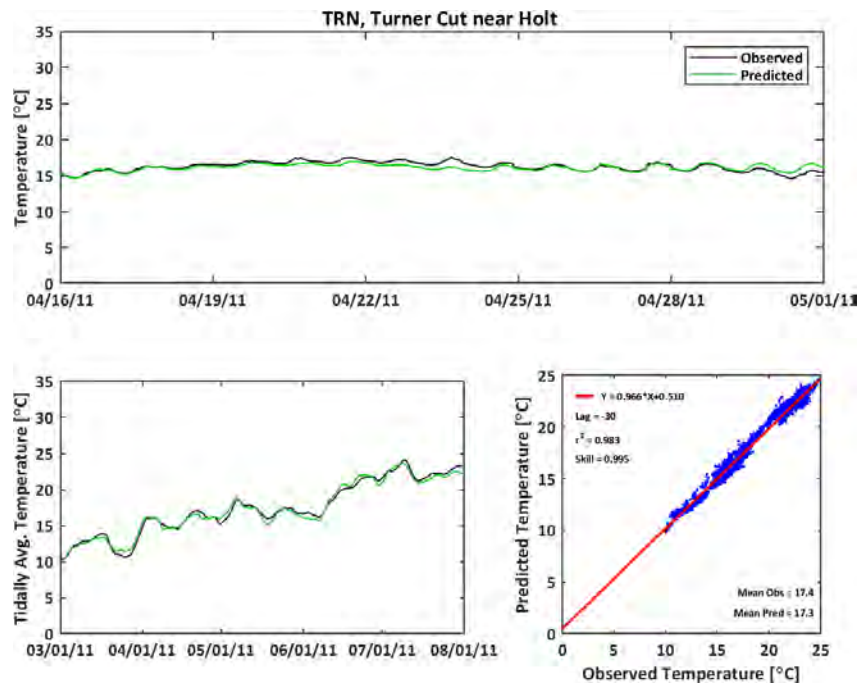


**Figure C-131**

**Observed and Predicted Temperature at Old River at Bacon Island (OBI) During 2011**

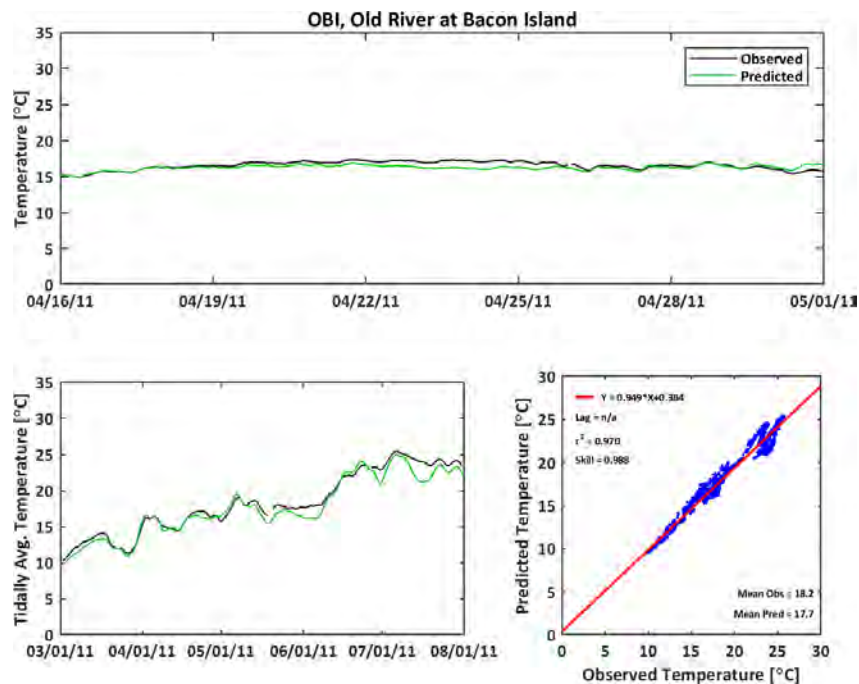


**Figure C-132**

**Observed and Predicted Temperature at Middle River at Middle River (MDM) During 2011**

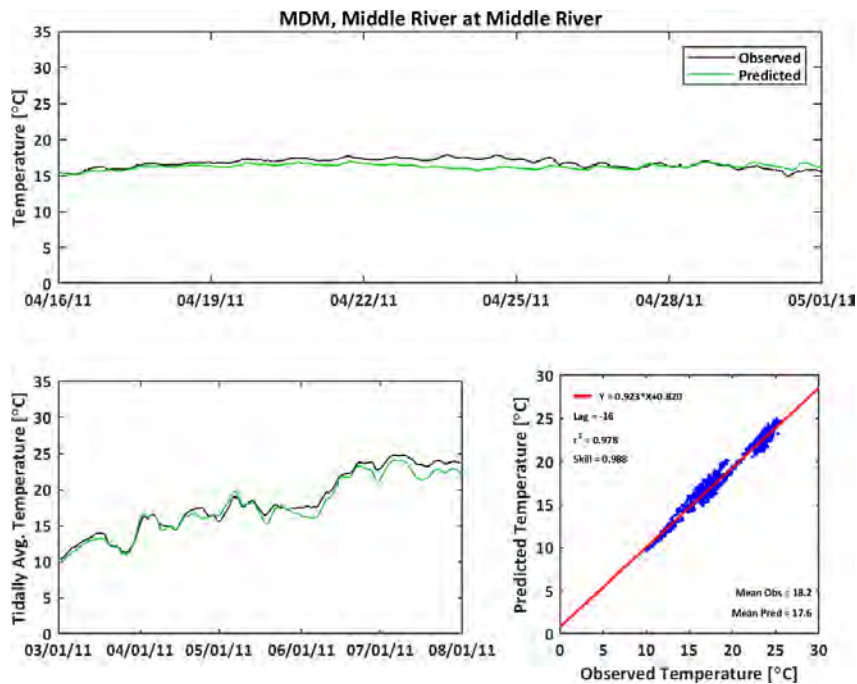


**Figure C-133**

**Observed and Predicted Temperature at Old River at Highway 4 (OH4) During 2011**

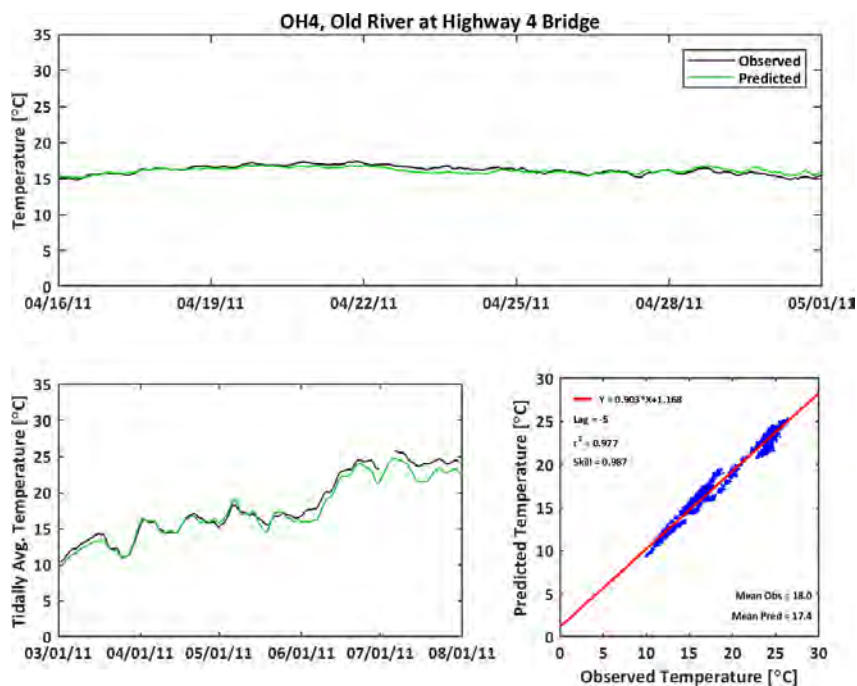


**Figure C-134**

**Observed and Predicted Temperature at Victoria Canal near Byron (VCU) During 2011**

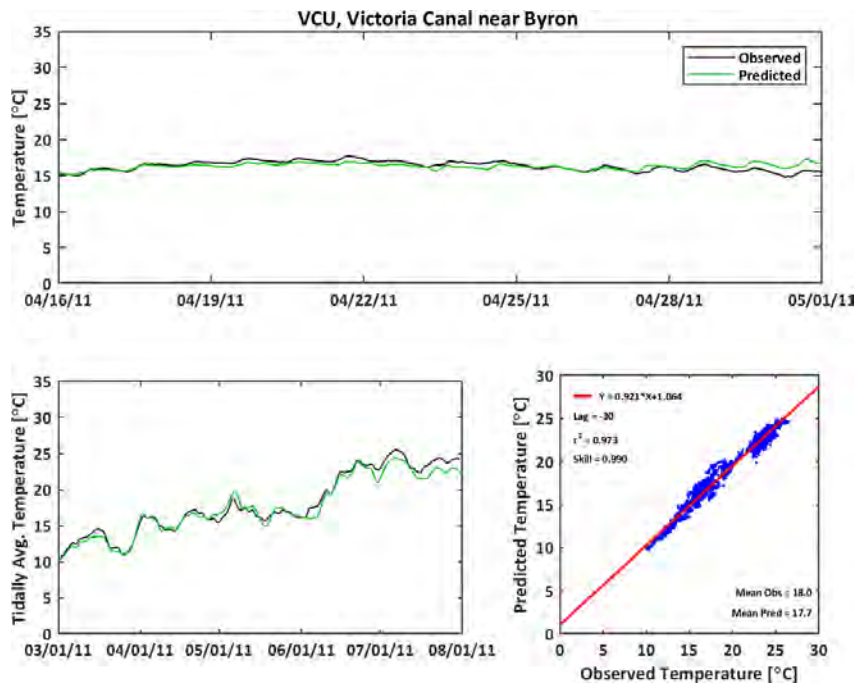


**Figure C-135**

**Observed and Predicted Temperature at Grant Line Canal near Clifton Court Ferry (GLC)  
During 2011**

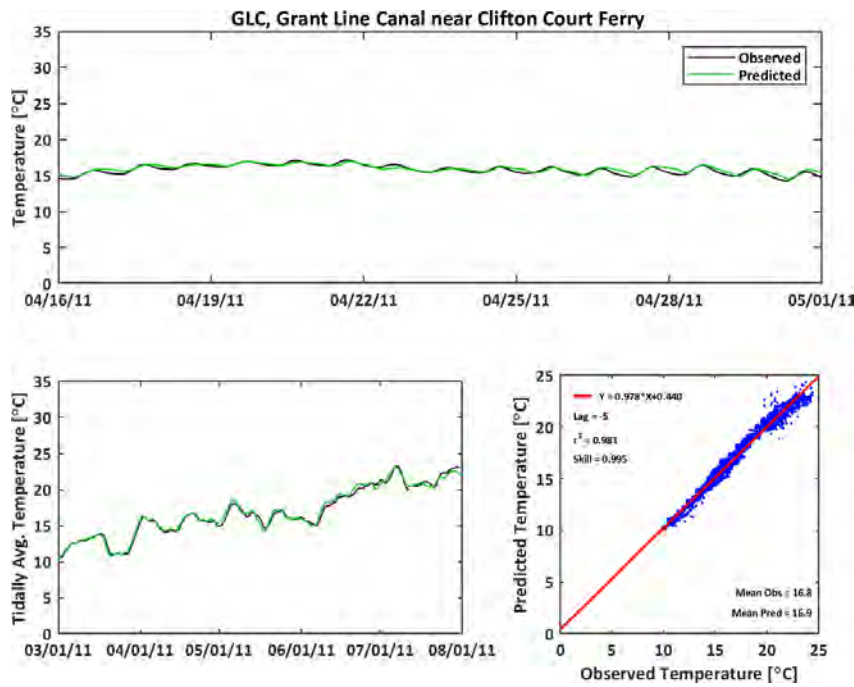


**Figure C-136**

**Observed and Predicted Temperature at San Joaquin River below Old River near Lathrop (SJL) During 2011**

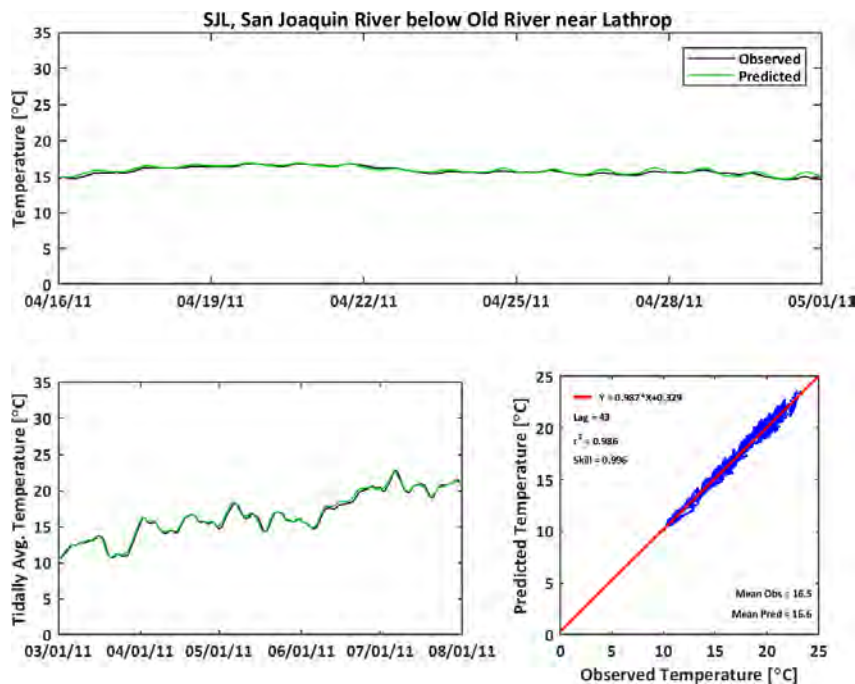


**Figure C-137**

**Observed and Predicted Temperature at San Joaquin River at Mossdale (MSD) During 2011**

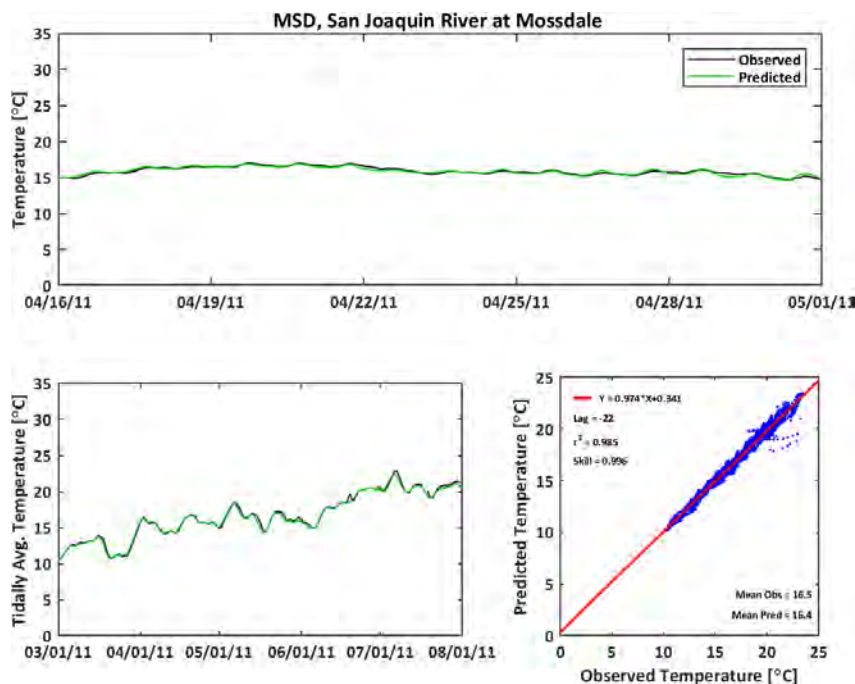


**Figure C-138**

**Observed and Predicted Temperature at Sacramento River at Rio Vista (SRV) During 2012**

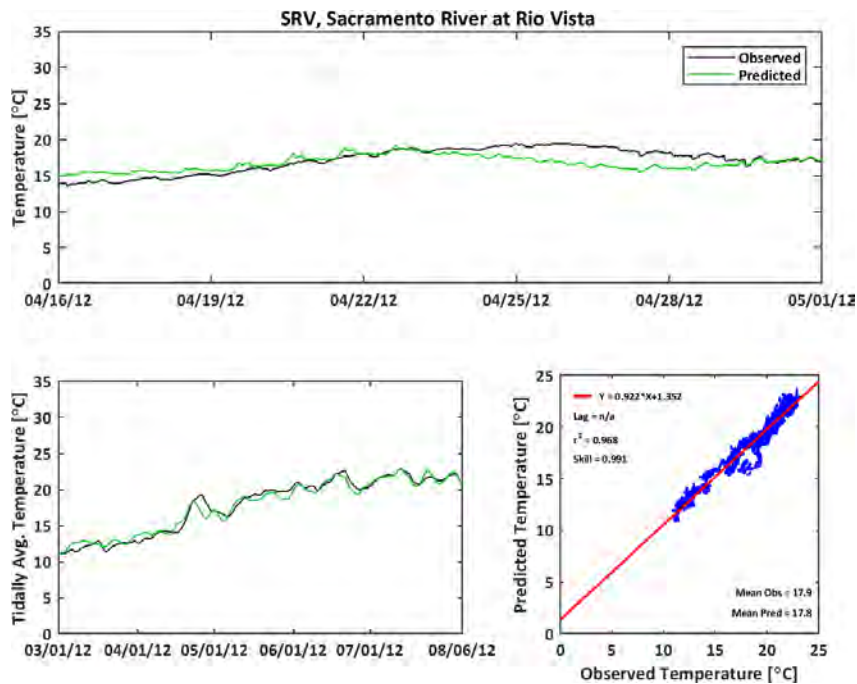


**Figure C-139**

**Observed and Predicted Temperature at San Joaquin River at Jersey Point (SJJ) During 2012**

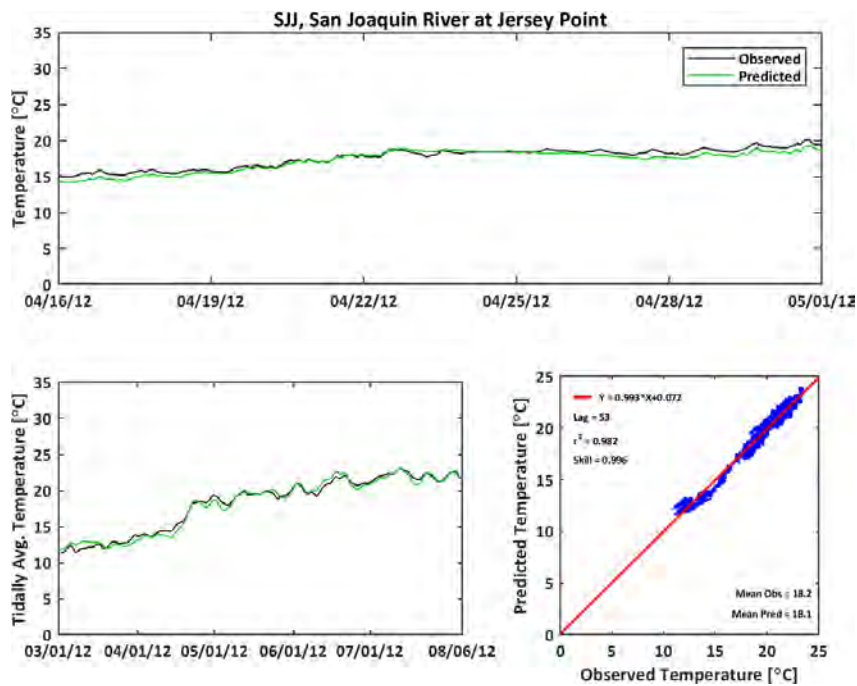


**Figure C-140**

**Observed and Predicted Temperature at Turner Cut near Holt (TRN) During 2012**

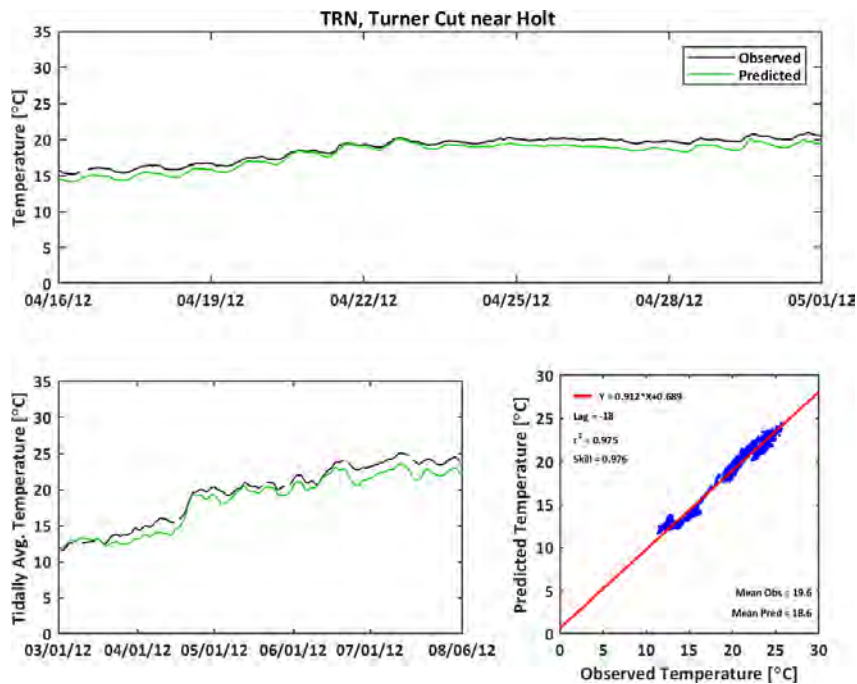


**Figure C-141**

**Observed and Predicted Temperature at Old River at Bacon Island (OBI) During 2012**

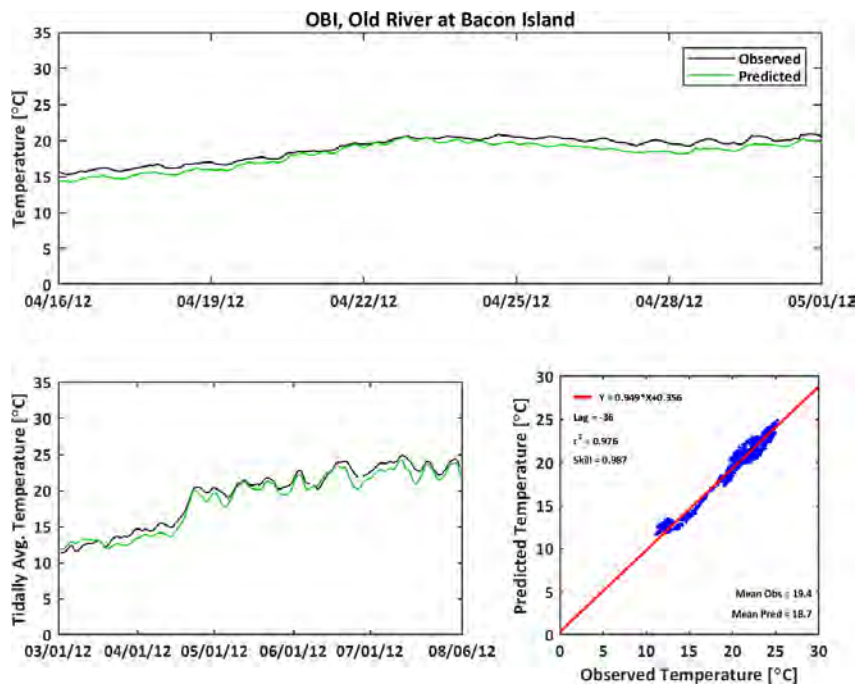


**Figure C-142**

**Observed and Predicted Temperature at Middle River at Middle River (MDM) During 2012**

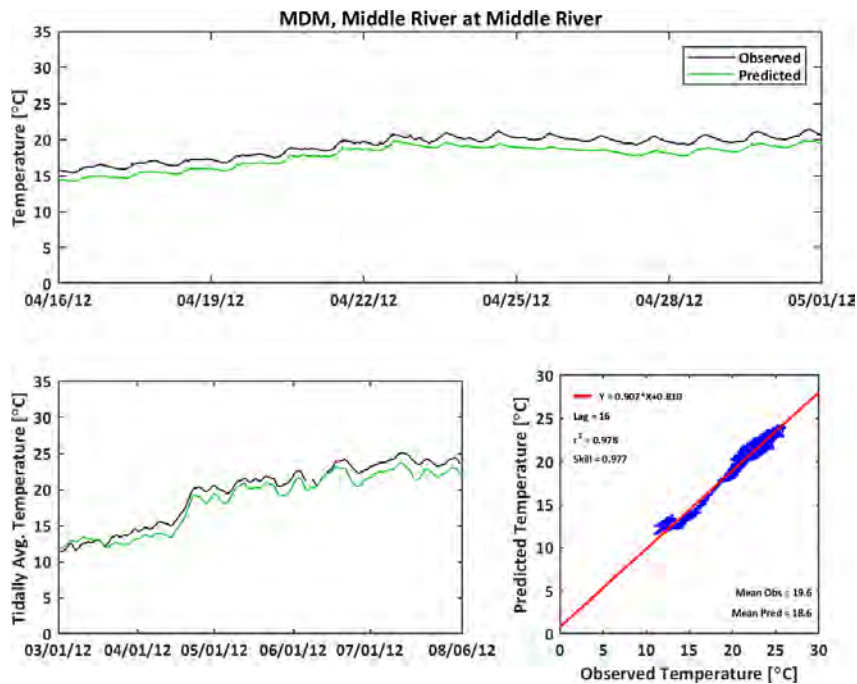


**Figure C-143**

**Observed and Predicted Temperature at Old River at Highway 4 (OH4) During 2012**

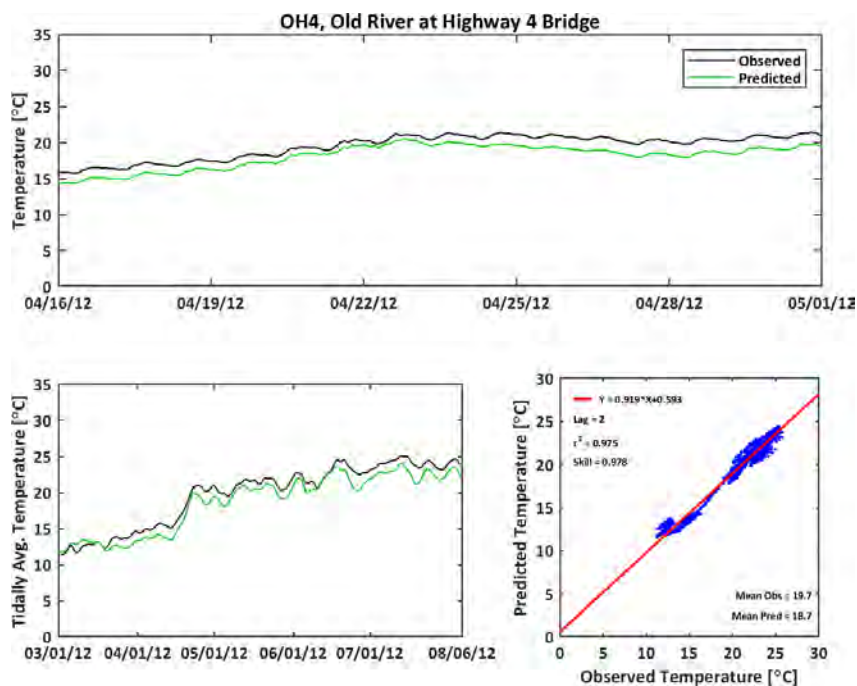


**Figure C-144**

**Observed and Predicted Temperature at Victoria Canal near Byron (VCU) During 2012**

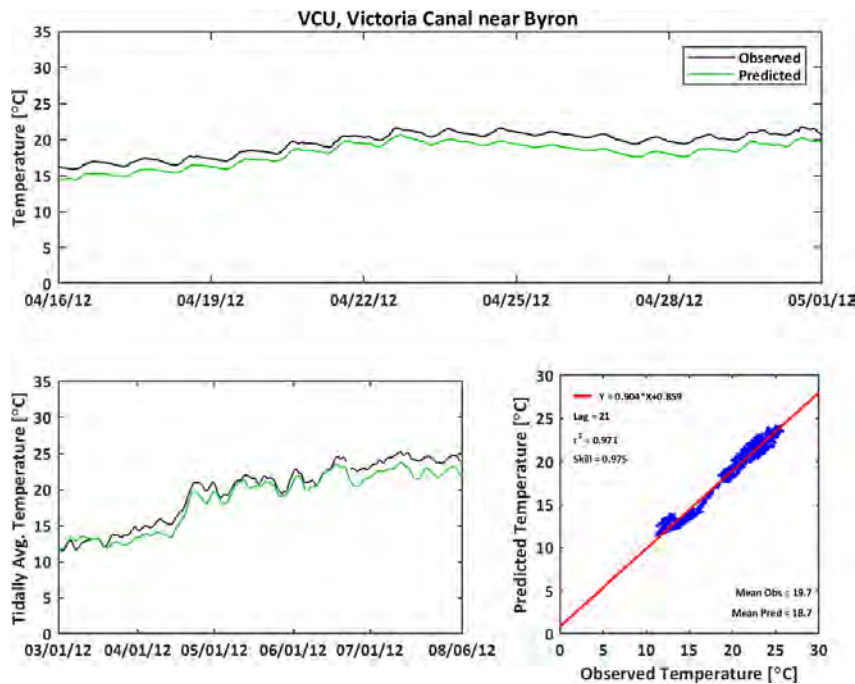


**Figure C-145**

**Observed and Predicted Temperature at Grant Line Canal near Clifton Court Ferry (GLC) During 2012**

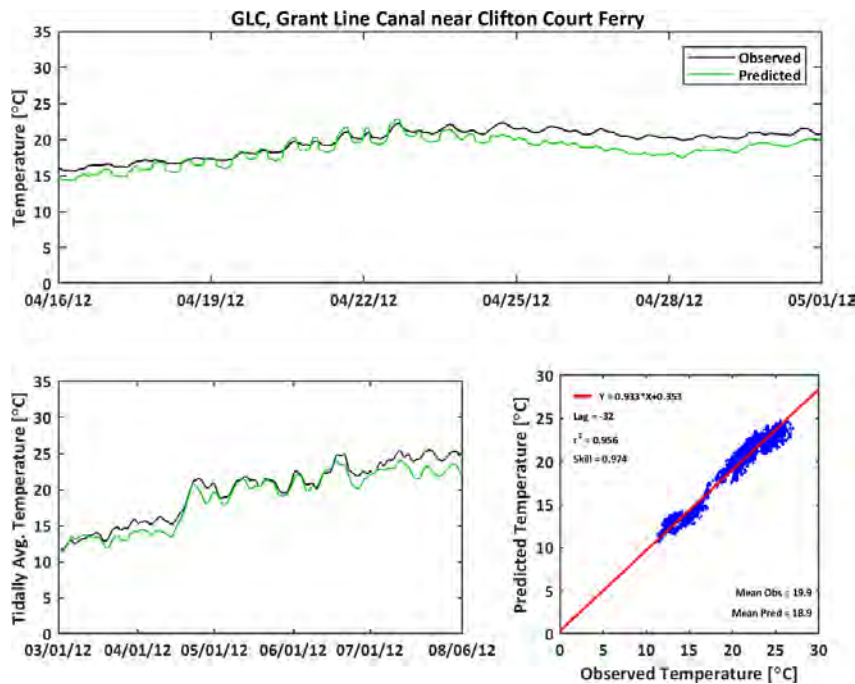


**Figure C-146**

**Observed and Predicted Temperature at San Joaquin River below Old River near Lathrop (SJL) During 2012**

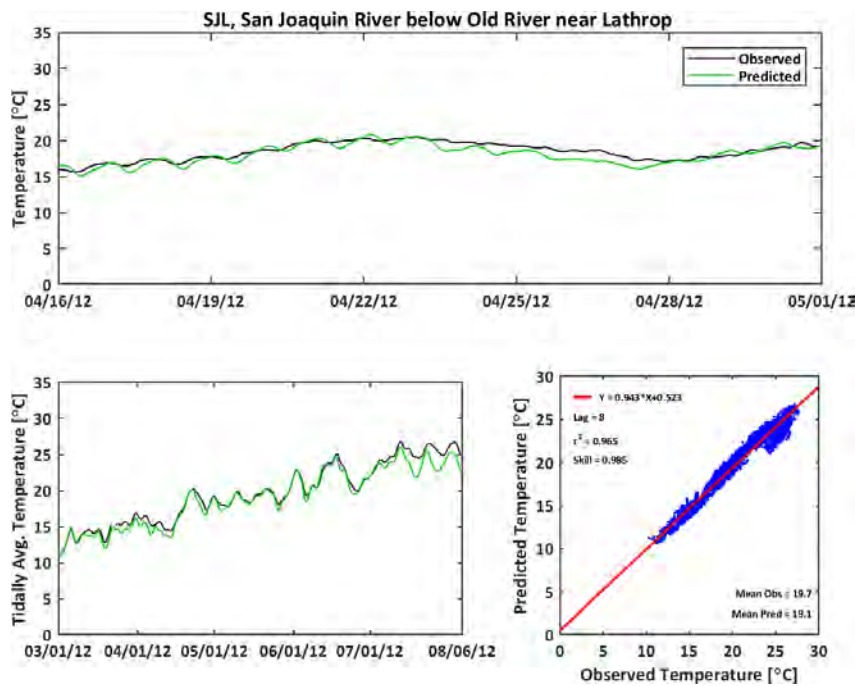


**Figure C-147**

**Observed and Predicted Temperature at San Joaquin River at Mossdale (MSD) During 2012**

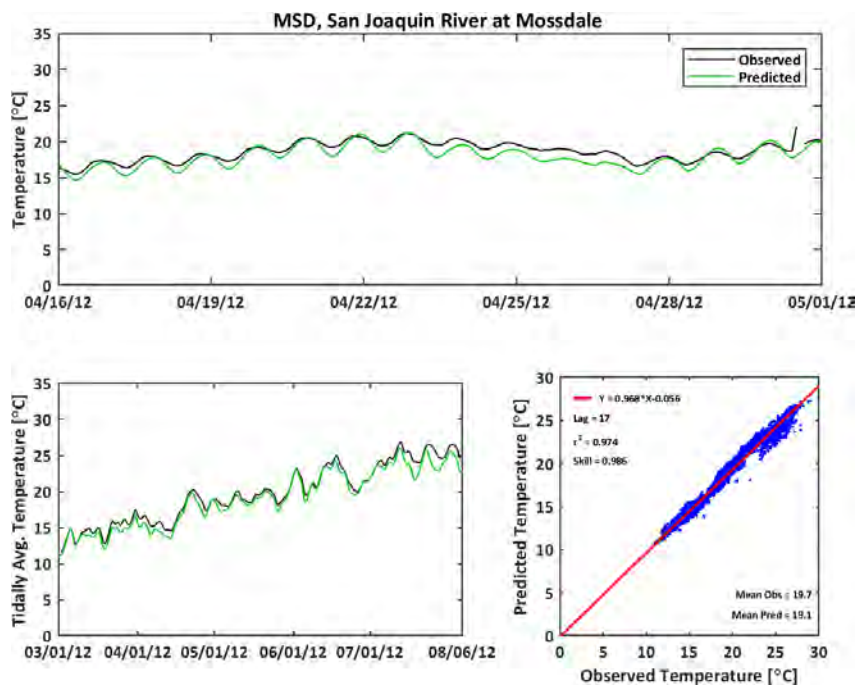


**Figure C-148**

**Observed and Predicted Temperature at Sacramento River at Rio Vista (SRV) During 2013**

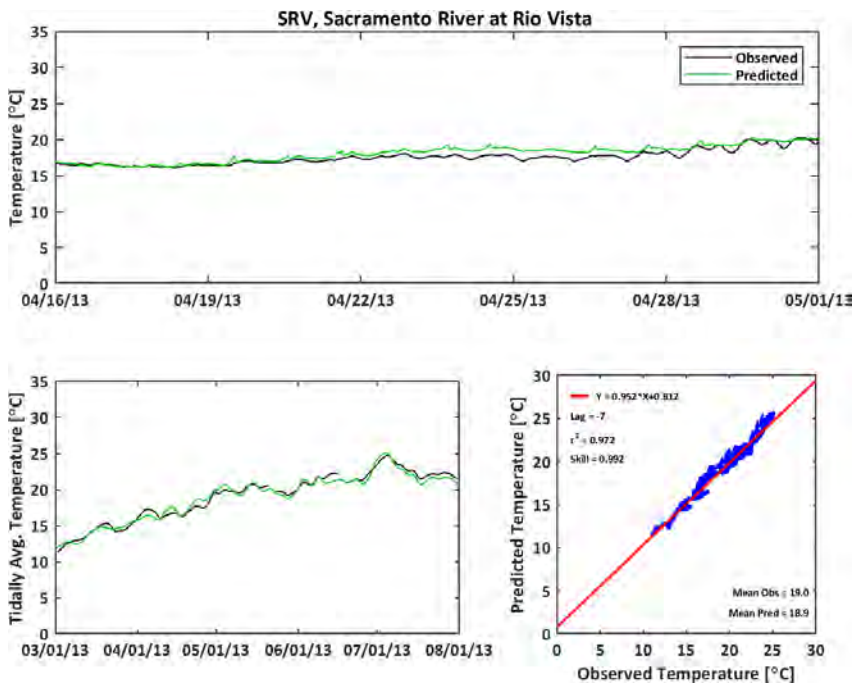


**Figure C-149**

**Observed and Predicted Temperature at San Joaquin River at Jersey Point (SJJ) During 2013**

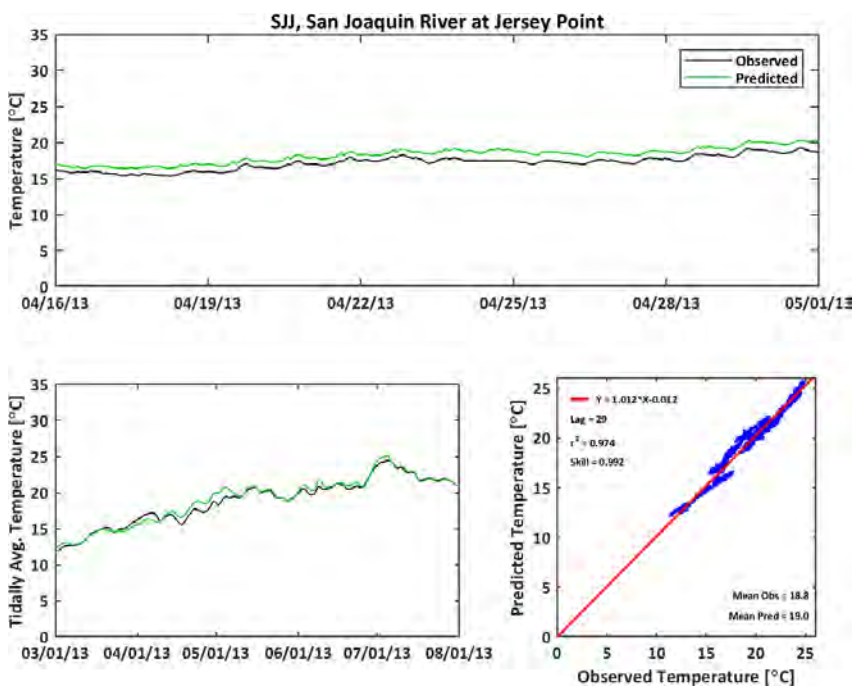


**Figure C-150**

**Observed and Predicted Temperature at Turner Cut near Holt (TRN) During 2013**

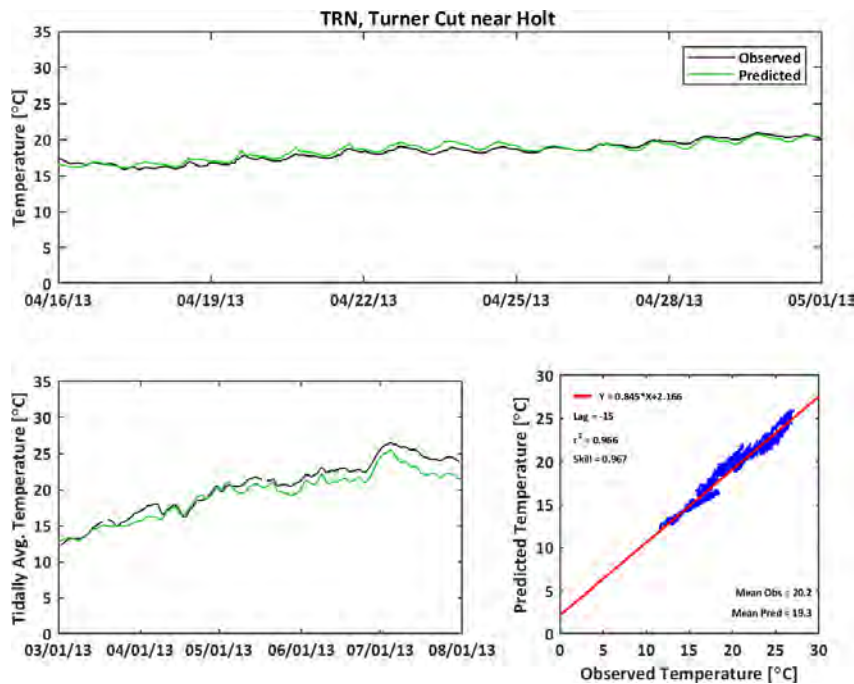


**Figure C-151**

**Observed and Predicted Temperature at Old River at Bacon Island (OBI) During 2013**

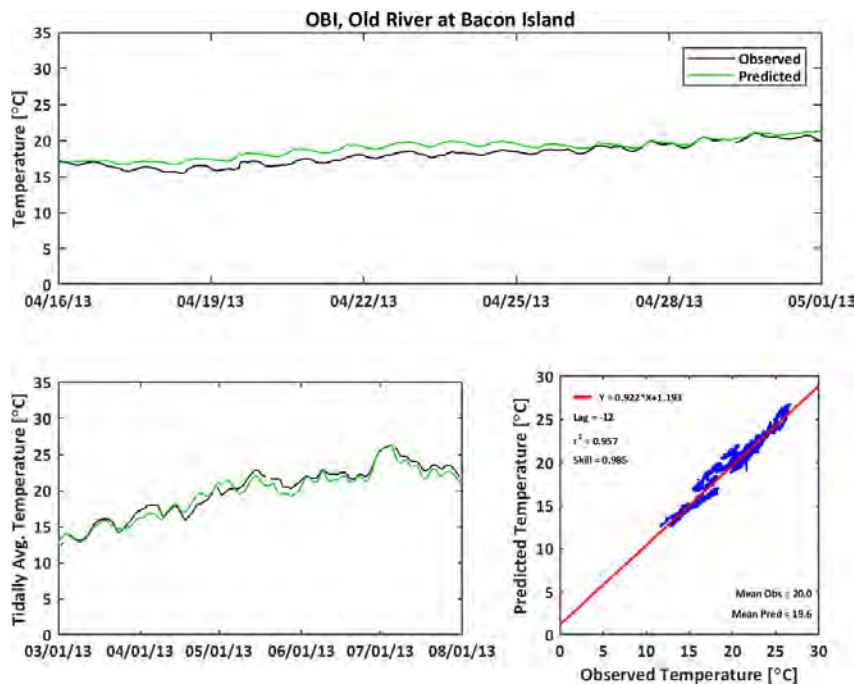


**Figure C-152**

**Observed and Predicted Temperature at Middle River at Middle River (MDM) During 2013**

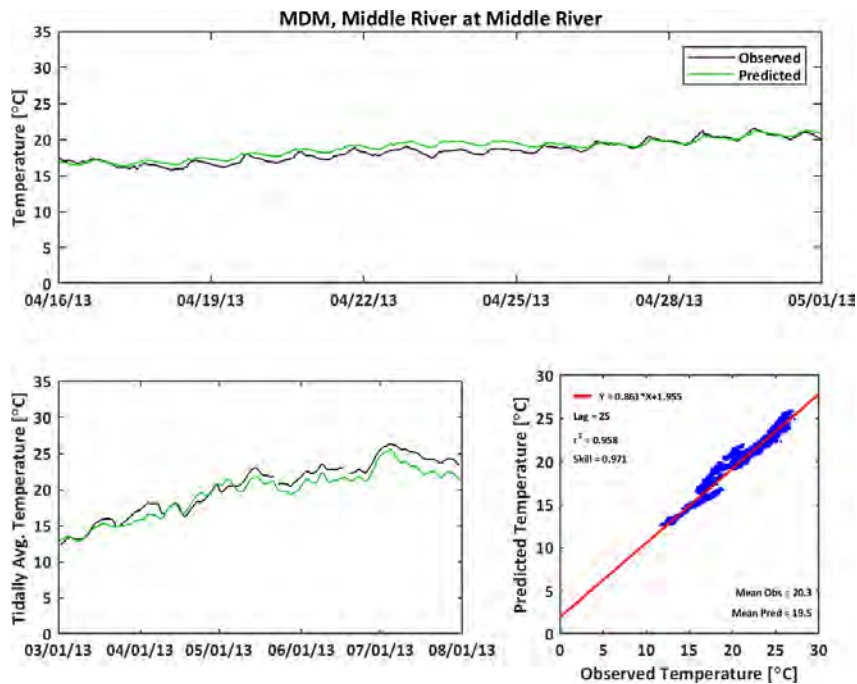


**Figure C-153**

**Observed and Predicted Temperature at Old River at Highway 4 (OH4) During 2013**

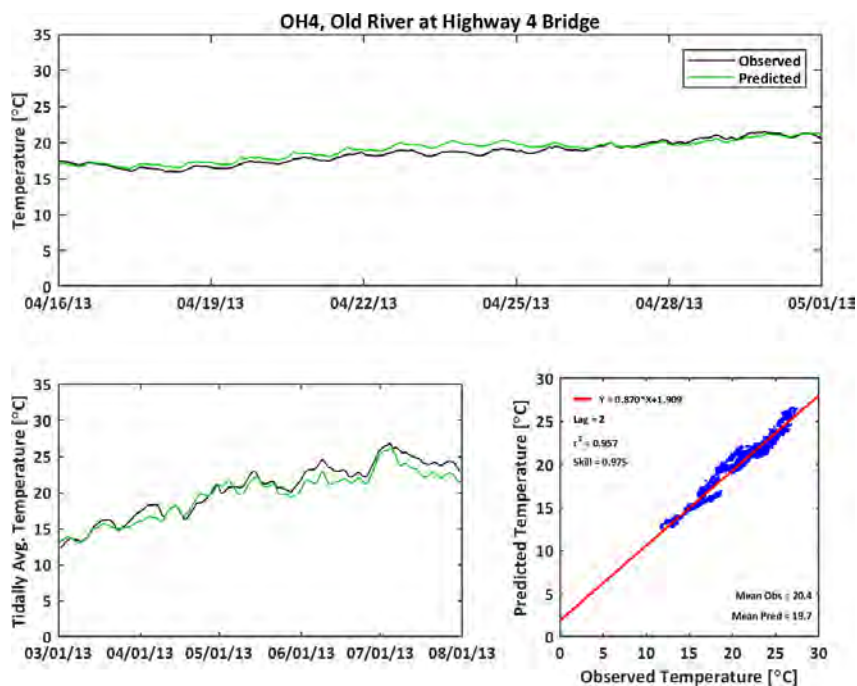


**Figure C-154**

**Observed and Predicted Temperature at Victoria Canal near Byron (VCU) During 2013**

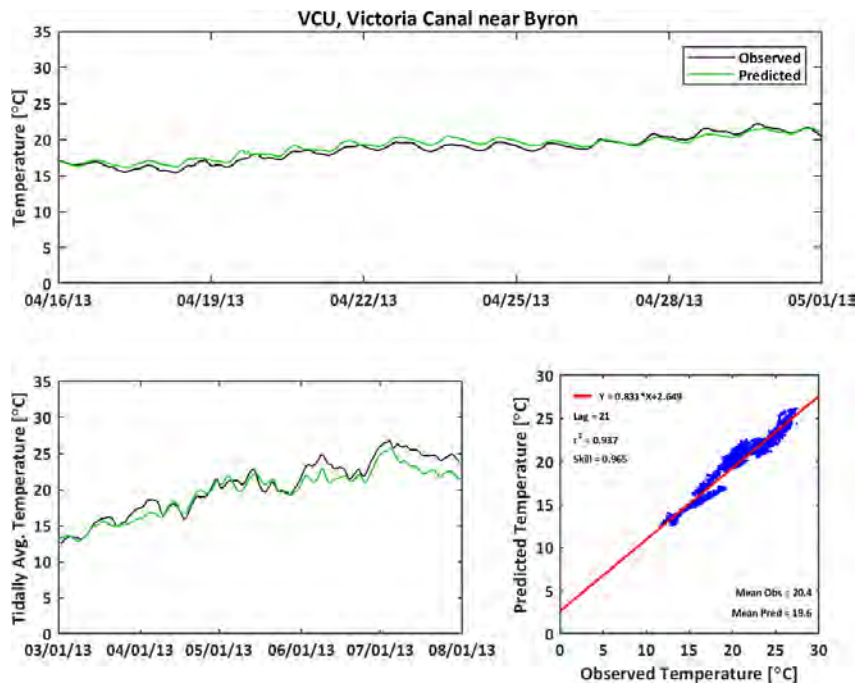


**Figure C-155**

**Observed and Predicted Temperature at Grant Line Canal near Clifton Court Ferry (GLC) During 2013**

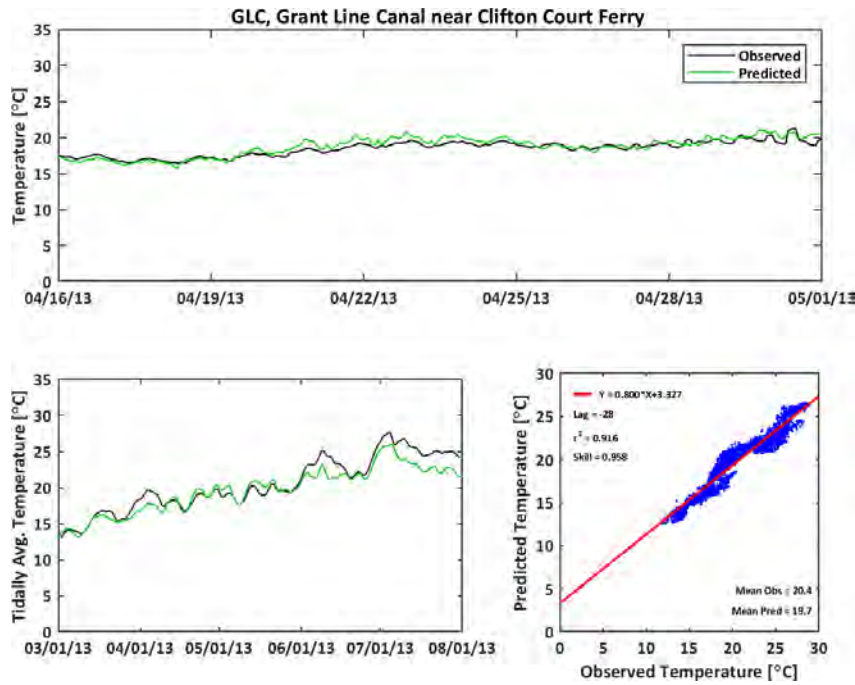


**Figure C-156**

**Observed and Predicted Temperature at San Joaquin River below Old River near Lathrop (SJL) During 2013**

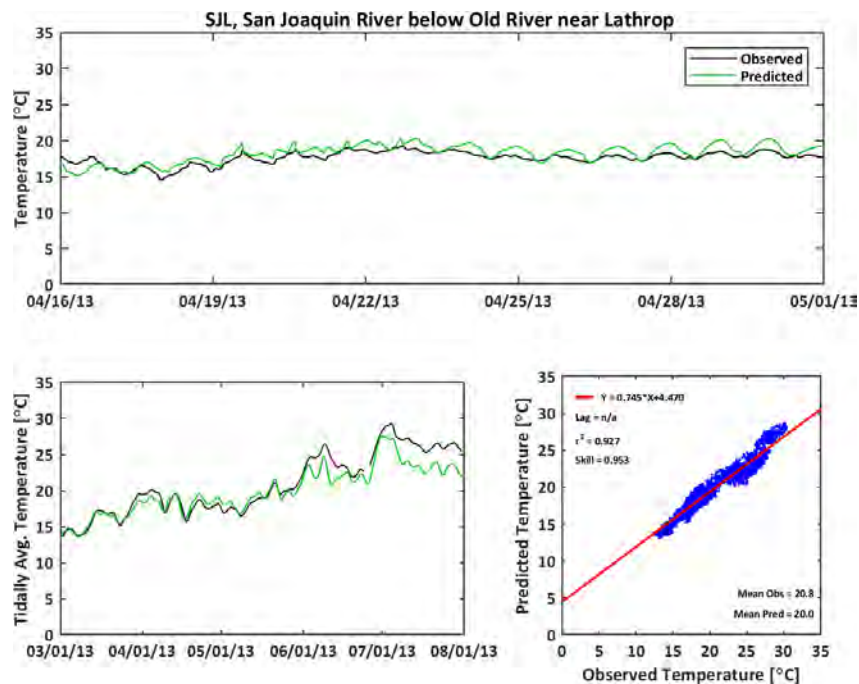


**Figure C-157**

**Observed and Predicted Temperature at San Joaquin River at Mossdale (MSD) During 2013**

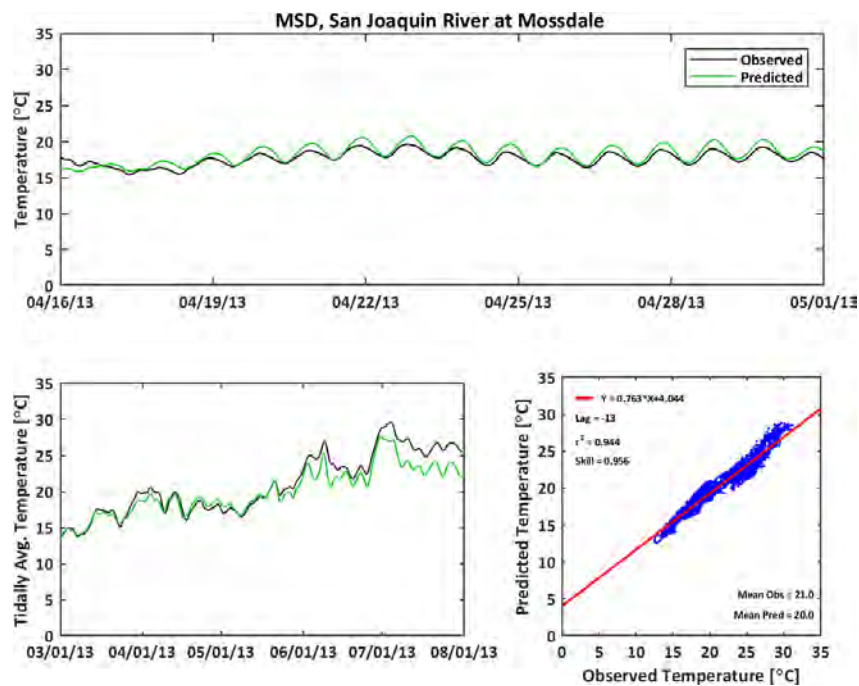


**Figure C-158**

**Observed and Predicted Temperature at Sacramento River at Rio Vista (SRV) During 2014**

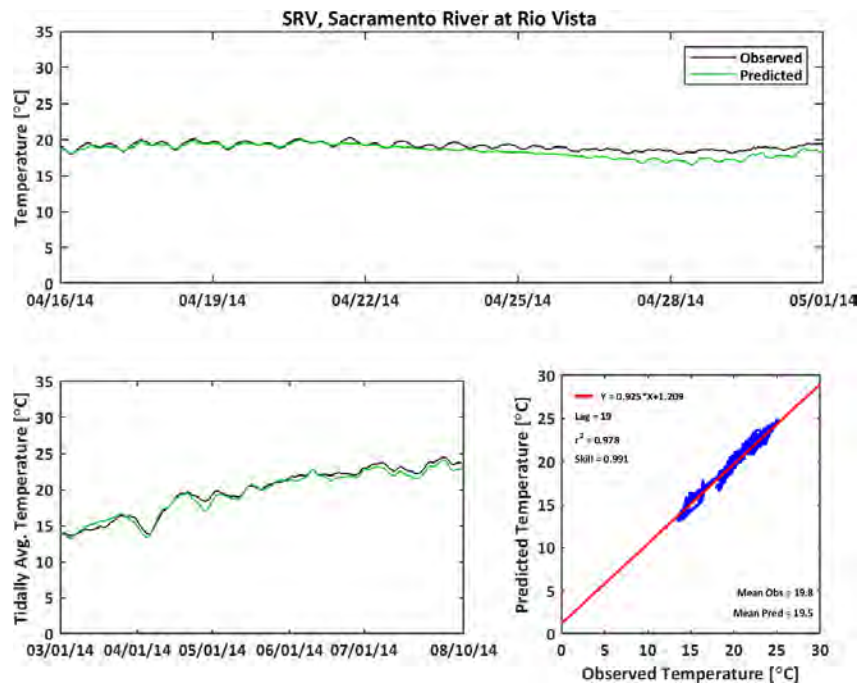


**Figure C-159**

**Observed and Predicted Temperature at San Joaquin River at Jersey Point (SJJ) During 2014**

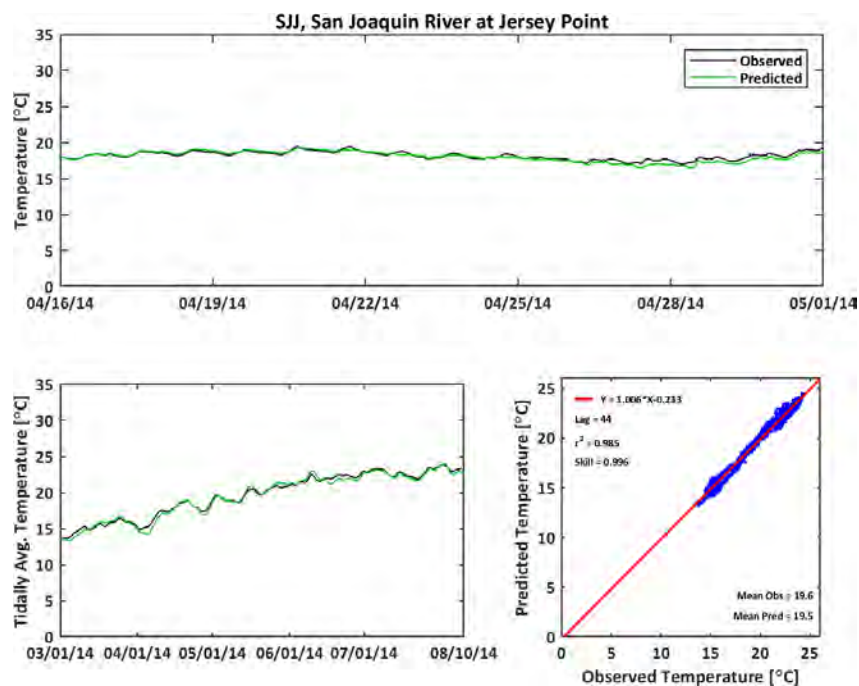


**Figure C-160**

**Observed and Predicted Temperature at Turner Cut near Holt (TRN) During 2014**

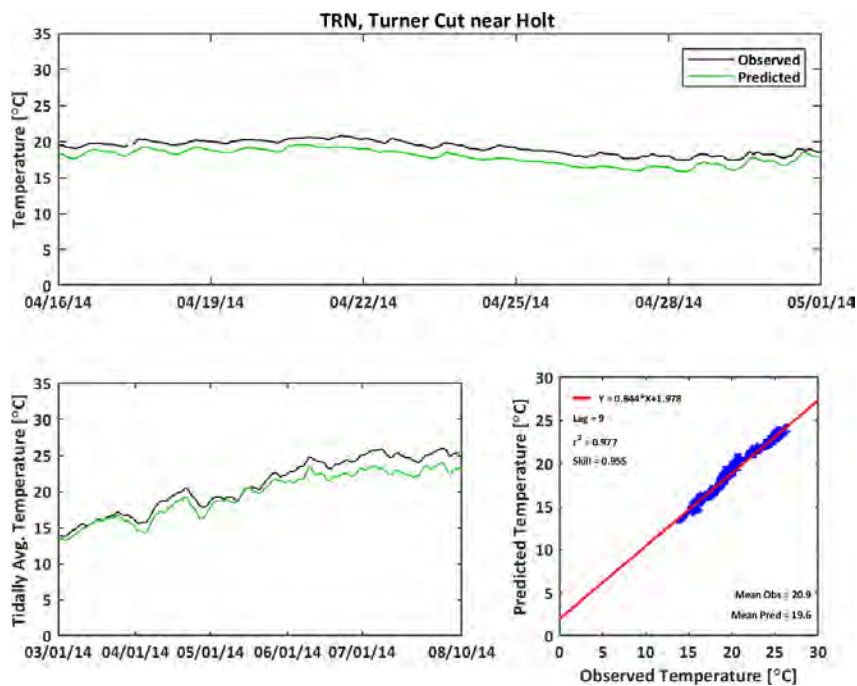


**Figure C-161**

**Observed and Predicted Temperature at Old River at Bacon Island (OBI) During 2014**

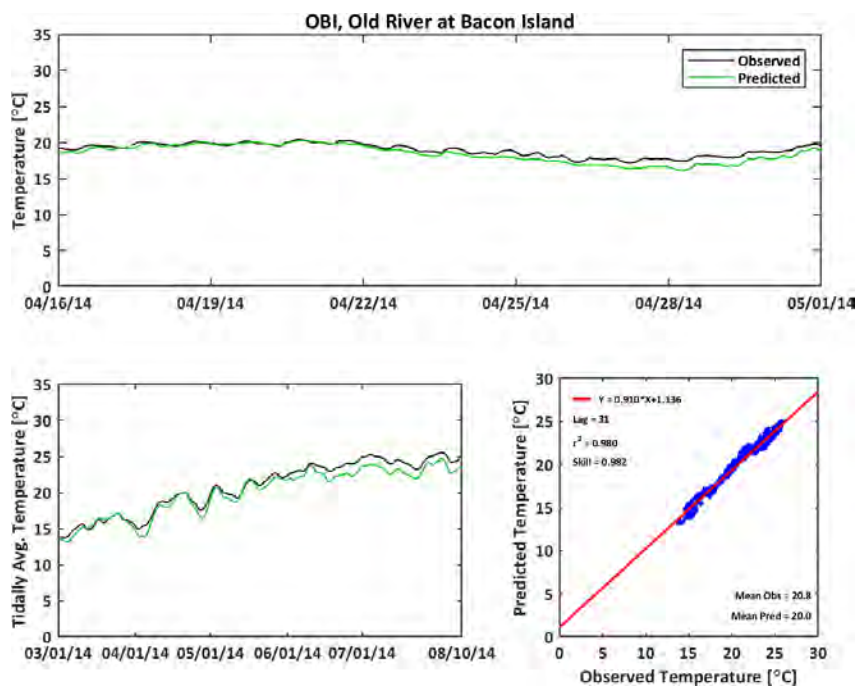


**Figure C-162**

**Observed and Predicted Temperature at Middle River at Middle River (MDM) During 2014**

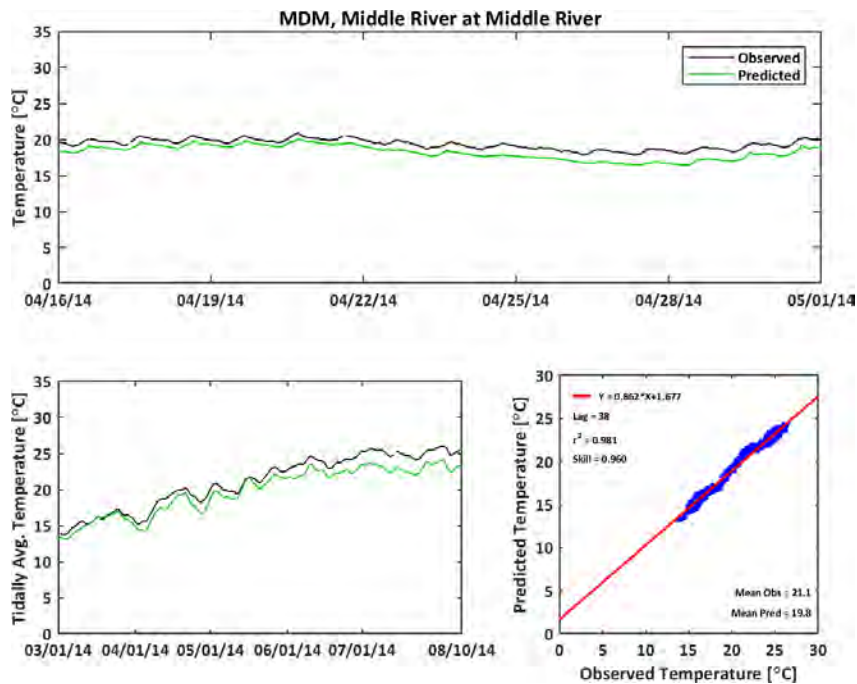


**Figure C-163**

**Observed and Predicted Temperature at Old River at Highway 4 (OH4) During 2014**

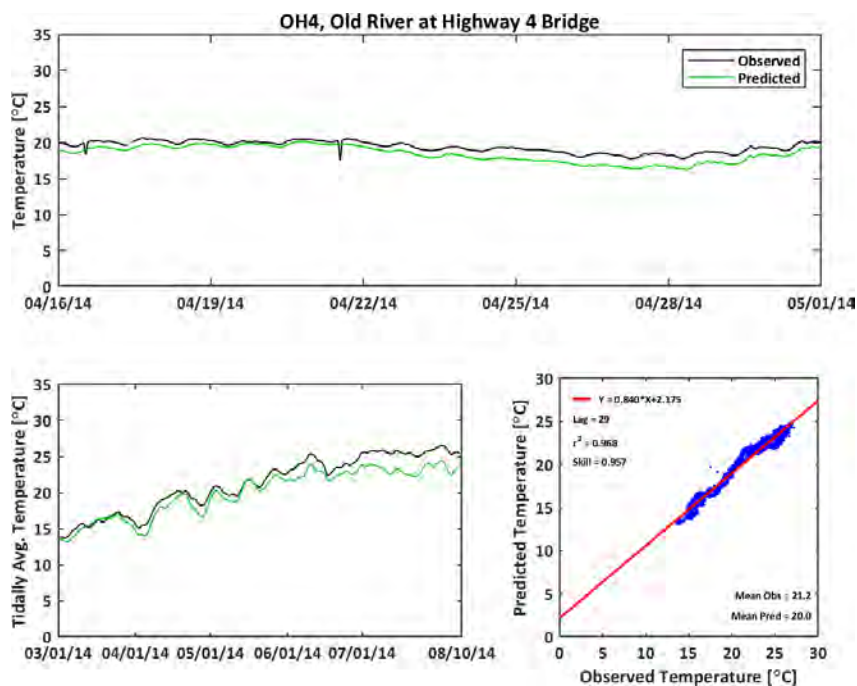


**Figure C-164**

**Observed and Predicted Temperature at Victoria Canal near Byron (VCU) During 2014**

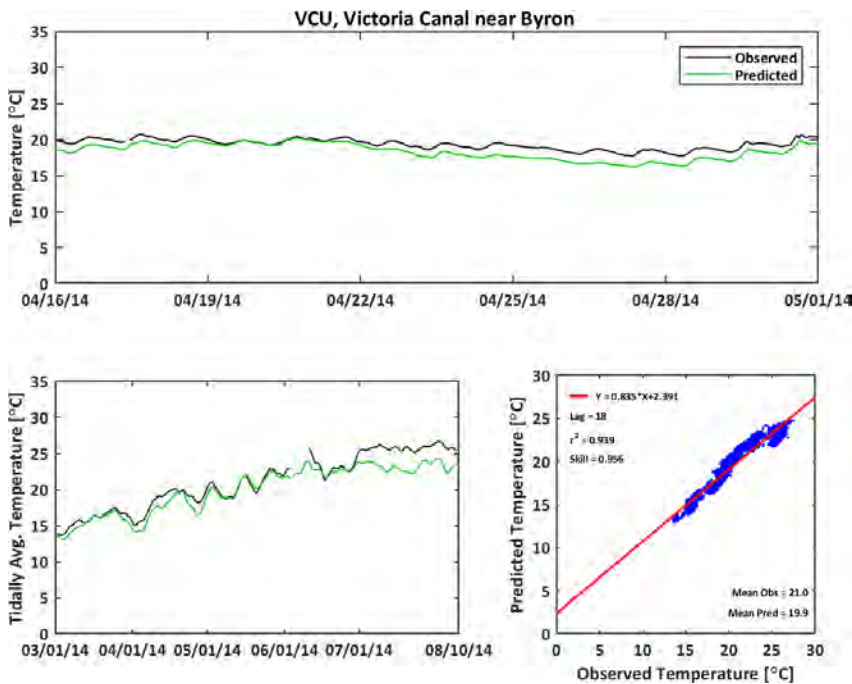


**Figure C-165**

**Observed and Predicted Temperature at Grant Line Canal near Clifton Court Ferry (GLC) During 2014**

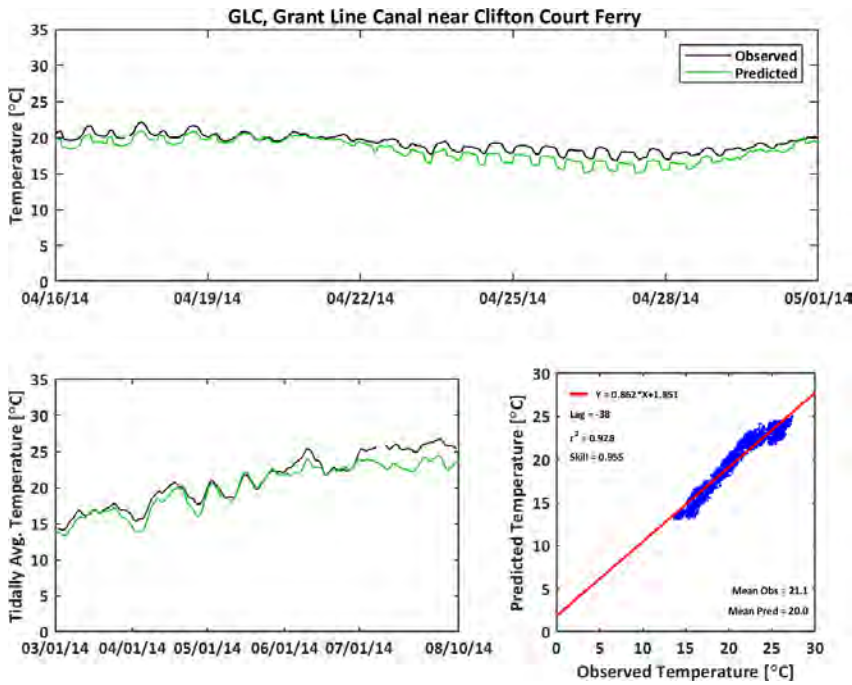


**Figure C-166**

**Observed and Predicted Temperature at Old River at Head (OH1) During 2014**

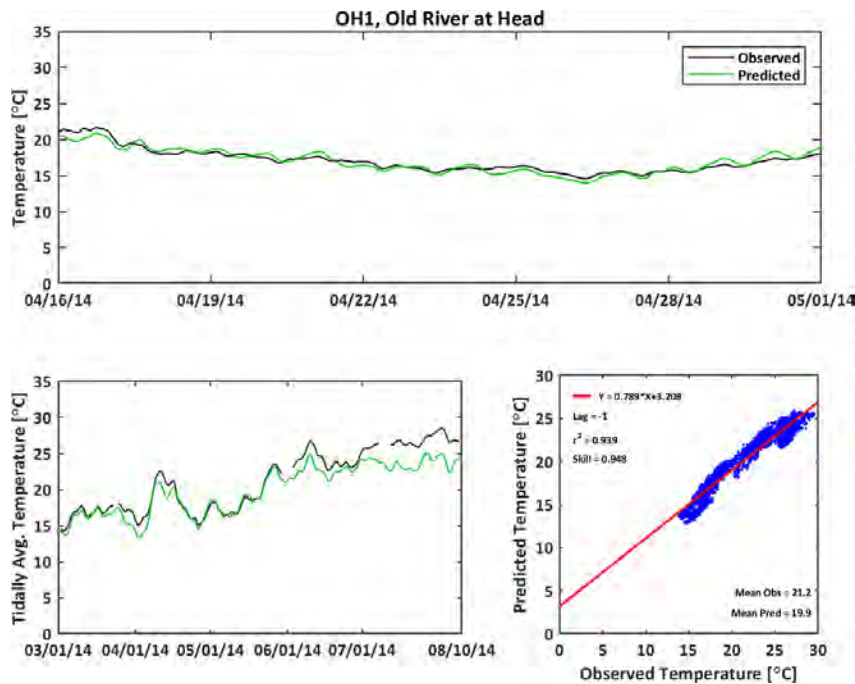


**Figure C-167**

**Observed and Predicted Temperature at San Joaquin River below Old River near Lathrop (SJL) During 2014**

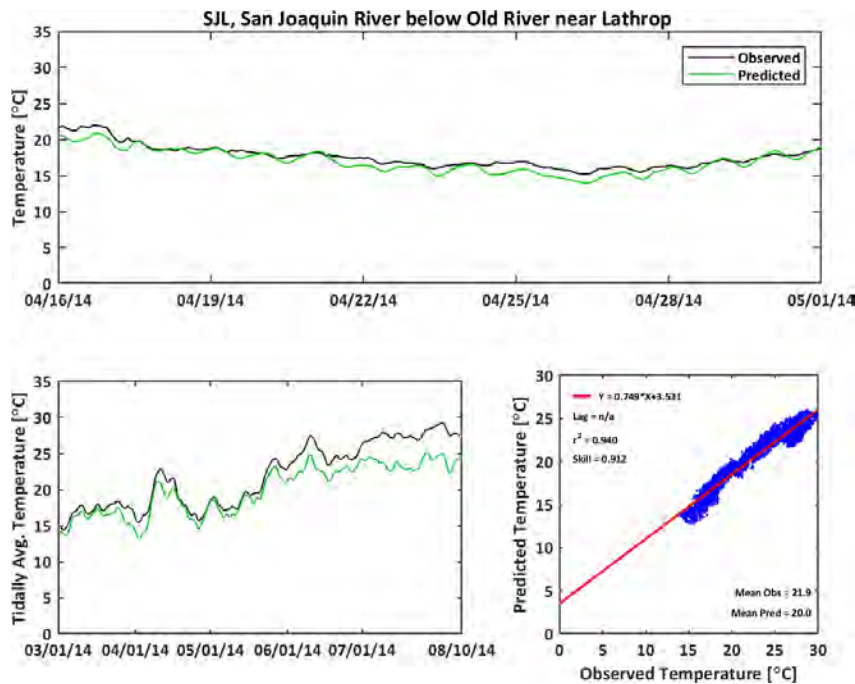


**Figure C-168**

**Observed and Predicted Temperature at San Joaquin River at Mossdale (MSD) During 2014**

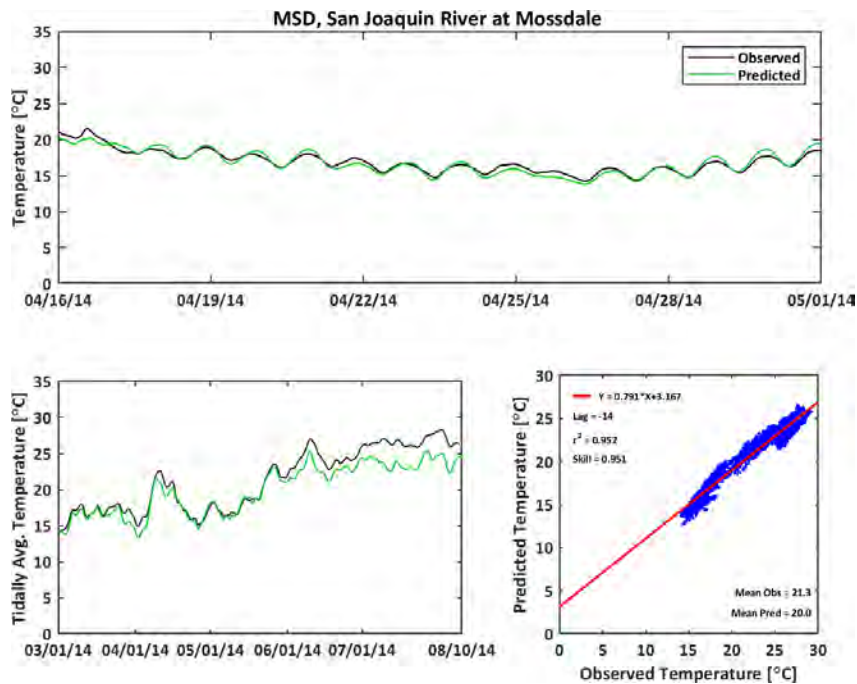


**Figure C-169**

**Observed and Predicted Temperature at Sacramento River at Rio Vista (SRV) During 2015**

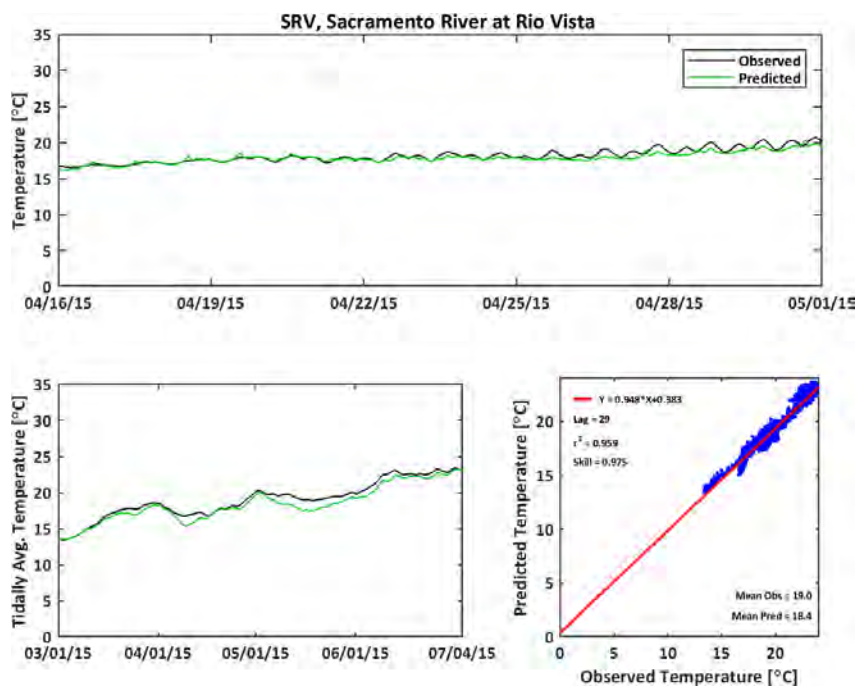


**Figure C-170**

**Observed and Predicted Temperature at San Joaquin River at Jersey Point (SJJ) During 2015**

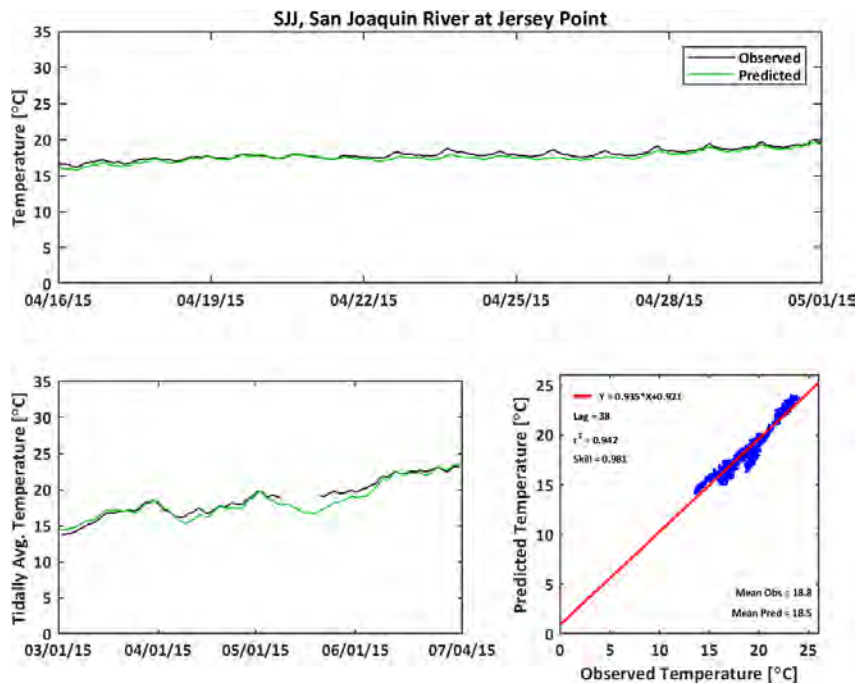


**Figure C-171**

**Observed and Predicted Temperature at Turner Cut near Holt (TRN) During 2015**

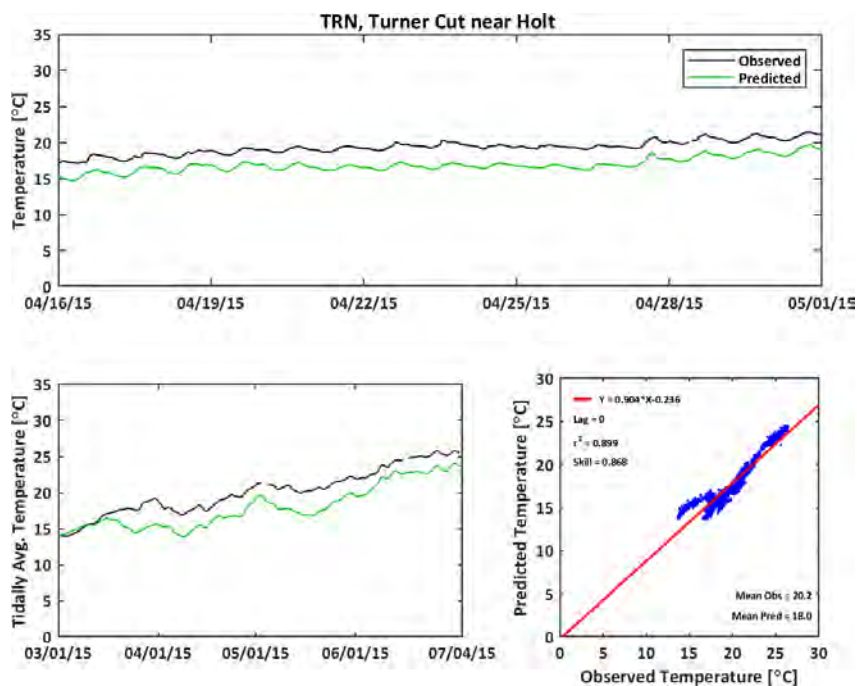


**Figure C-172**

**Observed and Predicted Temperature at Old River at Bacon Island (OBI) During 2015**

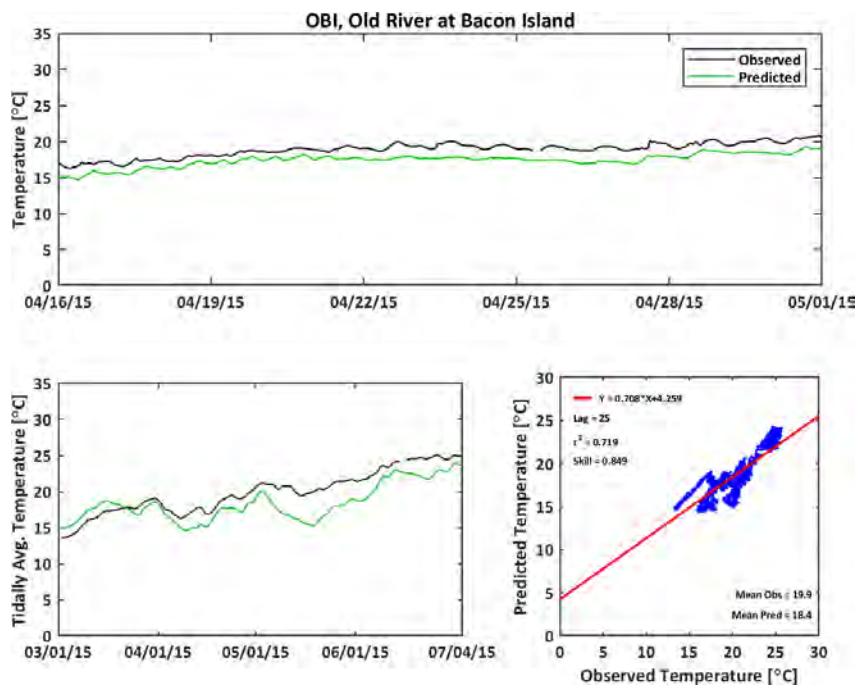


**Figure C-173**

**Observed and Predicted Temperature at Middle River at Middle River (MDM) During 2015**

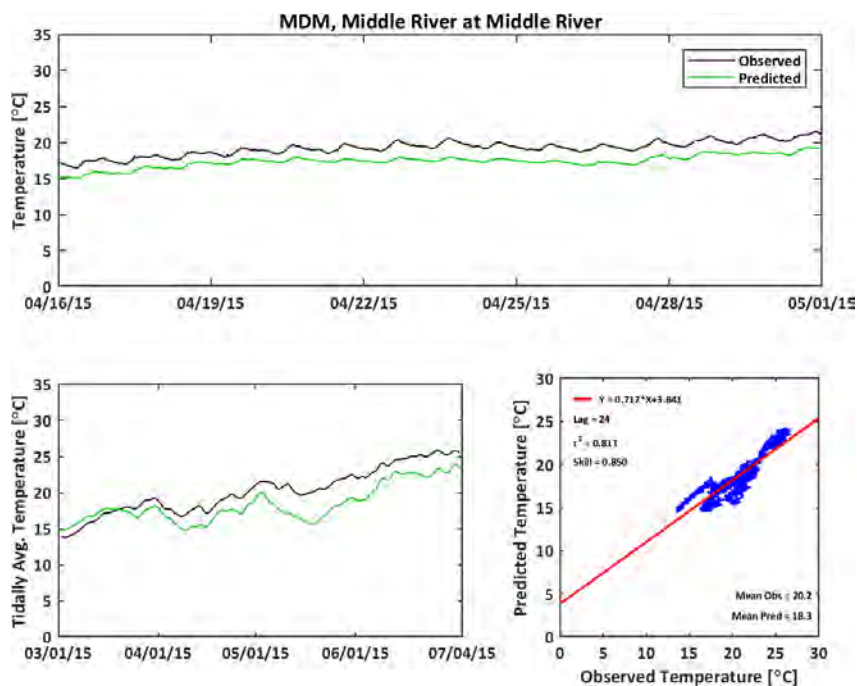


**Figure C-174**

**Observed and Predicted Temperature at Old River at Highway 4 (OH4) During 2015**

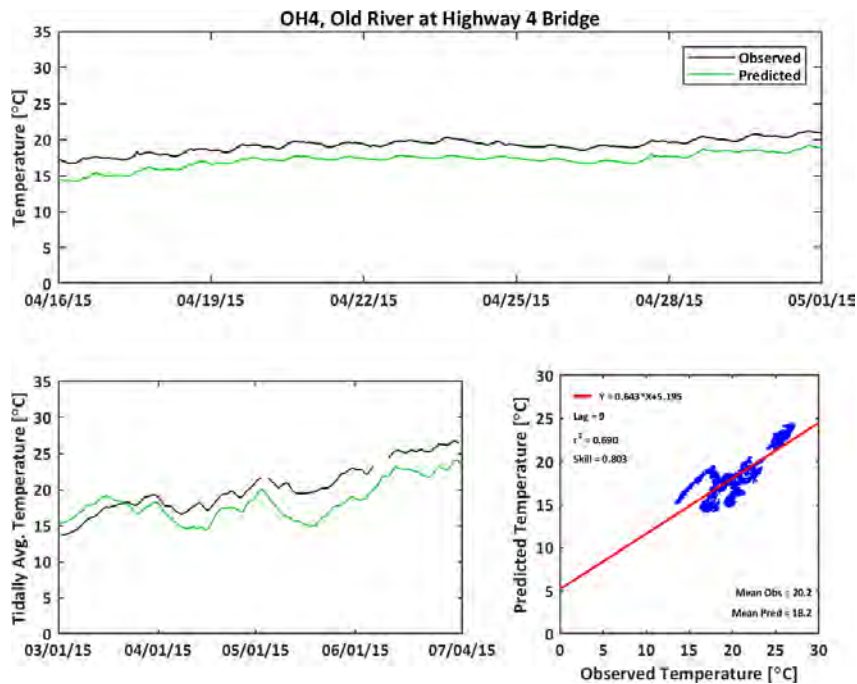


**Figure C-175**

**Observed and Predicted Temperature at Victoria Canal near Byron (VCU) During 2015**

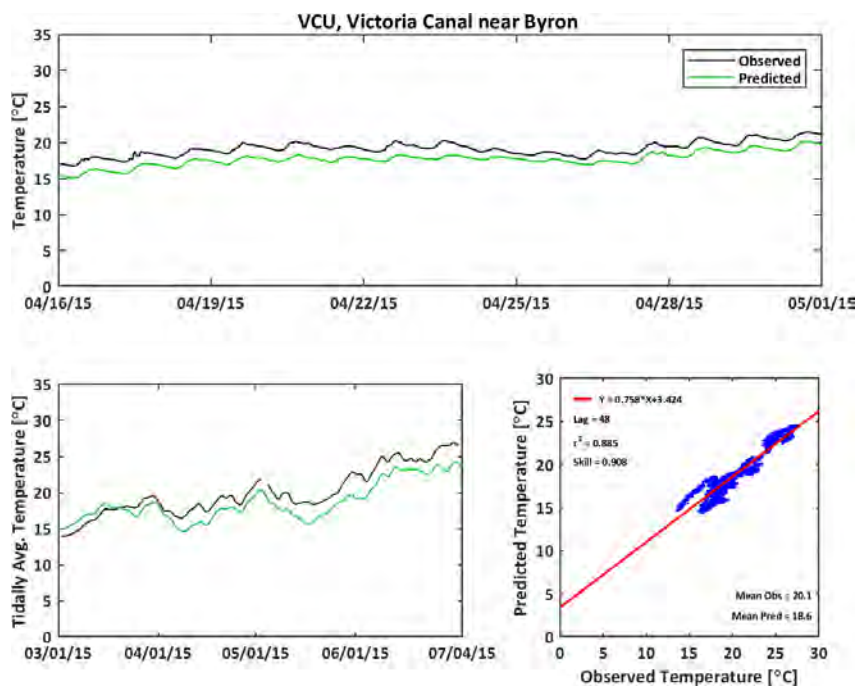


**Figure C-176**

**Observed and Predicted Temperature at Grant Line Canal near Clifton Court Ferry (GLC) During 2015**

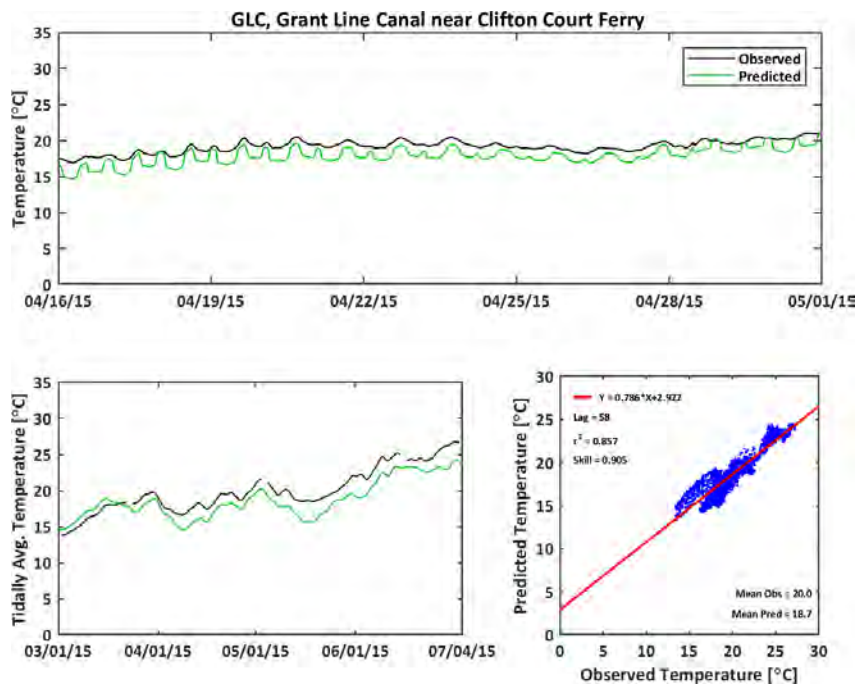


**Figure C-177**

**Observed and Predicted Temperature at Old River at Head (OH1) During 2015**

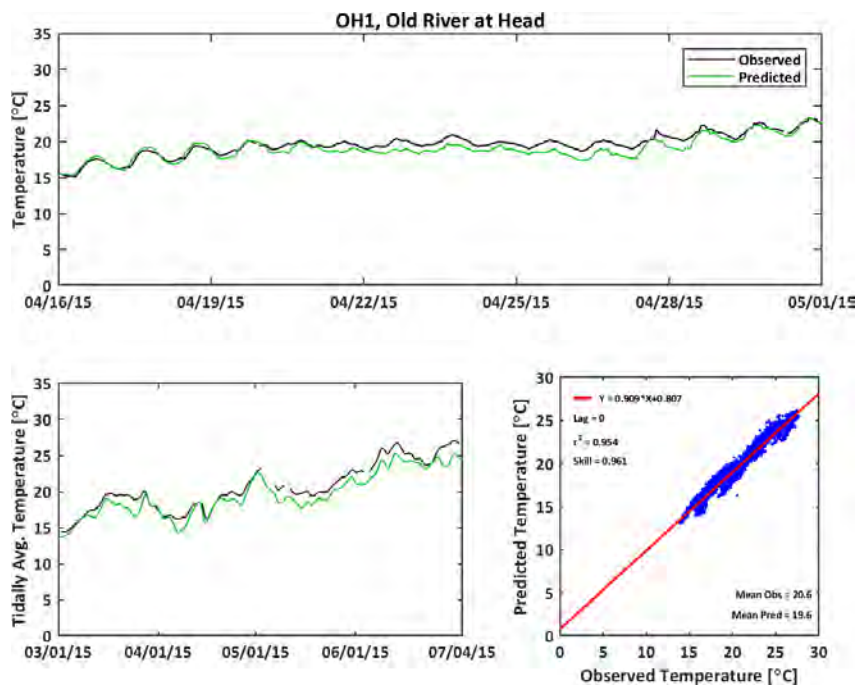


**Figure C-178**

**Observed and Predicted Temperature at San Joaquin River below Old River near Lathrop (SJL) During 2015**

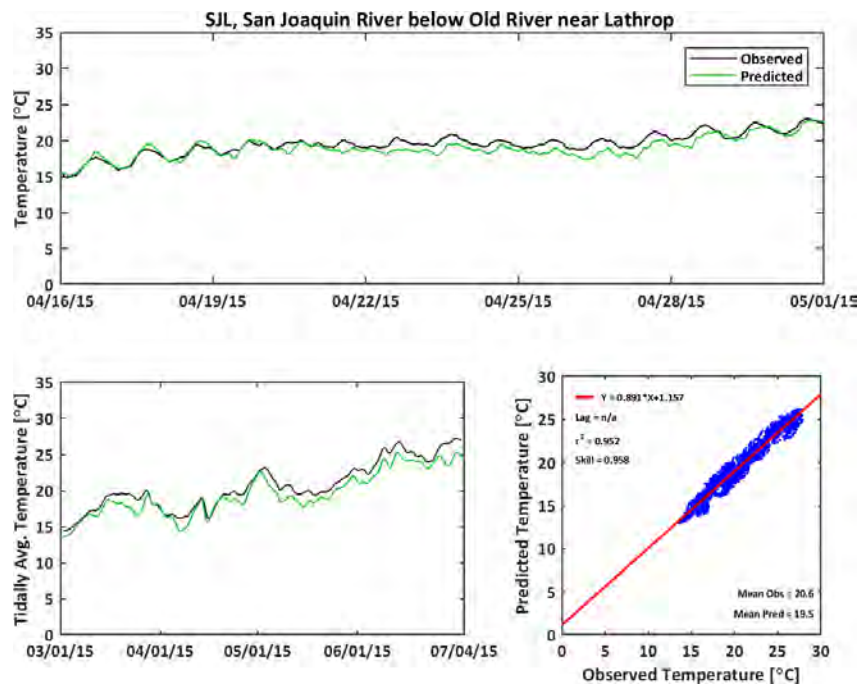


**Figure C-179**

**Observed and Predicted Temperature at San Joaquin River at Mossdale (MSD) During 2015**

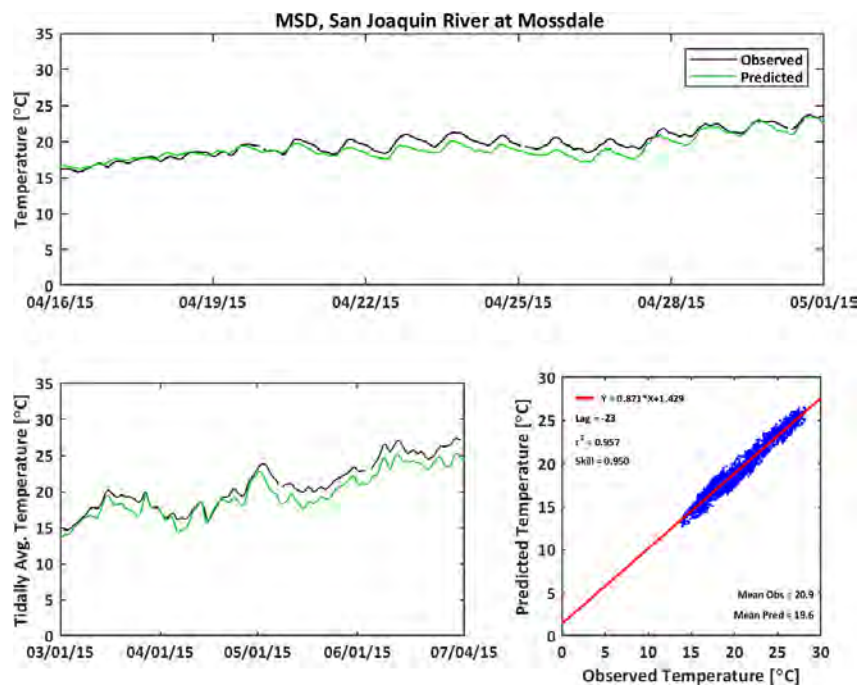


**Figure C-180**

**Observed and Predicted Temperature at Sacramento River at Rio Vista (SRV) During 2016**

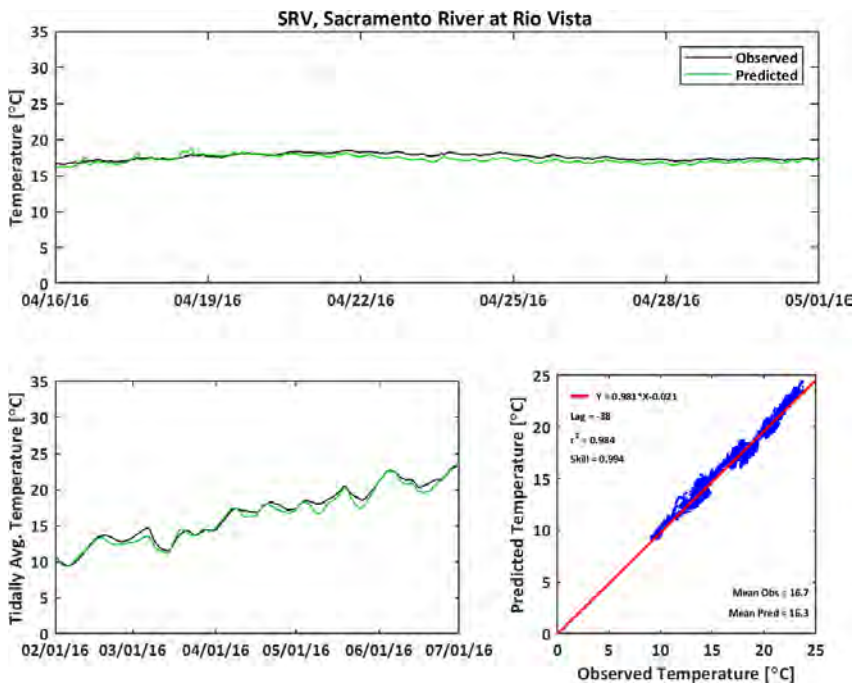


**Figure C-181**

**Observed and Predicted Temperature at San Joaquin River at Jersey Point (SJJ) During 2016**

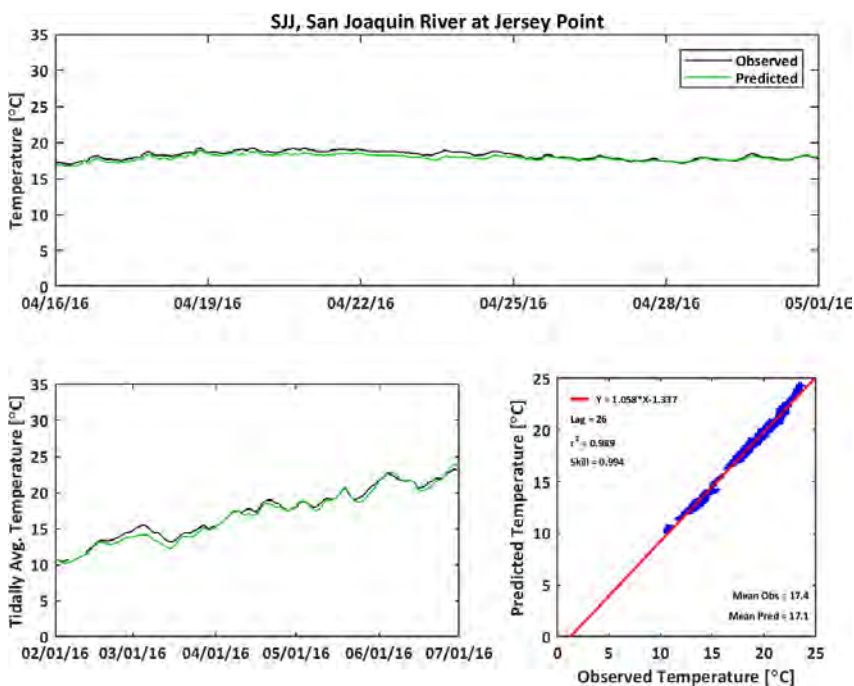


**Figure C-182**

**Observed and Predicted Temperature at Turner Cut near Holt (TRN) During 2016**

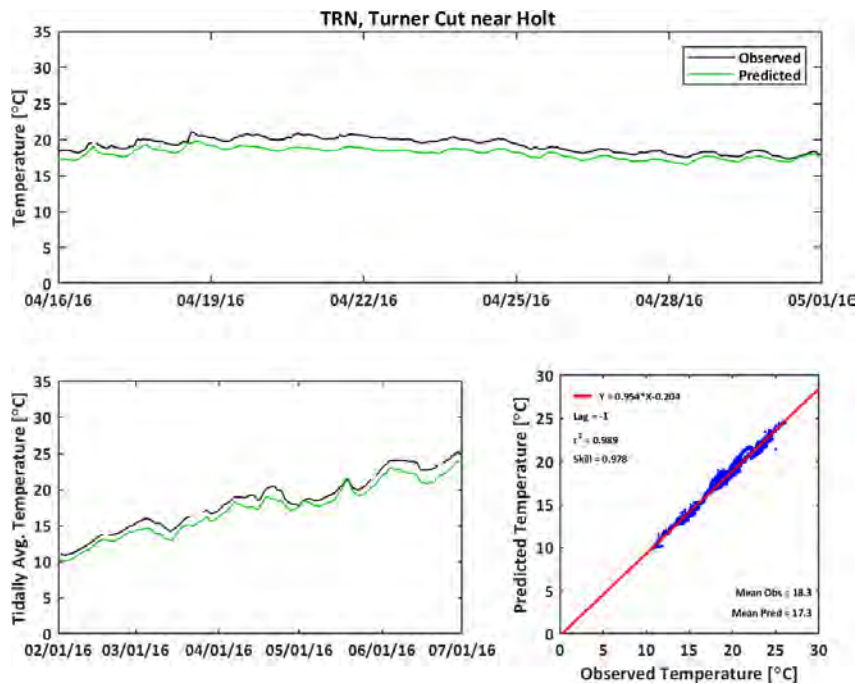


**Figure C-183**

**Observed and Predicted Temperature at Old River at Bacon Island (OBI) During 2016**

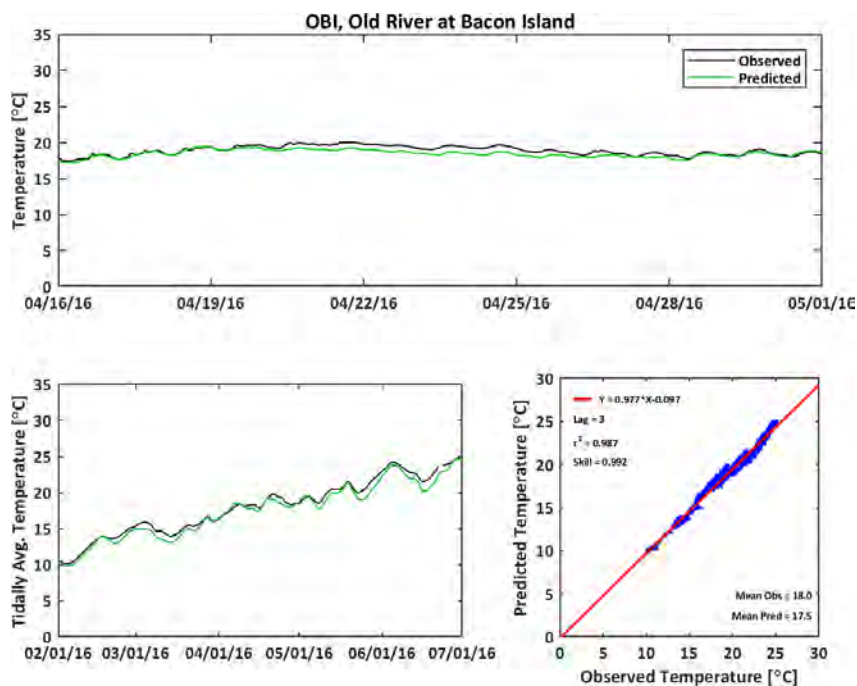


**Figure C-184**

**Observed and Predicted Temperature at Middle River at Middle River (MDM) During 2016**

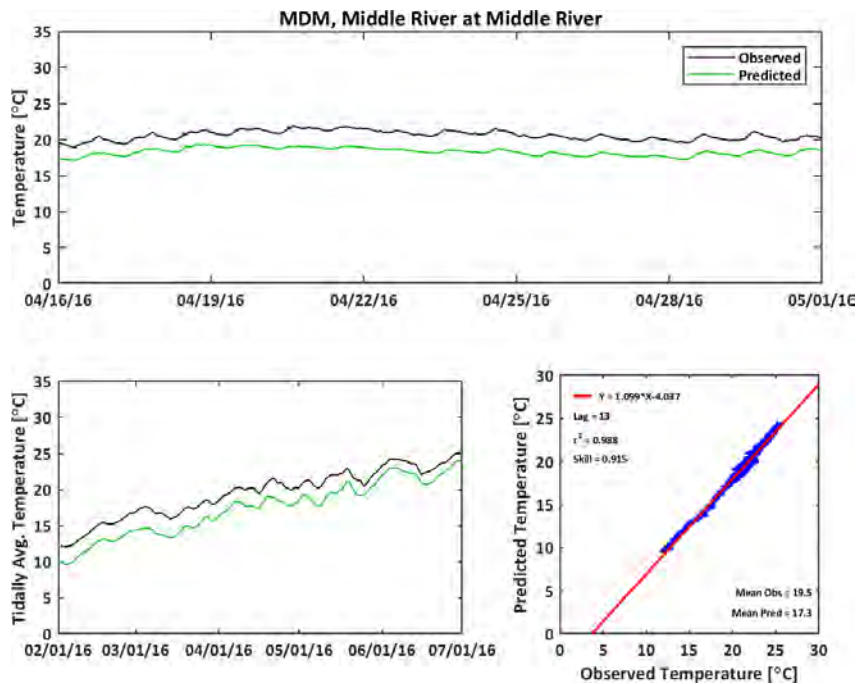


**Figure C-185**

**Observed and Predicted Temperature at Old River at Highway 4 (OH4) During 2016**

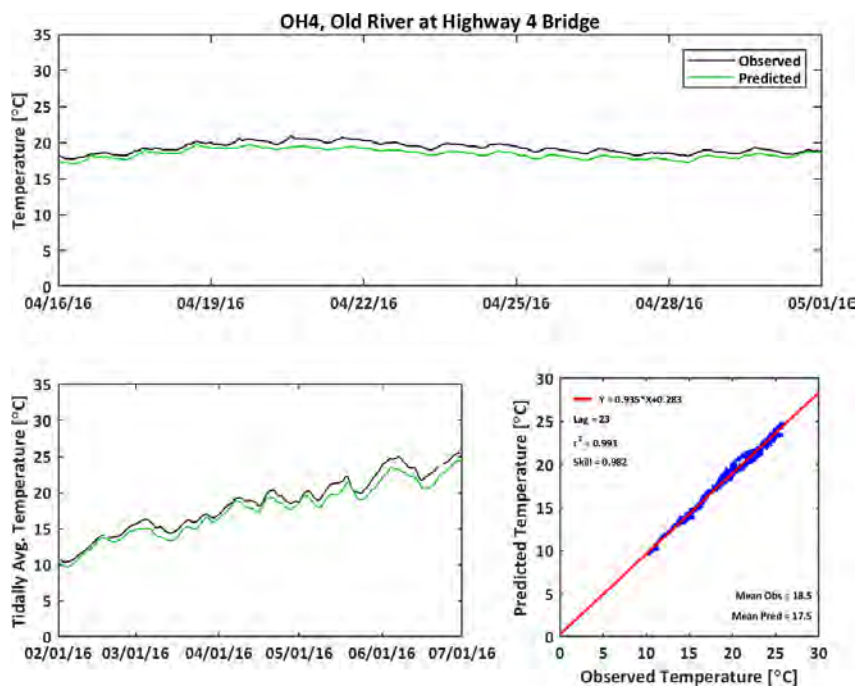


**Figure C-186**

**Observed and Predicted Temperature at Victoria Canal near Byron (VCU) During 2016**

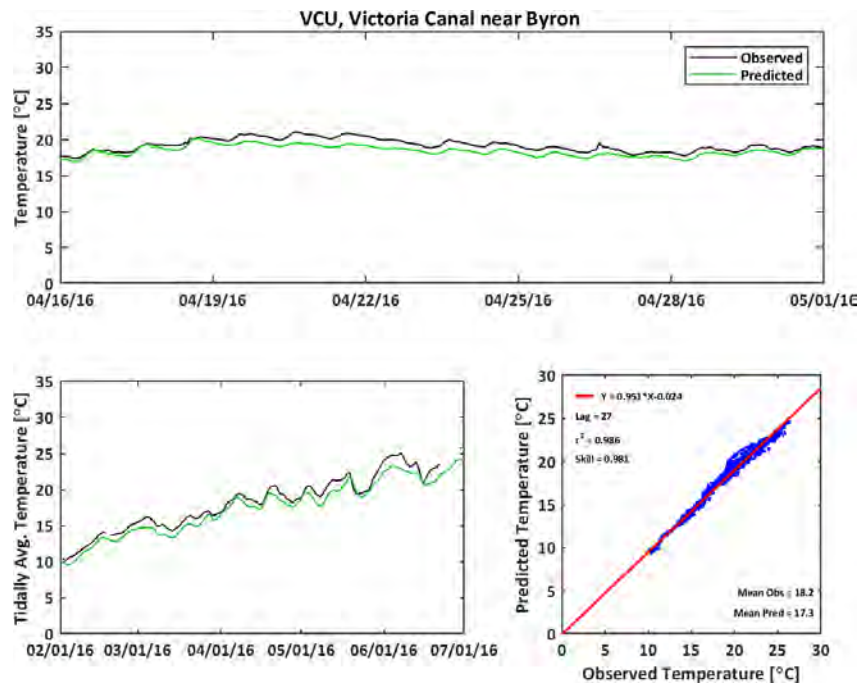


**Figure C-187**

**Observed and Predicted Temperature at Grant Line Canal near Clifton Court Ferry (GLC)  
During 2016**

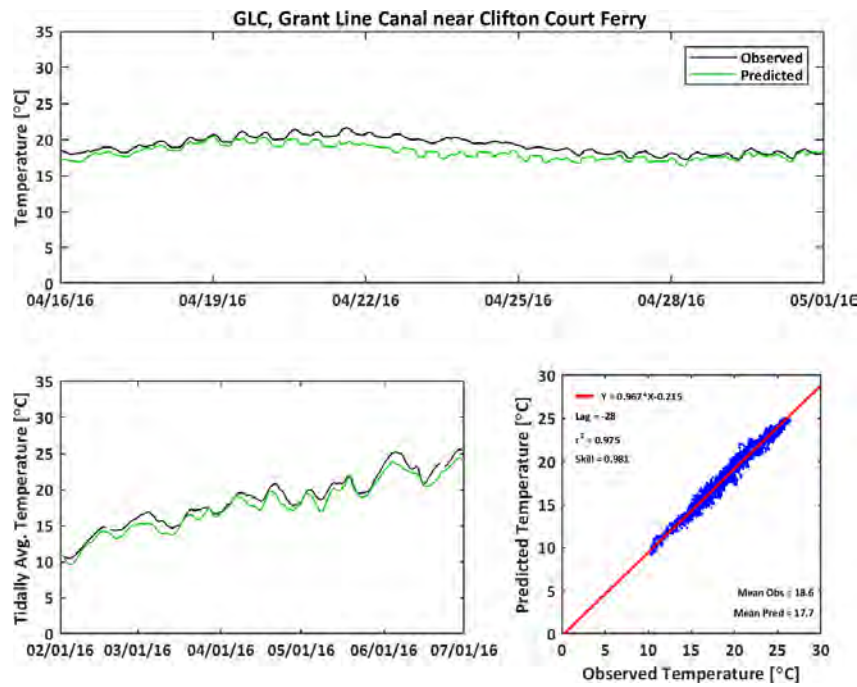


**Figure C-188**

**Observed and Predicted Temperature at Old River at Head (OH1) During 2016**

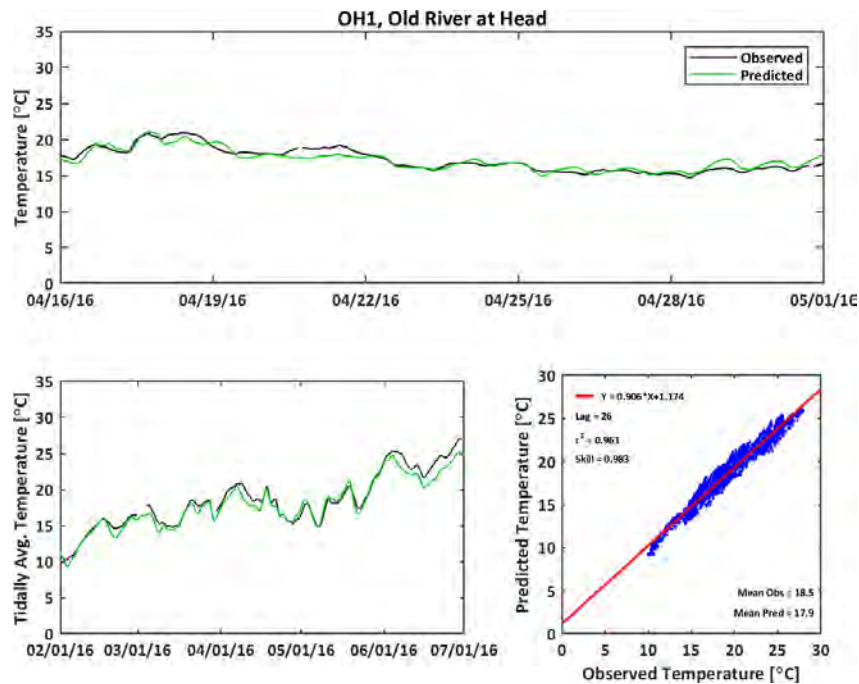


**Figure C-189**

**Observed and Predicted Temperature at San Joaquin River below Old River near Lathrop (SJL) During 2016**

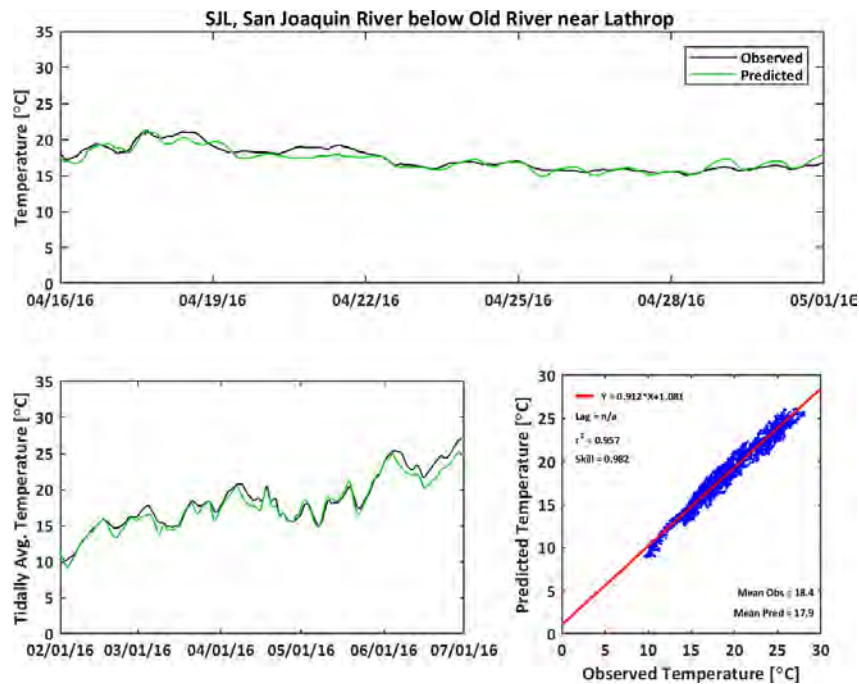
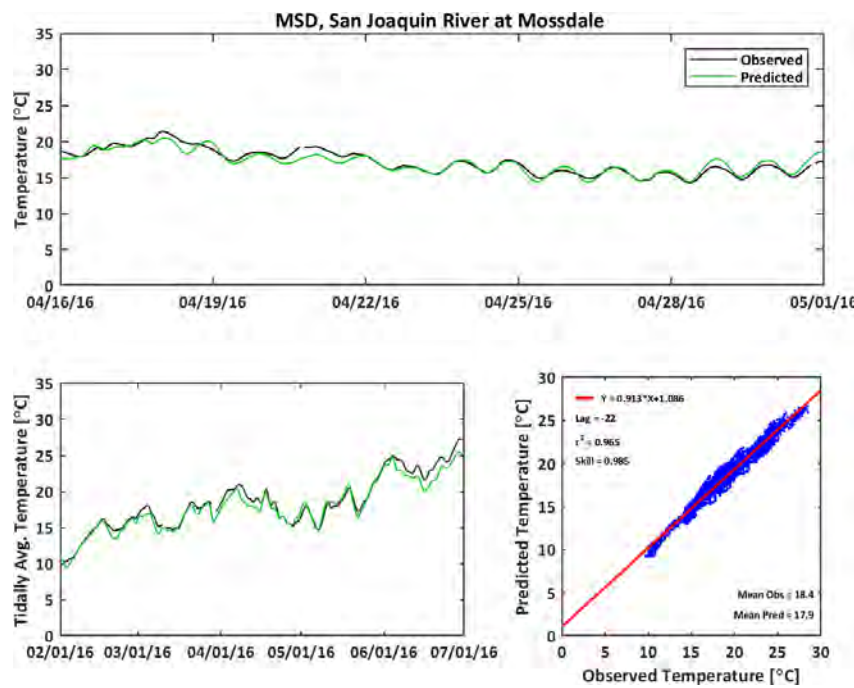


**Figure C-190**

**Observed and Predicted Temperature at San Joaquin River at Mossdale (MSD) During 2016**



## Appendix D

### Supplemental Fish Data and Model Outputs

---



## Appendix D

### Supplemental Fish Data and Model Outputs

---



## D.1 Fish Detection Summaries

**Table D.1-1 Head of Old River Junction**

Year	Fish Detection Dates	Barrier In	Barrier Out	Median Hours Spent	Number of Fish Detected	Active Migr %	Avg FL (mm)	Min FL (mm)	Max FL (mm)	Release Groups					Total Fish Released
										R1	R2	R3	R4	R5	
2011	3/22–7/14	--	--	2.53	785	90%	280	175	396	3/22–3/26	5/3–5/7	5/17–5/21	5/22–5/26	6/15–6/17	2,196
2012	4/5–7/2	4/1	6/4	1.7	802	97%	230	115	305	4/4–4/7	5/1–5/6	5/18–5/23	--	--	1,435
2013	3/7–6/8	--	--	2.3	907	90%	215	119	300	3/6–3/9	4/3–4/6	5/8–5/11	--	--	1,425
2014	3/28–6/9	4/8	6/9	7.1	599	73%	245	181	281	3/25–3/29	4/24–4/27	5/21–5/24	--	--	958
2015	3/6–5/19	4/3	6/1	17.1	485	58%	238	106	287	3/4–3/7	3/25–3/28	4/22–4/25	--	--	1,427
2016	2/26–6/7	4/1	6/1	2.2	1002	93%	250	148	292	2/24–2/27	3/16–3/19	4/27–4/30	--	--	1,440

Notes:

Active migrators were defined as fish that passed through Head of Old River junction within one completed tidal cycle (24.8 hours). This amount of time would be consistent with total Head of Old River to Chippis Island travel time of 1.4 to 34.9 days (Buchanan et al. 2021<sup>1</sup>).

--: no fish were released

Avg: average

FL: fork length

Max: maximum

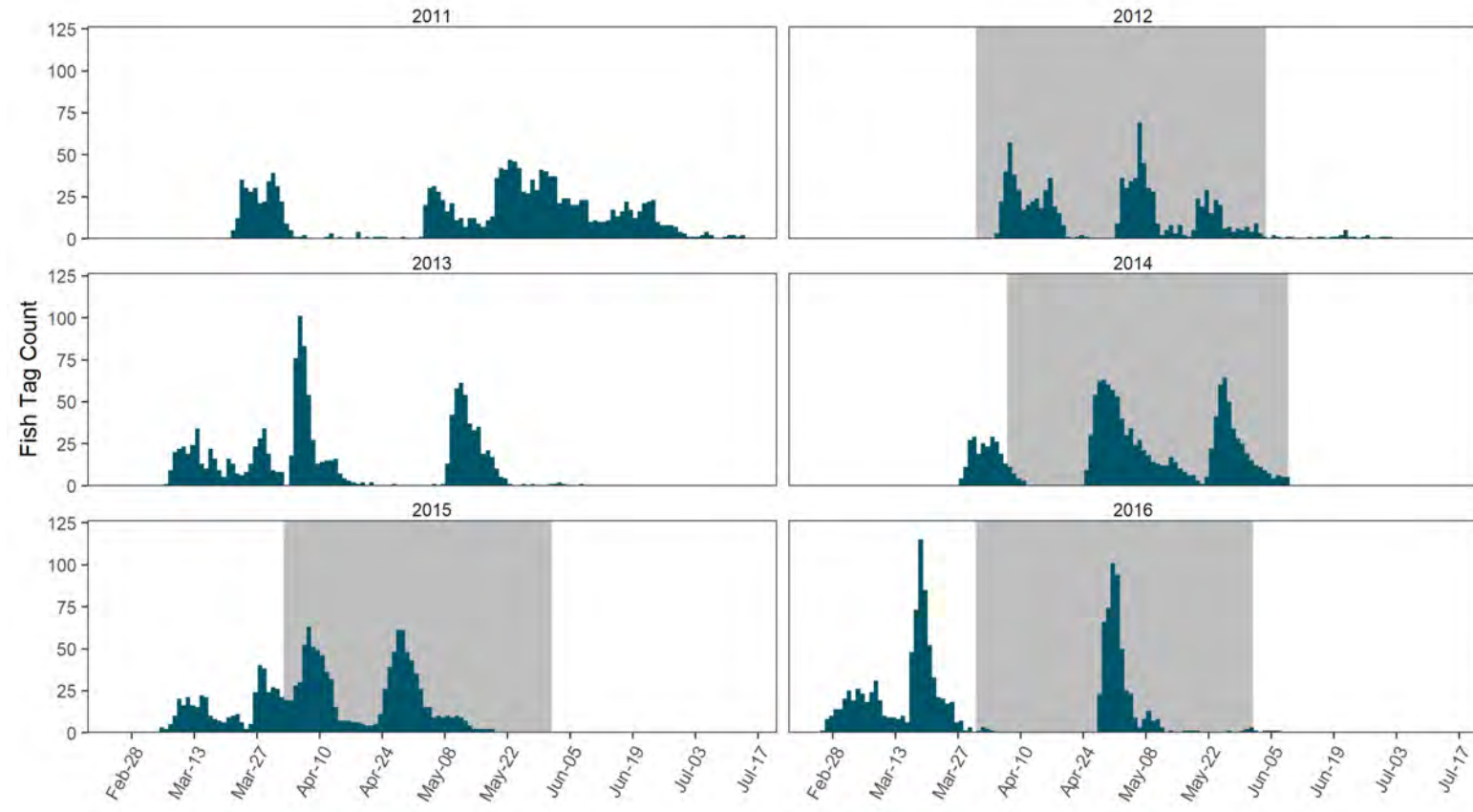
Migr: migrator

Min: minimum

mm: millimeter

<sup>1</sup> Buchanan, R.A., E. Buttermore, and J. Israel, 2021. "Outmigration Survival of a Threatened Steelhead Population Through a Tidal Estuary." *Canadian Journal of Fisheries and Aquatic Sciences* 78(12):1869–1886.

**Figure D1-1**  
**Head of Old River Juvenile Steelhead Tag Counts by Day with Barrier Presence**



Note:  
Gray background shows the Head of Old River barrier presence.

**Table D.1-2 Turner Cut Junction**

Year	First Fish Detection	Last Fish Detection	Barrier In	Barrier Out	Median Hours Spent	Number of Fish	Avg FL (mm)	Min FL (mm)	Max FL (mm)	Release Groups		
										R1	R2	R3
2013	4/8	5/22	--	--	7.85	29	221	180	252	3/6–3/9	4/3–4/6	5/8–5/11
2015	3/15	5/9	4/3	6/1	9.19	91	246	202	280	3/4–3/7	3/25–3/28	4/22–4/25
2016	3/6	5/30	4/1	6/1	9.6	456	255	196	292	2/24–2/27	3/16–3/19	4/27–4/30

**Table D.1-3 Water Project Area**

Year	First Fish Detection	Last Fish Detection	Barrier In	Barrier Out	Median Hours Spent	Number of Fish	Avg FL (mm)	Min FL (mm)	Max FL (mm)	Release Groups		
										R1	R2	R3
2014	3/30	6/11	4/8	6/9	26.3	118	241	181	275	3/25–3/29	4/24–4/27	5/21–5/24
2015	3/11	5/20	4/3	6/1	29.4	218	236	139	287	3/4–3/7	3/25–3/28	4/22–4/25
2016	2/28	6/21	4/1	6/1	11.4	454	248	148	281	2/24–2/27	3/16–3/19	4/27–4/30

## D.1.1 Fish Observed Transition Frequency Tables

The frequency tables count the number of times each pair of states were observed in successive observation times (Figures D.1.1-1, D.1.1-2, and D.1.1-3). The tables are not used to decide what transitions are allowed to occur, since the model works in continuous time. These transition frequency tables count the transitions between states over a time interval, not in real time. There can be observed transitions between state r and s over an interval even if  $q_{rs} = 0$ , because the process may have passed through one or more intermediate states in the middle of the interval (Jackson 2019<sup>2</sup>). Similarly, successive observations of the same state do not rule out that the process may have passed through one or more intermediate states in the middle of the interval.

**Figure D.1.1-1**  
**Observed Number of State Transitions for Head of Old River Junction**

A			B				
	U	D	T	U	D	T	
U	[3576	3476	1833]	U	[1344	1021	1743]
D	809	2529	340	D	67	833	324
T	36	28	672	T	36	26	569

Barrier Installed    Barrier Not Installed

Notes:

Panel A is the overall state table that the model is fitted to. For state transition matrices, starting states are listed as rows ("from"), and finishing states are listed as columns ("to"). For example, fish transitioned from state U to state D 3,476 times. Panel B shows the observed number of state transitions during periods when the barrier was installed versus when the barrier was not installed.

D: downstream

T: distributary

U: upstream

<sup>2</sup> Jackson, C., 2019. "msm: Multi-State Markov and Hidden Markov Models in Continuous Time." Reference manual for version 1.6.8. December 16, 2019. Accessed on October 7, 2020. Available at: <https://cran.r-project.org/web/packages/msm/index.html>.

**Figure D.1.1-2**  
**Observed Number of State Transitions for Turner Cut Junction**

	U	D	T
U	460	571	136
D	130	402	29
T	22	5	47

Notes:

For state transition matrices, starting states are listed as rows ("from"), and finishing states are listed as columns ("to"). For example, fish transitioned from state U to state D 571 times.

**Figure D.1.1-3**  
**Observed Number of State Transitions for Water Project Area**

	C	R	W	V
C	1494	115	78	243
R	227	692	251	0
W	118	241	404	0
V	0	0	0	0

Notes:

For state transition matrices, starting states are listed as rows ("from"), and finishing states are listed as columns ("to"). For example, fish transitioned from state C to state R 227 times.

C: Central Valley Project (CVP)

R: Clifton Court Forebay radial gates

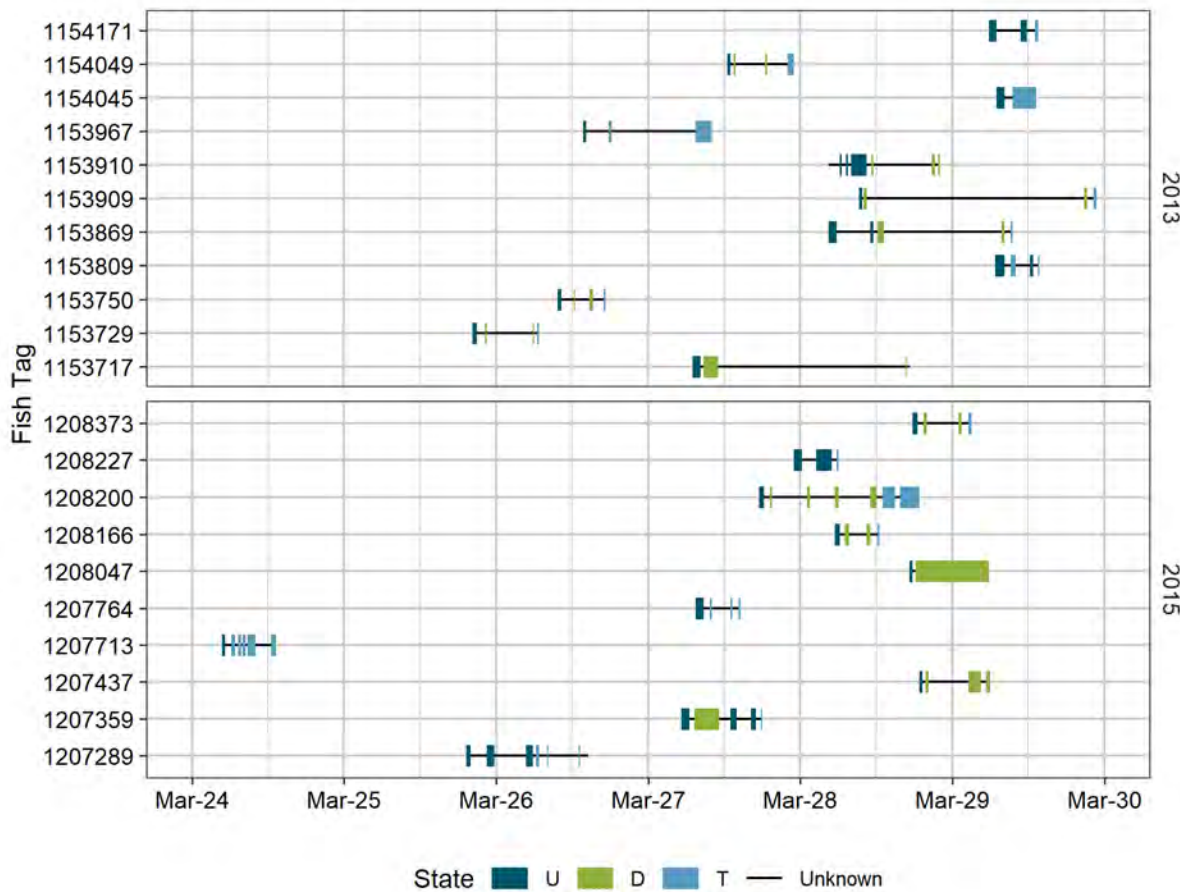
V: Central Valley Project salvage tank

W: West Canal

## D.2 Observed Fish Detection Histories

**Figure D.2-1**

**Example Observed Detection Histories at Head of Old River Junction for Subset of Study Fish in Late March**

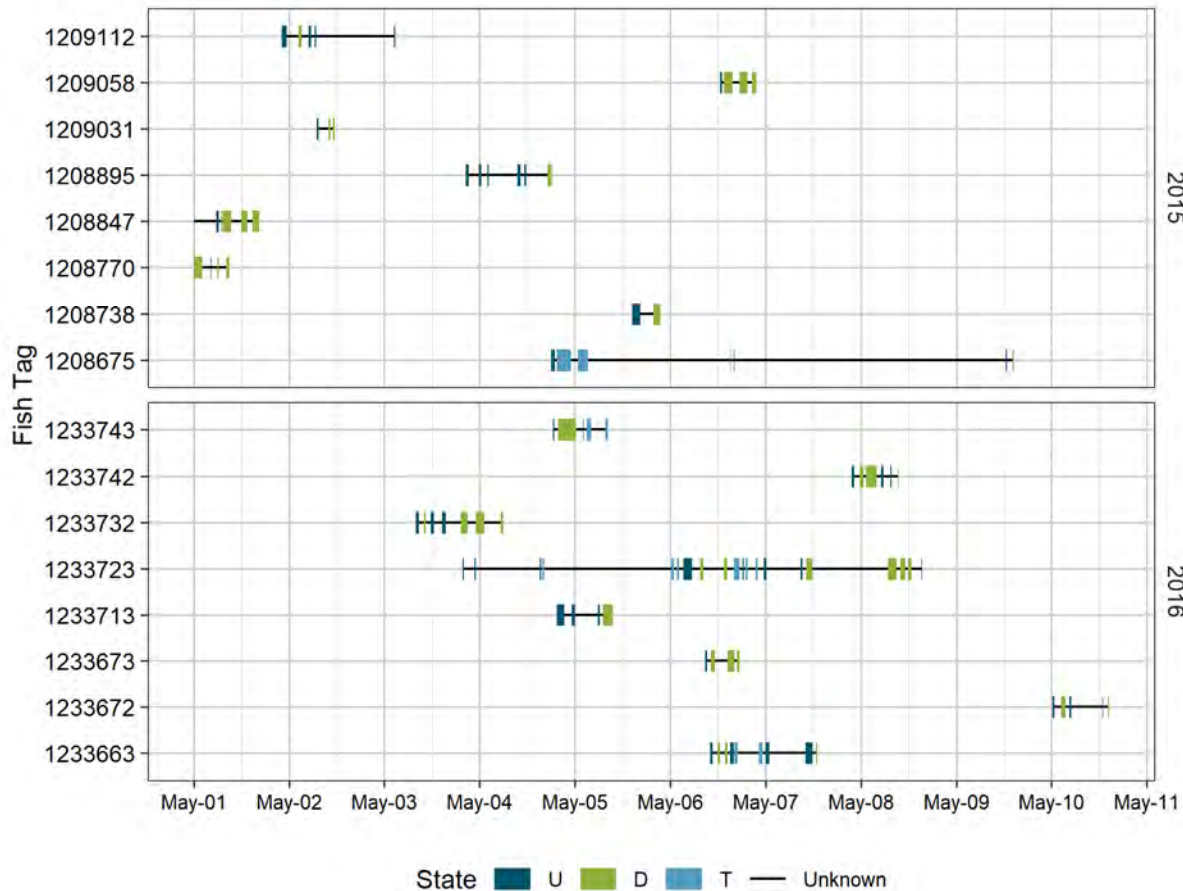


**Notes:**

Each line represents an individual fish detection history. Thick colored lines represent presence at a single state, while thin black lines represent periods when the fish was not detected.

**Figure D.2-2**

**Example Observed Detection Histories at Turner Cut Junction for a Subset of Study Fish in Early March**

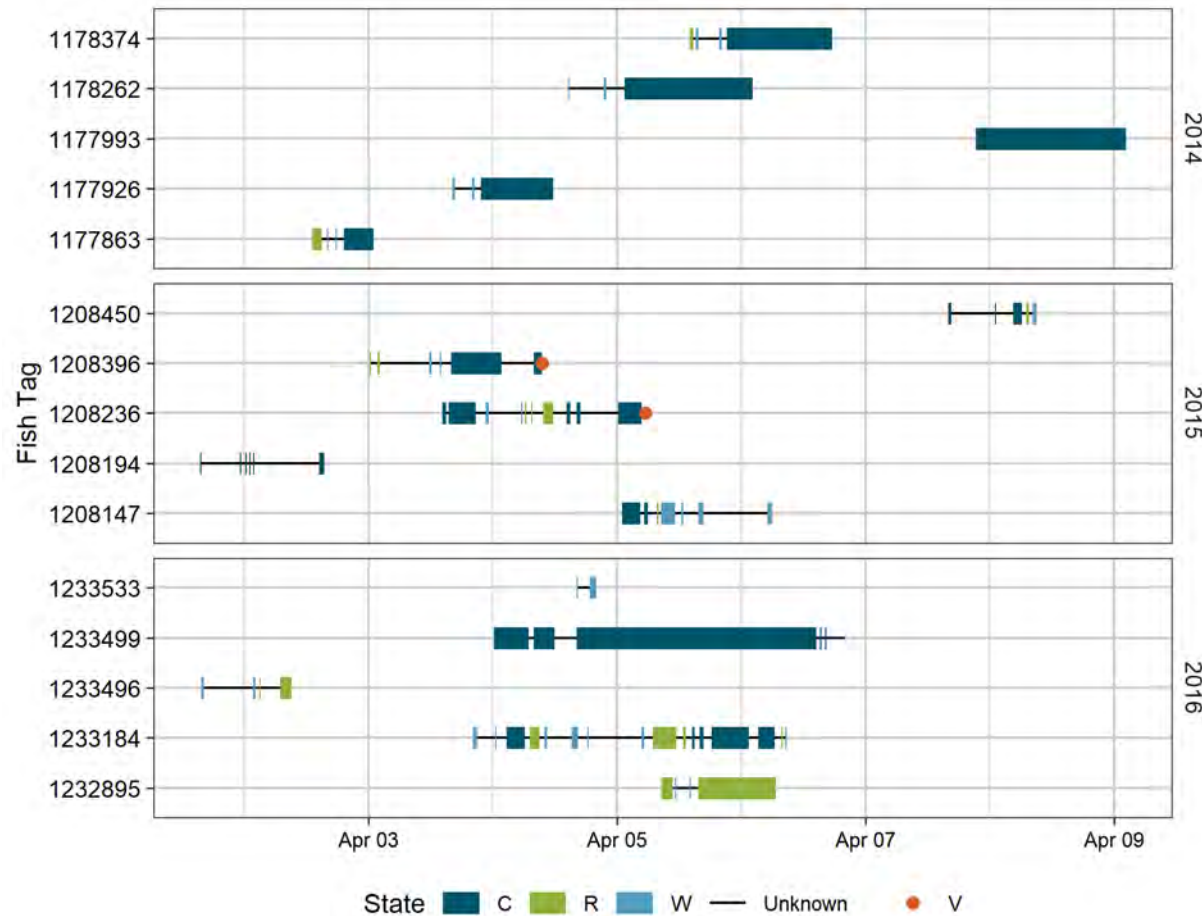


**Notes:**

Each line represents an individual fish detection history. Thick colored lines represent presence at a single state, while thin black lines represent periods when the fish was not detected.

**Figure D.2-3**

**Example Observed Detection Histories at Water Project Export Facilities Area for a Subset of Study Fish in Early April**



Notes:

Each line represents an individual fish detection history. Thick colored lines represent presence at a single state, while thin black lines represent periods when the fish was not detected.

### D.3 Additional Example Period Transitions for HOR

In addition to the high flow with barrier not installed (March 17 to March 21, 2016) and low flow with the barrier installed (May 22 to May 26, 2016) periods present in the main text, transition probabilities were modeled for a period of low flow with the barrier not installed (April 5 to April 9, 2013). Transition probabilities during this period were substantially similar to the higher flow period in 2016 and were therefore not presented in the main text. There were no instances of high flow with barrier installed to evaluate.

**Figure D.3-1**  
**Example Transition Probabilities at Head of Old River over a 3-Day Period (April 5 to April 9, 2013)**

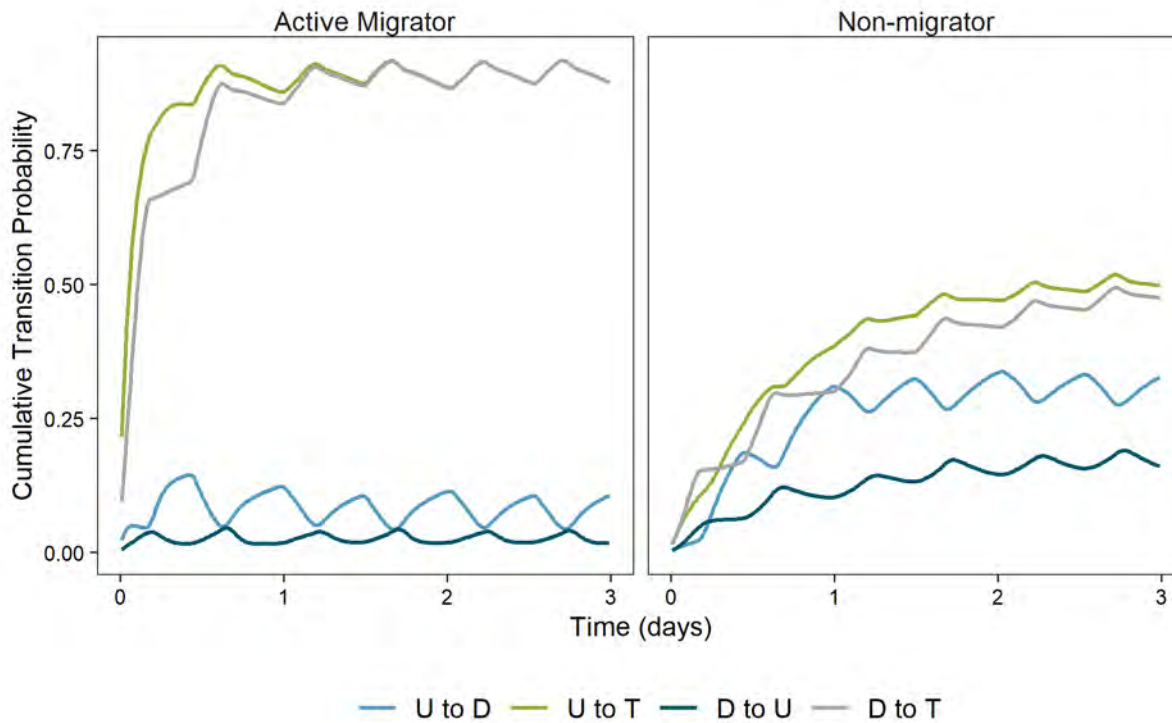
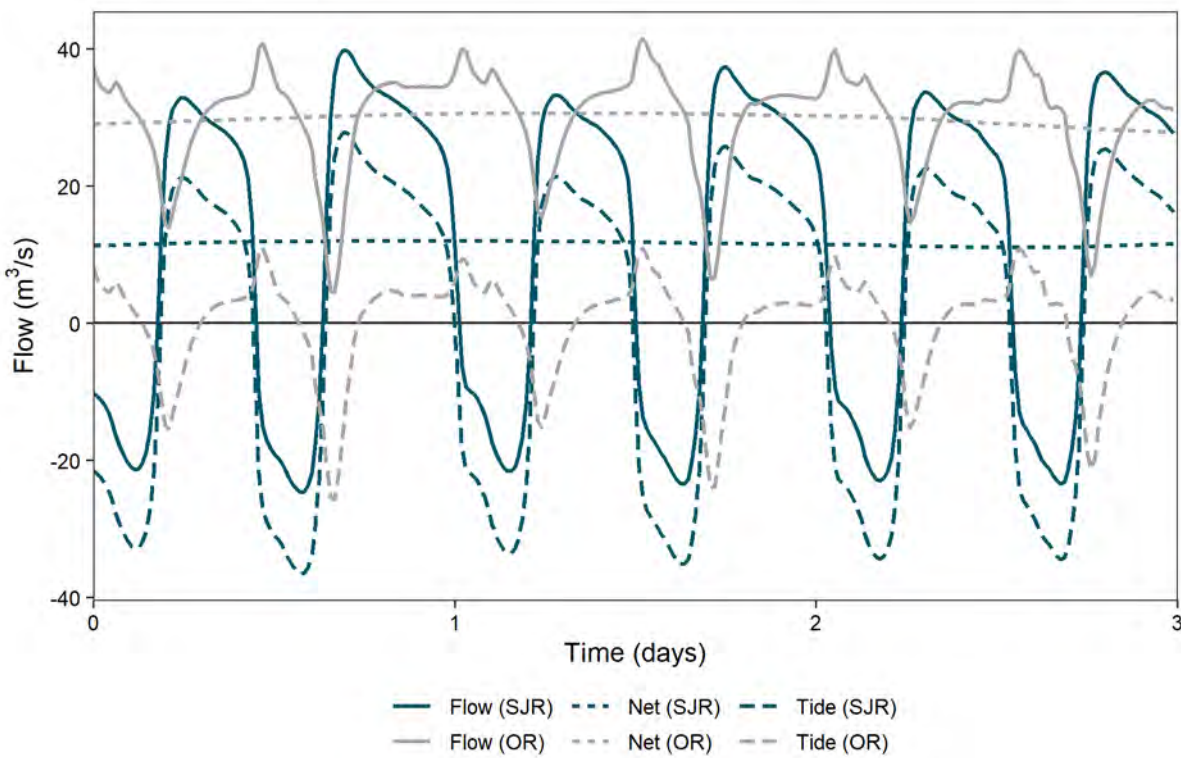


**Figure D.3-2**

**Flow Conditions at Head of Old River over a 3-Day Period (April 5 to April 9, 2013)**



Notes:

OR: Old River

SJR: San Joaquin River

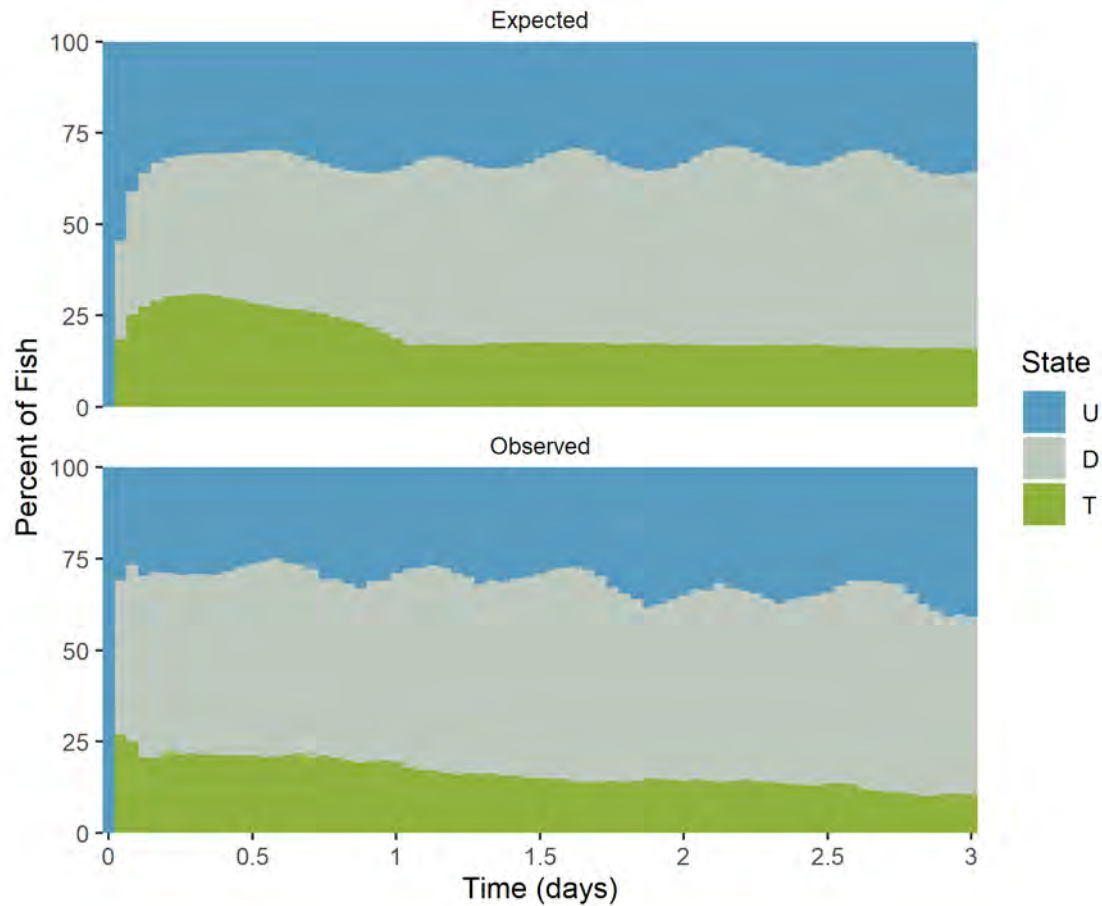
## D.4 Model Performance Plots

Prevalence plots help determine how well a fitted multistate model describes an irregularly observed process by comparing observed data with fitted or expected data under the model (Jackson 2011<sup>3</sup>, Jackson 2019). A set of expected counts can be produced by assuming process begins at a common time for all individuals. If at this common time each individual is in state 0, then if  $n(t)$  individuals are under observation at time  $t$ , the expected number of individuals in state  $r$  at time  $t$  is  $n(t)*P(t)_{0,r}$  (Jackson 2019). If the covariates vary between individuals, they averaged over the covariates observed in the data (Jackson 2019). The observed and expected percentages in each state can then be plotted against time.

---

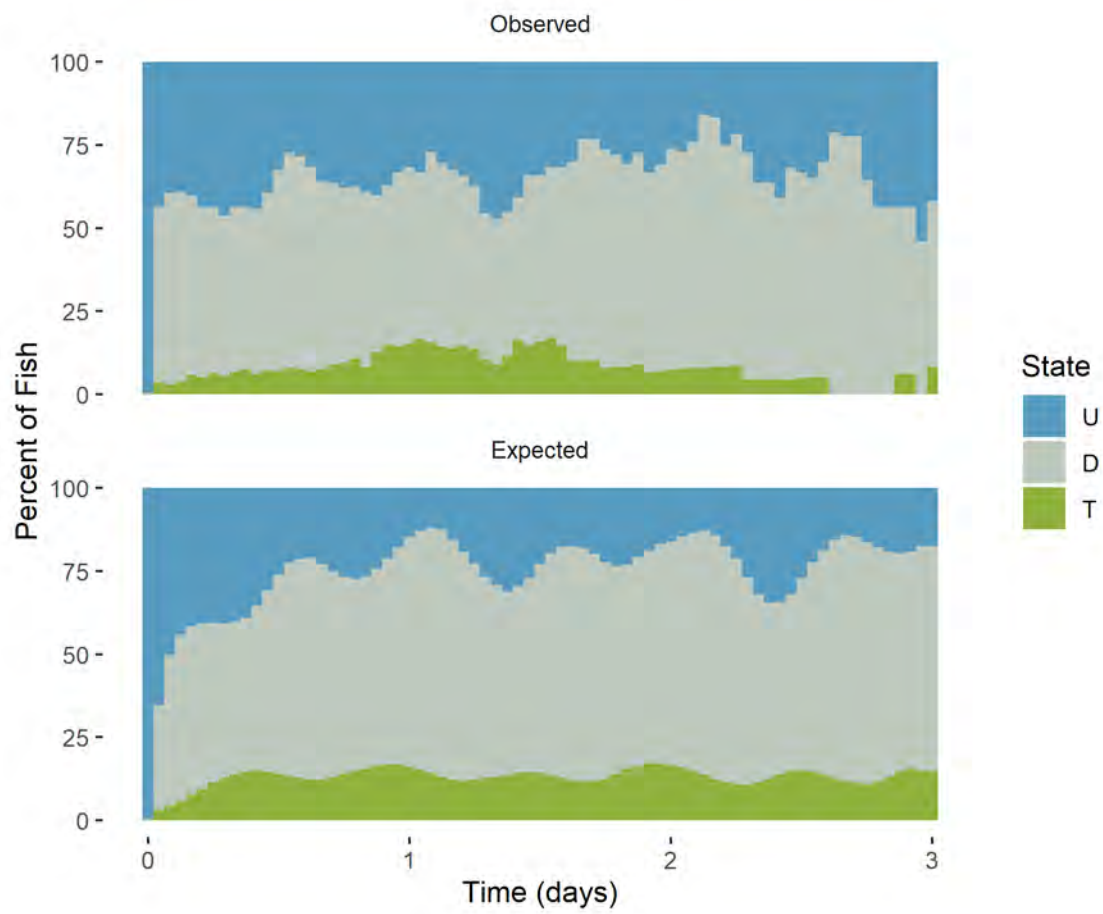
<sup>3</sup> Jackson, C.H., 2011. "Multi-State Models for Panel Data: The *msm* Package for R." *Journal of Statistical Software* 38(8). Available at: <https://doi.org/10.18637/jss.v038.i08>.

**Figure D.4-1**  
**Head of Old River Prevalence**



Notes:  
U: upstream, D: downstream, T: distributary

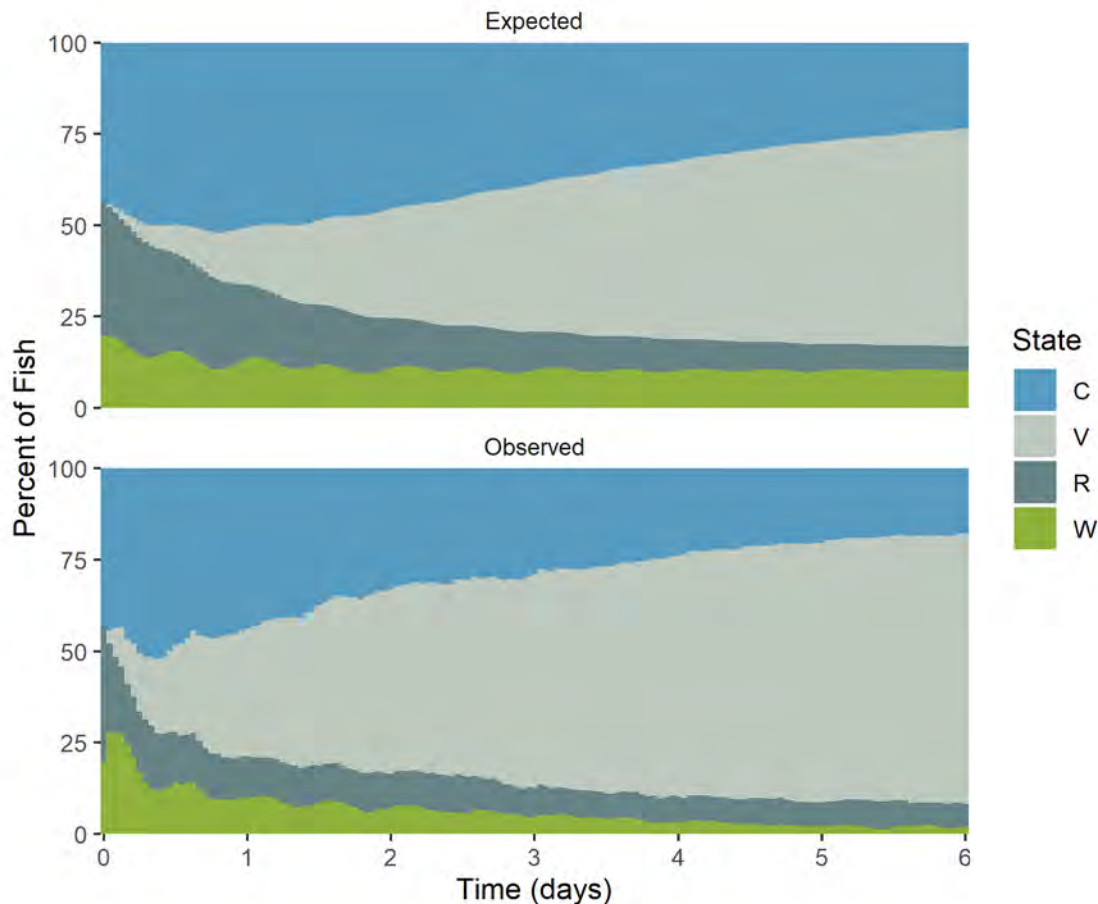
**Figure D.4-2**  
**Turner Cut Prevalence**



Notes:

U: upstream, D: downstream, T: distributary

**Figure D.4-3**  
**Water Project Export Facilities Area Prevalence**



Notes:

C: CVP, V: CVP salvage tank, R: Clifton Court Forebay radial gates, W: West Canal.